Gold-Catalysed Functionalisations of Yndiamides



Zixuan Tong

The Queen's College
University of Oxford

A thesis submitted to the Board of the Faculty of Physical Sciences
in partial fulfilment of the requirements for the degree of

Doctor of Philosophy

Trinity Term 2023

Gold-Catalysed Functionalisations of Yndiamides

Zixuan Tong Doctor of Philosophy

The Queen's College Trinity 2023

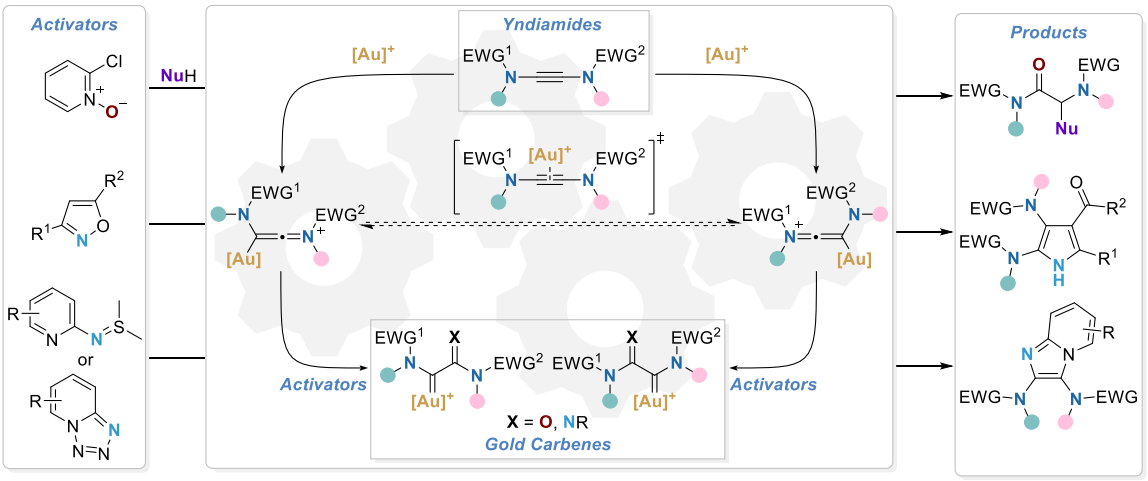
Yndiamides, doubly nitrogen-substituted alkynes, have been explored by our group in the past few years due to their unique reactivity profiles compared to their better-established ynamide relatives. Gold-catalysed functionalisation of alkynes has gained significant importance over the past decade, however, the potential utility of gold-catalysed functionalisation of yndiamides remained unexplored. As an exploration into this uncharted territory, three projects have been completed with a further project ongoing:

(i) In Chapter II, a gold-catalysed oxidative functionalisation of yndiamides with pyridine *N*-oxides *via* α-oxo gold Fischer carbenes is described. An array of unnatural amino acid derivatives was produced. Regioselectivity could be achieved by introducing subtle steric bias between two nitrogen substituents.

(ii) In Chapter III, a gold-catalysed cyclisation of yndiamides with isoxazoles *via* α-imino gold Fischer carbenes was achieved. A broad scope of polysubstituted 2,3-diaminopyrroles was acquired. The same steric control was found to be effective in establishing regioselectivity. In addition, the reaction outcome could be switched to a formal [5+2] cyclisation by using benzisoxazoles as the activator.

(iii) In Chapter IV, computational investigations were conducted to explore the mechanism of the gold-catalysed cyclisation of yndiamides with isoxazoles. This revealed that the key to its regioselectivity was a low-barrier gold π-complex-like transition state which established a Curtin-Hammett scenario for isoxazole addition.

(iv) In Chapter V, the discovery of tetrazolo[1,5-*a*]pyridines as novel nitrene transfer reagents is presented. Their reactivity difference compared to that of pyridyl sulfilimines for the functionalisation of yndiamides *via* α-imino gold Fischer carbenes is discussed.



Through the aforementioned four projects, a variety of protocols to functionalise yndiamides with various activators *via* α-gold carbenes has been successfully established. Combined with computational tools, a detailed mechanism has been revealed, including the underlying principles that control the regiochemical outcomes. This study is expected to serve as the door into new possibilities for gold- or other transition metal-catalysed yndiamide functionalisations.

Declaration

The work presented in this thesis was conducted in the Department of Chemistry at the University of Oxford. This thesis is the result of my own work and contains no results obtained by others or through collaboration except where explicitly stated in the text. The work presented has not been submitted, either partially or in full, for any qualification at this or any other institution.

Aspects of this work have been included in the following publications:

1. Z. Tong, O. L. Garry, P. J. Smith, Y. Jiang, S. J. Mansfield, E. A. Anderson, *Org. Lett.* **2021**, 23, 4888–4892.
2. Z. Tong, P. J. Smith, H. D. Pickford, K. E. Christensen, E. A. Anderson, *Manuscript Submitted*, **2023**.

Contributions have also been made to the following publications:

1. Y. Jiang, R. E. McNamee, P. J. Smith, A. Sozanschi, Z. Tong, E. A. Anderson, *Chem. Soc. Rev.* **2021**, 50, 58–71.
2. P. J. Smith, Y. Jiang, Z. Tong, H. D. Pickford, K. E. Christensen, J. Nugent, E. A. Anderson, *Org. Lett.* **2021**, 23, 6547–6552.
3. P. J. Smith, Z. Tong, J. Ragus, P. Solon, K. W. Shimkin and E. A. Anderson, *Org. Lett.* **2022**, 24, 7522–7526.

Table of Contents

Acknowledgement vi

Abbreviations viii

Chapter I: Introduction to Yndiamides 1

1.1 Yndiamides: Past and present 2

1.1.1 Ynamides: Predecessors of yndiamides 2

1.1.2 Synthesis of Yndiamides 3

1.1.3 Previously Reported Yndiamide Reactivities 6

1.2 Gold-Catalysed Oxidative Functionalisations of Alkynes 13

1.3 Conclusion: Project Objectives and Challenges 15

Chapter II: Gold(I)-Catalysed Functionalisation of Yndiamides with Pyridine *N*-Oxides 17

2.1 Introduction 18

2.1.1 Gold-Catalysed Oxidative Functionalisation of Ynamides with Pyridine N-oxides 18

2.1.2 Concepts of This Work and Initial Attempts 25

2.2 Results and Discussion 28

2.2.1 Optimisation of Conditions 28

2.2.2 Nucleophile Scope and Robustness Tests 30

2.2.3 Derivatisation of Products 34

2.2.4 Regioselectivity Studies 35

2.2.5 Mechanistic Proposal 40

2.3 Conclusions 42

Chapter III: Gold(I)-Catalysed Cyclisation of Yndiamides with Isoxazoles 43

3.1 Introduction 44

3.1.1 Gold-Catalysed Functionalisation of Ynamides with Isoxazoles 44

3.1.2 Concepts of This Work 52

3.2 Results and Discussion 53

3.2.1 Optimisation of Conditions *53*

3.2.2 Isoxazole Scope *56*

3.2.3 Derivatisation of Products *59*

3.2.4 Regioselectivity Studies *61*

3.2.5 Mechanistic Proposal *63*

3.2.6 Reactions with Benzisoxazoles and Anthranils *65*

3.2.7 Attempts to Construct Polycyclic N-Heterocycles *67*

3.3 Conclusions 71

Chapter IV: Computational Investigation of Regioselective Gold(I)-Catalysed Cyclisation of Yndiamides with Isoxazoles 73

4.1 Introduction 74

4.1.1 DFT Studies on Gold-Catalysed Functionalisation of Ynamides with Isoxazoles *74*

4.1.2 DFT Studies on Regioselective Gold-Catalysed Functionalisation of Alkynes *80*

4.1.3 Design of this Work *84*

4.2 Results and Discussion 85

4.2.1 Evaluation of Level of Theory *85*

4.2.2 Catalytic Cycles for Symmetic Yndiamide *91*

4.2.3 Catalytic Cycle for Non-symmetric Yndiamide *99*

4.3 Conclusions 101

Chapter V: Gold-Catalysed Functionalisation of Yndiamides with Sulfilimines or Tetrazolo[1,5-*a*]pyridines 103

5.1 Introduction 104

5.1.1 Gold-Catalysed Functionalisation of Ynamides with Azides *104*

5.1.2 Gold-Catalysed Functionalisation of Ynamides with Sulfilimines *108*

5.1.3 Concepts of This Work and Initial Attempts *112*

5.2 Results and Discussion 113

5.2.1 Gold-Catalysed Functionalisation of Yndiamides with Sulfilimines *113*

5.2.2 Gold-Catalysed Functionalisation of Yndiamides with Tetrazolo[1,5-a]pyridines .118

5.3 Conclusions 124

Chapter VI: Conclusions and Future Directions.....125

6.1 Conclusions 126

6.2 Future Directions.....127

6.2.1 Asymmetric Gold(I)-Catalysed Functionalisation of Yndiamides with Pyridine N-Oxides.....127

6.2.2 Gold(I)-Catalysed Functionalisation of Yndiamides via Vinyl Gold Carbenes.....128

6.2.3 Gold-Catalysed Functionalisation of Yndiamides with Tetrazoles 130

6.3 Closing Remarks 131

Chapter VII: Experimental Section 133

7.1 Materials and Physical Measurements 134

7.2 General Procedures 135

7.2.1 Synthesis of Yndiamides and Corresponding Coupling Partners.....135

7.2.2 Synthesis of Oxygen- or Nitrogen-Transfer Reagents.....138

7.2.3 General Procedures for Gold-catalysed Functionalisations 141

7.3 Chapter II Characterisation Data.....144

7.3.1 Regioselectivity: Determination of the regioisomeric ratio.....144

7.3.2 Sulfonamides and Phosphoramidates 146

7.3.3 1,1-Dibromoenamides.....153

7.3.4 Yndiamides.....156

7.3.5 Au(I) Pre-Catalysts.....164

7.3.6 Pyridine N-Oxides 165

7.3.7 Nucleophiles.....166

7.3.8 Oxidative Functionalisation Products 170

7.3.9 Brønsted Acid-Catalysed Double Substitution.....184

7.3.10 Miscellaneous.....188

7.4 Chapter III Characterisation Data 190

7.4.1 Regioselectivity Studies 190

7.4.2 Sulfonamides and Phosphoramidates 198

7.4.3 1,1-Dibromoenamides 201

7.4.4 Yndiamides 202

7.4.5 Isoxazoles and Benzo[d]isoxazoles 207

7.4.6 Gold-catalyzed Cyclisation of Yndiamides with Isoxazoles 225

7.4.7 Derivatizations of the 2,3-Diaminopyrroles 253

7.4.8 Gold-catalyzed Cyclisation of Yndiamides with Benzisoxazoles 256

7.4.9 X-Ray Crystallography 263

7.5 Chapter IV Computational Details 267

7.5.1 Computational Methods 267

7.5.2 Cartesian Coordinates and Energy Data of All Computed Structures 268

7.6 Chapter V Characterisation Data 326

7.6.1 Sulfilimines 326

7.6.2 Tetrazolo[1,5-a]pyridines 333

7.6.3 Gold-catalysed Functionalisation of Yndiamides with Sulfilimines or Tetrazolo[1,5-a]pyridines 339

7.6.4 Miscellaneous 353

7.6.5 X-Ray Crystallography 354

7.7 Chapter VI Characterisation Data 356

7.7.1 HPLC Traces 356

7.7.2 Sulfonamides 357

7.7.3 1,1-Dibromoenamides 358

7.7.4 Yndiamides 359

7.7.5 Transfer Reagents 360

7.7.6 Gold-Catalysed Functionalisaion Products 362

7.7.7 Miscellaneous.....*364*

7.7.8 X-Ray Crystallography.....*364*

Reference**.....367**

Acknowledgement

I would like to express my sincerest gratitude to the following people, without their help, I would not be where I am today. First of all, I would like to thank Ed for offering me the position to join his group, and for his priceless advice, continued support, and burning enthusiasm over the past years. The years I spent studying in the group under his guidance were among the most memorable and fruitful adventures of my life, and, I believe, this thesis will be the best reward for this experience. Thank you, Ed!

I would also like to extend my thanks to many individuals who provided me with invaluable academic support: Philip, Julia and Tim for making up Team Yndiamide; a special thanks goes to Philip for kindly leading me through the tough process of making my first batch of yndiamide, and also to Nils for being my 'sifu' in computational chemistry; my dear 'office bay-mates' and 'F10 labmates' Ayan, Bahskar, Beth, Guoduan, Helena, Jieyan, Jeremy, Marie, Marius, Pavle, Philip, Priyansh and Ryan for our chemistry discussions and especially Ayan, Bahskar, Jeremy and Marius for tirelessly approving my 'usually-safe-but-occasionally-risky' experiment ideas; Eddie, Marie, Marius, Pavle and Priyansh for technical support on the HPLC, glovebox and CombiFlash (and many other fancy gadgets we have in the group); Helena, Yasmine and Dr Kirsten Christensen for their generous help on X-ray crystallography.

A huge thank you to all the past and present members of the EAA group with whom I shared a wonderful time in the CRL: Beth, Helena, Jeremy, Nils and Philip for the refreshing tea breaks; Ana, Ayan, Hannah, Jeremy, Marius, Ryan and Yasmine for all the pub nights; my 'fellow foodies' Jisook, Kenny, Ryan and Yasmine for all the gourmet outings; and really everyone in the group, you are all good friends and I will miss you all!

Of course, I would not have accomplished this much without the support from my family and my partner. Thank you, Mum and Dad, for your continued support and encouragement along the way! Thank you, Qingrui, for everything you did that made me a better person and for being part of my life, I love you so much!

Abbreviations

1,10-phen	1,10-phenanthroline
Ac	Acetyl
app.	apparent
Ar	Generic aryl group
Ar^F	3,5-Bis(trifluoromethyl) phenyl
atm	Standard atmospheric pressure
ATR	Attenuated total reflection
bbeda	Bis-benzylidene ethylenediamine
BHT	2,6-Di-*tert*-butyl-4-methylphenol
BINAP	([1,1'-Binaphthalene]-2,2'-diyl)bis(diphenylphosphane)
Bn	Benzyl
Boc	*tert*-Butyloxycarbonyl
Bpin	Pinacolboryl
***c*-Hex / Cy**	Cyclohexyl
cod	Cycloocta-1,5-diene
COSY	Homonuclear correlation spectroscopy
Cp	Cyclopentadienyl
CPCM	Conductor-like polarisable continuum model
DBE	1,2-Dibromoethane
DBU	Diazabicyclo[5.4.0]undec-7-ene
DCE	1,2-Dichloroethane
DCM	Dichloromethane
DDQ	2,3-Dichloro-5,6-dicyano-1,4-benzoquinone
Decomp.	Decomposition
DFT	Density functional theory
DIAD	Diisopropyl azodicarboxylate
DMF	*N*,*N*-Dimethylformamide
dmfu	Dimethyl fumarate
DMSO	Dimethylsulfoxide
dppe	1,2-Bis(diphenylphosphino) ethane
dppm	1,2-Bis(diphenylphosphino) methane
E^+	Generic electrophile
ECP	Effective core potential
e.e.	Enantiomeric excess
eq. / equiv.	Equivalent(s)
ESI	Electrospray ionisation
Et	Ethyl
EWG	Generic electron-withdrawing group
FT-IR	Fourier-transform infrared spectroscopy
HA / H–A	Generic Brønsted acid
Het	Generic heteroaryl group
HFIP	Hexafluoroisopropanol
HMBC	Heteronuclear multiple bond correlation
HOMO	Highest occupied molecular orbital
HPLC	High-performance liquid chromatography
HRMS	High-resolution mass spectrometry
HSQC	Heteronuclear single quantum correlation
IEFPCM	Integral equation formalism version of the polarisable continuum model

IPA	Isopropanol
***i*-Pr**	Isopropyl
J	Coupling constant
L	Generic ligand
LG	Generic leaving group
m	Meta
M	mol dm^{-3}
Me	Methyl
m.p.	Melting point
Ms	Methanesulfonyl
M. S.	Molecular sieves
NBO	Natural bond orbital
NBS	*N*-Bromosuccinimide
***n*-Bu / Bu**	*normal*-Butyl
NCS	*N*-Chlorosuccinimide
***n*-Hept**	*normal*-Heptyl
***n*-Hex**	*normal*-Hexyl
NMR	Nuclear magnetic resonance
NOESY	Nuclear Overhauser effect spectroscopy
***n*-Pr**	*normal*-Propyl
n.r.	No reaction
Nu^- / NuH	Generic nucleophile
o	Ortho
p	Para
pc	Piece
PG	Generic protecting group
Pic	2-Pyridinecarboxylate
Ph	Phenyl
Py	Generic pyridine group
Qn	Generic quinoline group
quant.	Quantitative
R	Generic carbon group
r.r.	Regioisomeric ratio
r.t.	Room temperature
SET	Single electron transfer
SMD	Solvation model based on density
Taut.	Tautomerisation
TBS	*tert*-Butyldimethylsilyl
***t*-Bu**	*tert*-Butyl
Temp	Temperature
TEMPO	(2,2,6,6-Tetramethyl piperidin-1-yl)oxyl
Tf	Trifluoromethanesulfonyl
TFA	Trifluoroacetic acid
THF	Tetrahydrofuran
TLC	Thin layer chromatography
TOF	Time of flight
LPLC	Low-pressure liquid chromatography
Ts	4-Methylbenzenesulfonyl / tosyl
UV	Ultraviolet
v/v	Volume by volume
w/w	Weight by weight

Long, long is my road, and far, far is the journey;

High and low, up and down, I'll search with will.

– Qu Yuan, *Li Sao*

CHAPTER

I

Introduction to Yndiamides

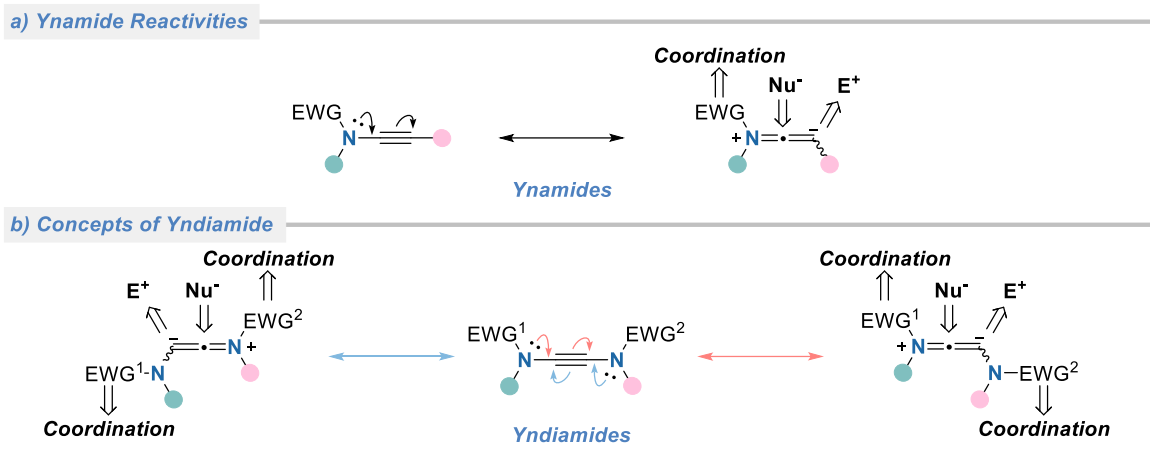
Yndiamides, doubly nitrogen-substituted alkynes, were developed by our group as a new tool for forming diverse nitrogen-containing compounds. Their electron-donating nitrogen atoms activate the central alkyne at both ends, offering distinct reactivity profiles compared to their well-established ynamide relatives; these doubly nitrogenated motifs also provide a facile entry to a wide library of complex aza-cycles and 1,2-diaminated products. At the time of writing, our group has reported several studies using yndiamides, yet a vast space of yndiamide chemistry remains unexplored. This chapter will briefly introduce the history of yndiamides and our previous work on them. Later sections of this introduction will focus on the development of gold-catalysed functionalisations of alkynes, and the challenges of applying such reactivity to yndiamides will be discussed.

1.1 Yndiamides: Past and present

1.1.1 Ynamides: Predecessors of yndiamides

In 1972, ynamides, alkynylamines featuring an electron-withdrawing group on the nitrogen atom, were first synthesised by Viehe and co-workers.[1] Synthetic routes towards ynamides have evolved greatly over the past few decades; modern synthetic methods for ynamide synthesis can be categorised into two classes: i) alkynylation of secondary amides with various reagents,[2-10] and ii) functionalisation of (pre-formed) chloro-/bromo-ynamides.[11, 12] Thanks to those efficient methods to a broad scope of ynamides, an ocean of ynamide reactions has been explored, and today, half a century after ynamides were first synthesised, they have become a highly versatile building block in organic synthesis.[13-20] Covered in this selection of review articles[13-20] are distinguished examples of ynamide chemistry, including but not limited to additions of various reagents across the central alkyne bond, cycloadditions, cycloisomerisations, ring-closing metathesis and generation of metal carbenes.

Most of those ynamide reactivities offer predictable regio- and/or stereo-chemical outcomes. This predictability originates from the polarisation of the central alkyne motif imposed by the donation of the nitrogen atom's lone pair of electrons (Scheme 1.01a). The electron-withdrawing group on the nitrogen atom also plays an important role in dictating the regio- and/or stereo-selectivity of ynamide chemistry. It increases the stability of the molecule by lowering the energy of the nitrogen lone pair, but can also serve as a potential chelation site for transformations such as directed carbometallation.[21-23]



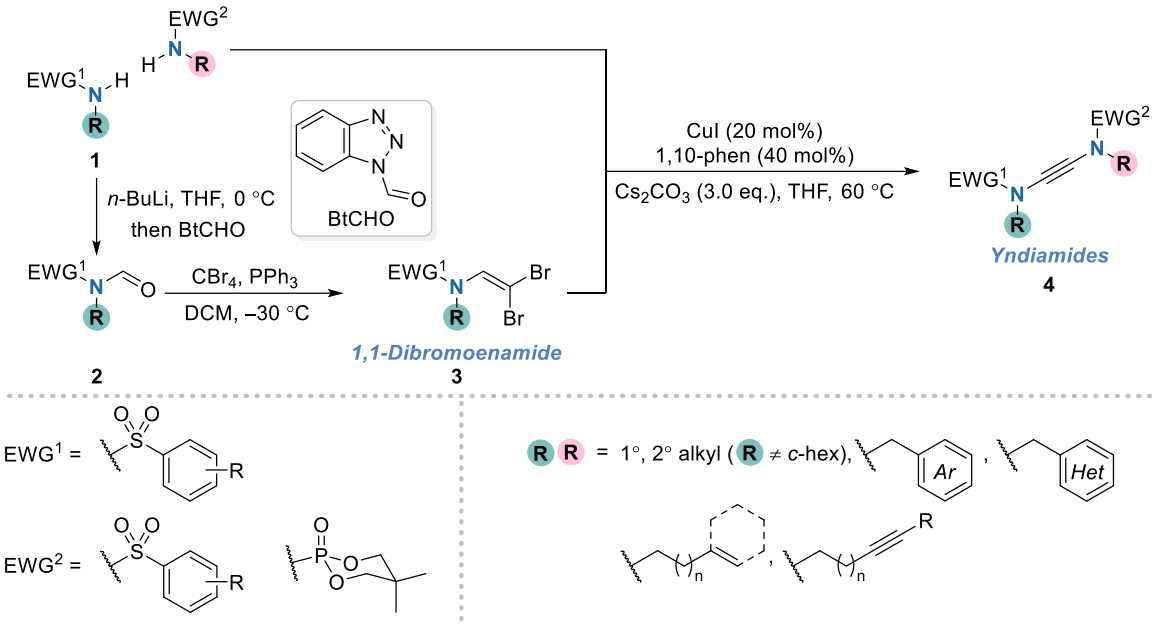
Scheme 1.01 a) General reactivity profiles of ynamides and b) concept of yndiamides.

Having seen the merits of the nitrogen substituent of ynamides, our group envisioned that yndiamides – alkynes bearing a nitrogen substituent at each end of the central alkyne moiety – would experience distinct polarisation effects of the orthogonal π-bonds of the alkyne from each nitrogen substituents (Scheme 1.01b) and thus exhibit different reactivities. In the DPhil thesis[24] and published work[25] of Steven Mansfield, a previous group member, the first and still the only known practical synthesis of yndiamides, together with a preliminary screening of yndiamide reactivities, were reported. In the same set of works, more fundamental aspects (e.g. crystallographic and spectroscopic properties) of yndiamides were compared to that of ynamides, which, combined with experimental discoveries, become the solid base of yndiamide chemistry. However, at the time of writing, yndiamides have not been utilised by other research groups. Nonetheless, our enthusiasm for exploring the chemistry of yndiamides remains strong; we have made and hope to continue to make contributions to this field of many possibilities.[26-28]

1.1.2 Synthesis of Yndiamides

Retrosynthetically, yndiamides can be traced back to two molecules of secondary amides **1** (usually sulfonamides or phosphoramidates) (Scheme 1.02).[24, 25] One of the sulfonamides was formylated to a tertiary formamide **2** which is then subjected to Ramirez *gem*-

dibromoolefination[29] to afford a 1,1-dibromoenamide **3**. Lastly, a copper-catalysed cross-coupling between the 1,1-dibromoenamide and the other secondary amide efficiently produces yndiamide **4**.

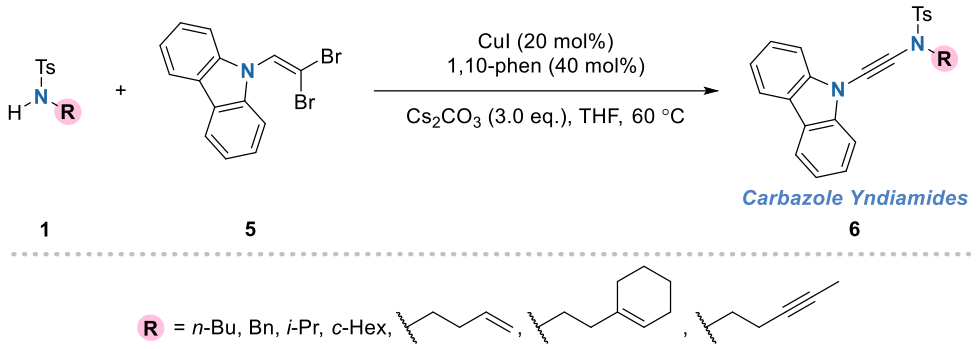


Scheme 1.02 Synthesis routes towards yndiamides.

This synthetic route is highly convergent; however, it is not without limitations. The major among these are i) the synthesis of 1,1-dibromoenamides and ii) the substrate scope of the copper-catalysed cross-coupling step. Through a brief exploration of the 1,1-dibromoenamide scope,[24, 25] only a limited selection of non-sterically-demanding *N*-sulfonyl formamide precursors were found to be competent in the Ramirez *gem*-dibromoolefination. As for the final cross-coupling reaction, although the reaction mechanism remained unclear, our experimental experiences suggest that a successful amide coupling partner must possess nucleophilicity that exceeds a certain threshold, given that the presence of a strong electron-withdrawing group (e.g., nosyl group or 3,5-bis(trifluoromethyl)benzenesulfonyl group) or a bulky sidechain (e.g., *tert*-butyl group) on these nucleophiles leads to failed reactions. The choices for electron-withdrawing groups

are therefore limited to either sulfonyl groups (usually tosyl group) or a phosphate diester group. The sidechains, on the other hand, are found to be more tolerant of different functionalities. Working examples include primary and secondary alkyl groups, benzyl groups, tethered alkenes/alkynes, and certain silyl ethers, acetals and esters are also tolerated.[24, 25]

Aiming to overcome the synthetic limitations and thus unlock new territories of yndiamides, attempts with a wider variety of coupling partners have continued. Recently, a class of novel carbazole yndiamides has been successfully synthesised by our group (Scheme 1.03).[26, 28, 30]



Scheme 1.03 Synthesis of carbazole yndiamides.

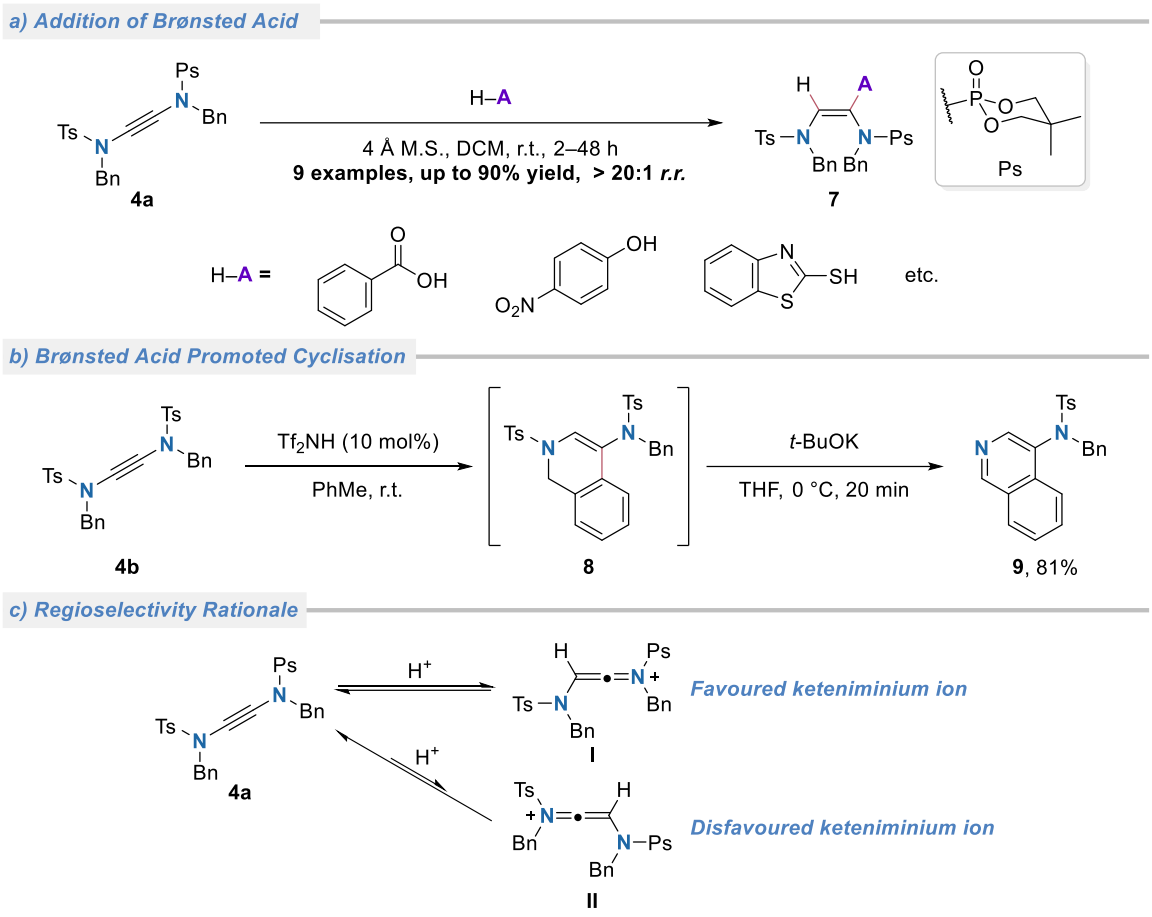
The use of carbazole instead of secondary sulfonamides in the formylation/Ramirez *gem*-dibromoolefination sequence afforded a 1,1-dibromovinyl carbazole **5**. The same copper-catalysed cross-coupling reaction condition used in the classic yndiamide synthesis proved effective in coupling **5** with different tosylamide partners to give a series of carbazole yndiamides **6**. This is considered our first breach through the bottleneck of yndiamide synthesis, however, a "tosyl-free" yndiamide synthesis has not yet been achieved. A need remains for the development of a brand-new synthetic strategy towards yndiamides that can broaden the scope of electron-withdrawing group selections, unlock wider yndiamide reactivities and create more opportunities for utilising yndiamides in synthesis.

1.1.3 Previously Reported Yndiamide Reactivities

Our group has made a number of contributions to the field of yndiamide chemistry over the past few years. Several transformations of yndiamides were discovered,[24, 26, 28, 31] which have served as valuable comparisons between yndiamides and their ynamide analogues. In this section, a selection of yndiamide reactions will be summarised, along with a discussion of some of their mechanistic aspects, thus introducing the distinctive reactivity profiles of yndiamides.

1.1.3a Brønsted Acids Addition to Yndiamides

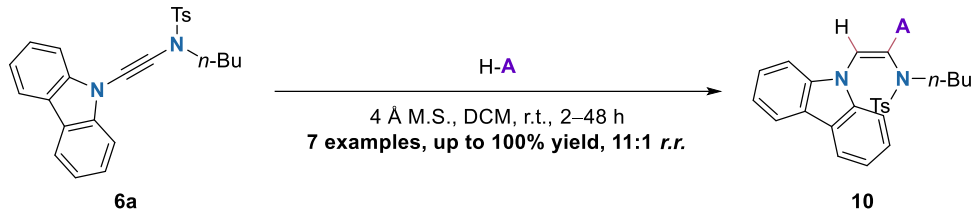
A Brønsted acid addition across the central C–C triple bond was developed to form *N*,*O*,*N*- and *N*,*S*,*N*-trisubstituted ketene acetals (Scheme 1.04a).[27, 31] Brønsted acids of pK_a ~6.5 – 7.5, including various carboxylic acids, electron-deficient phenols and thiols, were found to be reactive in addition to the non-symmetric yndiamide **4a**, delivering *N*,*X*,*N*-type trisubstituted ketene acetal products **7** with good regio- and stereo-selectivity. However, carbon-based Brønsted acids such as 1,3-dicarbonyl equivalents and HCl were shown to be either non-reactive or destructive. A Brønsted acid-promoted cyclisation of symmetric yndiamide **4b** was also achieved by using a non-nucleophilic Brønsted acid catalyst (Scheme 1.04b). Dihydroisoquinoline **8** was obtained as the product, which could be de-tosylated in a one-pot process by treatment with *t*-BuOK to produce an aminoisoquinoline **9**. This reaction was tested on non-symmetric yndiamide **4a** as well, however, only mediocre regioselectivity was observed.



Scheme 1.04 Reactions of yndiamides with Brønsted acid: addition, acid-promoted cyclisation and regioselectivity rationale.

The underlying principles that confer regioselectivity in both reactions of non-symmetric yndiamides (Brønsted acid addition and Brønsted acid-promoted cyclisation) are still unclear. Our proposed rationale (Scheme 1.04c) is that the regio-chemical outcome is mainly influenced by the different electronic properties of the two electron-withdrawing groups on the nitrogen atoms (in this case, Ts vs. Ps). The protonation of the yndiamide is favoured at the alkyne carbon distal to the phosphate diester (Ps) group, forming the keteniminium ion **I** predominantly, and thus leading to the formation of the major regioisomer observed. Such bias in protonation suggests that the Ps group is a weaker electron-withdrawing group than the Ts group. This conclusion is also supported by the fact that peaks of the benzylic hydrogen and carbon atoms in the TsNHBn molecule appear more deshielded than those in the PsNHBn molecule in their NMR spectrum.

Following the synthesis of carbazole yndiamides **6**, their reactivities in Brønsted acid additions were also studied (Scheme 1.05).[28] Similar to that of classic yndiamides, all of the selected Brønsted acids (including HCl which, in the case of a classic yndiamide, leads to the decomposition of the Ps group) were shown to be competent. The yields were comparable to that of classic yndiamide, although a weakly negative correlation with the bulk of the acid was observed. Moreover, regioselectivity was found to be reduced in all cases, suggesting the possible influence of both steric and electronic factors of the nitrogen substituents. Interestingly, contrary to reactions of classic yndiamides, the major regioisomers observed in Brønsted acid additions to carbazole yndiamides were found to prefer protonation proximal to the carbazole moiety, which indicates that the carbazole motif offers poorer stabilisation of the corresponding keteniminium ion intermediate. More studies on factors that control the regioselectivities of carbazole yndiamides are ongoing.



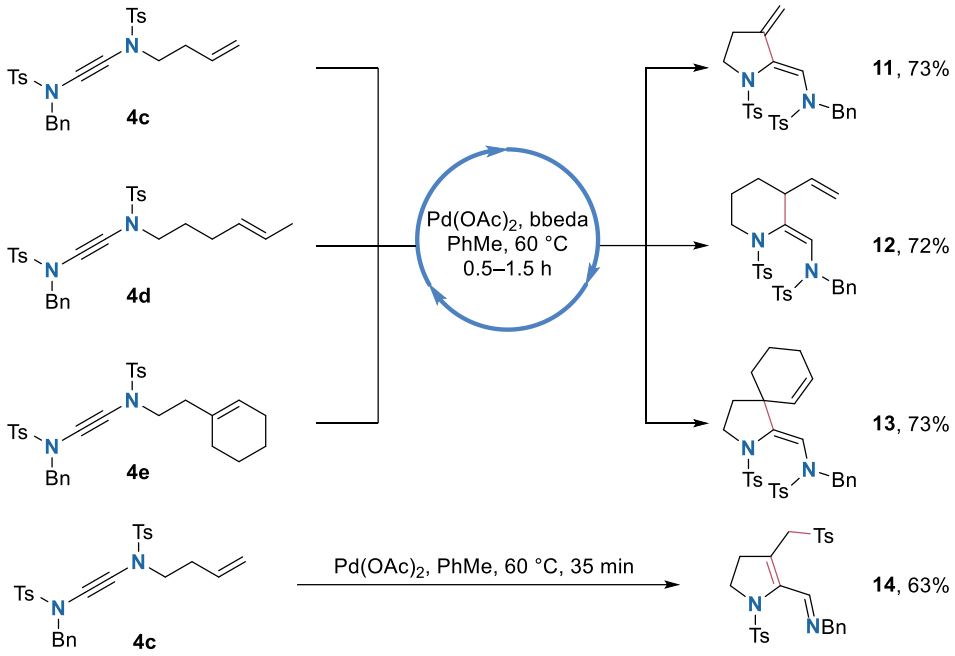
6a **10**

Scheme 1.05 Brønsted acid additions to novel carbazole yndiamide.

1.1.3b Ring-Forming Reactions of Yndiamides

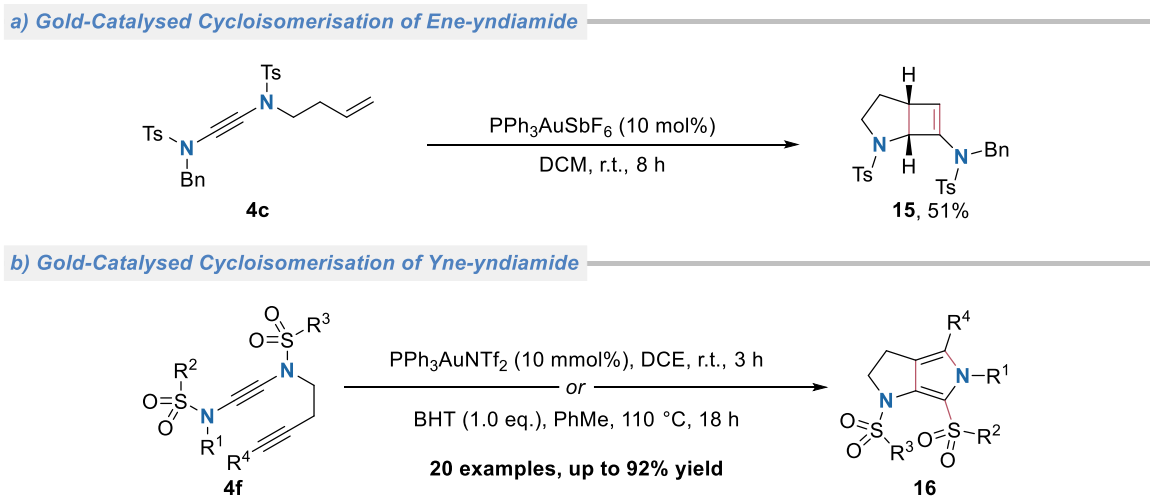
Ynamides have gained popularity in organic synthesis because their unique atom connectivity makes them very convenient precursors to a wide range of complex *N*-heterocycles.[18] With an additional nitrogen substituent, yndiamides are expected to grant access to a broader scope of even more sophisticated ring systems. To illustrate the applicability of yndiamides in such reactions, a variety of ring-forming reactions of yndiamides were developed by our group, which constituted the main body of the DPhil thesis of previous group member Philip Smith.[24-26]

Palladium-catalysed cycloisomerisation of ene-yndiamides (Scheme 1.06) formed 1,3- (**11**) and 1,4-dienes (**12**). A spirocycle **13** was also observed, and an unexpected tosyl-migrated product **14** was acquired when the reaction was carried out in the absence of the bbeda ligand, which is in contrast to ynamides whose palladium-catalysed cycloisomerisation required the presence of such ligand.[32]



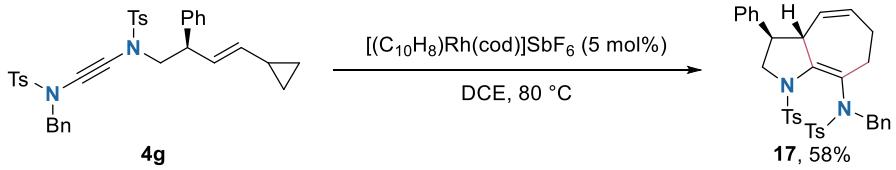
Scheme 1.06 Palladium-catalysed cycloisomerisation of ene-yndiamides.

In the presence of gold(I) catalysts, ene-yndiamide **4c** was isomerised to cyclobutenamide (Scheme 1.07a, **15**) as a single diastereomer. The use of yne-yndiamides **4f** under similar conditions led to the formation of tetrahydropyrrolopyrroles **16**, as the result of a formal [3+2] cycloaddition and tandem 1,2-sulfonyl migration (Scheme 1.07b).[26, 33] Subsequent optimisations revealed that the latter reactions could also proceed under thermal conditions, albeit requiring the addition of radical inhibitor BHT and extended reaction time.



Scheme 1.07 Gold-catalysed cycloisomerisation of yndiamides.

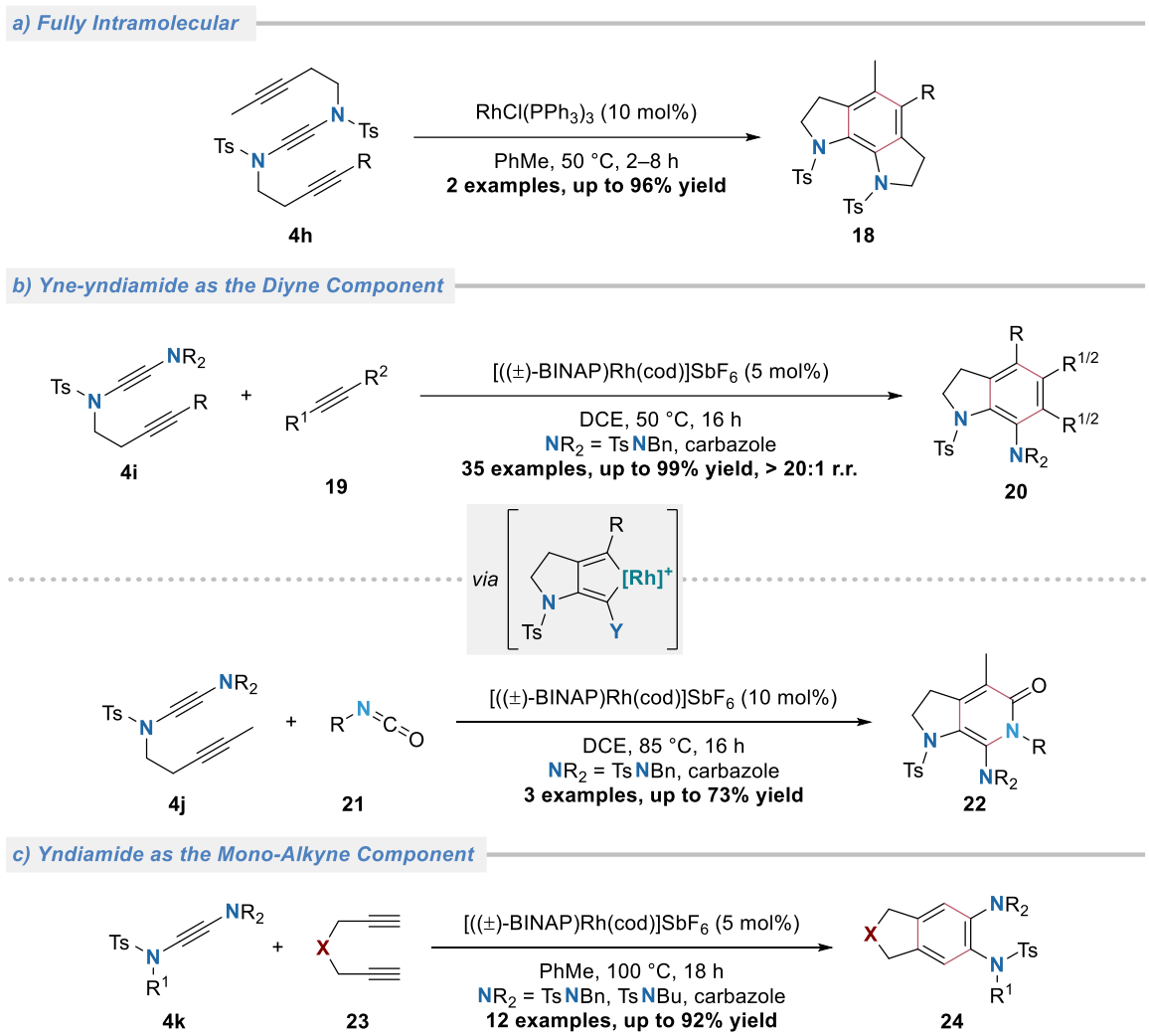
Rhodium-catalysed cycloisomerisation and cyclotrimerisation of yndiamides were also explored. A vinylcyclopropane yndiamide **4g** was successfully converted to a 5,7-fused ring system **17** as a single diastereomer (Scheme 1.08), however requiring harsher conditions compared to analogous ynamides.[34, 35]



Scheme 1.08 Rhodium-catalysed cycloisomerisation of vinylcyclopropane yndiamide.

The rhodium-catalysed [2+2+2] cyclotrimerisation of yndiamides was achieved using different combinations of diynes and mono-alkynes (Scheme 1.09).[25, 26, 30] Using Wilkinson's catalyst a fully intramolecular cyclotrimerisation of diyne-yndiamide **4h** could be achieved to form the tricyclic hexahydropyrroloindole **18** (Scheme 1.09a). The partially intermolecular cycloisomerisation of yndiamides can be categorised into two classes: i) yne-yndiamides serving as the diyne components; ii) yndiamides serving as the mono-alkyne components. For the first class, yne-yndiamides **4i** were found to be a reactive partner with external mono-alkynes **19** using [((±)-BINAP)Rh(cod)]SbF_6 as the catalyst to

form a regioisomeric mixture of indoline products **20** (Scheme 1.09b). The regioselectivity exhibited a strong correlation with the electronic properties of the external alkyne, as electron-rich alkynes gave excellent regioselectivity, while electron-poor alkynes produced modest selectivity.

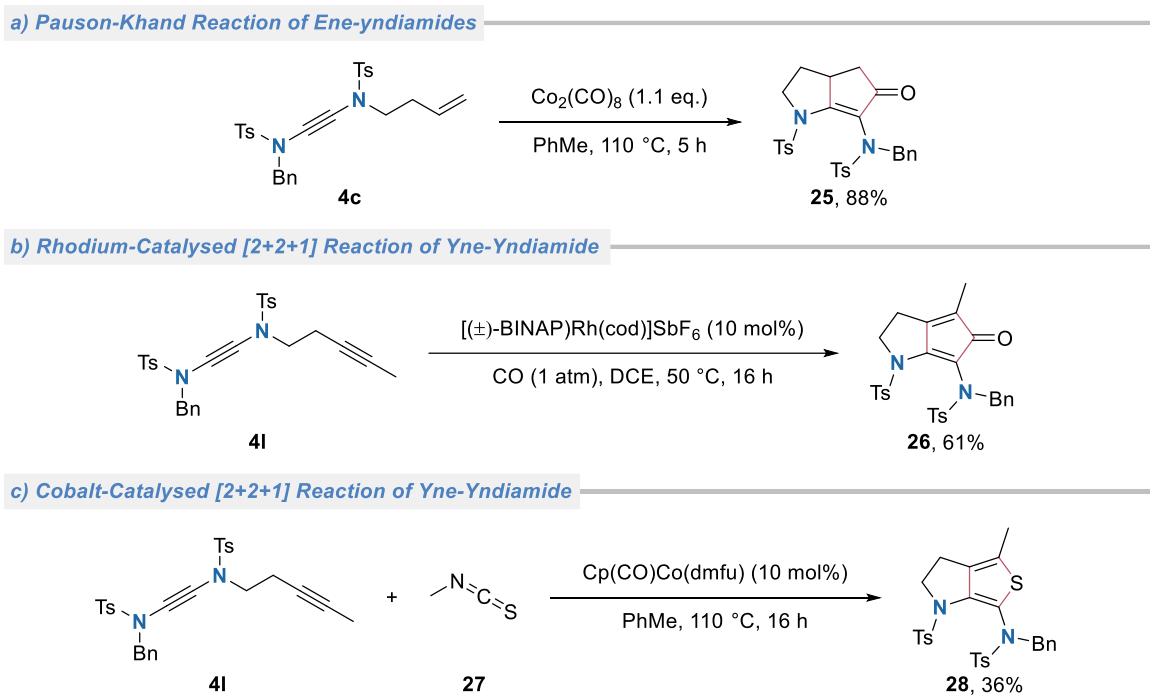


Scheme 1.09 Rhodium-catalysed cyclotrimerisation of yndiamides.

Unexpectedly, the use of carbazole yndiamide achieved regioselectivity even when reacting with electron-poor alkynes (which are known to give poor selectivity when reacting with classic yndiamides). Computational analysis suggested that the reaction proceeded *via* the generation and subsequent alkyne migratory insertion of a rhodacycle species; however, our preliminary results on the regioselectivity-determining factors were

inconclusive.[26] Our group's initial tests also demonstrated that such rhodacycle intermediates generated from yne-yndiamides **4j** could be trapped by using isocyanates **21**, delivering diaminopyridones **22** in good yields (Scheme 1.09b).

Simple yndiamides **4k** (*N*-benyzl- or *N*-butyl-substituted), including carbazole yndiamides, could serve as the mono-alkyne components in insertion into the rhodacycle intermediates generated from diynes **23** to produce 1,2-phenylenediamine derivatives **24**, albeit requiring elevated reaction temperature and extended reaction time (Scheme 1.09c). Either intermolecular or intramolecular [2+2+2] cyclotrimerisation between yndiamides and nitriles was also successful in the presence of cobalt or Lewis acid catalysts.[26] However, due to their limited examples and unoptimised reaction conditions, they are not discussed in detail in this section.



Scheme 1.10 [2+2+1] cycloadditions of yndiamides.

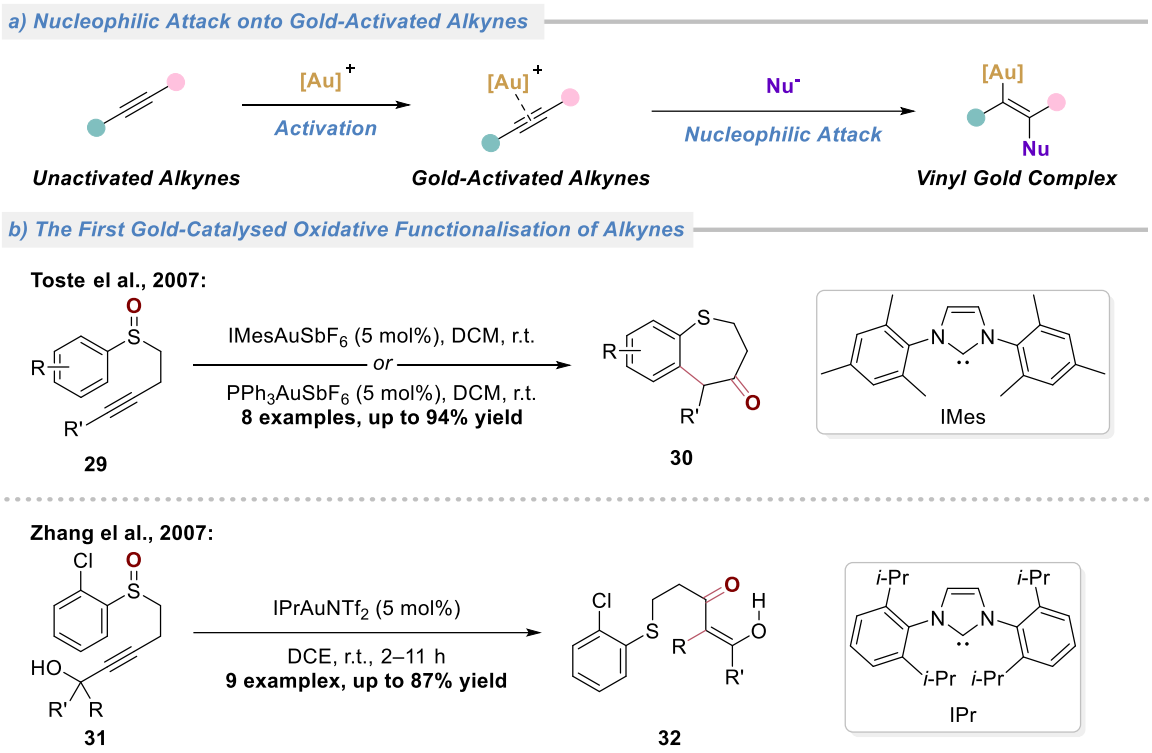
Yndiamides are also capable of undergoing [2+2+1] cycloadditions (Scheme 1.10). A Pauson-Khand reaction was performed on ene-yndiamide **4c** to give sulfonamide

cyclopentenenone **25** (Scheme 1.10a). Under rhodium-catalysed conditions and an atmosphere of carbon monoxide, yne-yndiamide **4l** underwent [2+2+1] cycloaddition to generate cyclopentadienenone **26** (Scheme 1.10b). Methylisothiocyanate **27**, in the presence of a cobalt catalyst, could also react with **4l**, leading to the formation of a diaminothiophene **28** (Scheme 1.10c).

1.2 Gold-Catalysed Oxidative Functionalisations of Alkynes

For a long time in human history, it was believed that gold was nothing more than a noble, inert (but good-looking) metal – until Schwemberger and Gordon reported the first use of gold(I) and gold(III) compounds as homogeneous catalysts in the complete chlorination of naphthalene.[36] More than half a century later, Teles and co-workers'[37] and Hayashi and co-workers'[38] research on the activation of alkynes with homogeneous gold(I) catalysts followed by nucleophilic attack from oxygen-centred nucleophiles (alcohols and water, respectively) showed the scientific community the great potential of gold(I) catalysts in organic synthesis and marked the beginning of a new era of gold-catalysed functionalisations of alkynes.[39]

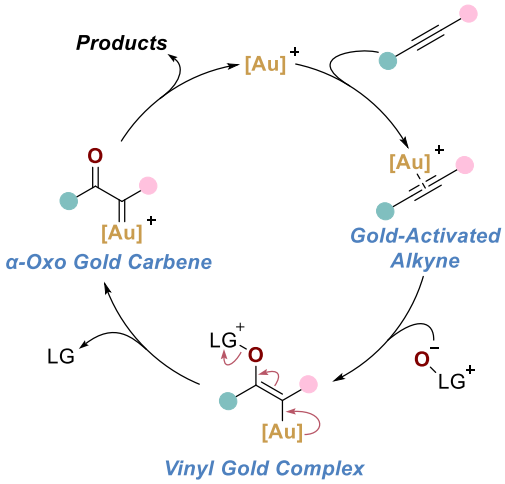
Due to relativistic effects, Au(I) complexes exhibit extraordinary alkyno-philicity that is rarely replaceable by other Lewis-acidic transition metal complexes.[39-41] The gold-activated alkynes showed heightened electrophilicity towards nucleophilic attack from nucleophiles which then leads to subsequent reactivities (Scheme 1.11a). Over the past decade, enormous amounts of various nucleophiles have been explored. These results were comprehensively reviewed in several review articles.[39, 42-49]



Scheme 1.11 a) Nucleophilic attack onto gold-activated alkynes; b) First reported examples of gold-catalysed oxidative functionalisation of alkynes by intramolecular oxygen transfer from a sulfinyl group.

Among all the nucleophiles explored, one of the most significant contributions is found in gold(I)-catalysed intramolecular redox reactions of sulfinyl alkynes developed independently by Toste *et al.*[50] and Zhang *et al.*[51] (Scheme 1.11b). Both groups explored the gold-catalysed rearrangement of sulfinyl alkynes and proposed that the reaction proceeded *via* an *α*-oxo gold carbene intermediate. This idea was further developed as a wide variety of N–O/S–O/C–O bond oxidants were discovered, and this concept is now recognised as a common approach to generate *α*-oxo gold carbenes from an alkyne motif (Scheme 1.12).[50-53] Similar to other gold-catalysed functionalisations of alkynes, the alkyne is first activated by the gold catalyst by complexation, which promotes nucleophilic attack by an oxidant (either internal or external) to form the vinyl gold complex. Through gold(I) π-back bonding, the X–O bond in the oxidant was cleaved, and a charge-neutral leaving group is extruded, generating the *α*-oxo gold carbenes which can be trapped (e.g., by

nucleophiles) to afford the product and to re-generate the gold catalyst to complete the cycle.



Scheme 1.12 Generalised catalytic cycle for gold-catalysed oxidative functionalisation of alkynes *via* generation of α-oxo gold carbenes.

This strategy completely avoids the use of hazardous α-diazo carbonyl compounds to generate α-oxo gold carbenes. Its tolerance of a wide scope of internal and external oxidants (i.e. nucleophiles) also unmasked new territories of gold-catalysed functionalisation of alkynes and thus opened up new opportunities to further expand the scope of this chemistry. Indeed, this methodology has gained enormous importance over the past decade in ynamide chemistry.[20, 54] Literature concerning this part will be reviewed in detail in later chapters.

1.3 Conclusion: Project Objectives and Challenges

Our group has developed several yndiamide-based methodologies, including Brønsted acid addition, Brønsted acid-promoted cyclisation, palladium-catalysed cycloisomerisation, rhodium-catalysed cycloisomerisation and cyclotrimerisation, and gold-catalysed cycloisomerisation/1,2-sulfonyl migration of yndiamides. Considering the crucial role gold catalysis played in alkyne chemistry, the vast majority of possible gold-catalysed

functionalisation reactions of yndiamides *via* gold carbenes remain unexplored. It is hoped that by filling this research gap we could make another contribution not only to yndiamide chemistry but also to more general alkyne and gold-catalysis chemistry.

However, the road ahead is not smooth; the major challenge we could foresee before starting this work was the problem of regioselectivity using non-symmetric yndiamides. In contrast to ynamides, whose regioselectivity is inherent, the pseudo-symmetry of the yndiamide would likely pose a great challenge in establishing regioselective transformations. It remains questionable whether the electronic control observed in regioselective Brønsted acid additions would hold for gold-catalysed processes.

In summary, the objectives of this study contain three parts: i) to test the feasibility of using yndiamides in gold-catalysed functionalisation *via* gold-carbenes; ii) to explore the limits of this reactivity; iii) to establish regioselectivity and investigate the regioselectivity-determining factors. In the following chapters, all three points will be addressed. In Chapter II, a gold-catalysed oxidative functionalisation of yndiamides with pyridine *N*-oxides was developed, representing the first example of generating and functionalising α-oxo gold carbenes from yndiamides. In Chapter III, a gold-catalysed cyclisation of yndiamides with isoxazoles *via* α-imino gold carbenes was achieved. In both chapters, regioselectivity could be established by introducing subtle steric bias between two nitrogen substituents. In Chapter IV, computational investigations were completed to reveal the key to this regioselectivity. Lastly, in Chapter V, a novel tetrazolo[1,5-*a*]pyridine nucleophile was synthesised and its reactivity with yndiamides was tested under gold-catalysed conditions.

C H A P T E R

II

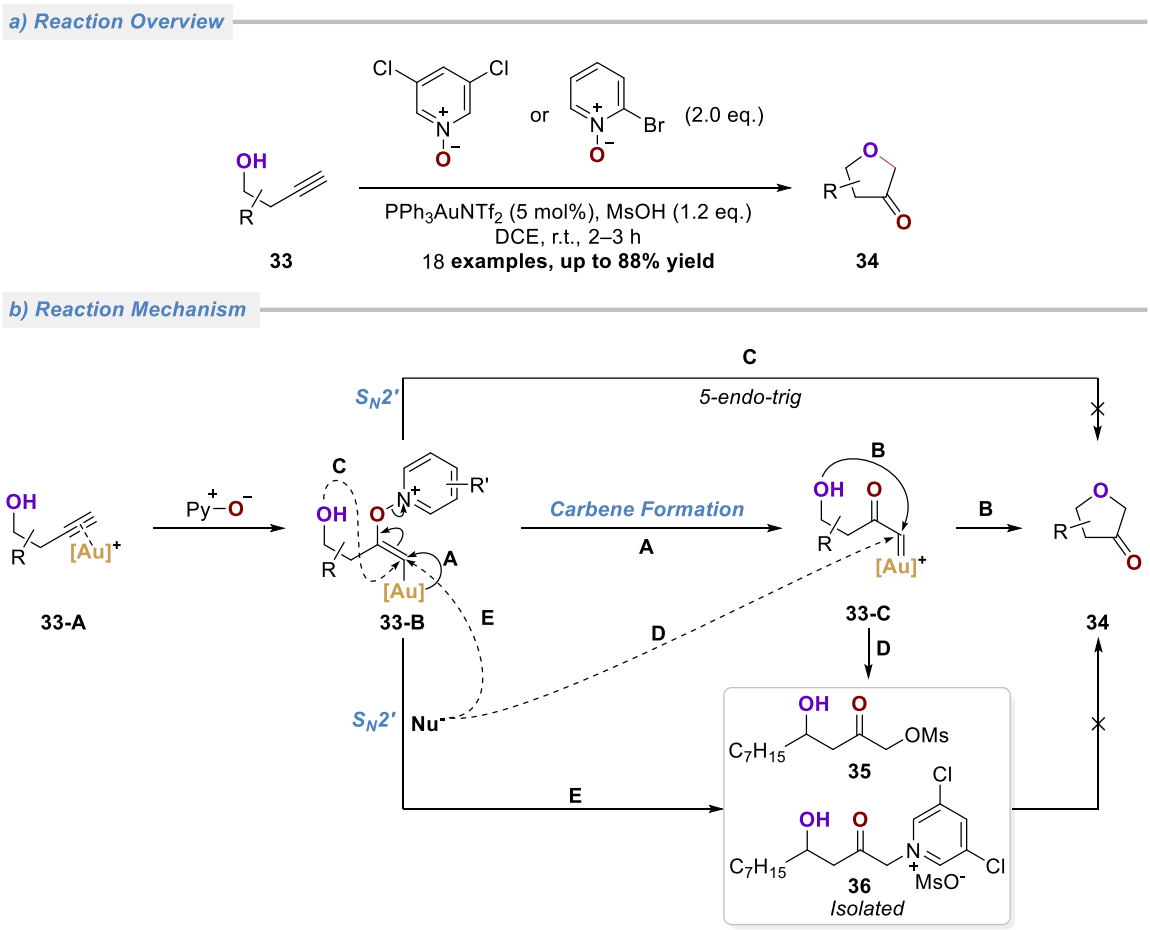
Gold(I)-Catalysed Functionalisation of Yndiamides with Pyridine *N*-Oxides

Pyridine *N*-oxides were reported as effective external oxidants in the gold-catalysed oxidative functionalisation of alkynes. In the past decade, they have received significant attention in ynamide chemistry, with multiple functionalisations of ynamides using pyridine *N*-oxides *via* α-oxo gold carbenes having been discovered. The excellent reactivity of pyridine *N*-oxides in this context provided an accessible entry point for the gold-catalysed oxidative functionalisation of yndiamides. In this chapter, we describe the gold-catalysed oxidation of yndiamides with pyridine *N*-oxides *via* α-oxo gold carbenes to generate unnatural amino acid derivatives. Regioselectivity can be achieved by introducing minor steric bias between the two nitrogen substituents of the yndiamide.

2.1 Introduction

2.1.1 Gold-Catalysed Oxidative Functionalisation of Ynamides with Pyridine *N*-oxides

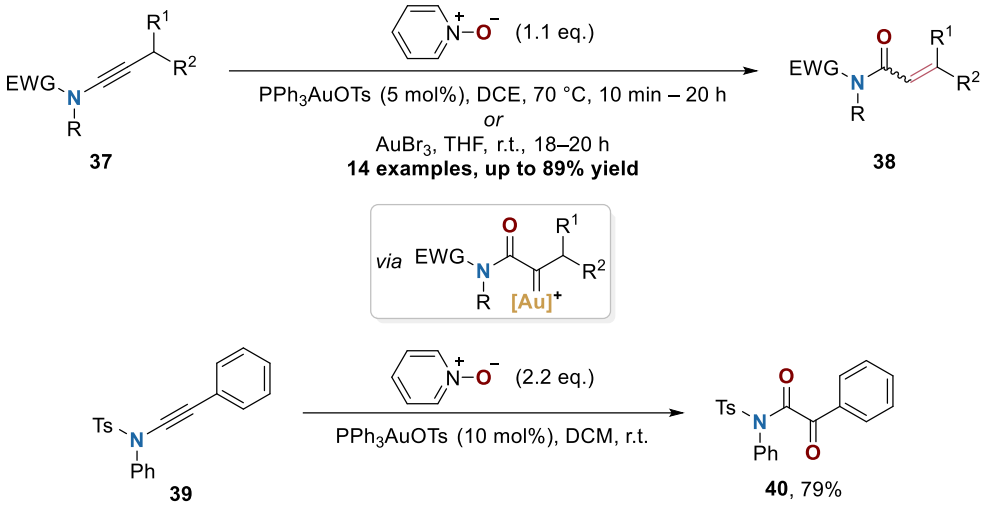
First reported by Zhang and co-workers, pyridine *N*-oxides were used as intermolecular oxygen atom transfer reagents to generate α-oxo gold carbenes from homopropargylic alcohols **33** for the synthesis of dihydrofuran-3-ones **34** (Scheme 2.01a).[55] This strategy was further developed into a common protocol to generate α-oxo gold carbenes without the need for using the hazardous α-diazo carbonyl compounds.[56]



Scheme 2.01 Gold-catalysed oxidative functionalisation of alkynes for the synthesis of dihydrofuran-3-ones *via* α-oxo gold carbenes.

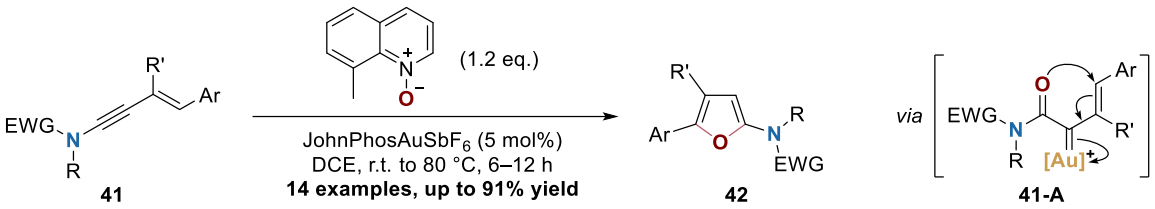
Their proposed reaction mechanism commenced with the nucleophilic attack onto the gold-activated alkyne **33-A** by the pyridine *N*-oxide reagent to give a vinyl gold complex **33-B**. Intramolecular O–H insertion from the gold carbene **33-C** (pathway **A** and **B**) was proposed as the most likely mechanism to deliver the final product **34**, since trapping of **33-B** using the intramolecular hydroxyl group to form **34** in an S_N2' manner was a disfavoured 5-*endo*-*trig* cyclisation (pathway **C**). Two side-products, mesylate **35** and pyridinium salt **36,** were isolated as crucial evidence of this mechanism (Scheme 2.01b). The formation of these compounds can be rationalised by either i) competitive nucleophilic attack by the MsOH or the pyridine species present in the reaction mixture onto the gold carbene **33-C** (pathways **A** and **D**); or ii) nucleophilic attack onto the *trans*-alkenyl gold complex **33-B** through an S_N2' mechanism (pathway **E**). However, the conversion of **35** and **36** to **34** was unsuccessful even under basic conditions, which suggested that side-products **35** and **36** were not stable intermediates *en route* to **34**. Zhang *et al.*'s report laid a solid foundation for the development of numerous subsequent works on gold-catalysed oxidative functionalisation of alkynes with pyridine *N*-oxides, which led to the prosperity of this field. Following their pioneering work, many other types of nucleophiles, including oxygen-based nucleophiles,[57-61] nitrogen-based nucleophiles,[62-64] and electron-rich aromatic systems (Friedel-Crafts-type reactivity),[65-68] were developed to efficiently trap the α-oxo gold carbene intermediates to form a broad scope of products.[52-54]

In 2011 Davies and co-workers published the first example of the site-specific generation/1,2-insertion cascade of α-oxo gold carbenes from ynamides **37** and pyridine *N*-oxide to access α,β-unsaturated carboxylic acid derivatives **38** (Scheme 2.02).[69] The reaction outcome was substrate-dependent, since, under similar conditions, an excess amount of pyridine *N*-oxide resulted in the formation of oxoacetamide **40** in good yield when ynamide **39** was used.



Scheme 2.02 Generation/1,2-insertion cascade of *α*-oxo gold carbenes from ynamides.

Shortly after Davies *et al.* demonstrated the feasibility of generating *α*-oxo gold carbenes from ynamides, Liu and co-workers reported a gold-catalysed synthesis of poly-substituted 2-aminofurans **42** *via* *α*-oxo gold carbenes **41-A** from ene-ynamides **41** and 8-methyl quinoline *N*-oxide through a formal [4+1] cycloaddition (Scheme 2.03).[70]

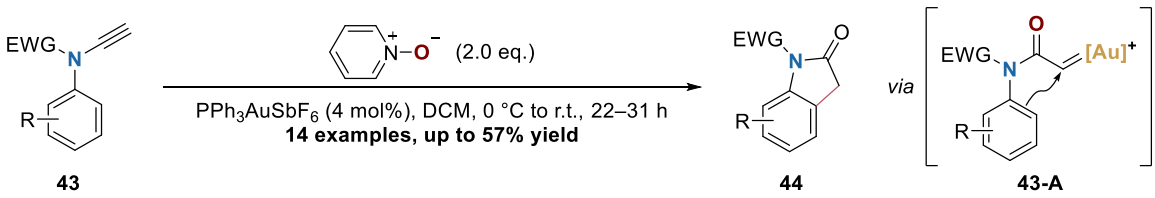


Scheme 2.03 Gold-catalysed synthesis of substituted 2-aminofurans via *α*-oxo gold carbenes. JohnPhos = (*o*-biphenyl)PCy_2.

In their proposed mechanism, the *α*-oxo gold carbene intermediate **41-A** generated from ene-ynamides **41** underwent an oxa-Nazarov cyclisation followed by a deprotonative aromatisation/protodeauration sequence to afford the 2-aminofuran products **42**. During their optimisation of conditions, an oxoacetamide similar to **40** was isolated as one of the major undesired side products, which, as the authors claimed, supported the presence and intermediacy of a gold-carbene species. Formation of such oxoacetamide side-products

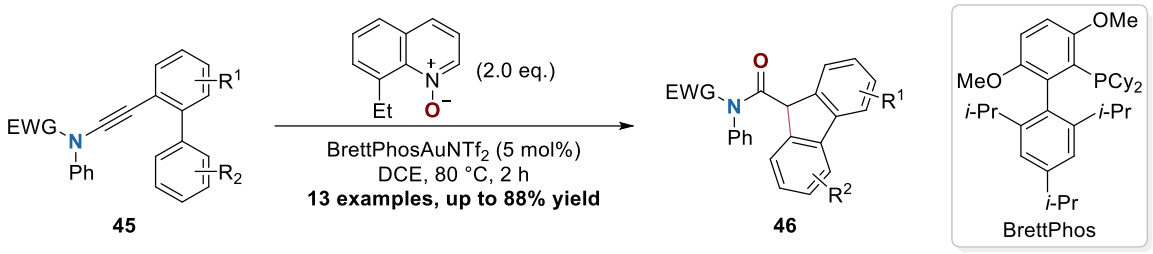
could be the result of trapping of the gold carbene by nucleophilic attack from the organic *N*-oxide. Similar mechanisms were often proposed for the gold-catalysed oxidative 1,2-difunctionalisation of alkynes.[71-73]

The Friedel-Crafts-type reactivity of *α*-oxo gold carbenes derived from ynamides was not explored until 2013 by Li and co-workers (Scheme 2.04).[74] Upon oxidation by pyridine *N*-oxide, *α*-oxo gold carbenes **43-A** were generated from terminal *N*-arylynamides **43**. Intramolecular Friedel-Crafts-type reaction of **43-A** followed by protodeauration gave oxindole **44**. It is worth noting that Li *et al.* did not observe any overoxidation products, but instead isolated *N*-tosylaniline as the major side-product, whose formation could be explained by a Wolff rearrangement/oxidation/hydrolysis cascade.[75]



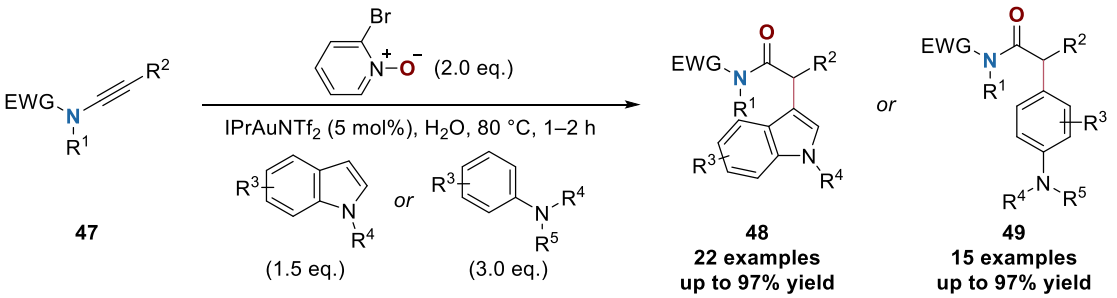
Scheme 2.04 Intramolecular Friedel-Crafts-type reaction of *α*-oxo gold carbenes generated from *N*-arylamides.

A similar strategy to employ *α*-oxo gold carbenes in intramolecular Friedel-Crafts-type reactions was also applied by Ye *et al.* in their work in 2014 on the gold-catalysed oxidation of *o*-alkynylbiaryls **45** for the synthesis of functionalised fluorenes **46** (Scheme 2.05).[76] A bulky gold catalyst BrettPhosAuNTf$_2$ was used in this reaction to inhibit the formation of the oxoacetamide side-product, which assumes that the increased bulkiness around the gold carbene motif could block the nucleophilic attack from the external quinoline *N*-oxide.



Scheme 2.05 Gold-catalysed oxidation of *o*-alkynylbiaryls for the synthesis of fluorenes.

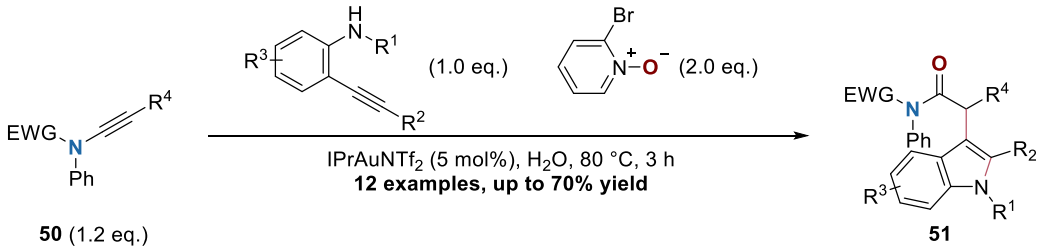
In the same year, the Ye group also reported the first intermolecular trapping of *α*-oxo gold carbenes generated from ynamides **47** with indoles or anilines (Scheme 2.06).[77] The reaction proceeded efficiently in water, affording a broad scope of carboxylic acid derivatives **48** (with indoles) and **49** (with anilines). Interestingly, the reaction exhibited excellent selectivity when water was used as the solvent, as only a trace amount of oxoacetamide side-product was observed. The authors suspected that this 'water effect' was because the water-soluble 2-bromopyridine *N*-oxide mainly exists in the aqueous phase while the insoluble organic species (ynamides and indole/aniline nucleophiles) and the gold catalyst formed a mesophase where 2-bromopyridine *N*-oxide was kept at a proper level that prevented the overoxidation.



Scheme 2.06 Intermolecular Friedel-Crafts-type reaction of *α*-oxo gold carbenes generated from ynamides.

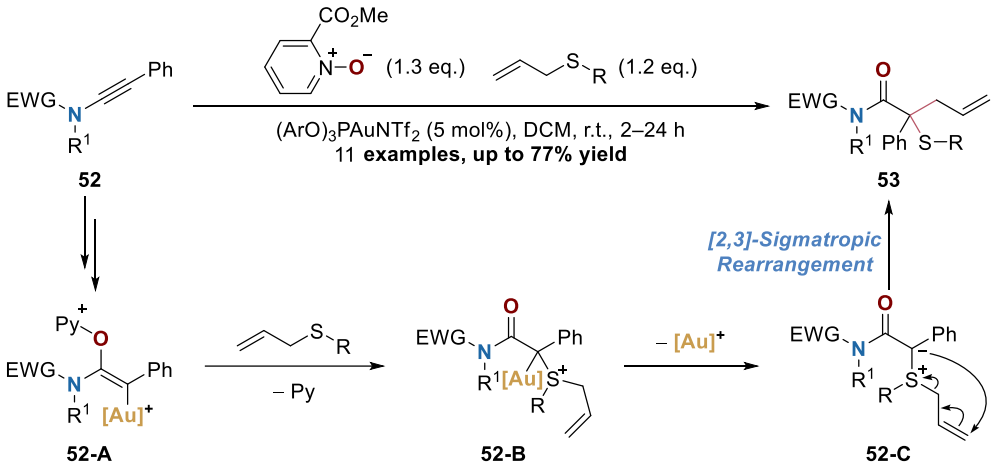
In addition to this work, Ye and co-workers also demonstrated a gold-catalysed tandem cycloisomerisation/functionalisation of *α*-oxo gold carbenes under similar conditions (Scheme 2.07).[78] By using *o*-alkynylanilines, indole nucleophiles, which were generated *in*

situ through a gold-catalysed cycloisomerisation, could trap the *α*-oxo gold carbenes generated from yndiamide **50** by the same gold catalyst to form amide products **51** in good yield. This strategy successfully expanded the scope of indole nucleophiles in such reactivity, while also providing a new type of concurrent tandem catalysis.



Scheme 2.07 Gold-catalysed tandem cycloisomerisation/functionalisation of *α*-oxo gold carbenes.

Studies that claimed a non-carbene-mediated mechanism were also reported. In 2014, the Davies group demonstrated a gold-catalysed oxidation/sulfur ylide rearrangement sequence on ynamides to deliver a range of sulfide-substituted amides **53** (Scheme 2.08).[79]

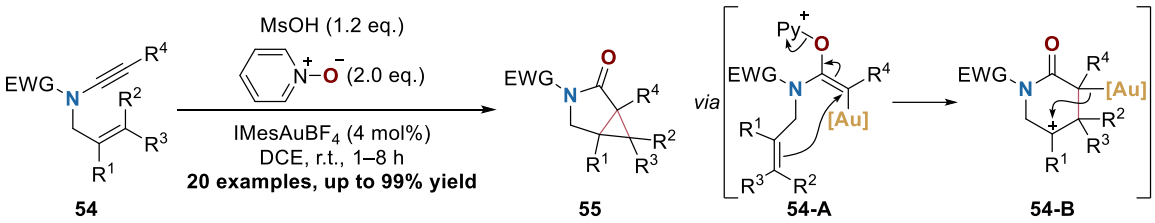


Scheme 2.08 Gold-catalysed oxidation/sulfur ylide rearrangement sequence on ynamides. Ar = 2,4-di-*tert*-butylphenyl.

The authors suggested that, instead of having the polarisable sulfide nucleophile attacking the positively-charged gold carbene intermediate, the attack onto the relatively charge-neutral vinyl gold complex **52-A** was favoured. The resulting sulfonium gold complex **52-**

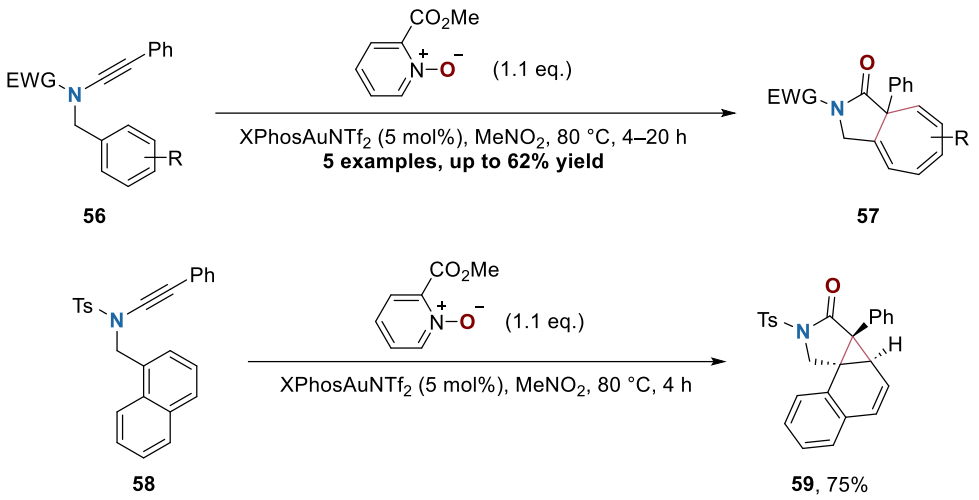
B could undergo deauration to form the sulfonium ylide **52-C**. Subsequent [2,3]-sigmatropic rearrangement of the sulfur ylide afforded the final product **53**. Recently, the same group illustrated a diastereoselective version of this reaction.[80] Since the diastereocontrol model did not involve gold chemistry, it is not discussed in detail here.

The cyclopropanation of ene-ynamides was not explored until 2013 the Li group described a gold-catalysed oxidative cyclopropanation of *N*-allylynamides **54** to synthesise 3-aza-bicyclo[3.1.0]hexan-2-ones **55** (Scheme 2.09).[81] Based on literature precedents on gold-catalysed cycloaddition/cycloisomerisation of similar ene-yne systems,[82-84] the authors proposed a mechanism without the generation of α-oxo gold carbenes. The proposed reaction pathway involved an intramolecular nucleophilic attack from the alkene group onto the vinyl gold complex **54-A** through an S_N2' mechanism to afford a 6-membered ring gold complex **54-B**. Subsequent deauration/ring contraction yielded the final product **55**.



Scheme 2.09 Gold-catalysed oxidative cyclopropanation of *N*-allylynamides.

In 2018 Davies and co-workers reported the first oxidative Büchner-type reaction of α-oxo gold carbenes generated from *N*-benzylynamides **56** (Scheme 2.10).[85] Apart from one example (**58**) that stopped at the arene cyclopropanation step (**59**), the rest all collapsed to the [5.3.0]azabicycle product **57**. Nonetheless, this work served as a great example showing the possibility of utilising ynamides-generated α-oxo gold carbenes in cyclopropanation reactions.



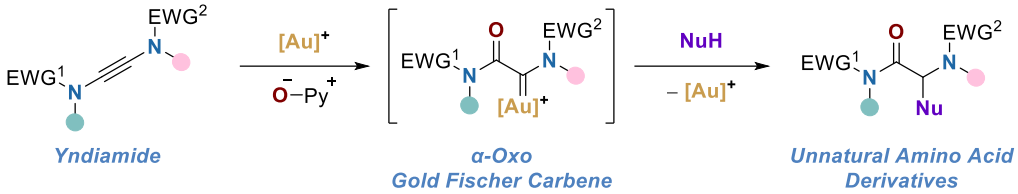
Scheme 2.10 Gold-catalysed oxidative Büchner-type reaction of *N*-benzylynamides. XPhos = dicyclohexyl(2',4',6'-triisopropyl-[1,1'-biphenyl]-2-yl)phosphane.

Besides gold-catalysed oxidation of ynamides with pyridine *N*-oxides, oxidative functionalisation of ynamides could also be achieved by using other sorts of oxidants (e.g. sulfoxides[86] and nitrones[87]) or other catalysts (zinc catalyst,[88] $NaBAr^F_4$ catalyst,[89] Brønsted acid catalyst,[90] and acridinium-based photocatalyst[91]). All those examples became great additions to the field of gold-catalysed oxidation of ynamides, demonstrating the versatility and expandability of this reactivity.

2.1.2 Concepts of This Work and Initial Attempts

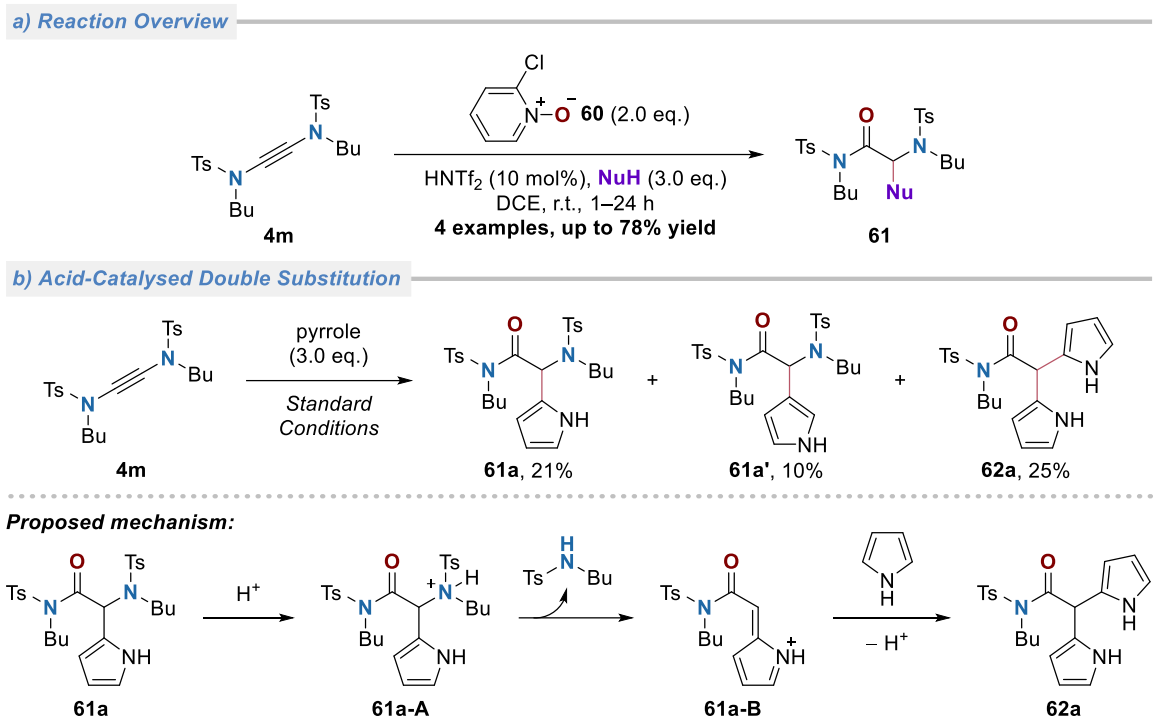
Concluding from the abovementioned literature precedents, pyridine *N*-oxides offer efficient access to a variety of *α*-oxo gold carbenes from various ynamides. The trapping of these gold carbene intermediates is usually achieved through simple nucleophilic attack or Friedel-Crafts-type reactivity. The straightforwardness of this approach makes it an ideal starting point to investigate if yndiamides are also competent in such reactivity. Therefore, inspired by the work of Ye *et al.*,[77] we designed a similar reaction involving yndiamide (Scheme 2.11). The successful reaction would lead to the formation of an unprecedented *α*-oxo gold Fischer carbene from yndiamide, which could subsequently be trapped by

external nucleophiles to yield unnatural amino acid derivatives. These motifs are of great significance in medicinal chemistry,[92] as well as in modifying protein structure and function.[93]



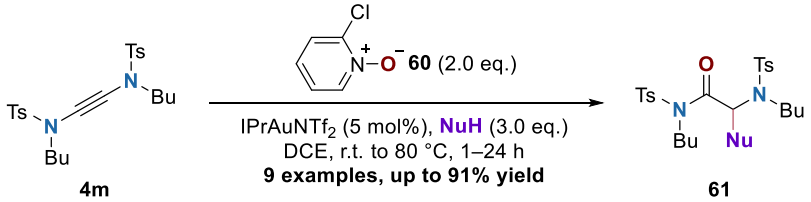
Scheme 2.11 Concept of this work.

Our group's initial attempts at such reactions, led by Olivia Garry, employed a Brønsted acid catalyst (Scheme 2.12a),[27] following Shin and co-workers who utilised chiral bis-isoquinoline *N*-oxides to enable enantioselective Brønsted acid-catalysed oxidative functionalisations of ynamides.[90] Although Garry successfully screened a small nucleophile scope, the progress was severely hampered by the discovery of an uncontrollable acid-catalysed double substitution (Scheme 2.12b). This undesired over-reactivity was attributed to the acid-catalysed elimination of the sulfonamide from the monosubstituted product **61a**, resulting in a highly electrophilic species **61a-B** that could be attacked by a second molecule of the nucleophile to generate the doubly-substituted product **62a**.



Scheme 2.12 Brønsted acid-catalysed oxidative functionalisation of yndiamide by Olivia Garry.

The uncontrollability observed during these Brønsted acid-catalysed reactions prompted the development of a gold-catalysed protocol. Moreover, as discussed later in this chapter, the acid-catalysed double-substitution created an opportunity to further derivatise the product **61**. Garry's Part II (Master's) thesis also reported a prototype gold-catalysed oxidative functionalisation of yndiamides (Scheme 2.13), which served as a foundation for our studies.



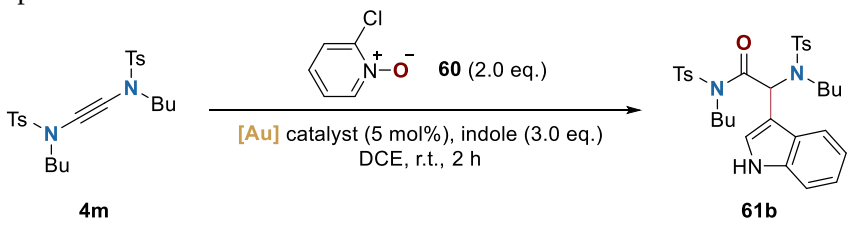
Scheme 2.13 Prototype gold-catalysed oxidative functionalisation of yndiamide **4m** by Olivia Garry.

2.2 Results and Discussion

2.2.1 Optimisation of Conditions

We initiated our studies by attempting to reproduce one of Garry's results. The reaction was tested using $IPrAuNTf_2$ as the catalyst, with yndiamide **4m** as the substrate, 2-chloropyridine *N*-oxide **60** as the oxidant, and indole as the nucleophile (Table 2.01, entry 1). Encouragingly, the desired product **61b** was isolated in good yield (82%), albeit with a small amount (~5%) of inseparable side products. Changing the gold catalyst to $Ph_3PAuNTf_2$ (Table 2.01, entry 2, 72%) or $Ph_3PAuSbF_6$ (Table 2.01, entry 3, 80%) did not improve the yield nor inhibit the formation of the side products.

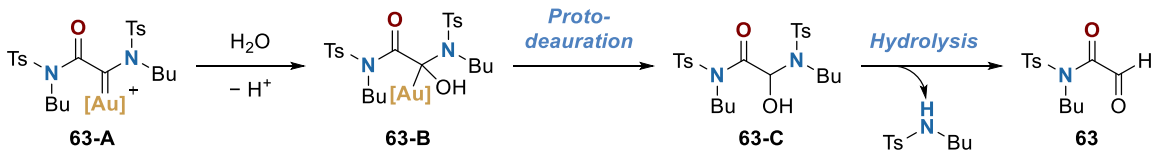
Table 2.01 Optimisation of conditions.



Entry	Catalyst	Solvent	Yield
1	$IPrAuNTf_2$[a]	DCE	82%[b]
2	PPh_3AuNTf_2	DCE	72%[b]
3	PPh_3AuSbF_6	DCE	80%[b]
4[c]	PPh_3AuNTf_2	DCE/H_2O (1:1)	-
5[d]	PPh_3AuNTf_2	DCE (dry)	59%
6[d]	$(4\text{-}MeOC_6H_4)_3PAuNTf_2$	DCE (dry)	41%
7[d]	$(4\text{-}FC_6H_4)_3PAuNTf_2$	DCE (dry)	42%
8[d]	$IPrAuNTf_2$[a]	DCE (dry)	81%
9[e]	$IPrAuNTf_2$[a]	DCE (dry)	81%

Reactions were conducted on 0.1 mmol scale with [**4m**] = 0.05 M; catalysts LAuX were generated *in situ* by pre-mixing the corresponding LAuCl and AgX salts; yields refer to isolated yields. [a] $IPrAuNTf_2$ was obtained commercially. [b] Products were isolated with ~5% inseparable impurities. [c] The reaction was conducted in the absence of indole. [d] Reactions were conducted in the presence of 3 Å molecular sieves. [e] The reaction was conducted at 0.5 M concentration, 1 h.

Extensive attempts were made to isolate and characterise the side products but to no avail. Upon comparison of the ^{1}H NMR spectra of the three experiments, it was evident that the side products were identical and exhibited a characteristic singlet peak at $\delta_H \sim 9.6$ ppm. It was hypothesised that the side products may contain an aldehyde species **63**, which could have resulted from the competitive trapping of the putative gold-carbene intermediate **63-A** by water (Scheme 2.14). This trapping would have generated an unstable hemiaminal species **63-C**, which would have been readily hydrolysed to the aldehyde **63** and *N*-butyl-tosylamide. To intentionally promote the formation of the suspected aldehyde side product, we performed a control experiment using a wet solvent in the absence of indole (Table 2.01, entry 4). However, we did not isolate the desired aldehyde side product but instead identified trace amounts of *N*-butyl-tosylamide in the crude reaction mixture. Unfortunately, with this evidence, we were unable to confirm or disprove our proposed mechanism (Scheme 2.15) since the source of this sulfonamide could have been either the hydrolysis of the suspected aldehyde **63-C** or a Wolff rearrangement/oxidation/hydrolysis cascade similar to what was proposed by Li *et al.*[74] Despite this, the experiment did demonstrate the sensitivity of yndiamides to water under the reaction conditions. We were pleased to find that the use of dry DCE and the inclusion of 3 Å molecular sieves successfully suppressed the formation of the side products, albeit at the expense of the yield (Table 2.01, entry 5).



Scheme 2.14 Proposed mechanism for the formation of side product by competitive trapping of gold carbene by water.

Several other phosphine/gold(I) complexes were screened, however, none were found to give an improved yield (Table 2.01, entries 6, 7). The NHC-gold(I) catalyst IPrAuNTf$_2$ was shown as the best-performing catalyst among our selections, delivering **61b** in an excellent yield of 81% (Table 2.01, entry 8). Notably, performing the reaction at a higher concentration (0.5 M) led to complete conversion within 1 hour and the same yield of 81% (Table 2.01, entry 9), which is consistent with Garry's previous findings.

2.2.2 Nucleophile Scope and Robustness Tests

With the optimised conditions in hand, the scope of the reaction was investigated with respect to the nucleophile (Figure 2.01). The reaction of yndiamide **4m** with indole as the nucleophile was found to be equally efficient at 1.0 mmol scale (0.48 g), yielding **61b** in 80% yield. As reported by Garry, the reaction also translated smoothly to electron-deficient indoles (5-nitro-indole and 5-bromo-indole), giving the corresponding product in high yield (81% yield for both).[27] The reactions with 5-methoxy-indole and *N*-methylindole also proved successful, leading to the formation of **61c** and **61d** in good yields (89% and 63% respectively), although the latter required an extended reaction time. Various pyrroles were also tested, and in accord with the results of Garry, the use of unsubstituted pyrrole gave 2-substituted pyrrole aminoamide exclusively in good yield (66%), whereas the use of *N*-methylpyrrole resulted in a regioisomeric mixture of C2 and C3 products in an overall yield of 84%,[27] 3,5-dimethylpyrrole was also a competent nucleophile, giving the C3 adduct **61e** in good yield (83%) at larger scales.

The introduction of activating substituents (e.g., 2-methoxy group) was necessary for benzofurans or benzothiophenes to deliver the corresponding products **61g** and **61h** in good yield (83% and 70% respectively) but at elevated temperatures. The parent unactivated heterocycles, however, did not react even at higher temperatures. Garry's survey of

phenol/anisole derivatives revealed that only those with multiple activating groups were reactive.[27] This conclusion was further supported by our testing with two additional

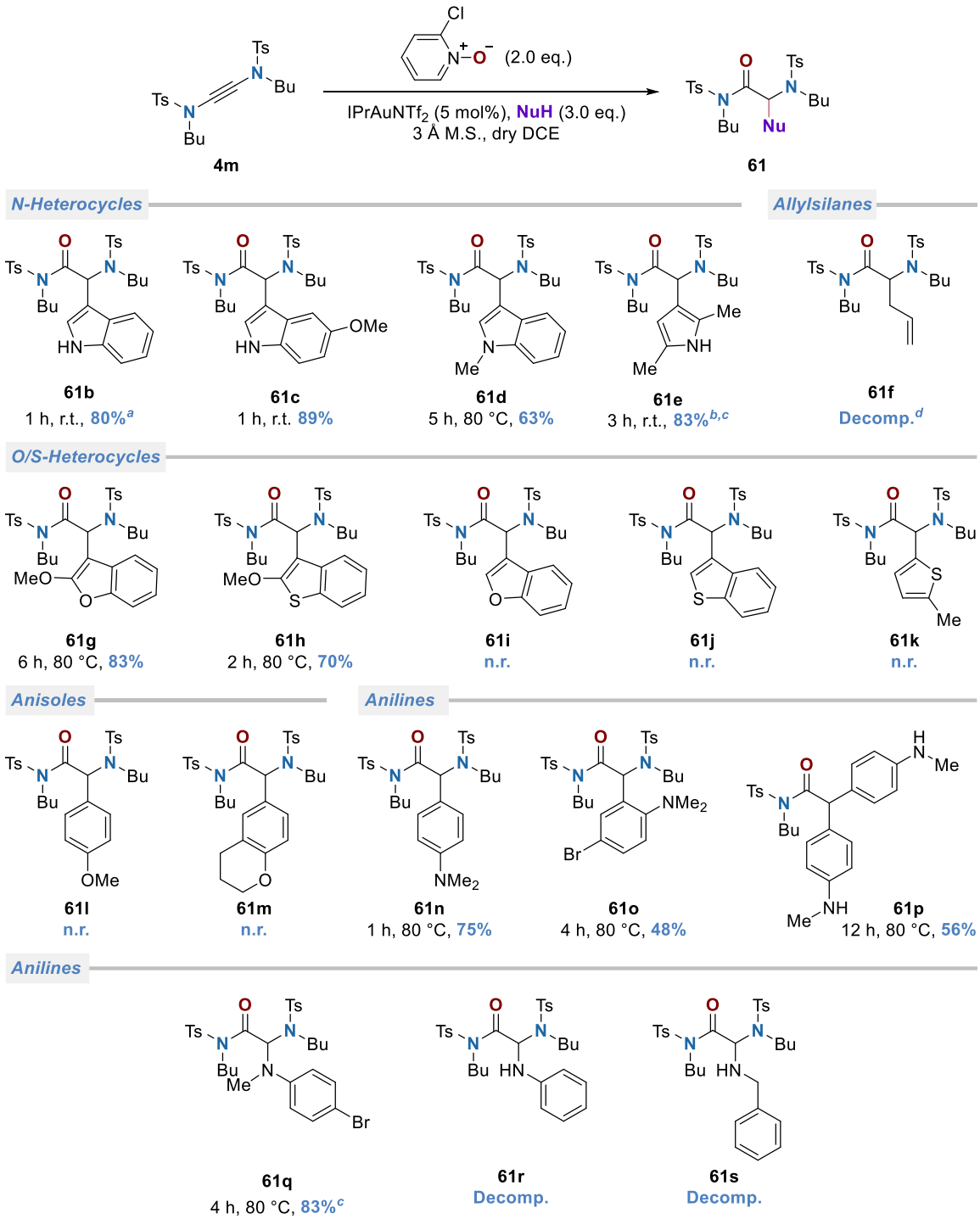


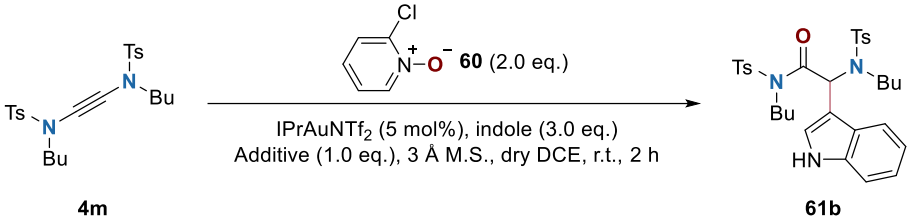
Figure 2.01 Nucleophile scope of gold-catalysed yndiamide oxidative functionalisation. Unless otherwise stated all reactions were performed at 0.1 mmol scale with [**4m**] = 0.5 M. Yields refer to isolated yields. [a] Reactions were performed on 1.0 mmol scale. [b] Reactions were performed on 0.2 mmol scale. [c] Reactions were performed at 0.4 mmol scale. [d] Allyltrimethylsilane was used as the nucleophile.

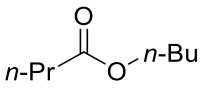
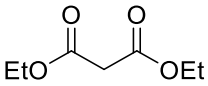
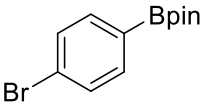
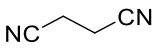
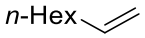
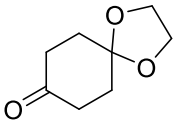
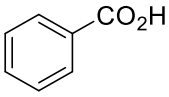
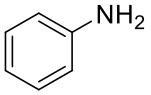
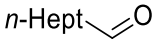
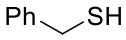
nucleophiles, anisole (**61l**) and chromane (**61m**); no reactions were observed in both cases. An interesting reaction pattern was observed for anilines. *N*,*N*-Dimethylaniline reacted efficiently at the *para* position, yielding the desired product **61n** in 75% yield, while in the presence of a blocking group at the *para* position, the reaction proceeded at the *ortho* position to produce **61o** in 48% yield. Similarly, an *N*-monosubstituted aniline underwent a reaction at the *para* position to form the double-substitution product **61p** in good yield (56%) through a similar mechanism discussed above (Scheme 2.12b), whereas in the case of the *para* position being masked, the reaction proceeded *via* the nitrogen atom to give **61q** in 83% yield. However, the parent aniline or benzylamine was found to be unreactive and only resulted in yndiamide decomposition, likely due to the addition of these reagents across the central alkyne triple bond, followed by decomposition of the corresponding products. Non-aryl carbon nucleophiles were also tested. A silyl enol ether was successfully utilised by Garry to produce the desired product in a low yield.[27] The use of allyltrimethylsilane, conversely, led only to decomposition of the yndiamide.

In addition to nucleophile scope screening, we conducted a series of robustness tests to assess the functional group tolerance of this transformation.[94, 95] The results were promising, as the reaction exhibited good tolerance towards a wide range of functional groups, with only one of the twelve external additives showing intolerance (Table 2.02). Ester groups, including a boronic ester, were well-tolerated in the reaction (Table 2.02, entries 2-4). The addition of a nitrile compound or an alkene species has no adverse effect on the yield (Table 2.02, entries 5-6). The reaction exhibited good tolerance towards carbonyl compounds such as ketones, aldehydes, as well as acetal protecting groups (Table 2.02, entries 7 and 10). Unexpectedly, when benzoic acid or aniline was added to the reaction, only a limited influence on the yield of **61b** was observed (Table 2.02, entries 8 and 9). This is likely due to the gold-catalysed functionalisation out-competed the latent Brønsted acid additions with

these reagents. The inclusion of pyridine or benzyl groups, however, did lead to a diminished yield of **61b** (Table 2.02, entries 11 and 12) presumably due to their ability to coordinate to the gold catalyst and thus inhibit the reaction.

Table 2.02 Robustness tests of gold-catalysed oxidative functionalisation of yndiamide.



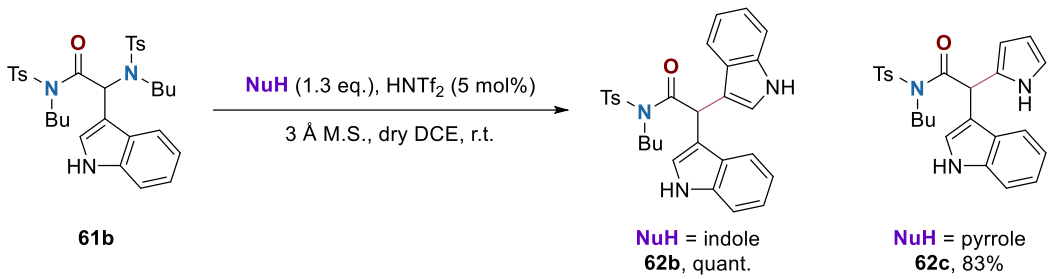
Entry	Additive	Yield	Additive Recovery Rate
1	-	94%	-
2		98%	68%
3		95%	91%
4		92%	100%
5		91%	100%
6		89%	28%
7		88%	81%
8		87%	94%
9		84%	100%
10		79%	21%
11		77%	- [a]
12		73%	87%
13		46%	63%

Reactions were conducted at 0.05 mmol scale with [**4m**] = 0.5 M; yields of **61b** and recovery rates of the additive were determined by ^{1}H NMR experiments with dimethylsulfone as the internal standard. [a] Recovery rate of the additive was unable to be determined due to peak overlap.

Finally, the reaction exhibited poor tolerance towards a 1,3-diol, which induced the formation of unidentified side products likely due to a competitive nucleophilic attack by the diol (Table 2.02, entry 13).

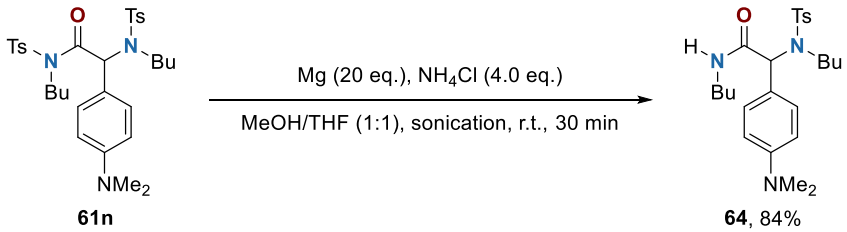
2.2.3 Derivatisation of Products

Our previous observation of double substitution under Brønsted acid-catalysed conditions (Scheme 2.12b) offers the potential for further functionalisation of the mono-substituted aminoamide products. To reduce the loading of the second nucleophile, we utilised the mono-substituted aminoamide product directly as the reactant. Surprisingly, our first attempt at the acid-catalysed substitution of the α-sulfonamide group in **61b** using an excess amount (1.3 eq.) of indole as the nucleophile with only 5 mol % $HNTf_2$ catalyst resulted in bis-indole acetamide **62a** in quantitative yield within 15 minutes of reaction time (Scheme 2.15). Pyrrole was also used as the nucleophile under similar conditions, affording the bis-heteroarylated product **62b** with 83% yield. Notably, the sparing solubility of the bis-heteroarylated products **62a** and **62b** in common solvents, except for DMSO, facilitated their separation from tosylamide by-products by washing and centrifugation. This unique feature, combined with the selectivity for the substitution of the α-tosylamido group, allowed us to identify the products efficiently and reliably in subsequent regioselectivity studies.



Scheme 2.15 Brønsted acid-catalysed double substitution of aminoamide **61b**.

Selective magnesium-mediated detosylation of aminoamide **61n** was achieved to deliver **64** with high yield (84%, Scheme 2.16),[96] which provided further differentiation of the two nitrogen substituents in **61n**. Despite the unclear mechanism of this detosylation reaction, it is speculated that the selectivity is derived from a favoured SET/N–S bond fission sequence of the more electron-deficient sulfonamide group. This mechanism is analogous to a SmI_2-mediated detosylation reaction. [97] Increasing the magnesium loading, extending reaction time or elevating reaction temperature proved insufficient to remove the second tosyl group. Therefore, it is suggested that stronger reducing conditions may be required to fully deprotect **61n**.

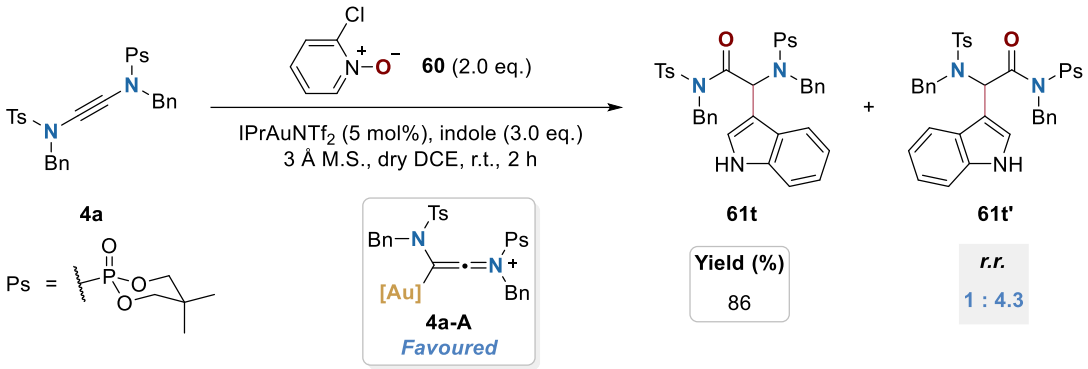


Scheme 2.16 Selective detosylation of aminoamide **61n**.

2.2.4 Regioselectivity Studies

As mentioned previously, ynamide functionalisations generally benefit from high regioselectivity due to the inherent polarisation of the central alkyne motif. Achieving high regioselectivity in yndiamide functionalisation is more challenging due to the presence of pseudo-symmetric nitrogen substituents that can both donate electron density to the central alkyne, in opposite directions (see Chapter I). In our previous studies on Brønsted acid addition to yndiamides, we were able to introduce an electronic bias between the two alkynyl carbons by using different electron-withdrawing groups on the nitrogen atom. This approach presumably enabled the preferential formation of one keteniminium ion intermediate over the other regioisomer, thus establishing regioselectivity (see Chapter I).[27,

[31] In this context, we were interested in examining whether this principle would also hold for controlling the regiochemical outcome of the gold-catalysed oxidative functionalisation of yndiamides. We synthesised and evaluated two non-symmetric yndiamides under our standard gold-catalysed oxidative functionalisation conditions, using indole as the nucleophile (Scheme 2.17).

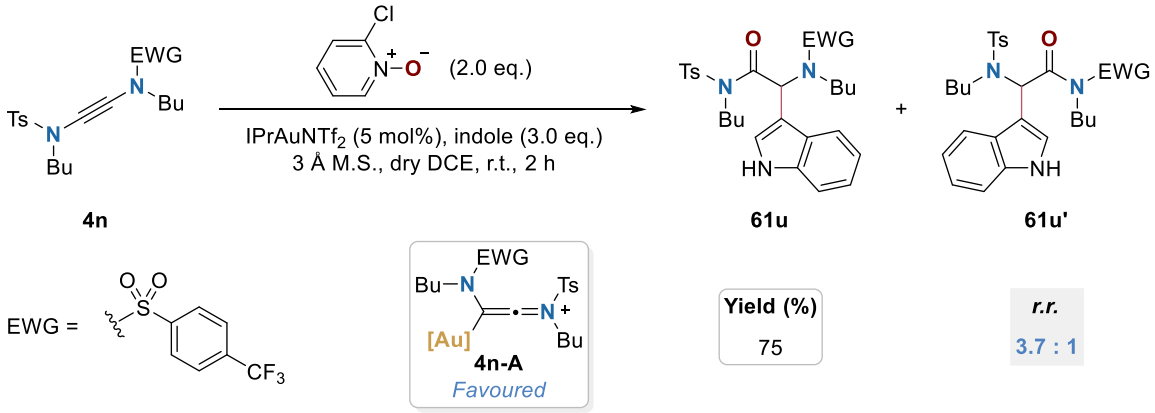


Scheme 2.17 Regioselectivity studies on yndiamide **4a**. Reactions were conducted at 0.1 mmol scale with [**4a**] = 0.5 M. Yields refer to the combined isolated yield of both isomers. Regioisomeric ratios (*r.r.*) were determined by ^{1}H NMR spectroscopic analysis of the crude reaction mixture.

Yndiamide **4a**, bearing a phosphate diester (Ps) group on one nitrogen atom, was the first to be tested in the reaction since it exhibited excellent regioselectivity in our previous studies.[27, 31] However, it only gave moderate regioselectivity (**61t**/**61t′**, *r.r.* = 1:4.3) despite a good overall yield (86%). Due to the inseparability of the two regioisomeric products and the inapplicability of the previously described Brønsted acid-catalysed double-substitution strategy for non-sulfonamide yndiamides, the structures of **61t**/**61t′** (as well as **61u**/**61u′**) were determined based on differences in TsCH_3 chemical shifts. We assumed that the tosyl signals proximal to the indole group are expected to appear more downfield than those distal to the indole moiety (similar effects on the proton chemical shifts were observed for many of the amino amide products **61**). The major regioisomer formed from yndiamide **4a** was identified as having the carbonyl group proximal to the phosphate diester group, which

is consistent with the hypothesis that the formation of keteniminium gold complex **4a-A** was favoured due to the phosphate diester group being less electron-withdrawing than the tosyl group.[27, 31]

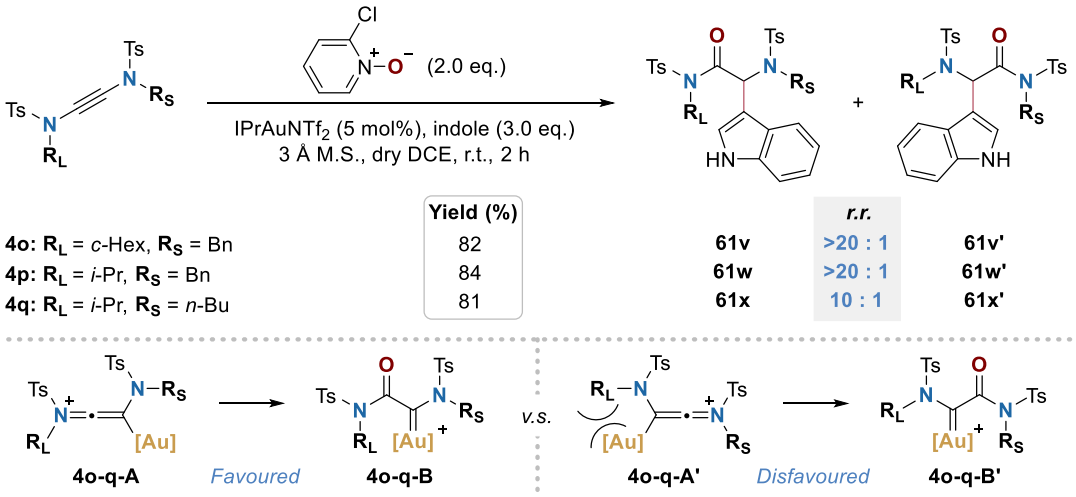
Yndiamide **4n** bearing a more electron-withdrawing 4-(trifluoromethyl)benzenesulfonyl group was next examined (Scheme 2.18). In contrast to yndiamide **4a**, in which case the formation of keteniminium gold complex **4a-A** was favoured, the keteniminium gold complex **4n-A** with the gold atom coordinated proximal to the tosyl groups would be formed preferentially. This hypothesis was supported by the regioselectivity now being inverted, however, no improvement in r.r. was observed. Since neither **4a** nor **4n** gave satisfactory *r.r.*, it was concluded that the regioselectivity of the gold-catalysed oxidative functionalisation of yndiamides could not be productively dictated by electronic factors.



Scheme 2.18 Regioselectivity studies on yndiamide **4n**. Reactions were conducted at 0.1 mmol scale with [**4n**] = 0.5 M. Yield refers to the combined isolated yield of both isomers. Regioisomer ratios (*r.r.*) were determined by ^{1}H NMR spectroscopic analysis of the crude reaction mixture.

Considering the significant difference in steric properties between a Brønsted acid catalyst, which is essentially a proton, and a gold catalyst, steric effects might be expected to play a much more pronounced role in determining the regiochemical outcome in a gold-catalysed reaction compared to a Brønsted acid-catalysed process. Given this premise, it was hypothesised that the use of non-symmetric yndiamides containing sterically-differentiated

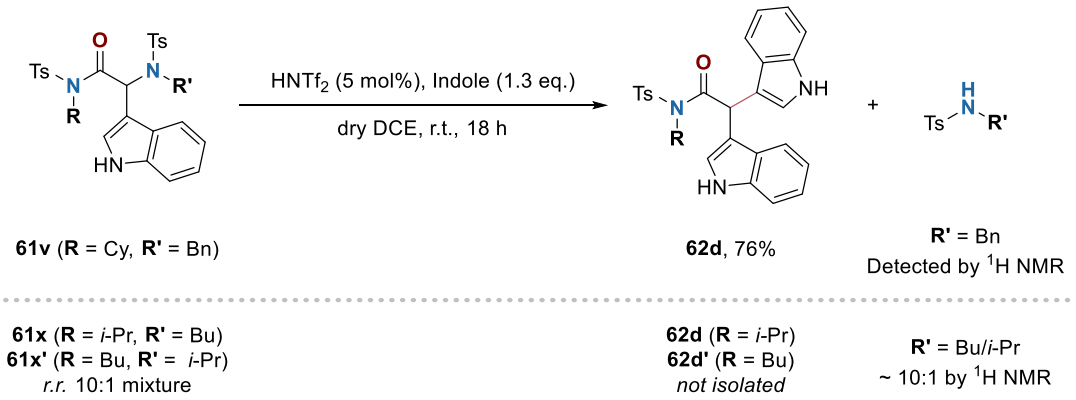
nitrogen substituents might enable regioselective gold-catalysed oxidative functionalisations. Encouragingly, yndiamide **4o**, featuring cyclohexyl and benzyl substituents, provided product **61v** with high regioselectivity (*r.r.* > 20:1) and an excellent yield of 82% (Scheme 2.19). To test the influence of decreased steric bias between the two substituents on regioselectivity, ynamides **4p** (*i*-Pr vs Bn) and **4q** (*i*-Pr vs *n*-Bu) were synthesised and tested in the reaction. The former also yielded the desired product **61w** as a single regioisomer with an excellent yield (84%), while the latter produced a regioisomeric mixture of **61x** and **61x′**, nonetheless with good *r.r.* (10:1) and yield (81%). These results demonstrate that even a single methyl branch α to the yndiamide nitrogen atom is sufficient to achieve high levels of regiocontrol in the functionalisation process.



Scheme 2.19 Regioselectivity studies on sterically-biased yndiamides. Reactions were conducted at 0.1 mmol scale, 0.5 M. Yields refer to the isolated yield of the major regioisomers. Yield for **61x**/**61x′** refers to the combined isolated yield of both products since they are inseparable. Regioisomeric ratios (*r.r.*) were determined by ^{1}H NMR spectroscopic analysis of the crude reaction mixture.

The structures of the major regioisomers were determined using various methods. The identities of **61v** and **61x** were confirmed by employing the Brønsted acid-catalysed double-substitution with indole as the nucleophile (Scheme 2.20a). The reaction produced

bis-indole acetamide **62d** in good yield (76%). Additionally, the *N*-benzyl-tosylamide was detected by ^{1}H NMR spectroscopic analysis of the crude reaction mixture. As **61x** and **61x′** were obtained as a mixture, bis-heteroarylated acetamide products were not isolated. However, ^{1}H NMR analysis revealed that a mixture of *N*-butyl-tosylamide and *N*-isopropyl-tosylamide in ~10:1 ratio was present in the reaction mixture, which was consistent with the previously measured r.r. value and supported the proposed structure of **61x** (Scheme 2.20). The structure of **61w** was confirmed by key HMBC interactions (see Chapter VII).

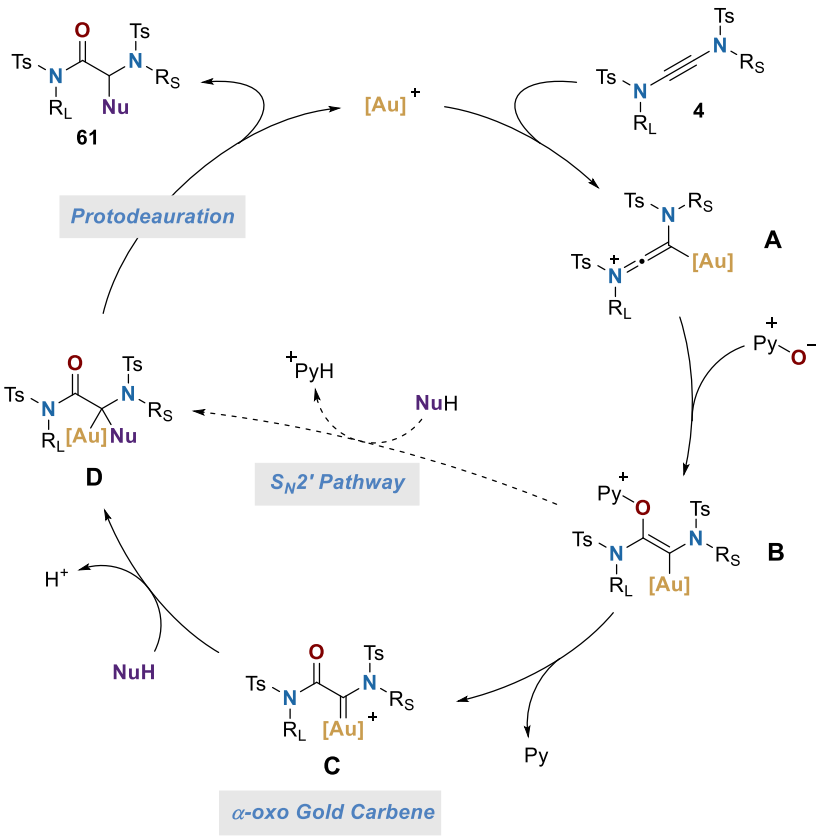


Scheme 2.20 Determination of structures of the major regioisomers **61v** and **61x**.

The carbonyl groups of the major regioisomers are located close to the bulkier nitrogen substituent, indicating that the gold complex preferentially engages the yndiamide proximal to the less-hindered nitrogen substituent. These results suggest a scenario of regiocontrol, where the formation of keteniminium gold complex **4o-q-A** is favoured over **4o-q-A′**, reducing the steric repulsion between the gold catalyst and the nitrogen substituent. As a result, **4o-q-B** becomes the predominant gold carbene species and thus leads to the formation of the major regioisomer.

2.2.5 Mechanistic Proposal

According to literature precedents reviewed earlier in this chapter, and on our observations of the regioselectivity of this transformation, a reaction mechanism is proposed that includes a possible regiocontrol scenario (Scheme 2.21). The regioselectivity is determined in the first step – the coordination of yndiamide **4** to the gold catalyst. Keteniminium gold complex **A**, with the gold atom bound distal to the bulkier nitrogen substituent to minimise steric repulsion, is formed predominantly. Based on our findings in Chapters III and IV, we hypothesised a Curtin-Hammett scenario for 2-chloropyridine *N*-oxide addition, giving vinyl gold complex **B**.



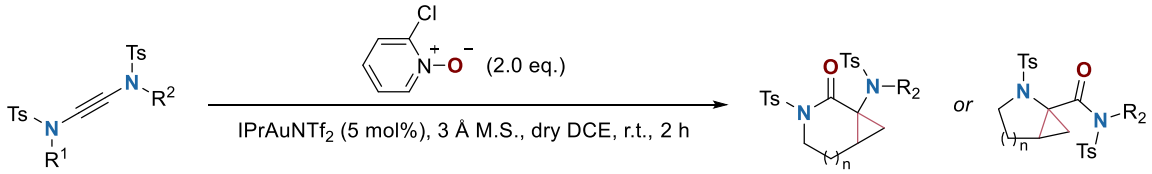
Scheme 2.21 Proposed reaction mechanism.

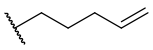
Two pathways are then possible from intermediate **B**, the first of which involves the formation of an *α*-oxo gold carbene **C** *via* loss of pyridine, as has been proposed for other

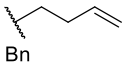
gold-catalysed oxidative processes on ynamides.[74, 76, 77] Attack from the nucleophile onto the gold carbene **D** affords adduct **D**, protodeauration of which gives the desired final product **60** and regenerates the gold catalyst to complete the cycle. Alternatively, vinyl gold complex **B** could undergo attack by the external nucleophile to directly generate adduct **D** *via* an S_N2' pathway, with loss of the pyridine leaving group.

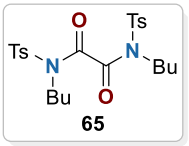
Inspired by the gold-catalysed cyclopropanation of ene-ynamides by Li and co-workers that was proposed to proceed *via* a non-carbene-mediated mechanism,[81] we envisioned that a similar reaction of ene-yndiamides under our gold-catalysed conditions could be a great opportunity for probing whether the reaction mechanism involves the generation of gold carbenes. We synthesised several ene-yndiamides and subjected them to gold-catalysed oxidative functionalisation in the absence of external nucleophiles (Table 2.02).

Table 2.02 Cyclopropanation experiments on ene-yndiamides.



4r: R_1 = 
R_2 = Bn

4c: R_1 = 
R_2 = Bn



65

Entry	Substrate	Deviation from Standard condition	Results
1	**4r**	None	Decomp.
2	**4c**	2-chloro-pyridine *N*-oxide (1.0 eq.) [**4c**] = 0.2 M, 0 °C	Decomp.
3	**4m**	With styrene (3.0 eq.)	Over-oxidation, and decomp.

Reactions were conducted on 0.1 mmol scale, 0.5 M.

However, regardless of the length of the carbon linker between the alkene and yndiamide motifs (**4r** and **4c**), no cyclopropanation products were found in either case (Table 2.02, entry 1, 2). Yndiamides applied in these reactions completely decomposed, even with a

reduced loading of the 2-chloropyridine *N*-oxide and lowered reaction temperature (Table 2.02, entry 2), giving non-analysable complicated results. A third attempt with yndiamide **4m** and styrene also failed to produce an intermolecular cyclopropanation product, instead giving an identifiable over-oxidation side product **65** (Table 2.02, entry 3). Attempts to trap any intermediate by approaches other than Friedel-Crafts-type reaction are thus unsuccessful; the search for other mechanistic probes or computational analyses to further investigate the reaction mechanism is ongoing.

2.3 Conclusions

In conclusion, we have developed the first gold-catalysed oxidative functionalisation of yndiamides to access unnatural amino acid derivatives, using a wide range of electron-rich π-nucleophiles. Through a series of robustness tests, the excellent tolerance of this transformation against external additives, covering a broad selection of functional groups, was highlighted. Furthermore, the aminoamide products obtained from this reaction have shown the potential for further derivatisation, including Brønsted acid-catalysed double-substitution with a second nucleophile, or selective detosylation. We have also demonstrated that minor steric differentiation between the two yndiamide nitrogen substituents can result in remarkable regioselectivity for non-symmetric substrates. While the proposed reaction mechanism involves the generation of *α*-oxo gold carbene intermediates, we could not disprove an alternative S_N2' pathway. Overall, our findings open up new possibilities in yndiamide chemistry – not least *via* oxidative functionalisations with other nucleophiles, which will be explored in the subsequent chapters.

C H A P T E R

III

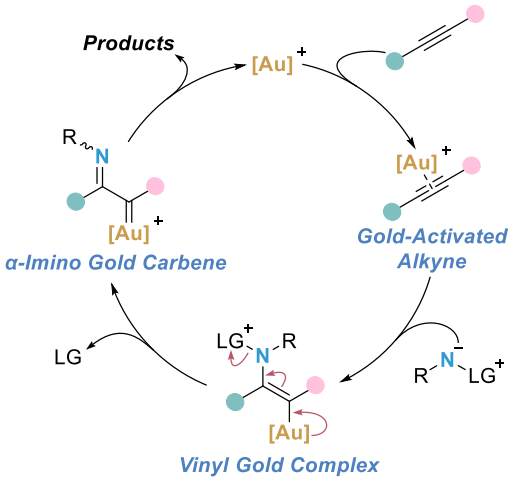
Gold(I)-Catalysed Cyclisation of Yndiamides with Isoxazoles

The generation and functionalisation of α-imino gold carbenes have attracted significant attention in the past decade. Among nitrogen-transfer reagents, isoxazoles have stood out as versatile building blocks for the atom-economic generation of α-imino gold carbene intermediates to access various complex azacycles. In this chapter, we describe the gold-catalysed cyclisation of yndiamides with isoxazoles *via* α-imino gold carbenes to deliver a library of highly substituted 2,3-diaminopyrroles. The reaction could be switched to a formal [5+2] cyclisation, leading to 1,4-oxazepines, by using benzisoxazoles as substrates. The regioselectivity was controlled by steric factors and could be achieved by introducing a subtle steric bias between the *N*-alkyl substituents on the yndiamide.

3.1 Introduction

3.1.1 Gold-Catalysed Functionalisation of Ynamides with Isoxazoles

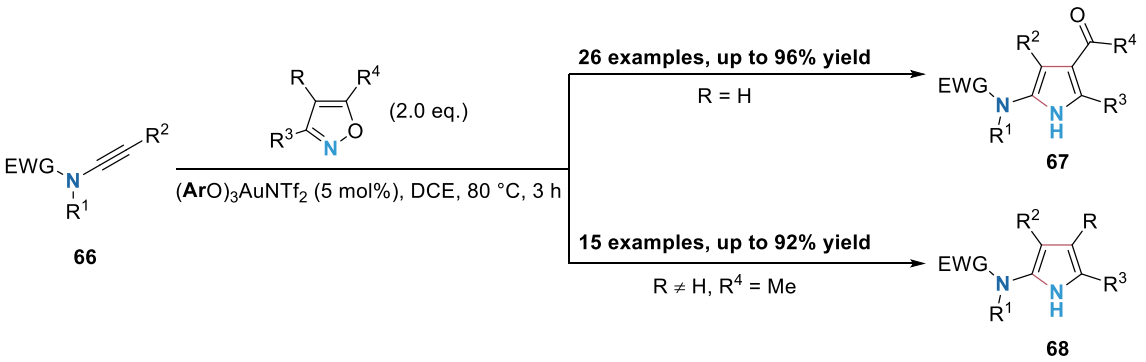
Over the past decade, gold-catalysed nitrene-transfer reactions have garnered considerable attention and have become a highly versatile tool for the synthesis of a diverse range of *N*-containing molecules, especially when combined with ynamides substrates.[18, 39, 54, 98-100] Several nitrene-transfer reagents (such as azides, pyridine-based or sulfur-based aza-ylides) have been developed, most of which operate *via* the mechanism depicted below (Figure 3.01).



Scheme 3.01 Generic representation of gold-catalysed nitrene-transfer reactions.

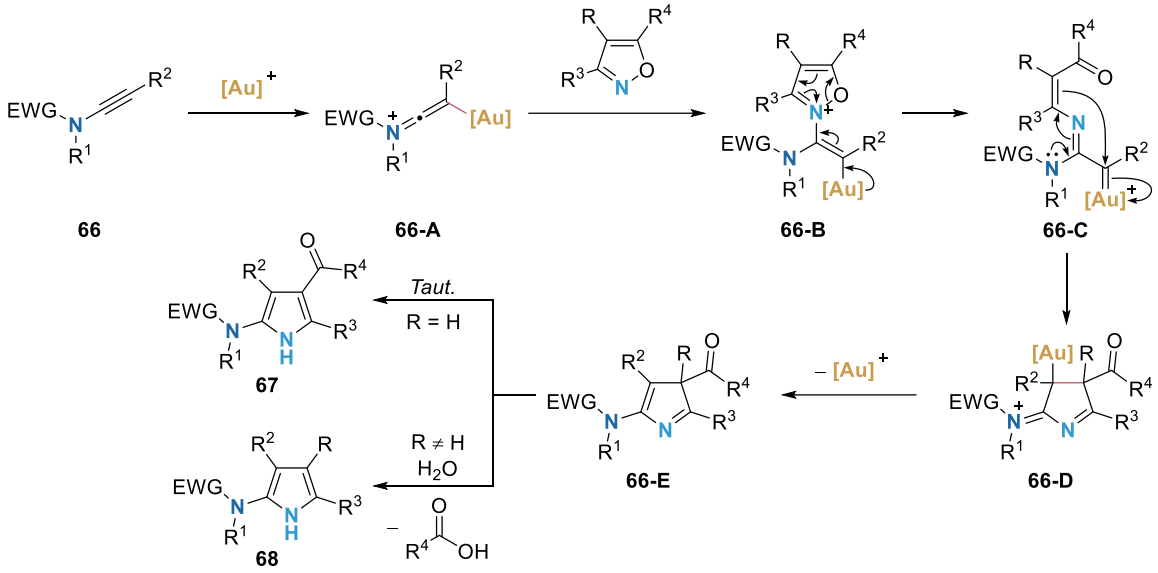
Similar to that of *α*-oxo gold carbene generation, the reaction is initiated by the coordination of the alkyne to the active gold catalyst. The nucleophilic nitrogen atom in the nitrene-transfer reagent attacks the gold-activated alkyne species to produce a vinyl gold complex. Subsequently, an *α*-imino gold carbene intermediate is generated upon the spontaneous loss of a charge-neutral leaving group (for instance, N_2 for azides, pyridine for pyridine-based aza-ylides, and thioethers for sulfur-based aza-ylides) by cleavage of a relatively weak N–X bond. The gold carbene species can then undergo a range of reactions (such as 1,2-migration, X–H insertion, cyclopropanation, etc.) to produce diverse products.

However, the above synthetic route to generate the carbene species has a drawback due to low atom economy as the expulsion of a leaving group from the reaction system is required. In 2015, Ye and co-workers introduced isoxazoles as novel nitrene-transfer reagents to achieve the atom-economic generation of *α*-imino gold carbenes from ynamides (Scheme 3.02).[101] The use of 4*H*-isoxazole resulted in the formation of acylated pyrrole products **67**, incorporating all atoms of the isoxazole. Deacylated products **68** were acquired using 4-substituted isoxazoles.



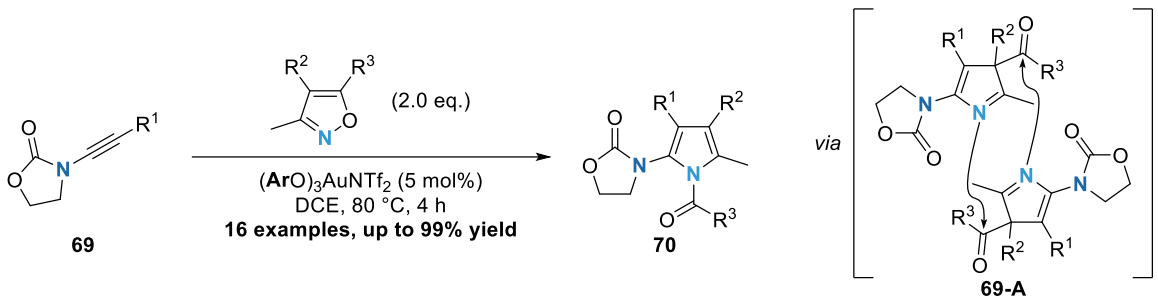
Scheme 3.02 Gold-catalysed formal [3+2] cycloaddition between ynamides and isoxazoles. Ar = 2,4-di-*tert*-butylphenyl.

With the aid of DFT calculations, the Ye group proposed a mechanism that modifies the conventional model (Scheme 3.03).[101] The catalytic cycle begins with the activation of the ynamide triple bond by the gold catalyst, followed by the nucleophilic attack of the isoxazole nitrogen atom to form the vinyl gold complex **66-B**. Then scission of the labile N–O bond in the isoxazole motif forms the *α*-imino gold carbene **66-C**.[102-104] The *α*-imino gold carbene intermediate **66-C**, bearing an α,β-unsaturated carbonyl sidechain, then undergoes 1,5-cyclisation to generate intermediate **66-D**. Subsequent deauration/tautomerization (R = H) produces **67**; alternatively, a deauration/deacylative aromatisation cascade can produce **68** (R ≠ H).



Scheme 3.03 Reaction mechanism for the gold-catalysed formal [3+2] cycloaddition between ynamides and isoxazoles.

In the same year, the Ye group further developed the latter reactivity, using oxazolidinone ynamides **69**, and reported gold-catalysed functionalisation with 4-substituted isoxazoles to synthesise fully substituted 2-aminopyrroles **70** (Scheme 3.04).[105] The formation of the major product was proposed to be the result of an intermolecular carbonyl exchange between two molecules of 3*H*-pyrrole intermediate **69-A**.

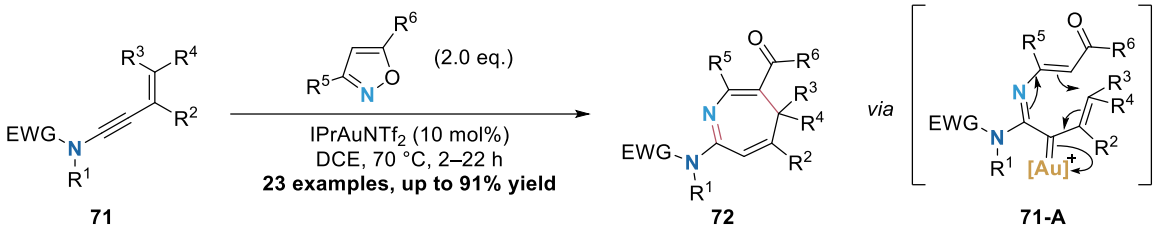


Scheme 3.04 Gold-catalysed formal [3+2] cycloaddition between oxazolidinone-ynamides and 4-substituted isoxazoles.

These two works by the Ye group represent the first two examples of gold-catalysed functionalisation of ynamides with isoxazoles. Following their seminal work, a variety of 'isoxazole-like' nitrene-transfer reagents were developed. In the following years, the Liu

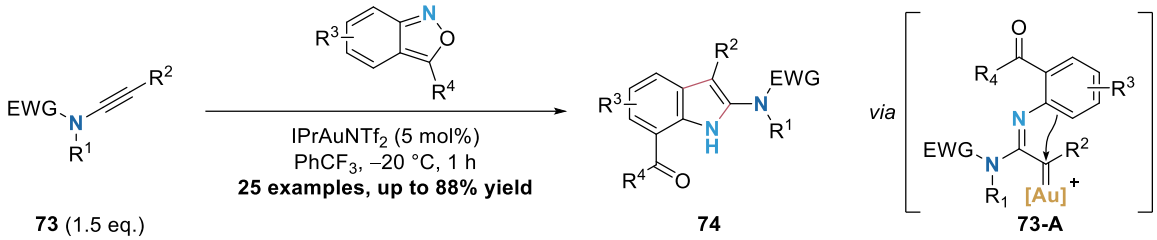
group reported several gold-catalysed functionalisations of non-polarised alkyne species (propiolates,[106] 1,4-diyn-3-ols,[107] and 1,2-dienyl-5-ynes[108]) with isoxazoles to construct various pyrrole-based aza-cycles. Recently, Davies and co-workers also demonstrated the gold-catalysed annulation of alkynyl thioethers with isoxazoles and anthranils to provide controlled access to 3-sulfenyl pyrroles or indoles.[109]

In 2018, Liu and co-workers reported the gold-catalysed [4+3] annulation of ene-ynamides and isoxazoles, which represents the first example of incorporating a 'non-isoxazole-originated' alkene in the cyclisation (Scheme 3.05).[110] The proposed reaction mechanism involves a 6π-cyclisation of the *α*-imino gold carbene species **71-A** generated from the nucleophilic attack/ring-opening sequence, followed by a deprotonation/protodeauration sequence to deliver the 4*H*-azepine products **72**.



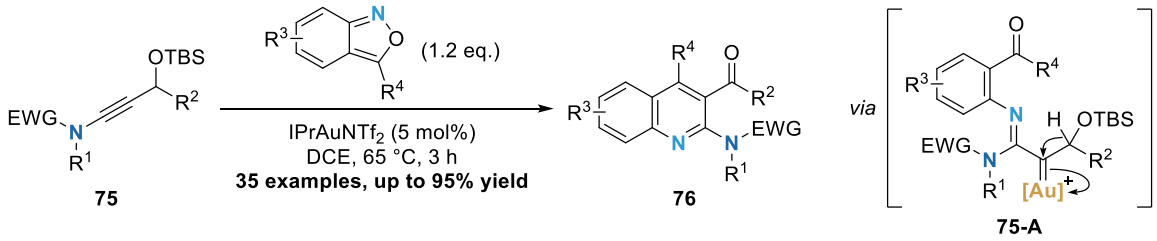
Scheme 3.05 Gold-catalyzed [4+3]-annulations of 3-en-1-ynamides with isoxazoles.

In 2016, Hashmi and co-workers first reported the use of anthranils, that is, benzo-annulated isoxazole analogues, in the gold-catalysed functionalisation of ynamides for the synthesis of 2-aminoindoles **74** under mild conditions (Scheme 3.06).[111] The transformation proceeds through regioselective C–H insertion of the *α*-imino gold carbene intermediate **73-A** into the *ortho* C–H bond.



Scheme 3.06 Gold-catalysed functionalisation of ynamides with anthranils.

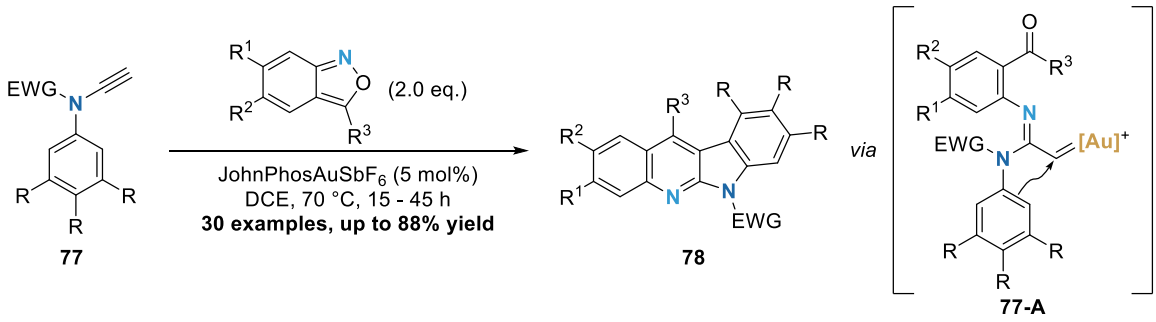
Following their earlier work, the Hashmi group reported the utilisation of propargyl silyl ethers **75** and anthranils in the gold-catalysed synthesis of quinolines **76** through a sequential ring-opening/1,2-H migration/protodeauration/Mukaiyama aldol cyclisation (Scheme 3.07).[112] In contrast to the previously discussed works that made use of the electrophilicity of the gold carbene carbon, this work demonstrated the umpolung reactivity of the gold carbene carbon atom. The proposed reaction mechanism invokes the *α*-imino gold carbene **75-A**, which can undergo a 1,2-H migration/protodeauration sequence to form a silyl enol ether. The following intramolecular Mukaiyama aldol condensation onto the aryl ketone yields the quinoline product **76**.



Scheme 3.07 Gold-catalysed synthesis of quinolines from propargyl silyl ethers and anthranils.

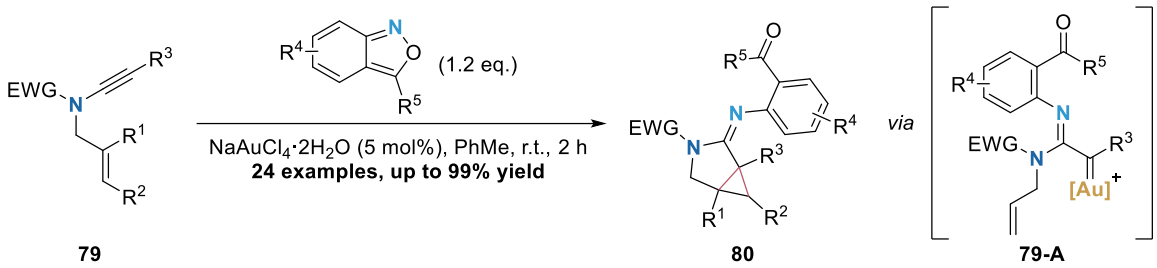
The Hashmi group continued to explore alternative strategies for the functionalisation of *α*-imino gold carbene intermediates. In their study on the gold-catalysed annulation of *o*-ethynylbiaryls with anthranils, a regiospecific C–H insertion/protodeauration/Friedel-Crafts-type cyclisation sequence was used to construct diverse '*N*-doped' polycyclic aromatic hydrocarbons.[113] Liu and co-workers applied a similar approach in the gold-catalysed annulation of *N*-aryl ynamides **77** with anthranils to synthesize 6*H*-indolo[2,3-

b]quinolines **78** *via* C–H insertion/protodeauration of the gold carbene **77-A** followed by intramolecular condensation (Scheme 3.08).[114] While terminal ynamides bearing electron-rich aryl groups were required for this transformation, anthranils of varied electronic properties were well tolerated, providing a broad scope of 6*H*-indolo[2,3-*b*]quinolines. Following this work, several other gold-catalysed syntheses of quinoline-based aza-heterocycles from various ynamides and anthranils were explored utilising this strategy.[115, 116] Their mechanisms are not discussed here due to their similarities with those already covered.



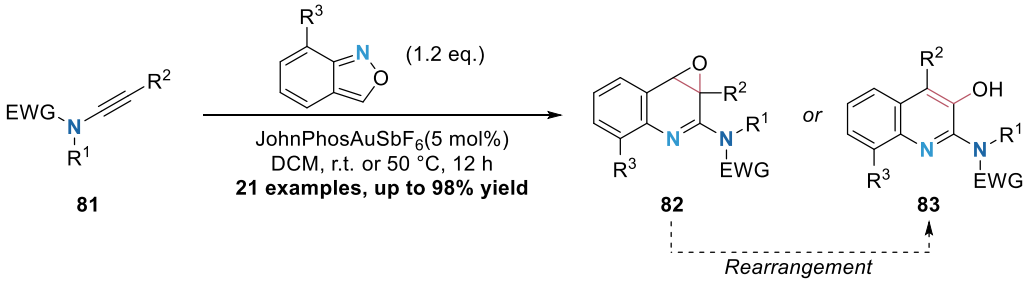
Scheme 3.08 Gold-catalyzed annulations of *N*-arylynamides with anthranils.

The abovementioned literature precedents adequately demonstrated the ability of isoxazole-based nitrene-transfer reagents in the formation of medium-sized ring structures, however, the application of those reagents in the synthesis of small-sized rings is relatively rare. The first gold-catalysed cyclopropanation of *N*-allyl ynamides **79** and anthranils was reported by Hashmi and co-workers for the synthesis of 3-azabicyclo[3.1.0]hexan-2-imines **80** *via* the generation of the gold carbene **79-A** (Scheme 3.09).[117] The reaction can accommodate anthranils with varied electronic properties and a wide selection of internal and external *N*-allyl ynamides**.**



Scheme 3.09 Gold(III)-catalysed cyclopropanation of anthranils with *N*-allyl ynamides.

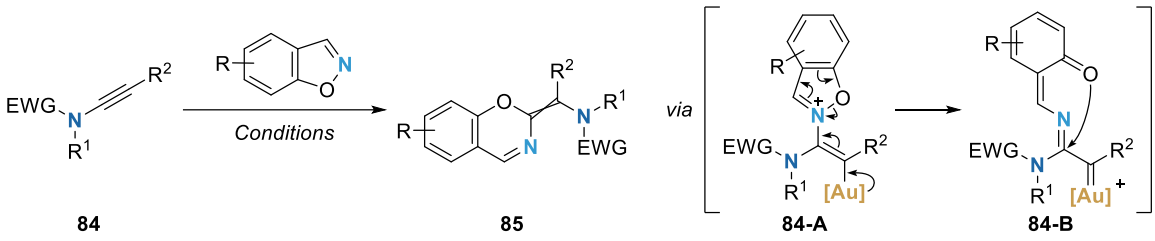
The same research group also demonstrated the gold-catalysed epoxidation of ynamides and anthranils.[118] In the presence of a gold(I) catalyst (JohnPhosAuSbF$_6$), the reaction proceeded towards the formal [4+2] cyclisation, yielding a range of quinoline oxides **82**, which in some cases undergo rearrangement to give 3-hydroxyl-quinolines **83** (Scheme 3.10).



Scheme 3.10 Gold(I)-catalyzed [4+2] epoxidation of ynamides with anthranils.

The gold-catalysed functionalisation of ynamides using benzo[*d*]isoxazoles, isomers of anthranils with different benzo-annulation positions, was investigated by several research groups. Reported independently by R.-S. Liu *et al.*[119] and Y. Liu *et al.*,[120] and later by Sahoo *et al.*,[121] the use of benzo[*d*]isoxazoles offered an interesting switchable reactivity between [5+1] and [5+2] cycloaddition. The reaction outcome was mainly controlled by the catalyst. The use of gold catalysts with bulky ligands led to formal [5+1] cycloaddition, delivering a mixture of *Z*- and *E*-benzo[*e*][1,3]oxazine derivatives **85** (Scheme 3.11). While R.-S. Liu and co-workers observed *Z*-selectivity with JohnPhosAuNTf$_2$ as the catalyst, the Y. Liu group and the Sahoo group reported the *E*-isomer as the major product using the

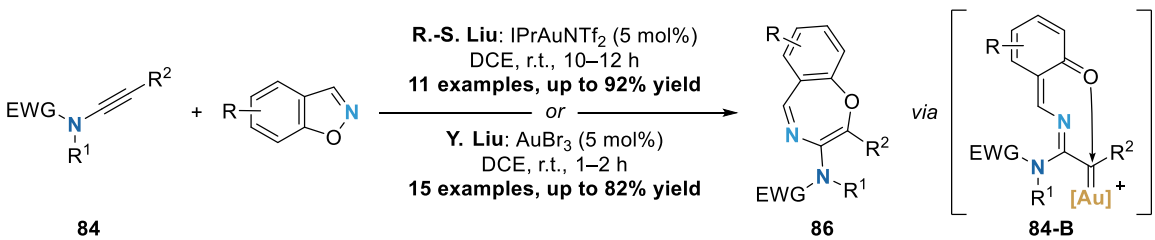
JohnPhosAu(MeCN)SbF_6 catalyst, which indicates the *Z*/*E*-selectivity might be affected by the choice of the counterion. All three groups proposed similar mechanisms that proceed through the generation of the α-imino gold carbene intermediate **84-B** by sequential N–O bond scission/ring-opening of vinyl gold complex **84-A**. Due to the bulky nature of the gold catalyst, nucleophilic attack from the carbonyl group onto the gold carbene is less favoured. Instead, a 6π-electrocyclisation can occur, followed by a 1,2-sulfonamide shift to furnish the final benzo[*e*][1,3]oxazine products **85**.



R.-S. Liu: JohnPhosAuNTf$_2$ (5 mol%), DCE, r.t., 11–13 h, **14 examples, up to 87% yield, *Z*/*E* = 15:1**
Y. Liu: JohnPhosAu(MeCN)SbF$_6$ (5 mol%), DCE, r.t., 1–9 h, **17 examples, up to 93% yield, *E*/*Z* = 12.5:1**
Sahoo: JohnPhosAu(MeCN)SbF$_6$ (5 mol%), $CHCl_3$, r.t., 4 h, **22 examples, up to 94% yield, *E*/*Z* = 6.1:1**

Scheme 3.11 Gold-catalyzed [5+1] cycloaddition of ynamides with benzo[*d*]isoxazoles.

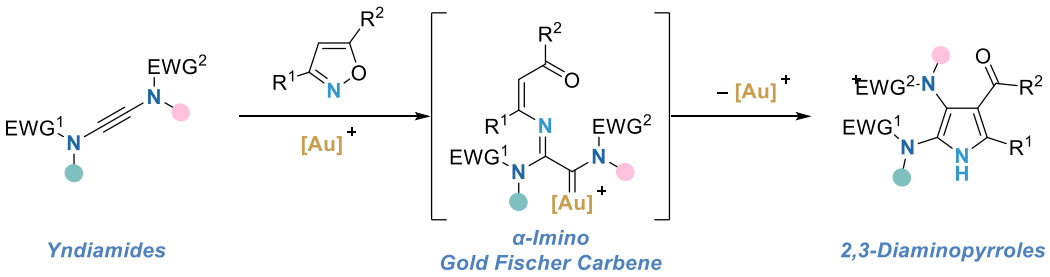
On the other hand, the use of a non-bulky gold(I) catalyst or gold(III) salt changes the outcome of the reaction from formal [5+1] to [5+2] cycloaddition, leading to the formation of benzo[*f*][1,4]oxazepines **86** (Scheme 3.12). Thanks to the non-bulky nature of the catalyst, the 6π Nazarov-type cyclisation of the α-imino gold carbene intermediate **84-B** is favoured, delivering the benzo[*f*][1,4]oxazepine products **86** upon deauration.



Scheme 3.12 Gold-catalyzed [5+2] cycloaddition of ynamides with benzo[*d*]isoxazoles.

3.1.2 Concepts of This Work

The above literature demonstrates the exceptional versatility of isoxazole-based nitrene-transfer reagents in the gold-catalysed functionalisation of ynamides, leading to the synthesis of complex azacycles. The functionalisation of the *α*-imino gold carbenes generated from this system ranges from simple one-step cyclisation to intricate poly-cyclisation cascades. The anthranil or benzo[*d*]isoxazole analogues also offer opportunities for switchable reactivities that can provide valuable insights for further mechanistic discussions. Therefore, the application of these nitrene-transfer reagents in the gold-catalysed functionalisation of yndiamides would represent a significant contribution to yndiamide chemistry and an improvement over previously described gold-catalysed functionalisation with pyridine *N*-oxides. In this regard, we designed a gold-catalysed formal [3+2] cyclization between yndiamides and 5-substituted isoxazoles that forms 2,3-diaminopyrroles through *α*-imino gold Fischer carbenes (Scheme 3.13).



Scheme 3.13 Concept of this work.

This transformation offers a straightforward route to explore the gold-catalysed functionalisation with isoxazoles while providing access to valuable products with potential utility in medicinal chemistry. Pyrroles are fundamental building blocks in medicinal chemistry, as evidenced by blockbuster drugs such as Atorvastatin which feature fully-substituted pyrrole cores (Figure 3.01);[122-124] the direct synthesis of highly decorated pyrroles is desirable, but challenging, particularly for those featuring heteroatom

substituents.[125] We also anticipated exploring the use of anthranils and benzo[*d*]isoxazoles in the reaction system for potential switchable reactivities.

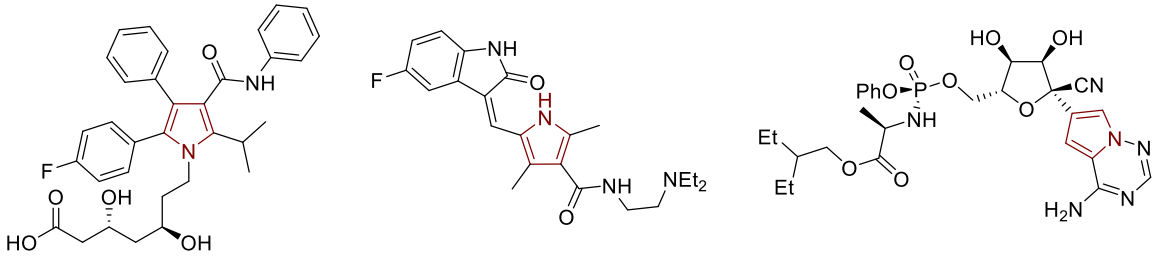


Figure 3.01 Polysubstituted pyrroles in medicinal chemistry.

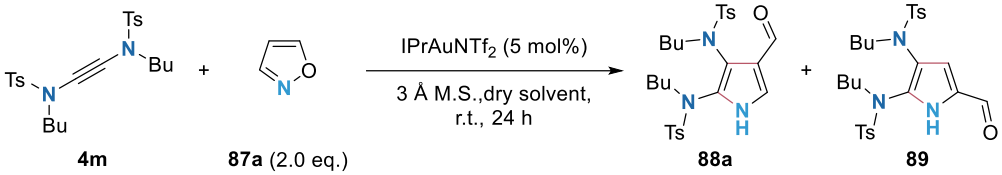
Our research focus will also include regioselectivity studies. Previously in Chapter II, we discovered that steric factors can effectively control regioselectivity. In this chapter, we employed this concept on this new reaction system and monitored their regiochemical outcome. In addition, since isoxazoles provide more points of attachment for substituents close to the nucleophilic centre, we also investigated the impact of different substituted isoxazoles on the regioselectivity of the reaction.

3.2 Results and Discussion

3.2.1 Optimisation of Conditions

For initial attempts, we applied the optimised reaction conditions previously developed for the gold-catalysed oxidative functionalisation of yndiamides with pyridine *N*-oxides, using yndiamide **4m** and isoxazole **87a** (Table 3.01, entry 1). Successful formation of the desired 2,3-diaminopyrrole product **88a** was observed in good yield (51% NMR yield; 60% isolated yield). To improve the yield of **88a**, different solvents were screened (Table 3.01).

Table 3.01 Optimisation of conditions: solvents screening.



Entry	Solvent	Yield	88a:89[a]
1	DCE	51% (60%)	> 20:1
2	DCM	51%	14:1
3	DBE	47%	> 20:1
4	$CHCl_3$	47%	> 20:1
5	MeCN	trace	-
6	DMSO	0%	-
7	DMF	0%	-
8	MeOH	0%	-
9	PhMe	19%	> 20:1
10	THF	6%	> 20:1
11	Neat[b]	28%	> 20:1

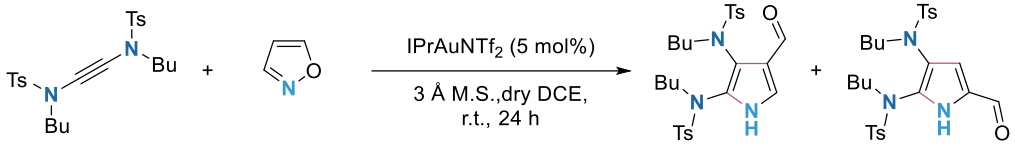
Reactions were conducted on 0.05 mmol scale with [**4m**] = 0.5 M; yields were determined by ^{1}H NMR spectroscopy using dimethyl sulfone as internal standard; yields in parentheses are isolated yields on 0.1 mmol scale. [a] Ratios between **88a** and **89** were determined by ^{1}H NMR spectroscopic analysis of the crude reaction mixture; [b] 0.1 mL of isoxazole was added as the solvent.

These optimisations revealed that halogenated (chlorinated and brominated) solvents were the most effective, providing optimal yields of the desired product **88a** when using DCE or DCM (Table 3.01, entries 1–4). However, dipolar aprotic and protic solvents resulted in decomposition of the yndiamide (Table 3.01, entries 5–8). Non-polar solvents and neat isoxazole led to reduced yields of **88a** (Table 3.01, entries 9–11). Interestingly, varying amounts of isomeric side product **89** were observed in entries with successful reactions, the structure of which was determined by X-ray crystallographic analysis (see Chapter VII). This isomer presumably arises from a 1,5-formyl shift in the final aromatization step in the catalytic cycle (see later).

To improve the yield of **88a**, the effect of varying the equivalents of isoxazole and the reaction concentration was evaluated (Table 3.02). An enhancement in the yield of the

product was observed when the quantity of isoxazole was increased. Nevertheless, even with a large excess amount of isoxazole, the resulting improvement in yield remained modest (Table 3.02, entries 1–3). Conversely, a reduction in yield and a decline in the **88a**:**89** ratio were evident upon dilution of the reaction (Table 3.02, entries 4–6).

Table 3.02 Optimisation of conditions: isoxazole equivalents and reaction concentration.



4m **87a** (**x** eq.) **88a** **89**

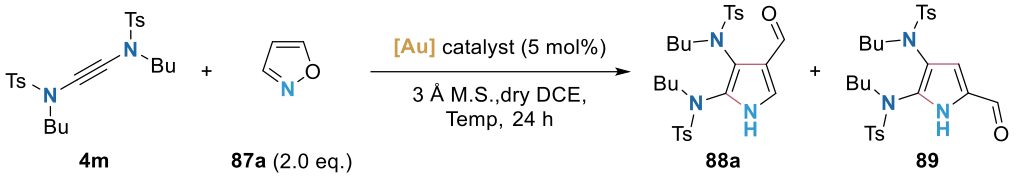
Entry	x	[4m]	Yield	88:89[a]
1	1.1	0.50 M	41%	17:1
2	1.5	0.50 M	44%	12:1
3	10	0.50 M	60%	12:1
4	2.0	0.25 M	47%	13:1
5	2.0	0.125 M	44%	11:1
6	2.0	0.05 M	41%	10:1

Reactions were conducted on 0.05 mmol scale; yields were determined by ^{1}H NMR spectroscopy using dimethyl sulfone as the internal standard. [a] Ratios between **88** and **89** were determined by ^{1}H NMR spectroscopic analysis of the crude reaction mixture.

Various gold catalysts were also screened (Table 3.03). The best result was obtained using $(ArO)_3PAuNTf_2$ (Ar = 2,4-di-*tert*-butylphenyl), which produced **88a** in an optimal yield of 77% (78% isolated) (Table 3.03, entry 3). Notably, $(ArO)_3PAuNTf_2$ exhibited remarkable reactivity and achieved complete conversion within 2 h. The presence of an active gold catalyst was found to be indispensable for the reaction, as no reactions were observed when no/non-activated gold catalyst or $AgNTf_2$ were used (Table 3.03, entries 7–9). Increasing the reaction temperature did not harm the yield or selectivity of the reaction (Table 3.03, entries 10–12) and was beneficial for several cases in our study of reaction scope (see the subsequent section). Application of the optimal conditions (Table 3.03, entry 3) on 1.0

mmol scale afforded **88a** in 75% isolated yield (Table 3.03, entry 13). However, a higher proportion of (separable) **89** was also generated.

Table 3.03 Optimisation of conditions: catalysts and temperature.



4m **87a** (2.0 eq.) **88a** **89**

Entry	Catalyst	Temp	Yield	88a:89[a]
1[b]	$AuCl_3$	r.t.	27%	4:1
2	$dppe(AuNTf_2)_2$[c]	r.t.	51%	5:1
3[b]	$(\mathbf{Ar}O)_3PAuNTf_2$	r.t.	77% (78%)	> 20:1
4	PPh_3AuNTf_2	r.t.	54%	6.8:1
5	$KAuBr_4{\cdot}2H_2O$	r.t.	55%	3.6:1
6	$PicAuCl_2$	r.t.	28%	7.8:1
7	-	r.t.	0%	-
8	$(ArO)_3PAuCl$	r.t.	0%	-
9	$AgNTf_2$	r.t.	0%	-
10[b]	$(\mathbf{Ar}O)_3PAuNTf_2$	40 °C	71%	> 20:1
11[b]	$(\mathbf{Ar}O)_3PAuNTf_2$	60 °C	71%	> 20:1
12[b]	$(\mathbf{Ar}O)_3PAuNTf_2$	80 °C	72%	> 20:1
13[b, d]	$(\mathbf{Ar}O)_3PAuNTf_2$	r.t.	(75%)	4.8:1

Reactions were conducted on 0.05 mmol scale with [**4m**] = 0.5 M; catalysts $LAuNTf_2$ were prepared *in situ* by premixing the corresponding LAuCl pre-catalyst and $AgNTf_2$; yields were determined by ^{1}H NMR spectroscopy using dimethyl sulfone as internal standard; yields in parentheses are isolated yields on 0.1 mmol scale; **Ar** = 2,4-di-*tert*-butylphenyl. [a] Ratios between **88a** and **89** was determined by ^{1}H NMR spectroscopic analysis of the crude reaction mixture. [b] Reaction completed after 2 h. [c] 2.5 mol% of the catalyst was used. [d] Reaction was conducted on 0.1 mmol scale, and completed after 3 h, **88a**:**89** was based on isolated products.

3.2.2 Isoxazole Scope

With optimised conditions in hand, the scope of the reaction was investigated using various 3,5-disubstituted isoxazoles (Figure 3.02). Initial attempts utilising 3,5-dimethylisoxazole resulted in the formation of the desired product **88b** (45%). However, the formation of considerable amounts of a side product (37%) was also observed. It was identified as 1,4-

oxazepine **90** with two possible structures, but at this stage, we were unable to distinguish between them. The formation of **90** could be the result of the competitive 1,7-cyclisation of the proposed gold carbene intermediate (see later).

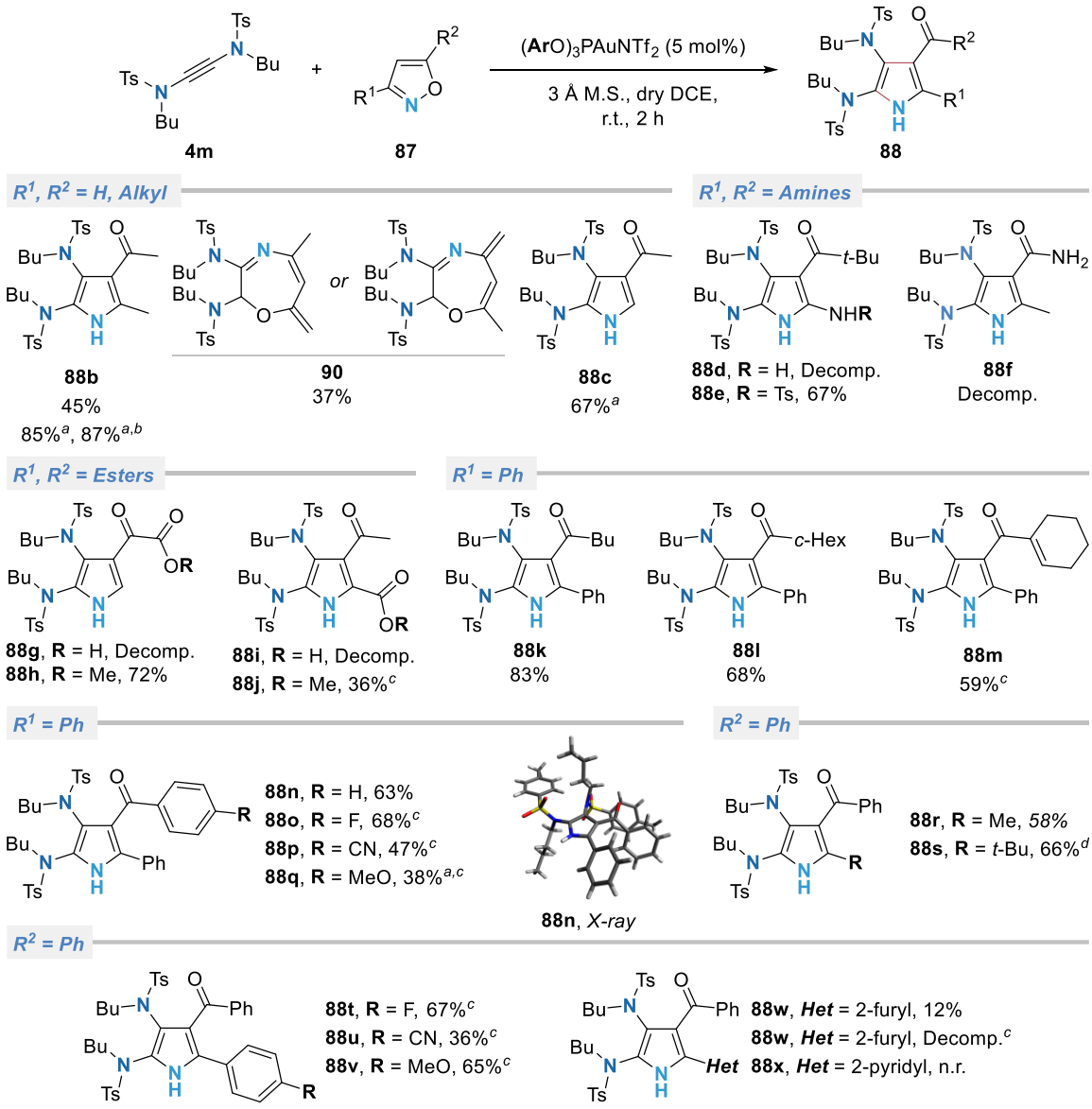


Figure 3.02 Isoxazole scope for gold(I)-catalysed yndiamide cyclisation. Unless otherwise stated all reactions were performed on 0.1 mmol scale at room temperature with [**4m**] = 0.5 M; **Ar** = 2,4-di-*tert*-butylphenyl; yields refer to isolated yields. [a] Reactions were treated with HCl (1.0 M in Et_2O, 1.0 eq.) for 30 min after full conversion of **4m** as indicated by TLC. [b] Reactions were performed on 1.0 mmol scale and reached completion after 3 h; [c] Reaction performed at 80 °C; [d] Reaction reached completion after 4 h.

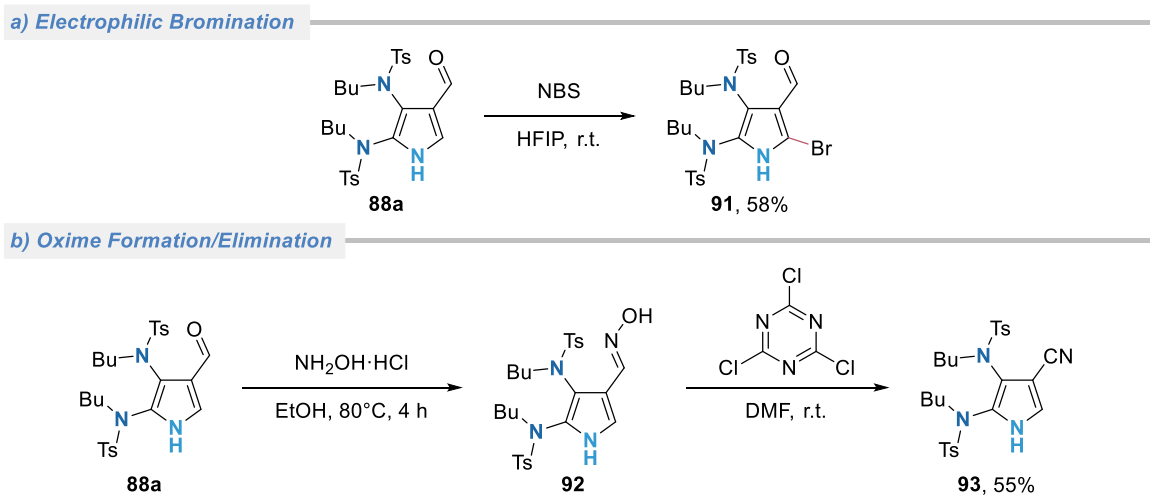
Fortunately, we discovered that treatment of the crude reaction mixture with ethereal HCl facilitated the smooth conversion of **90** to **88b**, resulting in an overall yield of 85% for **88b**. This technique proved to be effective on 1.0 mmol scale (0.48 g), producing **88b** in an excellent yield of 87%. The reaction also performed well with monosubstituted 5-methylisoxazole, producing trisubstituted pyrrole **88c** with a good yield of 67%. The use of sulfonamidoisoxazole led to the production of the rarely-seen tris-aminopyrrole **88e** in a yield of 67%. Methyl esters were accommodated at either the 3- or 5-position of the isoxazole, resulting in the formation of **88h** (72%) and **88j** (36%), albeit the latter reaction necessitated heating to 80 °C, presumably due to the reduced nucleophilicity of the adjacent nitrogen atom when in proximity to an electron-withdrawing group. However, the inclusion of unprotected amino or carboxylic groups at either the 3- or 5-position of the isoxazole resulted in the degradation of the yndiamide, formation of the desired pyrrole products (**88d**, **88f**, **88g**, and **88i**) was not detected, likely due to the addition to the yndiamide triple bond and subsequent decomposition of the products.

Isoxazole substituent effects were further investigated by introducing aryl groups to either R^1 or R^2 (or both). To evaluate the effect of substituents at the 5-position, a range of 3-phenylisoxazoles was employed. Alkyl groups at the 5-position were well-tolerated, providing **88k** and **88l** in good yields (83% and 68% respectively). For substrates with sp^2-hybridised substituents at the 5-position, conversion required heating (80 °C), with **88m** being produced in a yield of 59% with a cyclohexenyl group. The use of 3,5-diphenylisoxazole produced **88n** (whose structure was confirmed by X-ray crystallographic analysis) in a satisfactory yield (63%), while other aryl groups were moderately accommodated (**88o–88q**). The substitution effects at the 3-position were assessed using a complementary series of 5-phenyl isoxazoles. Alkyl substitution was well-tolerated (**88r** and **88s**), while 3-aryl isoxazoles required heating (**88t–88v**); for these substrates, electron-

rich aryl isoxazoles performed better than electron-poor ones. The incorporation of heteroaryl groups was found to be unfavourable. When a 5-furyl group was introduced, the yield of product **88w** was low (12%) and only decomposition was observed upon heating. Similarly, no observable reactions were detected with the inclusion of a 5-pyridyl group, presumably due to the pyridine group coordinating to the active gold catalyst and thus inhibiting the reaction.

3.2.3 Derivatisation of Products

To showcase the potential of the 2,3-diaminopyrrole products, further functionalisation was investigated. Electrophilic bromination[126] of pyrrole **88a** was performed, resulting in the formation of **91** in good yield (58%, Scheme 3.14a). The formyl group in **88a** was also transformed into an oxime **92**, which was subsequently dehydrated[127] to produce cyanopyrrole **93** in a 55% yield (Scheme 3.14b).

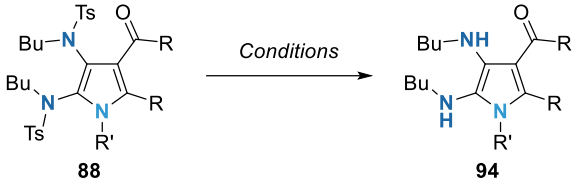


Scheme 3.14 Derivatisation of the pyrrole product **88a**.

The detosylation of the pyrrole products was also studied, expecting that deprotecting the two sulfonamide substituents could open up venues for further functionalisation (Table 3.04). However, initial attempts using the previously applied conditions (Scheme 2.16, Mg

(20 eq.), NH_4Cl (4 eq.), THF/MeOH (1:1), sonication, r.t.) on pyrrole **88a** failed to produce the desired 2,3-diaminopyrrole **94a** and only decomposition of the starting material was observed (Table 3.04, entries 1 – 2).

Table 3.04 Attempted detosylation of **88**.



88 94

Entry	SM	R	R′	Conditions	Results
1	**88a**	H	H	Mg (20 eq.), THF/MeOH (1:1) sonication, r.t.	Decomp.
2	**88a**	H	H	Mg (20 eq.), THF/MeOH (1:1), stirring, r.t.	Decomp.
3	**88a**	H	H	Mg (20 eq.), NH_4Cl (4.0 eq.) THF/MeOH (1:1), r.t.	Decomp.
4	**88a**	H	H	TfOH (2.4 eq.) DCE, 80 °C	Decomp.
5	**88y**	H	Boc	Mg (20 eq.), NH_4Cl (4.0 eq.) THF/MeOH (1:1), r.t.	Decomp.
6	**88c**	Me	H	Mg (20 eq.), NH_4Cl (4.0 eq.) THF/MeOH (1:1), r.t.	Decomp.
7	**88c**	Me	H	SmI_2 (20 eq.), pyrrolidine (2.0 eq.) H_2O (28 eq.), THF, r.t.	Decomp.

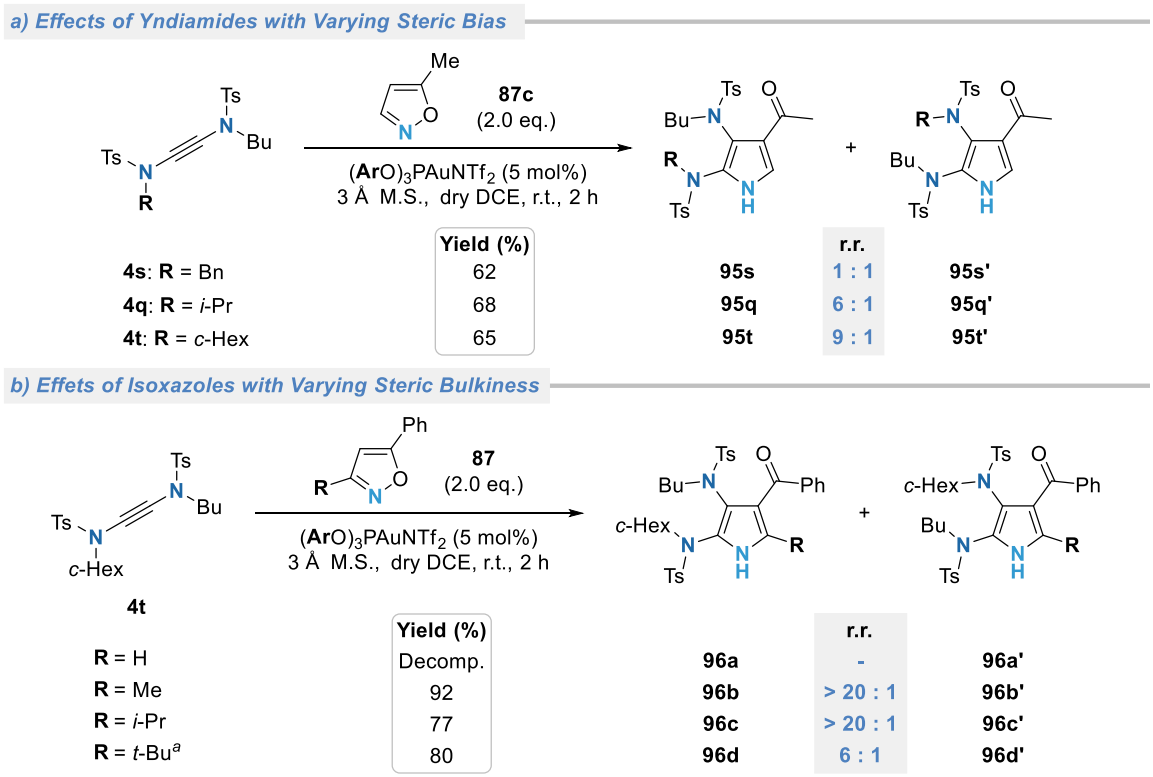
Reactions were conducted on 0.1 mmol scale.

Increasing the acidity of the reaction mixture (Table 3.04, entry 3) or using another literature-reported detosylation condition for sulfonamides[128] (Table 3.04, entry 4) also resulted in complete degradation of the starting material. It was suspected that the removal of the electron-withdrawing tosyl groups in **88a** would significantly increase the electron density on the pyrrole ring, rendering the detosylated product too unstable to isolate. To stabilise the desired electron-rich product, we synthesised **88y** with an electron-

withdrawing carbamate group attached to the pyrrole nitrogen atom. However, when **88y** was subjected to magnesium-promoted detosylation (Table 3.04, entry 5), a complicated reaction mixture was obtained. Similarly, the use of fully substituted pyrrole **88c** proved to be ineffective in producing the detosylated product **94c** under the magnesium-promoted detosylation conditions (Table 3.04, entry 6), or the well-established SmI_2-mediated conditions[97] (Table 3.04, entry 7).

3.2.4 Regioselectivity Studies

In our previous work on the oxidative functionalisation of yndiamides *via* α-oxo gold carbenes in Chapter II, we observed that steric effects played a more significant role than electronic effects in achieving regiocontrol. Similarly, this principle was tested in the present study of the regioselective functionalisation of asymmetric yndiamides with isoxazoles (Scheme 3.15). We explored the steric effects of a series of yndiamides (**4s**, **4q**, **4t**) with varying levels of difference in steric bulk between the two nitrogen atoms using 5-methylisoxazole (Scheme 3.15a). As the steric bulk of one of the alkyl groups relative to the other (*n*-Bu) substituent increased, the regioselectivity also increased up to *r.r.* 9:1 for yndiamide **4t** (*n*-Bu vs. *c*-Hex, **95t**/**95t'**). This trend indicates that similar to α-oxo-gold carbenes, there is a preference for the less-hindered alkyne carbon of the yndiamide to coordinate to the bulky gold complex. Since in the previous scenario, the isoxazole was required to attack the yndiamide at the 'bulkier' end (i.e. at the cyclohexyl-substituted terminus), it would be interesting to study the ability of **4t** to undergo regioselective cyclisation with isoxazoles featuring increasing steric hindrance adjacent to the nucleophilic nitrogen atom. To achieve this, 5-phenyl substituted isoxazoles with differently-sized 3-alkyl substituents were tested for regioselectivity (Scheme 3.15b).

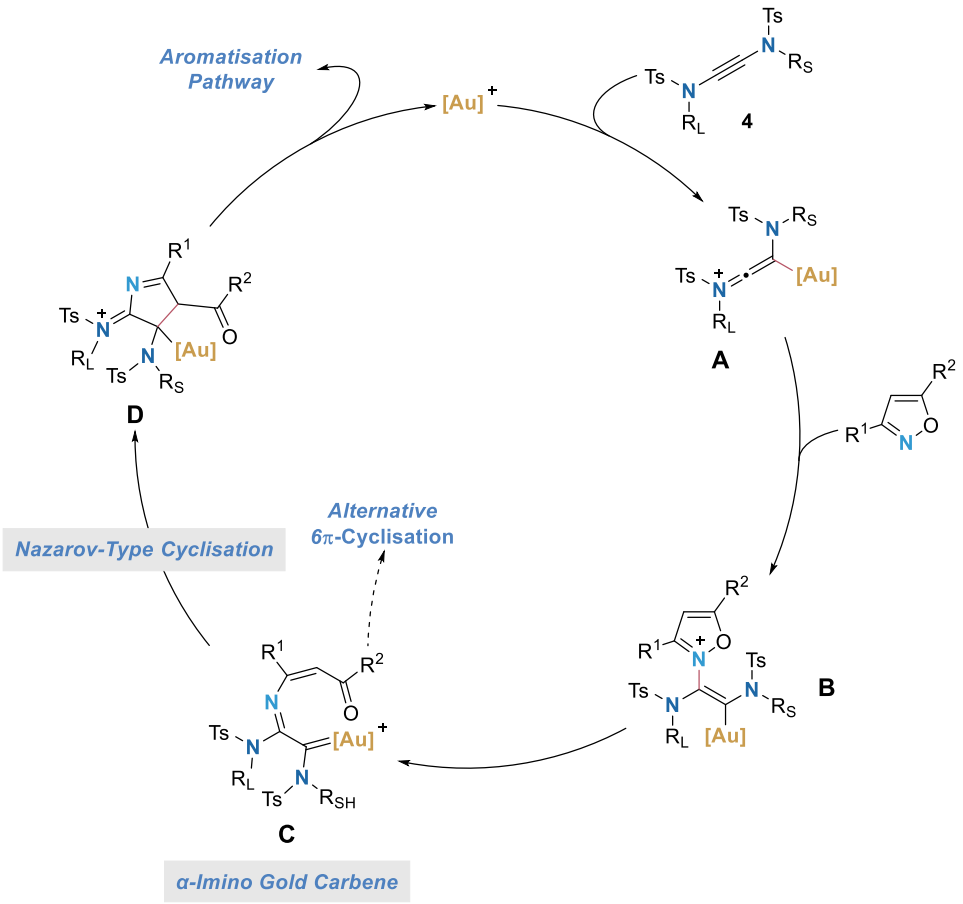


Scheme 3.15 Regioselectivity studies of the gold-catalysed functionalisation of asymmetric yndiamides with isoxazoles. Reactions were conducted on 0.1 mmol scale with [**4**] = 0.5 M; **Ar** = 2,4-di-*tert*-butylphenyl; yields are isolated yields of both regioisomers; r.r. was determined by ^{1}H NMR spectroscopic analysis of the isolated mixture of regioisomers; the identity of the major regioisomer was assigned by NOESY experiments. [a] Reaction completed after 24 h.

Although the use of 5-phenylisoxazole led to decomposition of the yndiamide, excellent selectivity was observed for methyl- or isopropyl-substituted isoxazoles (R = Me, **96b**/**96b′**, *r.r.* > 20:1; R = *i*-Pr, **96c**/**96c′**, *r.r.* > 20:1). The introduction of a *t*-Bu group on the isoxazole ring required an extended reaction time, however, a satisfactory level of regioselectivity was obtained (**96d**/**96d′**, *r.r.* 6:1). These findings suggest that the steric demands of the gold phosphite complex play a dominant role in the formation of the pyrrole product featuring the bulkier nitrogen substituent at the 2-position, even when challenged with a *tert*-butyl substituent on the nucleophile.

3.2.5 Mechanistic Proposal

Based on the work by Ye *et al.*[101] and our experimental observations, we proposed a catalytic cycle to account for the formation of the major pyrrole product as well as other minor side products (Scheme 3.16 – 3.18).

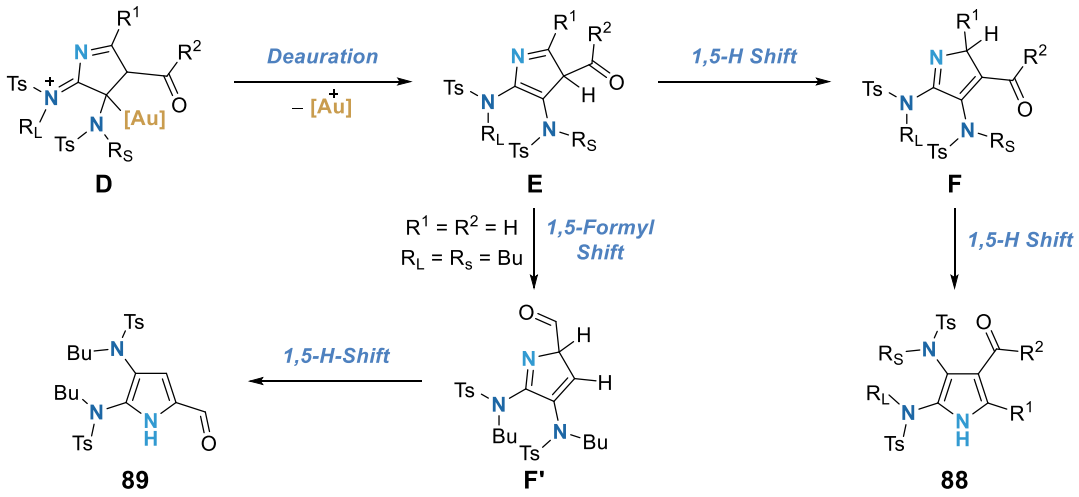


Scheme 3.16 Proposed reaction mechanism for the main catalytic cycle.

The reaction is initiated by the coordination of the yndiamide to the gold catalyst, preferentially using the less-hindered alkynyl carbon to form the keteniminium gold complex **A** (Scheme 3.16). The keteniminium gold complex **A** is then subjected to the nucleophilic attack from the nitrogen atom in the isoxazole reagent, which delivers the vinyl gold complex **B**. Subsequent N–O bond cleavage and isoxazole ring opening afford the α-imino gold Fischer carbene intermediate **C**. This gold carbene intermediate can

undergo two distinct cyclisations that lead to different products. The first pathway involves a 4π Nazarov-type cyclisation,[129, 130] leading to intermediate **D**, followed by aromatisation to deliver the major pyrrole product (Scheme 3.17). The second pathway involves an alternative 6π-electrocyclisation,[120, 131] generating the 1,4-oxazepine side product that has been identified previously (Scheme 3.18).

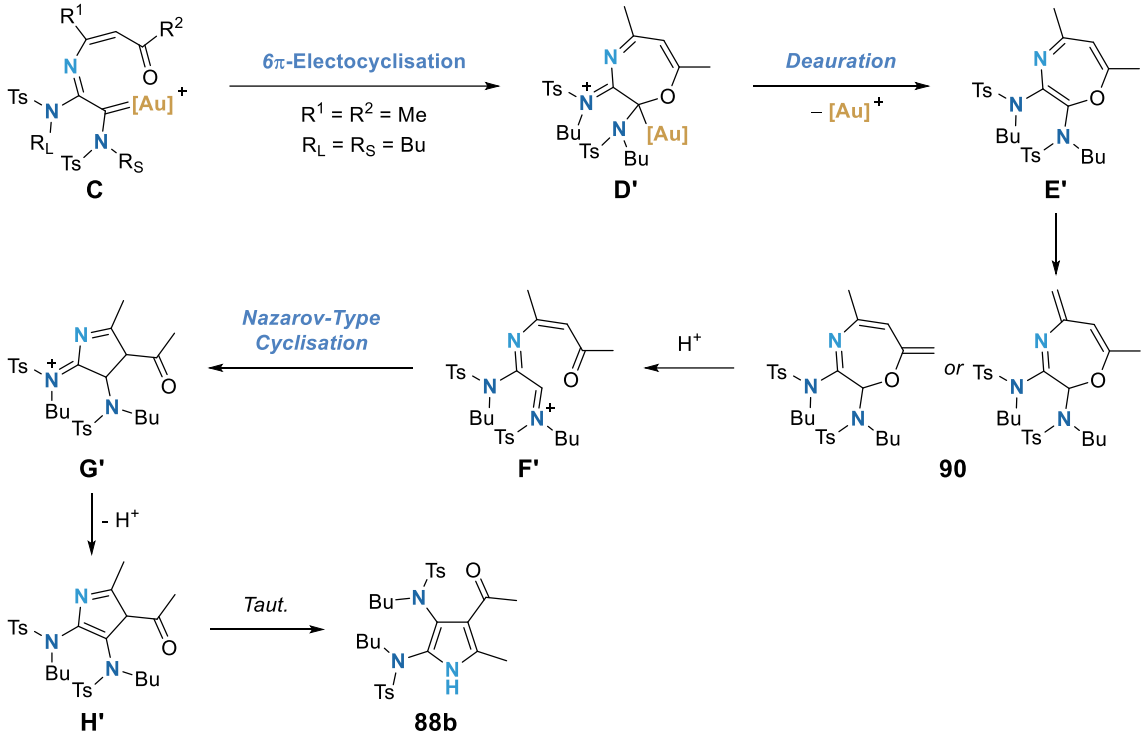
After the 4π Nazarov-type cyclisation and deauration, the 3*H*-pyrrole species **E** is formed, which can undergo two possible tautomerisation/aromatisation mechanisms to give the corresponding products (Scheme 3.17). Although the presence of trace Brønsted acid, such as water, in the reaction mixture may facilitate the tautomerisation/aromatisation of intermediate **E**, it is also plausible for **E** to undergo two consecutive 1,5-hydride shifts (*via* **F**) to generate the major pyrrole product **88** or a 1,5-formyl shift/hydride shift sequence (*via* **F′**) to produce the minor product **89**.



Scheme 3.17 Proposed reaction mechanism for the aromatisation of **D**.

An alternative pathway from the gold carbene intermediate involves the *α*-imino gold carbene intermediate **C** undergoing a 6π-electrocyclisation, resulting in the formation of the 7-membered ring intermediate **D′** (Scheme 3.18). Subsequent deauration leads to the production of a 1,4-oxazepine product **E′** that can readily undergo tautomerisation to yield

two possible structures as the side product **90**. Unfortunately, we were unable to identify which of the two structures correspond to the actual isolated side product. However, treating this species with ethereal HCl (1 M) induces ring-opening to generate the same iminium ion intermediate **F′**. The intermediate **F′** can undergo the 4π Nazarov-type cyclisation once again, followed by deprotonation, resulting in the formation of the 3*H*-pyrrole intermediate **H′** (*via* **G′**). The tautomerisation of **H′** eventually yields the pyrrole product **88b**.

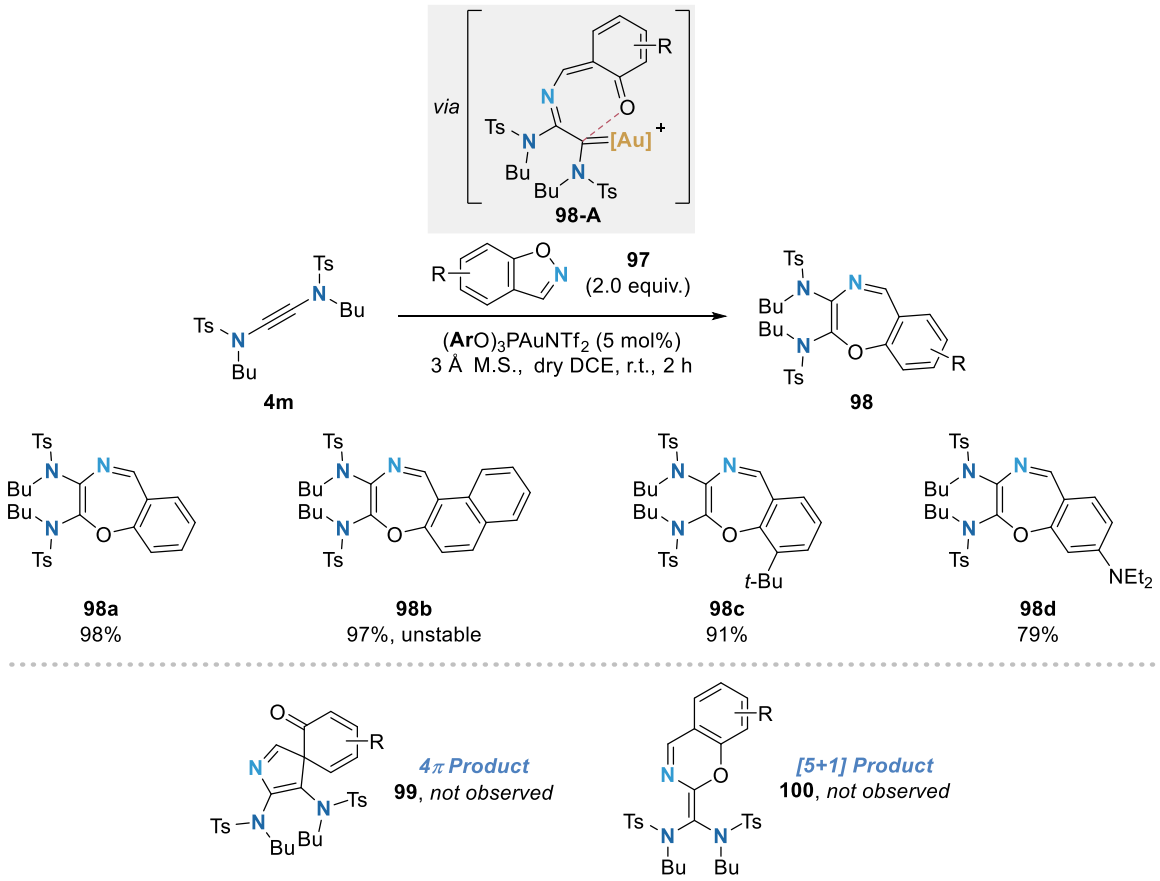


Scheme 3.18 Proposed reaction mechanism to account for the formation of the side products and its acid-catalysed transformation to the pyrrole product.

3.2.6 Reactions with Benzisoxazoles and Anthranils

Based on the proposed mechanism, we raised the question of whether the selection between 4π- and 6π-electrocyclisation could be influenced by employing different benzo-annulated isoxazole nucleophiles instead of isoxazoles. In the case of benzo[*d*]isoxazoles **97**, 6π-electrocyclisation would allow for the rearomatisation of the benzene ring from the gold

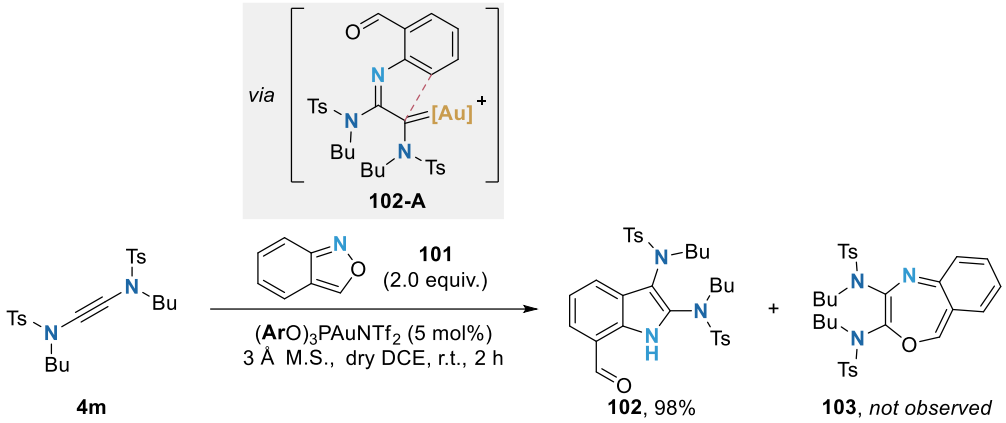
carbene intermediate **98-A**, whereas 4π-electrocyclisation would lead to the formation of a spirocyclic product **99** that is less likely to undergo aromatisation. In comparison to the gold-catalysed functionalisation of ynamides with benzo[*d*]isoxazoles, where the use of bulky gold(I) catalyst led to formal [5+1] cycloaddition,[119-121] we found that the reactions of yndiamides with benzo[*d*]isoxazoles instead afforded a series of diamino-1,4-benzoxazepine products **98a**–**98d** in excellent yields ranging from 79% to 98%, and the [5+1] product **100** was not observed (Scheme 3.19).



Scheme 3.19 Reactivity of yndiamides towards benzo[*d*]isoxazoles. Reactions were conducted on 0.1 mmol scale with [**4m**] = 0.5 M; **Ar** = 2,4-di-*tert*-butylphenyl; yields refer to isolated yields.

The reaction with anthranil **101** proceeded similarly to analogous reactions on ynamides,[111] resulting in the formation of only the 2,3-diamino-substituted formyl indole **102** in nearly

quantitative yield (98%) *via* C–H insertion of the gold carbene intermediate **102-A**, and the [5+2] product **103** was not observed (Scheme 3.20).



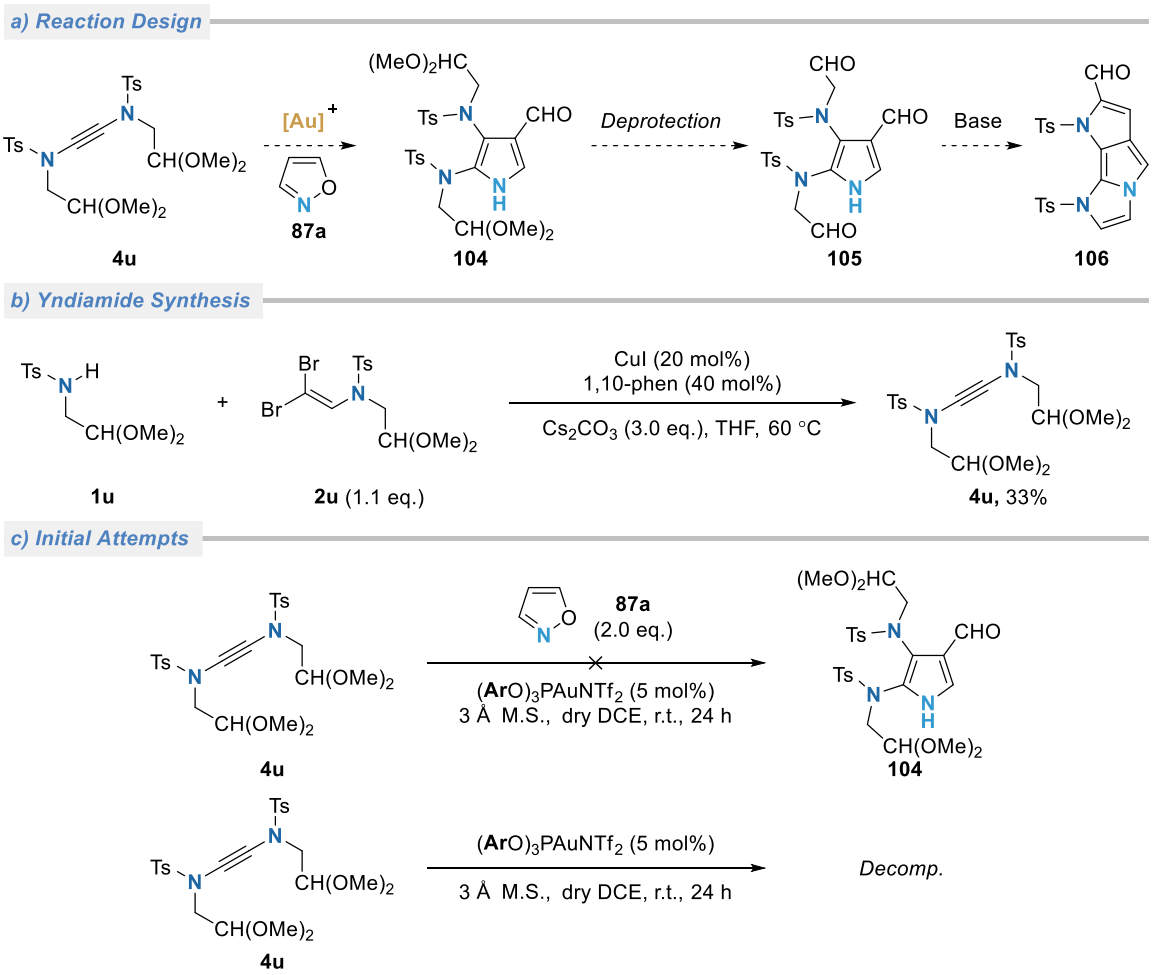
Scheme 3.20 Reactivity of yndiamides with anthranil. The reaction was conducted on 0.1 mmol scale with [**4m**] = 0.5 M; **Ar** = 2,4-di-*tert*-butylphenyl; yield refers to isolated yield.

3.2.7 Attempts to Construct Polycyclic *N*-Heterocycles

Literature precedents for gold-catalysed functionalisation of ynamides with isoxazole-type nitrene-transfer reagents show that transformations that deliver sophisticated *N*-heterocycles often involve the participation of the substituent on the ynamide nitrogen atom in the cyclisation process.[110, 112, 114-117] However, such involvement of the nitrogen substituents was absent in our studies on yndiamides, and we thus envisaged that the use of yndiamides bearing substituents that can be further functionalised could serve as perfect examples to emphasise the significant utility and versatility of this transformation in the synthesis of *N*-containing compounds of greater molecular complexity.

Our first design involved the use of yndiamide **4u** with acetal substituents on both nitrogen atoms (Scheme 3.21a). The gold-catalysed formal [3+2] cycloaddition between **4u** and isoxazole would generate 2,3-diaminopyrrole **104**. Subsequent global deprotection and base-promoted double cyclisation would lead to the formation of the tricyclic compound **106**. However, although yndiamide **4u** was successfully synthesised (Scheme 3.21b), its

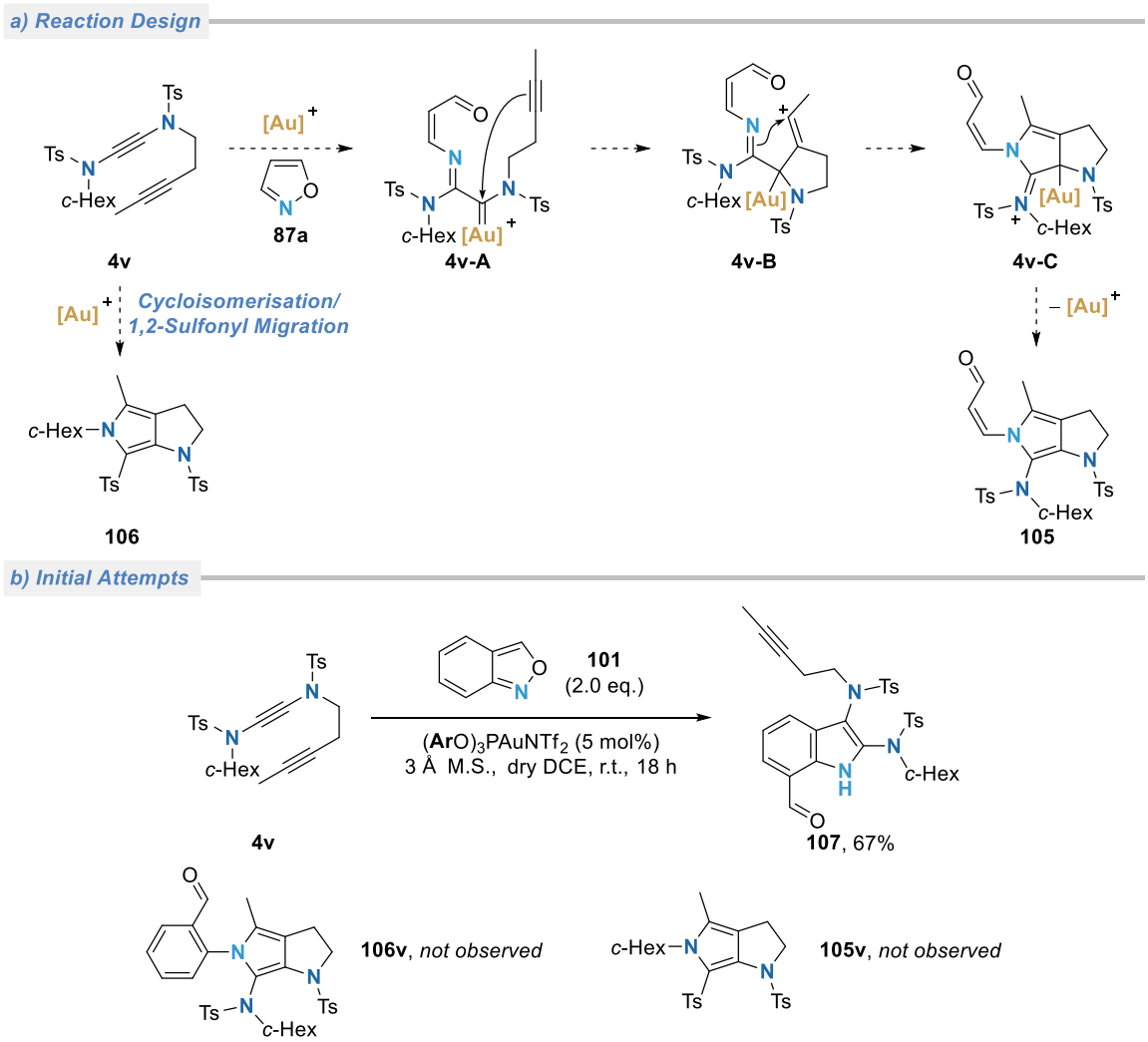
gold-catalysed cyclisation with isoxazole failed to produce the desired product **104**, likely due to Lewis acid-mediated deprotection of the acetals.[132, 133] This was supported by the decomposition of **4u** under the same gold-catalysed condition in the absence of **87a** (Scheme 3.21c).



Scheme 3.21 Gold-catalysed [3+2] cycloaddition/deprotection/double cyclisation cascade. **Ar** = 2,4-di-*tert*-butylphenyl.

Inspired by the work of Liu *et al.*, which incorporated the alkene groups of ene-ynamides in the gold-catalysed cyclisation with isoxazoles,[110] we envisioned that similar reactivity could be achieved by utilising an yndiamide with an alkyne sidechain. In this context, we designed yne-yndiamide **4v** bearing a bulky cyclohexyl group at the other terminus to facilitate the regiospecific generation of the α-imino gold carbene intermediate **4v-A**. This

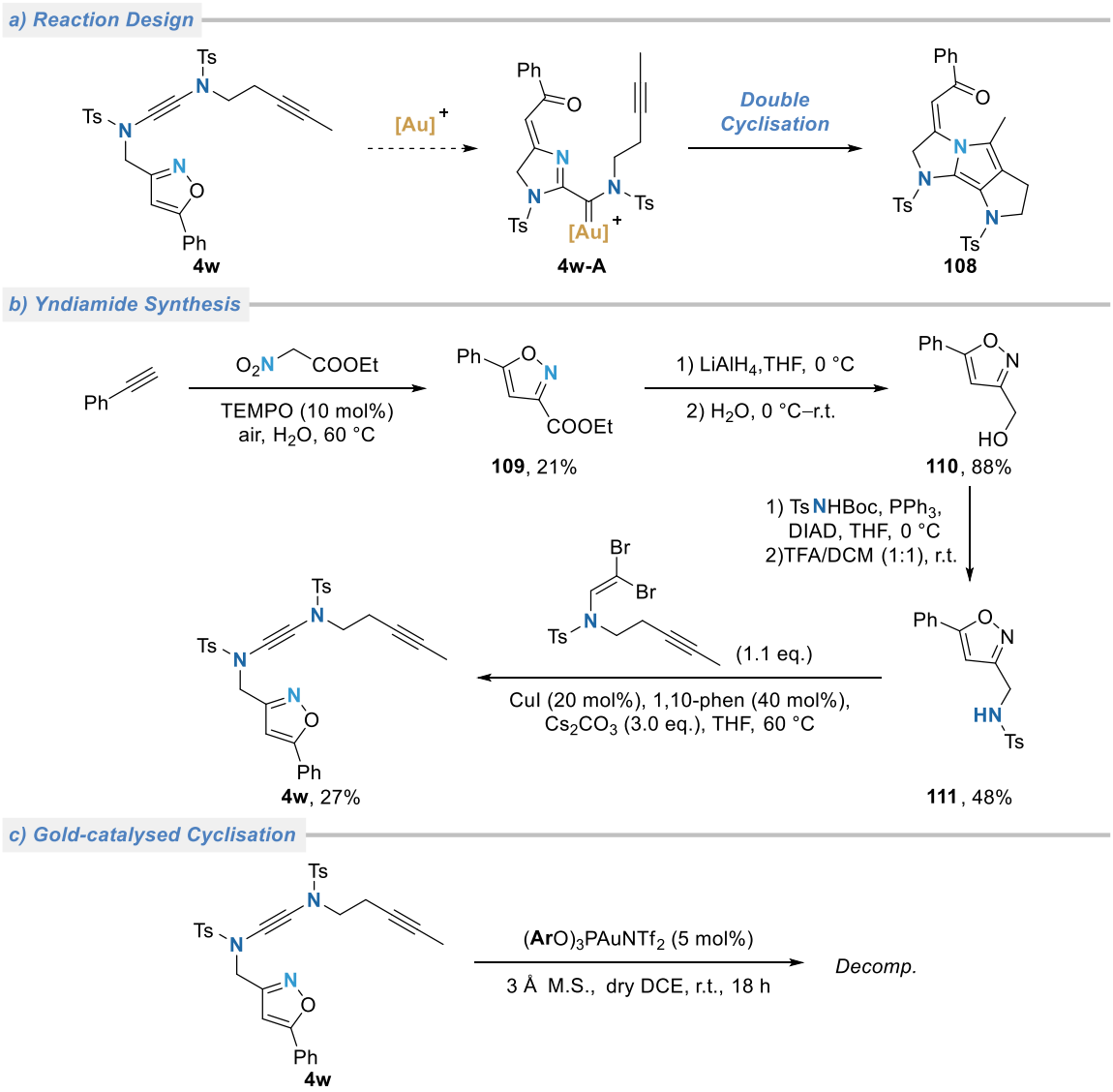
intermediate could then be trapped by the homopropargyl side chain to give the vinyl cation **4v-B**,[116] which upon subsequent cyclisation/deauration sequence might yield pyrrolopyrrole **105** (Scheme 3.22a). It is worth noting that the yne-yndiamide described above was also anticipated to undergo gold-catalysed cycloisomerisation/1,2-sulfonyl migration to produce **106**, as reported by Philip J. Smith in previous studies.[26, 33] Yndiamide **4v** was synthesised with ease using our established protocol.[24, 25]



Scheme 3.22 Gold-catalysed cyclisation of yne-yndiamide and anthranil. **Ar** = 2,4-di-*tert*-butylphenyl.

Instead of isoxazoles, anthranil **101** was used as the nitrene-transfer reagent in anticipation of reducing the efficiency of cyclisation from the parent aryl ring, thereby allowing time

for the involvement of the alkynyl side chain. Despite efforts made, neither of the pyrrolopyrrole products (**106v** or **105v**) was detected. Instead, the 2,3-diaminoindole **107** was successfully obtained in good yield with high regioselectivity (67%, *r.r.* > 20:1) (Scheme 3.22b).



Scheme 3.23 Gold-catalysed intramolecular cyclisation of isoxazole tethered yne-yndiamide. **Ar** = 2,4-di-*tert*-butylphenyl.

The unsuccessful incorporation of the alkyne sidechain into the cyclisation process was attributed to competitive gold carbene formal C–H insertion into the parent aryl ring. To address this issue, a new model was developed, utilising yndiamide **4w** featuring an isoxazole motif tethered to the other terminus of the yndiamide (Scheme 3.23a). The

corresponding *α*-imino gold carbene intermediate **4w-A** was expected to contain a 5-membered ring that would fix the geometry of the imine moiety, deflecting the *α,β*-unsaturated carbonyl sidechain away from the gold carbene motif. A double cyclisation process from the gold carbene intermediate (similar to the one depicted in Scheme 3.22a) would subsequently generate the tricyclic product **108**. After exploring multiple strategies to synthesise yndiamide **4w**, an effective route was established (Scheme 3.23b). Initially, an oxidative [3+2] cycloaddition between phenylacetylene and ethyl nitroacetate was performed to generate the isoxazole carboxylate **109** (21%).[134] Subsequent reduction of the carboxylate produced alcohol **110** (88%), which was then subjected to a Mitsunobu reaction/Boc-deprotection sequence to yield the isoxazole-tethered tosylamide **111** (48% over two steps). The desired yndiamide **4w** was synthesised from **111** and the corresponding 1,1-dibromoenamide[26] using our established protocol.[24, 25] However, subjecting the yndiamide to the gold-catalysed cyclisation conditions resulted only in decomposition of the starting material, with no observable products (Scheme 3.23c).

3.3 Conclusions

In conclusion, we have demonstrated the gold-catalyzed formal [3+2] cycloaddition between yndiamides and isoxazoles to synthesise 2,3-diaminopyrroles. Consistent with our findings in Chapter II, steric effects played a significant role in achieving the regiocontrol of this transformation. Excellent regioselectivity was established for asymmetric yndiamides by introducing steric differentiation between the two alkyl substituents on the nitrogen atom. Furthermore, in addition to the unusual 1,2-formyl migration product, the reaction also allowed for a switch in ring-size selectivity using different benzannulated isoxazole nucleophiles. While the use of benzo[*d*]isoxazles resulted in the formation of 1,4-oxazepine products, a 2,3-diaminoindole product was produced when anthranil was used.

A comprehensive reaction mechanism was proposed to account for the formation of the major pyrrole products, as well as all the side products. Our mechanistic proposal will be further supported by computational analysis which will also provide insight into the regioselectivity of this transformation (see Chapter IV). Apart from DFT calculations, we continued to look into opportunities to extend the scope of this transformation to polycyclisation for the construction of *N*-containing molecules of greater complexity. We believe this reported chemistry could be of significant utility for the synthesis of medicinally relevant scaffolds and will make a substantial contribution towards the future development of yndiamide chemistry.

C H A P T E R

IV

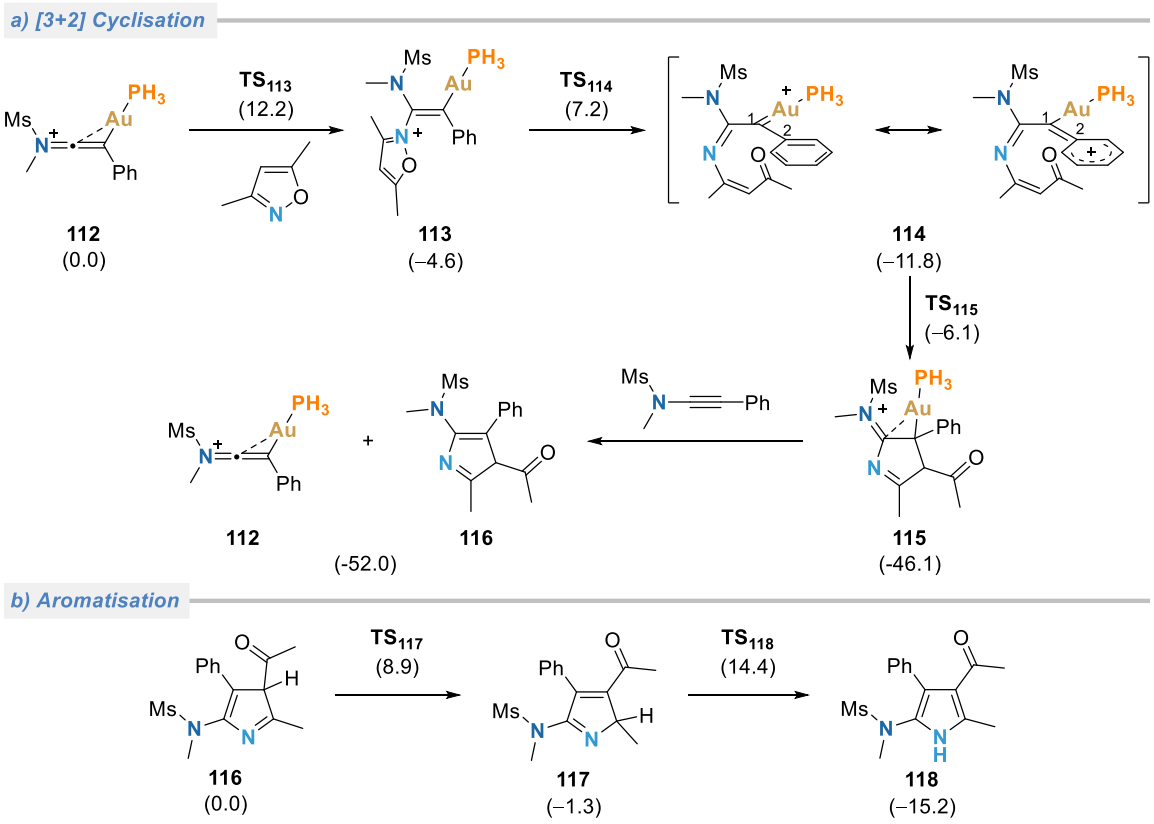
Computational Investigation of Regioselective Gold(I)-Catalysed Cyclisation of Yndiamides with Isoxazoles

The reaction mechanism of gold-catalysed functionalisation of ynamides with isoxazole-type nitrene-transfer reagents is well supported by extensive computational analyses in related literature. However, DFT rationalisation of regioselectivity remains rare, likely due to the intrinsic polarisation of the ynamide. In this chapter, we applied computational chemistry methods to support our proposed mechanism for the gold-catalysed cyclisation of the symmetric yndiamide with isoxazoles in Chapter III. Besides, a variation of the catalytic cycle using a non-symmetric yndiamide was also studied, which revealed that the key to the regioselectivity was a low-barrier gold π-complex-like transition state which established a Curtin-Hammett scenario for isoxazole addition.

4.1 Introduction

4.1.1 DFT Studies on Gold-Catalysed Functionalisation of Ynamides with Isoxazoles

In the first reported example of gold-catalysed cyclisation between ynamides and isoxazoles by the group of Ye, thorough DFT investigations were conducted to establish a basic model for this transformation (Scheme 4.01).[101] Several simplifications were made in their computational model: i) the catalytic gold species was simplified as H_3PAu^+;[135, 136] ii) the non-coordinating NTf_2^- counterion was excluded.



Scheme 4.01 Reaction energy profiles of the gold-catalysed [3+2] cycloaddition of ynamide and isoxazole, and aromatisation towards the pyrrole product. Relative free energies (ΔG_{sol}, kcal mol^{-1}) of key intermediates and transition states were computed at the CPCM(1,2-dichloroethane)-M06/6-31+G(d)/SDD(Au) level of theory at 298 K/1 M.

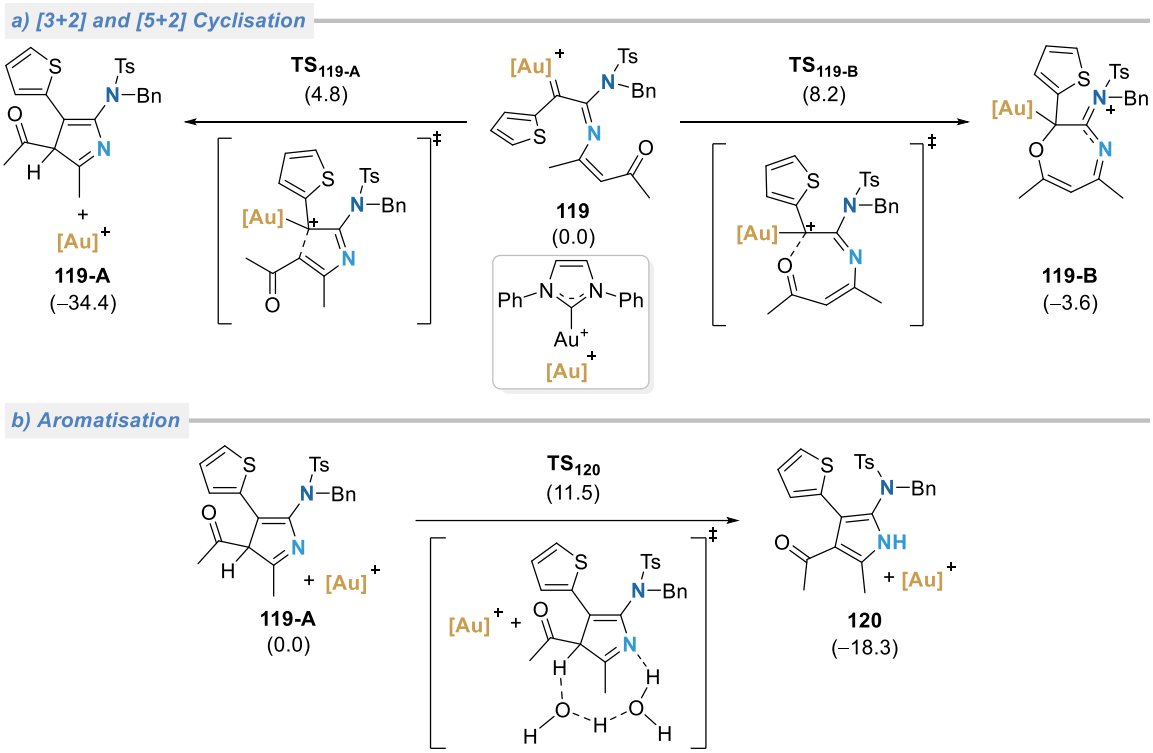
Furthermore, Ye and co-workers found that initial ligand exchange between the $H_3PAuNTf_2$ species and the ynamide is barrierless and slightly exothermic. The main catalytic cycle was initiated by the formation of the keteniminium gold species **112** (Scheme 4.01a). A moderate free activation energy barrier (**TS_{113}**, $\Delta G^{\ddagger}_{sol}$ = 12.2 kcal mol^{-1}) was observed when **112** was subjected to nucleophilic attack by the 3,5-dimethylisoxazole, resulting in the formation of a vinyl gold complex **113** (ΔG_{sol} = −4.6 kcal mol^{-1}). The formation of the gold carbene intermediate **114** by isoxazole ring-opening was energetically favoured (ΔG_{sol} = −7.2 kcal mol^{-1}), with an activation energy barrier of 11.8 kcal mol^{-1} (**TS_{114}**).

The phenyl group of the ynamide played a significant role in stabilising the gold carbene intermediate, as demonstrated by the increased Wiberg bond index of the C^1–C^2 bond and the greater positive charge on the C^2 carbon compared to that of the methyl variant (where the phenyl group was replaced with a methyl group). It is worth noting that the imine moiety in the gold carbene intermediate **114** had an *E*-geometry, which facilitated the intramolecular cyclisation (**TS_{115}**, $\Delta G^{\ddagger}_{sol}$ = 5.7 kcal mol^{-1}), leading to intermediate **115** with a substantial energy gain (ΔG_{sol} = −40.0 kcal mol^{-1}). The subsequent substrate exchange between **115** and a second molecule of the ynamide regenerated the keteniminium species **112** and produced the 3*H*-pyrrole **116**, which could later undergo aromatisation.

Ye *et al.* proposed two consecutive H-migrations as the aromatisation pathway from **116** to the final pyrrole product **118** (Scheme 4.01b). Both migrations were thermodynamically favoured (ΔG_{sol} = −1.3 kcal mol^{-1} and ΔG_{sol} = −13.9 kcal mol^{-1} respectively), though the latter required a higher free activation energy (**TS_{117}**, $\Delta G^{\ddagger}_{sol}$ = 8.9 kcal mol^{-1} vs. **TS_{118}**, $\Delta G^{\ddagger}_{sol}$ = 15.7 kcal mol^{-1}).

More recently, Yang and co-workers conducted extensive DFT investigations to gain insight into the cyclisation mechanism of ynamides and isoxazoles under gold-catalysed

conditions in the presence of water (Scheme 4.02).[137] Their computed reaction energy profiles of the gold-catalysed [3+2] cyclisation of ynamide and isoxazole were consistent with the results of Ye *et al.*[101] In addition, the authors also modelled the less-favoured [5+2] cycloaddition pathway (Scheme 4.02a). This transformation proceeded by overcoming a higher reaction activation energy barrier (**TS$_{119\text{-A}}$**, $\Delta G^{\ddagger}_{sol}$ = 4.8 kcal mol^{-1} vs. **TS$_{119\text{-B}}$**, $\Delta G^{\ddagger}_{sol}$ = 8.2 kcal mol^{-1}), yielding a 1,4-oxazepine intermediate **119-B** (ΔG_{sol} = −3.6 kcal mol^{-1}).

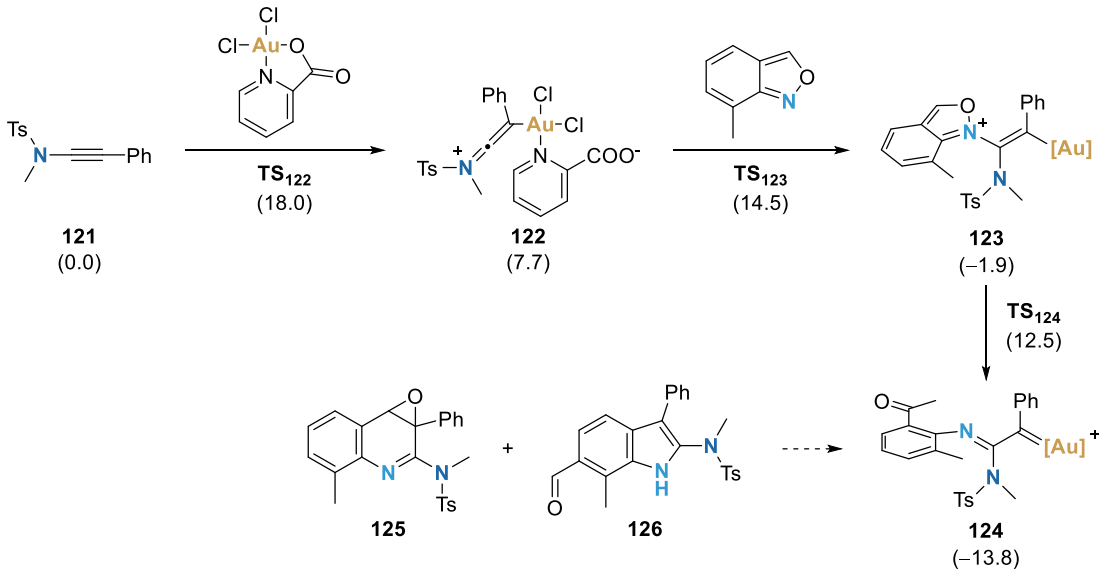


Scheme 4.02 Reaction energy profiles of the gold-catalysed [3+2]/[5+2] cycloaddition of ynamide and isoxazole, and aromatisation towards the pyrrole product. Relative free energies (ΔG_{sol}, kcal mol^{-1}) of key intermediates and transition states were computed at the SMD(1,2-dichloroethane)-M06-2X/6-311++G(d,p)/LANL2DZ(Au)//IEFPCM(1,2-dichloroethane)-M06-2X/6-31G(d,p)/LANL2DZ(Au) level of theory at 298 K/1 M.

In contrast to the Ye group's proposal of a stepwise *H*-migration sequence for the aromatisation of the 3*H*-pyrrole intermediate, Yang *et al.* suggested that the process could occur through water-mediated tautomerisation of the 3*H*-pyrrole intermediate **119-A**, resulting in the formation of the pyrrole product **120** (ΔG_{sol} = −18.3 kcal mol^{-1}) by

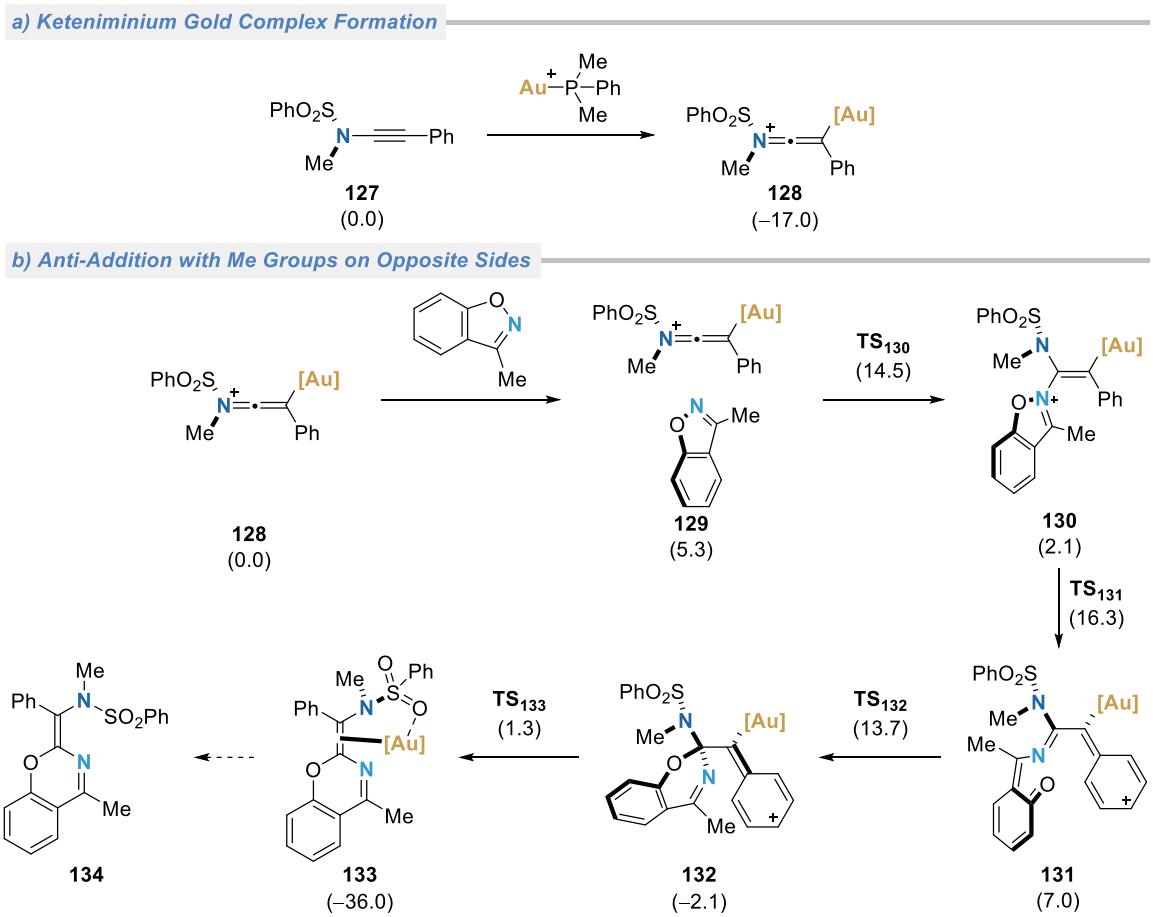
overcoming a relatively low activation energy barrier (**TS$_{120}$**, $\Delta G^{\ddagger}_{sol}$ = 11.5 kcal mol^{-1}) (Scheme 4.02b).

In their study on gold-catalysed tunable [3+2] and [4+2] annulations of ynamides and anthranils, the Hashmi group offered valuable DFT-assisted mechanistic discussions that shed light on the reaction pathways involved (Scheme 4.03).[118] Unlike the ligand exchange reaction observed between ynamide and gold(I) catalyst, a similar process between ynamide **121** and gold(III) catalyst to form keteniminium gold complex **122** was found to be moderately endergonic (ΔG_{sol} = 7.7 kcal mol^{-1}), necessitating a relatively large free activation energy of 18.0 kcal mol^{-1} (**TS$_{122}$**). The subsequent nucleophilic attack by the anthranil nitrogen atom was found to be thermodynamically favoured (ΔG_{sol} = −9.6 kcal mol^{-1}), yielding the vinyl gold complex **123** with a lower energy barrier (**TS$_{123}$**, $\Delta G^{\ddagger}_{sol}$ = 6.8 kcal mol^{-1}).



Scheme 4.03 Reaction energy profiles of gold-catalysed tunable [3+2]/[4+2] annulations of ynamide and anthranils. Relative free energies (ΔG_{sol}, kcal mol^{-1}) of key intermediates and transition states were computed at the SMD(DCM)-M06/def2-TZVP//CPCM(DCM)-M06/6-31G(d)/LANL2DZ(Au) level of theory at 298 K/1 M.

The subsequent formation of gold carbene **124** *via* anthranil ring opening was found to be significantly irreversible ($\Delta G_{sol} = -11.9$ kcal mol^{-1}), although it required a free activation energy of 14.4 kcal mol^{-1} (**TS$_{124}$**). It is noteworthy that the imine group of the gold carbene intermediate was in the *Z*-geometry, causing the aryl ring to be positioned away from the gold carbene moiety. Although the existence of the *E*-imine isomer of the gold carbene **124** was not reported by Hashmi *et al.*, it is reasonable to hypothesise the presence of such an isomer during the formation of final products **125** and **126**, where the corresponding C=N bond geometries were inverted.



Scheme 4.04 Reaction energy profiles of the gold-catalysed ring expansion and 1,2-migration of ynamide and 3-methylbenzo[*d*]isoxazole. Relative free energies (ΔG°, kcal mol^{-1}) of key intermediates and transition states were computed at the M06/6-31+G(2d,p)/def2-QZVP(Au)//B3LYP/6-31G(d,p)/LANL2DZ(Au) level of theory at 298 K.

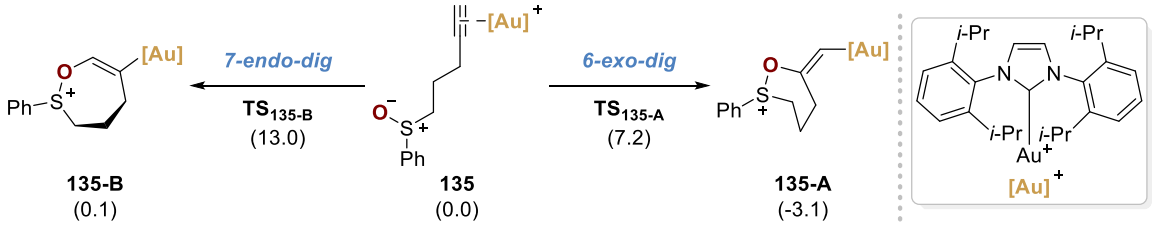
Sahoo and co-workers made another important contribution to this field through the investigation of the gold-catalysed ring expansion and 1,2-migration cascade of ynamides and benzo[*d*]isoxazoles (Scheme 4.04).[121] The authors initiated their DFT investigations with the addition of the active gold catalyst to the model ynamide **127** (Scheme 4.04a). The process was energetically favoured and occurred without a free activation energy barrier ($\Delta G° = -17.0$ kcal mol^{-1}), forming the keteniminium gold complex **128**. Sahoo *et al.* further examined the subsequent nucleophilic attack by the 3-methylbenzo[*d*]isoxazole with varying stereochemistry (*anti* vs. *syn*) and methyl group positioning. They concluded that the *anti*-addition of the 3-methylbenzo[*d*]isoxazole with the two methyl groups on opposite sides was the most favoured pathway (Scheme 4.04b).

Optimisation of **128** and 3-methylbenzo[*d*]isoxazole in this orientation led to adduct **129** ($\Delta G° = 5.3$ kcal mol^{-1}), from which the C–N bond was formed *via* $\mathbf{TS_{130}}$ ($\Delta G^{‡} = 9.2$ kcal mol^{-1}) while releasing a Gibbs Free energy of −3.2 kcal mol^{-1}. The resulting vinyl gold complex **130** could undergo N–O bond cleavage to deliver the α-imino gold carbene **131** by overcoming a free activation energy barrier of 14.2 kcal mol^{-1} ($\mathbf{TS_{131}}$). Contrary to the abovementioned literature that reported exergonic generation of the gold carbene,[101, 118, 137] the formation of **131** required an input of Gibbs Free energy of 4.9 kcal mol^{-1}, likely due to the presence of an unstable *ortho*-quinone methide motif. From the gold carbene **131**, a 6π-electrocyclisation could take place to provide intermediate **132** ($\Delta G° = -9.1$ kcal mol^{-1}) through $\mathbf{TS_{132}}$ ($\Delta G^{‡} = 6.7$ kcal mol^{-1}). **132** could then undergo a kinetically facile ($\mathbf{TS_{133}}$, $\Delta G^{‡} = 3.3$ kcal mol^{-1}) and thermodynamically favoured ($\Delta G° = -33.9$ kcal mol^{-1}) 1,2-sulfonamide migration to yield **133**, which upon deauration resulted in the formation of the *E*-benzo[*e*][1,3]oxazine product **134** observed experimentally.

4.1.2 DFT Studies on Regioselective Gold-Catalysed Functionalisation of Alkynes

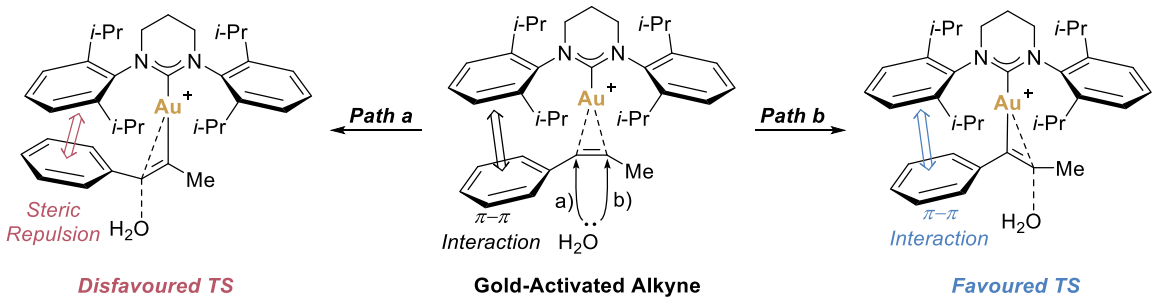
The literature reports discussed earlier describe similar reaction mechanisms and energy profiles for the functionalisation of ynamides with isoxazole-type nitrene-transfer reagents using gold catalysts. However, these studies did not focus on the origin of the regioselectivity. In contrast, the regioselectivity of gold-catalysed transformations of non-polarised alkynes is commonly observed and has been more thoroughly investigated by computational methods. This section highlights some of the representative works on DFT investigations of the regioselectivity of gold-catalysed transformations of alkynes.

As the gold-catalysed transformation of alkynes typically begins with the nucleophilic attack on the gold-activated alkyne species, the regioselectivity is often explained by the natural charge/electrophilicity bias between the two alkynyl carbon atoms.[138, 139] Various alternative arguments have also been proposed to account for the preferential attack on one alkynyl carbon over the other. Zhang *et al.* suggested a 7-*endo-dig* vs. 6-*exo-dig* scenario to explain the regioselectivity observed in the gold-catalysed rearrangement of alkynyl aryl sulfoxides (Scheme 4.05).[135] For terminal alkynes, the two intramolecular cyclisation pathways displayed a significant difference in activation energy barrier (**$TS_{135\text{-}A}$** vs. **$TS_{135\text{-}B}$**, $\Delta\Delta G^{\ddagger}_{sol}$ = 5.8 kcal mol^{-1}), resulting in the predominant formation of the 6-membered ring intermediate **135-A**.



Scheme 4.05 Key step of the regioselective gold-catalysed rearrangement of alkynyl aryl sulfoxides. Relative free energies (ΔG_{sol}, kcal mol^{-1}) of key intermediates and transition states were computed at the SMD(DCM)- PBE1PBE/6-31+G**/SDD(Au) level of theory at 298 K/1 M.

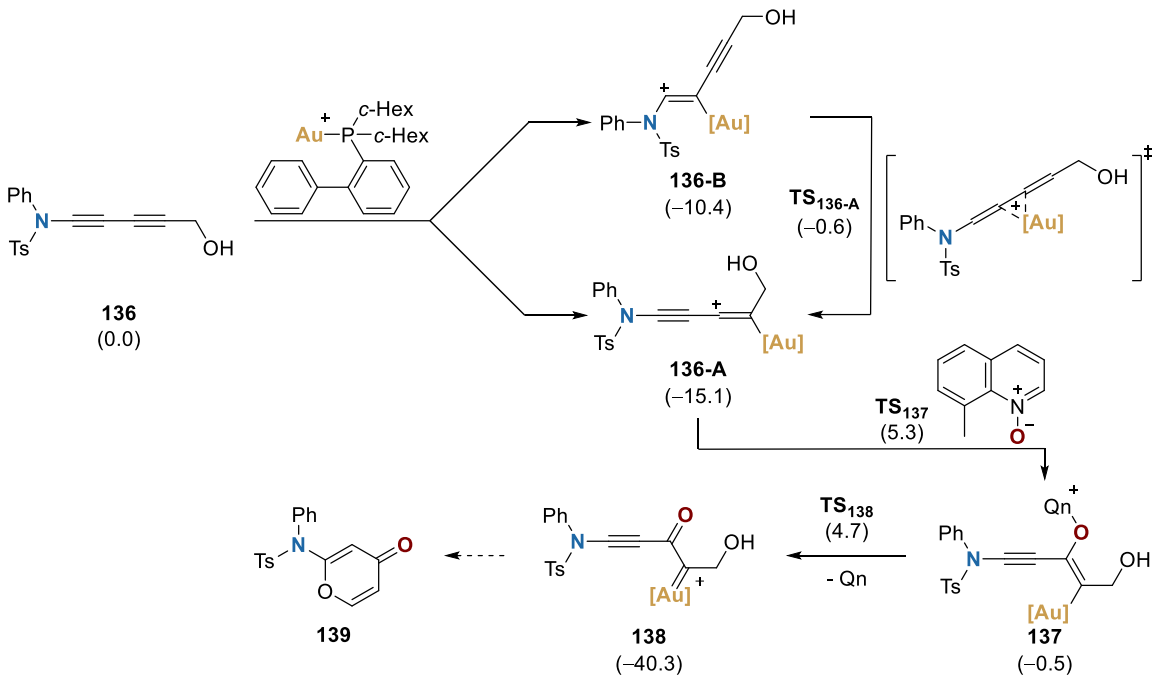
The Asachenko group proposed a hypothesis to explain the observed regioselectivity in the gold-catalysed hydration of alkyne, attributing it to the π-π interaction between the ligand and the alkyne substrate (Scheme 4.06).[140] The authors suggested that the nucleophilic attack by the water molecule through **Path a** would inevitably increase the steric repulsion between the aryl ring and the ligand, resulting in this pathway being disfavoured. Conversely, the nucleophilic attack on the alkynyl carbon distal to the aryl ring (**Path b**) would not encounter this drawback and therefore become the preferred pathway, leading to the major regioisomer observed experimentally.



Scheme 4.06 Hypothesised regio-control model of the regioselective gold-catalysed hydration of alkynes.

It is noteworthy that the literature examples discussed above depict the gold-activated non-polarised alkyne species as gold π-complexes, in which both alkynyl carbon atoms are coordinated to the gold centre without significant bias. As a result, the selective attack of the nucleophile on either of the alkynyl carbons is essential in determining the regioselectivity of the reaction. However, for polarised alkynes such as ynamides, the gold-activated alkyne species are depicted as allene-like gold complexes, requiring the use of different models to explain the observed regioselectivity.

Liu and colleagues suggested that the preferential formation of the gold complex **136-A** over **136-B** was the key factor determining the observed regioselectivity in the gold-catalysed oxidations of 1,3-diynamides (Scheme 4.07).[141]

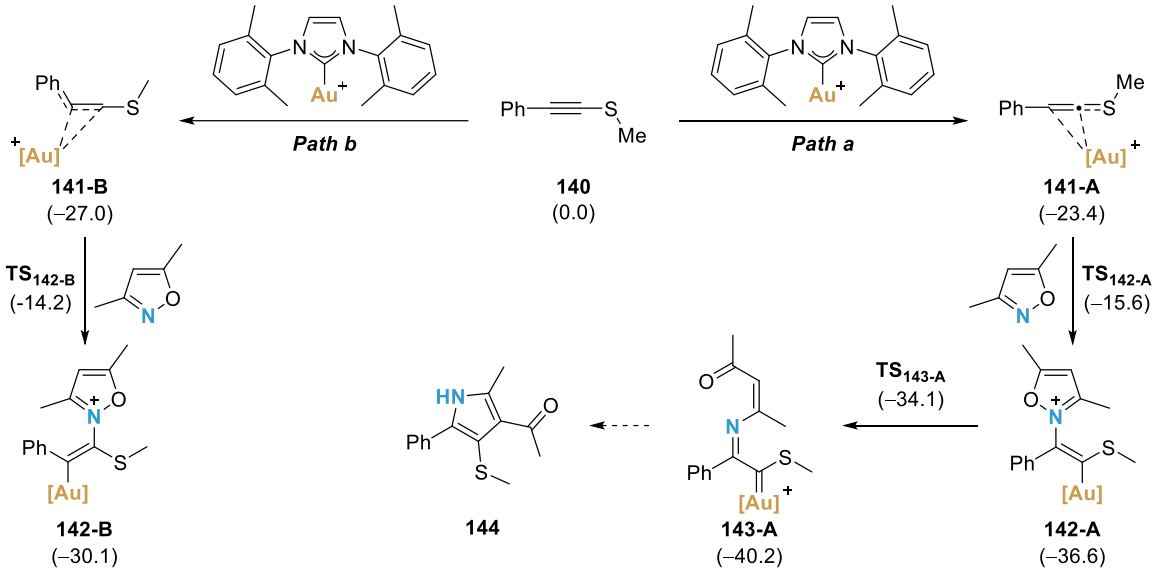


Scheme 4.07 Reaction energy profiles of the gold-catalysed oxidation of 1,3-diynamides. Relative free energies (ΔG_{sol}, kcal mol^{-1}) of key intermediates and transition states were computed at the CPCM(DCM)-B3LYP/6-311G**++/LANL2DZ(Au)+s,p(Au)//B3LYP/6-311G**/LANL2DZ(Au) level of theory at 298 K/1 M.

Feasible formation of two potential gold-activated alkyne species, **136-A** (ΔG_{sol} = −15.1 kcal mol^{-1}) and **136-B** (ΔG_{sol} = −10.4 kcal mol^{-1}) could occur from the reaction of 1,3-diynamide **136** with the gold catalyst. Moreover, the authors discovered that the less stable **136-B** could convert to **136-A** *via* **TS$_{136\text{-A}}$** ($\Delta G^{\ddagger}_{sol}$ = 11.0 kcal mol^{-1}), leading to the preferential formation of the intermediate **136-A**. The ensuing nucleophilic attack by 8-methylquinoline *N*-oxide through **TS$_{137}$** ($\Delta G^{\ddagger}_{sol}$ = 20.4 kcal mol^{-1}) was identified as the rate-determining step, resulting in the formation of the vinyl gold complex **137** (ΔG_{sol} = 14.6 kcal mol^{-1}). Following this, *α*-oxo gold carbene intermediate **138** (ΔG_{sol} = −39.8 kcal mol^{-1}) could be readily generated by overcoming a small activation energy barrier (**TS$_{138}$**, $\Delta G^{\ddagger}_{sol}$ = 5.2 kcal mol^{-1}). The gold carbene **138** could then undergo multiple transformations to produce the final product **139**.

Recently, the group of Yang presented an explanation for the observed regioselectivity of the gold-catalysed coupling between alkynyl thioether **140** and isoxazoles (Scheme

4.08).[142] The initial steps of the catalytic cycle resulted in the formation of two possible gold complexes: **141-A** *via* **Path a** ($\Delta G_{sol} = -23.4$ kcal mol^{-1}) and **141-B** via **Path b** ($\Delta G_{sol} = -27.0$ kcal mol^{-1}). Despite the fact that the formation of **141-B** *via* **Path b** was thermodynamically favoured, this contradicted the observed regioselectivity. However, the nucleophilic attack by 3,5-dimethylisoxazole onto the gold complex **141-A** occurred by overcoming a lower activation energy barrier (**TS$_{142\text{-A}}$**, $\Delta G^{\ddagger}_{sol} = 7.8$ kcal mol^{-1}) compared to that of **141-B** (**TS$_{142\text{-B}}$**, $\Delta G^{\ddagger}_{sol} = 12.8$ kcal mol^{-1}). The lower activation energy suggested a more favourable reaction through **Path a** to the vinyl gold complex **142-A** ($\Delta G_{sol} = -13.2$ kcal mol^{-1}), which aligned with experimental observations.[109]



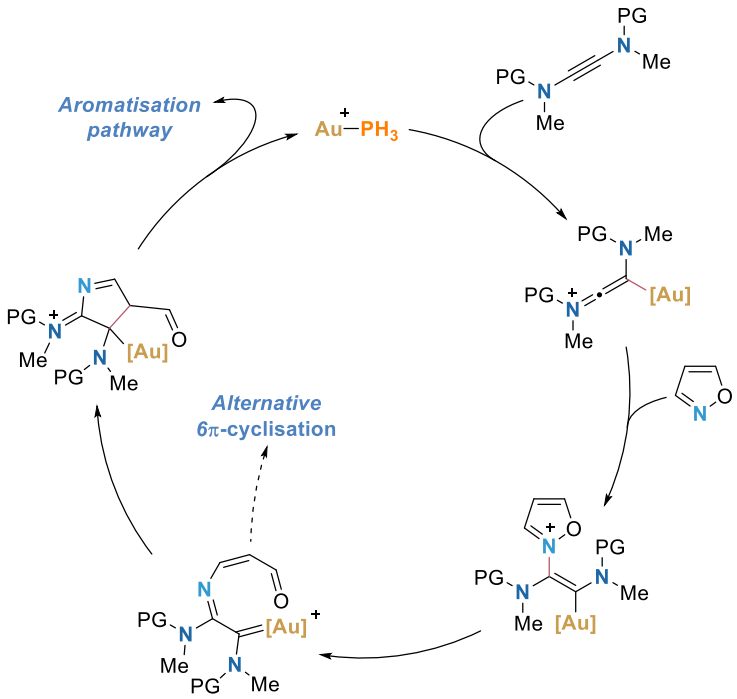
Scheme 4.08 Reaction energy profiles of the gold-catalysed coupling between alkynyl thioether and isoxazole. Relative free energies (ΔG_{sol}, kcal mol^{-1}) of key intermediates and transition states were computed at the IEFPCM($PhCF_3$)-B3LYP-D3(BJ)/6-311++G(d,p)/LANL2DZ(Au)//B3LYP/6-31G(d,p)/LANL2DZ(Au) level of theory at 298 K/1 M.

The authors also found that the interaction between sulfur and the gold centre was crucial to the regioselectivity, as demonstrated by further distortion/interaction analysis of **TS$_{142\text{-A}}$** and **TS$_{142\text{-B}}$**. The intermediate **142-A** underwent isoxazole ring-opening to generate the gold

carbene **143-A** *via* $\mathbf{TS_{143\text{-}A}}$ ($\Delta G^{\ddagger}_{sol}$ = 2.5 kcal mol^{-1}), which was subjected to subsequent transformations to afford the final product **144**.

4.1.3 Design of this Work

The above-reviewed literature reports presented consistent mechanisms and reaction energy profiles of the gold-catalysed functionalisation of ynamides and isoxazole-type nitrene-transfer reagents. However, there is a relative dearth of DFT investigations into the regioselectivity of these transformations. Despite this, selected examples of gold-catalysed functionalisation of various alkynes still provide multiple possible models to explain the observed regioselectivity. Therefore, we propose the utilisation of computational chemistry methods to corroborate our suggested reaction mechanism for the gold-catalysed cyclisation of yndiamides and isoxazoles (as described in Chapter III) and to provide insight into the crucial steps that determine the regioselectivity.



Scheme 4.09 Simplified model of gold-catalysed cyclisation of symmetric yndiamide and isoxazole for DFT calculations. PG = benzenesulfonyl.

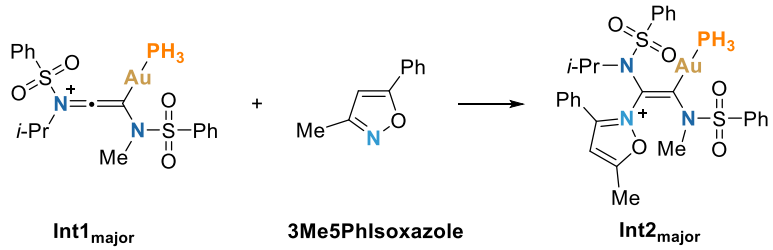
Our initial goal is to obtain a comprehensive understanding of the entire catalytic cycle using a symmetrical yndiamide, including the investigation of side product formation pathways. To minimise computational expenses, we have simplified the system by i) utilising H_3PAu^+ as the catalytic gold species;[101, 135, 136] ii) replacing the electron-withdrawing groups on the yndiamide with benzenesulfonyl groups and downsizing the alkyl substituents on the nitrogen atoms to methyl groups; and iii) employing the non-substituted isoxazole (Scheme 4.09).

Upon the completion of the first stage, we expect the discovery of rate-determining steps that can be important to the regioselectivity. The application of an asymmetric yndiamide (Me vs. *i*-Pr) in combination with 3-methyl-5-phenylisoxazole in these steps will be examined to establish a plausible explanation for the observed regioselectivity,

4.2 Results and Discussion

4.2.1 Evaluation of Level of Theory

We began our investigation by performing benchmark tests on a range of functionals and basis sets. To assess the effectiveness of different levels of theory, we chose to model the addition of 3-methyl-5-phenylisoxazole (**3Me5PhIsoxazole**) to the keteniminium gold complex (**Int1$_{major}$**) as our test transformation (Scheme 4.10).



Scheme 4.10 Model transformation for benchmarking.

Different functionals (M06,[143] M06-L,[144] PBE,[145] PBE0,[146] TPSS,[147] B2PLYP[148] with D3BJ dispersion[149, 150]) and MP2[151] method, combined with 6-31+G(d) basis set[152] for H,

C, N, O, P and S and an SDD pseudopotential[153] for Au, were screened, using the optimised geometry at M06/6-31+G(d)/SDD(Au) level of theory. The solvation effects of 1,2-dichloroethane were simulated by the IEFPCM model.[154] More accurate electronic energies of the same geometry were acquired at the CPCM(1,2-dichloroethane)-DLPNO-CCSD(T)/def2-TZVPP//IEFPCM(1,2-dichloroethane)-M06/6-31+G(d)/SDD(Au) level of theory.[155-158] Upon comparison of the change in electronic energies of the model reaction, noticeable inconsistencies were found among the outcomes produced by different functionals (Figure 4.01).

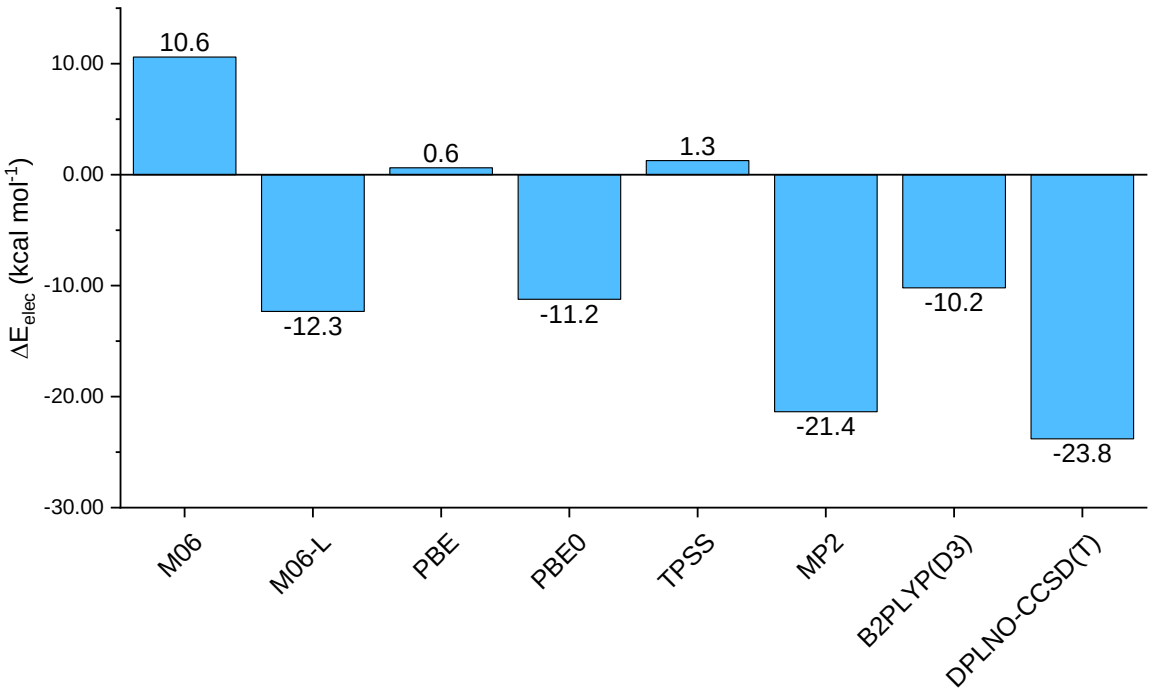


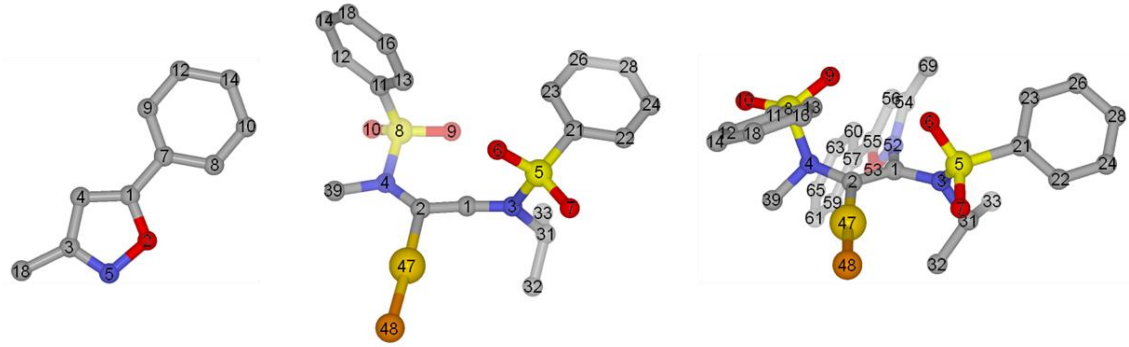
Figure 4.01 Comparison of electronic energies calculated at IEFPCM(1,2-dichloroethane)-[Functional]/6-31+G(d)/SDD(Au)//IEFPCM(1,2-dichloroethane-M06/6-31+G(d)/SDD(Au), or CPCM(1,2-dichloroethane)-DLPNO-CCSD(T)/def2-TZVPP//IEFPCM(1,2dichloroethane) -M06/6-31+G(d)/SDD(Au) level of theory. Relative electronic energies $\Delta E_{elec} = \Delta E_{elec}(\mathbf{Int2_{major}}) - [\Delta E_{elec}(\mathbf{3Me5PhIsoxazole}) + \Delta E_{elec}(\mathbf{Int1_{major}})]$.

While the MP2 method yielded an electronic energy profile that most closely resembled that of the single-point energy of the DLPNO-CCSD(T) method (performed upon M06-geometry), employment of the 'double-hybrid' MP2-like B2PLYP(D3) functional led to a

markedly distinct energy outcome. The absence of a discernible pattern in the electronic energy profiles computed from the selected functionals indicated their inadequacy in furnishing reliable electronic energies for our reaction system.

In light of the inconsistent results obtained in our previous investigations, we hypothesised that the dissimilarities in the stationary point geometries generated by the selected functionals might be responsible. As a consequence, single-point calculations utilising different functionals on the same geometry obtained at the M06/6-31+G(d)/SDD(Au) level of theory may not accurately reflect the actual performance of the selected functionals. With this in mind, we performed geometry optimisation of the same test reaction using several functionals (M06, M06-L, PBE, TPSS) and MP2 method in combination with a 6-31+G(d) basis set for H, C, N, O, P and S and SDD pseudopotential for Au. Table 4.01 presents a comparison of some of the geometry attributes for each optimised structure. All of the optimised structures demonstrated a high degree of geometric consistency, with variations concentrated primarily around the central N–C–C–N motif of **Int1$_{major}$**. The considerable deviation in dihedral angles was not unexpected, given that the C1, C2, and N3 atoms were highly co-linear, despite the overall geometry distortion being relatively slight.

Table 4.01 Comparison of optimised geometries from different functionals.



3Me5PhIsoxazole $Int1_{major}$ $Int2_{major}$

		M06	*M06-L*	*PBE*	*TPSS*	*MP2*
3Me5Ph Isoxazole	D(2-1-7-8)/°	0.0	0.0	0.0	0.0	31.3
	D(1-2-5-3)/°	0.0	0.0	0.0	0.0	−0.3
	B(2-5)/Å	1.39	1.40	1.41	1.42	1.40
	A(5-3-18)/°	120.4	120.0	120.1	119.8	120.3
Int1 $_{major}$	B(2-47)/Å	2.13	2.12	2.08	2.09	2.06
	A(4-2-47)/°	123.5	122.2	128.3	122.2	124.6
	A(47-2-1)/°	105.3	107.4	107.8	109.2	107.2
	B(47-48)/Å	2.34	2.32	2.31	2.32	2.32
	D(4-2-1-3)/°	147.2	126.1	110.1	123.1	160.8
	D(47-2-1-3)/°	−32.7	−60.7	−70.7	−62.0	−19.1
Int2 $_{major}$	B(2-47)/Å	2.09	2.08	2.07	2.06	2.04
	A(4-2-47)/°	121.1	120.9	121.0	120.5	121.8
	A(47-2-1)/°	122.3	123.5	120.8	123.4	123.4
	B(47-48)/Å	2.37	2.35	2.34	2.34	2.33
	D(4-2-1-3)/°	176.3	175.1	173.7	175.7	175.8
	D(47-2-1-3)/°	−0.1	−2.3	−5.9	−5.8	0.2
	B(1-52)/Å	1.44	1.44	1.44	1.45	1.44
	A(53-52-1)/°	115.5	115.3	115.0	114.5	115.3
	D(53-52-1-3)/°	114.7	117.1	115.9	113.1	119.0

The structures were visualised using CYLview20.[159] Hydrogens were omitted for clarity. A = bond angle; B = bond length; D = dihedral angle.

Upon analysis of electronic energy profiles, it became apparent that the selected functionals produced divergent outcomes (Figure 4.02). While the M06-L functional and the MP2 method aligned closely with the results obtained from the previous single-point calculations (Figure 4.01), the PBE and TPSS methods generated significant changes in relative electronic energies. As a result, these methods were excluded from further benchmarks.

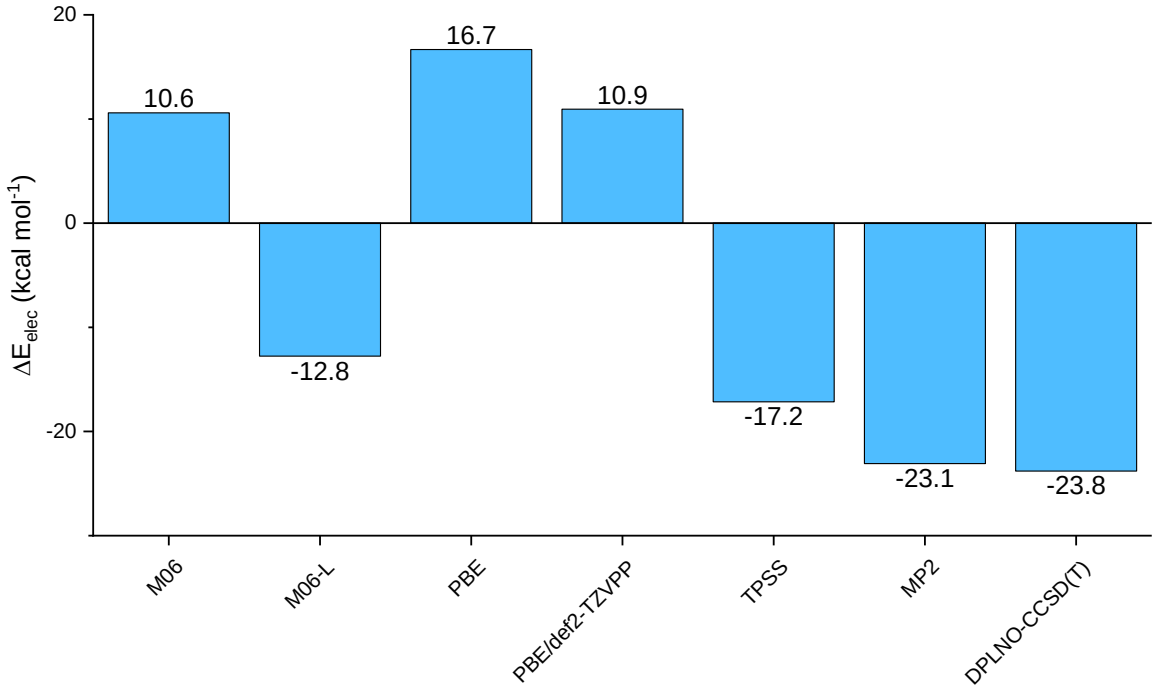


Figure 4.02 Comparison of electronic energies calculated at IEFPCM(1,2-dichloroethane)-[Functional]/6-31+G(d)/SDD(Au), or CPCM(1,2-dichloroethane)-DLPNO-CCSD(T)/def2-TZVPP//IEFPCM(1,2-dichloroethane)-M06/6-31+G(d)/SDD(Au) level of theory. Relative electronic energies ΔE_{elec} = ΔE_{elec}(**Int2$_{major}$**) – [ΔE_{elec}(**3Me5PhIsoxazole**) + ΔE_{elec}(**Int1$_{major}$**)].

Despite the MP2 method being the closest to the DLPNO-CCSD(T) method in terms of accuracy, we decided to avoid its usage in anticipation that the combination of a cheaper functional for geometry optimisation and the DLPNO-CCSD(T) for electronic energy refinement could serve as a good compromise between efficiency and accuracy. Given that the optimised geometries obtained at the M06 functional better resemble those at the MP2 method (see Table 4.01) and that the M06 functional was extensively used in literature for comparable reaction systems,[101, 118, 121] we proceeded with this method for our studies. Following this finding, we conducted additional geometry optimisation tests using the M06 functional combined with various basis sets to evaluate the influence of basis sets on the computed electronic energies (Figure 4.03).

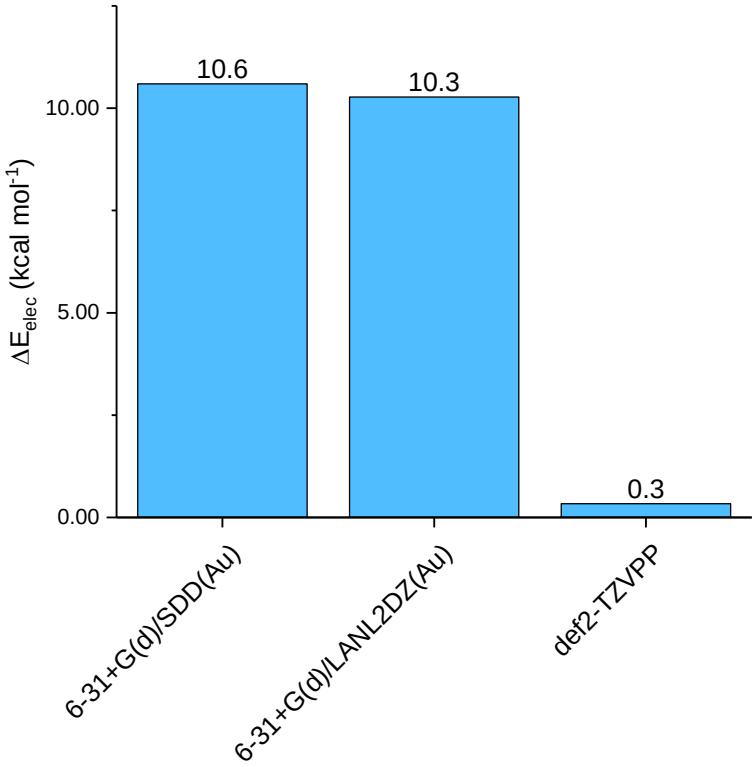


Figure 4.03 Comparison of electronic energies calculated at IEFPCM(1,2-dichloroethane)-M06/[basis set] level of theory. Relative electronic energies ΔE_{elec} = ΔE_{elec}(**Int2$_{major}$**) – [ΔE_{elec}(**3Me5PhIsoxazole**) + ΔE_{elec}(**Int1$_{major}$**)].

Changing the pseudopotential used for the gold atom from SDD to LANL2DZ (D95V[160] basis set plus double-ζ Los Alamos ECP[161-163]) had no discernible effect on the overall relative electronic energy outcome. However, the use of the def2-TZVPP basis set, which only uses an inner core def2-ECP,[153] caused the relative electronic energy outcome to deviate, yet still far from the 'gold standard' DLPNO-CCSD(T) results.

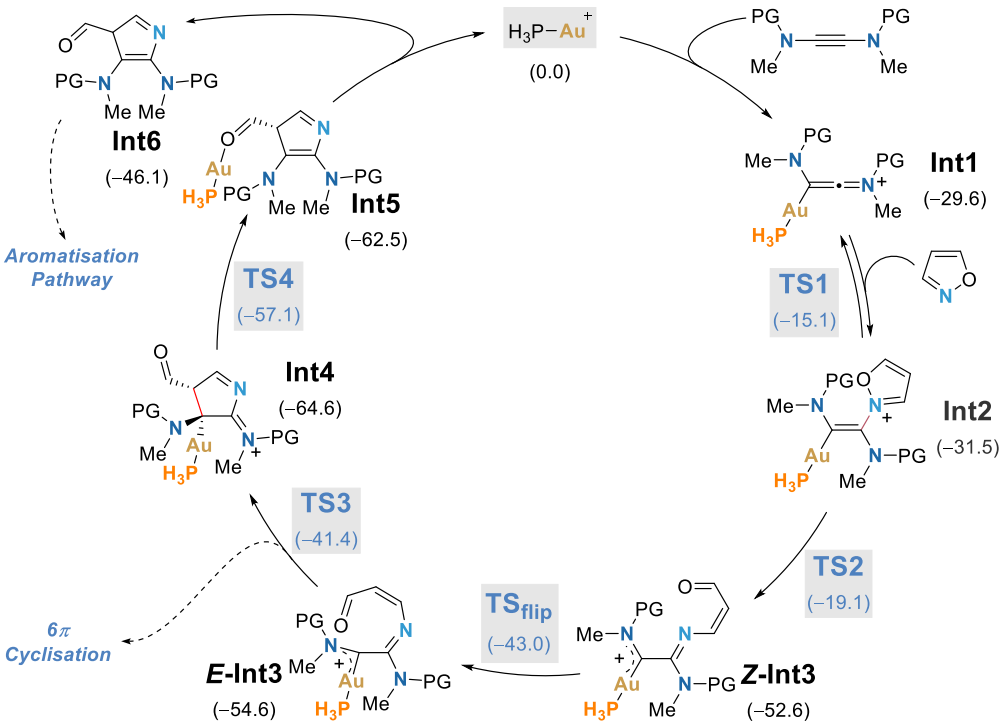
At this point, we regret to conclude that the screened functionals and basis sets did not yield consistent results. Therefore, following the computational work conducted by Ye *et al.* on a similar reaction on ynamides,[101] we have opted to use a similar IEFPCM(1,2-dichloroethane)-M06/6-31+G(d)/SDD(Au) level of theory for geometry optimisations, followed by refinement of electronic energies at the CPCM(1,2-dichloroethane)-DLPNO-CCSD(T)/def2-TZVPP level of theory at 298 K. The free energy of each species in the solution was calculated using the following formula:

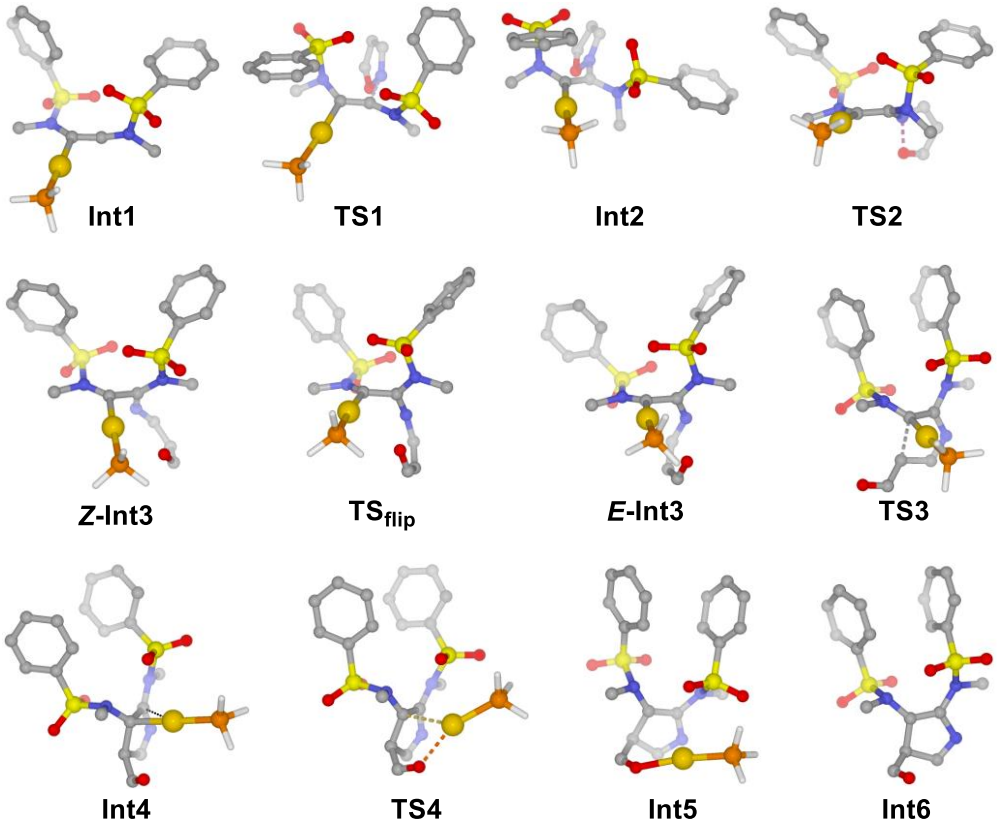
$$G_{sol} = E_{elec}(\text{DLPNO-CCSD(T)}) + [G(M06) - E_{elec}(M06)] + \Delta G^{1\,atm \rightarrow 1\,M}$$

where E_{elec}(DLPNO-CCSD(T)) is the electronic energy calculated at the CPCM(1,2-dichloroethane)-DLPNO-CCSD(T)/def2-TZVPP level of theory; G(M06) and E_{elec}(M06) are the free energy and electronic energy calculated at the IEFPCM(1,2-dichloroethane)-M06/6-31+G(d)/SDD(Au) level of theory, respectively; $\Delta G^{1\,atm \rightarrow 1\,M}$ = RTln(24.5) = 1.89 kcal mol^{-1} is the correction to free energy for conversion from the standard state (1 atm) to solution state (1 M).

4.2.2 Catalytic Cycles for Symmetic Yndiamide

The catalytic cycle for symmetric yndiamide was first explored (Scheme 4.11). The yndiamide's initial reaction with the active gold species results in the formation of the keteniminium-gold complex **Int1**. This process, similar to other literature reports,[101, 121, 141, 142] is barrier-less and energetically favourable (ΔG_{sol} = −29.6 kcal mol^{-1}). Subsequently, **Int1** undergoes nucleophilic attack by the isoxazole, yielding the triply nitrogen-substituted vinyl gold complex **Int2**. The activation barrier for this transformation is 14.5 kcal mol^{-1} (**TS1**). **Int2** and **Int1** are close in free energy (ΔG_{sol} = −1.9 kcal mol^{-1}), implying that these species exist in equilibrium. The subsequent opening of the isoxazole ring leads to the formation of the α-imino gold Fischer carbene intermediate ***Z*-Int3** with moderate activation energy (**TS2**, $\Delta G^{\ddagger}_{sol}$ = 12.4 kcal mol^{-1}).





Scheme 4.11 Main catalytic cycle for symmetric yndiamide. Relative Gibbs Free energies (ΔG_{sol}, kcal mol^{-1}) of key intermediates and transition states were calculated at CPCM(1,2-dichloroethane)-DLPNO-CCSD(T)/def2-TZVPP//IEFPCM(1,2-dichloroethane)-M06/6-31+G(d)/SDD(Au) level of theory at 298 K/1 M. 3D structures were visualised by CYLview20.[159] C–H hydrogens were hidden for clarity.

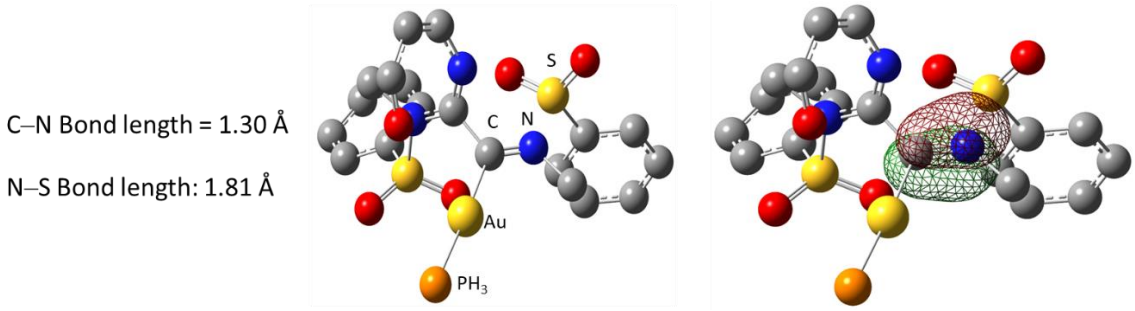


Figure 4.04 3D structure of ***Z*-Int3** (left) and visualisation of its HOMO−24 (isovalue = 0.05) showing the conjugation between the nitrogen atom and the gold carbene moiety (right) computed at the IEFPCM(1,2-dichloroethane)-M06/6-31+G(d)/SDD(Au) level of theory at 298 K/1 M. Both structures were visualised by GaussView6.[164] All hydrogens are hidden for clarity.

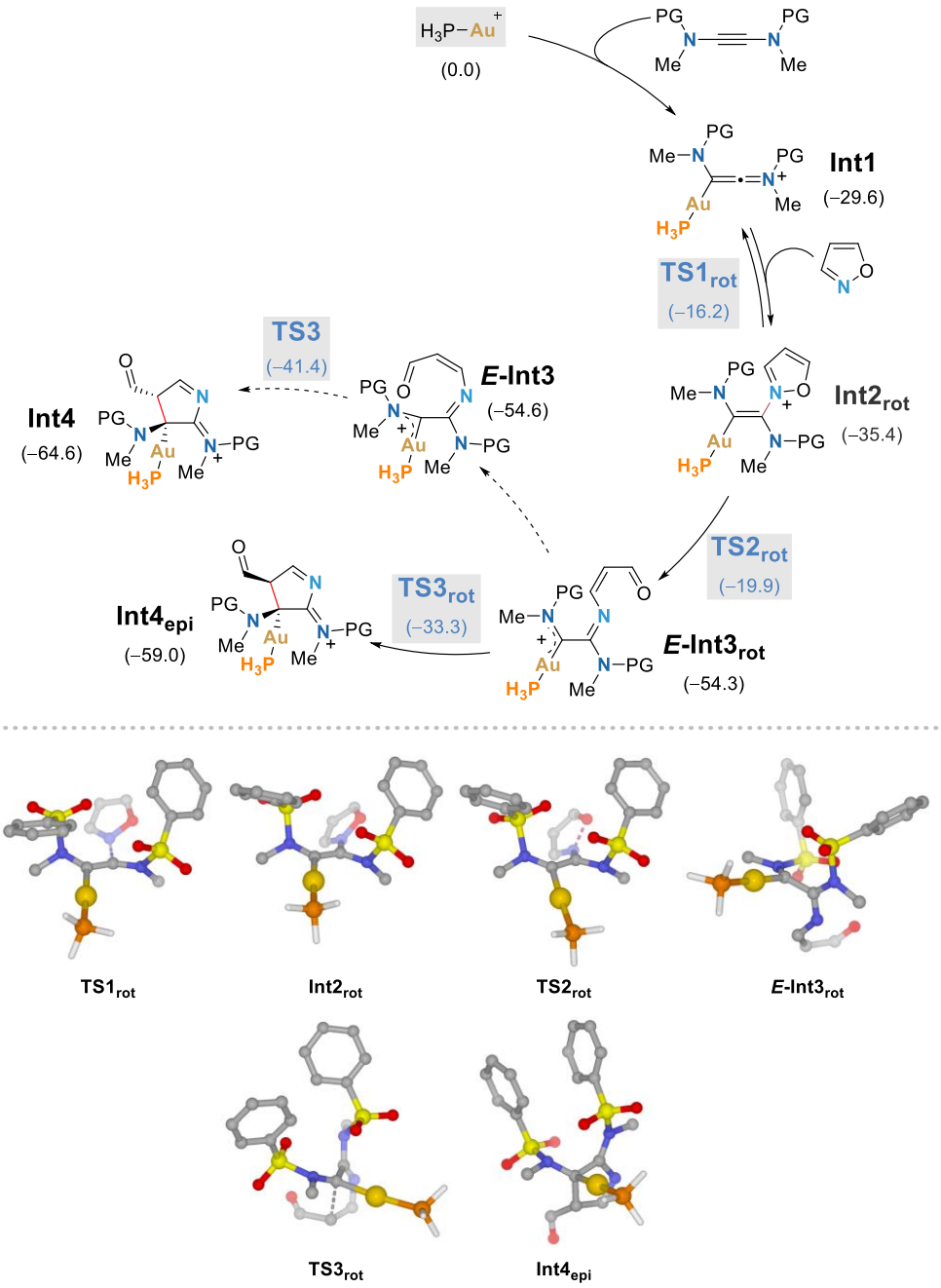
This transformation is significantly exergonic ($\Delta G_{sol} = -21.1$ kcal mol^{-1}) due to the Fischer carbene nitrogen atom's additional stabilisation, making the process irreversible. As a result, the reaction's regioselectivity is likely to be determined during this step. Through NBO analysis of the intermediate ***Z*-Int3** several structural traits are observed (Figure 4.04): i) the C–N bond has enhanced double bond character with a bond length of 1.30 Å, similar to that of the C=N bond, and a Wiberg bond index of 1.545; ii) the N–S bond is weakened, with a bond length of 1.81 Å, which is longer than that of **Int1** (1.72 Å), and a Wiberg bond index of 0.575. Concluding from these facts, we believe they resulted in a great stabilisation effect from the neighbouring nitrogen atom, which contributes to the large ΔG_{sol} from **Int2** to ***Z*-Int3** and strongly favours the gold carbene formation.

***Z*-Int3** can undergo a geometrical inversion to form the slightly more stable ***E*-Int3** *via* **TS$_{flip}$** ($\Delta G^{\ddagger}_{sol}$ = 9.6 kcal mol^{-1}), followed by a 4π Nazarov-type cyclisation[129, 130] to produce the cyclic intermediate **Int4** (**TS3**, $\Delta G^{\ddagger}_{sol}$ = 13.2 kcal mol^{-1}). The formyl group in **Int4** appears to facilitate the subsequent deauration step, leading to the formation of the acyl-gold complex **Int5**, which releases the 3*H*-pyrrole intermediate **Int6** and regenerates the gold complex to complete the catalytic cycle.

In addition to the catalytic cycle discussed above (Scheme 4.11), an alternative pathway has been modelled where the isoxazole attacks the keteniminium-gold complex in a

different orientation (Scheme 4.12), resulting in various rotamers of the intermediates and transition states. The energy profiles of both cycles are identical until the formation of **Int1**. In this alternative pathway, the isoxazole approaches the yndiamide to produce **Int2$_{rot}$**, a rotamer of **Int2** *via* **TS1$_{rot}$** ($\Delta G^{\ddagger}_{sol}$ = 13.4 kcal mol^{-1}). The main difference between **TS1$_{rot}$**/**Int2$_{rot}$** and **TS1**/**Int2** is the dihedral angle between the plane of the isoxazole and the plane of the yndiamide moiety. Despite that **Int2$_{rot}$** is more stable than **Int2**, its subsequent ring-opening to produce the gold carbene ***E*-Int3$_{rot}$** *via* **TS2$_{rot}$** is more difficult ($\Delta G^{\ddagger}_{sol}$ = 15.5 kcal mol^{-1}).

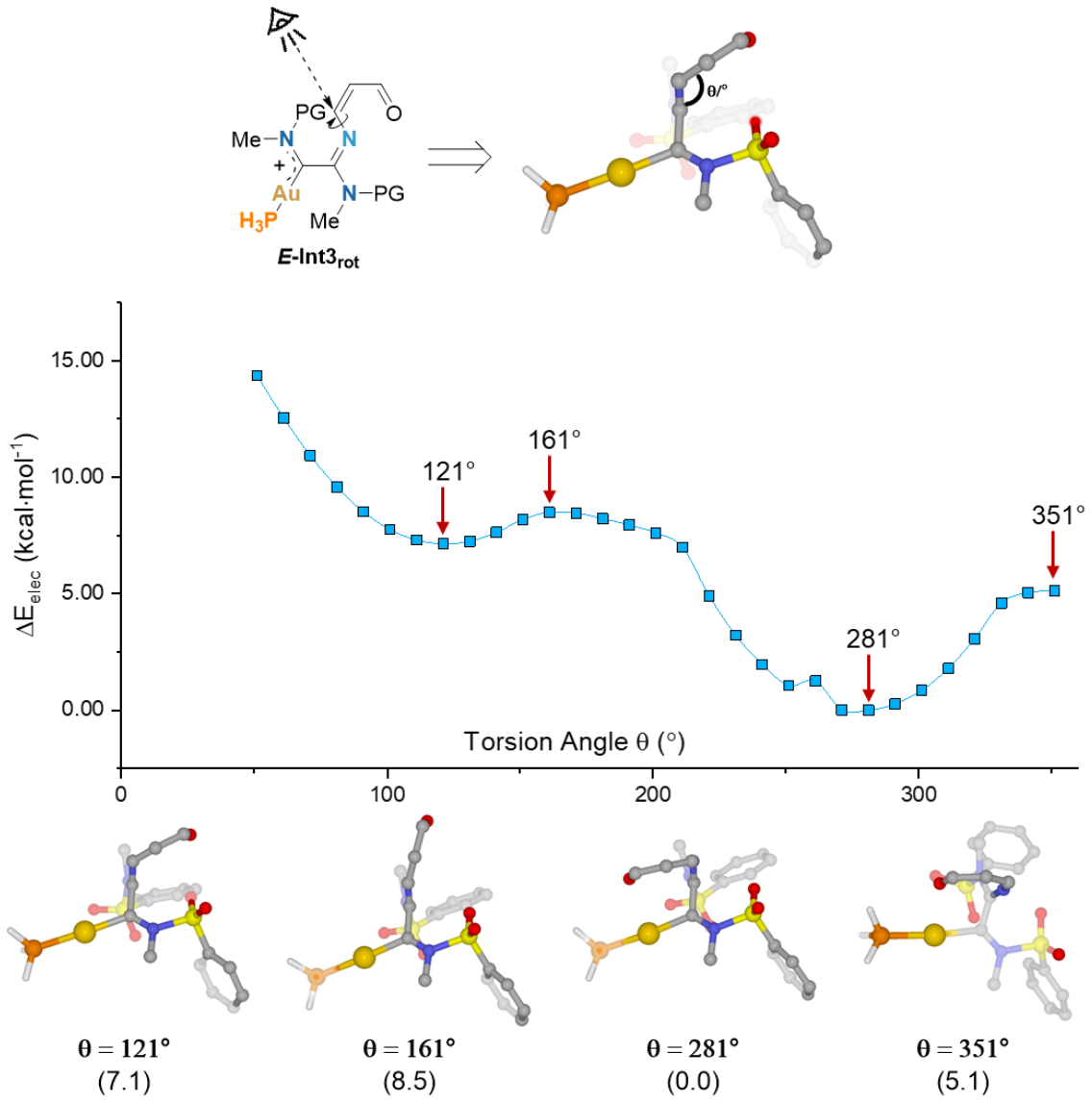
We suspected the presence of a Curtin-Hammett scenario in this gold carbene generation step. Assuming a facile conversion between **Int2$_{rot}$** and **Int2** through C–N bond rotation, the more stable **Int2$_{rot}$** would become the predominant intermediate that reacts through a transition state of lower energy (that is, **TS2**). As a result, the mechanism we presented in Scheme 4.12 might be the less-favoured pathway. Attempts have been made to find the rotational barrier between **Int2$_{rot}$** and **Int2**, but they were all to no avail.



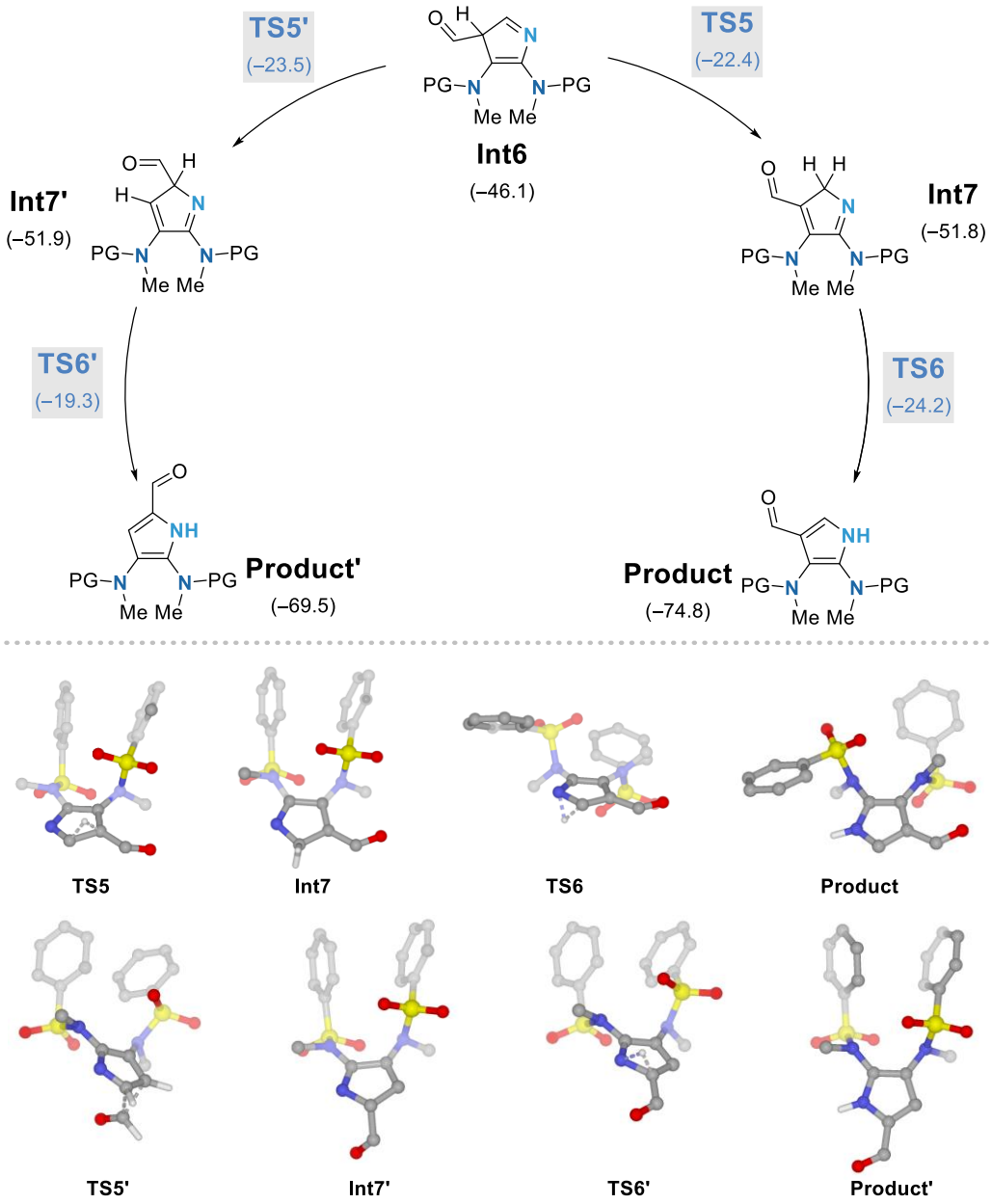
Scheme 4.12 Alternative mechanism for symmetric yndiamide with the nucleophilic attack by isoxazole with different relative orientations. Relative Gibbs Free energies (ΔG_{sol}, kcal mol^{-1}) of key intermediates and transition states were calculated at CPCM(1,2-dichloroethane)-DLPNO-CCSD(T)/def2-TZVPP//IEFPCM(1,2-dichloroethane)-M06/6-31+G(d)/SDD(Au) level of theory at 298 K/1 M. 3D structures were visualised by CYLview20.[159] C-H hydrogens were hidden for clarity.

Thanks to the relative orientation between the isoxazole and yndiamide moiety in **Int2$_{rot}$**, the resulting gold carbene ***E*-Int3$_{rot}$** from the previous step will have the imine part in *E*-geometry. However, the *α,β*-unsaturated carbonyl side-chain of ***E*-Int3$_{rot}$** lies in a

conformation that orients the C=C bond further away from the gold carbene motif, compared to that of ***E*-Int3**, it needs to overcome a much higher activation energy barrier to cyclize ($\Delta G^{\ddagger}_{sol}$(**TS3$_{rot}$**) = 21.0 kcal mol^{-1} vs. $\Delta G^{\ddagger}_{sol}$(**TS3**) = 13.2 kcal mol^{-1}). Considering the rotamer nature of ***E*-Int3$_{rot}$** compared to ***E*-Int3**, we envisioned that ***E*-Int3$_{rot}$** can readily convert to ***E*-Int3** through conformational change and cyclize through the more favoured **TS3**.



Scheme 4.05 Relaxed potential energy surface scan of the rotation around the C-N bond in ***E*-Int3$_{rot}$**. Relative electronic energies (ΔE_{elec}, kcal mol^{-1}) were computed at IEFPCM(1,2-dichloroethane)-M06/6-31+G(d)/SDD(Au) level of theory at 298 K/1 M. 3D structures were visualised by CYLview20.[159] C-H hydrogens were hidden for clarity.

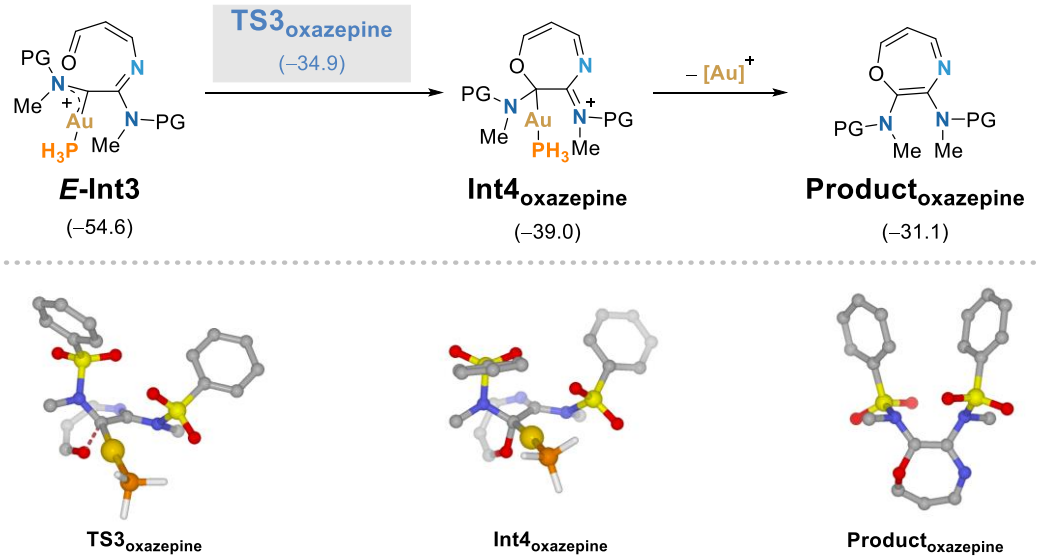


Scheme 4.13 Aromatisation pathway for **Int6**. Relative Gibbs Free energies (ΔG_{sol}, kcal mol^{-1}) of key intermediates and transition states were calculated at CPCM(1,2-dichloroethane)-DLPNO-CCSD(T)/def2-TZVPP//IEFPCM(1,2-dichloroethane)-M06/6-31+G(d)/SDD(Au) level of theory at 298 K/1 M. 3D structures were visualised by CYLview20.[159] Some C–H hydrogens were hidden for clarity.

In this context, we performed a relaxed potential energy surface scan of the rotation around the C-N bond in ***E*-Int3$_{rot}$** (Scheme 4.05). The result revealed a small rotational barrier (~ 1.4 kcal mol^{-1}), indicating that ***E*-Int3** is the principal reactive gold carbene intermediate in

our reaction system. Combining the findings above, we are confident to conclude that the pathway we discussed above (Scheme 4.12) is less-favoured.

Continuing from the main catalytic cycle (Scheme 4.11), the aromatisation of **Int6** may be achieved through two consecutive 1,5-hydride shifts (*via* **TS5** and **TS6**) to yield the **Product** (Scheme 4.13). The free activation energies required for these two transformations are relatively high ($\Delta G^{\ddagger}_{sol}$ = 23.7 kcal mol^{-1} and $\Delta G^{\ddagger}_{sol}$ = 27.6 kcal mol^{-1}), but from a thermodynamic point of view, this process is extremely favoured (ΔG_{sol} = −28.7 kcal mol^{-1} over two steps). Alternatively, a 1,5-formyl shift/hydride shift sequence (*via* **TS5′** and **TS6′**) could give the minor product **Product′**. Although the first 1,5-formyl shift occurs by overcoming a slightly smaller free activation energy barrier ($\Delta G^{\ddagger}_{sol}$ = 22.6 kcal mol^{-1}), the subsequent 1,5-hydride shift to furnish **Product′** proceeds through a high-barrier **TS6′** ($\Delta G^{\ddagger}_{sol}$ = 32.6 kcal mol^{-1}), rendering this pathway less-favoured.



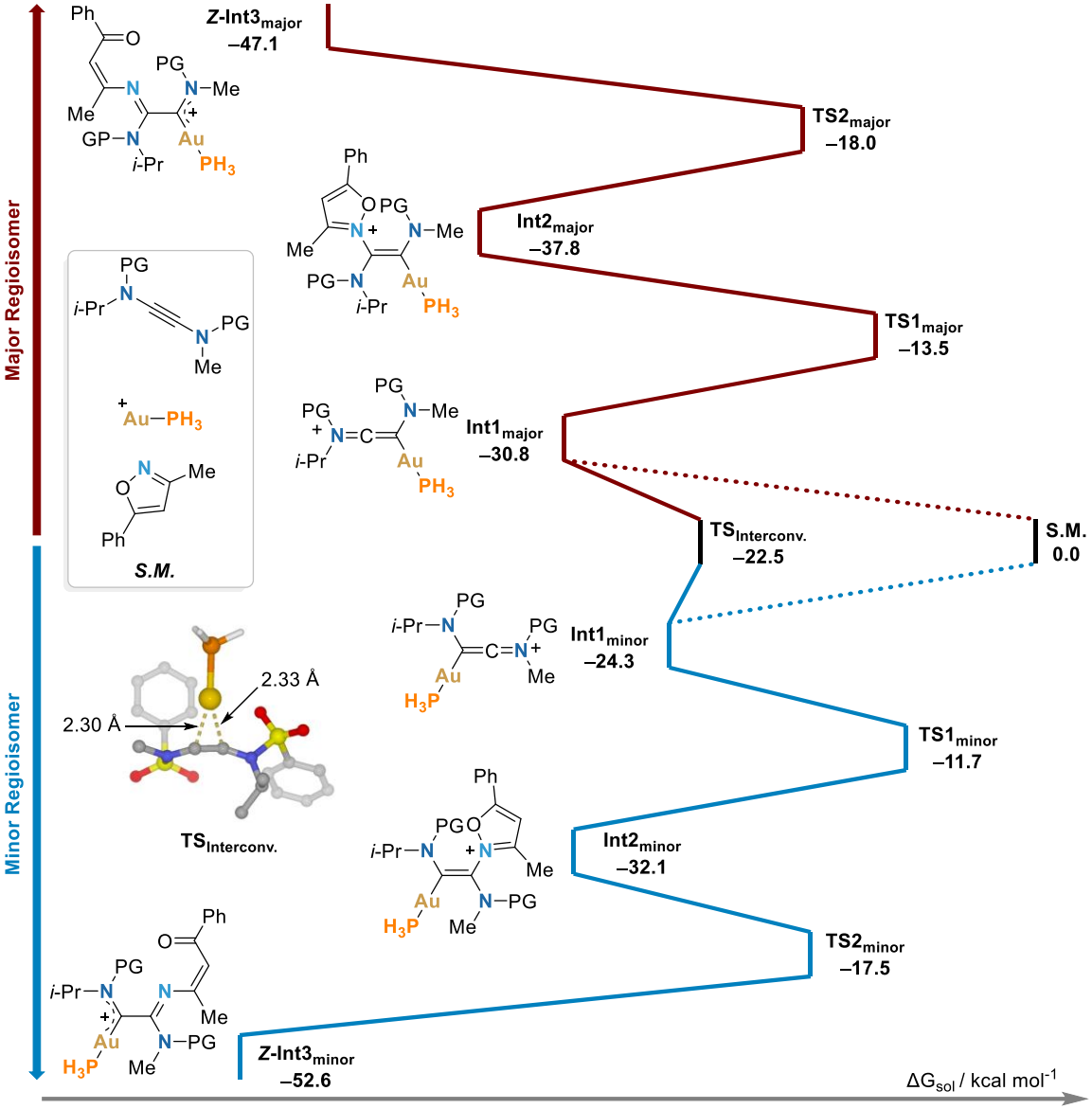
Scheme 4.14 1,4-Oxazepine formation pathway from ***E*-Int3**. Relative Gibbs Free energies (ΔG_{sol}, kcal mol^{-1}) of key intermediates and transition states were calculated at CPCM(1,2-dichloroethane)-DLPNO-CCSD(T)/def2-TZVPP//IEFPCM(1,2-dichloroethane)-M06/6-31+G(d)/SDD(Au) level of theory at 298 K/1 M. 3D structures were visualised by CYLview20.[159] C–H hydrogens were hidden for clarity.

The appearance of a 1,4-oxazepine byproduct in some cases, such as **90**, may be linked to an alternative pathway for the formation of a seven-membered ring, which branches off from the main catalytic cycle at ***E*-Int3** (Scheme 4.14). Within this pathway, both the 6π electrocyclisation[120, 131] and the following deauration are strongly disfavoured, requiring large activation energy (**TS3$_{oxazepine}$**, $\Delta G^{\ddagger}_{sol}$ = 19.7 kcal mol^{-1}). The change in free energy was also positive (ΔG_{sol} = 23.5 kcal mol^{-1} over two steps), suggesting that this pathway is non-spontaneous. This conclusion, however, contradicts our experimental observations where such byproducts were indeed isolated under mild conditions. We attributed this inconsistency to the over-simplification of the model reactions, and we anticipate increasing the complexity of the model reactions could help us better explain our experimental results.

4.2.3 Catalytic Cycle for Non-symmetric Yndiamide

Upon obtaining an understanding of the catalytic cycle for symmetric yndiamides, our objective was to comprehend the observed regioselectivity when using non-symmetric yndiamides. As discussed earlier, regioselectivity is likely to be determined at or before the rate-determining step of ***Z*-Int3** formation. To gain further insight into this, additional reaction energy profiles were computed up to this point for a non-symmetric yndiamide featuring methyl and isopropyl substituents with 3-methyl-5-phenylisxoazole (Scheme 4.15). This substrate can react with the active gold catalyst to form two regioisomeric keteniminium-gold complexes (**Int1$_{major}$** and **Int1$_{minor}$**). The formation of these complexes is highly exergonic and barrierless, implying that this process is irreversible. This finding also suggests that if the regioselectivity was determined at this point by the preferential formation of the more stable **Int1$_{major}$** over **Int1$_{minor}$**, there would be no room for the isoxazole reagent to influence the regioselectivity, which conflicts with our experimental

observations. Pleasingly, an unprecedented π-complex transition state with a low energy barrier (**$TS_{interconv.}$**) was identified, where the gold is coordinated to the centre of the C-C triple bond with the bond lengths between the gold and two alkynyl carbon atoms being nearly identical.



Scheme 4.15 Reaction energy profiles of regioselectivity determining steps for non-symmetric yndiamide. PG = benzenesulfonyl. Relative Gibbs Free energies (ΔG_{sol}, kcal mol^{-1}) of key intermediates and transition states were calculated at CPCM(1,2-dichloroethane)-DLPNO-CCSD(T)/def2-TZVPP//IEFPCM(1,2-dichloroethane)-M06/6-31+G(d)/SDD(Au) level of theory at 298 K/1 M. 3D structures were visualised by CYLview20.[159] Some C–H hydrogens were hidden for clarity.

The presence of $\mathbf{TS_{interconv.}}$ allows the interconversion of $\mathbf{Int1_{major}}$ and $\mathbf{Int1_{minor}}$ ($\Delta G^{\ddagger}_{sol}$ = 1.8 kcal mol^{-1}, ΔG_{sol} = −6.5 kcal mol^{-1}). It also indicates that the subsequent regioselectivity-determining step operates under a Curtin-Hammett scenario. Sterically undemanding isoxazole nucleophiles (e.g. 3-methyl-5-phenylisoxazole as shown in Scheme 4.15) can attack $\mathbf{Int1_{major}}$ *via* $\mathbf{TS1_{major}}$ ($\Delta G^{\ddagger}_{sol}$ = 17.3 kcal mol^{-1}) which is of lower barrier compared to $\mathbf{TS1_{minor}}$ ($\Delta\Delta G^{\ddagger}_{sol}$ = 1.8 kcal mol^{-1}). Consequently, $\mathbf{Int2_{major}}$ is primarily formed, and the major regioisomer product is eventually produced. As the bulkiness of the isoxazole nucleophile increases, the energy difference between $\mathbf{TS1_{major}}$ and $\mathbf{TS1_{minor}}$ is expected to decrease, owing to the increased steric repulsion between the isoxazole and the bulkier nitrogen substituent, resulting in lower observed regioselectivity.

4.3 Conclusions

In summary, we have conducted a comprehensive DFT investigation of the reaction mechanism for the gold-catalysed cyclisation of yndiamides with isoxazoles. The catalytic cycle for symmetric yndiamide was initially explored, providing detailed reaction energy profiles. Our analysis indicated that the formation of the *α*-imino gold carbene intermediate was the rate-determining step of the overall transformation. Furthermore, we computed the energy profiles for the aromatisation pathway, which includes the 1,5-formyl shift/1,5-hydride shift sequence, and the alternative 6π-electrocyclisation from the gold carbene intermediates, to account for the generation of several by-products. Building on our understanding of the reaction mechanism for symmetric yndiamide, we investigated the regioselectivity exhibited by non-symmetric yndiamide. Our calculations demonstrated a Curtin-Hammett scenario in which a gold π-complex-like transition state was crucial for the interconversion of alkenyl-gold complexes, and consequently, in determining the regiochemical outcome. Our studies represent the first attempt to understand the underlying

principle that dictates the regioselectivity of yndiamide transformations. We hope that our effort could spur further investigations and provide valuable inspiration to the field of DFT rationalisation of the regioselectivity of gold-catalysed functionalisation of alkynes.

C H A P T E R

V

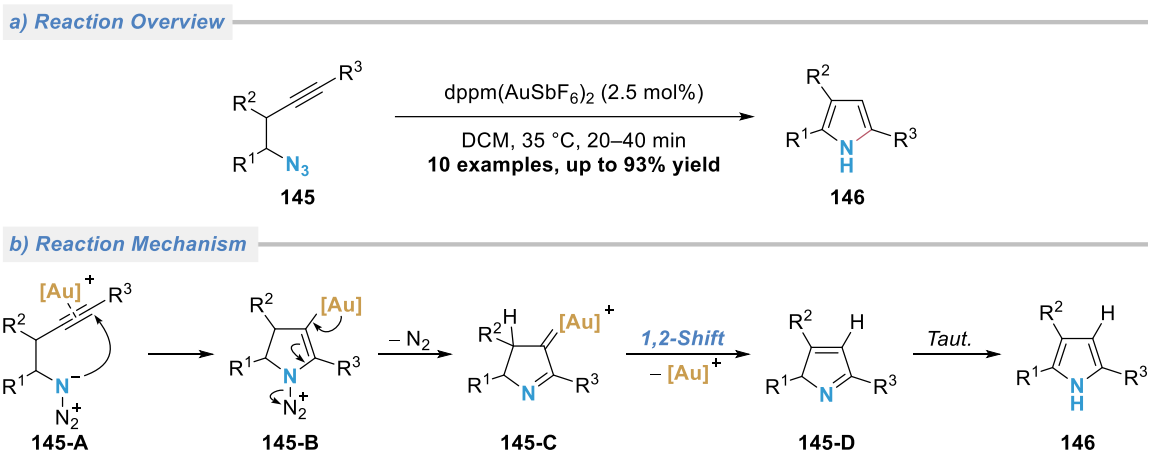
Gold-Catalysed Functionalisation of Yndiamides with Sulfilimines or Tetrazolo[1,5-*a*]pyridines

Sulfilimines, also known as sulfur-based aza-ylides, have been established as an alternative to organic azides in the functionalisation of ynamides *via* α-imino gold carbenes to construct a variety of *N*-heterocycles. This chapter presents an ongoing project on the gold-catalysed functionalisation of yndiamides with sulfilimines for the synthesis of imidazo[1,2-*a*]pyridines. Furthermore, the development of tetrazolo[1,5-*a*]pyridines as novel nitrene transfer reagents equivalent to sulfilimines is also discussed, for gold-catalysed functionalisation of yndiamides that produce the same imidazo[1,2-*a*]pyridine products.

5.1 Introduction

5.1.1 Gold-Catalysed Functionalisation of Ynamides with Azides

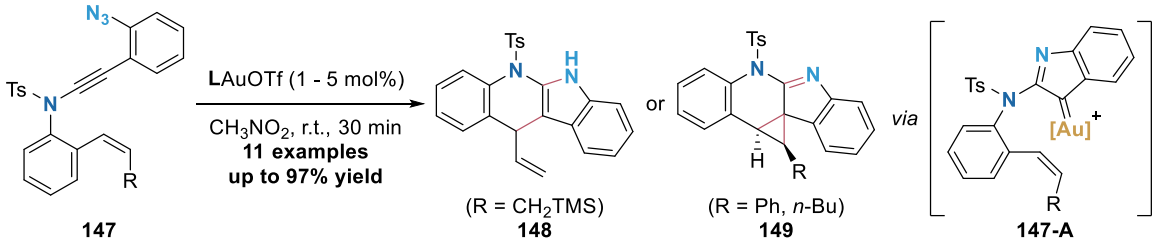
As early as 2005, Toste and co-workers reported the gold-catalysed cyclisation of homopropargyl azides **145** *via* α-imino gold carbenes to access highly substituted pyrroles **146** (Scheme 5.01a).[165]



Scheme 5.01 Gold-catalysed functionalisation of homopropargyl azides for the synthesis of highly-substituted pyrroles.

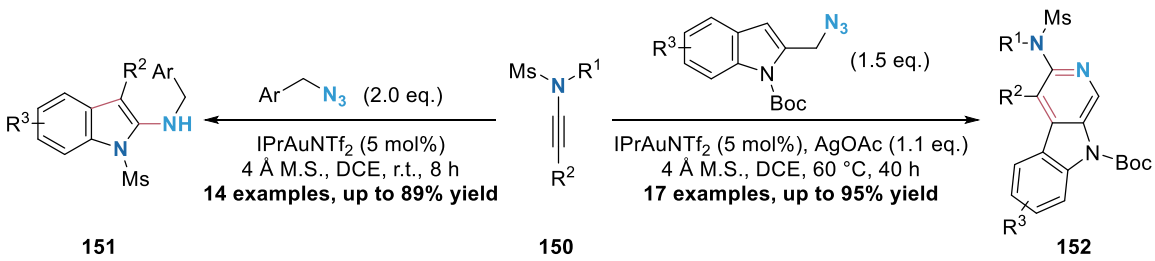
The Toste group proposed an acetylenic Schmidt reaction mechanism for this transformation (Scheme 5.01b). Specifically, the process was initiated from the gold-activated alkyne **145-A**, followed by a 5-*endo*-*dig* cyclisation event from the azide group to form the vinyl gold complex **145-B**. The loss of a nitrogen molecule then yielded an α-imino gold carbene **145-C**, which underwent a 1,2-shift leading to the regeneration of the gold catalyst and the formation of 2*H*-pyrrole **145-D**. The latter compound further tautomerised to the final product **146**. Undoubtedly, the groundbreaking work of Toste and co-workers has stimulated much research on the functionalisation of alkynes *via* α-imino gold carbenes. As such, over the past decade, a plethora of transformations involving the generation of α-imino gold carbenes from alkynes with internal or external azides have

been discovered.[54, 98] Ynamides, known for their versatility as building blocks for *N*-containing cyclic compounds, have also attracted significant attention in this field.[15, 16, 100, 166] In 2014, Ohno and co-workers reported the first application of (azido)ynamides **147** in the gold-catalysed cascade cyclisation to construct various indoloquinolines **148** and **149** *via* *α*-imino gold carbene **147-A** (Scheme 5.02).[167]



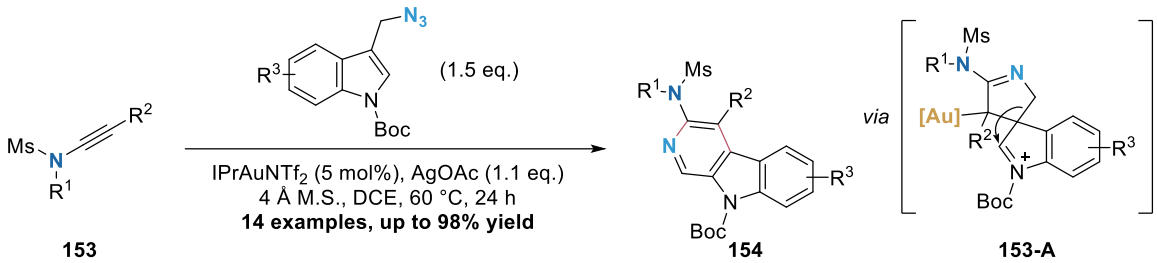
Scheme 5.02 Gold-catalysed cascade cyclisation of (azido)ynamides for the construction of indoloquinolines. **L** = $[4\text{-}(CF_3)C_6H_4]_3P$.

Shortly after, Ye and co-workers demonstrated the generation of *α*-imino gold carbenes from the gold-catalysed intermolecular reaction of ynamides **150** and azides (Scheme 5.03).[168] The use of benzyl azides delivered 2-aminoindoles **151**, while indolyl azides led to the formation of pyrido[2,3-*b*]indoles **152**. Despite the divergent products, the two reactions followed a similar mechanism where the *α*-imino gold carbene was inserted into the neighbouring C–H bond followed by protodeauration and tautomerisation/oxidation to yield the final products.



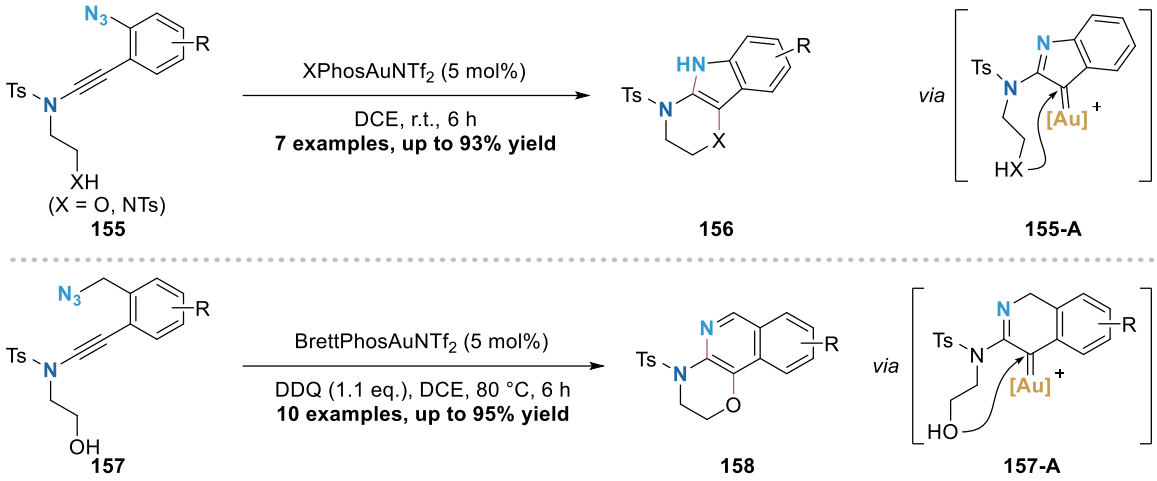
Scheme 5.03 Gold-catalysed intermolecular reaction of ynamides and azides.

The same research group also reported an unexpected 1,2-alkyl migration variation of the aforementioned reactivity with indolyl azide (Scheme 5.04).[169] Upon nucleophilic attack onto the gold carbene from the neighbouring indole moiety, a spirocyclic intermediate **153-A** was generated, which could undergo a sequential 1,2-alkyl shift/protodeauration/oxidation to furnish the *β*-carbolines **154** as the final product.



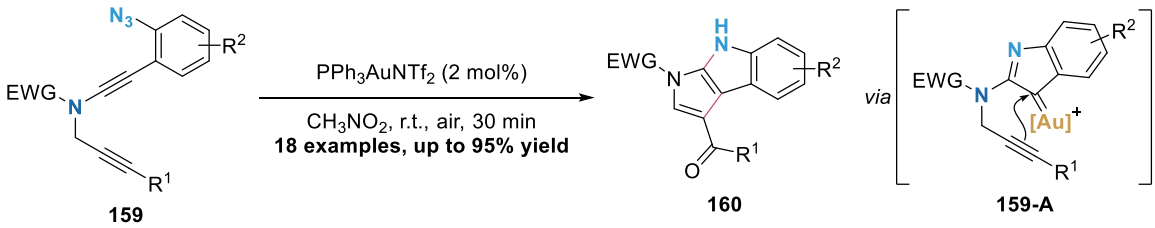
Scheme 5.04 Gold-catalysed intermolecular reaction of ynamides with 3-indolyl azides *via* 1,2-alkyl migration.

The Ye group further took advantage of the X–H bond insertion reactivity of the gold carbene and developed the gold-catalysed cascade cyclisations of (azido)ynamides to synthesise various indole- or isoquinoline-based *N*-containing tricyclic compounds (Scheme 5.05).[170, 171] In the case of aryl azide tethered ynamides **155**, the procedure produced a series of [1,4]oxazino[3,2-*b*]indoles or 1*H*-pyrazino[2,3-*b*]indoles **156** *via* O–H or N–H insertion of the gold carbene **155-A**. On the other hand, the use of benzyl azide tethered ynamides **157** delivered a range of valuable [1,4]oxazino[3,2-*c*]isoquinolines **158** through an O–H insertion/oxidation sequence from the gold carbene **157-A**.



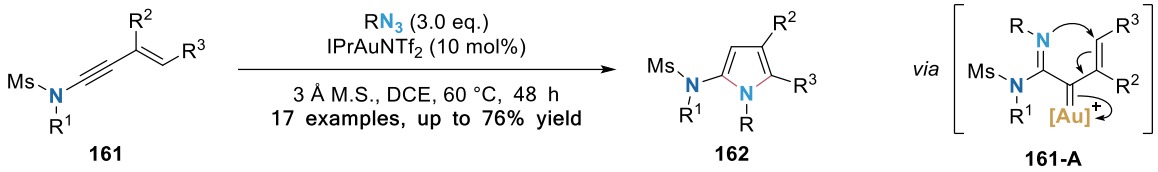
Scheme 5.05 Gold-catalysed cascade cyclisation of (azido)ynamides for the synthesis of indole- or isoquinoline-based *N*-containing tricyclic compounds.

Besides X–H bonds, internal alkynes could also serve as nucleophiles to trap the *α*-imino gold carbene intermediate, as demonstrated by Ye and co-workers' research on the gold-catalysed cyclisation of (azido)diynamides **159** (Scheme 5.06).[172] The authors reported a controllable divergent synthesis of different *N*-heterocycles where the use of a copper catalyst in the presence of external oxidants led to the formation of pyrrolo[3,4-*c*]quinolin-1-ones, while pyrrolo[2,3-*b*]indoles **160** were acquired under gold-catalysed conditions. The proposed mechanism involves the generation of the *α*-imino gold carbene **159-A**, which was trapped by the internal alkyne motif. The resulting vinyl cationic intermediate could undergo nucleophilic attack by water, followed by a deauration/tautomerisation/oxidation sequence to afford the final product **160**.



Scheme 5.06 Gold-catalysed cyclisation of (azido)diynamides for the synthesis of pyrrolo[2,3-*b*]indoles.

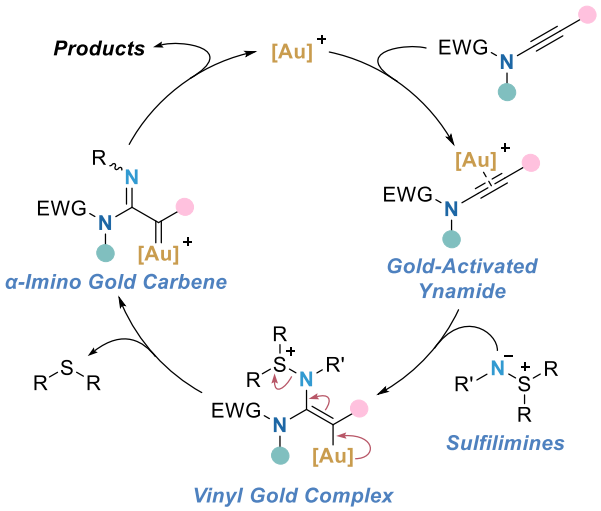
The aza-Nazarov cyclisation of the α-imino gold carbene intermediate generated from ene-ynamides **161** was also realised by the group of Ye to construct functionalised 2-aminopyrroles **162** (Scheme 5.07).[129] The transformation involved the generation of gold carbene **161-A**, followed by a 4π-electrocyclisation/protodeauration cascade to deliver the final product.



Scheme 5.07 Gold-catalysed aza-Nazarov cyclisation of ene-ynamides with azides for the synthesis of functionalised pyrroles.

5.1.2 Gold-Catalysed Functionalisation of Ynamides with Sulfilimines

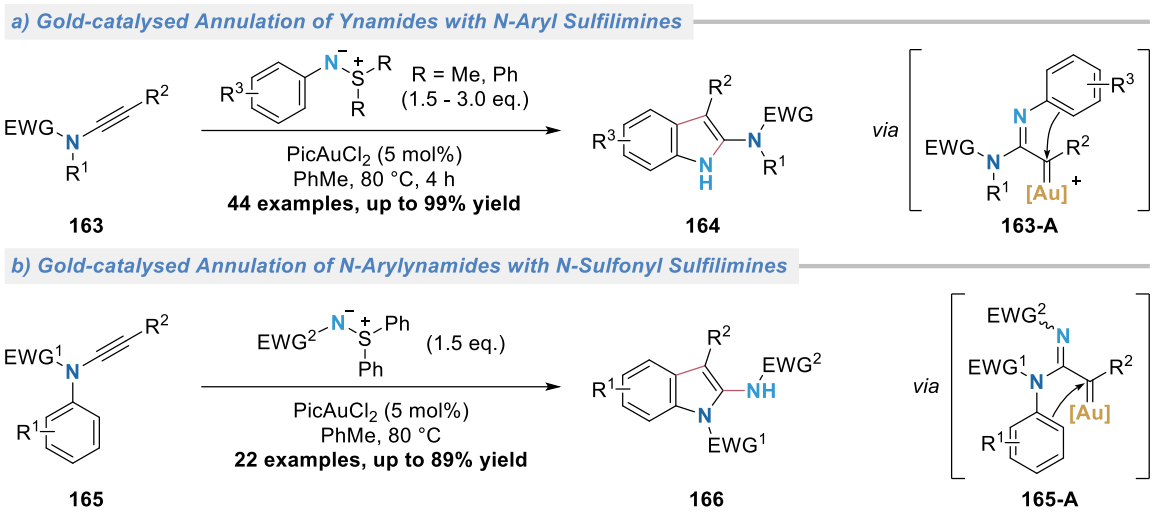
The literature reviewed above demonstrates the great potential and versatility of gold-catalysed functionalisation of ynamides with azides for the synthesis of complex *N*-heterocycles. Azide reagents, however, are often associated with drawbacks such as i) functional group intolerance; ii) toxicity and potential explosivity; and iii) relatively limited use in the intermolecular functionalisation of ynamides.[173] To overcome these limitations, aza-ylides have emerged as promising alternatives for azides, and sulfur-based aza-ylides, or sulfilimines, have stood out among others as a new generation of nitrene transfer reagents. Although first demonstrated by Zhang and Li,[174] the use of sulfilimines in the gold-catalysed nitrene transfer to ynamides was not well developed until the Hashmi group reported a collection of gold(III)-catalysed intermolecular annulation between ynamides and sulfilimines to deliver a broad scope of *N*-heterocycles *via* α-imino gold carbenes.[175-178] Similar to the previously discussed mechanism for gold-catalysed nitrene-transfer reactions with alkynes (Scheme 3.01), a catalytic cycle was proposed for the gold-catalysed functionalisation of ynamides with sulfilimines (Scheme 5.08).



Scheme 5.08 Reaction mechanism for the gold-catalysed functionalisation of ynamides with sulfilimines *via* *α*-imino gold carbenes.

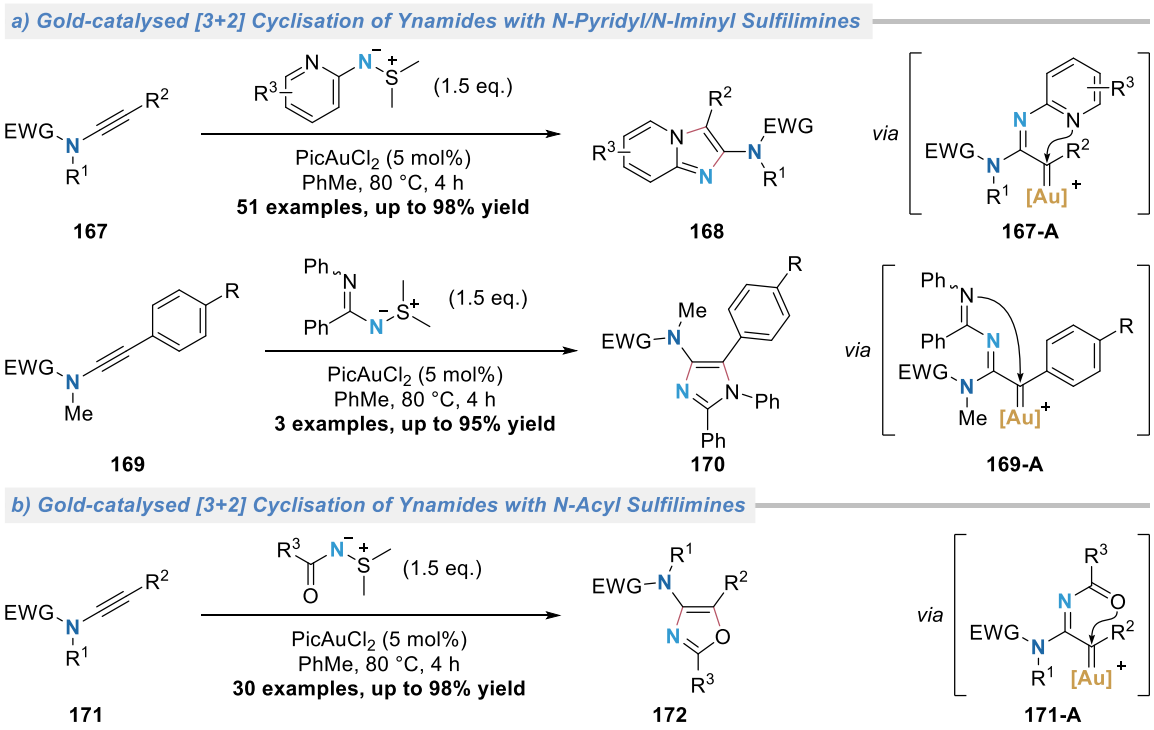
The reaction begins with the formation of the keteniminium-gold complex *via* the interaction of the gold catalyst with the ynamide. The nucleophilic attack of the sulfilimine reagent at the *N*-terminus of the keteniminium-gold complex formed a vinyl gold complex which could be converted to the *α*-imino gold carbene through the extrusion of the thioether group by N–S bond cleavage. Various approaches were employed to trap the gold carbene intermediate, producing a wide spectrum of aza-heterocyclic products.

The gold carbene could insert into the *ortho* C–H bond of the aryl groups introduced by *N*-aryl sulfilimines, delivering 2-aminoindoles **164** (Scheme 5.09a).[175] A similar gold-catalysed C–H annulation of *N*-arylynamides was also observed when using *N*-sulfonyl sulfilimines, resulting in the formation of 2-aminoindoles **166** (Scheme 5.09b).[178]



Scheme 5.09 Gold-catalysed annulation of ynamides with sulfilimines *via* C-H insertion.

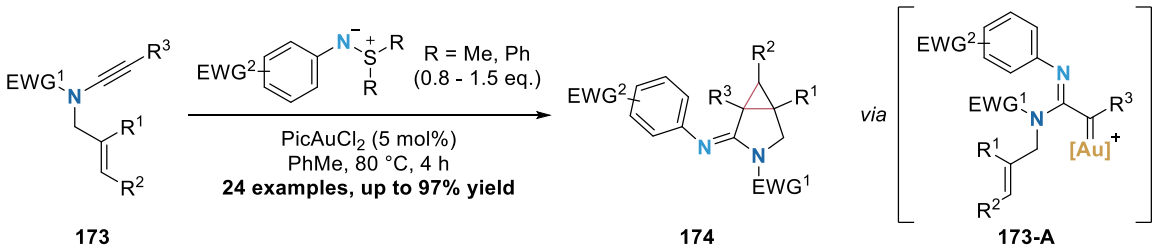
In addition to exhibiting C–H insertion reactivity, the α-imino gold carbenes that arise from the reaction between ynamides and sulfilimines are capable of participating in formal 1,3-dipolar cycloadditions (Scheme 5.10).



Scheme 5.10 Gold-catalysed [3+2] cyclisation of ynamides with sulfilimines.

The use of *N*-pyridyl or *N*-iminyl sulfilimines led to the formation of a variety of imidazole-based scaffolds **168** or **170** (Scheme 5.10a),[175, 176] whereas the use of *N*-acyl sulfilimines resulted in the synthesis of a range of 4-aminooxazoles **172** (Scheme 5.10b).[177]

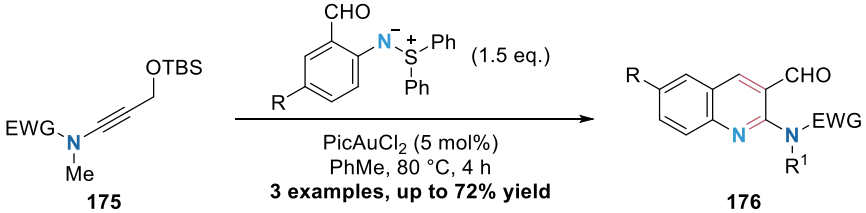
The Hashmi group also accomplished the generation of various 3-aza-bicyclo[3.1.0]hexan-2-imines **174** through the cyclopropanation of the *α*-imino gold carbene intermediate derived from ene-ynamide **173** (Scheme 5.11).[175] The reaction exhibited tolerance towards sulfilimines with electron-withdrawing groups, as well as different *N*-allyl ynamides.



173 **174** **173-A**

Scheme 5.11 Gold-catalysed cyclopropanation of ene-ynamide with sulfilimines.

In addition to the one-step cyclisation reactions of the gold carbenes mentioned above, Hashmi and co-workers performed a 1,2-H shift/Mukaiyama aldol condensation sequence on the gold carbene generated from ynamides **175**, resulting in the production of 4-acylquinolines **176** (Scheme 5.12).[175] This cascade reaction of the α-imino gold carbene was also applied in a previous study by the same group on the gold-catalysed synthesis of quinolines from propargyl silyl ethers and anthranils,[112] providing a new method to construct this motif.



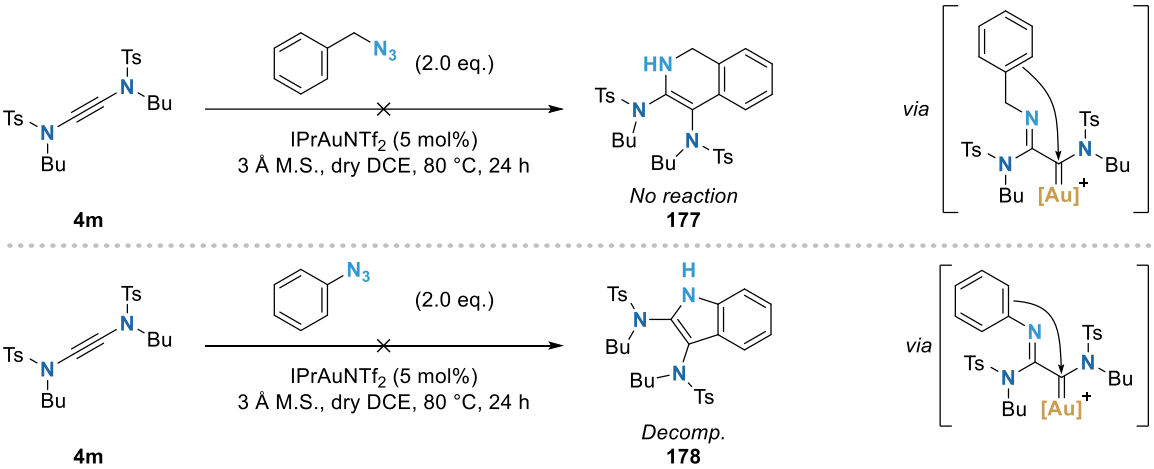
175 **176**

Scheme 5.12 Gold-catalysed 1,2-H shift/Mukaiyama aldol condensation sequence for the construction of 4-acylquinolines.

5.1.3 Concepts of This Work and Initial Attempts

The literature examples discussed above showcase the effectiveness of organic azides and sulfilimines in the generation of complex *N*-heterocyclic compounds. Despite their lower atom economy in comparison to isoxazole reagents (as discussed in Chapter III), they remain a prominent choice for nitrene transfer reactions in gold catalysis. Therefore, we anticipated that the application of yndiamides in such transformations could open up new chemical space in the gold-catalysed functionalisation of yndiamides, and become another addition to yndiamide chemistry.

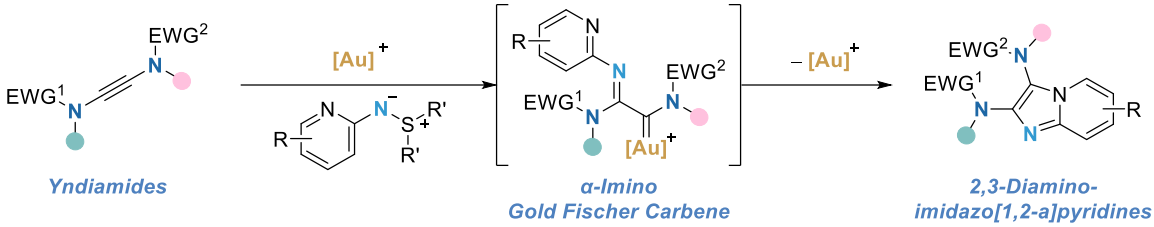
However, our initial attempts at the gold-catalysed cyclisation with yndiamides and benzyl or phenyl azide proved unsuccessful, indicating that these 'original' nitrene source reagents are not suitable for the gold-catalysed functionalisation of yndiamides (Scheme 5.13).



Scheme 5.13 Attempted gold-catalysed cyclisation of yndiamide with organic azides.

As a result, we shifted our research focus to the use of sulfilimines for the generation and functionalisation of α-imino gold carbenes from yndiamides (Scheme 5.14). We expect that the use of *N*-pyridyl sulfilimines would generate an *α*-imino gold Fischer carbene intermediate with a pyridyl sidechain. Subsequent cyclisation from the pyridyl group onto the gold carbene should produce the 2,3-diamino-imidazo[1,2-*a*]pyridine products.

Imidazo[1,2-*a*]pyridines are important pharmacophores for many bioactive compounds,[179] and the direct and facile synthesis of these frameworks, especially the poly-aminated derivatives, is of significant synthetic interest and medicinal importance.



Scheme 5.14 Concept of the gold-catalysed functionalisation of yndiamides with sulfilimines.

5.2 Results and Discussion

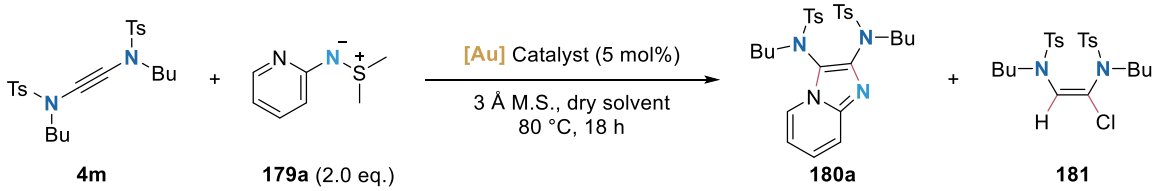
5.2.1 Gold-Catalysed Functionalisation of Yndiamides with Sulfilimines

5.2.1a Optimisation of Conditions

To initiate our studies, we implemented the previously optimised conditions for the gold-catalysed oxidative functionalisation of yndiamides with pyridine *N*-oxides, while using yndiamide **4m** and *N*-pyridyl sulfilimine **179a** instead (Table 5.01, entry 1). Unfortunately, the intended imidazo[1,2-*a*]pyridine product **180a** was not observed, and instead, we obtained an HCl adduct **181** of the yndiamide in good yield (64%, Table 5.01, entry 1). It was hypothesised that this undesired side product resulted from the sulfilimine-assisted elimination of HCl from the solvent, followed by Brønsted acid addition to the yndiamide. Although switching the solvent to toluene suppressed this side reaction, it also resulted in decreased reactivity, as evidenced by the low conversion of **4m** and the absence of identifiable products (Table 5.01, entry 2). Encouragingly, the utilisation of $PicAuCl_2$[175-178, 180] as catalyst furnished **180a** in good yield (60% NMR yield, 61% isolated yield), despite incomplete conversion (Table 5.01, entry 3). Time-dependent TLC analysis suggested that the conversion was stopped even if there was still starting material left. We

conducted a brief screening of various other commonly used gold catalysts, but none of them could enhance the yield or conversion, which further highlighted the superiority of the $PicAuCl_2$ catalyst (Table 5.01, entries 4, 5).

Table 5.01 Optimisation of conditions: solvent and catalyst.



4m **179a** (2.0 eq.) **180a** **181**

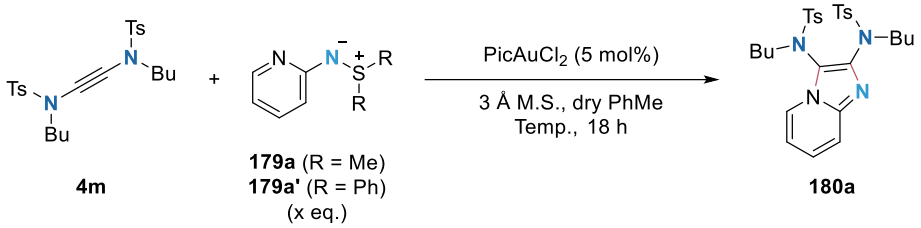
Entry	Catalyst	Solvent	180a Yield	181 Yield	Conversion
1	$IPrAuNTf_2$ [a]	DCE	-	64%	(100%)
2	$IPrAuNTf_2$ [a]	PhMe	-	-	12%
3	$PicAuCl_2$	PhMe	60% (61%)	-	73% (69%)
4	$(\mathbf{Ar}O)_3PAuNTf_2$	PhMe	7%	-	15%
5	$Ph_3PAuNTf_2$	PhMe	-	-	0%

Reactions were conducted on 0.05 mmol scale with [**4m**] = 0.50 M; yields and conversions were determined by ^1H NMR spectroscopy using dimethyl sulfone as internal standard; yields in parentheses are isolated yields on 0.1 mmol scale; conversions in parentheses were calculated based on recovered unreacted yndiamide on 0.1 mmol scale; catalysts $LAuNTf_2$ were prepared *in situ* by premixing the corresponding LAuCl pre-catalyst and $AgNTf_2$; **Ar** = 2,4-di-*tert*-butylphenyl; [a] $IPrAuNTf_2$ was commercially available.

We attributed the incomplete consumption of the yndiamide substrate to the coordination of the pyridine moiety of the sulfilimine reagent to the gold catalyst, thereby inhibiting the reaction. To mitigate this effect, we attempted several strategies (Table 5.02). Elevation of the reaction temperature (Table 5.02, entries 1, 2), decreasing the concentration (Table 5.02, entries 3 – 5), or reducing the sulfilimine equivalent (Table 5.02, entries 6, 7) improved the conversion of **4m**, however, no positive influence was observed on the overall yield. Increasing the loading of the gold catalyst resulted in higher conversion but still did not enhance the yield of **180a** (Table 5.02, entry 8). Additionally, no reaction was observed

when using an *S,S*-diphenyl sulfilimine (Table 5.02, entry 9). While we look forward to opportunities to further optimise the reaction conditions, it was decided to use the initial set of reaction conditions (Table 5.01, entry 3) to continue our studies.

Table 5.02 Optimisation of conditions: attempts to improve the conversion.



Entry	Temperature	[4m]	x	Yield	Conversion
1	r.t.	0.50 M	2.0	-	0%
2	100 °C	0.50 M	2.0	46%	91%
3	80 °C	0.25 M	2.0	53%	69%
4	80 °C	0.10 M	2.0	47%	68%
5	80 °C	0.05 M	2.0	56%	81%
6	80 °C	0.50 M	1.6	44%	59%
7	80 °C	0.50 M	1.2	56%	77%
8[a]	80 °C	0.50 M	2.0	58%	81%
9[b]	80 °C	0.50 M	2.0	-	0%

Reactions were conducted on 0.05 mmol scale with **179a** unless stated otherwise; yields and conversions were determined by ^{1}H NMR spectroscopy using dimethyl sulfone as internal standard; [a] Reaction was conducted with $PicAuCl_2$ (10 mol%); [b] **179a′** was used.

5.2.1b Sulfilimine Scope

A brief sulfilimine scope was explored using the relatively well-performing reaction condition in hand (Figure 5.01).

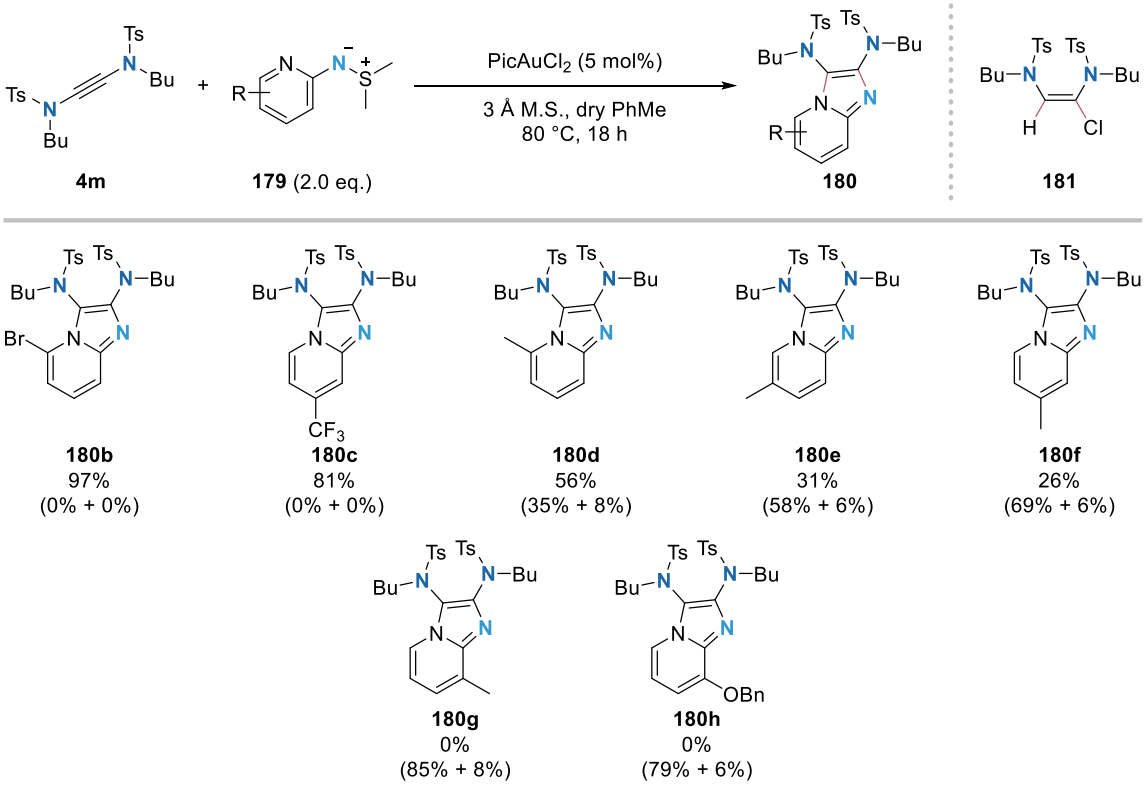
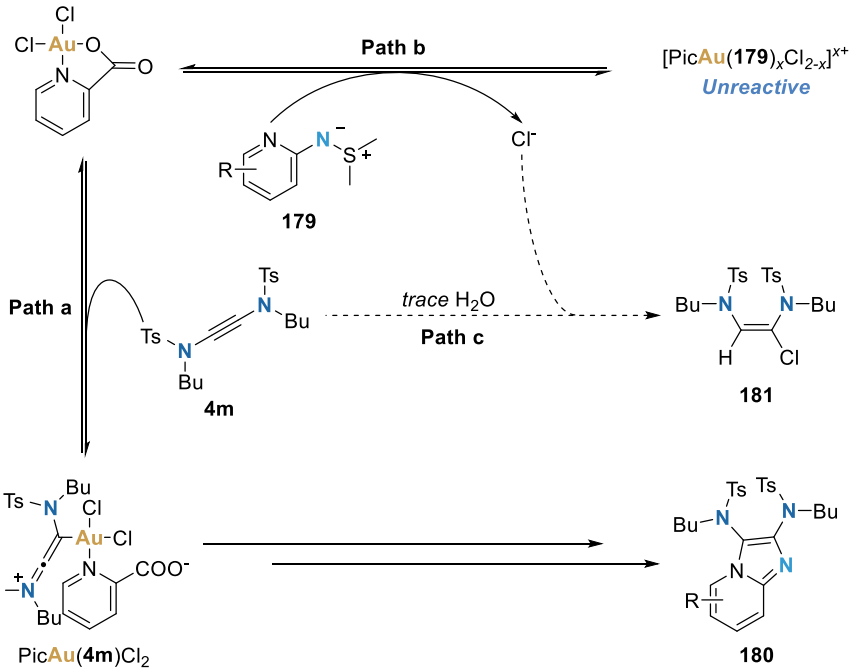


Figure 5.01 Sulfilimine scope for gold(III)-catalysed yndiamide cyclisation. Unless otherwise stated all reactions were performed on 0.1 mmol scale with [**4m**] = 0.5 M; yields refer to isolated yields; yields in parentheses refer to isolated yields of the unreacted yndiamide **4m** and the HCl adduct **181** respectively.

The application of electron-deficient sulfilimines yielded the desired products with excellent yield (**180b**, 97%; **180c**, 81%). In both cases, the yndiamide was completely consumed, which supports our conjecture that the inhibition in conversion previously observed was a result of the coordination of the sulfilimine reagent to the gold catalyst. Methylation at the 2-, 3-, or 4-position of the pyridine ring was tolerated, delivering the corresponding products at compromised yields (**180d**, 56%; **180e**, 31%; **180f**, 26%). However, the inclusion of substituents at the 5-position of the pyridine ring (**180g** and **180h**) impeded the transformation, as no imidazo[1,2-*a*]pyridine products were obtained, and instead, a significant portion of the yndiamide substrate was recovered.

Surprisingly, minor amounts of the HCl adduct **181** were isolated in all cases involving non-electron-deficient sulfilimines, which presumably derive from the $PicAuCl_2$ catalyst,

the only source of chloride in the reaction system. The yield of **181** never exceeded 10%, since only 5 mol% of the $PicAuCl_2$ was used in the reaction. These results helped us to propose a possible model for the inhibitory effects of the sulfilimine reagents on the gold(III)-catalysed transformation of yndiamides (Scheme 5.15). Based on Hashmi *et al.*'s investigation into the mechanism of the $PicAuCl_2$-catalysed functionalisation of ynamides,[118] the keteniminium gold complex PicAu(**4m**)Cl_2 is formed by the displacement of the carboxylate group in the gold catalyst by yndiamide **4m** (**path a**). PicAu(**4m**)Cl_2 can be converted to imidazo[1,2-*a*]pyridines **180** through a similar mechanism as discussed earlier in Scheme 5.08.



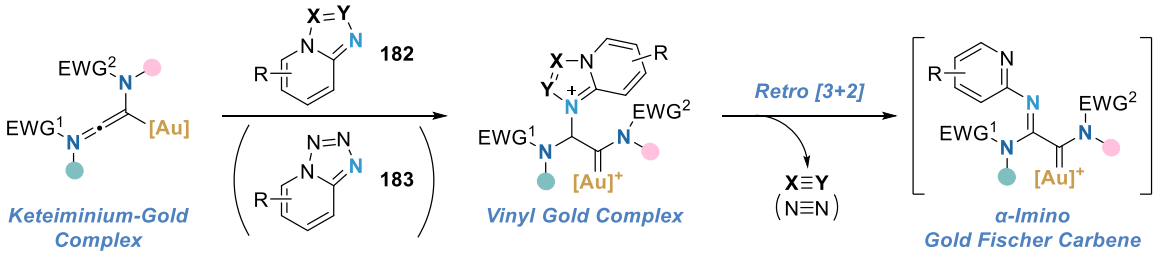
Scheme 5.15 Proposed mechanism for the inhibitory effects of the sulfilimine reagents.

A further possibility is a ligand exchange equilibrium between the $PicAuCl_2$ catalyst and the sulfilimine reagent **179**, which generates an unreactive gold species $[PicAu(\mathbf{179})_xCl_{2-x}]^{x+}$ upon the loss of chloride anions (**path b**). The desired reaction to form **180** would proceed efficiently on the premise that both ligand exchange processes (**path a** and **path b**) were in equilibrium. However, as evidenced by the formation of the HCl adduct **181**, the

chloride anions released from the gold complex can react with the yndiamide **4m** through Brønsted acid addition with trace water (or other H^+ source) in the reaction (with/without the participation of the gold catalyst) (**path c**). These side reactions can shift the equilibrium established in **path b**, leading to the irreversible degradation of the active $PicAuCl_2$ catalyst to the unreactive $[PicAu(\mathbf{179})_xCl_{2-x}]^{x+}$ species. Ultimately, this scenario results in incomplete conversion and low yield of the desired product.

5.2.2 Gold-Catalysed Functionalisation of Yndiamides with Tetrazolo[1,5-*a*]pyridines

Based on our hypothesis that the presence of unmasked pyridine moiety in the nitrene transfer reagent would hinder the gold-catalysed functionalisation of yndiamides through catalyst poisoning, we imagined the inclusion of a transient protecting group on the pyridine nitrogen atom would be the antidote to the catalyst poisoning. In this context, we designed a novel class of nitrene transfer reagents, **182**, featuring a pyridine-fused ring framework (Scheme 5.16). The nucleophilic attack of the keteniminium-gold complex by the nitrene transfer reagent **182** would form a vinyl gold complex which could be converted to the α-imino gold carbene through a retro [3+2] cyclisation. To the best of our knowledge, such mode of reactivity has not been explored in the generation of α-oxo gold carbenes from ynamides and has only been rarely studied in the generation of α-imino gold carbenes.[181] The gold carbene intermediate can undergo formal [3+2] cyclisation again with the pyridine moiety to generate the imidazo[1,2-*a*]pyridine products as discussed above in Scheme 5.14. Inspired by the works of the Chattopadhyay group on the switchable reactivity of tetrazolo[1,5-*a*]pyridines between traditional click chemistry and denitrogenative annulation,[182, 183] we envisaged that tetrazolo[1,5-*a*]pyridines **183** (**X** = **Y** = N) could be competent nitrene transfer reagents in this mode of reactivity.



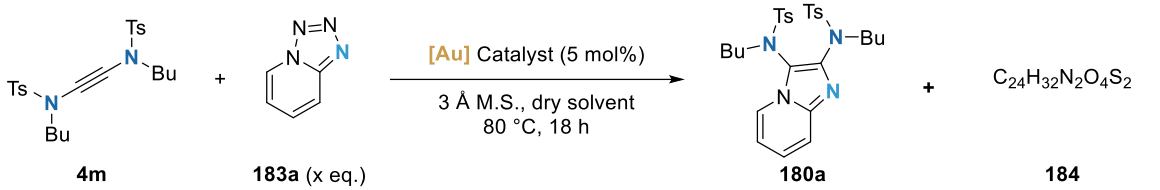
Scheme 5.16 Concept of the gold-catalysed functionalisation of yndiamides with tetrazolo[1,5-*a*]pyridines.

5.2.2a Optimisation of Conditions

In our initial attempt to functionalise yndiamides **4m** with tetrazolo[1,5-*a*]pyridine **183a** (crystal structure included in Chapter VII) under the conditions previously employed for the gold-catalysed reaction with sulfilimines, the desired product **180a** was not observed (Table 5.03, entry 1). Instead, an unknown product **184** was isolated in 23% yield (Table 5.03, entry 1). The chemical formula of **184** was confirmed by HRMS as an isomer of the yndiamide **4m**; however, we were unable to identify its structure through spectroscopic analysis, or X-ray crystallographic analysis. Switching to the (**Ar**O)$_3$PAuNTf$_2$ (**Ar** = 2,4-di-*tert*-butylphenyl) catalyst successfully improved the yield of **180a**, yet still with a significant amount of **184** present in the reaction mixture (Table 5.03, entry 2). The use of DCE as the solvent further enhanced the yield of **180a** while suppressing the formation of **184** (Table 5.03, entry 3).

The presence of compound **184** is likely due to the gold-catalysed isomerisation of yndiamide **4m**, but the reaction mechanism remains unclear. Interestingly, this side product was not observed in our previous studies on the gold-catalysed functionalisation of yndiamides with pyridine *N*-oxides, isoxazoles, or sulfilimines, indicating that this isomerisation pathway is solvent- and/or catalyst-dependent and only occurs in the absence of (reactive) oxygen- or nitrogen-transfer reagents. A control experiment was performed without the addition of nitrene transfer reagents (Table 5.03, entry 4). **184** was produced at a good yield (55%), providing strong evidence for the latter claim.

Table 5.03 Optimisation of conditions.



Entry	Catalyst	Solvent	x	180a Yield	184 Yield
1	$PicAuCl_2$	PhMe	2.0	-	(23%)
2	(**Ar**O)$_3$PAuNTf$_2$	PhMe	2.0	46%	39%
3	(**Ar**O)$_3$PAuNTf$_2$	DCE	2.0	58%	23%
4	(**Ar**O)$_3$PAuNTf$_2$	DCE	0	-	55%
5	(**Ar**O)$_3$PAuNTf$_2$	DCE	3.0	(80%)	-
6	(**Ar**O)$_3$PAuNTf$_2$	DCE	5.0	(93%)	-
7 [a]	(**Ar**O)$_3$PAuNTf$_2$	DCE	2.0	(75%)	-
8 [b]	(**Ar**O)$_3$PAuNTf$_2$	DCE	2.0	(58%)	-
9 [c]	(**Ar**O)$_3$PAuNTf$_2$	DCE	2.0	(79%)	-
10 [d]	(**Ar**O)$_3$PAuNTf$_2$	DCE	2.0	69% (68%)	-
11 [d]	(**Ar**O)$_3$PAuNTf$_2$	DCE	0	-	-

Reactions were conducted under a nitrogen atmosphere on 0.05 mmol scale with [**4m**] = 0.50 M; yields were determined by ^{1}H NMR spectroscopy using dimethyl sulfone as internal standard; yields in parentheses are isolated yields on 0.1 mmol scale; catalysts $LAuNTf_2$ were prepared *in situ* by premixing the corresponding LAuCl pre-catalyst and $AgNTf_2$; **Ar** = 2,4-di-*tert*-butylphenyl. [a] The yndiamide was added to the reaction in 3 portions with a 2 h time interval in between. [b] The yndiamide was added to the reaction in 10 portions with a 1 h time interval in between. [c] The yndiamide was added to the reaction in 4 portions with a 2 h time interval in between. [d] The reaction was conducted under air.

Increasing the amount of tetrazolo[1,5-*a*]pyridine reagent in the reaction was found to effectively suppress the undesired isomerisation of the yndiamide and improve the yield of **180a** (Table 5.03, entries 5–6). Similarly, the slow addition of the yndiamide to the reaction also had a positive impact on the yield of the desired product (Table 5.03, entries 7–9). However, both approaches have drawbacks: using a large excess of the tetrazolo[1,5-

a]pyridine reagent would result in unnecessary material waste, while the slow addition of the yndiamide was not scalable.

Notably, it was observed that the improved yields in entries 7 – 9 of Table 5.03 might indicate that it was unnecessary to conduct this reaction under an inert atmosphere since during the process of slow addition of the yndiamide, the reaction vial was repeatedly exposed to air, which led to significant contamination of the nitrogen atmosphere inside. Building upon this observation, the reaction was tested under air (Table 5.03, entry 10). Remarkably, **180a** was isolated in good yield (68%), and the formation of **184** was not detected. This unforeseen outcome implied that the reaction could potentially benefit from exposure to air, as the gold-catalysed isomerisation of yndiamide might be inhibited by components in the air, most likely oxygen. A control experiment was conducted under air without adding the tetrazolo[1,5-*a*]pyridine **183a**, but this only resulted in decomposition of the yndiamide starting material **4m** (Table 5.03, entry 11). Hence, the conditions outlined in entry 10 of Table 5.03 were deemed appropriate as a practical and efficient approach for the gold-catalysed functionalisation of yndiamides using tetrazolo[1,5-*a*]pyridines.

5.2.2b Tetrazolo[1,5-*a*]pyridine Scope

With optimised conditions in hand, the scope of the reaction was investigated using various tetrazolo[1,5-*a*]pyridines (Figure 5.02). The use of electron-rich or phenyl-substituted tetrazolo[1,5-*a*]pyridines afforded the desired product at excellent yields (**180i**, 93%; **180j**, 91%). Methylation at the 2-position of the pyridine ring was well-tolerated, yielding **180d** at a good yield (56%); however, methylation at the 4-position led to incomplete conversion of the yndiamide, and the corresponding product **180f** was isolated at only 37% yield. Using tetrazolo[1,5-*a*]quinoline **183k** in the reaction produced **180k** in low yield (18%) with a significant amount of **184** (38%) formed. The tetrazolo[1,5-*a*]pyridine reagent bearing a

dimethyl acetal group was also examined, and although the overall yield was good (69%), partial deprotection of the dimethyl acetal group was observed leading to some of the aldehyde product being formed (**180m**, 27%).

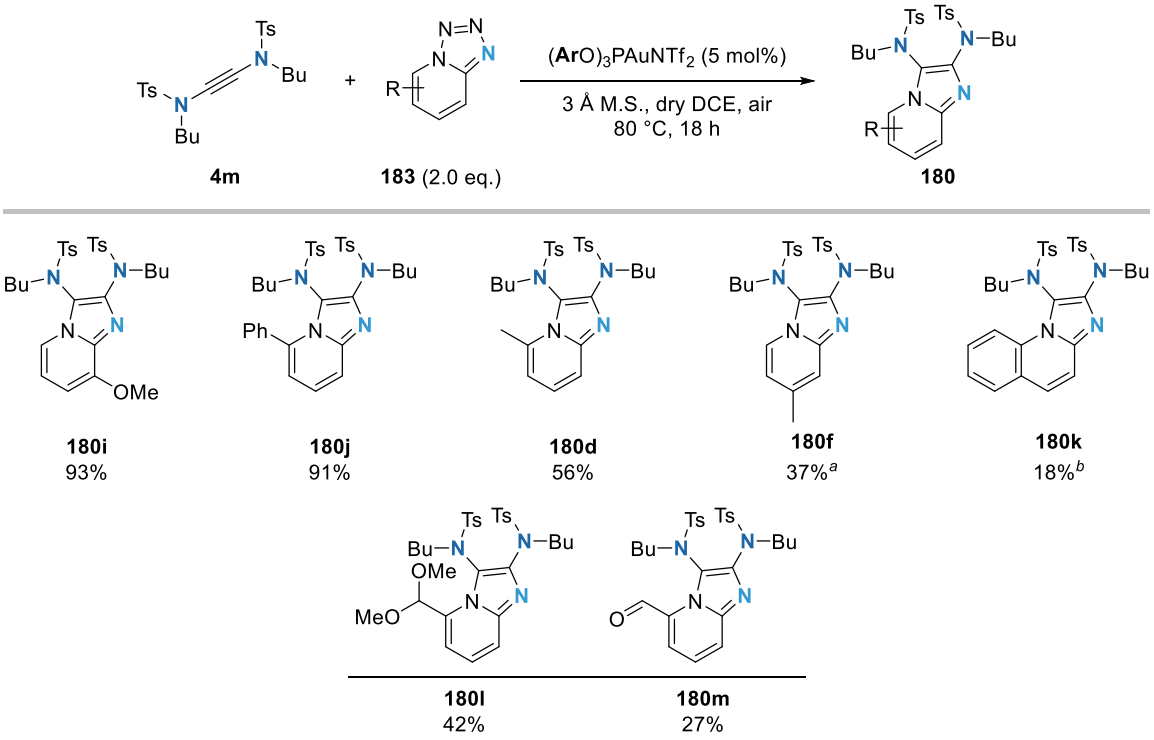
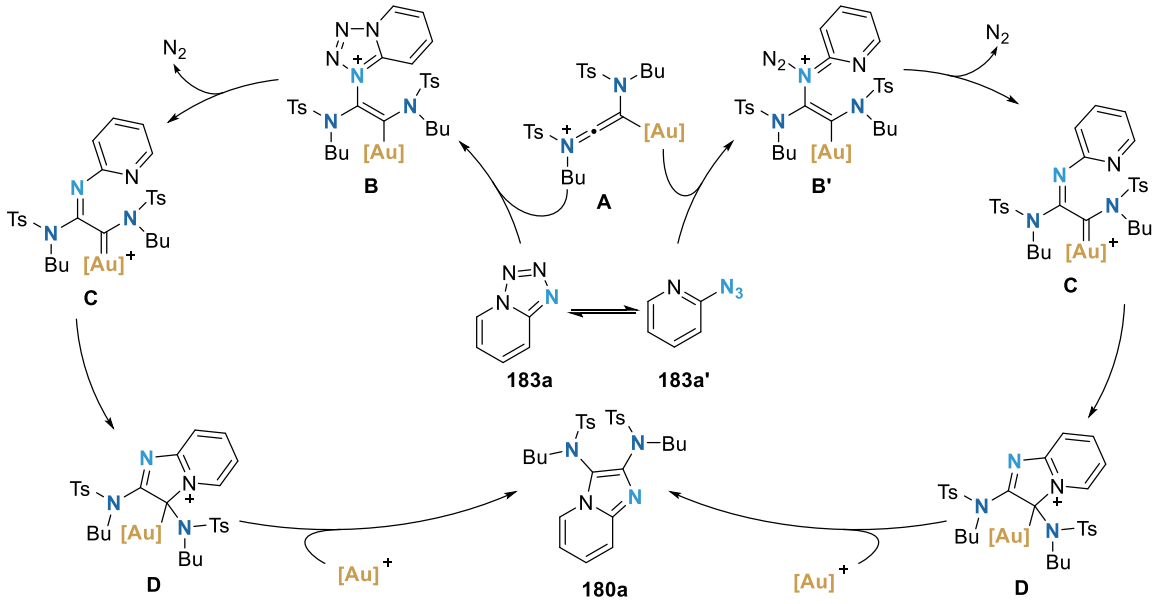


Figure 5.02 Tetrazolo[1,5-*a*]pyridine scope for gold-catalysed yndiamide cyclisation. Unless otherwise stated all reactions were performed under air and on 0.1 mmol scale with [**4m**] = 0.5 M; **Ar** = 2,4-di-*tert*-butylphenyl; yields refer to isolated yields of **180**. [a] 33% of the unreacted yndiamide was recovered. [b] 38% of **184** was isolated from the reaction mixture as well.

5.2.2c Mechanistic Proposal

Two possible reaction mechanisms for this transformation are shown in Scheme 5.17. Similar to all the mechanisms discussed in previous chapters, the reaction is initiated by the formation of the keteniminium gold complex **A** (not shown in Scheme 5.17). The subsequent nucleophilic attack onto **A** can, however, occur by two different pathways, as the tetrazolo[1,5-*a*]pyridine **183a** and the 2-azidopyridine **183a′** may co-exist in equilibrium.[184-188] In the case of **183a** serving as the nucleophile, vinyl gold complex **B** will

be formed, which can undergo further (formal) retro [3+2] cycloaddition to generate *α*-imino gold carbene **C**. On the other hand, in the case of **183a′** serving as the nucleophile, vinyl gold complex **B′** will be formed and the same gold carbene intermediate **C′** can be generated in a mechanism analogous to the cases of organic azides (see Scheme 5.01).



Scheme 5.17 Proposed reaction mechanism.

The same gold carbene intermediate **C** will be formed regardless of the different mechanisms. It can then participate in a [3+2] cyclisation event with the pyridine sidechain to form intermediate **D**, subsequent deauration of which delivers the final product **180a**. Unfortunately, based on the experimental results we collected, we are currently unable to differentiate between the two reaction pathways, and we look forward to opportunities to probe the proposed mechanisms.

5.3 Conclusions

To summarise, we have presented a prototype protocol for the gold-catalysed functionalisation of yndiamides with sulfilimines to synthesise imidazo[1,2-*a*]pyridines, which are important motifs in medicinal chemistry. However, the conversion rate of the reaction was hindered by the sulfilimine potentially poisoning the gold catalyst. To address this limitation, we employed tetrazolo[1,5-*a*]pyridines as novel nitrene transfer reagents to construct the same imidazo[1,2-*a*]pyridine scaffolds. The optimisation of conditions revealed that the gold-catalysed functionalisation of yndiamide with imidazo[1,2-*a*]pyridines benefited from exposure to air, resulting in reduced side product formation. Our proposed reaction mechanism for the gold-catalysed functionalisation of yndiamides with tetrazolo[1,5-*a*]pyridines involved two possible pathways since the tetrazolo[1,5-*a*]pyridine reagents may isomerise *in situ* to 2-azidopyridines. We are eagerly awaiting opportunities to further explore both transformations, more optimisation of conditions, investigation of the reaction scope and regioselectivity studies. We believe, upon the complete development of these two strategies, they will become another significant contribution to the growing diversity of yndiamide chemistry.

C H A P T E R

VI

Conclusions and Future Directions

Previous chapters have demonstrated the versatility and utility of the gold-catalysed functionalisations of yndiamides in the construction of a diverse array of 1,2-diaminated compounds, most of which are of high synthetic interest and potential medicinal importance. Regioselectivity in these transformations could be achieved by simple approaches, and thorough DFT investigations have also shed light on the regioselectivity-determining scenarios. This chapter will summarise our major findings and research progress so far, and will also discuss potential future directions that these methodologies can take to expand their applicability.

6.1 Conclusions

Chapter II described the gold(I)-catalysed oxidation of yndiamides with pyridine *N*-oxides to synthesise unnatural amino acid derivatives. It represents the first example of the generation and functionalisation of *α*-oxo gold Fischer carbene intermediates from yndiamides.

Following this project, Chapter III explored the gold(I)-catalysed cyclisation of yndiamides with isoxazoles to deliver a series of highly substituted 2,3-diaminopyrroles *via* *α*-imino gold Fischer carbenes. Furthermore, a switchable reactivity between [3+2] and [5+2] cyclisation could be achieved by using benzisoxazoles. In both of the projects above, remarkable regioselectivity could be established by introducing subtle steric bias between the two alkyl substituents on the nitrogen atoms of the yndiamides.

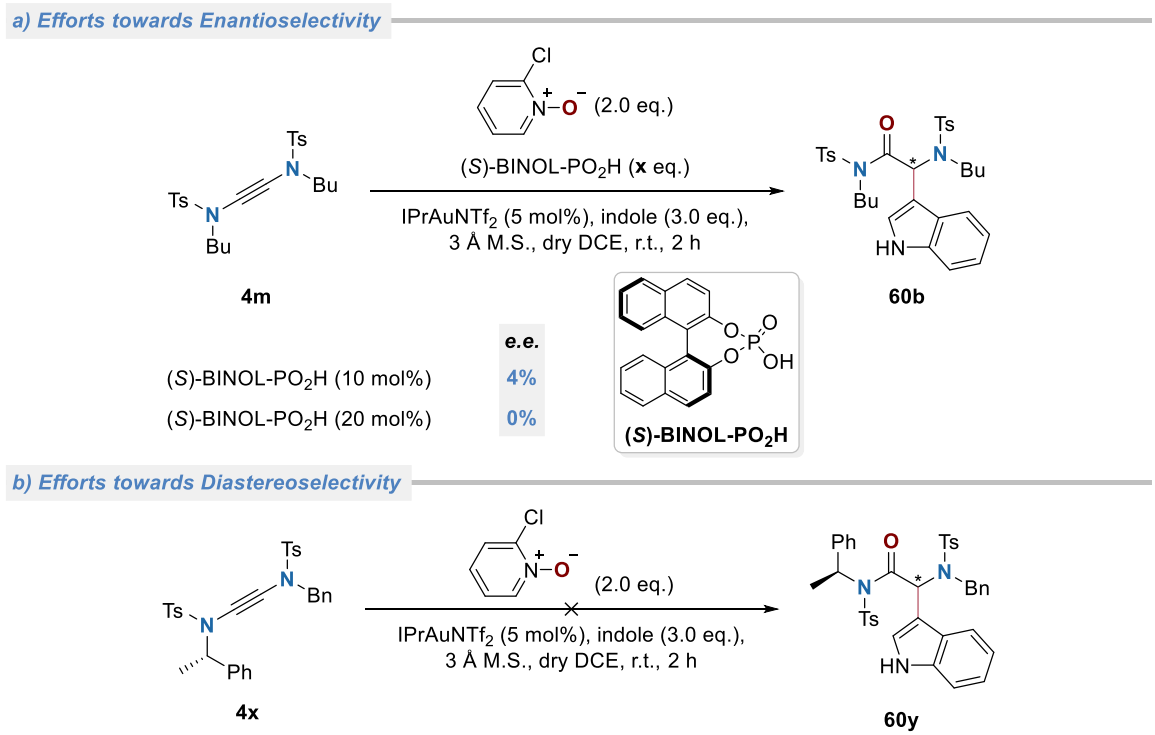
Based on the experimental data collected in Chapter III, Chapter IV presented the DFT investigation of the reaction mechanism for the gold-catalysed cyclisation of yndiamides and isoxazoles. The reaction energy profile of the symmetric yndiamide included the main catalytic cycle leading to the major product, as well as pathways accounting for the formation of all the side products. Moreover, studies of the catalytic cycle concerning non-symmetric yndiamides revealed a Curtin-Hammett-type scenario for isoxazole addition as the key to the regioselectivity.

Finally, Chapter V introduced an ongoing project on the gold-catalysed functionalisation of yndiamides with sulfilimines for the synthesis of imidazo[1,2-*a*]pyridines. In addition, the development of a novel nitrene-transfer reagent, tetrazolo[1,5-*a*]pyridines, in the generation of *α*-imino gold Fischer carbenes from yndiamides was also discussed.

6.2 Future Directions

6.2.1 Asymmetric Gold(I)-Catalysed Functionalisation of Yndiamides with Pyridine *N*-Oxides

The development of effective synthesis towards enantioenriched (unnatural) amino acid derivatives has long been a hotspot in biological and medicinal chemistry research.[189, 190] We are hopeful that the exploration of the asymmetric gold(I)-catalysed functionalisation of yndiamides with pyridine *N*-oxides (Chapter II) will become a great addition to this field. Commonly applied strategies in asymmetric gold catalysis involve the use of chiral ligands,[191, 192] or chiral counterions.[193-195]



Scheme 6.01 Efforts towards asymmetric gold(I)-catalysed functionalisation of yndiamides and pyridine *N*-oxides. Reactions were conducted on 0.1 mmol scale with [**4**] = 0.50 M; *e.e.* was determined by chiral HPLC.

However, our previous experimentation with chiral ligands failed to produce any enantioselectivity.[27] We then shifted our focus to the application of chiral phosphoric acids

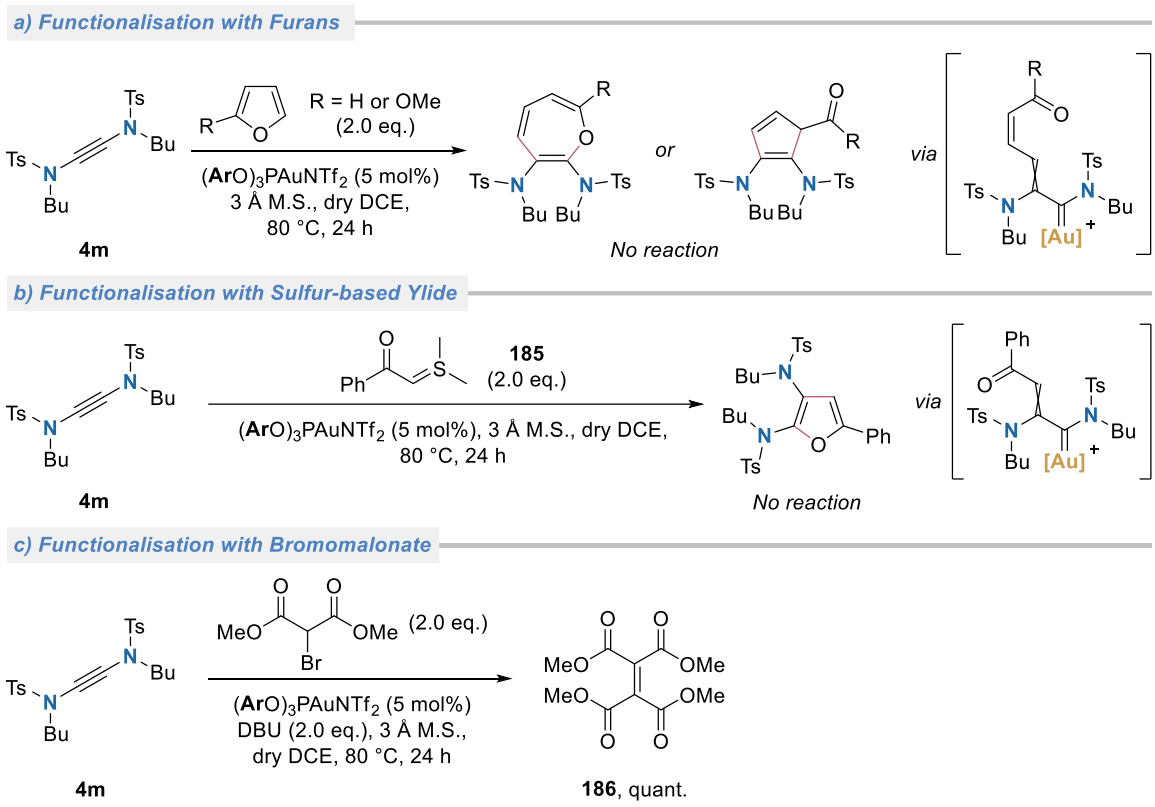
as a potential chiral proton source in the reaction (Scheme 6.01a). Unfortunately, our initial attempts resulted in no improvement of the enantiomeric excess, despite raising the amount of the chiral phosphoric acid additive employed (Scheme 6.01a). Having experienced failure in achieving the enantioselectivity of this transformation, we imagined diastereoselectivity could be established using a chiral yndiamide **4x**. However, subjecting such yndiamide **4x** under the standard conditions led to unanalyzable complex results (Scheme 6.01b), presumably due to imperfect regioselectivity and/or gold-catalysed isomerisation of yndiamide (similar to that observed in Chapter V).

Our enthusiasm and interest in further exploring this direction remain strong. Based on our current findings, we speculated that the utilisation of a ligand designed and synthesised *ad hoc* or the use of chiral *N*-oxides[90] might be the solution to this problem.

6.2.2 Gold(I)-Catalysed Functionalisation of Yndiamides *via* Vinyl Gold Carbenes

The successful and facile generation of α-imino gold carbenes from yndiamides with various nitrene-transfer reagents (Chapter III and Chapter V) prompted us to investigate the possibility of forming vinyl gold carbenes from yndiamides through similar mechanisms. Currently, catalytic methods for the generation of vinyl gold carbene intermediates primarily involve various carbene transfer pathways,[196-200] while the utilisation of external vinyl-transfer reagents for such purpose has not been reported. In this context, we tested several potential vinyl-transfer reagents (Scheme 6.02). Furans (Scheme 6.02a) and sulfur-based ylide **185** (Scheme 6.02b) were both unreactive with yndiamide **4m** even at elevated reaction temperatures and extended reaction times. The use of 2-bromomalonate, however, resulted in the dimerisation (**186**)[201] of the bromomalonate in quantitative yield. While these results did not meet our initial expectations, we still highly

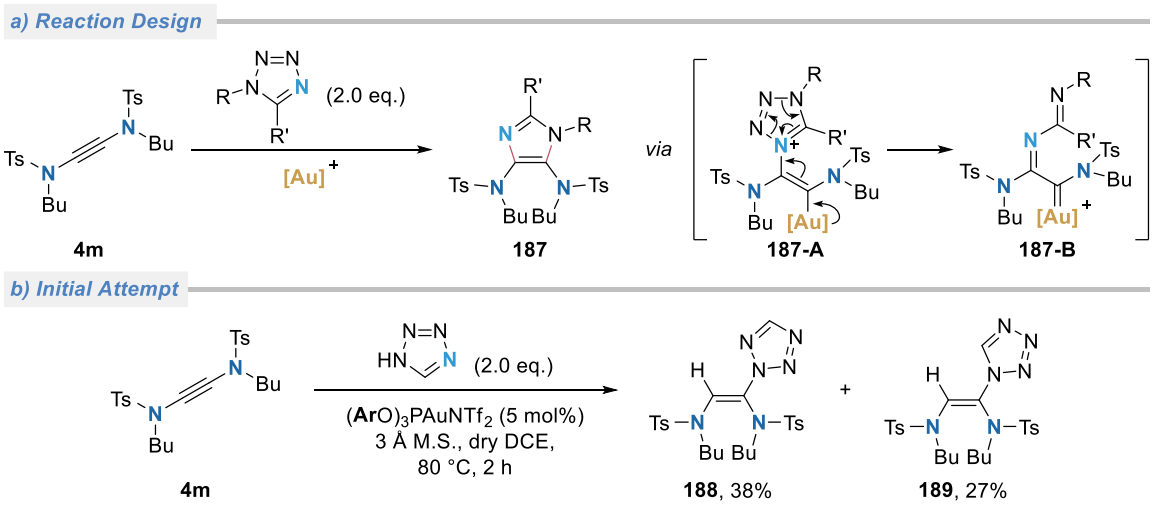
value the insights we gained from these studies. These initial results suggest the need for further optimisation of reaction conditions and the screening of other vinyl-transfer reagents to achieve the generation of vinyl gold carbenes. The successful development of this mode of reactivity would enable us to construct a broader range of 1,2-diaminated cyclic compounds from yndiamides, and thus we are motivated to continue exploring this direction.



Scheme 6.02 Efforts towards gold(I)-catalysed functionalisation of yndiamides with vinyl-transfer reagents. Reactions were conducted on 0.1 mmol scale with [**4m**] = 0.50 M; **Ar** = 2,4-di-*tert*-butylphenyl.

6.2.3 Gold-Catalysed Functionalisation of Yndiamides with Tetrazoles

Chapter V disclosed an ongoing project concerning the use of tetrazolo[1,5-*a*]pyridines in the generation of *α*-imino gold carbenes from yndiamides. Despite the successful reactions, our proposed reaction mechanism (Scheme 5.17) remains ambiguous. In an effort to probe the reaction mechanism, and to expand the scope of the tetrazolo[1,5-*a*]pyridine reagents, we anticipated the use of tetrazoles in the reaction to forge diaminoimidazoles **187** (Scheme 6.03a). Since the generation of the *α*-imino gold carbene intermediate **187-B** can only be from the retro [3+2] cyclisation of the vinyl gold complex **187-A**, the successful application of tetrazoles in this transformation would serve as strong evidence to our previously proposed reaction mechanism in Scheme 5.17. However, our initial attempt only resulted in the formation of a mixture of two hydroarylation products **188** (crystal structure available) and **189** at moderate yield (38% for **188** and 27% for **189**) (Scheme 6.03b). This finding suggests that multiple substitutions on the isoxazole ring might be necessary for the desired reaction, and further optimisation of reaction conditions is also required. It nonetheless may offer other opportunities for yndiamide functionalisation via heterocycle addition reactions.



Scheme 6.03 Gold-catalysed functionalisation of yndiamides with tetrazoles; **Ar** = 2,4-di-*tert*-butylphenyl.

6.3 Closing Remarks

In the opening chapter of this thesis, we identified three objectives of this study; and here, in the closing chapter, we feel confident to announce that all three questions have been properly answered. Yndiamides are inarguably competent and powerful substrates in gold-catalysed functionalisations to build a diverse array of 1,2-diaminated compounds. Several oxygen- and nitrogen-transfer reagents were explored, showcasing the great versatility and utility of this reactivity; and regioselectivity could be established in most cases. These findings not only broaden the horizon of yndiamide chemistry but also provide points for in-depth DFT-assisted mechanistic discussions which are rarely seen in the literature concerning ynamides. We hope that this work can serve as a great entry point and solid foundation for the future expedition into the vast unknown space of yndiamide chemistry.

C H A P T E R

VII

Experimental Section

7.1 Materials and Physical Measurements

Reagents and Solvents: All reagents were purchased from commercial suppliers and used as received without dilution or further purification unless stated otherwise. Anhydrous solvents were obtained from solvent dispenser units having been passed through an activated alumina column under nitrogen. Anhydrous DCE was prepared by refluxing commercially purchased non-anhydrous DCE over calcium hydride followed by distillation onto 3 Å molecular sieves under nitrogen.

Chromatography: Reactions were monitored by TLC on Merck Kieselgel 60 aluminium-back TLC plated with UV254 fluorescent indicator. Spots were visualised by quenching of UV fluorescence under 254 nm radiation or by $KMnO_4$ or vanillin staining. Flash column chromatography was performed on silica gel (Merck Geduran® Si 60 (40 – 63 μm)) using the solvent system described per compound. Preparative LPLC was performed by a Teledyne CombiFlash® Rf200 Chromatography system using the disposable flash column and solvent condition described per compound. HPLC was carried out on an Agilent 1200 series HPLC system under UV (210 – 254 nm) detection. Stationary and mobile phase conditions were described per analysis.

NMR Spectroscopy: ^{1}H, ^{13}C, ^{19}F, and ^{31}P NMR spectra were obtained by a Bruker AVIII400 HD Nanobay, a Bruker NEO 400 Nanobay or a Bruker AVIII HD 500 instrument at room temperature using TOPSPIN software. Assignments were determined either based on unambiguous chemical shift/coupling patterns or from COSY and/or HSQC experiments. Peak multiplicities are defined as: s = singlet, d = doublet, t = triplet, q = quartet, quin. = quintet, sext. = sextet, hept. = heptet, oct. = octet, m = multiplet, brs. = broad singlet, app. = apparent. Coupling constants (*J*) are reported to the nearest 0.1 Hz.

Infrared Spectroscopy: All infrared spectra were recorded by a Bruker Tensor 27 FT-IR spectrometer on a sample thin film prepared on a diamond ATR module. Maximum absorption (ν_{max}) was reported in wavenumbers (cm^{-1}).

Mass Spectrometry: HRMS were measured by a Bruker Microflex TOF spectrometer using electrospray ionisation (ESI). Mass-to-charge ratios are calculated to 4 decimal places from the molecular formula, and all reported experimental results are within 5 ppm of difference compared to the calculated ones.

Melting Points: Melting points were measured on a Griffin melting point apparatus and are reported without correction.

Optical Rotation: Optical rotations were recorded on a Perkin-Elmer 241 or 341 polarimeter with a 1 dm path length cell (using the sodium D line, 589 nm). Specific rotations ($[\boldsymbol{\alpha}]_D^{25}$) are given in deg dm^2 g^{-1}. Concentration (*c*) is reported in g/100 mL.

7.2 General Procedures

7.2.1 Synthesis of Yndiamides and Corresponding Coupling Partners

7.2.1a Synthesis of Sulfonamides

Modified from a literature procedure.[202] To a solution of corresponding amine (1.1 eq.) and triethylamine (1.2 eq.) in DCM (1 mL $mmol^{-1}$ of amine substrate) at 0 °C was slowly added the corresponding sulfonyl chloride (1.0 eq.). The reaction mixture was then warmed to room temperature and stirred until completion by TLC. Upon completion, the reaction mixture was diluted with water and extracted three times with DCM. The organic layer was combined, washed with 1 M HCl, then with brine, and dried over Na_2SO_4. The solvent was removed *in vacuo* to afford the product, which was used without further purification unless stated otherwise.

7.2.1b Synthesis of Phosphoramidates

Modified from a literature procedure.[203] To a heat gun-dried round-bottom flask equipped with a stirrer bar was added 2,2-dimethylpropane-1,3-diol (1.0 eq.). The flask was purged under high vacuum for 30 s and backfilled with nitrogen (the vacuum cycle was repeated twice more). DCM (anhy., 2 mL $mmol^{-1}$ of diol) and triethylamine (3.3 eq.) were added to the flask before it was cooled to 0 °C. While stirring, phosphoryl chloride (1.0 eq.) was added dropwise to the solution. The mixture was stirred at 0 °C for 30 min before the corresponding amine (1.3 eq.) was added slowly. The reaction was then gradually warmed to room temperature and stirred until completion by TLC. Upon completion, the reaction was diluted with water and extracted three times with DCM. The organic phase was combined, dried over Na_2SO_4, and then concentrated *in vacuo* to give the crude phosphoramidate product which was purified by flash chromatography or recrystallisation as described per compound.

7.2.1c Synthesis of 1,1-Dibromoenamides

According to our previous work.[25]

Step 1: To a heat gun-dried round-bottom flask equipped with a stirrer bar was added corresponding sulfonamide (1.0 eq.). The flask was purged under high vacuum for 30 s and backfilled with argon (the vacuum cycle was repeated twice more). The sulfonamide was then dissolved in THF (anhy., 6 mL $mmol^{-1}$ of sulfonamide substrate) and cooled to 0 °C. While stirring at 0 °C, an *n*-butyllithium solution in hexane (1.1 eq.) was added dropwise. The reaction mixture was stirred at 0 °C for another 30 min when a persistent colour change occurred which indicates complete lithiation.

In another heat gun-dried round-bottom flask was added 1*H*-benzotriazole-1-carboxaldehyde (BtCHO)[204] (1.2 eq.). The flask was purged under high vacuum for 30 s

and backfilled with argon (this process was repeated twice more). THF (2.5 mL $mmol^{-1}$ of BtCHO) was added, and the resulting solution was added dropwise to the previously prepared lithiated sulfonamide solution at 0 °C. The reaction mixture was gradually warmed to room temperature and stirred until completion by TLC. Upon completion, it was quenched by pouring into a separatory funnel containing Et_2O and 2 M K_2CO_3 solution. The reaction flask was also rinsed alternately with Et_2O and water into the same separatory funnel. The organic layer was separated, washed three times with 2 M K_2CO_3 solution, dried over Na_2SO_4, and concentrated *in vacuo* to give the crude formamide which was used in the next step without further purification.

Step 2: To a heat gun-dried round-bottom flask equipped with a stirrer bar was added triphenylphosphine (4.0 eq.). The flask was purged under high vacuum for 30 s and backfilled with argon (this process was repeated twice more). DCM (anhy., 6 mL $mmol^{-1}$ of formamide substrate) was added, and the mixture was stirred to dissolution at −30 °C. A solution of tetrabromomethane (2.0 eq.) in DCM (anhy., 1 mL $mmol^{-1}$ of formamide substrate) was prepared in a similar way. While stirring at −30 °C the tetrabromomethane solution was added slowly to the triphenylphosphine solution and the mixture was stirred at –30 °C until it turned into deep orange.

To a heat gun-dried flask was added the previously prepared crude formamide (1.0 eq.). The flask was then purged under high vacuum for 30 s and backfilled with argon (this process was repeated twice more). DCM (anhy., 3 mL $mmol^{-1}$ of formamide substrate) was added and the resulting solution was added dropwise to the deep orange solution prepared previously at −30 °C. The reaction mixture was slowly warmed to room temperature and stirred until completion by TLC. The reaction mixture was concentrated *in vacuo* and purified by flash chromatography in the stated eluent to afford the 1,1-dibromoenamide product.

7.2.1d Synthesis of Yndiamides

According to our previous work.[25] To a heat gun-dried flask equipped with a stirrer bar was added the corresponding sulfonamide or phosphoramidate (1.0 eq.), 1,1-dibromoenamide (1.1 eq.), and 1,10-phenanthroline (40 mol%). The vial was purged under high vacuum for 10 min and backfilled with argon (the vacuum cycle was repeated twice more). Then the flask was placed inside the glovebox where CuI (20 mol%) and Cs_2CO_3 (3.0 eq.) were added. The flask was removed from the glovebox and, again, purged under high vacuum for 30 s and then backfilled with argon. THF (anhy., 3.3 mL $mmol^{-1}$ of sulfonamide substrate) was added, and the mixture was stirred vigorously at 60 °C until completion by TLC. The reaction mixture was cooled to room temperature and filtered through a Celite® pad (eluted with EtOAc). The filtrate was concentrated *in vacuo* and purified by flash chromatography using the stated eluent to afford the yndiamide product.

7.2.2 Synthesis of Oxygen- or Nitrogen-Transfer Reagents

7.2.2a Synthesis of Pyridine *N*-Oxide

Modified from a literature procedure.[205] To a solution of 3-chlorobenzene-1-carboperoxoic acid (3.0 eq.) in DCM (1.3 M) was added the corresponding pyridine (1.0 eq.) dropwise. The mixture was stirred at room temperature overnight. Upon completion, the reaction mixture was washed three times with 10% NaOH solution and the combined aqueous phases were extracted six times with $CHCl_3$. The organic phase was combined, dried over Na_2SO_4, concentrated *in vacuo,* and purified by flash chromatography in the stated eluent to give the pyridine *N*-oxide.

7.2.2b Synthesis of 3,5-Substituted Isoxazoles

Modified from a literature procedure.[206] To a solution of hydroxylamine hydrochloride (1.05 eq.) in 1:1 *t*-BuOH/H_2O (0.25 M) was added the corresponding aldehyde (1.00 eq.) and NaOH (1.05 eq.). The reaction was stirred at room temperature until completion by TLC. Chloramine T trihydrate (1.05 eq.) was then added in small portions, followed by copper sulfate pentahydrate (3 mol%), copper turning (1 pc, *ca.* 50 mg) and the corresponding alkyne (1.05 eq.). The reaction mixture was adjusted to ~ pH 6 by adding 1 M NaOH solution, and then it was stirred at room temperature until completion by TLC. Upon completion, the reaction was poured onto ice, and dilute aqueous ammonia was added to remove all the copper salts. The crude product was collected by filtration and further purified by recrystallization or column chromatography (described per compound) to give the final product.

7.2.2c Synthesis of Benzo[*d*]isoxazoles

Step 1: In a round-bottom flask was mixed the corresponding salicylaldehyde (1.0 eq.), hydroxylamine hydrochloride (1.5 eq.) and $NaHCO_3$ (2.0 eq.) in EtOH (0.5 M). The reaction mixture was stirred at room temperature until completion by TLC. Upon completion, the reaction mixture was diluted with water and extracted three times with DCM. The organic layer was combined, dried over Na_2SO_4, and concentrated *in vacuo* to give the crude salicylaldoxime which was used in the next step without further purification.

Step 2: *Modified from a literature procedure.*[207] To a heat gun-dried flask was added the crude salicylaldoxime (1.00 eq.) prepared in the previous step and PPh_3 (1.25 eq.). The flask was purged under high vacuum for 30 s and backfilled with argon (this cycle was repeated twice more). Anhydrous THF (0.05 M) was added to dissolve the starting material, and the solution was cooled to 0 °C in an ice bath. DIAD (1.20 eq.) was added slowly to

the solution over 1 h. The reaction mixture was then warmed to room temperature, concentrated *in vacuo* and purified by column chromatography (column conditions described per reaction) to afford the final product.

7.2.2d Synthesis of Sulfilimines

Modified from a literature procedure.[177] In a round-bottom flask containing a stirrer bar, was dissolved the corresponding amine substrate (1.0 eq.) and dimethyl sulfide (1.1 eq.) in anhydrous DCM (1.6 mL per mmol of amine substrate). The solution was then cooled to −20 °C before NCS (1.1 eq.) was added as solid. The mixture was then stirred at −20 °C until completion by TLC. Upon completion, a sodium methoxide solution (25% w/w in MeOH, 1.1 eq.) was added, and the mixture was stirred overnight before the reaction was diluted with water and extracted three times with DCM. The organic phase was combined, dried over Na_2SO_4, concentrated *in vacuo*, and purified by column chromatography (column conditions described per compound) to afford the sulfilimines product.

7.2.2e Synthesis of Tetrazolo[1,5-*a*]pyridines

Modified from a literature procedure.[208] In a round-bottom flask equipped with a stirrer bar was dissolved the corresponding 2-bromopyridine (1.0 eq.) in EtOH/H_2O (7 : 3 v/v, 5 mL per mmol of the 2-bromopyridine substrate). The solution was degassed before sodium azide (3.0 eq.), CuI (10 mol%), *N*,*N*′-dimethylethylenediamine (15 mol%), and sodium ascorbate (5 mol%) were added. The mixture was then stirred and refluxed at 120 °C until completion by TLC. Upon completion, the reaction mixture was diluted with water (6 mL per mmol of the 2-bromopyridine substrate). The pH of the solution was adjusted to ~ 9 before it was extracted 3 times with DCM. The organic phase was combined, washed with brine, and dried over Na_2SO_4. The solvent was removed *in vacuo* and purified by column

chromatography (conditions described per compound) to afford the tetrazolo[1,5-*a*]pyridine product.

7.2.3 General Procedures for Gold-catalysed Functionalisations

7.2.3a Synthesis of Gold(I) Pre-catalysts

Modified from a literature procedure.[209] Inside the glovebox, to a heat gun-dried vial equipped with a stirrer bar was added chloro(dimethylsulfide)gold(I) (1.0 eq.). The vial was then removed from the glovebox and kept in the dark. The vial was purged under high vacuum for 30 s and backfilled with argon. DCM (anhy., 0.1 M) was added to dissolve the chloro(dimethylsulfide)gold(I). A solution of the corresponding ligand (0.1 M in anhydrous DCM) was prepared in a similar way. The ligand solution was then added to the previously prepared chloro(dimethyl sulfide)gold(I) solution while stirring at room temperature. The reaction mixture was stirred for 2 h at room temperature under argon in the dark, then the solvent was removed *in vacuo* to give the Au(I) pre-catalyst.

7.2.3b Gold-Catalysed Functionalisation of Yndiamide with Pyridine *N*-Oxide

To a heat gun-dried vial containing 3 Å molecular sieves and a stirrer bar was added yndiamide (1.0 eq.), 2-chloropyridine *N*-oxide (2.0 eq.). The vial was then purged under high vacuum for 30 s and backfilled with argon (the vacuum cycle was repeated twice more). The vial was then moved inside a glovebox where it was charged with $IPrAuNTf_2$ (5 mol%). The vial was then removed from the glovebox and the corresponding nucleophile (3.0 eq.) and DCE (anhy., 0.5 M of yndiamide) were added (if the nucleophile is non-volatile, it was added together with yndiamide and 2-chloropyridine *N*-oxide). The mixture was stirred under an argon atmosphere in the dark until completion by TLC. Upon

completion, it was concentrated *in vacuo* and purified by flash chromatography using the stated eluent to give the product.

7.2.3c Robustness Tests

In a heat gun-dried vial containing 3 Å molecular sieves and a stirrer bar was added *N*,*N*'-(ethyne-1,2-diyl)bis(*N*-butyl-4-methylbenzenesulfonamide) (24 mg, 0.050 mmol, 1.0 eq.), 2-chloropyridine *N*-oxide (13 mg, 0.10 mmol, 2.0 eq.), indole (18 mg, 0.15 mmol, 3.0 eq.). The vial was then purged under high vacuum for 30 s and backfilled with argon (the vacuum cycle was repeated twice more). The vial was then moved inside a glovebox where it was charged with $IPrAuNTf_2$ (2.0 mg, 2.3 μmol, 5 mol%). The vial was then removed from the glovebox, and corresponding external additive (1.0 eq.) and DCE (anhy., 0.1 mL) were added (if the additive is non-volatile, it was added together with yndiamide and 2-chloropyridine *N*-oxide). The reaction mixture was then stirred at room temperature under an argon atmosphere in the dark for 2 h. The mixture was then concentrated *in vacuo* and dimethylsulfone (5 mg) was added to the residue as the internal standard for subsequent ^1H NMR analysis. The NMR yield of *N*-butyl-2-((*N*-butyl-4-methylphenyl)sulfonamido)-2-(1*H*-indol-3-yl)-*N*-tosylacetamide was thus determined.

7.2.3d Gold-Catalysed Cyclisation of Yndiamides with Isoxazoles

To a heat gun-dried vial containing a stirrer bar and 3 Å molecular sieves was added the corresponding yndiamide (1.0 eq.). The vial was purged under high vacuum for 30 s and backfilled with argon (this vacuum cycle was repeated twice more). The vial was then moved into the glovebox where chloro[tris(2,4-di-*tert*-butylphenyl)phosphite]gold(I) (5 mol%) and silver bis(trifluoromethanesulfonyl)imide (5 mol%) were added. DCE (anhy., 0.5 M) and the corresponding isoxazole (2.0 eq.) were added after the vial was removed

from the glovebox (the isoxazole reagent was added to the vial together with yndiamide before moving into the glovebox if it is non-volatile). The reaction mixture was stirred at the stated temperature under an argon atmosphere in the dark until completion by TLC. Upon completion, unless otherwise stated, the reaction mixture was concentrated *in vacuo* and purified by column chromatography (column conditions described per compound) to give the final product.

7.2.3e Gold-Catalysed Functionalisation of Yndiamides with Sulfilimines

To a heat gun-dried vial containing a stirrer bar and 3 Å molecular sieves were added the corresponding yndiamide (1.0 eq.) and sulfilimine (2.0 eq.). The vial was purged under high vacuum for 30 s and backfilled with argon (this vacuum cycle was repeated twice more). The vial was then moved into the glovebox where dichloro(2-pyridinecarboxylato)gold (5 mol%) was added. Toluene (anhy., 0.5 M) was added after the vial was removed from the glovebox. The reaction mixture was stirred at 80 °C under nitrogen atmosphere in the dark until completion by TLC. Upon completion, the reaction mixture was concentrated *in vacuo* and purified by column chromatography (column conditions described per compound) to give the final product.

7.2.3f Gold-catalysed Functionalisation of Yndiamides with tetrazolo[1,5-*a*]pyridines

To a glass vial containing a stirrer bar and 3 Å molecular sieves were added the corresponding yndiamide (1.0 eq.) and tetrazolo[1,5-*a*]pyridine (2.0 eq.). The vial was left uncapped and moved into the glovebox where chloro[tris(2,4-di-*tert*-butylphenyl)phosphite]gold(I) (5 mol%) and silver bis(trifluoromethanesulfonyl)imide (5 mol%) were added. The vial was then removed from the glovebox and still left open to air before DCE (anhy., 0.5 M) was added and the vial was capped with a screw cap

immediately afterwards. The reaction mixture was stirred at 80 °C in dark until completion by TLC. Upon completion, the reaction mixture was concentrated *in vacuo* and purified by column chromatography (column conditions described per compound) to give the final product.

7.3 Chapter II Characterisation Data

7.3.1 Regioselectivity: Determination of the regioisomeric ratio

The r.r. between **61t**/**61t′** and **61u**/**61u′** were determined by ^{1}H NMR spectroscopic analysis of the corresponding crude reaction mixture (Figure 7.01 – 7.02).

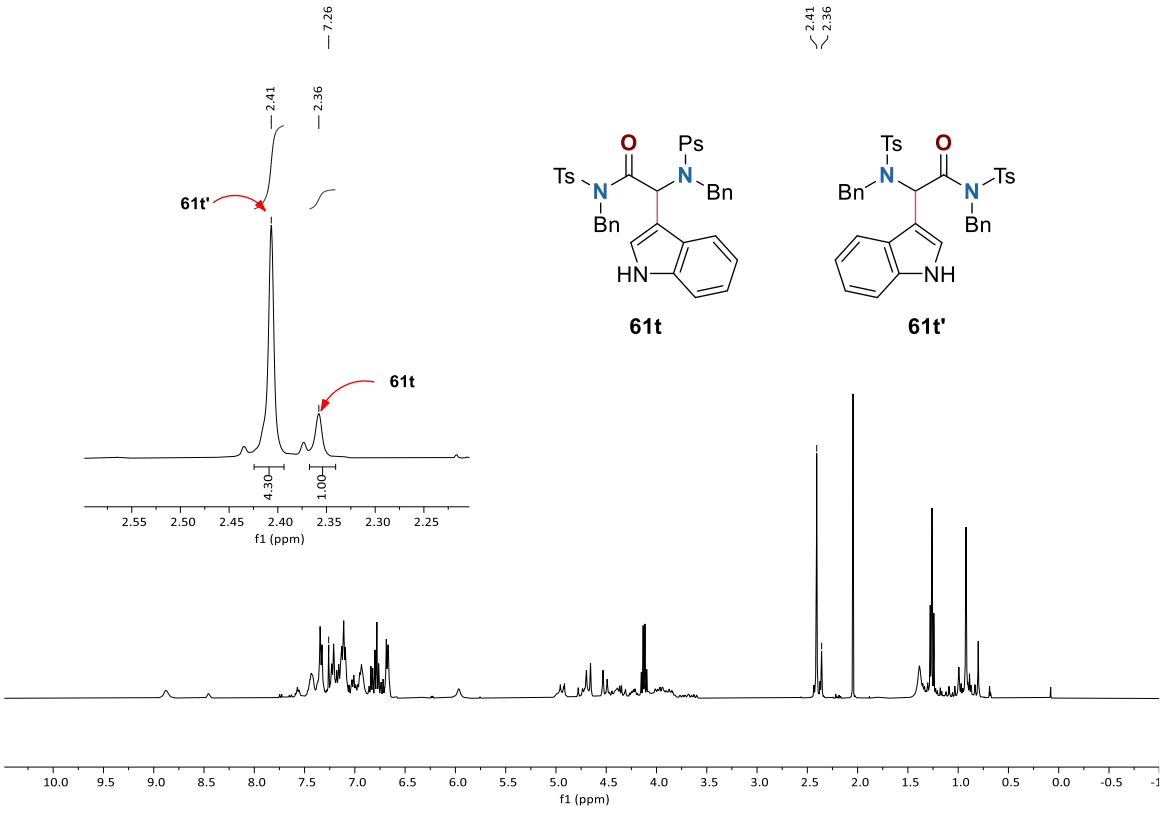


Figure 7.01 ^{1}H NMR Spectrum of **61t**/**61t′** mixture. Integrated peak: TsCH_3, showing that **61t**:**61t′** ≃ 1:4.3.

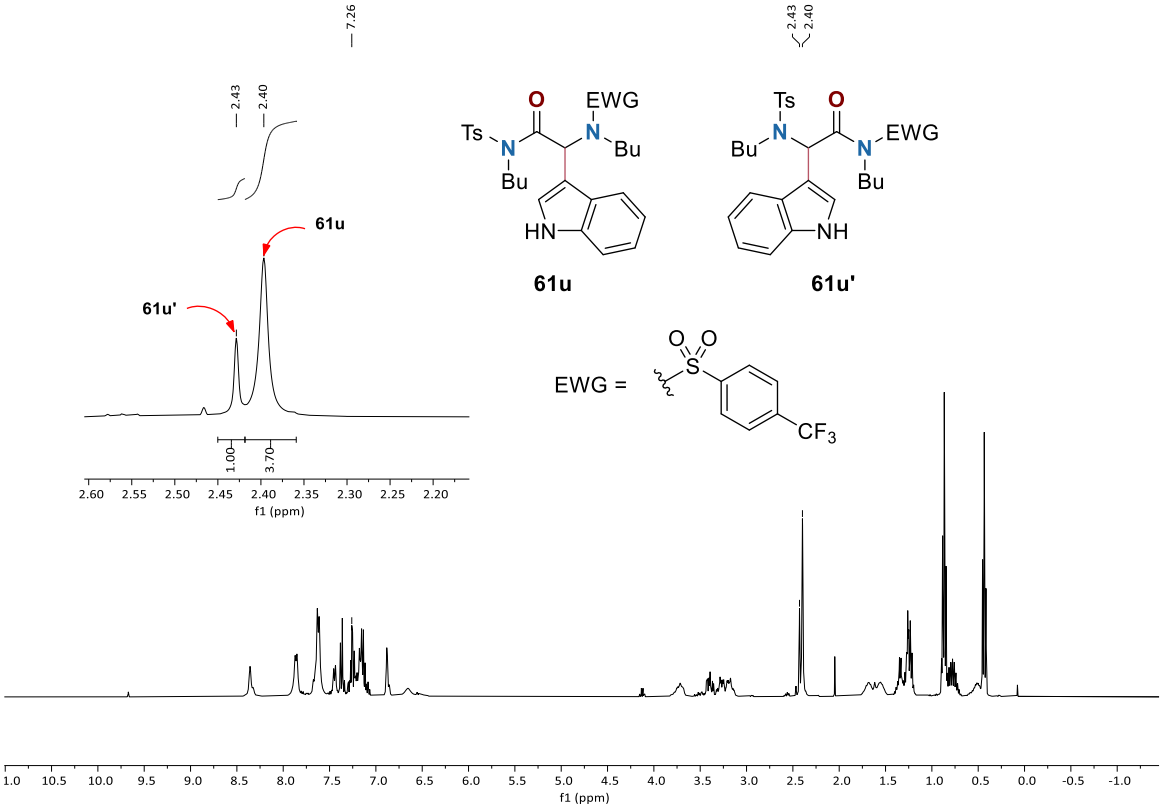


Figure 7.02 ^{1}H NMR Spectrum of **61u**/**61u′** mixture. Integrated peak: TsCH_3, showing that **61u**:**61u′** ≈ 3.7:1.

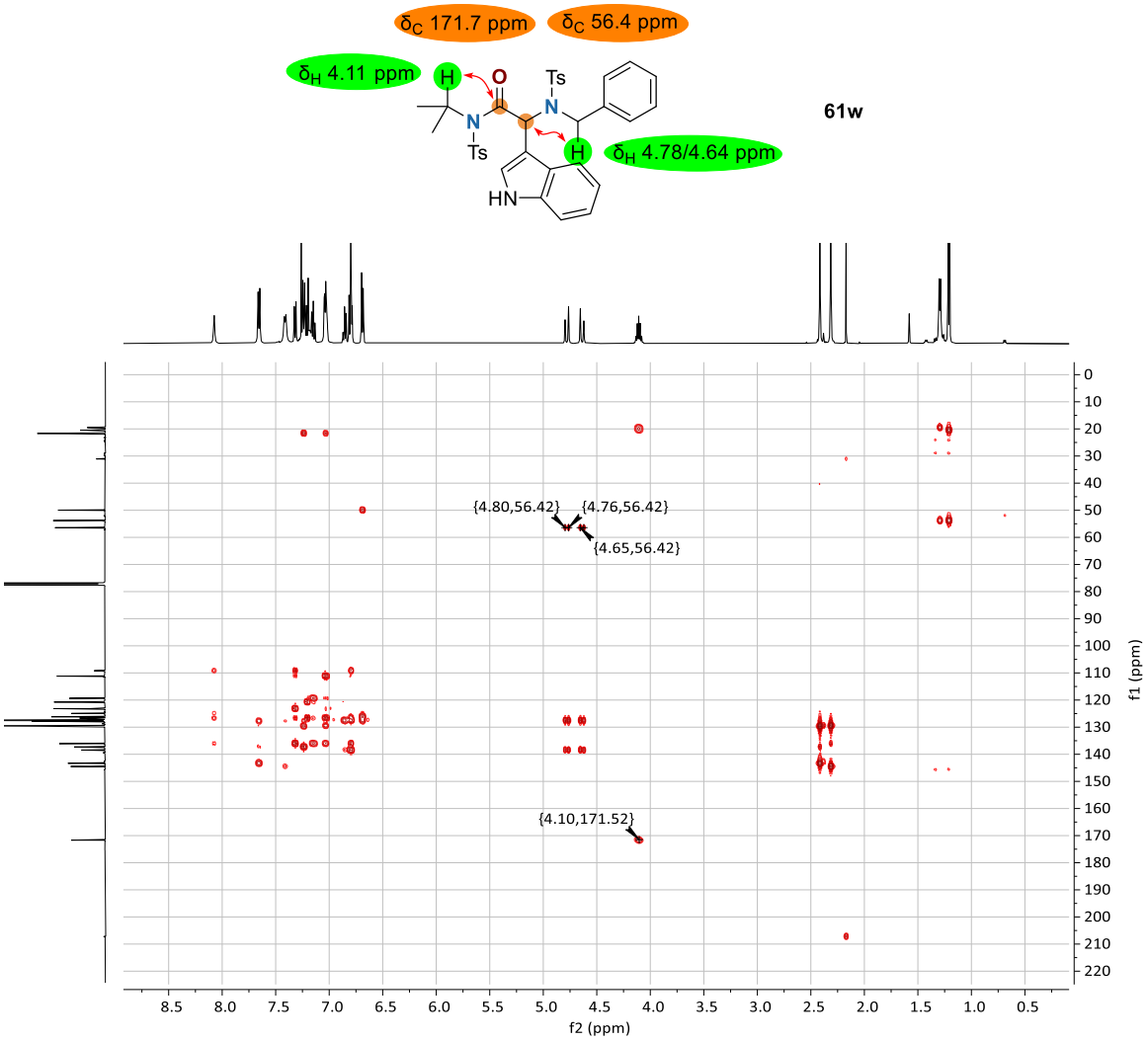
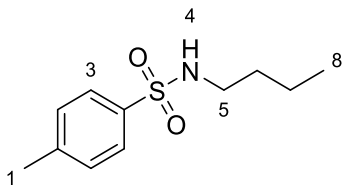


Figure 7.03 ^{1}H – ^{13}C HMBC (500 MHz / 126 MHz, $CDCl_3$) of **3w**. The picked peaks show the marked correlation between protons and carbons in **3w**, confirming its structure is as proposed.

7.3.2 Sulfonamides and Phosphoramidates

N-Butyl-4-methylbenzenesulfonamide, 1a



ZT020

Synthesised from *n*-butylamine (5.7 mL, 57.7 mmol, 1.1 eq.), triethylamine (8.8 mL, 63.0 mmol, 1.2 eq.) and 4-toluenesulfonylchloride (10.0 g, 52.5 mmol, 1.0 eq.) with general

procedure **7.2.1a**. Recrystallisation from DCM/pentane afforded the title compound (10.8 g, 47.6 mmol, 91%) as a colourless solid.

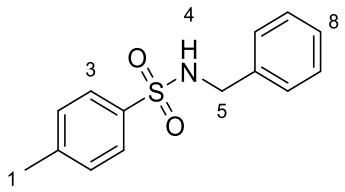
IR (thin film, ν_{max}/cm^{-1}) 3281, 2960, 2873, 1599, 1425, 1323, 1158, 1093, 815, 623.

^{1}H NMR (400 MHz, $CDCl_3$) δ_H 7.75 (2H, d, *J* = 8.1 Hz, H3), 7.31 (2H, d, *J* = 8.1 Hz, H2), 4.38 (1H, s, H4), 2.98 – 2.88 (2H, m, H5), 2.43 (3H, s, H1), 1.50 – 1.38 (2H, m, H6), 1.35 – 1.22 (2H, m, H7), 0.85 (3H, t, *J* = 7.3 Hz, H8).

^{13}C NMR (101 MHz, $CDCl_3$) δ_C 143.4, 137.1, 129.8, 127.2, 43.0, 31.7, 21.6, 19.8, 13.6.

Data are consistent with literature values.[202]

***N*-Benzyl-4-methylbenzenesulfonamide, 1b**



ZT125

Synthesised from benzylamine (6.3 mL, 57.7 mmol, 1.1 eq.), triethylamine (8.8 mL, 63.0 mmol, 1.2 eq.) and 4-methylbenzenesulfonyl chloride (10.0 g, 52.5 mmol, 1.0 eq.) with general procedure **7.2.1a**. Recrystallisation from DCM/pentane afforded the title compound (13.5 g, 51.5 mmol, 98%) as a colourless solid.

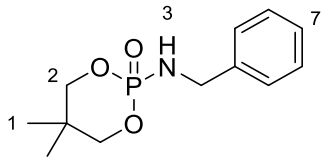
IR (thin film, ν_{max}/cm^{-1}) 3269, 1599, 1454, 1320, 1155, 1058, 906, 812, 729, 662;

^{1}H NMR (400 MHz, $CDCl_3$) δ_H 7.76 (2H, d, *J* = 8.3 Hz, H3), 7.33 – 7.24 (5H, m, H2, H7, H8), 7.22 – 7.17 (2H, m, H6), 4.73 (1H, s, H4), 4.12 (2H, d, *J* = 5.7 Hz, H5), 2.44 (3H, s, H1);

^{13}C NMR (101 MHz, $CDCl_3$) δ_C 143.7, 137.1, 136.4, 129.9, 128.8, 128.1, 128.0, 127.3, 47.4, 21.7.

Data are consistent with literature values.[210]

2-(Benzylamino)-5,5-dimethyl-1,3,2-dioxaphosphinane 2-oxide, 1c



ZT128

Synthesised from 2,2-dimethylpropane-1,3-diol (4.50 g, 42.8 mmol, 1.0 eq.), triethylamine (15.0 g, 0.15 mol, 3.4 eq.), phosphoryl chloride (4.0 mL, 42.8 mmol, 1.0 eq.) and benzylamine (5.5 g, 51.3 mmol, 1.2 eq.) with general procedure **7.2.1b**. Recrystallisation from EtOAc/pentane afforded the title compound (9.20 g, 36 mmol, 84%) as a colourless solid.

IR (thin film, ν_{max}/cm^{-1}) 3152, 2959, 2878, 1455, 1370, 1262, 1224, 1131, 1059, 1003, 945, 912, 892, 823, 775, 724, 694, 628;

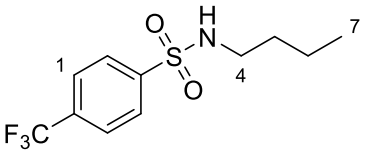
^{1}H NMR (400 MHz, $CDCl_3$) δ_H 7.38 – 7.28 (4H, m, H5, H6), 7.33 – 7.22 (1H, m, H7), 4.35 – 4.26 (2H, m, H2), 4.18 (2H, d, *J* = 10.0 Hz, H4), 3.82 (2H, dd, *J* = 19.9, 11.2 Hz, H2), 3.14 (1H, s, H3), 1.20 (3H, s, H1), 0.89 (3H, s, H1);

^{13}C NMR (101 MHz, $CDCl_3$) δ_C 139.3 (d, $^{3}J_{C–P}$ = 6.3 Hz), 128.7, 127.6, 127.4, 76.4 (d, $^{2}J_{C–P}$ = 5.4 Hz), 45.5, 32.0 (d, $^{3}J_{C–P}$ = 4.9 Hz), 22.2, 20.9. *Note: the two H1 methyl groups show two different peaks.*

^{31}P NMR (162 MHz, $CDCl_3$) δ_P 5.04;

Data are consistent with literature values.[203]

***N*-Butyl-4-(trifluoromethyl)benzenesulfonamide, 1d**



ZT093

Synthesised from *n*-butylamine (0.9 mL, 9.1 mmol, 1.1 eq.), triethylamine (1.4 mL, 9.8 mmol, 1.2 eq.) and 4-(trifluoromethyl)benzenesulfonyl chloride (2.00 g, 8.2 mmol, 1.0 eq.) with general procedure **7.2.1a**. Recrystallisation from DCM/pentane afforded the title compound (2.17 g, 7.8 mmol, 94%) as a colourless solid.

m.p. 76 – 78 °C;

R_f 0.36 ($CHCl_3$);

IR (thin film, ν_{max}/cm^{-1}) 3265, 2980, 1325, 1161, 1128, 1064, 1016, 839, 716;

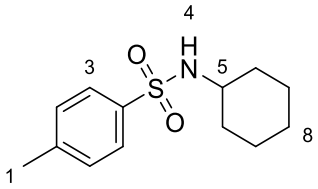
^{1}H NMR (500 MHz, $CDCl_3$) δ_H 8.00 (2H, d, *J* = 8.2 Hz, H2), 7.79 (2H, d, *J* = 8.2 Hz, H1), 4.55 (1H, t, *J* = 5.4 Hz, H3), 2.99 (2H, app. q, *J* = 6.7 Hz, H4), 1.46 (2H, app. quin., *J* = 7.3 Hz, H5), 1.30 (2H, app. sext., *J* = 7.3 Hz, H6), 0.86 (3H, t, *J* = 7.3 Hz, H7).

^{13}C {^{19}F} NMR (126 MHz, $CDCl_3$) δ_C 143.8, 134.5, 127.7, 126.4, 123.4, 43.2, 31.7, 19.8, 13.6.

^{19}F NMR (471 MHz, $CDCl_3$) δ_F -63.13;

HRMS (ESI) m/z: $[M + H]^+$ Calcd for $C_{11}H_{15}O_2NF_3S$ 282.0770, found 282.0771.

***N*-Cyclohexyl-4-methylbenzenesulfonamide, 1e**



ZT099

Synthesised from cyclohexylamine (3.3 mL, 28.9 mmol, 1.1 eq.), triethylamine (4.4 mL, 31.5 mmol, 1.2 eq.) and 4-methylbenzenesulfonyl chloride (5.00 g, 26.2 mmol, 1.0 eq.) with general procedure **7.2.1a**. *N*-cyclohexyl-4-methylbenzenesulfonamide (6.20 g, 24.5 mmol, 93%) was isolated as a colourless solid, which could be used without further purification.

m.p. 75 – 76 °C;

R_f 0.30 ($CHCl_3$);

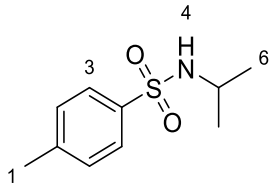
IR (thin film, ν_{max}/cm^{-1}) 3275, 2932, 2856, 1451, 1321, 1157, 1093, 1080, 993, 914, 883, 814, 752, 664;

^{1}H NMR (400 MHz, $CDCl_3$) δ_H 7.77 (2H, d, *J* = 8.2 Hz, H3), 7.29 (2H, d, *J* = 8.2 Hz, H2), 4.68 (1H, d, *J* = 7.5 Hz, H4), 3.18 – 3.05 (1H, m, H5), 2.42 (3H, s, H1), 1.81 – 1.68 (2H, m, H6), 1.68 – 1.57 (2H, m, H7), 1.55 – 1.43 (1H, m, H8), 1.29 – 1.02 (5H, m, H6, H7, H8);

^{13}C NMR (101 MHz, $CDCl_3$) δ_C 143.2, 138.7, 129.7, 127.1, 52.7, 34.0, 25.3, 24.8, 21.6.

Data are consistent with literature values.[211]

***N*-Isopropyl-4-methylbenzenesulfonamide, 1f**



ZT213

Synthesised from isopropylamine (2.4 mL, 28.9 mmol, 1.1 eq.), triethylamine (4.4 mL, 31.5 mmol, 1.2 eq.) and 4-methylbenzenesulfonyl chloride (5.00 g, 26.2 mmol, 1.0 eq.) with general procedure **7.2.1a**. The title compound (5.46 g, 25.6 mmol, 98%) was obtained as a colourless solid, which was used without further purification.

R_f 0.26 ($CHCl_3$);

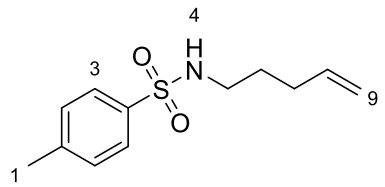
IR (thin film, ν_{max}/cm^{-1}) 3277, 2975, 1599, 1426, 1323, 1302, 1143, 1093, 1001, 892, 815, 751, 664;

^{1}H NMR (400 MHz, $CDCl_3$) δ_H 7.77 (2H, d, *J* = 8.3 Hz, H3), 7.29 (2H, d, *J* = 8.3 Hz, H2), 4.69 – 4.50 (1H, brs., H4), 3.50 – 3.36 (1H, m, H5), 2.42 (3H, s, H1), 1.06 (6H, d, *J* = 6.5 Hz, H6);

^{13}C NMR (101 MHz, $CDCl_3$) δ_C 143.3, 138.3, 129.8, 127.2, 46.2, 23.9, 21.6.

Data are consistent with literature values.[212]

4-Methyl-*N*-(pent-4-en-1-yl)benzenesulfonamide, 1g



ZT257

Modified from a literature procedure.[213] In a round-bottom flask equipped with a stirrer bar were mixed 4-methylbenzenesulfonamide (0.69 g, 4.00 mmol, 1.0 eq.), 5-bromo-1-pentene (0.52 mL, 4.40 mmol, 1.1 eq.), and K_2CO_3 (1.1 g, 8.00 mmol, 2.0 eq.) in acetone (6 mL). The reaction mixture was then stirred and refluxed at 60 °C until completion by TLC. Upon completion, the reaction mixture was concentrated *in vacuo*, quenched with saturated aqueous NH_4Cl, and extracted three times with Et_2O. The organic phase was combined, dried over Na_2SO_4, concentrated *in vacuo* and purified by column chromatography (silica gel, 20% EtOAc/pentane) to afford the title compound (0.65 g, 2.72 mmol, 68%) as a pale yellow viscous oil.

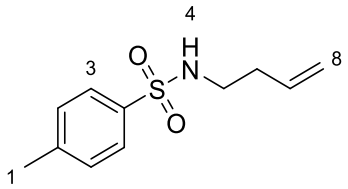
IR (thin film, ν_{max}/cm^{-1}) 3280, 2936, 1425, 1323, 1157, 1094, 913, 814, 663.

^{1}H NMR (400 MHz, $CDCl_3$) δ_H 7.75 (2H, d, *J* = 8.2 Hz, H3), 7.30 (2H, d, *J* = 8.2 Hz, H2), 5.70 (1H, ddt, *J* = 17.0, 10.2, 6.7 Hz, H8), 5.01 – 4.90 (2H, m, H9), 4.57 (1H, s, H4), 2.95 (2H, app. q, *J* = 6.9 Hz, H5), 2.43 (3H, s, H1), 2.04 (2H, app. q, *J* = 7.1 Hz, H7), 1.56 (2H, app. quin., *J* = 7.2 Hz, H6).

^{13}C NMR (101 MHz, $CDCl_3$) δ_C 143.5, 137.4, 137.1, 129.8, 127.2, 115.7, 42.8, 30.8, 28.8, 21.6.

Data are consistent with literature values.[214]

***N*-(But-3-en-1-yl)-4-methylbenzenesulfonamide, 1h**



ZT207

Modified from a literature procedure.[213] A mixture of 4-bromo-but-1-ene (3.0 mL, 29.6 mmol, 1.0 eq.), 4-methylbenzenesulfonamide (5.57 g, 32.5 mmol, 1.3 eq.) and K_2CO_3 (12.3 g, 88.7 mmol, 3.0 eq.) in acetone (60 mL) was heated at reflux (60 °C) until completion as monitored by TLC. The reaction mixture was then cooled to room temperature and concentrated *in vacuo*. Water was added to dissolve the residual, and the aqueous phase was extracted three times with DCM. The organic phase was combined, dried over Na_2SO_4, concentrated *in vacuo* and purified by flash chromatography (silica gel, 20% EtOAc/pentane) to afford the title compound (2.40 g, 10.7 mmol, 36%) as a pale-yellow viscous oil.

R_f 0.44 (20% EtOAc/pentane);

IR (thin film, ν_{max}/cm^{-1}) 3279, 2927, 1426, 1322, 1156, 1093, 918, 814, 662;

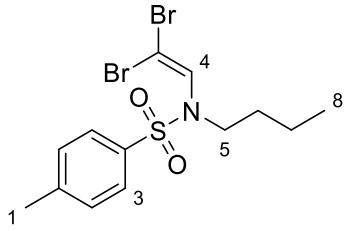
^{1}H NMR (400 MHz, $CDCl_3$) δ_H 7.74 (2H, d, *J* = 8.1 Hz, H3), 7.31 (2H, d, *J* = 8.1 Hz, H2), 5.62 (1H, ddt, *J* = 17.1, 10.3, 6.9 Hz, H7), 5.11 – 4.98 (2H, m, H8), 4.45 (1H, s, H4), 3.02 (2H, app. q, *J* = 6.6 Hz, H6), 2.43 (3H, s, H1), 2.25 – 2.15 (2H, m, H5);

^{13}C NMR (101 MHz, $CDCl_3$) δ_C 143.6, 137.1, 134.3, 129.9, 127.3, 118.4, 42.2, 33.7, 21.7.

Data are consistent with literature values.[215]

7.3.3 1,1-Dibromoenamides

***N*-Butyl-*N*-(2,2-dibromovinyl)-4-methylbenzenesulfonamide, 2a**



This reaction was repeated multiple times, and a clean NMR spectrum could be found under experiment entry ZT023.

Synthesised from *N*-butyl-4-methylbenzenesulfonamide (2.50 g, 11.0 mmol, 1.0 eq.), *n*-butyllithium in hexane (2.5 M in hexane, 4.8 mL, 12.0 mmol, 1.1 eq.), BtCHO (1.94 g, 13.2 mmol, 1.2 eq.), triphenylphosphine (11.6 g, 44.0 mmol, 4.0 eq.), tetrabromomethane (7.30 g, 22.0 mmol, 2.0 eq.) with general procedure **7.2.1c**. Purification by flash chromatography (silica gel, 5% EtOAc/pentane) afforded the title compound (4.00 g, 9.8 mmol, 89%) as a colourless solid.

m.p. 83 – 85 °C;

R_f 0.33 (5% EtOAc/pentane);

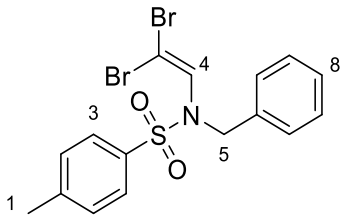
IR (thin film, ν_{max}/cm^{-1}) 2959, 2932, 2871, 1598, 1459, 1353, 1165, 1090, 1031, 860, 814, 717, 656.

^{1}H NMR (400 MHz, $CDCl_3$) δ_H 7.69 (2H, d, *J* = 8.5 Hz, H3), 7.33 (2H, d, *J* = 8.5 Hz, H2), 6.64 (1H, s, H4), 3.30 (2H, t, *J* = 7.5 Hz, H5), 2.44 (3H, s, H1), 1.54 – 1.45 (2H, m, H6), 1.33 (2H, app. sext., *J* = 7.3 Hz, H7), 0.90 (3H, t, *J* = 7.3 Hz, H8).

^{13}C NMR (101 MHz, $CDCl_3$) δ_C 144.2, 135.7, 131.7, 130.0, 127.5, 95.7, 49.1, 30.6, 21.7, 20.0, 13.8.

HRMS (ESI) m/z: $[M + H]^+$ Calcd for $C_{13}H_{18}{}^{79}Br_2NO_2S$ 409.9420; Found 409.9419.

***N*-Benzyl-*N*-(2,2-dibromovinyl)-4-methylbenzenesulfonamide, 2b**



ZT139, ZT140

Synthesised from *N*-benzyl-4-methylbenzenesulfonamide (4.00 g, 15.3 mmol, 1.0 eq.), *n*-butyllithium (2.0 M in hexane, 8.4 mL, 16.8 mmol, 1.1 eq.), BtCHO (2.93 g, 19.9 mmol, 1.3 eq.), tetrabromomethane (10.2 g, 30.6 mmol, 2.0 eq.), and triphenylphosphine (16.1 g, 61.2 mmol, 4.0 eq.) with general procedure **7.2.1c**. Purification by flash chromatography (silica gel, 20% EtOAc/pentane) afforded the title compound (1.43 g, 3.21 mmol, 21%) as a colourless solid.

m.p. 126 – 127 °C;

R_f 0.67 (20% EtOAc/pentane);

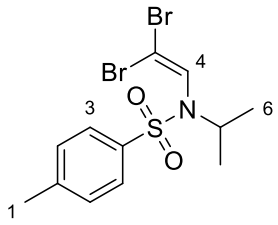
IR (thin film, ν_{max}/cm^{-1}) 3064, 1700, 1598, 1495, 1455, 1401, 1163, 1091, 1028, 900, 815, 760, 729, 697, 657;

^{1}H NMR (400 MHz, $CDCl_3$) δ_H 7.73 (2H, d, *J* = 8.3 Hz, H3), 7.38 – 7.25 (7H, m, H2, H6, H7, H8), 6.63 (1H, s, H4), 4.55 (2H, s, H5), 2.46 (3H, s, H1);

^{13}C NMR (101 MHz, $CDCl_3$) δ_C 144.4, 136.0, 135.2, 131.5, 130.0, 128.8, 128.7, 128.2, 127.6, 97.2, 52.9, 21.8.

Data are consistent with literature values.[25]

***N*-(2,2-Dibromovinyl)-*N*-isopropyl-4-methylbenzenesulfonamide, 2f**



ZT228, ZT229

Synthesised from *N*-isopropyl-4-methylbenzenesulfonamide (2.00 g, 9.38 mmol, 1.0 eq.), *n*-butyllithium (1.4 M in hexane, 7.4 mL, 10.4 mmol, 1.1 eq.), BtCHO (1.68 g, 11.3 mmol, 1.3 eq.), tetrabromomethane (6.22 g, 18.8 mmol, 2.0 eq.), and triphenylphosphine (9.84 g, 37.5 mmol, 4.0 eq.) with general procedure **7.2.1c**. Column chromatography (silica gel, 10% EtOAc/pentane) afforded the title compound (1.91 g, 4.8 mmol, 51%) as a colourless solid.

m.p. 100 °C;

R_f 0.42 (10% EtOAc/pentane);

IR (thin film, ν_{max}/cm^{-1}) 2979, 1597, 1349, 1161, 1007, 858, 812, 721, 651;

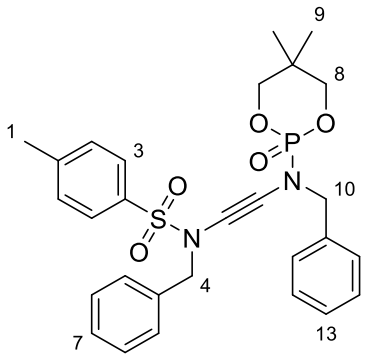
^{1}H NMR (400 MHz, $CDCl_3$) δ_H 7.72 (2H, d, *J* = 8.0 Hz, H3), 7.31 (2H, d, *J* = 8.0 Hz, H2), 6.46 (1H, s, H4), 4.20 (1H, hept., *J* = 7.0 Hz, H5), 2.43 (3H, s, H1), 1.03 (6H, d, *J* = 6.7 Hz, H6).

^{13}C NMR (101 MHz, $CDCl_3$) δ_C 144.0, 136.9, 129.9, 128.1, 127.6, 105.1, 52.8, 21.7, 20.6;

HRMS (ESI) m/z: $[M + H]^+$ Calcd for $C_{12}H_{16}{}^{79}Br_2NO_2S$ 395.9263; Found 395.9263.

7.3.4 Yndiamides

_N_-Benzyl-_N_-((benzyl(5,5-dimethyl-2-oxido-1,3,2-dioxaphosphinan-2-yl)amino)ethynyl)-4-methyl-benzenesulfonamide, 4a



ZT167

Synthesised from 2-(benzylamino)-5,5-dimethyl-1,3,2-dioxaphosphinane 2-oxide (209 mg, 0.82 mmol, 1.0 eq.)**,** _N_-benzyl-_N_-(2,2-dibromovinyl)-4-methylbenzenesulfonamide (402 mg, 0.90 mmol, 1.1 eq.), CuI (31 mg, 0.16 mmol, 0.20 eq.), 1,10-phenanthroline (59 mg, 0.33 mmol, 0.40 eq.) and Cs_2CO_3 (802 mg, 2.5 mmol, 3.0 eq.) with general procedure **7.2.1d**. Column chromatography (silica gel, 50% EtOAc/pentane) afforded the title compound (171 mg, 0.32 mmol, 39%) as a brown solid.

m.p. 118 °C;

R_f 0.28 (50% EtOAc/pentane);

IR (thin film, ν_{max}/cm^{-1}) 2970, 1597, 1409, 1359, 1289, 1168, 1059, 1009, 815, 726, 701;

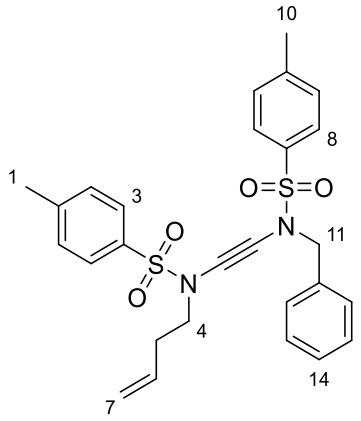
^{1}H NMR (400 MHz, $CDCl_3$) δ_H 7.57 (2H, d, J = 8.3 Hz, H3), 7.34 – 7.29 (3H, m, Ph*H*), 7.29 – 7.17 (7H, m, H2 + Ph*H*), 7.16 – 7.09 (2H, m, Ph*H*), 4.39 – 4.32 (4H, m, H4, H10), 3.97 – 3.79 (4H, m, H8), 2.44 (3H, s, H1), 1.10 (3H, s, H9), 0.69 (3H, s, H9);

^{13}C NMR (101 MHz, $CDCl_3$) δ_C 144.4, 136.8 (d, $^3J_{C-P}$ = 1.5 Hz), 135.1, 134.9, 129.7, 129.4, 128.6 (2C), 128.5, 128.4, 127.9, 127.8, 79.4 (d, $^2J_{C-P}$ = 7.3 Hz), 73.1 (d, $^2J_{C-P}$ = 5.1 Hz), 64.9 (d, $^3J_{C-P}$ = 5.0 Hz), 55.9, 55.8 (d, $^2J_{C-P}$ = 7.5 Hz), 31.9 (d, $^3J_{C-P}$ = 7.3 Hz), 21.9, 21.8, 20.6;

^{31}P NMR (162 MHz, $CDCl_3$) δ_P -4.97.

Data are consistent with literature values.[25]

_N_-Benzyl-_N_-(((_N_-(but-3-en-1-yl)-4-methylphenyl)sulfonamido)ethynyl)-4-methylbenzenesulfonamide, 4c



ZT212

Synthesised from 4-methyl-*N*-(but-3-en-1-yl)benzenesulfonamide (106 mg, 0.50 mmol, 1.0 eq.), *N*-benzyl-*N*-(2,2-dibromovinyl)-4-methylbenzenesulfonamide (245 mg, 0.55 mmol, 1.1 eq.), CuI (19 mg, 0.10 mmol, 0.20 eq.), 1,10-phenanthroline (36 mg, 0.20 mmol, 0.40 eq.) and Cs_2CO_3 (489 mg, 1.50 mmol, 3.0 eq.) with general procedure **7.2.1d**. Column chromatography (silica gel, 20% EtOAc/pentane) afforded the title compound (206 mg, 0.41 mmol, 81%) as a colourless solid.

R_f 0.44 (20% EtOAc/pentane);

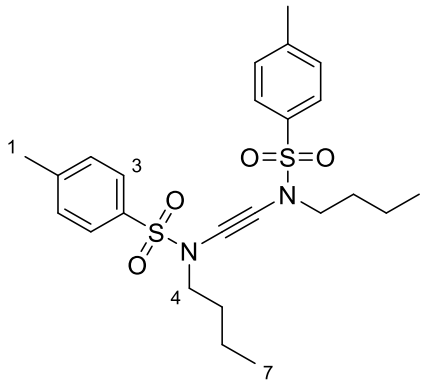
IR (thin film, ν_{max}/cm^{-1}) 3033, 1597, 1411, 1362, 1167, 1089, 813, 752, 656;

^{1}H NMR (400 MHz, $CDCl_3$) δ_C 7.67 (2H, d, *J* = 8.3 Hz, TsC*H*), 7.59 (2H, d, *J* = 8.3 Hz, TsC*H*), 7.30 – 7.22 (7H, m, H2, H9, H13, H14), 7.20 – 7.15 (2H, m, H12), 5.52 (1H, ddt, *J* = 17.1, 10.4, 6.8 Hz, H6), 4.97 – 4.85 (2H, m, H7), 4.49 (2H, s, H11), 3.25 (2H, t, *J* = 7.2 Hz, H4), 2.43 (6H, overlapping singlet, H1, H10), 2.05 (2H, tdd, *J* = 6.9, 5.4, 1.2 Hz, H5);

^{13}C NMR (101 MHz, $CDCl_3$) δ_C 144.7, 144.6, 135.1, 135.0, 134.8, 133.7, 129.8, 129.8, 128.9, 128.6, 128.3, 127.8, 127.7, 117.6, 69.7, 69.6, 56.1, 51.2, 32.1, 21.8 (2C).

Data are consistent with literature values.[25]

***N*,*N'*-(Ethyne-1,2-diyl)bis(*N*-butyl-4-methylbenzenesulfonamide), 4m**



This reaction was repeated multiple times, and a clean NMR spectrum could be found under experiment entry ZT045.

Synthesised from *N*-butyl-4-methylbenzenesulfonamide (355 mg, 1.56 mmol, 1.0 eq.), *N*-butyl-*N*-(2,2-dibromovinyl)-4-methylbenzenesulfonamide (720 mg, 1.75 mmol, 1.1 eq.), CuI (60 mg, 0.32 mmol, 0.20 eq.), 1,10-phenanthroline (113 mg, 0.63 mmol, 0.40 eq.) and Cs_2CO_3 (1.53 g, 4.68 mmol, 3.0 eq.) with general procedure **7.2.1d.** Column chromatography (silica gel, 10% EtOAc/pentane) afforded the title compound (458 mg, 0.96 mmol, 62%) as a colourless solid.

m.p. 63 – 65 °C;

R_f 0.28 (10% EtOAc/pentane);

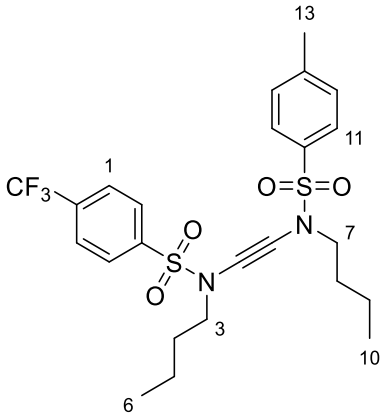
IR (thin film, ν_{max}/cm^{-1}) 2960, 2933, 2873, 1598, 1460, 1412, 1365, 1171, 1090, 1027, 814, 708, 675, 656;

^{1}H NMR (400 MHz, $CDCl_3$) δ_H 7.71 (4H, d, *J* = 8.4 Hz, H3), 7.31 (4H, d, *J* = 8.4 Hz, H2), 3.32 (4H, t, *J* = 7.2 Hz, H4), 2.45 (6H, s, H1), 1.53 (4H, app. quin., *J* = 7.4 Hz, H5), 1.28 (4H, app. sext., *J* = 7.5 Hz, H6), 0.87 (6H, t, *J* = 7.4 Hz, H7);

^{13}C NMR (101 MHz, $CDCl_3$) δ_C 144.5, 135.2, 129.8, 127.7, 69.0, 51.6, 30.0, 21.8, 19.5, 13.7;

HRMS (ESI) m/z: $[M + Na]^+$ Calcd for $C_{24}H_{32}O_4N_2NaS_2$ 499.1696; Found 499.1696.

***N*-Butyl-*N*-(((*N*-butyl-4-(trifluoromethyl)phenyl)sulfonamido)ethynyl)-4-methylbenzenesulfonamide, 4n**



ZT112, ZT121, ZT225

Synthesised from *N*-butyl-4-(trifluoromethyl)benzene-sulfonamide (311 mg, 1.10 mmol, 1.0 eq.**),** *N*-butyl-*N*-(2,2-dibromovinyl)-4-methylbenzene-sulfonamide (500 mg, 1.22 mmol, 1.1 eq.), CuI (42 mg, 0.22 mmol, 0.20 eq.), 1,10-phenanthroline (80 mg, 0.44 mmol, 0.40 eq.) and Cs_2CO_3 (1.08 g, 3.3 mmol, 3.0 eq.) with general procedure **7.2.1d**. Column chromatography (silica gel, 20% Et_2O/pentane) afforded the title compound (330 mg, 0.62 mmol, 57%) as a colourless oil.

R_f 0.38 (20% Et_2O/pentane);

IR (thin film, ν_{max}/cm^{-1}) 2962, 2066, 1694, 1405, 1323, 1169, 1137, 1063, 910, 732;

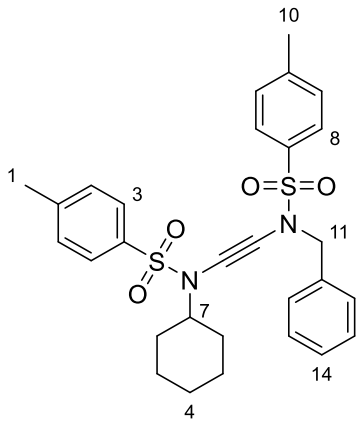
^{1}H NMR (500 MHz, $CDCl_3$) δ_H 7.98 (2H, d, *J* = 8.3 Hz, H1), 7.79 (2H, d, *J* = 8.3 Hz, H2), 7.68 (2H, d, *J* = 8.2 Hz, H11), 7.31 (2H, d, *J* = 8.2 Hz, H12), 3.38 – 3.31 (4H, m, H3, H7), 2.45 (3H, s, H13), 1.58 – 1.48 (4H, m, H4, H8), 1.34 – 1.21 (4H, m, H5, H9), 0.88 (6H, t, *J* = 7.4 Hz, H6, H10).

^{13}C {^{19}F} NMR (126 MHz, $CDCl_3$) δ_C 144.8, 141.4, 135.2, 135.1, 129.9, 128.3, 127.7, 126.4, 123.3, 69.5, 68.3, 51.9, 51.5, 30.1, 30.0, 21.8, 19.52, 19.49, 13.7 (2C).

^{19}F NMR (471 MHz, $CDCl_3$) δ_F -63.15.

HRMS (ESI) m/z: $[M + H]^+$ Calcd for $C_{24}H_{30}F_3N_2O_4S_2$ 531.1594; Found 531.1594.

***N*-Benzyl-*N*-(((*N*-cyclohexyl-4-methylphenyl)sulfonamido)ethynyl)-4-methylbenzenesulfon-amide, 4o**



ZT165

Synthesised from *N*-cyclohexyl-4-methylbenzenesulfonamide (254 mg, 1.00 mmol, 1.0 eq.**),** *N*-benzyl-*N*-(2,2-dibromovinyl)-4-methylbenzenesulfonamide (490 mg, 1.10 mmol, 1.1 eq.), CuI (38 mg, 0.20 mmol, 0.20 eq.), 1,10-phenanthroline (73 mg, 0.41 mmol, 0.40 eq.) and Cs_2CO_3 (980 mg, 3.0 mmol, 3.0 eq.) with general procedure **7.2.1d**. Column chromatography (silica gel, 30% Et_2O/pentane) afforded the title compound (278 mg, 0.52 mmol, 52%) as a yellow solid.

IR (thin film, ν_{max}/cm^{-1}) 2934, 2858, 1598, 1454, 1363, 1168, 1089, 909, 732, 662;

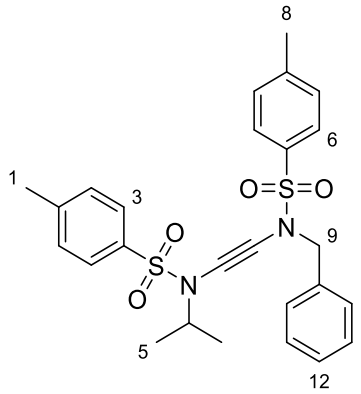
^{1}H NMR (400 MHz, $CDCl_3$) δ_H 7.68 (2H, d, *J* = 8.3 Hz, TsC*H*), 7.62 (2H, d, *J* = 8.4 Hz, TsC*H*), 7.30 – 7.23 (7H, m, H2, H9, H13, H14), 7.21 – 7.15 (2H, m, H12), 4.53 (2H, s, H11), 3.64 (1H, tt, *J* = 11.6, 4.1 Hz, H7), 2.48 – 2.38 (6H, m, H1, H10), 1.63-1.53 (2H, m,

H5), 1.53 – 1.44 (1H, m, H4), 1.43 – 1.33 (2H, m, H6), 1.25 – 1.08 (2H, m, H5), 1.04 – 0.88 (2H, m, H6), 0.87 – 0.73 (1H, m, H4);

^{13}C NMR (101 MHz, $CDCl_3$) δ_C 144.6, 144.3, 136.5, 135.1, 135.0, 129.8, 129.7, 129.1, 128.5, 128.2, 127.9, 127.5, 70.6, 67.7, 59.4, 56.1, 30.8, 25.4, 24.8, 21.8, 21.8.

Data are consistent with literature values.[25]

_N_-Benzyl-_N_-(((_N_-isopropyl-4-methylphenyl)sulfonamido)ethynyl)-4-methylbenzenesulfonamide, 4p



ZT231

Synthesised from *N*-benzyl-4-methylbenzenesulfonamide (131 mg, 0.50 mmol, 1.0 eq.), *N*-(2,2-dibromovinyl)-*N*-isopropyl-4-methylbenzenesulfonamide (219 mg, 0.55 mmol, 1.1 eq.), CuI (19 mg, 0.10 mmol, 0.20 eq.), 1,10-phenanthroline (36 mg, 0.20 mmol, 0.40 eq.) and Cs_2CO_3 (490 mg, 1.50 mmol, 3.0 eq.) with general procedure **7.2.1d**. Column chromatography (silica gel, 10% DCM + 20% Et_2O/pentane) afforded the title compound (107 mg, 0.22 mmol, 43%) as a colourless oil.

R_f 0.49 (10% DCM + 20% Et_2O/pentane);

IR (thin film, ν_{max}/cm^{-1}) 2981, 1598, 1417, 1360, 1167, 1089, 909, 814, 728, 673, 657;

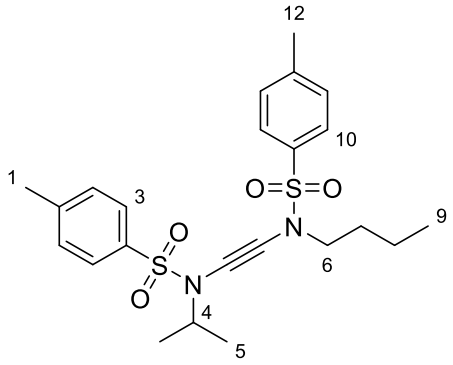
^{1}H NMR (400 MHz, $CDCl_3$) δ_H 7.70 (2H, d, *J* = 8.3 Hz, TsC*H*), 7.62 (2H, d, *J* = 8.3 Hz, TsC*H*), 7.31 – 7.24 (7H, m, H2, H7, H11, H12), 7.23 – 7.16 (2H, m, H10), 4.53 (2H, s,

H9), 4.07 (1H, hept., *J* = 6.6 Hz, H4), 2.44 (6H, overlapping singlet, H1, H8), 0.82 (6H, d, *J* = 6.6 Hz, H5);

^{13}C NMR (101 MHz, $CDCl_3$) δ_C 144.6, 144.3, 136.2, 135.1, 134.9, 129.79, 129.75, 129.0, 128.6, 128.3, 127.9, 127.5, 71.0, 66.8, 56.0, 52.4, 21.8 (2C), 20.6;

HRMS (ESI) m/z: $[M + H]^+$ Calcd for $C_{26}H_{29}O_4N_2S_2$ 497.1563; Found 497.1559.

_N_-Butyl-_N_-(((_N_-isopropyl-4-methylphenyl)sulfonamido)ethynyl)-4-methylbenzenesulfonamide, 4q



ZT246

Synthesised from *N*-butyl-4-methylbenzenesulfonamide (114 mg, 0.50 mmol, 1.0 eq.**),** *N*-(2,2-dibromovinyl)-*N*-isopropyl-4-methylbenzenesulfonamide (219 mg, 0.55 mmol, 1.1 eq.), CuI (19 mg, 0.10 mmol, 0.20 eq.), 1,10-phenanthroline (36 mg, 0.20 mmol, 0.40 eq.) and Cs_2CO_3 (490 mg, 1.50 mmol, 3.0 eq.) with general procedure **7.2.1d**. Column chromatography (silica gel, 10% DCM + 20% Et_2O/pentane) afforded the title compound (153 mg, 0.33 mmol, 66%) as a colourless oil;

R_f 0.69 (10% DCM + 20% Et_2O/pentane);

IR (thin film, ν_{max}/cm^{-1}) 2962, 1597, 1417, 1361, 1168, 1090, 972, 909, 814, 728, 672, 655;

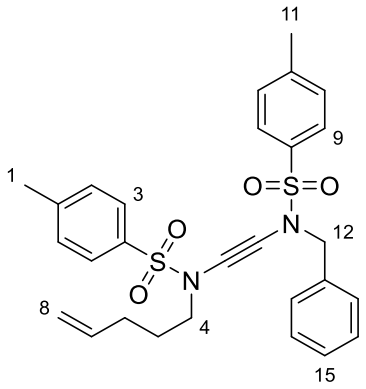
^{1}H NMR (400 MHz, $CDCl_3$) δ_H 7.72 (4H, overlapping doublet, *J* = 8.3 Hz, H3, H10), 7.34 – 7.28 (4H, m, H2, H11), 4.18 (1H, hept., *J* = 6.6 Hz, H4), 3.36 (2H, t, *J* = 7.2 Hz, H6),

2.44 (6H, s, H1, H12), 1.55 (2H, app. quin., J = 7.4 Hz, H7), 1.30 (2H, app. sext., J = 7.4 Hz, H8), 1.02 (6H, d, J = 6.6 Hz, H5), 0.88 (3H, t, J = 7.4 Hz, H9);

^{13}C NMR (101 MHz, $CDCl_3$) δ_C 144.5, 144.4, 136.2, 135.2, 129.8 (2C), 127.8, 127.6, 70.8, 65.8, 52.4, 51.5, 30.0, 21.8, 20.9, 19.5, 13.7 (2C);

HRMS (ESI) m/z: $[M + H]^+$ Calcd for $C_{23}H_{31}O_4O_2S_2$ 463.1720; Found 463.1721.

***N*-Benzyl-4-methyl-*N*-(((4-methyl-*N*-(pent-4-en-1-yl)phenyl)sulfonamido)ethynyl) benzenesulfonamide, 4r**



ZT204

Synthesised from 4-methyl-*N*-(pent-4-en-1-yl)benzenesulfonamide (120 mg, 0.50 mmol, 1.0 eq.**),** *N*-benzyl-*N*-(2,2-dibromovinyl)-4-methylbenzenesulfonamide (245 mg, 0.55 mmol, 1.1 eq.), CuI (19 mg, 0.10 mmol, 0.20 eq.), 1,10-phenanthroline (36 mg, 0.20 mmol, 0.40 eq.) and Cs_2CO_3 (489 mg, 1.50 mmol, 3.0 eq.) with general procedure **7.2.1d**. Column chromatography (20% EtOAc/pentane) afforded the title compound as a colourless solid (165 mg, 0.32 mmol, 63%).

m.p. 80 – 81 °C;

R_f 0.48 (20% EtOAc/pentane);

IR (thin film, ν_{max}/cm^{-1}) 2928, 1597, 1411, 1362, 1167, 1089, 813, 753, 657;

^{1}H NMR (500 MHz, $CDCl_3$) δ_H 7.68 (2H, d, J = 8.3 Hz, Ts*H*), 7.61 (2H, d, J = 8.3 Hz, Ts*H*), 7.31 – 7.23 (7H, m, H2, H10, H14, H15), 7.20 – 7.15 (2H, m, H13), 5.63 (1H, ddt, J

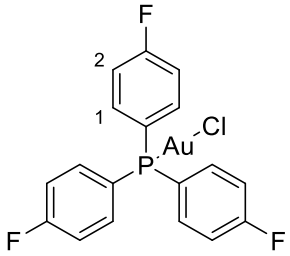
= 16.9, 10.4, 6.6 Hz, H7), 4.97 – 4.89 (2H, m, H8), 4.50 (2H, s, H12), 3.19 (2H, t, *J* = 7.2 Hz, H4), 2.44 (6H, s, H1, H11), 1.92 – 1.84 (2H, m, H6), 1.43 (2H, app. quin., *J* = 7.3 Hz, H5);

^{13}C NMR (126 MHz, $CDCl_3$) δ_C 144.6, 144.5, 137.2, 134.99, 134.96, 134.8, 129.77, 129.76, 128.9, 128.6, 128.3, 127.8, 127.6, 115.5, 69.8, 69.3, 56.0, 51.2, 30.2, 26.9, 21.8 (2C).

HRMS (ESI) m/z: $[M + H]^+$ Calcd for $C_{28}H_{31}O_4N_2S_2$ 523.1720; Found 523.1719.

7.3.5 Au(I) Pre-Catalysts

Chloro[tris(4-fluorophenyl)phosphine]gold(I)



ZT030

Synthesised from chloro(dimethylsulfide)gold(I) (30 mg, 0.10 mmol, 1.0 eq.) and tris(4-fluorophenyl) phosphine (32 mg, 0.10 mmol, 1.0 eq.) using general procedure **7.2.3a**. The title compound (56 mg, 0.10 mmol, quant.) was isolated as a grey solid.

IR (thin film, ν_{max}/cm^{-1}) 2980, 1589, 1496, 1396, 1302, 1235, 1161, 1103, 913, 828, 732, 640;

^{1}H NMR (400 MHz, $CDCl_3$) δ_H 7.57 – 7.43 (6H, m, H2), 7.25 – 7.14 (6H, m, H1);

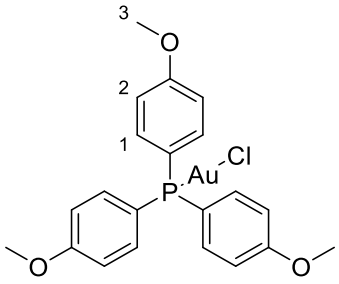
^{13}C NMR (101 MHz, $CDCl_3$) δ_C 165.2 (dd, $^1J_{C–F}$ = 255.8 Hz, $^4J_{C–P}$ = 2.7 Hz), 136.3 (dd, $^3J_{C–F}$ = 8.9 Hz, $^2J_{C–P}$ = 15.8 Hz), 124.2 (dd, $^4J_{C–F}$ = 3.5 Hz, $^1J_{C–P}$ = 65.4 Hz), 117.0 (dd, $^2J_{C–F}$ = 21.7 Hz, $^3J_{C–P}$ = 13.4 Hz);

^{19}F NMR (377 MHz, $CDCl_3$) δ_F -105.46 (d, $J_{F–P}$ = 2.9 Hz);

^{31}P NMR (162 MHz, $CDCl_3$) δ_P 30.71 (q, $J_{P–F}$ = 2.9 Hz).

Data are consistent with literature values.[216]

Chloro[tris(4-methoxyphenyl)phosphine]gold(I)



ZT032

Synthesised from chloro(dimethylsulfide)gold(I) (30 mg, 0.10 mmol, 1.0 eq.) and tris(4-methoxy)phosphine (36 mg, 0.10 mmol, 1.0 eq.) using general procedure **7.2.3a.** The title compound (59 mg, 0.10 mmol, 99%) was isolated as a colourless solid.

IR (thin film, ν_{max}/cm^{-1}) 2970, 2837, 1593, 1568, 1500, 1459, 1407, 1293, 1256, 1179, 1106, 1026, 828, 800, 731;

^{1}H NMR (400 MHz, $CDCl_3$) δ_H 7.43 (6H, dd, $^{3}J_{H-P}$ = 12.7, $^{3}J_{H-H}$ = 8.8 Hz, H1), 6.95 (6H, dd, $^{3}J_{H-H}$ = 8.8 Hz, $^{4}J_{P-H}$ = 1.9 Hz, H2), 3.84 (9H, s, H3);

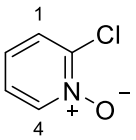
^{13}C NMR (101 MHz, $CDCl_3$) δ_C 162.5 (d, $^{4}J_{C-P}$ = 2.3 Hz), 135.7 (d, $^{2}J_{C-P}$ = 15.4 Hz), 120.6 (d, $^{1}J_{C-P}$ = 68.0 Hz), 114.9 (d, $^{3}J_{C-P}$ = 13.1 Hz), 55.6;

^{31}P NMR (162 MHz, $CDCl_3$) δ_P 29.30.

Data are consistent with literature values.[216]

7.3.6 Pyridine N-Oxides

2-Chloropyridine *N*-oxide, 60



This reaction was repeated multiple times, and a clean NMR spectrum could be found under experiment entry ZT029.

Synthesised from 2-chloropyridine (1.5 mL, 15.9 mmol, 1.0 eq.) and 3-chlorobenzene-1-carboperoxoic acid (8.21 g, 47.6 mmol, 3.0 eq.) with general procedure **7.2.2a**. Column chromatography (silica gel, 10% MeOH/DCM) afforded the title compound (1.79 g, 14 mmol, 87%) as a grey solid.

IR (thin film, ν_{max}/cm^{-1}) 3414, 3106, 1663, 1468, 1421, 1273, 1251, 1144, 1084, 1042, 846, 765, 703.

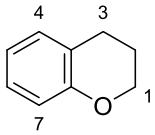
^{1}H NMR (400 MHz, $CDCl_3$) δ_H 8.39 – 8.29 (1H, m, Ar*H*), 7.54 – 7.45 (1H, m, Ar*H*), 7.26 – 7.15 (2H, m, Ar*H*).

^{13}C NMR (101 MHz, $CDCl_3$) δ_H 142.2, 140.8, 127.4, 125.8, 124.0.

Data are consistent with literature values.[217]

7.3.7 Nucleophiles

Chromane



ZT061

Modified from a literature procedure.[218] In a vial was dissolved 4-chromanone (300 mg, 2.02 mmol, 1.0 eq.) in acetic acid (1.5 mL). In a round-bottom flask equipped with a stirrer bar, was suspended zinc dust (3.31 g, 50.6 mmol, 25 eq.) in acetic acid (12 mL). While stirring, the 4-chromanone solution was added to the zinc dust suspension. Then the mixture was stirred and refluxed at 100 °C for 18 h. Upon completion by TLC, it was cooled to room temperature and was quenched by adding saturated K_2CO_3 solution. The mixture was filtered through a Celite® pad, and the filtrate was extracted three times with EtOAc. The

organic layers were combined, washed with brine, dried over $MgSO_4$, and concentrated *in vacuo* to give the crude product which was filtered through a silica plug pre-soaked with pentane to give chromane (161 mg, 1.20 mmol, 59%) as a pale-yellow oil.

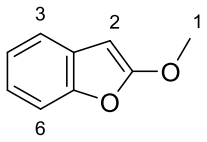
IR (thin film, ν_{max} / cm^{-1}) 2935, 1581, 1489, 1455, 1227, 1151, 1064, 1008, 753;

^{1}H NMR (400 MHz, $CDCl_3$) δ_H 7.14 – 7.01 (2H, m, Ar*H*), 6.89 – 6.77 (2H, m, Ar*H*), 4.23 – 4.16 (2H, m, H3), 2.80 (2H, t, *J* = 6.5 Hz, H1), 2.07 – 1.97 (2H, m, H2);

^{13}C NMR (101 MHz, $CDCl_3$) δ_C 155.1, 129.9, 127.3, 122.4, 120.2, 116.8, 66.6, 25.0, 22.5.

Data are consistent with literature values.[218]

2-Methoxybenzofuran



ZT107, ZT156, ZT111, ZT162

Step 1: To a heat gun-dried flask equipped with a stirrer bar was dissolved benzofuran (0.55 mL, 4.98 mmol, 1.0 eq.) in anhydrous THF (5.0 mL). The solution was cooled to -40 °C, and while stirring a solution of *n*-butyllithium (2.5 M in hexane, 3.0 mL, 7.5 mmol, 1.5 eq.) was added dropwise. The reaction mixture was kept at -40 °C for 1 h before a solution of iodine (1.90 g, 7.47 mmol, 1.5 eq.) in anhydrous THF (5.0 mL) was added dropwise. The mixture was gently warmed to room temperature and stirred until completion by TLC. Upon completion, the reaction mixture was washed twice with saturated $Na_2S_2O_3$ solution. The aqueous phase was then extracted three times with EtOAc. The organic phase was combined, washed with brine, and dried over $MgSO_4$. The solvent was removed *in vacuo* to give the crude 2-iodobenzofuran (1.18 g, 4.82 mmol, 97%) which was used in the next step without further purification.

Step 2: To a heat gun-dried flask equipped with a stirrer bar was added 2-iodobenzofuran (0.50 g, 2.05 mmol, 1.0 eq.) and CuI (78 mg, 0.41 mmol, 0.20 eq.). The flask was purged under high vacuum for 30 s and backfilled with argon (this vacuum cycle was repeated twice more). A sodium methoxide solution was prepared by dissolving sodium (345 mg, 15.0 mmol, 7.3 eq.) in anhydrous methanol (3.6 mL) under argon. Then the sodium methoxide solution was added to the flask containing 2-iodobenzofuran and CuI, after which the reaction mixture was stirred at 60 °C under argon until completion by TLC. Upon completion, the mixture was filtered through a Celite® pad, concentrated *in vacuo* and purified by column chromatography (silica gel, pentane) to afford the title compound (233 mg, 1.57 mmol, 77%) as a yellowish-green oil.

R_f 0.18 (pentane);

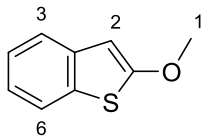
IR (thin film, ν_{max}/cm^{-1}) 2941, 1606, 1460, 1435, 1352, 1327, 1297, 1249, 1207, 1177, 1042, 954, 744;

^{1}H NMR (400 MHz, $CDCl_3$) δ_H 7.40 – 7.36 (1H, m, Ar*H*), 7.35 – 7.30 (1H, m, Ar*H*), 7.20 – 7.09 (2H, m, Ar*H*), 5.53 (1H, s, H2), 3.98 (3H, s, H1);

^{13}C NMR (101 MHz, $CDCl_3$) δ_C 164.4, 149.1, 129.8, 123.1, 121.7, 119.2, 110.3, 75.9, 57.9.

Data are consistent with literature values.[219]

2-Methoxybenzothiophene



ZT133, ZT157, ZT138, ZT163

Step 1: To a heat gun-dried flask equipped with a stirrer bar was added benzothiophene (700 mg, 5.22 mmol, 1.0 eq.). The flask was purged under high vacuum for 30 s and backfilled with argon. Anhydrous THF (5.0 mL) was added to dissolve the benzothiophene.

A solution of iodine (2.00 g, 7.88 mmol, 1.5 eq.) in anhydrous THF (5.0 mL) was also prepared in a similar method. The benzothiophene solution was cooled to -40 °C, and while stirring a solution of *n*-butyllithium (2.0 M in hexane, 4.0 mL, 11.0 mmol, 1.5 eq.) was added dropwise. The reaction mixture was kept at -40 °C for 1 h before the iodine solution was added slowly. The mixture was gently warmed to room temperature and stirred until completion by TLC. Upon completion, the reaction mixture was washed twice with saturated $Na_2S_2O_3$ solution, then the aqueous phase was extracted three times with EtOAc. The organic phase was combined, washed with brine, and dried over $MgSO_4$. The solvent was removed *in vacuo* to give the crude 2-iodobenzothiophene (1.22 g, 4.69 mmol, 90%) as a brown solid which was used in the next step without further purification.

Step 2: To a heat gun-dried flask equipped with a stirrer bar was added 2-iodobenzothiophene (500 mg, 1.92 mmol, 1.0 eq.) and CuI (73 mg, 0.38 mmol, 0.20 eq.). The flask was purged under high vacuum for 30 s and backfilled with argon (this vacuum cycle was repeated twice more). A sodium methoxide solution was prepared by dissolving sodium (400 mg, 17.4 mmol, 9.1 eq.) in anhydrous methanol (5 mL) under argon. Then the sodium methoxide solution was added to the flask containing 2-iodobenzothiophene and CuI, after which the reaction mixture was stirred at 60 °C under argon until completion by TLC. Upon completion, the mixture was cooled to room temperature, filtered through a Celite® pad, concentrated *in vacuo* and purified by column chromatography (silica gel, pentane) to afford the title compound (153 mg, 0.93 mmol, 49%) as a yellow solid.

m.p. 39 – 41 °C;

R_f 0.28 (pentane);

IR (thin film, ν_{max}/cm^{-1}) 3063, 2932, 2828, 1567, 1543, 1448, 1424, 1259, 1209, 1195, 1157, 1066, 1018, 989, 782, 742, 723, 623;

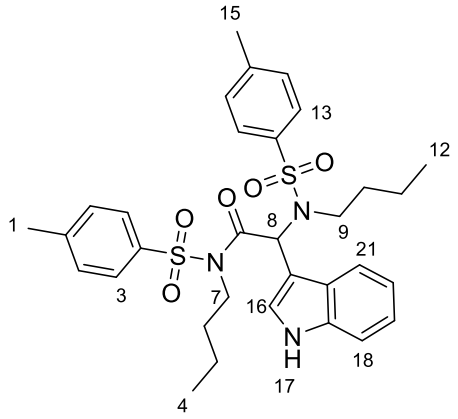
^{1}H NMR (400 MHz, $CDCl_3$) δ_H 7.69 – 7.61 (1H, m, Ar*H*), 7.60 – 7.53 (1H, m, Ar*H*), 7.36 – 7.28 (1H, m, Ar*H*), 7.27 – 7.18 (1H, m, Ar*H*), 6.37 (1H, s, H2), 3.99 (3H, s, H1);

^{13}C NMR (101 MHz, $CDCl_3$) δ_C 165.7, 138.8, 132.0, 124.6, 122.6, 122.0, 121.9, 98.3, 59.8.

Data are consistent with literature values.[219]

7.3.8 Oxidative Functionalisation Products

_N_-Butyl-2-((_N_-butyl-4-methylphenyl)sulfonamido)-2-(1_H_-indol-3-yl)-_N_-tosylacetamide, 61b



ZT040

Synthesised from *N*,*N*'-(ethyne-1,2-diyl)bis(*N*-butyl-4-methylbenzenesulfonamide) (50 mg, 0.10 mmol, 1.0 eq.), 2-chloropyridine *N*-oxide (27 mg, 0.21 mmol, 2.0 eq.), indole (37 mg, 0.32 mmol, 3.0 eq.), and $IPrAuTf_2$ (4.5 mg, 5.2 μmol, 5 mol%) in anhydrous DCE (0.2 mL) at room temperature for 1 h with general procedure **7.2.3b**. Column chromatography (silica gel, 20% EtOAc/pentane) afforded the title compound (52 mg, 85 μmol, 81%) as a colourless solid.

m.p. 143 – 144 °C;

R_f 0.11 (20% EtOAc/pentane);

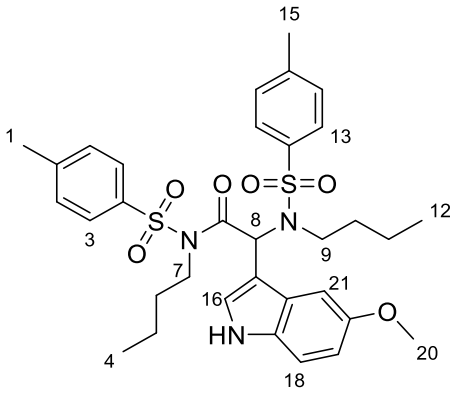
IR (thin film, ν_{max} / cm^{-1}) 3379, 2959, 2873, 1698, 1597, 1494, 1459, 1337, 1248, 1161, 1086, 1008, 913, 813, 775, 730, 670;

^{1}H NMR (400 MHz, $CDCl_3$) δ_H 8.42 (1H, s, H17), 7.77 – 7.54 (4H, m, H3, H18, H19), 7.35 (2H, d, *J* = 8.1 Hz, H13), 7.28 – 7.14 (5H, m, H2, H14, H21), 7.12 – 7.04 (1H, m, H20), 6.83 (1H, s, H16), 6.56 (1H, s, H8), 3.76 – 3.64 (1H, m, H9), 3.45 – 3.16 (3H, m, H7, H9), 2.44 – 2.37 (6H, m, H1, H15), 1.76 – 1.47 (2H, m, H6), 1.42 – 1.28 (1H, m, H10), 1.31 – 1.17 (2H, m, H5), 0.86 (3H, t, *J* = 7.4 Hz, H4), 0.82 – 0.67 (2H, m, H11), 0.62 – 0.49 (1H, m, H10), 0.43 (3H, t, *J* = 7.4 Hz, H12);

^{13}C NMR (101 MHz, $CDCl_3$) δ_C 171.0, 144.5, 143.2, 137.0, 136.4, 136.2, 129.6, 129.5, 128.2, 127.6, 126.4, 125.0, 123.3, 120.9, 118.8, 111.6, 108.1, 55.5, 46.9, 46.2, 32.7, 32.0, 21.8, 21.7, 20.2, 19.8, 13.7, 13.3;

HRMS (ESI) m/z: $[M + Na]^+$ Calcd for $C_{32}H_{39}O_5N_3NaS_2$ 632.2223; Found 632.2222.

N-Butyl-2-((*N*-butyl-4-methylphenyl)sulfonamido)-2-(5-methoxy-1*H*-indol-3-yl)-*N*-tosylacetamide, 61c



ZT095

Synthesised from *N*,*N*'-(ethyne-1,2-diyl)bis(*N*-butyl-4-methylbenzenesulfonamide) (50 mg, 0.10 mmol, 1.0 eq.), 2-chloropyridine *N*-oxide (27 mg, 0.21 mmol, 2.0 eq.), and 5-methoxyindole (47 mg, 0.32 mmol, 3.0 eq.) in anhydrous DCE (0.2 mL) at room temperature for 1 h according to general procedure **7.2.3b**. Column chromatography (silica gel, 20% EtOAc/pentane) afforded the title compound (60 mg, 94 μmol, 89%) as a colourless solid.

m.p. 174 – 176 °C;

R_f 0.15 (20% EtOAc/pentane);

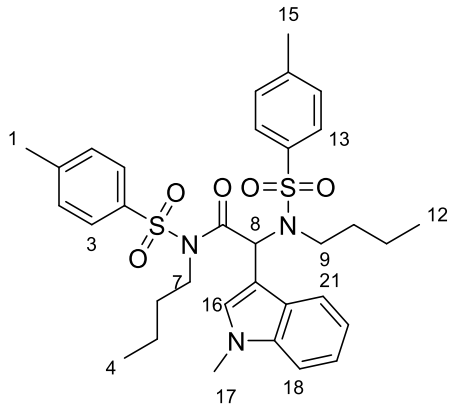
IR (thin film, ν_{max}/cm^{-1}) 3384, 2959, 2873, 1700, 1626, 1597, 1490, 1460, 1441, 1338, 1214, 1164, 1086, 1058, 1021, 1004, 911, 812, 731, 669, 652;

^{1}H NMR (400 MHz, $CDCl_3$) δ_H 8.18 (1H, s, H17), 7.79 – 7.52 (4H, m, H3, H18, H19), 7.26 – 7.11 (5H, m, H2, H14, H21), 6.93 – 6.76 (3H, m, H13, H16), 6.53 (1H, brs., H8), 3.77 (3H, s, H20), 3.74 – 3.62 (1H, m, H9), 3.48 – 3.35 (1H, m, H9), 3.34 – 3.20 (2H, m, H7), 2.40 (6H, s, H1, H15), 1.76 – 1.47 (2H, m, H6), 1.43 – 1.25 (1H, m, H10), 1.28 – 1.18 (2H, m, H5), 0.90 – 0.70 (5H, m, H4, H11), 0.70 – 0.55 (1H, m, H10), 0.44 (3H, t, *J* = 7.3 Hz, H12);

^{13}C NMR (101 MHz, $CDCl_3$) δ_C 171.1, 155.1, 144.5, 143.2, 137.3, 136.4, 131.2, 129.7, 129.5, 128.2, 127.6, 127.1, 125.5, 114.0, 112.4, 107.9, 100.0, 55.9, 55.5, 46.9, 46.2, 32.7, 31.9, 21.8, 21.7, 20.2, 19.8, 13.7, 13.4;

HRMS (ESI) m/z: $[M + Na]^+$ Calcd for $C_{33}H_{41}O_6N_3NaS_2$ 662.2329; Found 662.2328.

_N_-Butyl-2-((_N_-butyl-4-methylphenyl)sulfonamido)-2-(1-methyl-1_H_-indol-3-yl)-_N_-tosylacetamide, 61d



ZT096

Synthesised from *N*,*N*'-(ethyne-1,2-diyl)bis(*N*-butyl-4-methylbenzenesulfonamide) (50 mg, 0.10 mmol, 1.0 eq.), 2-chloropyridine *N*-oxide (27 mg, 0.21 mmol, 2.0 eq.), and 1-methylindole (40 μL, 0.32 mmol, 3.0 eq.) in anhydrous DCE (0.2 mL) at 80 °C for 5 h with general procedure **7.2.3b**. Column chromatography (silica gel, 20% EtOAc/pentane) afforded the product **3f** (41 mg, 66 μmol, 63%) as a colourless solid.

m.p. 164 – 166 °C;

R_f 0.24 (20% EtOAc/pentane);

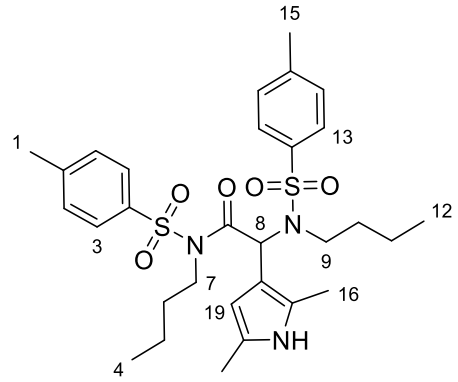
IR (thin film, ν_{max} / cm^{-1}) 3027, 2960, 2874, 1699, 1467, 1335, 1161, 1086, 1028, 999, 920, 813, 750, 666;

^{1}H NMR (400 MHz, $CDCl_3$) δ_H 7.75 – 7.54 (4H, m, H3, H18, H19), 7.38 – 7.31 (1H, m, H21), 7.30 – 7.26 (2H, m, H14), 7.23 – 7.12 (4H, m, H2, H13), 7.12 – 7.06 (1H, m, H16), 6.60 (1H, s, H20), 6.51 (1H, s, H8), 3.81 – 3.68 (1H, m, H9), 3.66 (3H, s, H17), 3.48 – 3.36 (1H, m, H9), 3.32 – 3.11 (2H, m, H7), 2.42 (6H, s, H1, H15), 1.77 – 1.52 (2H, m, H6), 1.43 – 1.28 (1H, m, H10), 1.31 – 1.19 (2H, m, H5), 0.88 (3H, t, *J* = 7.4 Hz, H4), 0.87 – 0.70 (2H, m, H11), 0.61 – 0.48 (1H, m, H10), 0.44 (3H, t, *J* = 7.4 Hz, H12);

^{13}C NMR (101 MHz, $CDCl_3$) δ_C 171.0, 144.3, 143.1, 137.2, 137.1, 136.5, 129.6, 129.4, 129.3, 128.3, 127.6, 127.4, 122.9, 120.6, 119.0, 109.5, 106.3, 55.3, 47.0, 46.0, 33.1, 32.6, 32.1, 21.8, 21.7, 20.2, 19.7, 13.7, 13.3;

HRMS (ESI) m/z: $[M + Na]^+$ calc. for $C_{33}H_{41}O_5N_3NaS_2$ 646.2380; Found 646.2375.

***N*-Butyl-2-((*N*-butyl-4-methylphenyl)sulfonamido)-2-(2,5-dimethyl-1*H*-pyrrol-3-yl)-*N*-tosyl-acetamide, 61e**



ZT126

Synthesised from *N*,*N*'-(ethyne-1,2-diyl)bis(*N*-butyl-4-methylbenzenesulfonamide) (0.10 g, 0.21 mmol, 1.0 eq.), 2-chloropyridine *N*-oxide (55 mg, 0.42 mmol, 2.0 eq.), 2,5-dimethylpyrrole (65 μL, 0.64 mmol, 3.0 eq.). and $IPrAuNTf_2$ (9.0 mg, 10 μmol, 5.0 mol%) in anhydrous DCE (0.4 mL) at 80 °C for 3 h with general procedure **7.2.3b**. Column chromatography (silica gel, 20% EtOAc/pentane) afforded the title compound (0.10 g, 0.17 mmol, 83%) as a yellow solid.

m.p. 94 °C;

R_f 0.24 (20% EtOAc/pentane);

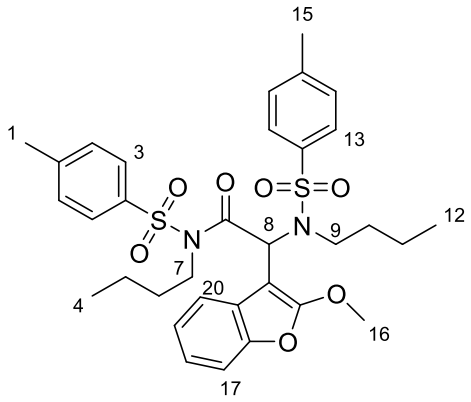
IR (thin film, ν_{max} / cm^{-1}) 3381, 2960, 1701, 1599, 1460, 1336, 1161, 1086, 1001, 920, 813, 756, 668;

^{1}H NMR (400 MHz, $CDCl_3$) δ_H 7.70 (1H, s, H17), 7.63 – 7.57 (4H, m, H3, H13), 7.23 (2H, d, *J* = 8.0 Hz, H2), 7.16 (2H, d, *J* = 7.9 Hz, H14), 6.19 (1H, s, H8), 5.26 (1H, d, *J* = 2.8 Hz, H19), 3.67 – 3.53 (1H, m, H9), 3.40 – 3.27 (1H, m, H9), 3.26 – 3.16 (2H, m, H7), 2.43 (3H, s, H1), 2.38 (3H, s, H15), 2.13 – 2.08 (6H, m, H16, H18), 1.69 – 1.60 (1H, m, H10), 1.58 – 1.41 (2H, m, H6, H10), 1.33 – 1.19 (2H, m, H5), 1.03 – 0.87 (5H, m, H4, H11), 0.82 – 0.71 (1H, m, H6), 0.65 (3H, t, *J* = 7.3 Hz, H12);

^{13}C NMR (101 MHz, $CDCl_3$) δ_C 171.2, 144.3, 142.9, 137.2, 136.6, 129.5, 129.4, 128.4, 127.6, 126.4, 125.8, 110.5, 106.8, 56.4, 46.7, 46.4, 32.9, 31.7, 21.8, 21.7, 20.3, 19.9, 13.8, 13.6, 12.9, 10.9.

HRMS (ESI) m/z: $[M + Na]^+$ Calcd for $C_{30}H_{41}N_3NaO_5S_2$ 610.2380; Found 610.2377.

***N*-Butyl-2-((*N*-butyl-4-methylphenyl)sulfonamido)-2-(2-methoxybenzofuran-3-yl)-*N*-tosylacetamide, 61g**



ZT137

Synthesised from *N*,*N'*-(ethyne-1,2-diyl)bis(*N*-butyl-4-methylbenzenesulfonamide) (50 mg, 0.10 mmol, 1.0 eq.), 2-chloropyridine *N*-oxide (27 mg, 0.21 mmol, 2.0 eq.), 2-methoxybenzofuran **(**47 mg, 0.32 mmol, 3.0 eq.). and $IPrAuNTf_2$ (4.5 mg, 5.2 μmol, 5.0 mol%) in anhydrous DCE (0.2 mL) at 80 °C for 6 h with general procedure **7.2.3b**. Column chromatography (10% EtOAc/pentane) afforded the title compound (56 mg, 88 μmol, 83%) as a yellow solid.

m.p. 139 – 140 °C;

R_f 0.14 (10% EtOAc/pentane);

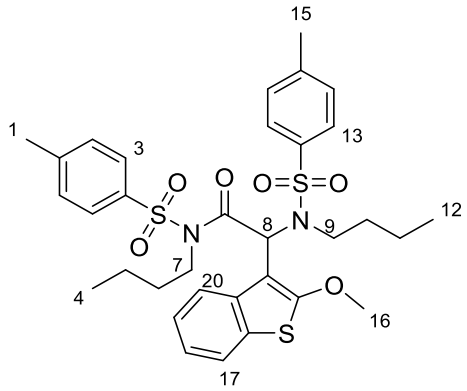
IR (thin film, ν_{max} / cm^{-1}) 2959, 1707, 1643, 1495, 1339, 1162, 1087, 1022, 1007, 925, 813, 750, 665;

^{1}H NMR (400 MHz, $CDCl_3$) δ_H 7.69 (2H, d, *J* = 7.9 Hz, H3), 7.56 (2H, d, *J* = 7.9 Hz, H13), 7.33 – 7.20 (4H, m, H2, H17, H18), 7.20 – 7.07 (4H, m, H14, H19, H20), 6.51 (1H, s, H8), 3.83 (3H, s, H16), 3.66 – 3.53 (1H, m, H9), 3.42 – 3.41 (2H, m, H7), 3.17 (1H, ddd, *J* = 15.6, 11.2, 5.0 Hz, H9), 2.44 – 2.36 (6H, m, H1, H15), 1.68 – 1.43 (3H, m, H6, H10), 1.32-1.17 (2H, m, H5), 0.98 – 0.71 (6H, m, H10, H11, H4), 0.51 (3H, t, *J* = 7.3 Hz, H12);

^{13}C NMR (101 MHz, $CDCl_3$) δ_C 169.6, 159.5, 148.1, 144.5, 143.1, 137.1, 136.4, 129.6, 129.4, 128.4, 127.7, 127.7, 124.0, 122.8, 118.8, 110.2, 86.2, 58.3, 54.9, 47.7, 47.2, 33.1, 31.8, 21.73, 21.67, 20.3, 19.9, 13.8, 13.4;

HRMS (ESI) m/z: $[M + Na]^+$ Calcd for $C_{33}H_{40}N_2NaO_7S_2$ 663.2169; Found 663.2165.

***N*-Butyl-2-((*N*-butyl-4-methylphenyl)sulfonamido)-2-(2-methoxybenzo[b]thiophen-3-yl)-*N*-tosylacetamide, 61h**



Synthesised from *N*,*N*'-(ethyne-1,2-diyl)bis(*N*-butyl-4-methylbenzenesulfonamide) (50 mg, 0.10 mmol, 1.0 eq.), 2-chloropyridine *N*-oxide (27 mg, 0.21 mmol, 2.0 eq.), 2-methoxybenzothiophene (52 mg, 0.32 mmol, 3.0 eq.). and $IPrAuNTf_2$ (4.5 mg, 5.2 μmol, 5.0 mol%) in anhydrous DCE (0.2 mL) at 80 °C for 2 h with general procedure **7.2.3b**. Column chromatography (10% EtOAc/pentane) afforded the title compound (48 mg, 73 μmol, 70%) as a colourless solid.

m.p. 145 – 146 °C;

R_f 0.11 (10% EtOAc/pentane);

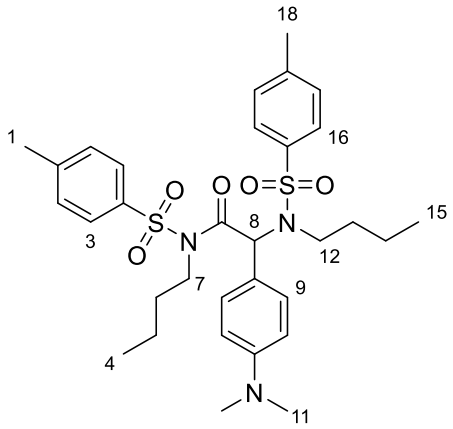
IR (thin film, ν_{max} / cm^{-1}) 2959, 2873, 1709, 1578, 1465, 1338, 1161, 1087, 1022, 997, 926, 813, 754, 668;

^{1}H NMR (400 MHz, $CDCl_3$) δ_H 7.84 (1H, d, *J* = 8.0 Hz, H20), 7.66 – 7.60 (3H, m, H3, H17), 7.55 – 7.45 (2H, m, H13), 7.41 (1H, app. t, *J* = 7.1 Hz, H18), 7.33 – 7.24 (1H, m, H19), 7.18 (2H, d, *J* = 7.2 Hz, H2), 7.11 (2H, d, *J* = 7.7 Hz, H14), 6.60 (1H, s, H8), 3.68 (3H, s, H16), 3.62 – 3.52 (1H, m, H9), 3.43 – 3.29 (2H, m, H7), 3.22 – 3.10 (1H, m, H9), 2.43 – 2.37 (6H, m, H1, H15), 1.68 – 1.55 (1H, m, H10), 1.47 – 1.31 (2H, m, H10, H11), 1.22-1.09 (2H, m, H6), 0.97 – 0.74 (5H, m, H4, H5), 0.57 – 0.39 (4H, m, H11, H12);

^{13}C NMR (101 MHz, $CDCl_3$) δ_C 169.6, 144.4, 143.0, 137.2, 136.8, 136.6, 130.3, 129.5, 129.4, 127.8, 127.7, 126.0, 123.8, 122.1, 121.3, 105.9, 61.4, 56.7, 47.9, 47.4, 32.9, 31.9, 28.9, 21.8, 21.7, 20.3, 19.9, 13.8, 13.4.

HRMS (ESI) m/z: $[M + Na]^+$ Calcd for $C_{33}H_{40}N_2NaO_6S_3$ 679.1941; Found 679.1938.

_N_-Butyl-2-((_N_-butyl-4-methylphenyl)sulfonamido)-2-(4-(dimethylamino)phenyl)-_N_-tosylacetamide, 61n



ZT046

Synthesised from *N*,*N*'-(ethyne-1,2-diyl)bis(*N*-butyl-4-methylbenzenesulfonamide) (50 mg, 0.10 mmol, 1.0 eq.), 2-chloropyridine *N*-oxide (27 mg, 0.21 mmol, 2.0 eq.), *N*,*N*-dimethylaniline (40 µL, 0.32 mmol, 3.0 eq.) and $IPrAuTf_2$ (4.5 mg, 5.2 µmol, 5 mol%) in

anhydrous DCE (0.2 mL) at 80 °C for 1 h according to general procedure **7.2.3b**. Column chromatography (10% EtOAc/pentane) afforded the title compound as a colourless solid (48 mg, 78 μmol, 75%).

m.p. 130 – 131 °C.

R_f 0.09 (10% EtOAc/pentane).

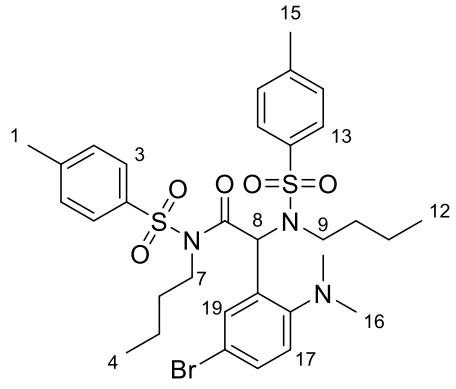
IR (thin film, ν_{max} / cm^{-1}) 2959, 2873, 2360, 1702, 1611, 1524, 1494, 1457, 1354, 1291, 1163, 1087, 1022, 1012, 919, 814, 773, 731, 714, 668.

^{1}H NMR (400 MHz, $CDCl_3$) δ_H 7.71 – 7.50 (4H, m, H3, H16), 7.23 (2H, d, *J* = 8.0 Hz, H2), 7.16 (2H, d, *J* = 8.1 Hz, H17), 6.95 – 6.87 (2H, m, H9), 6.63 – 6.54 (2H, m, H10), 6.22 (1H, s, H8), 3.70 – 3.52 (1H, m, H12), 3.40 – 3.27 (1H, m, H4), 3.26 – 3.04 (2H, m, H4, H12), 2.96 (6H, s, H11), 2.44 (3H, s, H1), 2.40 (3H, s, H18), 1.70 – 1.47 (2H, m, H13), 1.45 – 1.33 (1H, m, H14), 1.30 – 1.20 (2H, m, H5), 0.94 – 0.82 (5H, m, H6, H15), 0.69 – 0.55 (4H, m, H7, H14).

^{13}C NMR (101 MHz, $CDCl_3$) δ_C 170.7, 150.9, 144.4, 143.0, 137.1, 136.5, 130.4, 129.5, 129.5, 128.4, 127.6, 119.8, 112.6, 62.5, 46.6, 46.1, 40.4, 32.7, 31.7, 21.8, 21.7, 20.2, 20.0, 13.7, 13.6.

HRMS (ESI) m/z: $[M + Na]^+$ Calcd for $C_{32}H_{43}N_3NaO_5S_2$ 636.2536; Found 636.2533.

2-(5-Bromo-2-(dimethylamino)phenyl)-*N*-butyl-2-((*N*-butyl-4-methylphenyl)sulfonamido)-*N*-tosylacetamide, 61o



ZT175

Synthesised from *N*,*N*'-(ethyne-1,2-diyl)bis(*N*-butyl-4-methylbenzenesulfonamide) (50 mg, 0.10 mmol, 1.0 eq.), 2-chloropyridine *N*-oxide (27 mg, 0.21 mmol, 2.0 eq.), 4-bromo-*N*,*N*-dimethylaniline (63 mg, 0.31 mmol, 3.0 eq.). and $IPrAuNTf_2$ (4.5 mg, 5.2 μmol, 5.0 mol%) in anhydrous DCE (0.2 mL) at 60 °C for 3 h with general procedure **7.2.3b**. Column chromatography (10% EtOAc/pentane) afforded the title compound (35 mg, 51 μmol, 48%) as a colourless solid.

m.p. 122 – 123 °C;

R_f 0.26 (10% EtOAc/pentane);

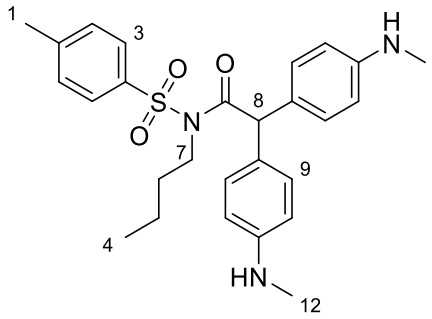
IR (thin film, ν_{max}/cm^{-1}) 2960, 1698, 1485, 1342, 1166, 1084, 813, 754, 715;

^{1}H NMR (400 MHz, $CDCl_3$) δ_H 7.72 (2H, d, *J* = 7.7 Hz, H3), 7.49 (2H, d, *J* = 8.1 Hz, H13), 7.41 (1H, dd, *J* = 8.5, 2.3 Hz, H18), 7.28 (2H, d, *J* = 7.7 Hz, H2), 7.18 (2H, d, *J* = 8.1 Hz, H12), 7.13 (1H, d, *J* = 8.5 Hz, H17), 6.62 (1H, s, H8), 6.58 (1H, s, H19), 3.94 – 3.77 (1H, m, H9), 3.43 (1H, ddd, *J* = 15.5, 11.1, 4.8 Hz, H7), 3.26 – 3.05 (2H, m, H7), 2.67 (6H, s, H16), 2.44 – 2.39 (6H, m, H1, H15), 2.05 – 1.91 (1H, m, H10), 1.88 – 1.73 (1H, m, H10), 1.49 – 1.38 (2H, m, H6), 1.34 – 1.20 (1H, m, H11), 1.02 (3H, t, *J* = 7.4 Hz, H4), 0.97 – 0.85 (2H, m, H5), 0.79 – 0.66 (1H, m, H11), 0.62 (3H, t, *J* = 7.3 Hz, H12);

^{13}C NMR (101 MHz, $CDCl_3$) δ_C 169.6, 152.9, 144.6, 143.7, 136.2, 135.6, 133.3, 131.9, 131.7, 129.6, 129.6, 128.6, 127.8, 124.0, 117.4, 57.8, 46.5, 46.1, 45.7, 32.9, 32.5, 21.8, 21.7, 20.2, 19.8, 13.9, 13.4;

HRMS (ESI) m/z: $[M + H]^+$ Calcd for $C_{32}H_{43}{}^{79}BrN_3O_5S_2$ 692.1822; Found 692.1816.

***N*-Butyl-2,2-bis(4-(methylamino)phenyl)-*N*-tosylacetamide, 61p**



ZT220

Synthesised from *N*,*N*'-(ethyne-1,2-diyl)bis(*N*-butyl-4-methylbenzenesulfonamide) (50 mg, 0.10 mmol, 1.0 eq.), 2-chloropyridine *N*-oxide (27 mg, 0.21 mmol, 2.0 eq.), *N*-methylaniline (35 μL, 0.32 mmol, 3.0 eq.). and $IPrAuNTf_2$ (4.5 mg, 5.2 μmol, 5.0 mol%) in anhydrous DCE (0.2 mL) at 80 °C for 12 h with general procedure **7.2.3b**. Column chromatography (40% EtOAc/pentane) afforded the title compound (28 mg, 58 μmol, 56%) as a yellow viscous oil.

R_f 0.27 (40% EtOAc/pentane);

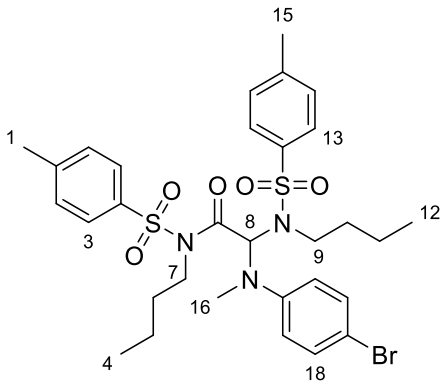
IR (thin film, ν_{max}/cm^{-1}) 3417, 2960, 1693, 1614, 1521, 1348, 1166, 1083, 812, 755, 668;

^{1}H NMR (400 MHz, $CDCl_3$) δ_H 7.68 (2H, d, *J* = 8.2 Hz, H3), 7.22 (2H, d, *J* = 8.2 Hz, H2), 6.83 (4H, d, *J* = 8.6 Hz, H9), 6.46 (4H, d, *J* = 8.6 Hz, H10), 5.32 (1H, s, H8), 3.82 – 3.73 (2H, m, H7), 3.68 – 2.88 (2H, brs., H11), 2.78 (6H, s, H12), 2.41 (3H, s, H1), 1.73 (2H, app. quin., *J* = 7.7 Hz, H6), 1.43 – 1.29 (2H, m, H5), 0.94 (3H, t, *J* = 7.4 Hz, H4);

^{13}C NMR (101 MHz, $CDCl_3$) δ_C 173.1, 148.5, 144.3, 137.0, 129.7, 129.5, 128.2, 127.4, 112.5, 55.2, 46.9, 32.8, 30.9, 21.7, 20.2, 13.8;

HRMS (ESI) m/z: $[M + H]^+$ Calcd for $C_{27}H_{34}N_3O_3S$ 480.2315; Found 480.2315.

2-((4-Bromophenyl)(methyl)amino)-*N*-butyl-2-((*N*-butyl-4-methylphenyl)sulfonamido)-*N*-tosylacetamide, 61q



ZT219

Synthesised from *N*,*N'*-(ethyne-1,2-diyl)bis(*N*-butyl-4-methylbenzenesulfonamide) (50 mg, 0.10 mmol, 1.0 eq.), 2-chloropyridine *N*-oxide (27 mg, 0.21 mmol, 2.0 eq.), and 4-bromo-*N*-methylaniline (40 μL, 0.32 mmol, 3.0 eq.) in anhydrous DCE (0.2 mL) at 80 °C for 4 h with general procedure **7.2.3b**. Column chromatography (10% EtOAc/pentane) afforded the title compound (59 mg, 87 μmol, 83%) as a colourless solid.

m.p. 126 – 127 °C;

R_f 0.23(10% EtOAc/pentane);

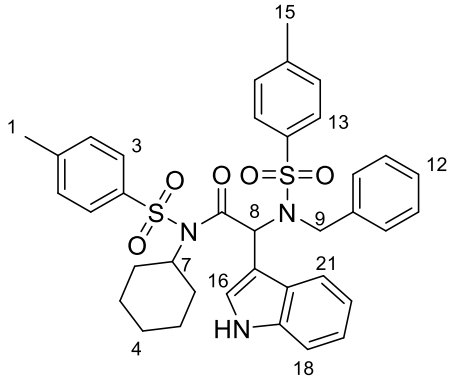
IR (thin film, ν_{max}/cm^{-1}) 2960, 2931, 2874, 1704, 1595, 1496, 1461, 1360, 1336, 1305, 1274, 1235, 1167, 1086, 981, 910, 813, 771, 731, 661;

^{1}H NMR (500 MHz, C_6D_6) δ_H 7.85 – 7.81 (2H, m, H3), 7.69 (2H, d, *J* = 6.7 Hz, H13), 7.21 (2H, d, *J* = 9.0 Hz, H18), 7.07 – 6.81 (1H, m, H8), 6.79 – 6.71 (4H, m, H14, H17), 6.69 (2H, d, *J* = 8.1 Hz, H2), 3.95 – 3.74 (1H, m, H9), 3.57 – 3.32 (2H, m, H7), 3.28 – 3.12 (1H, m, H9), 2.44 (3H, s, H16), 1.90 (3H, s, H1), 1.87 – 1.72 (6H, m, H16, H10, H15), 1.32 – 1.20 (1H, m, H6), 1.12 (2H, app. sext., *J* = 7.4 Hz, H5), 1.05 – 0.93 (2H, m, H11), 0.75 (3H, t, *J* = 7.4 Hz, H4), 0.64 (3H, t, *J* = 7.4 Hz, H12);

^{13}C NMR (126 MHz, C_6D_6) δ_C 167.5, 146.1, 144.5, 143.1, 137.2, 132.6, 129.6, 129.5, 128.4, 128.2, 128.0, 115.3, 112.7, 73.2, 46.9, 46.0, 34.3, 33.0, 32.6, 21.2, 21.2, 20.6, 20.4, 13.7, 13.7;

HRMS (ESI) m/z: $[M + Na]^+$ Calcd for $C_{31}H_{40}O_5N_3{}^{79}BrNaS_2$ 700.1485; Found 700.1482.

2-((*N*-Benzyl-4-methylphenyl)sulfonamido)-*N*-cyclohexyl-2-(1*H*-indol-3-yl)-*N*-tosylacetamide, 61v



ZT182

Synthesised from *N*-benzyl-*N*-(((*N*-cyclohexyl-4-methylphenyl)sulfonamido)ethynyl)-4-methylbenzene sulfonamide (54 mg, 0.10 mmol, 1.0 eq.), 2-chloropyridine *N*-oxide (26 mg, 0.21 mmol, 2.0 eq.), indole (36 mg, 0.31 mmol, 3.0 eq.), and $IPrAuTf_2$ (4.0 mg, 4.6 μmol, 5 mol%) in anhydrous DCE (0.2 mL) at room temperature for 2 h with general procedure **7.2.3b**. Column chromatography (20% EtOAc/pentane) afforded the title compound (55 mg, 82 μmol, 82%) as a colourless oil.

R_f 0.15 (20% EtOAc/pentane);

IR (thin film, ν_{max}/cm^{-1}) 3384, 2934, 2855, 1696, 1336, 1158, 1089, 992, 813, 757, 666;

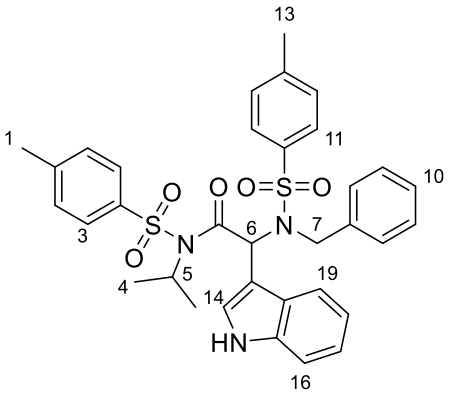
^{1}H NMR (400 MHz, $CDCl_3$) δ_H 8.12 (1H, s, H17), 7.65 (2H, d, *J* = 8.0 Hz, H3), 7.41 (2H, d, *J* = 7.1 Hz, H13), 7.34 (1H, d, *J* = 7.9 Hz, H18), 7.25 – 7.11 (5H, m, H2, H8, H20, H21), 7.07 – 6.99 (3H, m, H14, H19), 6.88 – 6.74 (4H, m, H11, H12, H16), 6.68 (2H, d, *J* = 6.8 Hz, H10), 4.77 (1H, d, *J* = 16.5 Hz, H9), 4.61 (1H, d, *J* = 16.5 Hz, H9), 3.68 (1H, tt, *J* =

12.0, 3.6 Hz, H7), 2.41 (3H, s, H1), 2.31 (3H, s, H15), 2.27-2.02 (2H, m, H5, H6), 1.80-1.71 (1H, m, H5), 1.66 – 1.56 (2H, m, H6), 1.55 – 1.46 (1H, m, H4), 1.21 – 1.04 (3H, m, H4, H5), 0.89 (1H, brs., H6);

^{13}C NMR (101 MHz, $CDCl_3$) δ_C 171.7, 144.4, 143.3, 138.5, 137.2, 136.3, 136.0, 129.6, 129.4, 127.8, 127.5, 127.4, 126.6, 126.1, 125.0, 123.1, 120.7, 119.1, 111.2, 109.0, 62.3, 56.5, 50.0, 30.3, 29.8, 29.1, 27.0, 26.8, 25.1, 21.7, 21.6; *Note: extra peaks are due to cyclohexyl group being diastereotopic.*

HRMS (ESI) m/z: $[M + Na]^+$ Calcd for $C_{37}H_{39}N_3NaO_5S_2$ 692.2223; Found 692.2219.

2-((*N*-Benzyl-4-methylphenyl)sulfonamido)-2-(1*H*-indol-3-yl)-*N*-isopropyl-*N*-tosylacetamide, 61w



ZT252

Synthesised from *N*-benzyl-*N*-(((*N*-isopropyl-4-methylphenyl)sulfonamido)ethynyl)-4-methylbenzene sulfonamide (50 mg, 0.10 mmol, 1.0 eq.), 2-chloropyridine *N*-oxide (26 mg, 0.21 mmol, 2.0 eq.), indole (36 mg, 0.31 mmol, 3.0 eq.), and $IPrAuTf_2$ (4.0 mg, 4.6 μmol, 5 mol%) in anhydrous DCE (0.2 mL) at room temperature for 2 h with general procedure **7.2.3b**. Column chromatography (20% EtOAc/pentane) afforded the title compound (53 mg, 84 μmol, 84%) as a colourless oil.

R_f 0.14 (20% EtOAc/pentane);

IR (thin film, ν_{max}/cm^{-1}) 3379, 2979, 1694, 1457, 1337, 1159, 1086, 983, 941, 813, 732, 668;

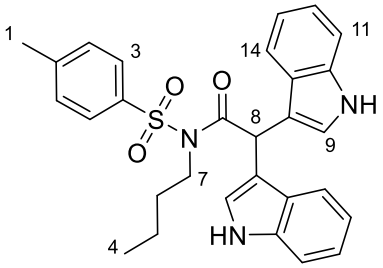
^{1}H NMR (500 MHz, $CDCl_3$) δ_H 8.07 (1H, s, H15), 7.66 (2H, d, *J* = 8.1 Hz, H3), 7.41 (2H, d, *J* = 7.5 Hz, H11), 7.32 (1H, d, *J* = 8.0 Hz, H16), 7.26 – 7.11 (5H, m, H2, H6, H18, H19), 7.07 – 6.99 (3H, m, H12, H17), 6.88 – 6.83 (1H, m, H10), 6.83 – 6.77 (3H, m, H9, H14), 6.69 (2H, d, *J* = 7.1 Hz, H8), 4.78 (1H, d, *J* = 16.4 Hz, H7), 4.64 (1H, d, *J* = 16.4 Hz, H7), 4.11 (1H, hept., *J* = 6.8 Hz, H5), 2.42 (3H, s, H1), 2.31 (3H, s, H13), 1.29 (3H, d, *J* = 6.8 Hz, H4), 1.21 (3H, d, *J* = 6.8 Hz, H4).

^{13}C NMR (126 MHz, $CDCl_3$) δ_C 171.7, 144.5, 143.3, 138.5, 137.3, 136.1 (2C), 129.6, 129.5, 127.80, 127.77, 127.6, 127.4, 126.7, 126.2, 124.9, 123.2, 120.7, 119.4, 111.2, 109.2, 56.4, 53.8, 50.0, 21.68, 21.65, 20.5, 19.5.

HRMS (ESI) m/z: $[M + Na]^+$ Calcd for $C_{34}H_{35}O_5N_3NaS_2$ 652.1910; Found 652.1906.

7.3.9 Brønsted Acid-Catalysed Double Substitution

_N_-Butyl-2-((_N_-butyl-4-methylphenyl)sulfonamido)-2-(1_H_-indol-3-yl)-_N_-tosylacetamide, 62b



ZT083

To a heat gun-dried vial equipped with a stirrer bar were added *N*-butyl-2-((*N*-butyl-4-methylphenyl)sulfonamido)-2-(1*H*-indol-3-yl)-*N*-tosylacetamide (40 mg, 66 μmol, 1.0 eq.) and indole (10 mg, 85 μmol, 1.3 eq.). The vial was purged under high vacuum for 30 s and backfilled with argon (the vacuum cycle was repeated twice more).

Bis(trifluoromethane)sulfonimide (1 mg, 3.6 μmol, 5 mol%) was added to the vial inside the glovebox, after which the vial was removed from the glovebox and anhydrous DCE (0.13 mL) was added to dissolve the reactants. The solution was stirred under argon for 15 min until a white precipitate was formed indicating the completion of the reaction. The solvent was removed *in vacuo*, and the residue was suspended in Et_2O. The mixture was centrifuged, and the precipitate was washed twice more with Et_2O. Finally, after drying *in vacuo*, the title compound (33 mg, 66 μmol, 100%) was collected as a colourless solid which required no further purification.

m.p. 216 °C (decomp.);

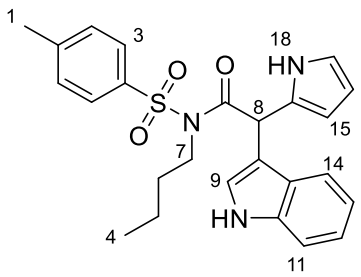
IR (thin film, ν_{max}/cm^{-1}) 3347, 2934, 1683, 1457, 1353, 1168, 1083, 1023, 814, 739;

^{1}H NMR (400 MHz, DMSO-d6) δ_H 10.91 (2H, s, H10), 7.72 (2H, d, *J* = 8.3 Hz, H3), 7.35 – 7.23 (6H, m, H2, H11, H14), 7.08 – 6.99 (2H, m, H12), 6.91 – 6.83 (2H, m, H13), 6.81 (2H, d, *J* = 2.4 Hz, H9), 5.83 (1H, s, H8), 3.92 – 3.83 (2H, m, H7), 2.36 (3H, s, H1), 1.67 – 1.54 (2H, m, H6), 1.32 – 1.18 (2H, m, H5), 0.81 (3H, t, *J* = 7.4 Hz, H4);

^{13}C NMR (101 MHz, DMSO-d6) δ_C 172.0, 144.2, 136.3, 136.3, 129.3, 127.7, 126.1, 124.0, 121.1, 118.5, 118.5, 111.9, 111.5, 46.5, 39.6, 32.5, 21.1, 19.4, 13.5;

HRMS (ESI) m/z: $[M - H]^-$ Calcd for $C_{29}H_{28}O_3N_3S$ 498.1857; Found 498.1854.

***N*-Butyl-2-(1*H*-indol-3-yl)-2-(1*H*-pyrrol-2-yl)-*N*-tosylacetamide, 62c**



ZT305

To a heat gun-dried vial equipped with a stirrer bar were added *N*-butyl-2-((*N*-butyl-4-methylphenyl)sulfonamido)-2-(1*H*-indol-3-yl)-*N*-tosylacetamide (122 mg, 0.2 mmol, 1.0 eq.). The vial was purged under high vacuum for 30 s and backfilled with argon (the vacuum cycle was repeated twice more). Inside the glovebox bis(trifluoromethane)sulfonimide (3 mg, 11 μmol, 5 mol%) was added to the vial, after which anhydrous DCE (0.40 mL) and pyrrole (17 mg, 0.26 mmol, 1.3 equiv.) were added to the reaction. The solution was then stirred at room temperature under argon for 3 h. Upon completion, the reaction mixture was concentrated *in vacuo*, and purified by column chromatography (30% EtOAc/pentane). The title compound (75 mg, 0.17 mmol, 83%) was collected as a colourless solid.

R_f 0.31 (30% EtOAc/pentane);

m.p. 145 °C (decomp.);

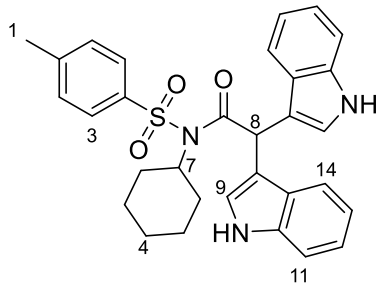
IR (thin film, ν_{max} / cm^{-1}) 3353, 2926, 2280, 1692, 1456, 1347, 1330, 1168, 1081, 880, 812, 718, 652;

^{1}H NMR (400 MHz, $CDCl_3$) δ_H 8.44 (1H, s, H18), 8.00 (1H, s, H10), 7.69 (2H, d, *J* = 8.4 Hz, H3), 7.37 – 7.29 (2H, m, H11, H14), 7.22 – 7.13 (3H, m, H2, H12), 7.03 (1H, ddd, *J* = 8.0, 7.1, 1.0 Hz, H13), 6.91 (1H, d, *J* = 2.0 Hz, H9), 6.64 – 6.61 (1H, m, H17), 6.06 (1H, app. q, *J* = 2.7 Hz, H16), 6.01 – 5.97 (1H, m, H15), 5.95 (1H, s, H8), 3.93 – 3.74 (2H, m, H7), 2.37 (3H, s, H1), 1.73 (2H, app. quin., *J* = 7.8 Hz, H6), 1.35 (2H, app. sext., *J* = 7.4 Hz, H5), 0.92 (3H, t, *J* = 7.4 Hz, H4);

^{13}C NMR (101 MHz, $CDCl_3$) δ_C 172.5, 144.7, 136.7, 136.4, 129.7, 127.9, 127.4, 126.2, 123.0, 122.6, 120.1, 118.9, 118.2, 113.0, 111.4, 108.1, 107.3, 47.2, 41.8, 32.4, 21.7, 20.2, 13.8;

HRMS (ESI) m/z: $[M + H]^+$ Calcd for $C_{25}H_{28}O_3N_3S$ 450.1846; Found 450.1846.

***N*-Cyclohexyl-2,2-di(1*H*-indol-3-yl)-*N*-tosylacetamide, 62d**



ZT244

To a heat gun-dried vial equipped with a stirrer bar were added *N*-benzyl-*N*-(((*N*-cyclohexyl-4-methylphenyl)sulfonamido)ethynyl)-4-methylbenzenesulfon-amide (50 mg, 75 μmol, 1.0 eq.) and indole (11 mg, 94 μmol, 1.3 eq.). The vial was purged under high vacuum for 30 s and backfilled with argon (the vacuum cycle was repeated twice more). Triflimide (1 mg, 3.7 μmol, 5 mol%) was also added to the vial inside the glovebox, after which anhydrous DCE (0.15 mL) was added to dissolve the reactants. The solution was then stirred under argon until a white precipitate was formed indicating the completion of the reaction. Next, the solvent was removed in vacuo, and Et_2O was added to suspend the residue. The mixture was centrifuged, and the precipitate was washed twice more with Et_2O. Finally, after drying *in vacuo*, the title compound (30 mg, 57 μmol, 76%) was collected as a colourless solid without further purification.

m.p. 254 °C (decomp.);

IR (thin film, ν_{max} / cm^{-1}) 3370, 2998, 2886, 1676, 1457, 1336, 1216, 1167, 1134, 1100, 1083, 954, 815, 741, 711, 652;

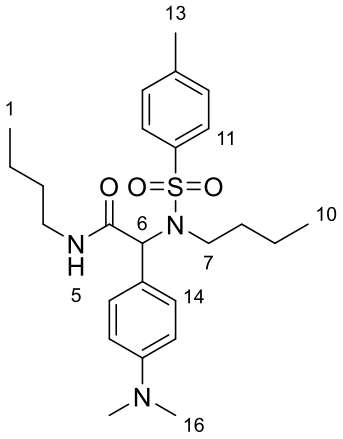
^{1}H NMR (400 MHz, DMSO-d6) δ_H 10.89 (2H, d, *J* = 1.9 Hz, H10), 7.69 (2H, d, *J* = 8.3 Hz, H3), 7.36 – 7.24 (6H, m, H2, H11, H14), 7.09 – 7.00 (2H, m, H12), 6.92 – 6.83 (4H, m, H9, H13), 5.97 (1H, s, H8), 4.20 (1H, tt, *J* = 11.9, 3.6 Hz, H7), 2.34 (3H, s, H1), 2.24 – 2.10 (2H, m, H6), 1.66 – 1.59 (2H, m, H6), 1.56 – 1.44 (3H, m, H4, H5), 1.11 – 0.95 (3H, m, H4, H5);

^{13}C NMR (101 MHz, DMSO-d6) δ_C 172.7, 144.0, 137.1, 136.2, 129.4, 127.4, 126.1, 124.0, 121.0, 118.7, 118.4, 112.1, 111.4, 60.8, 40.8, 30.7, 26.0, 24.8, 21.0;

HRMS (ESI) m/z: $[M - H]^-$ Calcd for $C_{31}H_{30}O_3N_3S$ 524.2013; Found 524.2015.

7.3.10 Miscellaneous

_N_-Butyl-2-((_N_-butyl-4-methylphenyl)sulfonamido)-2-(4-(dimethylamino)phenyl)acetamide, 64



ZT240

Modified from a literature procedure.[96] To a heat gun-dried vial was added *N*-Butyl-2-((*N*-butyl-4-methylphenyl)sulfonamido)-2-(4-(dimethylamino)phenyl)-*N*-tosylacetamide (62 mg, 0.10 mmol, 1.0 eq.), magnesium turnings (50 mg, 2.1 mmol, 20 eq.) and NH_4Cl (22 mg, 0.41 mmol, 4.0 eq.). The vial was then purged under high vacuum for 30 s and backfilled with argon (the vacuum cycle was repeated twice more). Anhydrous MeOH/THF (1:1 v/v, 2 mL) was added to the vial, and the mixture was sonicated under an argon atmosphere for 30 min. Upon completion, the reaction mixture was concentrated *in vacuo*, filtered through a Celite® pad and eluted with EtOAc. Subsequent flash chromatography (20% EtOAc/pentane) afforded the title compound (39 mg, 85 mmol, 84%) as a pale-yellow oil.

R_f 0.20 (20% EtOAc/pentane);

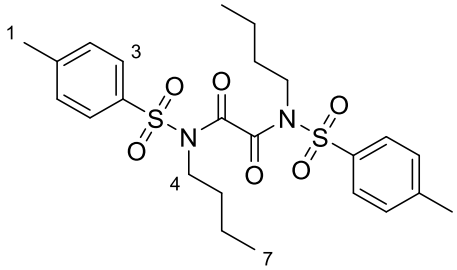
IR (thin film, ν_{max}/cm^{-1}) 3306, 2981, 1682, 1614, 1522, 1333, 1161, 1089, 908, 730, 660;

^{1}H NMR (400 MHz, $CDCl_3$) δ_H 7.69 (2H, d, *J* = 8.4 Hz, H11), 7.27 (2H, d, *J* = 8.4 Hz, H12), 6.91 (2H, d, *J* = 8.7 Hz, H14), 6.56 (2H, d, *J* = 8.7 Hz, H15), 6.23 (1H, t, *J* = 5.4 Hz, H5), 5.36 (1H, s, H6), 3.34 – 3.15 (3H, m, H4, H7), 3.01 – 2.87 (7H, m, H7, H16), 2.43 (3H, s, H13), 1.55 – 1.40 (3H, m, H3, H8), 1.38 – 1.28 (2H, m, H2), 1.17 – 1.00 (3H, m, H8, H9), 0.92 (3H, t, *J* = 7.3 Hz, H1), 0.74 (3H, t, *J* = 7.2 Hz, H10);

^{13}C NMR (101 MHz, $CDCl_3$) δ_C 169.9, 150.5, 143.4, 137.3, 130.7, 129.6, 127.5, 121.4, 112.2, 64.3, 46.3, 40.5, 39.5, 32.5, 31.6, 21.7, 20.2, 20.1, 13.9, 13.7;

HRMS (ESI) m/z: $[M + Na]^+$ Calcd for $C_{25}H_{37}O_3N_3NaS$ 482.2448; Found 482.2450.

***N*^{1},*N*^{2}-Dibutyl-*N*^{1},*N*^{2}-ditosyloxalamide, 65**



ZT227

Modified from a literature procedure.[220] To a solution of triethylamine (1.6 mL, 11.5 mmol, 2.4 eq.) and oxalyl chloride (0.4 mL, 4.66 mmol, 1.0 eq.) in DCM (20 mL) at 0 °C was added dropwise a solution of *N*-butyl-4-methylbenzenesulfonamide (2.33 g, 10.3 mmol, 2.2 eq.) in DCM (10 mL). The reaction mixture was warmed to room temperature and stirred overnight. The reaction was then quenched with water, extracted three times with DCM, concentrated in vacuo and purified by column chromatography (silica gel, DCM) to give the title compound (701 mg, 1.38 mmol, 30%) as a colourless viscous oil.

R_f 0.56 (DCM);

IR (thin film, ν_{max}/cm^{-1}) 2960, 1672, 1364, 1215, 1169, 1089, 1026, 909, 816, 730, 665;

^{1}H NMR (400 MHz, $CDCl_3$) δ_H 7.98 (4H, d, *J* = 8.3 Hz, H3), 7.37 (4H, d, *J* = 8.3 Hz, H2), 3.62 – 3.50 (2H, m, H4), 3.49 – 3.37 (2H, m, H4), 2.45 (6H, s, H1), 1.71 – 1.52 (4H, m, H5), 1.28 (4H, app. sext., *J* = 7.4 Hz, H6), 0.87 (6H, t, *J* = 7.4 Hz, H7);

^{13}C NMR (101 MHz, $CDCl_3$) δ_C 162.6, 145.6, 134.8, 130.1, 128.8, 45.4, 29.2, 21.9, 20.2, 13.7.

HRMS (ESI) m/z: $[M + H]^+$ Calcd for $C_{24}H_{33}N_2O_6S_2$ 509.1775; Found 509.1775.

7.4 Chapter III Characterisation Data

7.4.1 Regioselectivity Studies

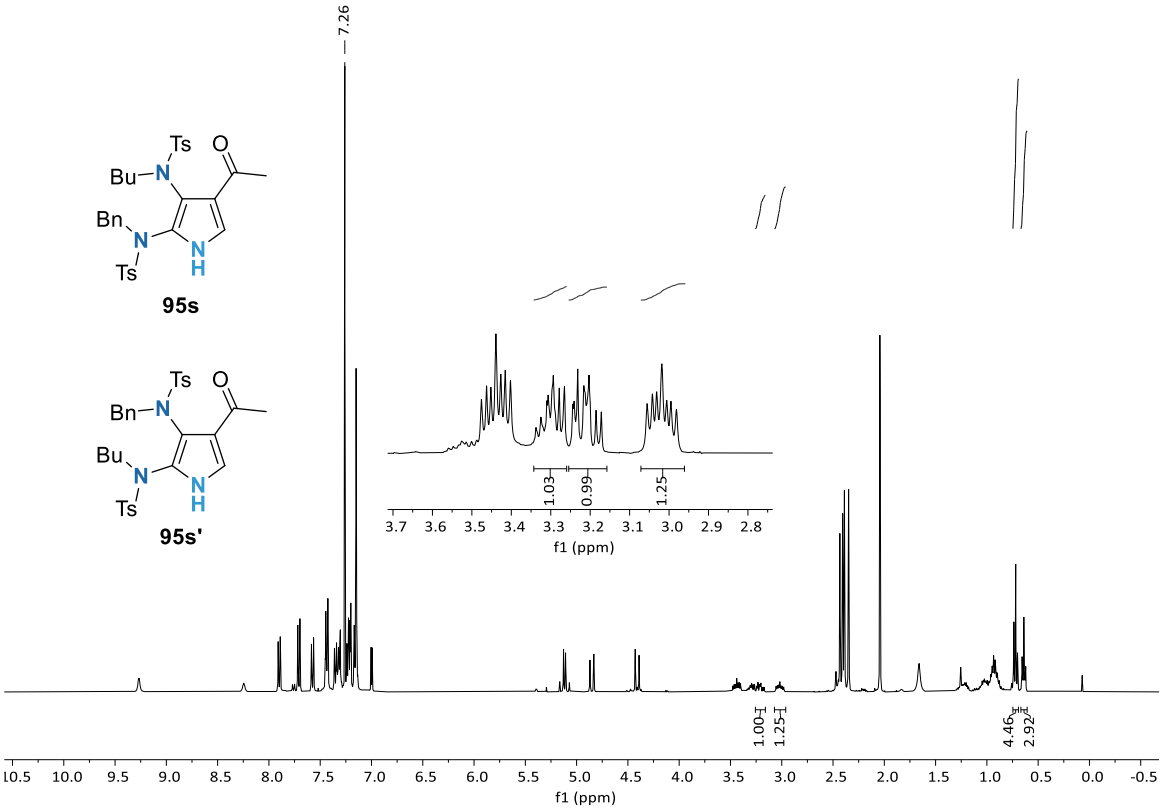


Figure 7.04 ^{1}H NMR (400 MHz, $CDCl_3$) of **95s/95s′** mixture. Integrated peak: BuCH_2, showing that **95s**:**95s′** ≈ 1:1. **HRMS** (ESI) m/z: [M + H]+ Calcd for $C_{31}H_{36}N_3O_5S_2$ 594.2091.; Found 594.2084.

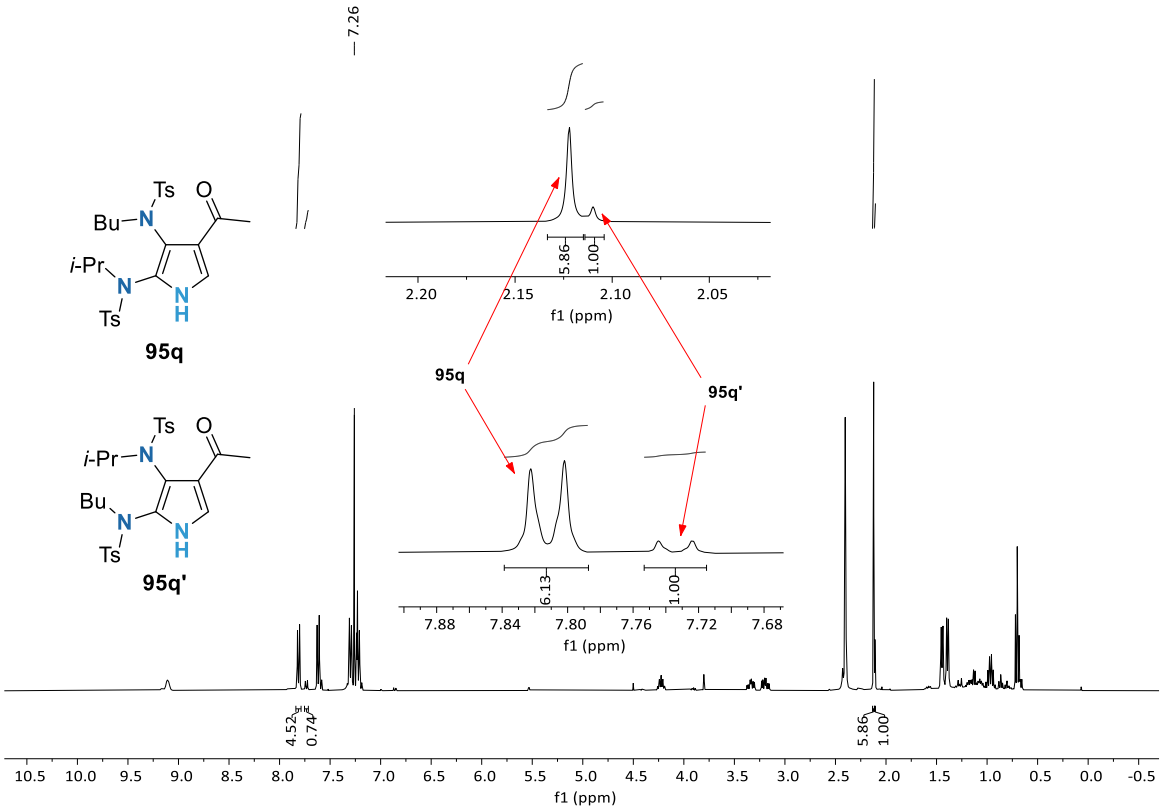


Figure 7.05 ^{1}H NMR (400 MHz, $CDCl_3$) of **95q/95q′** mixture. Integrated peak: Ts*H* and C(=O)C*H*$_3$, showing that **95q:95q′** ≈ 6:1. The structure of **95q** was confirmed in the latter NOESY experiment (Figure 7.06). HRMS (ESI) m/z: $[M + H]^+$ Calcd for $C_{27}H_{36}N_3O_5S_2$ 546.2091.; Found 546.2081.

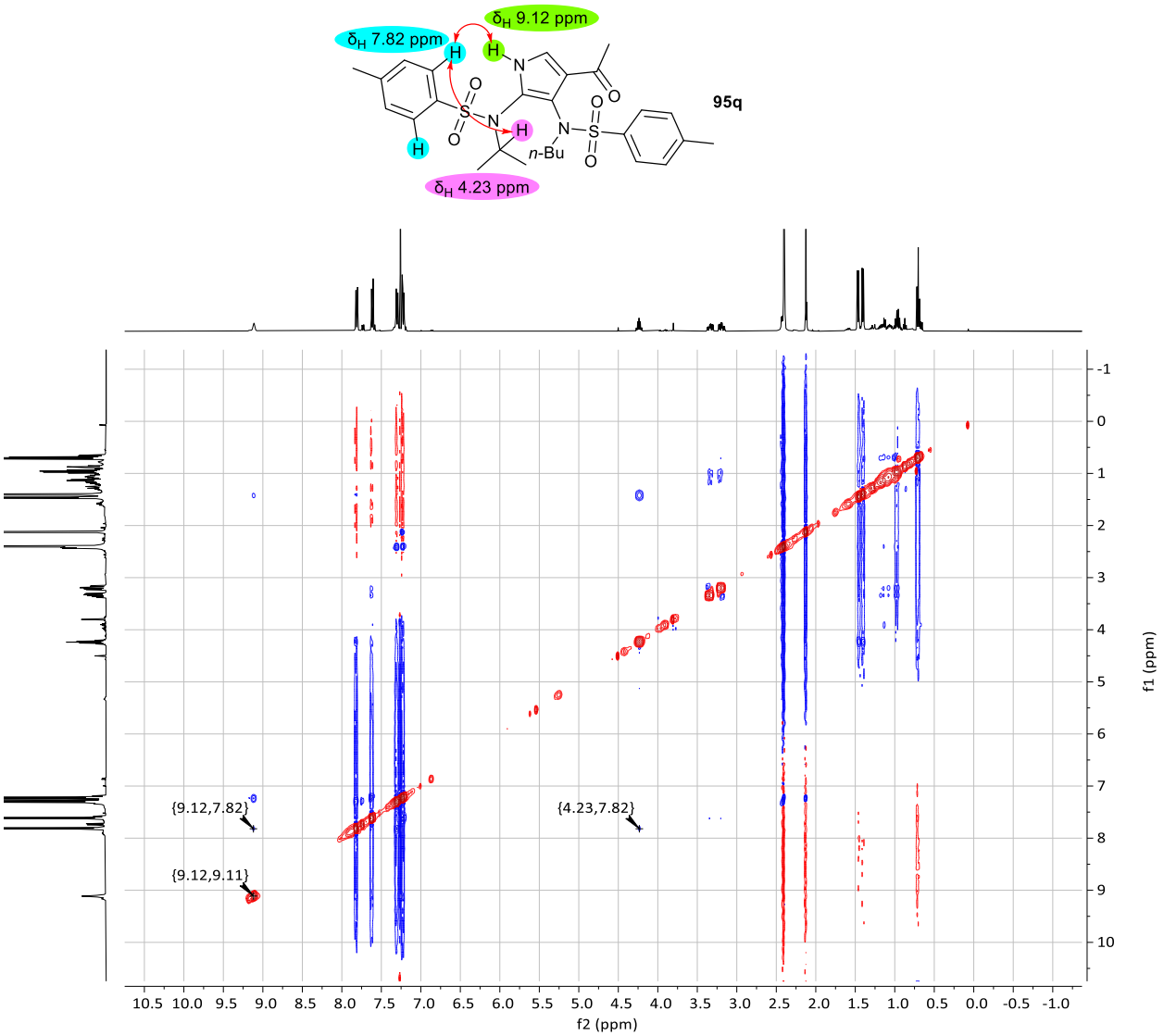


Figure 7.06 $^{1}H - {}^{1}H$ NOESY (400 MHz, $CDCl_3$) of **95q/95q′** mixture. The picked peaks show the marked correlation between protons in **95q**, confirming its structure is as proposed and it is the major regioisomer in the mixture.

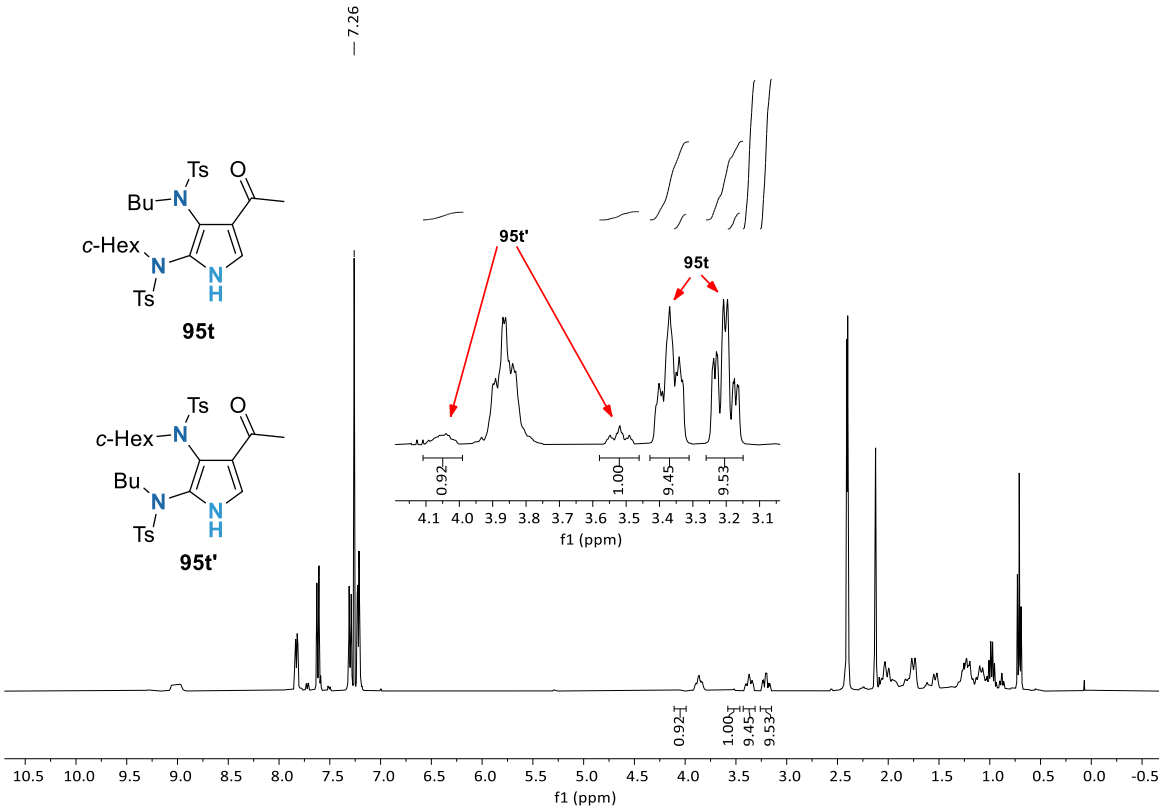


Figure 7.07 ^{1}H NMR (400 MHz, $CDCl_3$) of **95t/95t′** mixture. Integrated peak: CyC*H* and one of BuCH_2, showing that **95t**:**95t′** ≈ 9:1. The structure of **95t** was confirmed in the latter NOESY experiment (Figure 7.08). **HRMS** (ESI) m/z: [M + H]+ Calcd for $C_{30}H_{40}N_3O_5S_2$ 586.2404.; Found 586.2401.

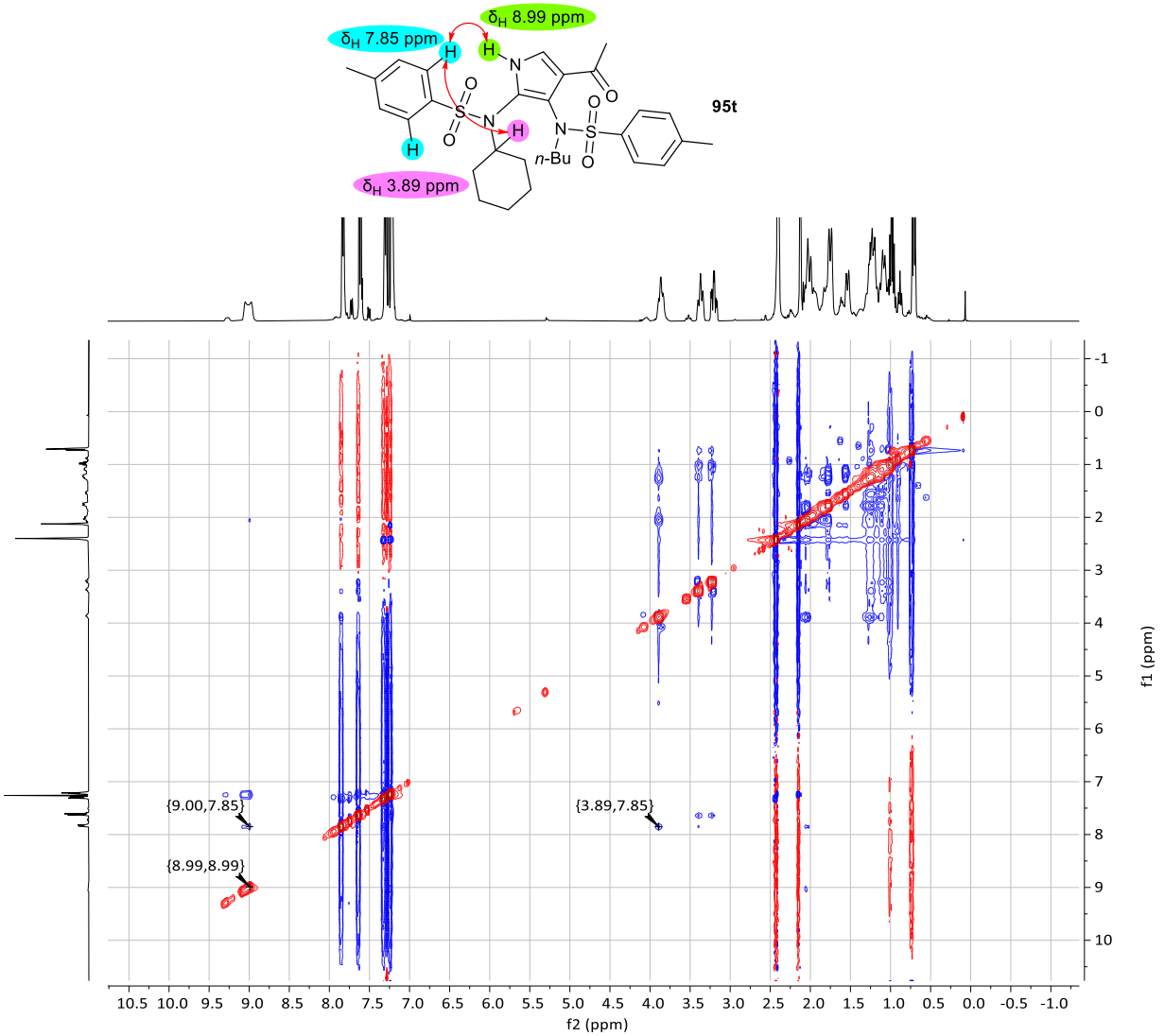


Figure 7.08 $^{1}H - {}^{1}H$ NOESY (400 MHz, $CDCl_3$) of **95t/95t′** mixture. The picked peaks show the marked correlation between protons in **95t**, confirming its structure is as proposed and it is the major regioisomer in the mixture.

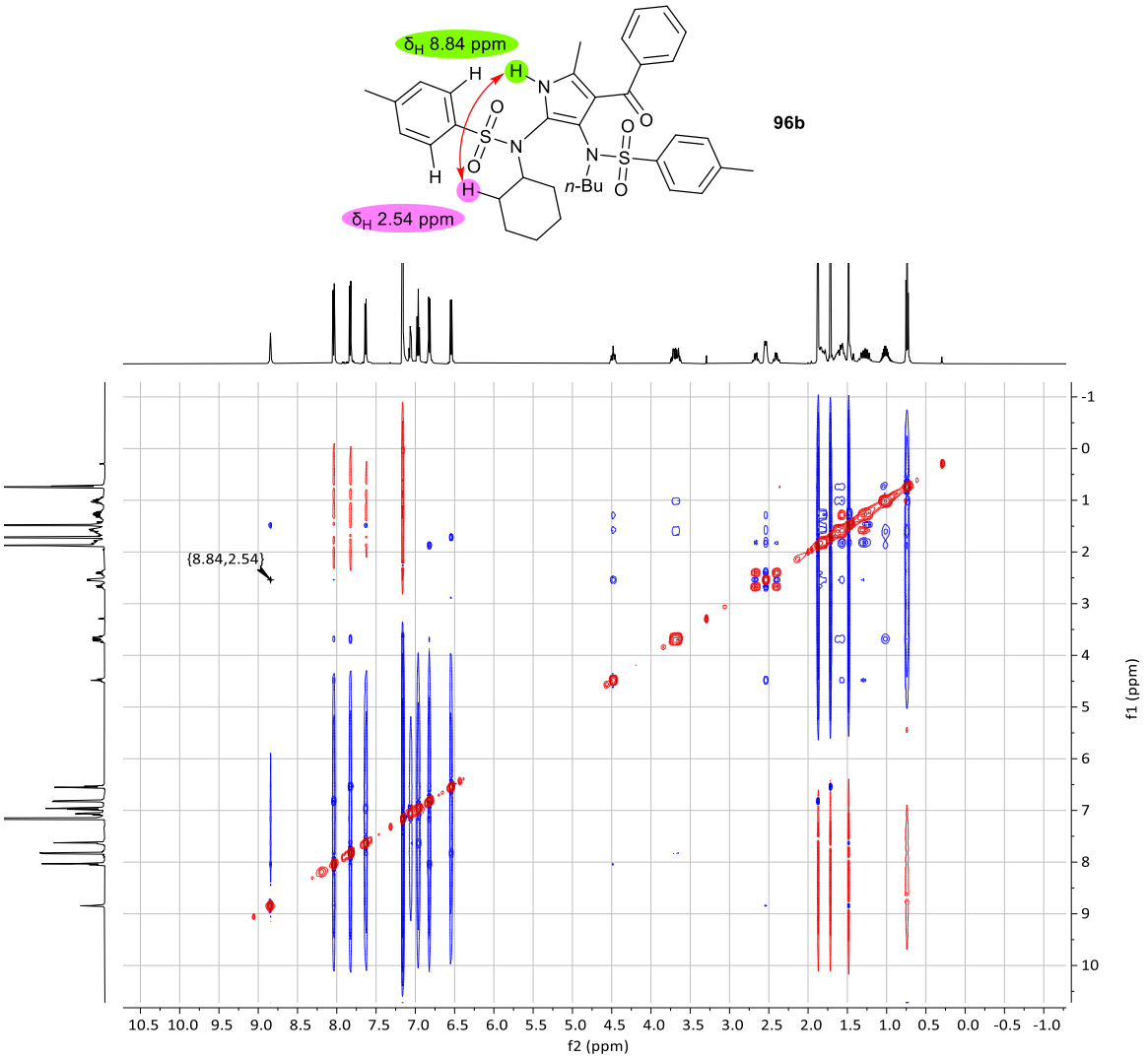


Figure 7.09 ^{1}H – ^{1}H NOESY (500 MHz, $CDCl_3$) of **96b**. The picked peaks show the marked correlation between protons in **96b**, confirming its structure is as proposed.

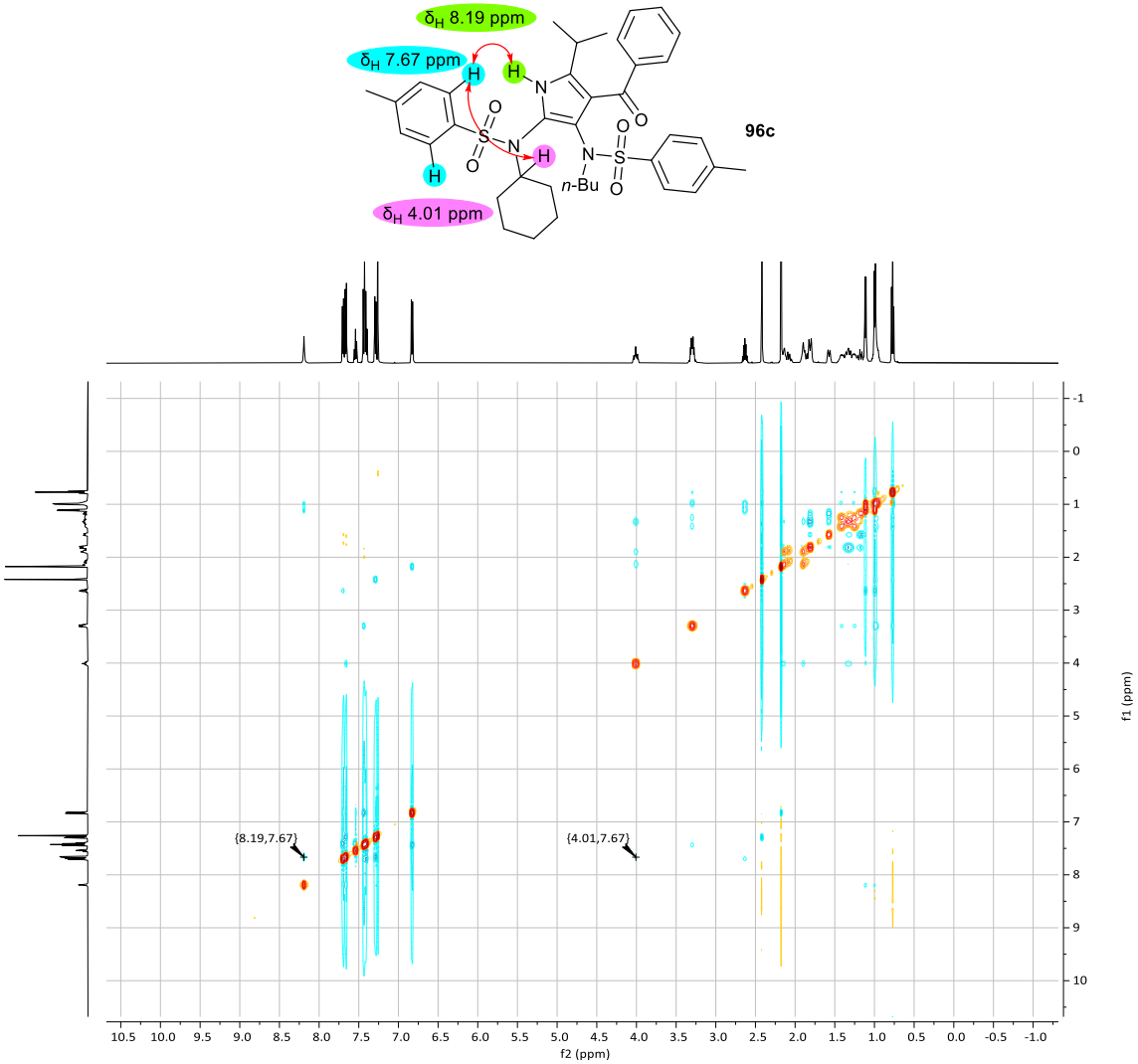


Figure 7.10 ^{1}H – ^{1}H NOESY (500 MHz, $CDCl_3$) of **96c**. The picked peaks show the marked correlation between protons in **96c**, confirming its structure is as proposed.

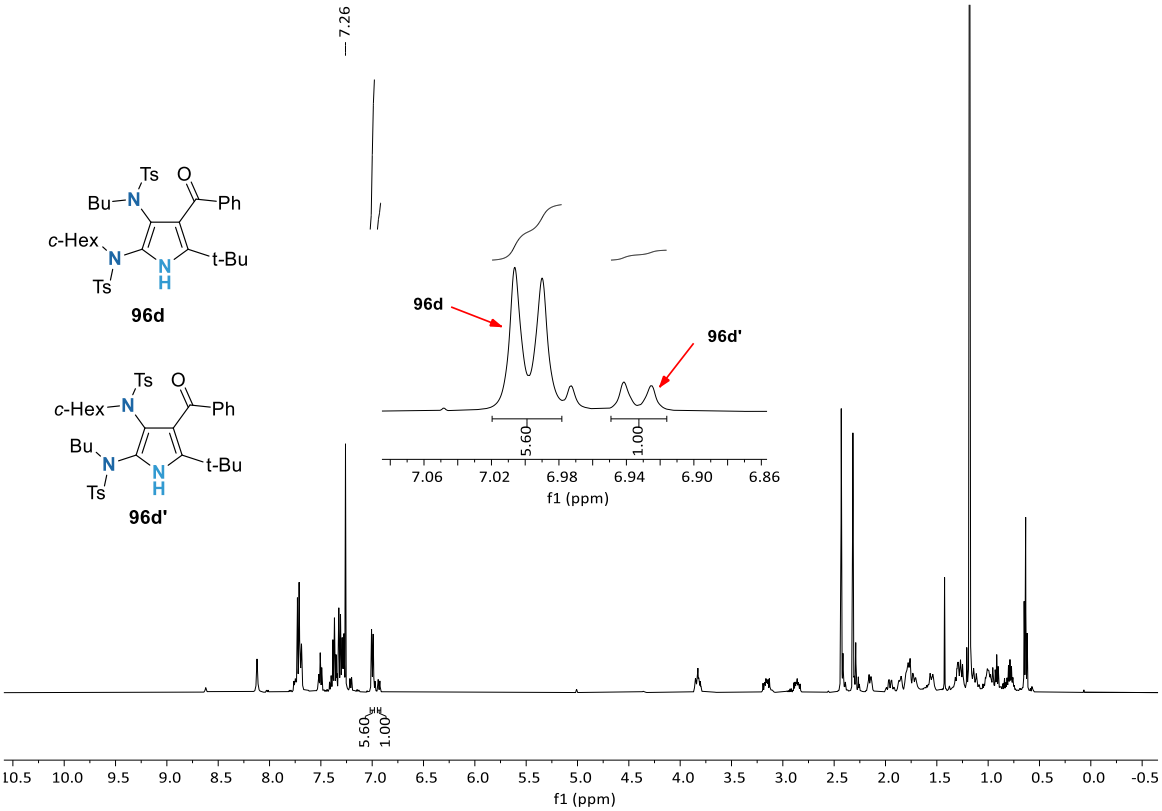


Figure 7.11 ^{1}H NMR (400 MHz, $CDCl_3$) of **96d/96d′** mixture. Integrated peak: Ts*H*, showing that **96d**:**96d′** ≈ 6:1. The structure of **96d** was confirmed in the latter NOESY experiment (Figure 7.11).

HRMS (ESI) m/z: [M + H]+ Calcd for $C_{39}H_{50}N_3O_5S_2$ 704.3187.; Found 704.3174.

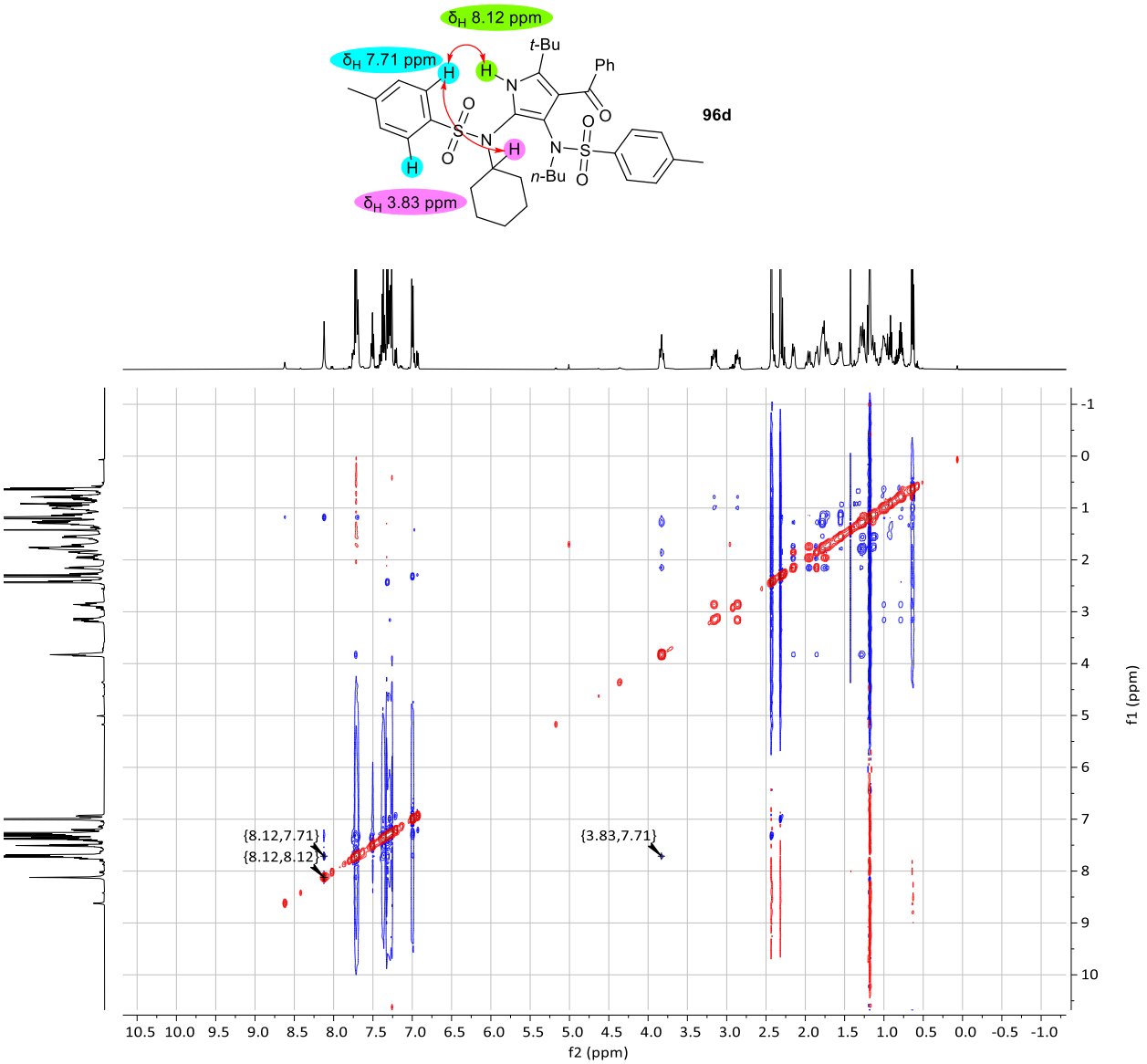
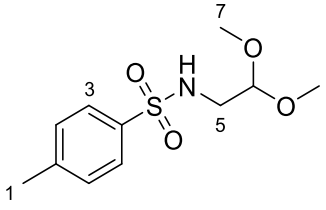


Figure 7.12 $^{1}H - {}^{1}H$ NOESY (400 MHz, $CDCl_3$) of **96d/96d′** mixture. The picked peaks show the marked correlation between protons in **96d**, confirming its structure is as proposed and it is the major regioisomer in the mixture.

7.4.2 Sulfonamides and Phosphoramidates

N-(2,2-Dimethoxyethyl)-4-methylbenzenesulfonamide, 1u



ZT436

Synthesised from 4-methylbenzenesulfonyl chloride (3.81 g, 20.0 mmol, 1.0 eq.), 2-aminoacetaldehyde dimethyl acetal (2.4 mL, 22.0 mmol, 1.1 eq.) and triethylamine (3.4 mL, 24.4 mmol, 1.2 eq.) in DCM (20 mL) with general procedure **7.2.1a**. The title compound (5.02 g, 19.4 mmol, 97%) was acquired as a pale-yellow oil without further purification.

R_f 0.41 (40% EtOAc/pentane)

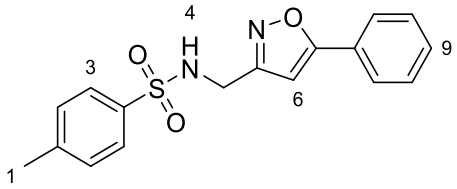
IR (thin film, ν_{max}/cm^{-1}) 3278, 2943, 1599, 1447, 1330, 1161, 1091, 815, 731, 664;

^{1}H NMR (400 MHz, $CDCl_3$) δ_H 7.74 (2H, d, *J* = 8.2 Hz, H3), 7.30 (2H, d, *J* = 8.2 Hz, H2), 4.73 (1H, brs., H4), 4.32 (1H, t, *J* = 5.6 Hz, H6), 3.31 (6H, s, H7), 3.02 (2H, d, *J* = 5.6 Hz, H5), 2.42 (3H, s, H1);

^{13}C NMR (101 MHz, $CDCl_3$) δ_C 143.7, 136.9, 129.9, 127.2, 102.7, 54.7, 44.7, 21.6.

Data are consistent with literature values.[221]

4-Methyl-*N*-((5-phenylisoxazol-3-yl)methyl)benzenesulfonamide, 111



ZT521, ZT523

Modified from a literature procedure.[222]

Step 1: To a heat gun-dried flask was added *tert*-butyl tosylcarbamate (1.81 g, 6.67 mmol, 1.0 eq.) and PPh_3 (2.10 g, 8.00 mmol, 1.2 eq.). The flask was purged under high vacuum for 30 s and backfilled with argon (this cycle was repeated twice more). Anhydrous THF (25 mL) and (5-phenylisoxazol-3-yl)methanol (1.40 mL, 8.00 mmol, 1.2 eq.) were added, and the solution was cooled to 0 °C in an ice bath. DIAD (1.6 mL, 8.00 mmol, 1.2 eq.) was added to the solution dropwise. The reaction mixture was then warmed slowly to room

temperature and stirred until completion by TLC. Upon completion, the reaction mixture was concentrated *in vacuo* and purified by column chromatography (silica gel, 0% → 10% → 20% EtOAc/pentane) to afford the crude *tert*-butyl ((5-phenylisoxazol-3-yl)methyl)(tosyl)carbamate which was used in the next step without further purification.

Step 2: In a round-bottom flask was dissolved the crude *tert*-butyl ((5-phenylisoxazol-3-yl)methyl)(tosyl)carbamate in DCM/TFA (20 mL, 1:1 v/v). The reaction mixture was stirred at room temperature for 2 h. Excess TFA was neutralized by adding saturated $NaHCO_3$ solution, and the mixture was extracted three times with DCM. The organic layer was combined, washed with brine, dried over Na_2SO_4, concentrated *in vacuo* and purified by column chromatography (silica gel, DCM) to afford the title compound (1.05 g, 3.20 mmol, 48%) as a colourless solid;

m.p. 152 – 153 °C;

R_f 0.12 (DCM);

IR (thin film, ν_{max}/cm^{-1}) 3314, 1456, 1414, 1326, 1157, 1092, 1068, 907, 846, 769, 693;

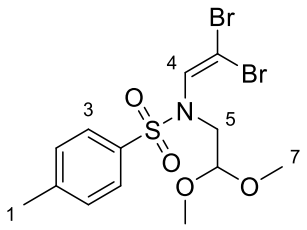
^{1}H NMR (400 MHz, DMSO) δ_H 8.28 (1H, s, H4), 7.79 – 7.71 (2H, m, H7), 7.67 (2H, d, *J* = 8.3 Hz, H3), 7.56 – 7.47 (3H, m, H8, H9), 7.33 (2H, d, *J* = 8.3 Hz, H2), 6.65 (1H, s, H6), 4.09 (2H, s, H5), 2.25 (3H, s, H1);

^{13}C NMR (101 MHz, DMSO) δ_C 169.0, 161.6, 142.9, 137.4, 130.4, 129.5, 129.3, 126.7, 126.6, 125.5, 99.7, 38.1, 20.8;

HRMS (ESI) m/z: $[M + H]^+$ Calcd for $C_{17}H_{17}N_2O_3S$ 329.0954; Found 329.0951.

7.4.3 1,1-Dibromoenamides

***N*-(2,2-Dibromovinyl)-*N*-(2,2-dimethoxyethyl)-4-methylbenzenesulfonamide, 2u**



ZT440, ZT441

Synthesised from *N*-(2,2-dimethoxyethyl)-4-methylbenzenesulfonamide (2.59 g, 10.0 mmol, 1.0 eq.), *n*-butyllithium (2.0 M in hexane, 5.5 mL, 11.0 mmol, 1.1 eq.), BtCHO (1.91 g, 13.0 mmol, 1.3 eq.), carbontetrabromide (9.95 g, 30.0 mmol, 3.0 eq.), triphenylphosphine (15.74 g, 60.0 mmol, 6.0 eq.) with general procedure **7.2.1c**. Column chromatography (silica gel, 10% → 20% EtOAc/pentane) afforded the title compound (3.13 g, 7.06 mmol, 71%) as a colourless solid.

m.p. 75 °C;

R_f 0.56 (20% EtOAc/pentane);

IR (thin film, ν_{max}/cm^{-1}) 2955, 2835, 1598, 1355, 1163, 1128, 1089, 1068, 871, 740, 660;

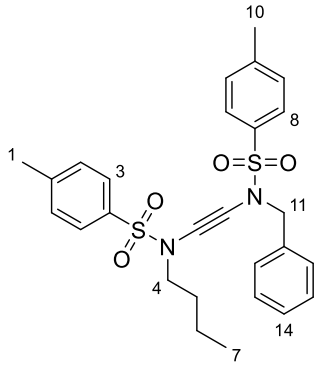
^{1}H NMR (500 MHz, $CDCl_3$) δ_H 7.69 (2H, d, *J* = 8.2 Hz, H3), 7.31 (2H, d, *J* = 8.2 Hz, H2), 6.76 (1H, s, H4), 4.54 (1H, t, *J* = 5.4 Hz, H6), 3.43 (2H, d, *J* = 5.4 Hz, H5), 3.37 (6H, s, H7), 2.43 (3H, s, H1);

^{13}C NMR (126 MHz, $CDCl_3$) δ_C 144.4, 135.9, 132.5, 129.9, 127.5, 103.2, 97.4, 54.6, 50.7, 21.7.

HRMS (ESI) m/z: $[M + Na]^+$ Calcd for $C_{13}H_{17}{}^{79}Br_2NO_4SNa$ 463.9137; Found 463.9138.

7.4.4 Yndiamides

_N_-Benzyl-_N_-(((_N_-butyl-4-methylphenyl)sulfonamido)ethynyl)-4-methylbenzenesulfonamide, 4s



ZT385

Synthesised from *N*-butyl-4-methylbenzenesulfonamide (455 mg, 2.00 mmol, 1.0 eq.), *N*-benzyl-*N*-(2,2-dibromovinyl)-4-methylbenzenesulfonamide (979 mg, 2.20 mmol, 1.1 eq.), CuI (76 mg, 0.40 mmol, 0.20 eq.), 1,10-phenanthroline (144 mg, 0.80 mmol, 0.40 eq.) and Cs_2CO_3 (1.95 g, 6.00 mmol, 3.0 eq.) with general procedure **7.2.1d**. Column chromatography (silica gel, 20% Et_2O + 10% DCM/pentane) afforded the title compound (689 mg, 1.35 mmol, 67%) as a colourless solid.

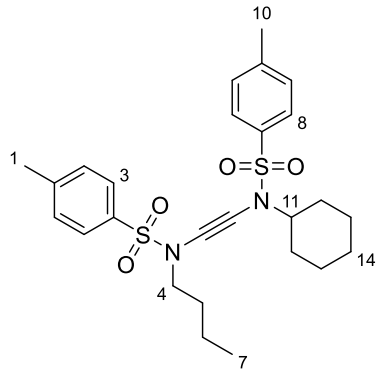
IR (thin film, ν_{max}/cm^{-1}) 2959, 2933, 1363, 1169, 1089, 814, 729;

^{1}H NMR (400 MHz, $CDCl_3$) δ_H 7.67 (2H, d, *J* = 8.3 Hz, TsC*H*), 7.60 (2H, d, *J* = 8.3 Hz, TsC*H*), 7.29 – 7.24 (7H, m, TsC*H*, H13, H14), 7.19 – 7.15 (2H, m, H12), 4.49 (2H, s, H11), 3.17 (2H, t, *J* = 7.2 Hz, H4), 2.44 (6H, s, H1, H10), 1.29 (2H, app. quin., *J* = 7.2 Hz, H5), 1.13 (2H, app. sext., *J* = 7.3 Hz, H6), 0.77 (3H, t, *J* = 7.3 Hz, H7);

^{13}C NMR (101 MHz, $CDCl_3$) δ_C 144.6, 144.5, 135.1, 134.8, 129.77, 129.75, 128.9, 128.5, 128.3, 127.8, 127.7, 69.9, 69.2, 56.1, 51.5, 29.8, 21.8, 19.4, 13.7. *Two peaks are obscured due to signal overlap.*

Data are consistent with literature values.[25]

***N*-Butyl-*N*-(((*N*-cyclohexyl-4-methylphenyl)sulfonamido)ethynyl)-4-methylbenzenesulfonamide, 4t**



ZT377

Synthesised from *N*-cyclohexyl-4-methylbenzenesulfonamide (507 mg, 2.00 mmol, 1.0 eq.)**,** *N*-butyl-*N*-(2,2-dibromovinyl)-4-methylbenzenesulfonamide (905 mg, 2.20 mmol, 1.1 eq.), CuI (76 mg, 0.40 mmol, 0.20 eq.), 1,10-phenanthroline (144 mg, 0.80 mmol, 0.40 eq.) and Cs_2CO_3 (1.95 g, 6.00 mmol, 3.0 eq.) with general procedure **7.2.1d**. Column chromatography (silica gel, 5% → 10% EtOAc/pentane) afforded the title compound (380 mg, 0.76 mmol, 38%) as a colourless solid.

m.p. 99 °C;

R_f 0.27 (10% EtOAc/pentane);

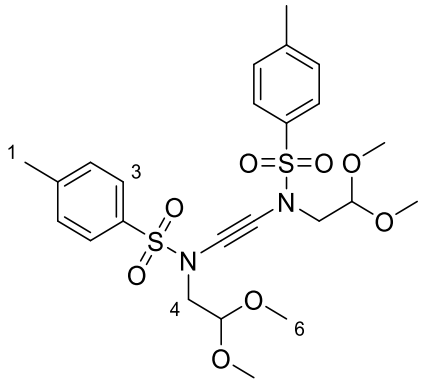
IR (thin film, ν_{max}/cm^{-1}) 2934, 2859, 1686, 1356, 1162, 1088, 814, 667;

^{1}H NMR (400 MHz, $CDCl_3$) δ_H 7.74 – 7.69 (4H, m, H3, H8), 7.32 – 7.27 (4H, m, H2, H9), 3.81 – 3.69 (1H, m, H11), 3.35 (2H, t, *J* = 7.2 Hz, H4), 2.44 (6H, s, H1, H10), 1.75 – 1.64 (2H, m, H12), 1.59 – 1.49 (5H, m, H5, H13, H14), 1.35 – 1.22 (6H, m, H6, H12, H13), 1.00 – 0.91 (1H, m, H14), 0.88 (3H, t, *J* = 7.4 Hz, H7);

^{13}C NMR (101 MHz, $CDCl_3$) δ_C 144.5, 144.3, 136.5, 135.2, 129.8, 127.8, 127.7, 127.6, 70.4, 66.8, 59.3, 51.5, 31.2, 30.0, 25.5, 25.0, 21.77, 21.76, 19.5, 13.7.

HRMS (ESI) m/z: $[M + Na]^+$ Calcd for $C_{26}H_{34}N_2N_aO_4S_2$ 525.1853, found 525.1853.

***N,N'*-(Ethyne-1,2-diyl)bis(*N*-(2,2-dimethoxyethyl)-4-methylbenzenesulfonamide). 4u**



ZT450

Synthesised from *N*-(2,2-dimethoxyethyl)-4-methylbenzenesulfonamide (259 mg, 1.00 mmol, 1.0 eq.), *N*-(2,2-dibromovinyl)-*N*-(2,2-dimethoxyethyl)-4-methylbenzenesulfonamide (487 mg, 1.10 mmol, 1.1 eq.), CuI (38 mg, 0.20 mmol, 0.20 eq.), 1,10-phenanthroline (72 mg, 0.40 mmol, 0.40 eq.), and Cs_2CO_3 (977 mg, 3.00 mmol, 3.0 eq.) with general procedure **7.2.1d**. Column chromatography (silica gel, 20% EtOAc/pentane), followed by second column chromatography (silica gel, 20% acetone/pentane) and recrystallization from DCM/pentane afforded the title compound (178 mg, 0.33 mmol, 33%) as a colourless solid;

m.p. 98 °C;

R_f 0.34 (20% acetone/pentane);

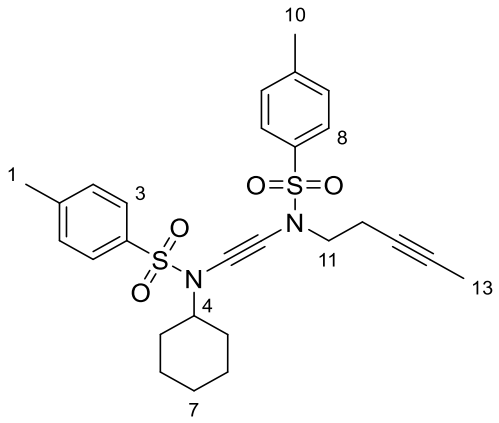
IR (thin film, ν_{max}/cm^{-1}) 2941, 1410, 1362, 1169, 1088, 910, 731, 658;

^{1}H NMR (400 MHz, $CDCl_3$) δ_H 7.72 (4H, d, *J* = 8.2 Hz, H3), 7.30 (4H, d, *J* = 8.2 Hz, H2), 4.50 (2H, t, *J* = 5.5 Hz, H5), 3.45 (4H, d, *J* = 5.5 Hz, H4), 3.30 (12H, s, H6), 2.44 (6H, s, H1);

^{13}C NMR (101 MHz, $CDCl_3$) δ_C 144.7, 135.1, 129.7, 128.0, 102.1, 69.4, 54.4, 53.0, 21.8;

HRMS (ESI) m/z: $[M + H]^+$ Calcd for $C_{24}H_{33}N_2O_8S_2$ 541.1673.; Found 541.1676.

***N*-Cyclohexyl-4-methyl-*N*-(((4-methyl-*N*-(pent-3-yn-1-yl)phenyl)sulfonamido)ethynyl)benzenesulfonamide, 4v**



ZT507

Synthesised from *N*-cyclohexyl-4-methylbenzenesulfonamide (253 mg, 1.00 mmol, 1.0 eq.), *N*-(2,2-dibromovinyl)-4-methyl-*N*-(pent-3-yn-1-yl)benzenesulfonamide (463 mg, 1.10 mmol, 1.1 eq.), CuI (38 mg, 0.20 mmol, 0.20 eq.), 1,10-phenanthroline (72 mg, 0.40 mmol, 0.40 eq.), and Cs_2CO_3 (977 mg, 3.00 mmol, 3.0 eq.) with general procedure **7.2.1d**. Column chromatography (silica gel, 5% Et_2O + 5% DCM/pentane → 10% Et_2O + 10%DCM/pentane) afforded the title compound (215 mg, 0.42 mmol, 42%) as a yellow oil;

R_f 0.24 (10% Et_2O + 10%DCM/pentane);

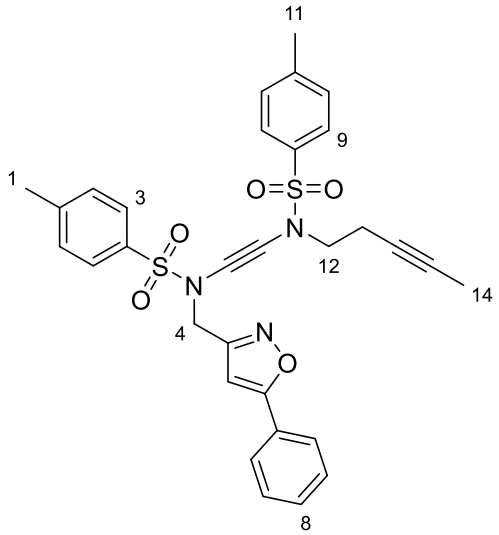
IR (thin film, ν_{max} / cm^{-1}) 2935, 2858, 1598, 1364, 1166. 1090, 912, 814, 732, 662;

^{1}H NMR (400 MHz, $CDCl_3$) δ_H 7.76 – 7.70 (4H, m, H3, H8), 7.30 (4H, overlapping doublet, *J* = 8.1 Hz, H2, H9), 3.75 (1H, brs., H4), 3.49 (2H, t, *J* = 8.1 Hz, H11), 2.44 (3H, s, H10), 2.43 (3H, s, H1), 2.39 – 2.32 (2H, m, H12), 1.73 – 1.65 (5H, m, H5, H13), 1.59 – 1.52 (3H, m, H6, H7), 1.33 – 1.19 (4H, m, H5, H6), 1.01 – 0.87 (1H, m, H7);

^{13}C NMR (101 MHz, $CDCl_3$) δ_C 144.6, 144.4, 136.3, 135.1, 129.81, 129.80, 127.9, 127.5, 77.9, 74.8, 69.9, 67.4, 59.4, 50.8, 31.1, 25.4, 24.9, 21.8, 21.8, 18.7, 3.6;

HRMS (ESI) m/z: $[M + H]^+$ Calcd for $C_{27}H_{33}N_2O_4S_2$ 513.1876.; Found 513.1866.

4-Methyl-*N*-(((4-methyl-*N*-((5-phenylisoxazol-3-yl)methyl)phenyl)sulfonamido)ethynyl)-*N*-(pent-3-yn-1-yl)benzenesulfonamide, 4w



ZT527

Synthesised from 4-methyl-*N*-((5-phenylisoxazol-3-yl)methyl)benzenesulfonamide (328 mg, 1.00 mmol, 1.0 eq.), *N*-(2,2-dibromovinyl)-4-methyl-*N*-(pent-3-yn-1-yl)benzenesulfonamide (463 mg, 1.10 mmol, 1.1 eq.), CuI (38 mg, 0.20 mmol, 0.20 eq.), 1,10-phenanthroline (72 mg, 0.40 mmol, 0.40 eq.), and Cs_2CO_3 (977 mg, 3.00 mmol, 3.0 eq.) with general procedure **7.2.1d**. Column chromatography (silica gel, 0 → 5% DCM + 10% Et_2O/pentane → 10% DCM + 20% Et_2O/pentane) afforded the title compound (161 mg, 0.27 mmol, 27%) as a yellow solid;

m.p. 119 – 120 °C;

R_f 0.34 (10%DCM + 20% Et2O/pentane);

IR (thin film, ν_{max}/cm^{-1}) 2921, 1614, 1367, 1168, 1090, 912, 814, 767, 730, 673;

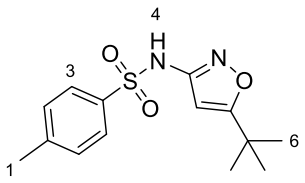
^{1}H NMR (400 MHz, $CDCl_3$) δ_H 7.75 – 7.64 (6H, m, H3, H6, H9), 7.48 – 7.40 (3H, m, H7, H8), 7.30 – 7.20 (4H, m, H2, H10), 6.50 (1H, s, H5), 4.71 (2H, s, H4), 3.43 (2H, t, *J* = 7.5 Hz, H12), 2.41 (3H, s, H1), 2.38 – 2.31 (2H, m, H13), 2.27 (3H, s, H11), 1.68 (3H, t, *J* = 2.5 Hz, H14);

^{13}C NMR (101 MHz, $CDCl_3$) δ_C 170.6, 159.6, 145.2, 144.9, 135.1, 134.5, 130.4, 130.0, 129.8, 129.1, 128.0, 127.5, 127.2, 125.9, 98.9, 78.1, 74.5, 69.8, 69.4, 50.8, 48.0, 21.8, 21.6, 18.7, 3.5;

HRMS (ESI) m/z: $[M + H]^+$ Calcd for $C_{31}H_{30}N_3O_5S_2$ 588.1621.; Found 588.1634.

7.4.5 Isoxazoles and Benzo[d]isoxazoles

***N*-(5-(*tert*-Butyl)isoxazol-3-yl)-4-methylbenzenesulfonamide, 87e**



ZT362

In a round-bottom flask containing a stirrer bar was dissolved 5-(*tert*-butyl)isoxazole-3-amine (463 mg, 3.30 mmol, 1.1 eq.) and pyridine (0.27 mL, 3.35 mmol, 1.1 eq.) in DCM (4 mL). The solution was cooled to 0 °C on an ice bath before a solution of 4-methylbenzenesulfonyl chloride (573 mg, 3.00 mmol, 1.0 eq.) in DCM (2 mL) was added dropwise. The reaction was slowly warmed to room temperature and stirred until completion by TLC. Upon completion, the reaction mixture was diluted with DCM and washed with 1 M HCl. The organic phase was collected, washed with saturated $NaHCO_3$ solution, then with brine, and finally dried over Na_2SO_4. The solvent was removed *in vacuo* and recrystallization from DCM/pentane afforded the title compound (578 mg, 1.96 mmol, 65%) as a pink solid;

m.p. 122 °C;

R_f 0.14 (DCM);

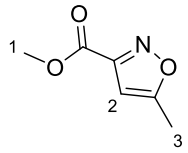
IR (thin film, ν_{max}/cm^{-1}) 3140, 2971, 1599, 1459, 1168, 1091, 908, 814, 732, 670;

^{1}H NMR (400 MHz, DMSO) δ_H 11.33 (1H, s, H4), 7.75 (2H, d, *J* = 8.2 Hz, H3), 7.40 (2H, d, *J* = 8.2 Hz, H2), 6.04 (1H, s, H5), 2.37 (3H, s, H1), 1.22 (9H, s, H6);

^{13}C NMR (101 MHz, DMSO) δ_C 181.1, 157.2, 143.8, 136.7, 129.7, 126.8, 92.3, 32.4, 28.2, 21.0;

HRMS (ESI) m/z: $[M + H]^+$ Calcd for $C_{14}H_{19}N_2O_3S$ 295.1111; Found 295.1111.

Methyl 5-methylisoxazole-3-carboxylate, 87j



ZT345

In a round-bottom flask containing a stirrer bar, was dissolved 5-methylisoxazole-3-carboxylic acid (256 mg, 2.01 mmol, 1.0 eq.). in MeOH (4 mL). Concentrated sulfuric acid (97 wt%, 55 µL, 1.01 mmol, 0.5 eq.) was added dropwise to the solution. The reaction mixture was stirred under reflux until completion by TLC. Upon completion, the reaction mixture was concentrated in vacuo, diluted with DCM, and washed with saturated $NaHCO_3$ solution. The organic phase was then collected, washed with brine, and dried over Na_2SO_4. The solvent was removed *in vacuo* to give the title compound (243 mg, 1.72 mmol, 85%) as a colourless solid;

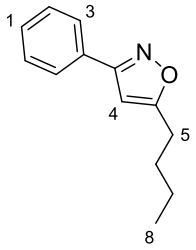
IR (thin film, ν_{max} / cm^{-1}) 3137, 2965, 1729, 1458, 1275, 1213, 1004, 918, 785, 729;

^{1}H NMR (400 MHz, $CDCl_3$) δ_H 6.40 (1H, s, H2), 3.95 (3H, s, H1), 2.48 (3H, s, H3);

^{13}C NMR (101 MHz, $CDCl_3$) δ_C 171.5, 160.7, 156.4, 102.4, 52.9, 12.4.

Data are consistent with literature values.[223]

5-Butyl-3-phenylisoxazole, 87k



ZT346

Synthesised from hydroxylamine hydrochloride (143 mg, 2.06 mmol, 1.05 eq.), benzaldehyde (0.20 mL, 2.06 mmol, 1.00 eq.), NaOH (82 mg, 2.06 mmol, 1.05 eq.), Chloramine T trihydrate (580 mg, 2.06 mmol, 1.05 eq.), copper sulfate pentahydrate (15 mg, 60 μmol, 3 mol%), copper turning (1 pc, *ca.* 50 mg), and hex-1-yne (0.24 mL, 2.09 mmol, 1.05 eq.) with general procedure **7.2.2b**. Column chromatography (5% EtOAc/pentane) afforded the title compound (209 mg, 1.04 mmol, 53%) as a pale yellow oil;

R_f 0.58 (5% EtOAc/pentane);

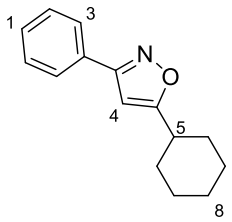
IR (thin film, ν_{max}/cm^{-1}) 2959, 2873, 1602, 1580, 1471, 1408, 908, 768, 731, 693;

^{1}H NMR (400 MHz, $CDCl_3$) δ_H 7.83 – 7.74 (2H, m, H3), 7.49 – 7.39 (3H, m, H1, H2), 6.28 (1H, s, H4), 2.80 (2H, t, *J* = 7.6 Hz, H5), 1.74 (2H, app. quin., *J* = 7.5 Hz, H6), 1.44 (2H, app. sext., *J* = 7.4 Hz, H7), 0.97 (3H, t, *J* = 7.4 Hz, H8);

^{13}C NMR (101 MHz, $CDCl_3$) δ_C 174.4, 162.5, 129.9, 129.6, 129.0, 126.9, 98.9, 29.8, 26.7, 22.3, 13.8.

Data are consistent with literature values.[224]

5-Cyclohexyl-3-phenylisoxazole, 87l



ZT364

Synthesised from hydroxylamine hydrochloride (286 mg, 4.12 mmol, 1.05 eq.), benzaldehyde (0.40 mL, 3.92 mmol, 1.00 eq.), NaOH (165 mg, 4.12 mmol, 1.05 eq.), Chloramine T trihydrate (1.16 g, 4.12 mmol, 1.05 eq.), copper sulfate pentahydrate (29 mg, 0.12 mmol, 3 mol%), copper turning (1 pc, *ca.* 50 mg), and ethynyl cyclohexane (0.54 mL, 4.12 mmol, 1.05 eq.) with general procedure **7.2.2b**. Column chromatography (5% → 10% EtOAc/pentane) afforded the title compound (391 mg, 1.72 mmol, 44%) as a colourless solid;

R_f 0.78 (10% EtOAc/pentane);

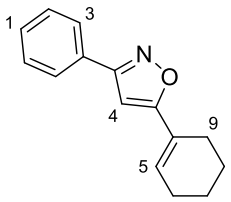
IR (thin film, ν_{max}/cm^{-1}) 2934, 2859, 1597, 1580, 1406, 924, 765, 690;

^{1}H NMR (400 MHz, $CDCl_3$) δH 7.83 – 7.76 (2H, m, H3), 7.48 – 7.39 (3H, m, H1, H2), 6.25 (1H, s, H4), 2.83 (1H, tt, *J* = 11.3, 3.6 Hz, H5), 2.15 – 2.07 (2H, m, H6), 1.88 – 1.80 (2H, m, H7), 1.78 – 1.70 (1H, m, H8), 1.56 – 1.36 (4H, m, H6, H7), 1.35 – 1.23 (1H, m, H8);

^{13}C NMR (101 MHz, $CDCl_3$) δ_C 178.5, 162.3, 129.9, 129.7, 129.0, 126.9, 97.2, 36.6, 31.4, 26.0, 25.8.

Data are consistent with literature values.[225]

5-(Cyclohex-1-en-1-yl)-3-phenylisoxazole, 87m



ZT363

Synthesised from hydroxylamine hydrochloride (286 mg, 4.12 mmol, 1.05 eq.), benzaldehyde (0.40 mL, 3.92 mmol, 1.00 eq.), NaOH (165 mg, 4.12 mmol, 1.05 eq.), Chloramine T trihydrate (1.16 g, 4.12 mmol, 1.05 eq.), copper sulfate pentahydrate (29 mg, 0.12 mmol, 3 mol%), copper turning (1 pc, *ca.* 50 mg), and 1-ethynylcyclohex-1-ene (0.48 mL, 4.12 mmol, 1.05 eq.) with general procedure **7.2.2b**. Column chromatography (5% → 10% EtOAc/pentane) afforded the title compound (467 mg, 2.07 mmol, 53%) as a colourless solid;

R_f 0.72 (10% EtOAc/pentane);

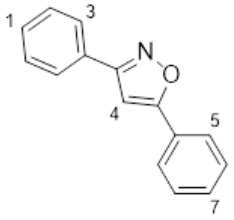
IR (thin film, ν_{max}/cm^{-1}) 2934, 1564, 1470, 1437, 1406, 920, 801, 766, 687;

^{1}H NMR (400 MHz, $CDCl_3$) δ_H 7.85 – 7.77 (2H, m, H3), 7.49 – 7.39 (3H, m, H1, H2), 6.66 (1H, tt, *J* = 4.0, 1.7 Hz, H5), 6.38 (1H, s, H4), 2.42 – 2.36 (2H, m, H9), 2.29 – 2.23 (2H, m, H6), 1.83 – 1.75 (2H, m, H8), 1.73 – 1.65 (2H, m, H7);

^{13}C NMR (101 MHz, $CDCl_3$) δ_C 171.8, 162.6, 130.3, 129.9, 129.6, 129.0, 126.9, 125.5, 96.3, 25.6, 25.4, 22.2, 21.9.

Data are consistent with literature values.[226]

3,5-Diphenylisoxazole, 87n



ZT324

Synthesised from hydroxylamine hydrochloride (215 mg, 3.09 mmol, 1.05 eq.), benzaldehyde (0.30 mL, 2.94 mmol, 1.00 eq.), NaOH (123 mg, 3.09 mmol, 1.05 eq.), Chloramine T trihydrate (870 mg, 3.09 mmol, 1.05 eq.), copper sulfate pentahydrate (22 mg, 88 μmol, 3 mol%), copper turning (1 pc, *ca.* 50 mg), and phenylacetylene (0.34 mL, 3.09 mmol, 1.05 eq.) with general procedure **7.2.2b**. Column chromatography (10% → 20% EtOAc/pentane) afforded the title compound (225 mg, 2.94 mmol, 35%) as a colourless solid.

R_f 0.10 (20% DCM/pentane);

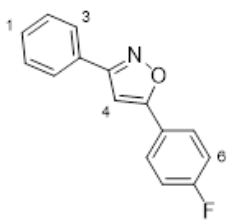
IR (thin film, ν_{max} / cm^{-1}) 3114, 3050, 1573, 1463, 1451, 1402, 950, 909, 763, 732, 691;

^{1}H NMR (400 MHz, $CDCl_3$) δ_H 7.93 – 7.81 (4H, m, H3, H5), 7.56 – 7.40 (6H, m, H1, H2, H6, H7), 6.84 (1H, s, H4);

^{13}C NMR (101 MHz, $CDCl_3$) δ_C 170.6, 163.1, 130.4, 130.2, 129.3, 129.2, 129.1, 127.7, 127.0, 126.0, 97.6.

Data are consistent with literature values.[227]

5-(4-Fluorophenyl)-3-phenylisoxazole, 87o



ZT330

Synthesised from hydroxylamine hydrochloride (151 mg, 2.16 mmol, 1.05 eq.), benzaldehyde (0.21 mL, 2.06 mmol, 1.00 eq.), NaOH (86 mg, 2.16 mmol, 1.05 eq.), Chloramine T trihydrate (609 mg, 2.16 mmol, 1.05 eq.), copper sulfate pentahydrate (15 mg, 62 μmol, 3 mol%), copper turning (1 pc, *ca.* 50 mg), and 1-ethynyl-4-fluorobenzene (260 mg, 2.16 mmol, 1.05 eq.) with general procedure **7.2.2b**. Recrystallization from DCM/pentane afforded the title compound (133 mg, 0.56 mmol, 27%) as a yellow solid;

IR (thin film, ν_{max}/cm^{-1}) 3115, 1617, 1501, 1462, 1418, 1237, 951, 844, 814, 768, 697;

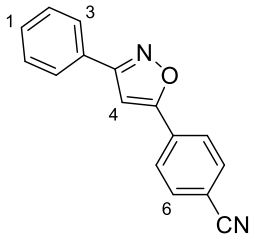
^{1}H NMR (400 MHz, $CDCl_3$) δ_C 7.90 – 7.79 (4H, m, H3, H5), 7.54 – 7.43 (3H, m, H1, H2), 7.23 – 7.15 (2H, m, H6), 6.78 (1H, s, H4);

^{13}C NMR (101 MHz, $CDCl_3$) δ_C 169.6, 164.0 (d, $^{1}J_{C-F}$ = 250.7 Hz), 163.2, 130.2, 129.2, 129.1, 128.1 (d, $^{3}J_{C-F}$ = 8.6 Hz), 127.0, 124.03 (d, $^{4}J_{C-F}$ = 3.2 Hz), 116.4 (d, $^{2}J_{C-F}$ = 22.2 Hz), 97.4;

^{19}F NMR (377 MHz, $CDCl_3$) δ_F -109.45.

Data are consistent with literature values.[228]

4-(3-Phenylisoxazol-5-yl)benzonitrile, 87p



ZT406

Synthesised from hydroxylamine hydrochloride (293 mg, 4.22 mmol, 1.05 eq.), benzaldehyde (0.41 mL, 4.02 mmol, 1.00 eq.), NaOH (169 mg, 4.22 mmol, 1.05 eq.), Chloramine T trihydrate (1.19 g, 4.22 mmol, 1.05 eq.), copper sulfate pentahydrate (30 mg, 0.12 mmol, 3 mol%), copper turning (1 pc, *ca.* 50 mg), and 1-ethynylbenzonitrile (536 mg,

4.22 mmol, 1.05 eq.) with general procedure **7.2.2b**. Column chromatography (10% → 20% EtOAc/pentane) afforded the title compound (335 mg, 1.36 mmol, 34%) as a colourless solid.

R_f 0.27 (10% EtOAc/pentane);

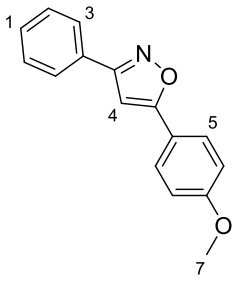
IR (thin film, ν_{max}/cm^{-1}) 3111, 2981, 2234, 1597, 1462, 1440, 819, 772, 698;

^{1}H NMR (600 MHz, $CDCl_3$) δ_H 7.95 (2H, d, *J* = 8.6 Hz, H6), 7.89 – 7.84 (2H, m, H3), 7.79 (2H, d, *J* = 8.6 Hz, H5), 7.55 – 7.46 (3H, m, H1, H2), 6.96 (1H, s, H4);

^{13}C NMR (151 MHz, $CDCl_3$) δ_C 168.3, 163.4, 133.0, 131.3, 130.5, 129.2, 128.7, 127.0, 126.4, 118.3, 113.8, 99.8.

Data are consistent with literature values.[229]

5-(4-Methoxyphenyl)-3-phenylisoxazole, 87q



ZT343

Synthesised from hydroxylamine hydrochloride (143 mg, 2.06 mmol, 1.05 eq.), benzaldehyde (0.20 mL, 2.06 mmol, 1.00 eq.), NaOH (82 mg, 2.06 mmol, 1.05 eq.), Chloramine T trihydrate (580 mg, 2.06 mmol, 1.05 eq.), copper sulfate pentahydrate (15 mg, 60 μmol, 3 mol%), copper turning (1 pc, *ca.* 50 mg), and 1-ethynyl-4-methoxybenzene (272 mg, 2.06 mmol, 1.05 eq.) with general procedure **7.2.2b**. Column chromatography (10% EtOAc/pentane) afforded the title compound (135 mg, 0.54 mmol, 27%) as a colourless solid;

R_f 0.31 (10% EtOAc/pentane);

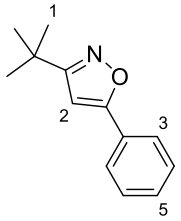
IR (thin film, ν_{max}/cm^{-1}) 2964, 2839, 1615, 1504, 1466, 1262, 1033, 767, 690;

^{1}H NMR (400 MHz, $CDCl_3$) δ_H 7.89 – 7.84 (2H, m, H3), 7.78 (2H, d, *J* = 9.0 Hz, H5), 7.51 – 7.44 (3H, m, H1, H2), 7.00 (2H, d, *J* = 9.0 Hz, H6), 6.71 (1H, s, H4), 3.87 (3H, s, H7);

^{13}C NMR (101 MHz, $CDCl_3$) δ_C 170.5, 163.1, 161.3, 130.1, 129.5, 129.0, 127.6, 127.0, 120.5, 114.6, 96.3, 55.6.

Data are consistent with literature values.[227]

3-(*tert*-Butyl)-5-phenylisoxazole, 87s



ZT355

Synthesised from hydroxylamine hydrochloride (202 mg, 2.91 mmol, 1.05 eq.), pivalaldehyde (0.30 mL, 2.76 mmol, 1.00 eq.), NaOH (116 mg, 2.90 mmol, 1.05 eq.), Chloramine T trihydrate (817 mg, 2.90 mmol, 1.05 eq.), copper sulfate pentahydrate (21 mg, 83 μmol, 3 mol%), copper turning (1 pc, *ca.* 50 mg), and phenylacetylene (0.32 mL, 2.91 mmol, 1.05 eq.) with general procedure **7.2.2b**. Column chromatography (5% EtOAc/pentane) afforded the title compound (223 mg, 1.11 mmol, 40%) as a yellow oil;

R_f 0.42 (5% EtOAc/pentane);

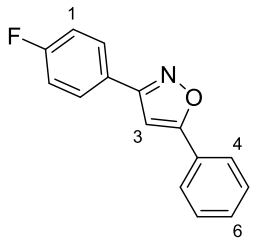
IR (thin film, ν_{max}/cm^{-1}) 2966, 1575, 1448, 1406, 1243, 906, 764, 690;

^{1}H NMR (400 MHz, $CDCl_3$) δ_H 7.80 – 7.73 (2H, m, H3), 7.48 – 7.38 (3H, m, H4, H5), 6.43 (1H, s, H2), 1.39 (9H, s, H1);

^{13}C NMR (101 MHz, $CDCl_3$) δ_C 172.8, 169.5, 130.0, 129.0, 128.0, 125.9, 97.5, 32.2, 29.7.

Data are consistent with literature values.[230]

3-(4-Fluorophenyl)-5-phenylisoxazole, 87t



ZT359

Synthesised from hydroxylamine hydrochloride (367 mg, 5.29 mmol, 1.05 eq.), 4-fluorobenzaldehyde (0.54 mL, 5.03 mmol, 1.00 eq.), NaOH (211 mg, 5.29 mmol, 1.05 eq.), Chloramine T trihydrate (1.49 g, 5.29 mmol, 1.05 eq.), copper sulfate pentahydrate (38 mg, 0.15 mmol, 3 mol%), copper turning (1 pc, *ca.* 50 mg), and phenylacetylene (0.58 mL, 5.29 mmol, 1.05 eq.) with general procedure **7.2.2b**. Column chromatography (10% EtOAc/pentane) afforded the title compound (484 mg, 2.02 mmol, 40%) as a colourless solid;

R_f 0.76 (10% EtOAc/pentane);

IR (thin film, ν_{max}/cm^{-1}) 3112, 1606, 1527, 1493, 1448, 1231, 845, 816, 765, 693;

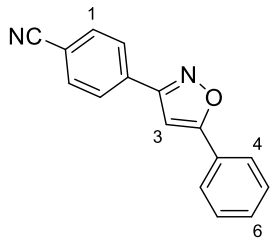
^{1}H NMR (400 MHz, $CDCl_3$) δ_H 7.90 – 7.81 (4H, m, H4, H2), 7.52 – 7.42 (3H, m, H1, H6), 7.21 – 7.13 (2H, m, H5), 6.79 (1H, s, H3);

^{13}C NMR (101 MHz, $CDCl_3$) δ_C 170.8, 164.0 (d, $^1J_{C-F}$ = 249.9 Hz), 162.2, 130.5, 129.2, 128.9 (d, $^3J_{C-F}$ = 8.4 Hz), 127.5, 126.0, 125.5 (d, $^4J_{C-F}$ = 3.4 Hz), 116.2 (d, $^2J_{C-F}$ = 21.9 Hz), 97.5;

^{19}F NMR (377 MHz, $CDCl_3$) δ_F -110.57.

Data are consistent with literature values.[231]

4-(5-Phenylisoxazol-3-yl)benzonitrile, 87u



ZT399

Synthesised from hydroxylamine hydrochloride (292 mg, 4.19 mmol, 1.05 eq.), 4-cyanobenzaldehyde (525 mg, 4.00 mmol, 1.00 eq.), NaOH (168 mg, 4.19 mmol, 1.05 eq.), Chloramine T trihydrate (1.18 g, 4.19 mmol, 1.05 eq.), copper sulfate pentahydrate (30 mg, 0.12 mmol, 3 mol%), copper turning (1 pc, *ca.* 50 mg), and phenylacetylene (0.46 mL, 4.19 mmol, 1.05 eq.) with general procedure **7.2.2b**. Column chromatography (20% EtOAc/pentane) afforded the title compound (324 mg, 1.32 mmol, 33%) as a yellow solid;

R_f 0.42 (20% EtOAc/pentane);

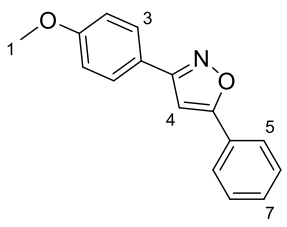
IR (thin film, ν_{max} / cm^{-1}) 3113, 1447, 908, 768, 732, 695;

^{1}H NMR (400 MHz, $CDCl_3$) δ_H 7.99 (2H, d, *J* = 8.6 Hz, H1), 7.87 – 7.83 (2H, m, H4), 7.78 (2H, d, *J* = 8.6 Hz, H2), 7.55 – 7.47 (3H, m, H5, H6), 6.86 (1H, s, H3);

^{13}C NMR (101 MHz, $CDCl_3$) δ_C 171.5, 161.6, 133.6, 132.9, 130.8, 129.3, 127.5, 127.1, 126.0, 118.5, 113.8, 97.5.

^{1}H NMR data is constituent with literature values, while we suspect the literature has misidentified their ^{13}C NMR peaks.[232]

3-(4-Methoxyphenyl)-5-phenylisoxazole, 87v



ZT360

Synthesised from hydroxylamine hydrochloride (300 mg, 4.32 mmol, 1.05 eq.), 4-methoxybenzaldehyde (0.50 mL, 4.11 mmol, 1.00 eq.), NaOH (173 mg, 4.33 mmol, 1.05 eq.), Chloramine T trihydrate (1.22 g, 4.32 mmol, 1.05 eq.), copper sulfate pentahydrate (31 mg, 0.12 mmol, 3 mol%), copper turning (1 pc, *ca.* 50 mg), and phenylacetylene (0.48 mL, 4.37 mmol, 1.06 eq.) with general procedure **7.2.2b**. Column chromatography (5% → 10% EtOAc/pentane) afforded the title compound (424 mg, 1.69 mmol, 41%) as a colourless solid;

R_f 0.42 (10% EtOAc/pentane);

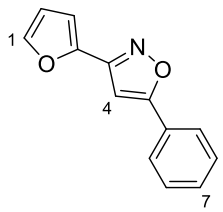
IR (thin film, ν_{max} / cm^{-1}) 3003, 2837, 1612, 1493, 1448, 1428, 1250, 1177, 1031, 837, 763, 686;

^{1}H NMR (400 MHz, $CDCl_3$) δ_H 7.86 – 7.78 (4H, m, H3, H5), 7.52 – 7.41 (3H, m, H6, H7), 7.00 (2H, d, *J* = 8.8 Hz, H2), 6.78 (1H, s, H4), 3.87 (3H, s, H1);

^{13}C NMR (101 MHz, $CDCl_3$) δ_C 170.3, 162.7, 161.2, 130.3, 129.1, 128.4, 127.8, 126.0, 121.9, 114.5, 97.4, 55.5.

Data are consistent with literature values.[227]

3-(Furan-2-yl)-5-phenylisoxazole, 87w



ZT353

Synthesised from hydroxylamine hydrochloride (176 mg, 2.54 mmol, 1.05 eq.), furan-2-carbaldehyde (0.20 mL, 2.41 mmol, 1.00 eq.), NaOH (101 mg, 2.54 mmol, 1.05 eq.), Chloramine T trihydrate (714 mg, 2.54 mmol, 1.05 eq.), copper sulfate pentahydrate (18

mg, 72 μmol, 3 mol%), copper turning (1 pc, *ca.* 50 mg), and phenylacetylene (0.28 mL, 2.54 mmol, 1.05 eq.) with general procedure **7.2.2b**. Column chromatography (5% → 10% → 20% EtOAc/pentane) afforded the title compound (124 mg, 0.59 mmol, 24%) as a colourless solid;

R_f 0.67 (20% EtOAc/pentane);

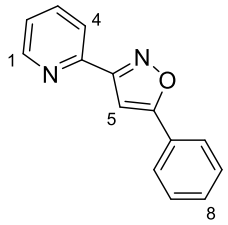
IR (thin film, ν_{max}/cm^{-1}) 3269, 2961, 1691, 1453, 1346, 1162, 1090, 669;

^{1}H NMR (400 MHz, $CDCl_3$) δ_H 7.85 – 7.80 (2H, m, H5), 7.58 (1H, dd, *J* = 1.8, 0.7 Hz, H1), 7.52 – 7.43 (3H, m, H6, H7), 6.96 (1H, dd, *J* = 3.4, 0.7 Hz, H3), 6.78 (1H, s, H4), 6.55 (1H, dd, *J* = 3.4, 1.8 Hz, H2);

^{13}C NMR (101 MHz, $CDCl_3$) δ_C 170.3, 155.5, 144.5, 144.0, 130.5, 129.2, 127.3, 126.0, 111.9, 110.3, 97.1.

Data are consistent with literature values.[233]

5-Phenyl-3-(pyridin-2-yl)isoxazole, 87x



This compound was synthesised by Philip J. Smith.

Synthesised from hydroxylamine hydrochloride (730 mg, 10.50 mmol, 1.05 eq.), picolinaldehyde (0.95 mL, 10.00 mmol, 1.00 eq.), NaOH (420 mg, 10.05 mmol, 1.05 eq.), Chloramine T trihydrate (2.96 g, 10.05 mmol, 1.05 eq.), copper sulfate pentahydrate (75 mg, 0.30 mmol, 3 mol%), copper turning (1 pc, *ca.* 50 mg), and phenylacetylene (1.2 mL, 10.93 mmol, 1.09 eq.) with general procedure **7.2.2b**. Column chromatography (10% → 20% EtOAc/pentane) afforded the title compound (242 mg, 1.09 mmol, 11%) as a beige solid;

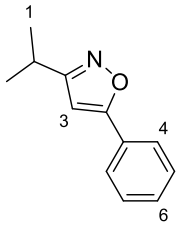
R_f 0.22 (10% EtOAc/pentane);

^{1}H NMR (400 MHz, $CDCl_3$) δ_H 8.72 (1H, ddd, *J* = 4.9, 1.8, 1.0 Hz, H1), 8.14 (1H, app. dt, *J* = 7.9, 1.1 Hz, H4), 7.88 – 7.85 (2H, m, H6), 7.82 (1H, app. td, *J* = 7.8, 1.8 Hz, H3), 7.52 – 7.45 (3H, m, H7, H8), 7.37 (1H, ddd, *J* = 7.6, 4.9, 1.2 Hz, H2), 7.20 (1H, s, H5);

^{13}C NMR (101 MHz, $CDCl_3$) δ_C 170.8, 164.0, 149.9, 148.8, 137.1, 130.4, 129.2, 127.6, 126.0, 124.7, 121.8, 98.5.

Data are consistent with literature values.[225]

3-Isopropyl-5-phenylisoxazole



ZT401

Synthesised from hydroxylamine hydrochloride (292 mg, 4.19 mmol, 1.05 eq.), isobutyraldehyde (0.37 mL, 4.00 mmol, 1.00 eq.), NaOH (168 mg, 4.19 mmol, 1.05 eq.), Chloramine T trihydrate (1.18 mg, 4.19 mmol, 1.05 eq.), copper sulfate pentahydrate (30 mg, 0.12 mmol, 3 mol%), copper turning (1 pc, *ca.* 50 mg), and phenylacetylene (0.46 mL, 4.19 mmol, 1.05 eq.) with general procedure **7.2.2b**. Column chromatography (5% EtOAc/pentane) afforded the title compound (343 mg, 1.83 mmol, 46%) as a yellow oil;

R_f 0.48 (5% EtOAc/pentane);

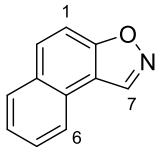
IR (thin film, ν_{max}/cm^{-1}) 2971, 2883, 1575, 1451, 1066, 948, 908, 764, 731, 690;

^{1}H NMR (500 MHz, $CDCl_3$) δ_H 7.79 – 7.74 (2H, m, H4), 7.46 – 7.38 (3H, m, H5, H6), 6.39 (1H, s, H3), 3.11 (1H, hept., *J* = 7.0 Hz, H2), 1.34 (6H, d, *J* = 7.0 Hz, H1);

^{13}C NMR (126 MHz, $CDCl_3$) δ_C 170.1, 169.6, 130.0, 129.0, 127.9, 125.8, 97.7, 26.7, 21.9.

Data are consistent with literature values.[234]

Naphtho[1,2-*d*]isoxazole, 97b



ZT469

Synthesised from 2-hydroxy-1-naphthaldehyde (1.72 g, 10.0 mmol, 1.0 eq.), hydroxylamine hydrochloride (1.04 g, 15.0 mmol. 1.5 eq.), $NaHCO_3$ (1.68 g, 20.0 mmol, 2.0 eq.), PPh_3 (3.28 g, 12.5 mmol, 1.25 eq.) and DIAD (2.4 mL, 12.2 mmol, 1.22 eq.) with general procedure **7.2.2c.** Column chromatography (silica gel, 0% → 10% → 20% Et_2O/pentane) afforded the title compound (738 mg, 4.36 mmol, 44%) as a colourless solid;

R_f 0.47 (20% Et_2O/pentane);

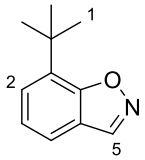
IR (thin film, ν_{max}/cm^{-1}) 3069, 1633, 1582, 1532, 1253, 1169, 930, 810, 753;

^{1}H NMR (400 MHz, $CDCl_3$) δ_H 9.10 (1H, d, *J* = 0.8 Hz, H7), 8.14 (1H, d, *J* = 8.1 Hz, H3), 8.02 – 7.92 (2H, m, H2, H6), 7.76 – 7.65 (2H, m, H1, H4), 7.57 (1H, ddd, *J* = 8.2, 7.2, 1.1 Hz, H5);

^{13}C NMR (101 MHz, $CDCl_3$) δ_C 162.4, 145.0, 131.8, 130.6, 129.2, 128.3, 126.9, 125.7, 123.3, 116.5, 110.4.

Data are consistent with literature values.[235]

7-(*tert*-Butyl)benzo[*d*]isoxazole, 97c



ZT479

Synthesised from 3-(*tert*-butyl)-2-hydroxybenzaldehyde (1.7 mL, 10.0 mmol, 1.0 eq.), hydroxylamine hydrochloride (1.04 g, 15.0 mmol. 1.5 eq.), $NaHCO_3$ (1.68 g, 20.0 mmol,

2.0 eq.), PPh_3 (3.28 g, 12.5 mmol, 1.25 eq.) and DIAD (2.4 mL, 12.2 mmol, 1.22 eq.) with general procedure **7.2.2c.** Column chromatography (silica gel, DCM) followed by recrystallization from DCM/pentane afforded the title compound (0.48 g, 2.74 mmol, 27%) as a colourless solid;

m.p. 76 °C;

R_f 0.61 (10% EtOAc/pentane);

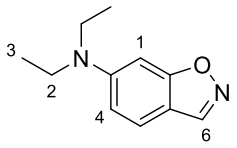
IR (thin film, ν_{max} / cm^{-1}) 2966, 2873, 1597, 1469, 1365, 1175, 908, 860, 751, 731;

^{1}H NMR (400 MHz, $CDCl_3$) δ_H 8.69 (1H, s, H5), 7.58 (1H, dd, *J* = 7.8, 1.1 Hz, H4), 7.43 (1H, dd, *J* = 7.4, 1.1 Hz, H2), 7.26 (1H, app. t, *J* = 7.6 Hz, H3), 1.53 (9H, s, H1);

^{13}C NMR (101 MHz, $CDCl_3$) δ 161.2, 146.3, 134.6, 126.2, 124.1, 122.0, 119.8, 34.6, 29.8;

HRMS (ESI) m/z: $[M + H]^+$ Calcd for $C_{11}H_{14}NO$ 176.1070; Found 176.1071.

***N*,*N*-Diethylbenzo[*d*]isoxazol-6-amine, 97d**



ZT478

Synthesised from 4-(diethylamino)-2-hydroxybenzaldehyde (1.93 g, 10.0 mmol, 1.0 eq.), hydroxylamine hydrochloride (1.04 g, 15.0 mmol. 1.5 eq.), $NaHCO_3$ (1.68 g, 20.0 mmol, 2.0 eq.), PPh_3 (3.28 g, 12.5 mmol, 1.25 eq.) and DIAD (2.4 mL, 12.2 mmol, 1.22 eq.) with general procedure **2.3.** Column chromatography (silica gel, DCM) afforded the title compound (1.28 g, 6.73 mmol, 67%) as a pink oil;

R_f 0.50 (DCM);

IR (thin film, ν_{max}/cm^{-1}) 2974, 1623, 1518, 1497, 1356, 1124, 803, 730;

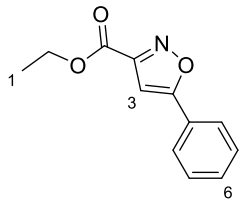
^{1}H NMR (400 MHz, $CDCl_3$) δ_H 8.44 (1H, d, *J* = 1.0 Hz, H6), 7.45 (1H, d, *J* = 8.8 Hz, H5), 6.71 (1H, dd, *J* = 8.8, 2.2 Hz, H4), 6.69 – 6.67 (1H, m, H1), 3.43 (4H, q, *J* = 7.1 Hz, H2), 1.21 (6H, t, *J* = 7.1 Hz, H3);

^{13}C NMR (101 MHz, $CDCl_3$) δ_C 165.2, 150.2, 145.7, 122.1, 110.8, 110.6, 89.6, 45.1, 12.5;

HRMS (ESI) m/z: $[M + H]^+$ Calcd for $C_{11}H_{15}N_2O$ 191.1179.; Found 191.1179.

^{1}H NMR data are consistent with literature values.[207]

Ethyl 5-phenylisoxazole-3-carboxylate, 109



ZT519

Modified from a literature procedure.[134] In a round-bottom flask was mixed phenylacetylene (5.5 mL, 50.1 mmol, 1.0 eq.), ethyl 2-nitroacetate (5.4 mL, 75.1 mL, 1.5 eq.) and TEMPO (783 mg, 5.01 mmol, 10 mol%) in water (100 mL). The mixture was stirred vigorously in the open air at 60 °C overnight. Upon completion, the reaction mixture was extracted three times with DCM. The organic phase was combined, dried over Na_2SO_4, concentrated *in vacuo* and purified by column chromatography (silica gel, 0 → 10% → 20% Et_2O/pentane) followed by recrystallization from pentane to give the title product (2.30 g, 10.6 mmol, 21%) as an orange solid.

R_f 0.57 (20% EtOAc/pentane);

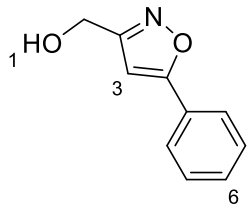
IR (thin film, ν_{max}/cm^{-1}) 3133, 2990, 1730, 1444, 1250, 1151, 1020, 772, 693;

^{1}H NMR (400 MHz, $CDCl_3$) δ_H 7.83 – 7.77 (2H, m, H4), 7.52 – 7.45 (3H, m, H5, H6), 6.92 (1H, s, H3), 4.47 (2H, q, *J* = 7.1 Hz, H2), 1.44 (3H, t, *J* = 7.1 Hz, H1);

^{13}C NMR (101 MHz, $CDCl_3$) δ_C 171.8, 160.2, 157.1, 130.9, 129.3, 126.7, 126.0, 100.0, 62.4, 14.3.

Data are consistent with literature values.[134]

(5-Phenylisoxazol-3-yl)methanol, 110



ZT520

Modified from a literature procedure.[236] In a heat gun-dried flask was added ethyl 5-phenylisoxazole-3-carboxylate (2.17 g, 10.0 mmol, 1.0 eq.). The flask was purged under high vacuum for 30 s and backfilled with argon (this cycle was repeated twice more). Anhydrous THF (20 mL) was added to dissolve the starting material and the resulting solution was cooled to 0 °C on an ice bath. $LiAlH_4$ (2.4 M in THF, 2.5 mL, 6.00 mmol, 0.60 eq.) was added dropwise. The reaction mixture was stirred at 0 °C for 1h and was then quenched carefully by adding water. The reaction mixture was acidified with 1M HCl, and extracted three times with EtOAc. The organic phase was combined, washed with brine, dried over Na_2SO_4 and concentrated *in vacuo* to afford the title compound (1.54 g, 8.79 mmol, 88%) as a pale yellow solid;

IR (thin film, ν_{max}/cm^{-1}) 3382, 2885, 1468, 1454, 1050, 1001, 766, 691;

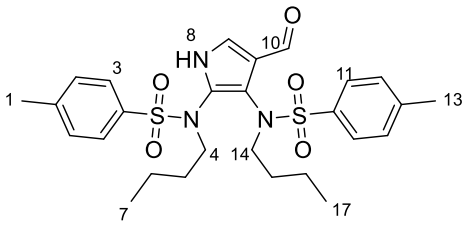
^{1}H NMR (400 MHz, $CDCl_3$) δ_H 7.80 – 7.72 (2H, m, H4), 7.49 – 7.41 (3H, m, H5, H6), 6.59 (1H, s, H3), 4.81 (2H, s, H2), 2.72 (1H, brs., H1);

^{13}C NMR (101 MHz, $CDCl_3$) δ_C 170.5, 164.3, 130.4, 129.1, 127.4, 126.0, 98.4, 57.2.

Data are consistent with literature values.[237, 238]

7.4.6 Gold-catalyzed Cyclisation of Yndiamides with Isoxazoles

***N*,*N'*-(4-Formyl-1*H*-pyrrole-2,3-diyl)bis(*N*-butyl-4-methylbenzenesulfonamide), 88a**



ZT288, ZT319-B

0.10 mmol scale: Synthesised from *N*,*N'*-(ethyne-1,2-diyl)bis(*N*-butyl-4-methylbenzene-sulfonamide) (48 mg, 0.10 mmol, 1.0 eq.), isoxazole (13 μL, 0.20 mmol, 2.0 eq.), chloro[tris(2,4-di-*tert*-butylphenyl)phosphite]gold(I) (4.4 mg, 5.0 μmol, 5 mol%) and silver bis(trifluoromethanesulfonyl)imide (2.0 mg, 5.2 μmol, 5 mol%) in DCE (anhy., 0.2 mL) with general procedure **7.2.3d** at room temperature for 2 h. Column chromatography (silica gel, 20% → 40% EtOAc/pentane) afforded the title compound (43 mg, 79 μmol, 78%) as a brown solid.

1 mmol scale: Synthesised from *N*,*N'*-(ethyne-1,2-diyl)bis(*N*-butyl-4-methylbenzene-sulfonamide) (477 mg, 1.00 mmol, 1.0 eq.), isoxazole (0.13 mL, 2.03 mmol, 2.0 eq.), chloro[tris(2,4-di-*tert*-butylphenyl)phosphite]gold(I) (44 mg, 5.0 μmol, 5 mol%) and silver bis(trifluoromethanesulfonyl)imide (20 mg, 0.05 mmol, 5 mol%) in DCE (anhy., 2.0 mL) with general procedure **7.2.3d** at room temperature for 2 h. Column chromatography (silica gel, 20% → 40% EtOAc/pentane) afforded the title compound (407 mg, 0.75 mmol, 75%) as a brown solid.

m.p. 138 °C (decomp.);

R_f 0.37 (40% EtOAc/pentane);

IR (thin film, ν_{max}/cm^{-1}) 3295, 2960, 2873, 1673, 1519, 1457, 1345, 1163, 1090, 814, 666;

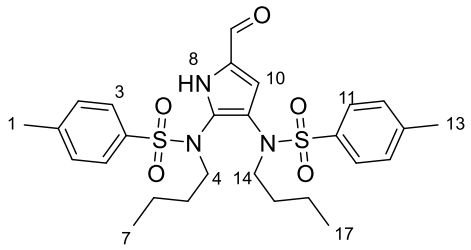
^{1}H NMR (500 MHz, C_6D_6) δ_H 9.18 (1H, s, H10), 8.97 (1H, s, H8), 7.98 (2H, d, *J* = 8.2 Hz, H3), 7.72 (2H, d, *J* = 8.2 Hz, H11), 6.88 (2H, d, *J* = 8.2 Hz, H2), 6.80 (2H, d, *J* = 8.2 Hz,

H12), 6.76 (1H, d, *J* = 3.7 Hz, H9), 4.25 – 4.14 (1H, m, H4), 4.01 – 3.92 (1H, m, H4), 3.61 – 3.48 (2H, m, H14), 1.88 (6H, s, H1, H13), 1.83 – 1.68 (2H, m, H5), 1.43 – 1.34 (1H, m, H15), 1.33 – 1.22 (3H, m, H6, H15), 0.94 (2H, app. sext., *J* = 7.4 Hz, H16), 0.85 (3H, t, *J* = 7.4 Hz, H7), 0.64 (3H, t, *J* = 7.4 Hz, H17);

^{13}C NMR (126 MHz, C_6D_6) δ_C 183.3, 143.9, 143.5, 137.7, 136.7, 130.0, 129.8, 128.6, 128.5, 127.4, 123.5, 122.9, 118.0, 52.1, 51.6, 32.2, 30.9, 21.19, 21.15, 20.3, 20.1, 14.0, 13.8.

HRMS (ESI) m/z: $[M + Na]^+$ Calcd for $C_{27}H_{35}O_5N_3NaS_2$ 568.1910; Found 568.1908.

***N*,*N'*-(5-Formyl-1*H*-pyrrole-2,3-diyl)bis(*N*-butyl-4-methylbenzenesulfonamide), 89**



ZT420-A

Synthesised from *N*,*N'*-(ethyne-1,2-diyl)bis(*N*-butyl-4-methylbenzenesulfonamide) (477 mg, 1.00 mmol, 1.0 eq.), isoxazole (0.13 mL, 2.03 mmol, 2.0 eq.), chloro[tris(2,4-di-*tert*-butylphenyl)phosphite]gold(I) (44 mg, 5.0 μmol, 5 mol%) and silver bis(trifluoromethanesulfonyl)imide (20 mg, 0.05 mmol, 5 mol%) in DCE (anhy., 2.0 mL) with general procedure **7.2.3d** at room temperature for 2 h. Column chromatography (silica gel, 20% EtOAc/pentane) afforded the title compound (85 mg, 0.16 mmol, 16%) as a yellow solid. Crystals suitable for X-ray diffraction were grown by vapour diffusion of pentane into a concentrated solution of the title compound in benzene.

m.p. 156 °C;

R_f 0.24 (20% EtOAc/pentane);

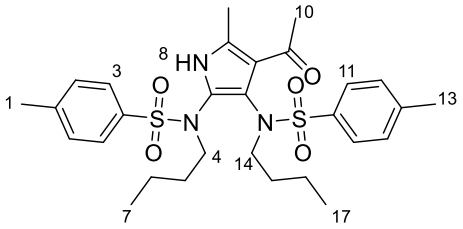
IR (thin film, ν_{max}/cm^{-1}) 3232, 2961, 2873, 1659, 1087, 1350, 1163, 1090, 814, 665;

^{1}H NMR (400 MHz, C_6D_6) δ_H 10.61 (1H, s, H8), 9.06 (1H, s, H9), 7.80 (2H, d, *J* = 8.3 Hz, H3), 7.66 (2H, d, *J* = 8.3 Hz, H11), 6.84 – 6.74 (4H, m, H2, H12), 6.29 (1H, d, *J* = 2.8 Hz, H10), 4.05 – 3.96 (2H, m, H4), 3.38 – 3.29 (2H, m, H14), 1.93 (3H, s, H1), 1.86 (3H, s, H13), 1.67 (2H, app. quin., *J* = 7.7 Hz, H5), 1.37 – 1.28 (2H, m, H15), 1.28 – 1.19 (2H, m, H6), 1.01 (2H, app. sext., *J* = 7.4 Hz, H16), 0.79 (3H, t, *J* = 7.4 Hz, H7), 0.73 (3H, t, *J* = 7.4 Hz, H17);

^{13}C NMR (101 MHz, C_6D_6) δ 178.5, 144.0, 143.5, 137.4, 137.1, 132.3, 129.9, 129.7, 128.5, 128.1, 127.7, 120.5, 118.2, 51.9, 50.7, 32.0, 30.4, 21.18, 21.16, 20.2, 20.0, 13.91, 13.85.

HRMS (ESI) m/z: $[M + H]^+$ Calcd for $C_{27}H_{36}O_5N_3S_2$ 546.2091; Found 546.2086.

***N,N'*-(4-Acetyl-5-methyl-1*H*-pyrrole-2,3-diyl)bis(*N*-butyl-4-methylbenzenesulfonamide), 88b**



ZT320-B, ZT322-B, ZT325

0.10 mmol scale: Synthesised from *N,N'*-(ethyne-1,2-diyl)bis(*N*-butyl-4-methylbenzene-sulfonamide) (48 mg, 0.10 mmol, 1.0 eq.), 3,5-dimethylisoxazole (20 μL, 0.20 mmol, 2.0 eq.), chloro[tris(2,4-di-*tert*-butylphenyl)phosphite]gold(I) (4.4 mg, 5.0 μmol, 5 mol%) and silver bis(trifluoromethanesulfonyl)imide (2.0 mg, 5.2 μmol, 5 mol%) in DCE (anhy., 0.2 mL) with general procedure **7.2.3d** at room temperature for 2 h. Upon completion, the reaction mixture was treated with HCl (1 M in Et_2O, 0.1 mL) for 30 min before it was concentrated *in vacuo* and purified by column chromatography (silica gel, 20% → 40% EtOAc/pentane) to give the title compound (49 mg, 85 μmol, 85%) as a beige solid.

1 mmol scale: Synthesised from *N,N'*-(ethyne-1,2-diyl)bis(*N*-butyl-4-methylbenzene-sulfonamide) (477 mg, 1.00 mmol, 1.0 eq.), 3,5-dimethylisoxazole (0.20 mL, 2.00 mmol, 2.0 eq.), chloro[tris(2,4-di-*tert*-butylphenyl)phosphite]gold(I) (44 mg, 5.0 μmol, 5 mol%) and silver bis(trifluoromethanesulfonyl)imide (20 mg, 0.05 mmol, 5 mol%) in DCE (anhy., 2.0 mL) with general procedure **7.2.3d** at room temperature for 3 h. Upon completion, the reaction mixture was treated with HCl (1 M in Et_2O, 1.0 mL) for 30 min, before it was concentrated in vacuo and purified by column chromatography (silica gel, 20% → 40% EtOAc/pentane), afforded the title compound (497 mg, 0.87 mmol, 87%) as a brown solid.

m.p. 130 °C (decomp.);

R_f 0.27 (40% EtOAc/pentane);

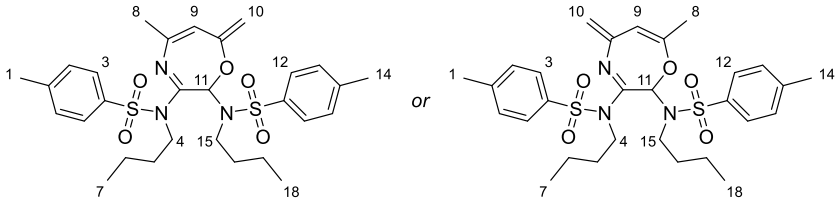
IR (thin film, ν_{max}/cm^{-1}) 3308, 2960, 2931, 2874, 1655, 1444, 1339, 1158, 1089, 910, 814, 731, 674;

^{1}H NMR (400 MHz, $CDCl_3$) δ_H 8.55 (1H, s, H8), 7.74 (2H, d, *J* = 8.2 Hz, H3), 7.60 (2H, d, *J* = 8.2 Hz, H11), 7.31 (2H, d, *J* = 8.2 Hz, H2), 7.23 (2H, d, *J* = 8.2 Hz, H12), 3.68 – 3.57 (1H, m, H4), 3.54 – 3.43 (1H, m, H4), 3.36 – 3.20 (2H, m, H14), 2.45 (3H, s, H10), 2.42 (3H, s, H1), 2.40 (3H, s, H13), 2.17 (3H, s, H9), 1.58 – 1.46 (2H, m, H5), 1.26 – 1.09 (4H, m, H6, H15), 1.05 – 0.93 (2H, m, H16), 0.86 (3H, t, *J* = 7.3 Hz, H7), 0.73 (3H, t, *J* = 7.3 Hz, H17);

^{13}C NMR (101 MHz, $CDCl_3$) δ_C 193.6, 144.3, 143.2, 137.0, 136.8, 130.5, 129.9, 129.4, 128.2, 127.8, 123.3, 120.2, 118.0, 52.0, 51.7, 31.5, 30.7, 30.6, 21.70, 21.67, 20.2, 19.8, 15.6, 13.9, 13.8.

HRMS (ESI) m/z: $[M - H]^-$ Calcd for $C_{29}H_{38}O_5N_3S_2$ 572.2258; Found 572.2263.

***N*,*N'*-(5-Methyl-7-methylene-2,7-dihydro-1,4-oxazepine-2,3-diyl)bis(*N*-butyl-4-methylbenzenesulfonamide) (left), or *N*,*N'*-(7-methyl-5-methylene-2,5-dihydro-1,4-oxaze-pine-2,3-diyl)bis(*N*-butyl-4-methylbenzenesulfonamide) (right), 90**



ZT320-A, ZT322-A

Synthesised from *N*,*N'*-(ethyne-1,2-diyl)bis(*N*-butyl-4-methylbenzenesulfonamide) (48 mg, 0.10 mmol, 1.0 eq.), 3,5-dimethylisoxazole (20 μL, 0.20 mmol, 2.0 eq.), chloro[tris(2,4-di-*tert*-butylphenyl)phosphite]gold(I) (4.4 mg, 5.0 μmol, 5 mol%) and silver bis(trifluoromethanesulfonyl)imide (2.0 mg, 5.2 μmol, 5 mol%) in DCE (anhy., 0.2 mL) with general procedure **7.2.3d** at room temperature for 2 h. Column chromatography (silica gel, 20% → 40% EtOAc/pentane) to give the title compound (21 mg, 0.37 mmol, 37%) as a colourless solid. The title compound (26 mg, 0.45 mmol, 45%) was also collected as a brown solid.

m.p. 145 °C (decomp.);

R_f 0.22 (20% EtOAc/pentane);

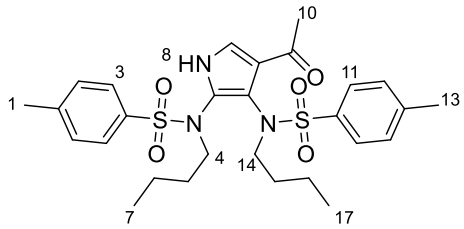
IR (thin film, ν_{max}/cm^{-1}) 2961, 2932, 2874, 2280, 1713, 1586, 1353, 1166, 1088, 812, 667;

^{1}H NMR (400 MHz, C_6D_6) δ_H 8.13 (2H, d, *J* = 8.3 Hz, Ts*H*), 7.79 (2H, d, *J* = 7.7 Hz, Ts*H*), 6.78 – 6.71 (4H, m, Ts*H*), 6.06 – 6.01 (1H, m, H9), 5.28 – 5.23 (1H, s, H10), 4.40 (1H, s, H10), 4.21 – 4.01 (2H, m, BuCH_2), 3.46 (1H, brs., H11), 3.26 (1H, ddd, *J* = 14.8, 11.0, 5.4 Hz, BuCH_2), 2.89 (1H, brs., BuCH_2), 1.94 – 1.69 (13H, m, TsCH_3, BuCH_2), 1.33 – 1.12 (4H, m, BuCH_2), 0.87 (3H, t, *J* = 7.4 Hz, BuCH_3), 0.82 (3H, t, *J* = 7.4 Hz, BuCH_3);

^{13}C NMR (101 MHz, C_6D_6) δ_C 201.9, 165.3, 155.7, 144.2, 143.6, 137.2, 137.1, 129.9, 129.4, 129.3, 128.17, 103.5, 65.2, 59.5, 48.4, 47.0, 32.7, 32.3, 28.3, 21.14, 21.09, 20.5, 20.2, 13.9, 13.8.

HRMS (ESI) m/z: $[M + H]^+$ Calcd for $C_{29}H_{40}O_5N_3S_2$ 574.2404; Found 574.2402.

***N,N'*-(4-Acetyl-1*H*-pyrrole-2,3-diyl)bis(*N*-butyl-4-methylbenzenesulfonamide), 88c**



ZT326-A

Synthesised from *N,N'*-(ethyne-1,2-diyl)bis(*N*-butyl-4-methylbenzenesulfonamide) (48 mg, 0.10 mmol, 1.0 eq.), 5-methylisoxazole (16.5 μL, 0.20 mmol, 2.0 eq.), chloro[tris(2,4-di-*tert*-butyl-phenyl)phosphite]gold(I) (4.4 mg, 5.0 μmol, 5 mol%) and silver bis(trifluoro-methanesulfonyl)imide (2.0 mg, 5.2 μmol, 5 mol%) in DCE (anhy., 0.2 mL) with general procedure **7.2.3d** at room temperature for 2 h. Upon completion, the reaction was treated with HCl (1.0 M in Et_2O, 0.1 mL) for 30 min at room temperature, after which column chromatography (silica gel, 20% → 40% EtOAc/pentane) afforded the title compound (38 mg, 68 μmol, 67%) as a beige solid.

m.p. 103 °C;

R_f 0.29 (40% EtOAc/pentane);

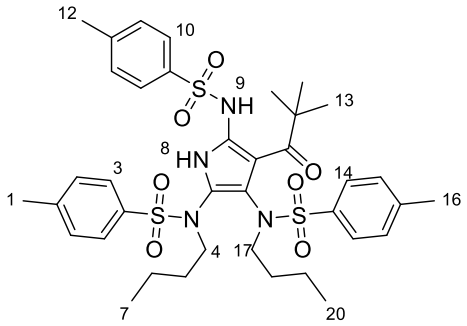
IR (thin film, ν_{max}/cm^{-1}) 3315, 2960, 2874, 1669, 1341, 1159, 1121, 910, 814, 731, 670;

^{1}H NMR (400 MHz, $CDCl_3$) δ_H 9.30 (1H, s, H8), 7.81 (2H, d, *J* = 8.2 Hz, H3), 7.51 (2H, d, *J* = 8.3 Hz, H11), 7.31 (2H, d, *J* = 8.2 Hz, H2), 7.23 – 7.16 (3H, m, H9, H12), 4.00 – 3.89 (1H, m, H4), 3.84 – 3.74 (1H, m, H4), 3.42 – 3.31 (1H, m, H14), 3.26 – 3.16 (1H, m, H14), 2.40 (3H, s, H1), 2.39 (3H, s, H13), 2.08 (3H, s, H10), 1.63 (2H, app. quin., *J* = 7.6 Hz, H5), 1.35 – 1.24 (2H, m, H6), 1.22 – 1.12 (1H, m, H15), 1.05 – 0.94 (3H, m, H15, H16), 0.88 (3H, t, *J* = 7.4 Hz, H7), 0.70 (3H, t, *J* = 7.1 Hz, H17);

^{13}C NMR (101 MHz, $CDCl_3$) δ_C 190.1, 144.3, 143.1, 136.6, 136.1, 129.9, 129.1, 128.4, 127.8, 127.4, 122.1, 121.6, 116.7, 51.8, 51.3, 31.8, 30.5, 27.3, 21.7 (2C), 20.1, 19.8, 13.9, 13.7;

HRMS (ESI) m/z: $[M + Na]^+$ Calcd for $C_{28}H_{37}N_3NaO_5S_2$ 582.2067; Found 582.2068.

***N,N'*-(5-((4-Methylphenyl)sulfonamido)-4-pivaloyl-1*H*-pyrrole-2,3-diyl)bis(*N*-butyl-4-methylbenzenesulfonamide), 88e**



ZT372

Synthesised from *N,N'*-(ethyne-1,2-diyl)bis(*N*-butyl-4-methylbenzenesulfonamide) (48 mg, 0.10 mmol, 1.0 eq.), *N*-(5-(*tert*-butyl)isoxazol-3-yl)-4-methylbenzenesulfonamide (60 mg, 0.20 mmol, 2.0 eq.), chloro[tris(2,4-di-*tert*-butyl-phenyl)phosphite]gold(I) (4.4 mg, 5.0 μmol, 5 mol%) and silver bis(trifluoromethanesulfonyl)imide (2.0 mg, 5.2 μmol, 5 mol%) in DCE (anhy., 0.2 mL) with general procedure **7.2.3d** at room temperature for 2 h. Column chromatography (silica gel, 5% → 10% → 20% EtOAc/pentane) afforded the title compound (52 mg, 0.67 mmol, 67%) as a colourless solid;

m.p. 93 °C (decomp.);

R_f 0.13 (20% EtOAc/pentane);

IR (thin film, ν_{max}/cm^{-1}) 3662, 2980, 2884, 1598, 1461, 1346, 1163, 1089, 910, 732, 668;

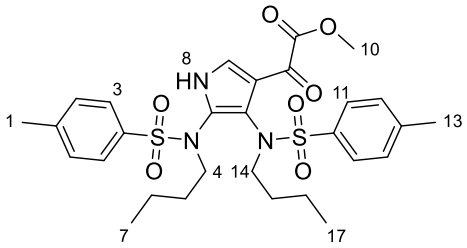
^{1}H NMR (400 MHz, $CDCl_3$) δ_H 8.67 (1H, s, H8), 7.86 (1H, s, H9), 7.71 (2H, d, *J* = 8.4 Hz, H3), 7.64 (2H, d, *J* = 8.4 Hz, H14), 7.46 (2H, d, *J* = 8.1 Hz, H10), 7.38 – 7.29 (4H, m, H2,

H15), 7.18 (2H, d, *J* = 8.1 Hz, H11), 3.78 – 3.65 (1H, m, H4), 3.62 – 3.51 (1H, m, H4), 3.30 – 3.19 (1H, m, H17), 2.45 (3H, s, H1), 2.42 (3H, s, H16), 2.35 (3H, s, H12), 1.85 – 1.69 (3H, m, H17, H5), 1.33 – 1.25 (2H, m, H6), 0.98 – 0.84 (13H, m, H7, H13, H18), 0.80 – 0.68 (5H, m, H19, H20), 0.66 – 0.51 (1H, m, H18);

^{13}C NMR (101 MHz, $CDCl_3$) δ 208.7, 145.1, 144.8, 143.7, 137.1, 136.2, 135.3, 130.6, 130.2, 129.7, 127.9, 127.4, 127.2, 123.7, 117.6, 117.2, 114.6, 51.4, 50.8, 44.7, 31.4, 30.4, 27.9, 21.8, 21.7, 21.6, 20.4, 19.4, 14.0, 13.8;

HRMS (ESI) m/z: $[M + H]^+$ Calcd for $C_{38}H_{51}N_4O_7S_3$ 771.2914; Found 771.2911.

Methyl 2-(4,5-bis((*N*-butyl-4-methylphenyl)sulfonamido)-1*H*-pyrrol-3-yl)-2-oxoacetate, 88h



ZT349

Synthesised from *N*,*N'*-(ethyne-1,2-diyl)bis(*N*-butyl-4-methylbenzenesulfonamide) (48 mg, 0.10 mmol, 1.0 eq.), methyl isoxazole-5-carboxylate (26 mg, 0.20 mmol, 2.0 eq.), chloro[tris(2,4-di-*tert*-butyl-phenyl)phosphite]gold(I) (4.4 mg, 5.0 μmol, 5 mol%) and silver bis(trifluoromethane-sulfonyl)imide (2.0 mg, 5.2 μmol, 5 mol%) in DCE (anhy., 0.2 mL) with general procedure **7.2.3d** at 80 °C for 2 h. Column chromatography (silica gel, 20% → 40% EtOAc/pentane) afforded the title compound (44 mg, 73 μmol, 72%) as a brown oil;

R_f 0.38 (40% EtOAc/pentane);

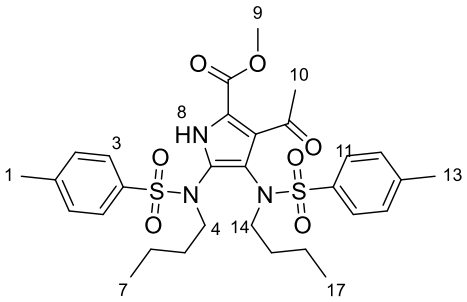
IR (thin film, ν_{max}/cm^{-1}) 3290, 2959, 1736, 1670, 1339, 1161, 1090, 910, 732, 666;

^{1}H NMR (400 MHz, $CDCl_3$) δ_H 9.56 (1H, s, H8), 7.78 (2H, d, *J* = 8.2 Hz, H3), 7.67 (1H, d, *J* = 3.9 Hz, H9), 7.46 (2H, d, *J* = 8.2 Hz, H11), 7.31 (2H, d, *J* = 8.2 Hz, H2), 7.17 (2H, d, *J* = 8.2 Hz, H12), 4.05 – 3.96 (1H, m, H4), 3.92 – 3.83 (1H, m, H4), 3.79 (3H, s, H10), 3.45 – 3.35 (1H, m, H14), 3.20 – 3.10 (1H, m, H14), 2.40 (3H, s, H1), 2.37 (3H, s, H13), 1.66 (2H, app. quin., *J* = 7.7 Hz, H5), 1.38 – 1.28 (2H, m, H6), 1.23 – 1.14 (1H, m, H15), 1.04 – 0.95 (3H, m, H15, H16), 0.90 (3H, t, *J* = 7.4 Hz, H7), 0.70 (3H, t, *J* = 7.1 Hz, H17);

^{13}C NMR (101 MHz, $CDCl_3$) δ_C 176.2, 162.8, 144.4, 143.4, 136.3, 135.6, 129.9, 129.2, 128.4, 128.2, 127.9, 126.7, 117.3, 116.8, 52.8, 51.9, 51.1, 32.0, 30.5, 21.70, 21.66, 20.1, 19.8, 13.9, 13.7;

HRMS (ESI) m/z: $[M + H]^+$ Calcd for $C_{29}H_{38}N_3O_7S_2$ 604.2146; Found 604.2144;

Methyl 3-acetyl-4,5-bis((N-butyl-4-methylphenyl)sulfonamido)-1*H*-pyrrole-2-carboxylate, 88j



ZT352, ZT373

Synthesised from *N*,*N'*-(ethyne-1,2-diyl)bis(*N*-butyl-4-methylbenzenesulfonamide) (48 mg, 0.10 mmol, 1.0 eq.), methyl 5-methylisoxazole-3-carboxylate (29 mg, 0.20 mmol, 2.0 eq.), chloro[tris(2,4-di-*tert*-butyl-phenyl)phosphite]gold(I) (4.4 mg, 5.0 µmol, 5 mol%) and silver bis(trifluoromethanesulfonyl)imide (2.0 mg, 5.2 µmol, 5 mol%) in DCE (anhy., 0.2 mL) with general procedure **7.2.3d** at 80 °C for 2 h. Column chromatography (silica gel, 10% → 20% EtOAc/pentane) afforded the title compound (22 mg, 36 µmol, 36%) as a yellow oil;

R_f 0.11 (20% EtOAc/pentane);

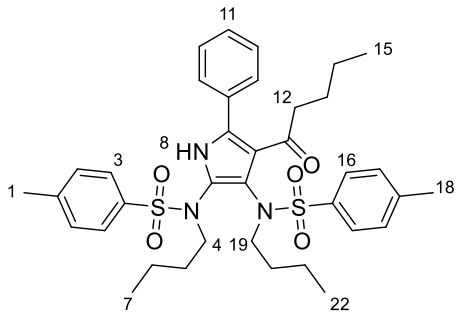
IR (thin film, ν_{max}/cm^{-1}) 3268, 2960, 1691, 1499, 1453, 1345, 1285, 1162, 1090, 859, 708;

^{1}H NMR (400 MHz, C_6D_6) δ_H 9.93 (1H, s, H8), 7.85 (2H, d, *J* = 8.2 Hz, H3), 7.73 (2H, d, *J* = 8.1 Hz, H11), 6.79 (2H, d, *J* = 8.2 Hz, H2), 6.68 (2H, d, *J* = 8.1 Hz, H12), 4.26 – 4.16 (1H, m, H4), 4.14 – 4.01 (1H, m, H4), 3.52 – 3.43 (1H, m, H14), 3.42 – 3.33 (1H, m, H14), 3.25 (3H, s, H9), 2.56 (3H, s, H10), 1.85 (3H, s, H1), 1.82 – 1.70 (5H, m, H5, H13), 1.41 – 1.28 (4H, m, H6, H15), 0.98 – 0.85 (2H, m, H16), 0.82 (3H, t, *J* = 7.4 Hz, H7), 0.64 (3H, t, *J* = 7.3 Hz, H17);

^{13}C NMR (101 MHz, C_6D_6) δ_C 198.2, 159.7, 144.2, 143.6, 137.5, 137.3, 131.0, 130.1, 129.7, 128.7, 128.62, 128.59, 117.2, 115.6, 51.6, 51.5, 51.3, 32.4, 31.9, 30.4, 21.1 (2C), 20.1, 20.0, 13.9, 13.8;

HRMS (ESI) m/z: $[M + H]^+$ Calcd for $C_{30}H_{40}N_3O_7S_2$ 618.2302; Found 618.2299.

***N*,*N'*-(4-Pentanoyl-5-phenyl-1*H*-pyrrole-2,3-diyl)bis(*N*-butyl-4-methylbenzenesulfonamide), 88k**



ZT350

Synthesised from *N*,*N'*-(ethyne-1,2-diyl)bis(*N*-butyl-4-methylbenzenesulfonamide) (48 mg, 0.10 mmol, 1.0 eq.), 5-butyl-3-phenylisoxazole (41 mg, 0.20 mmol, 2.0 eq.), chloro[tris(2,4-di-*tert*-butyl-phenyl)phosphite]gold(I) (4.4 mg, 5.0 μmol, 5 mol%) and silver bis(trifluoromethane-sulfonyl)imide (2.0 mg, 5.2 μmol, 5 mol%) in DCE (anhy., 0.2 mL) with general procedure **7.2.3d** at room temperature for 2 h. Column chromatography

(silica gel, 10% → 20% EtOAc/pentane) afforded the title compound (57 mg, 84 μmol, 83%) as a colourless solid;

m.p. 164 °C;

R_f 0.53 (20% EtOAc/pentane);

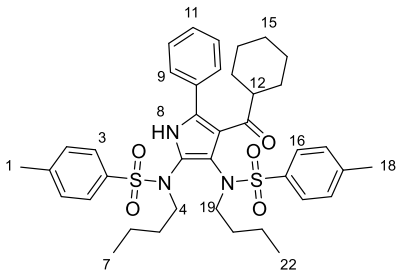
IR (thin film, ν_{max}/cm^{-1}) 3292, 2959, 1667, 1455, 1337, 1159, 1090, 909, 730, 665;

^{1}H NMR (400 MHz, $CDCl_3$) δ_H 8.79 (1H, s, H8), 7.73 (2H, d, *J* = 8.2 Hz, H16), 7.59 (2H, d, *J* = 8.2 Hz, H3), 7.46 – 7.40 (3H, m, H10, H11), 7.39 – 7.35 (2H, m, H12), 7.30 (2H, d, *J* = 8.2 Hz, H17), 7.20 (2H, d, *J* = 8.2 Hz, H2), 3.82 (2H, td, *J* = 7.2, 2.8 Hz, H19), 3.38 – 3.23 (2H, m, H4), 2.41 (3H, s, H18), 2.38 (3H, s, H1), 2.30 – 2.20 (1H, m, H12), 2.06 – 1.94 (1H, m, H12), 1.66 (2H, app. quin., *J* = 7.9 Hz, H20), 1.35 – 1.17 (6H, m, H5, H13, H21), 1.05 – 0.95 (4H, m, H6, H14), 0.92 (3H, t, *J* = 7.4 Hz, H22), 0.76 – 0.67 (6H, m, H7, H15);

^{13}C NMR (101 MHz, $CDCl_3$) δ_C 198.6, 144.3, 143.2, 137.0, 136.7, 132.1, 131.6, 129.9, 129.3, 129.1, 128.9 (2C), 128.2, 127.8, 125.5, 120.9, 117.5, 52.4, 51.5, 42.4, 31.8, 30.6, 25.9, 22.1, 21.7, 21.6, 20.1, 19.9, 13.9, 13.9, 13.8;

HRMS (ESI) m/z: $[M + H]^+$ Calcd for $C_{37}H_{48}N_3O_5S_2$ 678.3030; Found 638.3027.

***N*,*N'*-(4-(Cyclohexanecarbonyl)-5-phenyl-1*H*-pyrrole-2,3-diyl)bis(*N*-butyl-4-methylbenzenesulfonamide), 88l**



ZT368

Synthesised from *N*,*N'*-(ethyne-1,2-diyl)bis(*N*-butyl-4-methylbenzenesulfonamide) (48 mg, 0.10 mmol, 1.0 eq.), 5-cyclohexyl-3-phenylisoxazole (46 mg, 0.20 mmol, 2.0 eq.), chloro[tris(2,4-di-*tert*-butyl-phenyl)phosphite]gold(I) (4.4 mg, 5.0 μmol, 5 mol%) and silver bis(trifluoromethane-sulfonyl)imide (2.0 mg, 5.2 μmol, 5 mol%) in DCE (anhy., 0.2 mL) with general procedure **7.2.3d** at room temperature for 2 h. Column chromatography (silica gel, 5% → 10% → 20% EtOAc/pentane) afforded the title compound (48 mg, 68 μmol, 68%) as a colourless solid;

m.p. 173 °C (decomp.);

R_f 0.41 (20% EtOAc/pentane);

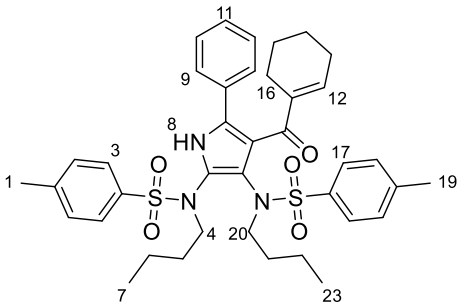
IR (thin film, ν_{max}/cm^{-1}) 3290, 2931, 1660, 1335, 1158, 1089, 908, 730;

^{1}H NMR (400 MHz, $CDCl_3$) δ_H 8.69 (1H, s, H8), 7.73 (2H, d, *J* = 8.2 Hz, H16), 7.66 (2H, d, *J* = 8.2 Hz, H3), 7.47 – 7.40 (5H, m, H9, H10, H11), 7.29 (2H, d, *J* = 8.2 Hz, H17), 7.23 (2H, d, *J* = 8.2 Hz, H2), 3.79 – 3.67 (1H, m, H19), 3.64 – 3.52 (1H, m, H19), 3.35 – 3.25 (1H, m, H4), 3.24 – 3.14 (1H, m, H4)., 2.47 – 2.36 (7H, m, H1, H12, H18), 1.66 – 1.44 (m, 7H, H13, H14, H15, H20), 1.32 – 1.16 (5H, m, H5, H15, H21), 1.11 – 0.92 (4H, m, H6, H13), 0.88 (3H, t, *J* = 7.3 Hz, H22), 0.85 – 0.70 (5H, m, H14, H7);

^{13}C NMR (101 MHz, $CDCl_3$) δ_C 201.3, 144.4, 143.2, 137.2, 136.7, 132.4, 132.2, 129.9, 129.3, 129.2, 129.1, 128.8, 128.4, 127.8, 124.9, 119.8, 118.3, 51.6, 51.5, 49.1, 31.6, 30.6, 30.0, 28.5, 26.1, 25.9, 25.6, 21.7, 21.6, 20.1, 19.8, 13.9, 13.8; *Note: extra peaks are due to cyclohexyl group being diastereotopic.*

HRMS (ESI) m/z: $[M + H]^+$ Calcd for $C_{39}H_{50}N_3O_5S_2$ 704.3186; Found 704.3182.

***N*,*N'*-(4-(Cyclohex-1-ene-1-carbonyl)-5-phenyl-1*H*-pyrrole-2,3-diyl)bis(*N*-butyl-4-methylbenzenesulfonamide), 88m**



ZT369-A

Synthesised from *N*,*N'*-(ethyne-1,2-diyl)bis(*N*-butyl-4-methylbenzenesulfonamide) (48 mg, 0.10 mmol, 1.0 eq.), 5-(cyclohex-1-en-1-yl)-3-phenylisoxazole (46 mg, 0.20 mmol, 2.0 eq.), chloro[tris(2,4-di-*tert*-butyl-phenyl)phosphite]gold(I) (4.4 mg, 5.0 μmol, 5 mol%) and silver bis(trifluoromethanesulfonyl)imide (2.0 mg, 5.2 μmol, 5 mol%) in DCE (anhy., 0.2 mL) with general procedure **7.2.3d** at 80 °C for 2 h. Column chromatography (silica gel, 5% → 10% → 20% EtOAc/pentane) afforded the title compound (42 mg, 60 μmol, 59%) as a colourless solid;

m.p. 218 °C (decomp.);

R_f 0.22 (10% EtOAc/pentane);

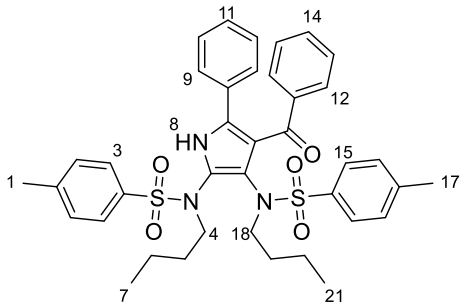
IR (thin film, ν_{max}/cm^{-1}) 3297, 2959, 2932, 1630, 1336, 1155, 1090, 910, 731, 664;

^{1}H NMR (400 MHz, $CDCl_3$) δ_H 8.91 (1H, s, H8), 7.71 (2H, d, *J* = 8.3 Hz, H17), 7.54 (2H, d, *J* = 8.2 Hz, H3), 7.37 – 7.27 (5H, m, H10, H11, H18), 7.20 – 7.13 (2H, m, H9), 7.11 (2H, d, *J* = 8.2 Hz, H2), 6.36 (1H, t, *J* = 3.8 Hz, H12), 4.06 – 3.96 (1H, m, H20), 3.95 – 3.83 (1H, m, H20), 3.31 (1H, td, *J* = 12.5, 5.2 Hz, H4), 3.16 (1H, td, *J* = 12.5, 5.2 Hz, H4), 2.40 (3H, s, H19), 2.35 (3H, s, H1), 2.11 – 1.98 (1H, m, H10), 1.97 – 1.82 (2H, m, H13, H16), 1.76 (2H, app. quin., *J* = 7.7 Hz, H21), 1.59 – 1.48 (1H, m, H16), 1.47 – 1.30 (5H, m, H14, H15, H22), 1.29 – 1.15 (2H, m, H5, H14), 1.16 – 1.00 (1H, m, H5), 1.00 – 0.86 (5H, m, H6, H23), 0.71 (3H, t, *J* = 7.3 Hz, H7);

^{13}C NMR (101 MHz, $CDCl_3$) δ_C 193.6, 144.5, 144.2, 143.0, 139.3, 136.9, 136.8, 132.2, 130.9, 129.9, 129.3, 128.7, 128.3, 128.2, 128.0, 127.7, 125.8, 119.4, 118.6, 52.7, 51.6, 32.0, 30.5, 26.1, 23.6, 21.9, 21.7 (2C), 21.6, 20.1, 19.9, 14.0, 13.7;

HRMS (ESI) m/z: $[M + H]^+$ Calcd for $C_{39}H_{48}N_3O_5S_2$ 702.3030; Found 702.3027.

***N,N'*-(4-Benzoyl-5-phenyl-1*H*-pyrrole-2,3-diyl)bis(*N*-butyl-4-methylbenzenesulfonamide), 88n**



ZT326-B, ZT329

Synthesised from *N,N'*-(ethyne-1,2-diyl)bis(*N*-butyl-4-methylbenzenesulfonamide) (48 mg, 0.10 mmol, 1.0 eq.), 3,5-diphenylisoxazole (45 mg, 0.20 mmol, 2.0 eq.), chloro[tris(2,4-di-*tert*-butyl-phenyl)phosphite]gold(I) (4.4 mg, 5.0 μmol, 5 mol%) and silver bis(trifluoromethane-sulfonyl)imide (2.0 mg, 5.2 μmol, 5 mol%) in DCE (anhy., 0.2 mL) with general procedure **7.2.3d** at room temperature for 2 h. Column chromatography (silica gel, 20% EtOAc/pentane) afforded the title compound (44 mg, 63 μmol, 63%) as a beige solid. Crystals suitable for X-ray crystallography were grown by vapour diffusion of pentane into a concentrated solution of the title compound in DCM.

m.p. 218 °C (decomp.);

R_f 0.39 (20% EtOAc/pentane);

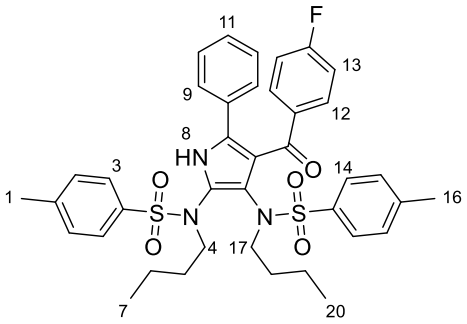
IR (thin film, ν_{max}/cm^{-1}) 3298, 2961, 2874, 1647, 1456, 1338, 1158, 1090, 908, 730, 696, 662;

^{1}H NMR (400 MHz, $CDCl_3$) δ_H 8.99 (1H, s, H8), 7.74 (2H, d, *J* = 8.2 Hz, H15), 7.46 (2H, d, *J* = 7.1 Hz, H12), 7.39 (2H, d, *J* = 8.2 Hz, H3), 7.31 (2H, d, *J* = 8.2 Hz, H16), 7.28 – 7.23 (1H, m, H14), 7.13 – 7.05 (7H, m, H9, H10, H11, H13), 6.76 (2H, d, *J* = 8.2 Hz, H2), 4.14 – 4.02 (1H, m, H18), 3.99 – 3.88 (1H, m, H18), 3.38 (1H, td, *J* = 12.4, 5.2 Hz, H4), 3.28 (1H, td, *J* = 12.4, 5.2 Hz, H4), 2.42 (3H, s, H17), 2.10 (3H, s, H1), 1.81 (2H, app. quin., *J* = 7.9 Hz, H19), 1.42 (2H, app. sext., *J* = 7.3 Hz, H20), 1.32 – 1.21 (1H, m, H5), 1.17 – 1.05 (1H, m, H5), 1.02 – 0.91 (5H, m, H6, H21), 0.73 (3H, t, *J* = 7.3 Hz, H7);

^{13}C NMR (101 MHz, $CDCl_3$) δ_C 191.6, 144.3, 143.0, 138.2, 136.7, 136.3, 132.2, 131.5, 131.1, 130.2, 129.9, 129.2, 128.5, 128.4, 128.2, 128.1, 127.7, 127.6, 126.4, 119.0, 118.7, 53.1, 51.7, 32.2, 30.7, 21.7, 21.4, 20.1, 19.9, 14.1, 13.7;

HRMS (ESI) m/z: $[M - H]^-$ Calcd for $C_{39}H_{42}N_3O_5S_2$ 696.2571; Found 696.2571.

***N*,*N'*-(4-(4-Fluorobenzoyl)-5-phenyl-1*H*-pyrrole-2,3-diyl)bis(*N*-butyl-4-methylbenzenesulfonamide), 88o**



ZT332, ZT338

Synthesised from *N*,*N'*-(ethyne-1,2-diyl)bis(*N*-butyl-4-methylbenzenesulfonamide) (48 mg, 0.10 mmol, 1.0 eq.), 5-(4-fluorophenyl)-3-phenylisoxazole (49 mg, 0.20 mmol, 2.0 eq.), chloro[tris(2,4-di-*tert*-butyl-phenyl)phosphite]gold(I) (4.4 mg, 5.0 μmol, 5 mol%) and silver bis(trifluoromethanesulfonyl)imide (2.0 mg, 5.2 μmol, 5 mol%) in DCE (anhy., 0.2 mL) with general procedure **7.2.3d** at 80 °C for 2 h. Column chromatography (silica gel,

10% EtOAc/pentane) afforded the title compound (48 mg, 67 μmol, 68%) as a colourless solid.

m.p. 185 °C (decomp);

R_f 0.13 (10% EtOAc/pentane);

IR (thin film, ν_{max}/cm^{-1}) 3293, 2963, 1650, 1597, 1338, 1151, 1090, 772, 732, 667;

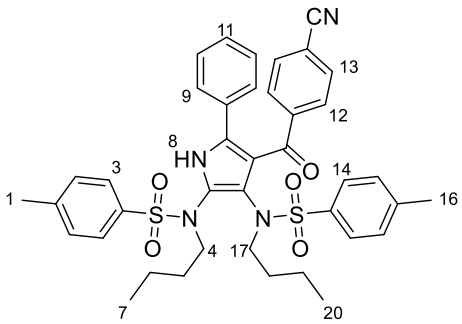
^{1}H NMR (500 MHz, $CDCl_3$) δ_H 9.03 (1H, s, H8), 7.73 (2H, d, *J* = 8.2 Hz, H3), 7.51 – 7.45 (2H, m, H12), 7.40 (2H, d, *J* = 8.2 Hz, H14), 7.31 (2H, d, *J* = 8.2 Hz, H2), 7.15 – 7.11 (3H, m, H9, H11), 7.10 – 7.06 (2H, m, H10), 6.81 (2H, d, *J* = 8.2 Hz, H15), 6.79 – 6.73 (2H, m, H13), 4.09 – 4.00 (1H, m, H17), 3.96 – 3.86 (1H, m, H17), 3.38 (1H, td, *J* = 12.5, 5.2 Hz, H4), 3.27 (1H, td, *J* = 12.5, 5.2 Hz, H4), 2.42 (3H, s, H1), 2.14 (3H, s, H16), 1.80 (2H, app. quin., *J* = 7.8 Hz, H18), 1.41 (2H, app. sext., *J* = 7.1 Hz, H19), 1.31 – 1.22 (1H, m, H5), 1.16 – 1.07 (1H, m, H5), 1.01 – 0.92 (5H, m, H6, H20), 0.73 (3H, t, *J* = 7.3 Hz, H7);

^{13}C NMR {^{19}F} (126 MHz, $CDCl_3$) δ_C 190.0, 165.2, 144.4, 143.1, 136.6, 136.3, 134.6, 132.6, 131.4, 130.9, 130.0, 129.2, 128.6, 128.40, 128.36, 128.1, 127.7, 126.5, 118.9, 118.5, 114.7, 53.0, 51.6, 32.1, 30.6, 21.7, 21.5, 20.1, 19.9, 14.0, 13.7;

^{19}F NMR (471 MHz, $CDCl_3$) δ_F -106.55.

HRMS (ESI) m/z: $[M - H]^-$ Calcd for $C_{39}H_{41}FN_3O_5S_2$ 714.2477; Found 714.2472.

***N*,*N'*-(4-(4-Cyanobenzoyl)-5-phenyl-1*H*-pyrrole-2,3-diyl)bis(*N*-butyl-4-methylbenzenesulfonamide), 88p**



ZT410

Synthesised from *N*,*N'*-(ethyne-1,2-diyl)bis(*N*-butyl-4-methylbenzenesulfonamide) (48 mg, 0.10 mmol, 1.0 eq.), 4-(3-phenylisoxazol-5-yl)benzonitrile (50 mg, 0.20 mmol, 2.0 eq.), chloro[tris(2,4-di-*tert*-butyl-phenyl)phosphite]gold(I) (4.4 mg, 5.0 μmol, 5 mol%) and silver bis(trifluoromethanesulfonyl)imide (2.0 mg, 5.2 μmol, 5 mol%) in DCE (anhy., 0.2 mL) with general procedure **7.2.3d** at 80 °C for 2 h. Column chromatography twice (silica gel, 10% → 20% EtOAc/pentane) afforded the title compound (34 mg, 47 μmol, 47%) as a yellow oil.

R_f 0.22 (20% EtOAc/pentane);

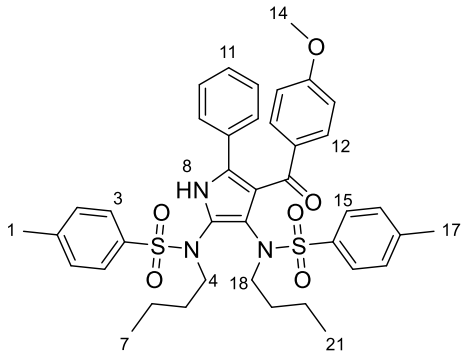
IR (thin film, ν_{max}/cm^{-1}) 3273, 2980, 2881, 2230, 1651, 1342, 1160, 1090, 910, 733;

^{1}H NMR (500 MHz, $CDCl_3$) δ_H 9.00 (1H, s, H8), 7.72 (2H, d, *J* = 8.2 Hz, H13), 7.53 (2H, d, *J* = 8.4 Hz, H14), 7.43 (2H, d, *J* = 8.1 Hz, H3), 7.37 (2H, d, *J* = 8.4 Hz, H15), 7.32 (2H, d, *J* = 8.2 Hz, H12), 7.17 – 7.10 (3H, m, H10, H11), 7.06 – 7.03 (2H, m, H9), 6.85 (2H, d, *J* = 8.1 Hz, H2), 4.04 – 3.86 (2H, m, H17), 3.37 (1H, td, *J* = 12.3, 5.3 Hz, H4), 3.28 (1H, td, *J* = 12.3, 5.3 Hz, H4), 2.42 (3H, s, H16), 2.15 (3H, s, H1), 1.77 (2H, app. quin., *J* = 7.8 Hz, H18), 1.46 – 1.35 (2H, m, H19), 1.30 – 1.20 (1H, m, H5), 1.17 – 1.07 (1H, m, H5), 1.01 – 0.92 (5H, m, H6, H20), 0.73 (3H, t, *J* = 7.3 Hz, H7);

^{13}C NMR (126 MHz, $CDCl_3$) δ_C 189.8, 144.5, 143.3, 141.8, 136.6, 136.4, 132.5, 131.5, 130.6, 130.3, 130.0, 129.3, 128.9, 128.8, 128.6, 128.1, 127.7, 126.8, 118.8, 118.3, 118.1, 115.1, 52.8, 51.6, 32.1, 30.7, 21.7, 21.5, 20.1, 19.9, 14.0, 13.8;

HRMS (ESI) m/z: $[M + Na]^+$ Calcd for $C_{40}H_{42}N_4O_5NaS_2$ 745.2489; Found 745.2482.

***N*,*N'*-(4-(4-Methoxybenzoyl)-5-phenyl-1*H*-pyrrole-2,3-diyl)bis(*N*-butyl-4-methylbenzenesulfonamide), 88q**



ZT348, ZT365

Synthesised from *N*,*N'*-(ethyne-1,2-diyl)bis(*N*-butyl-4-methylbenzenesulfonamide) (48 mg, 0.10 mmol, 1.0 eq.), 5-(4-methoxyphenyl)-3-phenylisoxazole (51 mg, 0.20 mmol, 2.0 eq.), chloro[tris(2,4-di-*tert*-butyl-phenyl)phosphite]gold(I) (4.4 mg, 5.0 μmol, 5 mol%) and silver bis(trifluoromethanesulfonyl)imide (2.0 mg, 5.2 μmol, 5 mol%) in DCE (anhy., 0.2 mL) with general procedure **7.2.3d** at 80 °C for 2 h. Upon completion, the reaction was treated with HCl (1.0 M in Et_2O, 0.1 mL) for 30 min at room temperature, after which column chromatography (silica gel, 10% → 20% EtOAc/pentane) afforded the title compound (28 mg, 38 μmol, 38%) as a pink solid;

m.p. 156 °C (decomp.);

R_f 0.26 (20% EtOAc/pentane);

IR (thin film, ν_{max}/cm^{-1}) 3293, 2961, 1644, 1599, 1338, 1257, 1158, 910, 732;

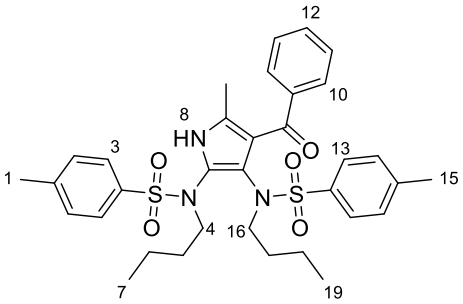
^{1}H NMR (400 MHz, $CDCl_3$) δ_H 8.96 (1H, s, H8), 7.73 (2H, d, *J* = 8.2 Hz, H15), 7.48 (2H, d, *J* = 8.9 Hz, H12), 7.37 (2H, d, *J* = 8.2 Hz, H3), 7.31 (2H, d, *J* = 8.2 Hz, H16), 7.16 – 7.10 (5H, m, H9, H10, H11), 6.80 (2H, d, *J* = 8.2 Hz, H2), 6.60 (2H, d, *J* = 8.9 Hz, H13), 4.12 – 4.02 (1H, m, H18), 4.00 – 3.88 (1H, m, H18) 3.75 (3H, s, H14), 3.41 – 3.30 (1H, m, H4), 3.25 – 3.14 (1H, m, H4), 2.41 (3H, s, H17), 2.15 (3H, s, H1), 1.81 (2H, app. quin., *J* = 7.8 Hz, H19), 1.42 (2H, app. sext., *J* = 7.3 Hz, H20), 1.29 – 1.19 (1H, m, H5), 1.15 – 1.04

(1H, m, H5), 0.98 (3H, t, *J* = 7.4 Hz, H21), 0.95 – 0.87 (2H, m, H6), 0.71 (3H, t, *J* = 7.3 Hz, H7);

^{13}C NMR (101 MHz, $CDCl_3$) δ_C 190.5, 163.0, 144.3, 143.0, 136.8, 136.4, 132.5, 131.3, 131.2, 130.4, 129.9, 129.2, 128.6, 128.09, 128.06 (2C), 127.7, 126.2, 119.1, 118.9, 113.0, 55.5, 52.9, 51.6, 32.1, 30.6, 21.7, 21.5, 20.0, 19.9, 14.1, 13.7;

HRMS (ESI) m/z: $[M + H]^+$ Calcd for $C_{40}H_{46}N_3O_6S_2$ 728.2823; Found 728.2819.

***N,N'*-(4-Benzoyl-5-methyl-1*H*-pyrrole-2,3-diyl)bis(*N*-butyl-4-methylbenzenesulfonamide), 88r**



ZT347

Synthesised from *N,N'*-(ethyne-1,2-diyl)bis(*N*-butyl-4-methylbenzenesulfonamide) (48 mg, 0.10 mmol, 1.0 eq.), 3-methyl-5-phenylisoxazole (32 mg, 0.20 mmol, 2.0 eq.), chloro[tris(2,4-di-*tert*-butyl-phenyl)phosphite]gold(I) (4.4 mg, 5.0 μmol, 5 mol%) and silver bis(trifluoromethanesulfonyl)imide (2.0 mg, 5.2 μmol, 5 mol%) in DCE (anhy., 0.2 mL) with general procedure **7.2.3d** at room temperature for 2 h. Column chromatography (silica gel, 10% → 15% → 20% EtOAc/pentane) afforded the title compound (37 mg, 58 μmol, 58%) as a colourless oil.

R_f 0.26 (20% EtOAc/pentane);

IR (thin film, ν_{max}/cm^{-1}) 3325, 2960, 1643, 1450, 1339, 1158, 1090, 909, 731;

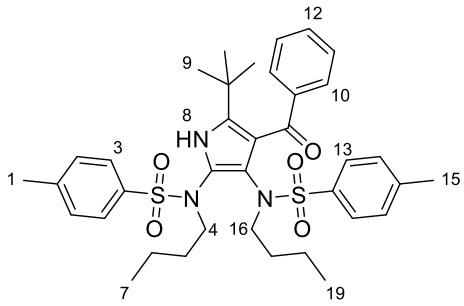
^{1}H NMR (400 MHz, $CDCl_3$) δ_H 8.80 (1H, s, H8), 7.74 (2H, d, *J* = 8.2 Hz, H13), 7.61 (2H, d, *J* = 7.0 Hz, H10), 7.52 (1H, t, *J* = 7.4 Hz, H12), 7.46 (2H, d, *J* = 8.2 Hz, H3), 7.43 – 7.37

(2H, m, H11), 7.31 (2H, d, *J* = 8.2 Hz, H14), 6.82 (2H, d, *J* = 8.2 Hz, H2), 4.03 – 3.91 (1H, m, H16), 3.88 – 3.77 (1H, m, H16), 3.33 – 3.18 (2H, m, H4), 2.41 (3H, s, H15), 2.12 (3H, s, H1), 1.91 (3H, s, H9), 1.75 – 1.67 (2H, m, H17), 1.40 – 1.30 (2H, m, H18), 1.25 – 1.15 (1H, m, H5), 1.10 – 1.00 (1H, m, H5), 0.97 – 0.88 (5H, m, H6, H19), 0.70 (3H, t, *J* = 7.3 Hz, H7);

^{13}C NMR (101 MHz, $CDCl_3$) δ_C 191.5, 144.2, 143.0, 139.8, 136.8, 136.4, 132.3, 129.9, 129.7, 129.3, 128.7, 128.3, 128.1, 127.7, 124.6, 119.1, 118.0, 52.8, 51.8, 32.0, 30.6, 21.7, 21.4, 20.1, 19.9, 14.5, 14.0, 13.7;

HRMS (ESI) m/z: $[M + H]^+$ Calcd for $C_{34}H_{42}N_3O_5S_2$ 636.2560; Found 636.2560.

***N*,*N'*-(4-Benzoyl-5-(tert-butyl)-1*H*-pyrrole-2,3-diyl)bis(*N*-butyl-4-methylbenzenesulfonamide), 88s**



ZT358, ZT375

Synthesised from *N*,*N'*-(ethyne-1,2-diyl)bis(*N*-butyl-4-methylbenzenesulfonamide) (48 mg, 0.10 mmol, 1.0 eq.), 3-(tert-butyl)-5-phenylisoxazole (41 mg, 0.20 mmol, 2.0 eq.), chloro[tris(2,4-di-*tert*-butyl-phenyl)phosphite]gold(I) (4.4 mg, 5.0 μmol, 5 mol%) and silver bis(trifluoromethanesulfonyl)imide (2.0 mg, 5.2 μmol, 5 mol%) in DCE (anhy., 0.2 mL) with general procedure **7.2.3d** at room temperature for 4 h. Column chromatography (silica gel, 5% → 10% EtOAc/pentane) afforded the title compound (45 mg, 66 μmol, 66%) as a colourless solid;

m.p. 64 °C ($CHCl_3$);

R_f 0.27 (10% EtOAc/pentane);

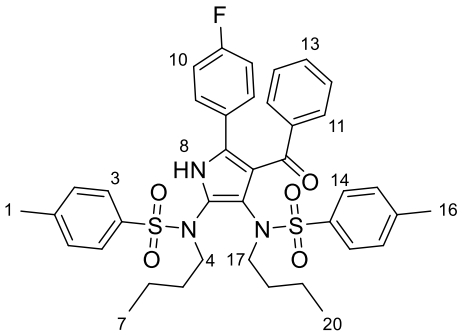
IR (thin film, ν_{max}/cm^{-1}) 2960, 1660, 1332, 1159, 1090, 1040, 910, 815, 732, 665;

^{1}H NMR (500 MHz, $CDCl_3$) δ_H 8.42 (1H, s, H8), 7.75 (2H, d, *J* = 6.9 Hz, H10), 7.69 (2H, d, *J* = 8.1 Hz, H13), 7.53 (1H, t, *J* = 7.4 Hz, H12), 7.43 – 7.37 (2H, m, H11), 7.31 (2H, d, *J* = 8.1 Hz, H14), 7.21 (2H, d, *J* = 8.2 Hz, H3), 6.98 (2H, d, *J* = 8.2 Hz, H2), 3.91 – 3.82 (1H, m, H16), 3.80 – 3.69 (1H, m, H16), 3.00 – 2.89 (1H, m, H4), 2.63 – 2.53 (1H, m, H4), 2.42 (3H, s, H15), 2.31 (3H, s, H1), 1.68 – 1.58 (2H, m, H17), 1.32 (2H, app. sext., *J* = 7.4 Hz, H18), 1.21 (9H, s, H9), 0.93 (3H, t, *J* = 7.4 Hz, H19), 0.90 – 0.83 (2H, m, H5), 0.73 – 0.63 (2H, m, H6), 0.58 (3H, t, *J* = 7.1 Hz, H7);

^{13}C NMR (126 MHz, $CDCl_3$) δ_C 195.8, 144.3, 143.1, 139.9, 137.1, 137.0, 135.4, 133.1, 130.4, 129.9, 129.2, 128.2, 128.1, 127.8, 121.4, 118.5, 117.9, 51.8, 51.5, 33.1, 31.6, 30.6, 30.1, 21.7, 21.6, 19.9, 19.8, 14.0, 13.6;

HRMS (ESI) m/z: $[M + H]^+$ Calcd for $C_{37}H_{48}N_3O_5S_2$ 678.3030; Found 678.3024.

***N*,*N'*-(4-Benzoyl-5-(4-fluorophenyl)-1*H*-pyrrole-2,3-diyl)bis(*N*-butyl-4-methylbenzenesulfonamide), 88t**



ZT366

Synthesised from *N*,*N'*-(ethyne-1,2-diyl)bis(*N*-butyl-4-methylbenzenesulfonamide) (48 mg, 0.10 mmol, 1.0 eq.), 3-(4-fluorophenyl)-5-phenylisoxazole (49 mg, 0.20 mmol, 2.0 eq.), chloro[tris(2,4-di-*tert*-butyl-phenyl)phosphite]gold(I) (4.4 mg, 5.0 μmol, 5 mol%) and

silver bis(trifluoromethane-sulfonyl)imide (2.0 mg, 5.2 μmol, 5 mol%) in DCE (anhy., 0.2 mL) with general procedure **7.2.3d** at 80°C for 2 h. Column chromatography (silica gel, 10% → 20% EtOAc/pentane) afforded the title compound (48 mg, 67 μmol, 67%) as a colourless solid;

m.p. 187 °C (decomp.);

R_f 0.11 (10% EtOAc/pentane);

IR (thin film, ν_{max}/cm^{-1}) 3293, 2960, 1648, 1532, 1453, 1337, 1158, 1090, 732;

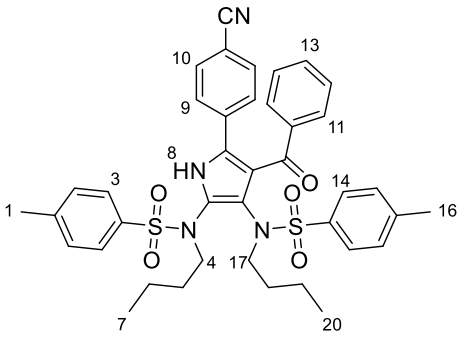
^{1}H NMR (400 MHz, $CDCl_3$) δ_H 9.09 (1H, s, H8), 7.73 (2H, d, *J* = 8.3 Hz, H14), 7.43 (2H, d, *J* = 7.1 Hz, H10), 7.39 (2H, d, *J* = 8.3 Hz, H3), 7.33 – 7.26 (3H, m, H13, H15), 7.14 – 7.02 (4H, m, H9, H11), 6.80 – 6.73 (4H, m, H2, H12), 4.12 – 4.00 (1H, m, H17), 3.95 – 3.84 (1H, m, H17), 3.37 (1H, td, *J* = 12.4, 5.2 Hz, H4), 3.26 (1H, td, *J* = 12.4, 5.2 Hz, H4), 2.42 (3H, s, H16), 2.10 (3H, s, H1), 1.81 (2H, app. quin., *J* = 7.7 Hz, H18), 1.41 (2H, app. sext., *J* = 7.2 Hz, H19), 1.33 – 1.18 (1H, m, H5), 1.19 – 1.03 (1H, m, H5), 1.02 – 0.90 (5H, m, H6, H20), 0.72 (3H, t, *J* = 7.3 Hz, H7);

^{13}C NMR (101 MHz, $CDCl_3$) δ_C 191.5, 162.5 (d, $^1J_{C-F}$ = 249.2 Hz), 144.4, 143.1, 138.1, 136.7, 136.2, 132.3, 130.6, 130.3, 130.2, 130.1, 129.9, 129.2, 128.0, 127.7 (2C), 127.4 (d, $^4J_{C-F}$ = 3.2 Hz), 126.5, 118.9 (d, $^2J_{C-F}$ = 22.2 Hz), 115.6 (d, $^3J_{C-F}$ = 21.9 Hz), 53.0, 51.7, 32.1, 30.6, 21.7, 21.4, 20.1, 19.9, 14.0, 13.7;

^{19}F NMR (377 MHz, $CDCl_3$) δ_F -112.68;

HRMS (ESI) m/z: $[M + H]^+$ Calcd for $C_{39}H_{43}FN_3O_5S_2$ 716.2623; Found 716.2618.

***N*,*N'*-(4-Benzoyl-5-(4-cyanophenyl)-1*H*-pyrrole-2,3-diyl)bis(*N*-butyl-4-methylbenzenesulfonamide), 88u**



ZT412

Synthesised from *N*,*N'*-(ethyne-1,2-diyl)bis(*N*-butyl-4-methylbenzenesulfonamide) (48 mg, 0.10 mmol, 1.0 eq.), 4-(5-phenylisoxazol-3-yl)benzonitrile (50 mg, 0.20 mmol, 2.0 eq.), chloro[tris(2,4-di-*tert*-butyl-phenyl)phosphite]gold(I) (4.4 mg, 5.0 μmol, 5 mol%) and silver bis(trifluoromethanesulfonyl)imide (2.0 mg, 5.2 μmol, 5 mol%) in DCE (anhy., 0.2 mL) with general procedure **7.2.3d** at 80 °C for 2 h. Column chromatography twice (silica gel, 10% → 20% EtOAc/pentane) afforded the title compound (26 mg, 36 μmol, 36%) as a yellow oil.

R_f 0.29 (20% EtOAc/pentane);

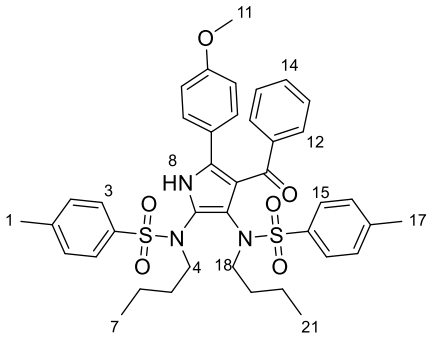
IR (thin film, ν_{max}/cm^{-1}) 3281, 2961, 2873, 2228, 1650, 1452, 1338, 1159, 1090, 911, 732;

^{1}H NMR (500 MHz, $CDCl_3$) δ_H 9.34 (1H, s, H8), 7.73 (2H, d, *J* = 8.3 Hz, H14), 7.46 (2H, d, *J* = 7.2 Hz, H11), 7.39 – 7.30 (7H, m, H3, H10, H13, H15), 7.19 (2H, d, *J* = 8.5 Hz, H9), 7.16 – 7.11 (2H, m, H12), 6.79 (2H, d, *J* = 8.0 Hz, H2), 4.09 – 3.99 (1H, m, H17), 3.96 – 3.86 (1H, m, H17), 3.35 (1H, td, *J* = 12.4, 5.1 Hz, H4), 3.21 (1H, td, *J* = 12.4, 5.1 Hz, H4), 2.43 (3H, s, H16), 2.13 (3H, s, H1), 1.81 (2H, app. quin., *J* = 7.7 Hz, H18), 1.47 – 1.34 (2H, m, H19), 1.26 – 1.17 (1H, m, H5), 1.14 – 1.05 (1H, m, H5), 1.01 – 0.89 (5H, m, H6, H20), 0.71 (3H, t, *J* = 7.3 Hz, H7);

^{13}C NMR (126 MHz, $CDCl_3$) δ_C 191.3, 144.6, 143.3, 137.8, 136.4, 136.1, 135.3, 132.9, 132.2, 130.1, 130.0, 129.3, 128.5, 128.5, 128.03, 127.98, 127.71, 127.69, 120.6, 119.4, 118.4, 111.4, 52.8, 51.5, 32.1, 30.6, 21.7, 21.5, 20.0, 19.9, 14.0, 13.7;

HRMS (ESI) m/z: $[M + H]^+$ Calcd for $C_{40}H_{43}N_4O_5S_2$ 723.2669; Found 723.2654.

***N,N'*-(4-Benzoyl-5-(4-methoxyphenyl)-1*H*-pyrrole-2,3-diyl)bis(*N*-butyl-4-methylbenzenesulfonamide), 88v**



ZT367

Synthesised from *N,N'*-(ethyne-1,2-diyl)bis(*N*-butyl-4-methylbenzenesulfonamide) (48 mg, 0.10 mmol, 1.0 eq.), 3-(4-methoxyphenyl)-5-phenylisoxazole (51 mg, 0.20 mmol, 2.0 eq.), chloro[tris(2,4-di-*tert*-butyl-phenyl)phosphite]gold(I) (4.4 mg, 5.0 μmol, 5 mol%) and silver bis(trifluoromethanesulfonyl)imide (2.0 mg, 5.2 μmol, 5 mol%) in DCE (anhy., 0.2 mL) with general procedure **7.2.3d** at 80℃ for 2 h. Column chromatography (silica gel, 20% EtOAc/pentane) afforded the title compound (48 mg, 66 μmol, 65%) as a pale yellow solid;

m.p. 180 ℃ (decomp.);

R_f 0.24 (20% EtOAc/pentane);

IR (thin film, ν_{max}/cm^{-1}) 3303, 2962, 1646, 1578, 1495, 1338, 1251, 1159, 1090, 732;

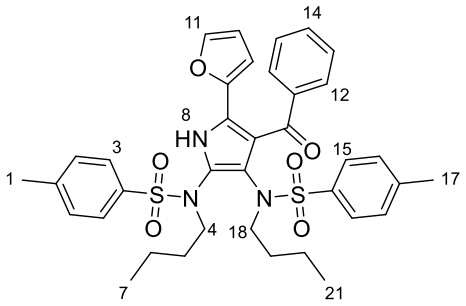
^{1}H NMR (400 MHz, $CDCl_3$) δ_H 8.93 (1H, s, H8), 7.74 (2H, d, *J* = 8.3 Hz, H15), 7.45 (2H, d, *J* = 7.1 Hz, H12), 7.39 (2H, d, *J* = 8.2 Hz, H3), 7.34 – 7.26 (3H, m, H14, H16), 7.13 –

7.07 (2H, m, H13), 7.00 (2H, d, *J* = 8.8 Hz, H9), 6.75 (2H, d, *J* = 8.2 Hz, H2), 6.62 (2H, d, *J* = 8.8 Hz, H10), 4.12 – 4.01 (1H, m, H18), 3.97 – 3.87 (1H, m, H18), 3.69 (3H, s, H11), 3.42 – 3.33 (1H, m, H4), 3.32 – 3.22 (1H, m, H4), 2.42 (3H, s, H17), 2.10 (3H, s, H1), 1.81 (2H, app. quin., *J* = 7.7 Hz, H19), 1.41 (2H, app. sext., *J* = 7.3 Hz, H20), 1.33 – 1.19 (1H, m, H5), 1.17 – 1.03 (1H, m, H5), 1.02 – 0.90 (5H, m, H6, H21), 0.72 (3H, t, *J* = 7.3 Hz, H7);

^{13}C NMR (101 MHz, $CDCl_3$) δ_C 191.6, 159.5, 144.2, 143.0, 138.2, 136.7, 136.3, 132.1, 131.8, 130.2, 129.9, 129.7, 129.2, 128.0, 127.7, 127.6, 126.0, 123.8, 119.0, 118.0, 114.0, 55.4, 53.1, 51.7, 32.1, 30.6, 21.7, 21.4, 20.1, 19.9, 14.0, 13.7;

HRMS (ESI) m/z: $[M + H]^+$ Calcd for $C_{40}H_{46}N_3O_6S_2$ 728.2823; Found 728.2820.

***N*,*N'*-(4-Benzoyl-5-(furan-2-yl)-1*H*-pyrrole-2,3-diyl)bis(*N*-butyl-4-methylbenzenesulfonamide), 88w**



ZT354, ZT356, ZT374

Synthesised from *N*,*N'*-(ethyne-1,2-diyl)bis(*N*-butyl-4-methylbenzenesulfonamide) (48 mg, 0.10 mmol, 1.0 eq.), 3-(furan-2-yl)-5-phenylisoxazole (43 mg, 0.20 mmol, 2.0 eq.), chloro[tris(2,4-di-*tert*-butyl-phenyl)phosphite]gold(I) (4.4 mg, 5.0 μmol, 5 mol%) and silver bis(trifluoromethanesulfonyl)imide (2.0 mg, 5.2 μmol, 5 mol%) in DCE (anhy., 0.2 mL) with general procedure **7.2.3d** at room temperature for 2 h. Column chromatography (silica gel, 5% → 10% → 20% EtOAc/pentane) afforded the title compound (8 mg, 12 μmol, 12%) as a yellow oil;

R_f 0.33 (20% EtOAc/pentane);

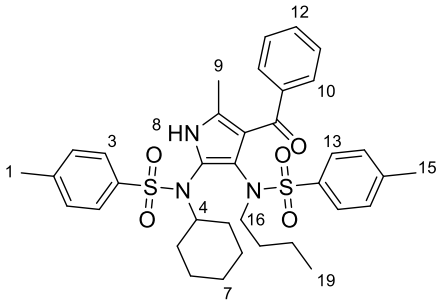
IR (thin film, ν_{max} / cm^{-1}) 3297, 2960, 2873, 1651, 1339, 1162, 1090, 731, 665;

^{1}H NMR (400 MHz, $CDCl_3$) δ_H 9.18 (1H, s, H8), 7.74 (2H, d, *J* = 8.3 Hz, H15), 7.67 (2H, d, *J* = 7.1 Hz, H12), 7.47 (1H, t, *J* = 7.4 Hz, H14), 7.38 (2H, d, *J* = 8.2 Hz, H3), 7.34 – 7.29 (4H, m, H13, H16), 7.23 (1H, dd, *J* = 1.8, 0.6 Hz, H11), 6.83 (2H, d, *J* = 8.2 Hz, H2), 6.15 (1H, dd, *J* = 3.5, 1.8 Hz, H10), 5.67 (1H, dd, *J* = 3.5, 0.6 Hz, H9), 3.98 – 3.87 (2H, m, H18), 3.35 – 3.24 (1H, m, H4), 3.21 – 3.09 (1H, m, H4), 2.42 (3H, s, H17), 2.17 (3H, s, H1), 1.74 (2H, app. quin., *J* = 7.9 Hz, H19), 1.44 – 1.32 (2H, m, H20), 1.23 – 1.01 (2H, m, H5), 0.96 (3H, t, *J* = 7.4 Hz, H21), 0.93 – 0.85 (2H, m, H6), 0.70 (3H, t, *J* = 7.3 Hz, H7);

^{13}C NMR (101 MHz, $CDCl_3$) δ_C 191.3, 144.7, 144.4, 143.2, 141.9, 138.4, 136.7, 136.4, 132.8, 130.04, 130.00, 129.3, 128.2, 128.0, 127.7, 125.8, 121.1, 118.7, 118.0, 111.8, 109.3, 52.6, 51.6, 32.0, 30.5, 21.7, 21.5, 20.0, 19.9, 14.0, 13.7;

HRMS (ESI) m/z: $[M + H]^+$ Calcd for $C_{37}H_{42}N_3O_6S_2$ 688.2510; Found 688.2506.

***N*-(4-Benzoyl-2-((*N*-cyclohexyl-4-methylphenyl)sulfonamido)-5-methyl-1*H*-pyrrol-3-yl)-*N*-butyl-4-methylbenzenesulfonamide, 96b**



ZT398

Synthesised from *N*-butyl-*N*-(((*N*-cyclohexyl-4-methylphenyl)sulfonamido)ethynyl)-4-methylbenzenesulfonam-ide (50 mg, 0.10 mmol, 1.0 eq.), 3-methyl-5-phenylisoxazole (32 mg, 0.20 mmol, 2.0 eq.), chloro[tris(2,4-di-*tert*-butyl-phenyl)phosphite]gold(I) (4.4 mg, 5.0 μmol, 5 mol%) and silver bis(trifluoromethanesulfonyl)imide (2.0 mg, 5.2 μmol, 5 mol%)

in DCE (anhy., 0.2 mL) with general procedure **7.2.3d** at room temperature for 2 h. Upon completion, HCl (1 M in Et_2O, 0.1 mL) was added to the reaction. The reaction mixture was stirred for 30 min before it was concentrated *in vacuo* and purified by column chromatography (silica gel, 20% → 40% Et_2O/pentane) afforded the title compound (61 mg, 92 μmol, 92%) as a yellow solid;

m.p. 114 – 115 °C;

R_f 0.13 (40% Et_2O/pentane);

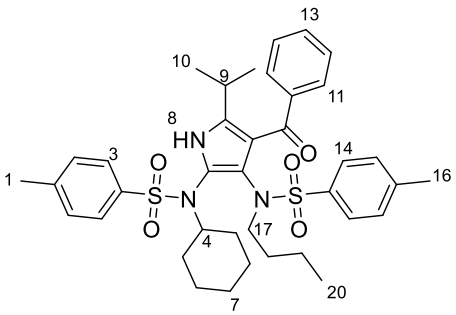
IR (thin film, ν_{max}/cm^{-1}) 3329, 2933, 1643, 1450, 1335, 1160, 1090, 909, 731;

^{1}H NMR (500 MHz, C_6D_6) δ_H 8.84 (1H, s, H8), 8.04 (2H, d, *J* = 8.3 Hz, H3), 7.83 (2H, d, *J* = 8.2 Hz, H13), 7.65 – 7.61 (2H, m, H10), 7.10 – 7.03 (1H, m, H12), 6.99 – 6.94 (2H, m, H11), 6.82 (2H, d, *J* = 8.3 Hz, H2), 6.54 (2H, d, *J* = 8.2 Hz, H14), 4.48 (1H, tt, *J* = 12.0, 3.7 Hz, H4), 3.77 – 3.61 (2H, m, H16), 2.72 – 2.36 (4H, m, H5), 1.90 – 1.79 (5H, m, H1, H6), 1.72 (3H, s, H15), 1.66 – 1.53 (3H, m, H6, H7), 1.51 – 1.45 (4H, m, H7, H9), 1.37 – 1.19 (2H, m, H17), 1.10 – 0.94 (2H, m, H18), 0.74 (3H, t, *J* = 7.4 Hz, H19);

^{13}C NMR (126 MHz, C_6D_6) δ_C 191.1, 143.7, 142.6, 140.7, 139.0, 137.7, 131.8, 129.9, 129.3, 128.8, 128.6, 128.5, 128.4, 126.0, 120.6, 119.9, 67.2, 53.0, 33.4, 32.2, 30.8, 26.9, 25.5, 21.1, 21.0, 20.6, 14.0, 13.9;

HRMS (ESI) m/z: $[M + H]^+$ Calcd for $C_{36}H_{44}N_3O_5S_2$ 662.2717; Found 662.2716.

_N_-(4-Benzoyl-2-((_N_-cyclohexyl-4-methylphenyl)sulfonamido)-5-isopropyl-1_H_-pyrrol-3-yl)-_N_-butyl-4-methylbenzenesulfonamide, 96c



ZT403

Synthesised from *N*-butyl-*N*-(((*N*-cyclohexyl-4-methylphenyl)sulfonamido)ethynyl)-4-methylbenzenesulfonamide (50 mg, 0.10 mmol, 1.0 eq.), 3-isopropyl-5-phenylisoxazole (38 mg, 0.20 mmol, 2.0 eq.), chloro[tris(2,4-di-*tert*-butyl-phenyl)phosphite]gold(I) (4.4 mg, 5.0 μmol, 5 mol%) and silver bis(trifluoromethanesulfonyl)imide (2.0 mg, 5.2 μmol, 5 mol%) in DCE (anhy., 0.2 mL) with general procedure **7.2.3d** at room temperature for 2 h. Upon completion, HCl (1 M in Et_2O, 0.1 mL) was added to the reaction. The reaction mixture was stirred for 12 h before it was concentrated *in vacuo* and purified by column chromatography (silica gel, 10% EtOAc/pentane) afforded the title compound (53 mg, 77 μmol, 77%) as a pink solid;

m.p. 183 °C (decomp.);

R_f 0.14 (10% EtOAc/pentane);

IR (thin film, ν_{max}/cm^{-1}) 2933, 2860, 1646, 1452, 1349, 1161, 909, 731;

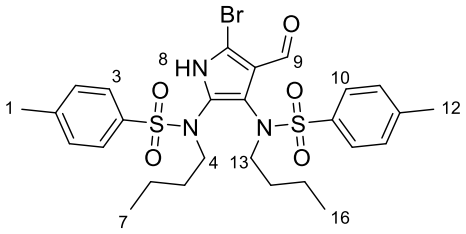
^{1}H NMR (500 MHz, $CDCl_3$) δ_C 8.19 (1H, s, H8), 7.70 (2H, d, *J* = 7.1 Hz, H11), 7.66 (2H, d, *J* = 8.2 Hz, H3), 7.54 (1H, t, *J* = 7.4 Hz, H13), 7.47 – 7.38 (4H, m, H12, H14), 7.29 (2H, d, *J* = 8.2 Hz, H2), 6.83 (2H, d, *J* = 8.1 Hz, H15), 4.01 (1H, tt, *J* = 11.6, 4.2 Hz, H4), 3.35 – 3.23 (2H, m, H17), 2.63 (1H, hept., *J* = 6.9 Hz, H9), 2.42 (3H, s, H1), 2.20 – 2.03 (5H, m, H5, H16), 1.92 – 1.78 (4H, m, H5, H6), 1.60 – 1.54 (1H, m, H7), 1.46 – 1.15 (5H, m, H6, H7, H18), 1.11 (3H, d, *J* = 6.9 Hz, H10), 1.02 – 0.94 (5H, m, H10, H19), 0.77 (3H, t, *J* = 7.3 Hz, H20);

^{13}C NMR (126 MHz, $CDCl_3$) δ_C 191.9, 144.2, 142.9, 140.0, 137.7, 137.1, 136.9, 132.5, 129.9, 129.8, 129.1, 128.2, 128.1, 127.7, 123.8, 120.2, 117.9, 65.8, 52.9, 33.1, 31.7, 31.1, 26.5 (2C), 26.1, 25.1, 23.9, 21.7, 21.5, 21.3, 20.2, 13.8; *Note: extra peaks are due to cyclohexyl and isopropyl groups being diastereotopic.*

HRMS (ESI) m/z: $[M + Na]^+$ Calcd for $C_{38}H_{47}N_3O_5NaS_2$ 712.2849; Found 712.2844.

7.4.7 Derivatizations of the 2,3-Diaminopyrroles

***N*,*N'*-(5-Bromo-4-formyl-1*H*-pyrrole-2,3-diyl)bis(*N*-butyl-4-methylbenzenesulfonamide), 91**



ZT432

Modified from a literature procedure.[126] To a stirred solution of *N*,*N'*-(4-formyl-1*H*-pyrrole-2,3-diyl)bis(*N*-butyl-4-methylbenzenesulfonamide) (55 mg, 0.10 mmol, 1.0 eq.) in HFIP (0.4 mL), NBS (20 mg, 0.11 mmol, 1.1 eq.) was added portion-wise. The reaction mixture was stirred at room temperature until completion by TLC (1 h). Upon completion, the reaction mixture was concentrated *in vacuo* and purified by column chromatography (silica gel, 20% → 30% → 40% Et_2O/pentane) to afford the title compound (36 mg, 58 μmol, 58%) as a yellow solid;

m.p. 91 °C;

R_f 0.26 (20% EtOAc/pentane);

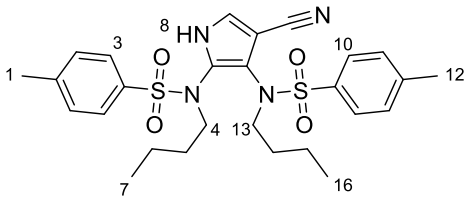
IR (thin film, ν_{max}/cm^{-1}) 3232, 2961, 1680, 1662, 1343, 1163, 1090, 910, 732;

^{1}H NMR (400 MHz, $CDCl_3$) δ_H 9.57 (1H, s, H8), 9.20 (1H, s, H9), 7.81 (2H, d, *J* = 8.2 Hz, H3), 7.53 (2H, d, *J* = 8.2 Hz, H10), 7.33 (2H, d, *J* = 8.2 Hz, H2), 7.24 (2H, d, *J* = 8.2 Hz, H11), 3.93 – 3.70 (2H, m, H4), 3.26 – 3.17 (2H, m, H13), 2.44 – 2.39 (6H, m, H1, H12), 1.65 (2H, app. quin., *J* = 7.6 Hz, H5), 1.36 – 1.26 (2H, m, H6), 1.19 – 1.09 (1H, m, H14), 1.07 – 0.94 (3H, m, H14, H15), 0.90 (3H, t, *J* = 7.4 Hz, H7), 0.71 (3H, t, *J* = 7.1 Hz, H16);

^{13}C NMR (101 MHz, $CDCl_3$) δ_C 183.3, 144.6, 143.9, 136.2, 135.8, 130.0, 129.5, 128.2, 127.9 (2C), 119.0, 118.0, 107.3, 51.6, 51.3, 31.8, 30.5, 21.7 (2C), 20.0, 19.8, 13.9, 13.7;

HRMS (ESI) m/z: $[M + H]^+$ Calcd for $C_{27}H_{35}N_3O_5{}^{79}BrS_2$ 624.1196; Found 624.1191.

***N,N'*-(4-cyano-1*H*-pyrrole-2,3-diyl)bis(*N*-butyl-4-methylbenzenesulfonamide), 93**



ZT439, ZT446

Step 1: To a vial equipped with a stirrer bar was added *N,N'*-(4formyl-1*H*-pyrrole-2,3-diyl)bis(*N*-butyl-4-methylbenzenesulfo-namide) (55 mg, 0.10 mmol, 1.0 eq.) and hydroxylamine hydrochloride (21 mg, 0.30 mmol, 3.0 eq.). EtOH (0.4 mL) was added to the vial and the resulting solution was refluxed at 80 °C for 4 h. The reaction mixture was then diluted with water and extracted three times with DCM. The organic phase was collected, washed with brine, and dried over Na_2SO_4. The solvent was removed *in vacuo* to afford the *N,N'*-(4-((hydroxyimino)methyl)-1*H*-pyrrole-2,3-diyl)bis(*N*-butyl-4-methyl-benzenesulfonamide) which was used in the next step without further purification.

Step 2: *Modified from a literature procedure.*[127] In a vial equipped with a stirrer bar, was dissolved cyanuric chloride (20 mg, 0.11 mmol, 1.1 eq.) in DMF (0.2 mL). The solution was stirred at room temperature until the disappearance of cyanuric chloride by TLC (overnight, 18 h). A solution of the oxime prepared in the previous step in DMF (0.2 mL) was then added and the reaction mixture was stirred at room temperature until completion by TLC. Upon completion, the reaction mixture was diluted with water and extracted three times with DCM. The organic phase was combined, washes with brine, and dried over Na_2SO_4. Column chromatography (silica gel, 20% → 40% EtOAc/pentane) afforded the title compound (30 mg, 55 μmol, 55%) as a brown solid;

m.p. 74 °C;

R_f 0.63 (40% EtOAc/pentane);

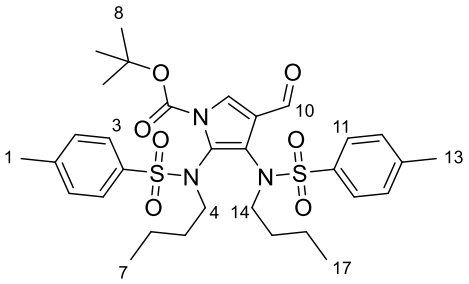
IR (thin film, ν_{max}/cm^{-1}) 3304, 2960, 2231, 1597, 1345, 1164, 1089, 910, 731, 665;

^{1}H NMR (400 MHz, $CDCl_3$) δ_H 9.50 (1H, s, H8), 7.74 (2H, d, *J* = 8.3 Hz, H3), 7.64 (2H, d, *J* = 8.3 Hz, H10), 7.33 – 7.27 (4H, m, H2, H11), 7.09 (1H, d, *J* = 3.5 Hz, H9), 3.92 – 3.83 (2H, m, H4), 3.30 – 3.13 (1H, brs, H13), 3.07 – 2.86 (1H, brs., H13), 2.42 (3H, s, H1), 2.40 (3H, s, H12), 1.61 (2H, app. quin., *J* = 7.7 Hz, H5), 1.37 – 1.27 (2H, m, H6), 1.12 – 0.94 (4H, m, H14, H15), 0.89 (3H, t, *J* = 7.4 Hz, H7), 0.70 (3H, t, *J* = 7.2 Hz, H16);

^{13}C NMR (101 MHz, $CDCl_3$) δ_C 144.6, 144.4, 136.3, 135.4, 130.0, 129.9, 128.3, 127.8, 125.7, 123.0, 118.6, 114.2, 93.2, 51.0, 50.7, 31.8, 30.1, 21.7, 21.7, 19.8, 19.7, 13.9, 13.6;

HRMS (ESI) m/z: $[M + H]^+$ Calcd for $C_{27}H_{35}N_4O_4S_2$ 543.2094; Found 543.2092.

***tert*-Butyl 2,3-bis((*N*-butyl-4-methylphenyl)sulfonamido)-4-formyl-1*H*-pyrrole-1-carboxylate, 88y**



ZT418

To a stirring solution of *N*,*N'*-(4-formyl-1*H*-pyrrole-2,3-diyl)bis(*N*-butyl-4-methylbenzenesulfonamide) (110 mg, 0.20 mmol, 1.0 eq.) and 4-dimethylaminopyridine (57 mg, 0.46 mmol, 2.3 eq.) in DCM (0.4 mL), a solution of di-*tert*-butyl dicarbonate (53 mg, 0.24 mmol, 1.2 eq.) in DCM (0.2 mL) was added slowly. The reaction mixture was stirred at room temperature until completion by TLC. Upon completion, the reaction was diluted with water and extracted twice with DCM. The organic phase was combined,

washed with brine, and dried over Na_2SO_4. Column chromatography (silica gel, 10% EtOAc/pentane) afforded the title compound (130 mg, 0.20 mmol, 100%) as a yellow oil;

R_f 0.35 (20% EtOAc/pentane);

IR (thin film, ν_{max}/cm^{-1}) 2980, 1772, 1690, 1345, 1159, 910, 732;

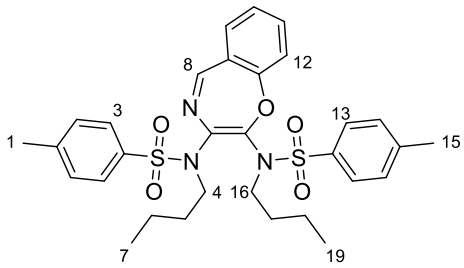
^{1}H NMR (500 MHz, $CDCl_3$) δ_H 9.13 (1H, s, H10), 7.85 (2H, d, *J* = 8.0 Hz, H3), 7.81 (1H, s, H9), 7.64 (2H, d, *J* = 8.3 Hz, H11), 7.33 – 7.27 (4H, m, H2, H12), 3.89 (1H, td, *J* = 12.4, 4.9 Hz, H4), 3.59 (1H, td, *J* = 12.4, 4.9 Hz, H4), 3.34 – 3.24 (2H, m, H14), 2.45 – 2.41 (6H, m, H1, H13), 1.87 – 1.76 (1H, m, H5), 1.75 – 1.66 (1H, m, H5), 1.61 (9H, s, H8), 1.25 (2H, app. sext., *J* = 7.4 Hz, H6), 1.12 – 0.93 (4H, m, H15, H16), 0.87 (3H, t, *J* = 7.4 Hz, H7), 0.69 (3H, t, *J* = 7.2 Hz, H17);

^{13}C NMR (126 MHz, $CDCl_3$) δ_C 184.2, 146.8, 144.0, 143.6, 138.3, 135.9, 129.7, 129.61, 129.58, 128.1, 127.8, 126.9, 123.5, 122.4, 87.1, 53.4, 51.5, 30.4, 29.7, 28.0, 21.8, 21.7, 20.3, 20.1, 14.0, 13.7;

HRMS (ESI) m/z: $[M + H]^+$ Calcd for $C_{32}H_{44}N_3O_7S_2$ 646.2615; Found 646.2613.

7.4.8 Gold-catalyzed Cyclisation of Yndiamides with Benzisoxazoles

***N*,*N'*-(Benzo[*f*][1,4]oxazepine-2,3-diyl)bis(*N*-butyl-4-methylbenzenesulfonamide), 98a**



ZT425

Synthesised from *N*,*N'*-(ethyne-1,2-diyl)bis(*N*-butyl-4-methylbenzenesulfonamide) (48 mg, 0.10 mmol, 1.0 eq.), benzo[d]isoxazole (20.5 μL, 0.20 mmol, 2.0 eq.), chloro[tris(2,4-di-

tert-butyl-phenyl)phosphite]gold(I) (4.4 mg, 5.0 μmol, 5 mol%) and silver bis(trifluoromethanesulfonyl)imide (2.0 mg, 5.2 μmol, 5 mol%) in DCE (anhy., 0.2 mL) with general procedure **7.2.3d** at room temperature for 2 h. Column chromatography (silica gel, 10% → 20% EtOAc/pentane) afforded the title compound (59 mg, 99 μmol, 98%) as a yellow solid;

m.p. 110 – 112 °C;

R_f 0.31 (20% EtOAc/pentane);

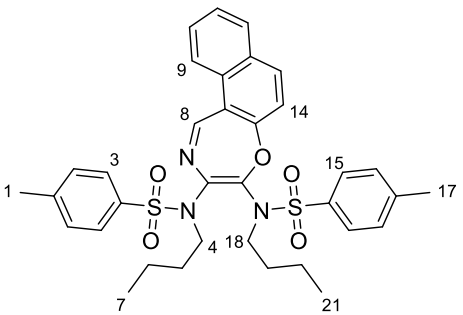
IR (thin film, ν_{max}/cm^{-1}) 2962, 2874, 1600, 1346, 1162, 1087, 1040, 814, 685, 658;

^{1}H NMR (400 MHz, C_6D_6) δ_H 8.30 (1H, s, H8), 8.15 (2H, d, *J* = 8.3 Hz, H13), 8.11 (2H, d, *J* = 8.3 Hz, H3), 6.93 – 6.82 (5H, m, H2, H9, H14), 6.83 – 6.76 (1H, m, H11), 6.69 (1H, app. t, *J* = 7.4 Hz, H10), 6.39 (1H, d, *J* = 8.1 Hz, H12), 4.25 – 3.85 (4H, m, H4, H16), 1.99 – 1.87 (8H, m, H1, H15, H17), 1.64 – 1.48 (2H, brs., H5), 1.32 – 1.22 (2H, m, H18), 1.15 – 1.05 (2H, m, H6), 0.79 (3H, t, *J* = 7.4 Hz, H19), 0.65 (3H, t, *J* = 7.3 Hz, H7);

^{13}C NMR (101 MHz, C_6D_6) δ_C 159.9, 159.1, 143.7, 143.2, 138.9, 138.4, 138.3, 133.6, 133.3, 129.6, 129.5, 129.4, 129.3, 129.2, 129.0, 125.5, 120.9, 51.0, 50.1, 31.1, 30.1, 21.2 (2C), 20.5, 20.2, 13.9, 13.8;

HRMS (ESI) m/z: $[M + H]^+$ Calcd for $C_{31}H_{38}N_3O_5S_2$ 596.2247; Found 596.2239.

***N*,*N'*-(Naphtho[1,2-*f*][1,4]oxazepine-3,4-diyl)bis(*N*-butyl-4-methylbenzenesulfonamide), *unstable*, 98b**



ZT481

Synthesised from *N*,*N'*-(ethyne-1,2-diyl)bis(*N*-butyl-4-methylbenzenesulfonamide) (48 mg, 0.10 mmol, 1.0 eq.), naphtho[1,2-*d*]isoxazole (34 mg, 0.20 mmol, 2.0 eq.), chloro[tris(2,4-di-*tert*-butylphenyl)phosphite]gold(I) (4.4 mg, 5.00 µmol, 5 mol%) and silver bis(trifluoromethanesulfonyl)imide (2.0 mg, 5.15 µmol**,** 5 mol%) in DCE (anhy., 0.2 mL) with general procedure **7.2.3d** at room temperature for 2 h. Upon completion, the reaction mixture was treated with HCl (1.0 M in Et_2O, 0.1 mL) for 30 min before it was concentrated *in vacuo* and purified by column chromatography (silica gel, 10% → 20% EtOAc/pentane) to afford the title compound (63 mg, 0.098 mmol, 97%) as a yellow oil.

R_f 0.34 (20% EtOAc/pentane);

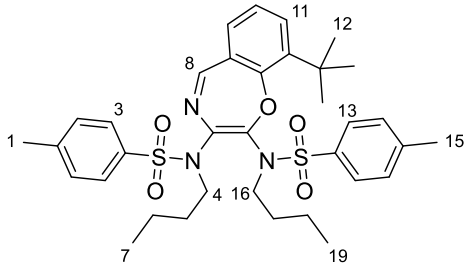
IR (thin film, ν_{max}/cm^{-1}) 2960, 2873, 1624, 1599, 1346, 1197, 1162, 1088, 1039, 816, 736, 663;

^{1}H NMR (400 MHz, $CDCl_3$) δ_H 9.14 (1H, s, H8), 8.09 (1H, d, *J* = 8.4 Hz, H9), 8.05 (2H, d, *J* = 8.3 Hz, H15), 7.87 – 7.83 (2H, m, H12, H13), 7.80 (2H, d, *J* = 8.3 Hz, H3), 7.67 (1H, app. t, *J* = 7.0 Hz, H10), 7.54 (1H, app. t, *J* = 7.5 Hz, H11), 7.41 (2H, d, *J* = 8.3 Hz, H16), 7.32 (2H, d, *J* = 8.3 Hz, H2), 6.46 (1H, d, *J* = 8.8 Hz, H14), 3.72 – 3.56 (4H, m, H4, H18), 2.51 (3H, s, H17), 2.46 (3H, s, H1), 1.79 – 1.63 (2H, m, H19), 1.36 – 1.20 (4H, m, H5, H20), 1.05 (2H, app. sext., *J* = 7.3 Hz, H6), 0.86 (3H, t, *J* = 7.4 Hz, H21), 0.64 (3H, t, *J* = 7.3 Hz, H20);

^{13}C NMR (101 MHz, $CDCl_3$) δ_C 159.5, 158.2, 144.2, 143.6, 137.7, 137.7, 137.0, 134.8, 133.4, 131.2, 131.1, 129.6, 129.4, 129.0, 128.68, 128.65, 128.63, 126.3, 122.8, 120.9, 120.0, 50.9, 49.8, 30.4, 29.7, 21.8, 21.7, 20.3, 19.9, 13.8, 13.6;

HRMS (ESI) m/z: $[M + H]^+$ Calcd for $C_{35}H_{40}N_3O_5S_2$ 646.2404; Found 646.2399.

***N,N'*-(9-(tert-Butyl)benzo[*f*][1,4]oxazepine-2,3-diyl)bis(*N*-butyl-4-methylbenzenesulfonamide), 98c**



ZT485

Synthesised from *N,N'*-(ethyne-1,2-diyl)bis(*N*-butyl-4-methylbenzenesulfonamide) (48 mg, 0.10 mmol, 1.0 eq.), 7-(*tert*-butyl)benzo[*d*]isoxazole (36 mg, 0.21 mmol, 2.0 eq.), chloro[tris(2,4-di-*tert*-butylphenyl)phosphite]gold(I) (4.4 mg, 5.00 µmol, 5 mol%) and silver bis(trifluoromethanesulfonyl)imide (2.0 mg, 5.15 µmol**,** 5 mol%) in DCE (anhy., 0.2 mL) with general procedure **7.2.3d** at room temperature for 2 h. Column chromatography (silica gel, 10% EtOAc/pentane) afforded the title compound (60 mg, 0.092 mmol, 91%) as a yellow oil;

R_f 0.16 (10% EtOAc/pentane);

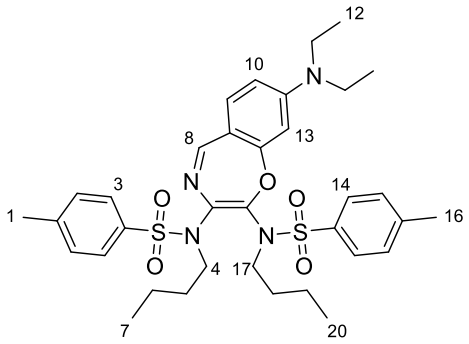
IR (thin film, ν_{max}/cm^{-1}) 2961, 2874, 1626, 1345, 1163, 1087, 909, 731, 658;

^{1}H NMR (400 MHz, $CDCl_3$) δ_H 8.22 (1H, s, H8), 7.92 (2H, d, *J* = 8.3 Hz, H13), 7.80 (2H, d, *J* = 8.3 Hz, H3), 7.46 (1H, dd, *J* = 7.2, 2.4 Hz, H9), 7.38 – 7.31 (4H, m, H2, H14), 7.22 – 7.12 (2H, m, H10, H11), 3.73 – 3.63 (1H, m, H16), 3.59 – 3.48 (1H, m, H16), 3.47 – 3.34 (2H, m, H4), 2.48 (3H, s, H15), 2.47 (3H, s, H1), 1.90 – 1.71 (3H, m, H5, H17), 1.52 – 1.39 (1H, m, H17), 1.34 – 1.25 (2H, m, H18), 1.23 – 1.11 (11H, m, H6, H12), 0.92 – 0.77 (6H, m, H7, H19);

^{13}C NMR (101 MHz, $CDCl_3$) δ_C 163.2, 163.1, 143.7, 143.6, 141.4, 139.6, 137.6, 137.5, 136.4, 131.7, 129.7, 129.3, 129.0, 128.6, 128.3, 128.1, 125.0, 52.5, 50.6, 35.1, 31.0, 30.2, 29.1, 21.71, 21.68, 20.4 (2C), 13.8 (2C);

HRMS (ESI) m/z: $[M + H]^+$ Calcd for $C_{35}H_{46}N_3O_5S_2$ 652.2873; Found 652.2874.

***N*,*N'*-(8-(Diethylamino)benzo[*f*][1,4]oxazepine-2,3-diyl)bis(*N*-butyl-4-methylbenzenesulfonamide), 98d**



ZT483

Synthesised from *N*,*N'*-(ethyne-1,2-diyl)bis(*N*-butyl-4-methylbenzenesulfonamide) (48 mg, 0.10 mmol, 1.0 eq.), *N*,*N*-diethylbenzo[*d*]isoxazol-6-amine (39 mg, 0.21 mmol, 2.0 eq.), chloro[tris(2,4-di-*tert*-butylphenyl)phosphite]gold(I) (4.4 mg, 5.00 µmol, 5 mol%) and silver bis(trifluoromethanesulfonyl)imide (2.0 mg, 5.15 µmol**,** 5 mol%) in DCE (anhy., 0.2 mL) with general procedure **7.2.3d** at room temperature for 2 h. Column chromatography (silica gel, 10% → 20% EtOAc/pentane) afforded the title compound (53 mg, 0.079 mmol, 79%) as a yellow solid;

m.p. 159 °C (decomp.);

R_f 0.16 (20% EtOAc/pentane);

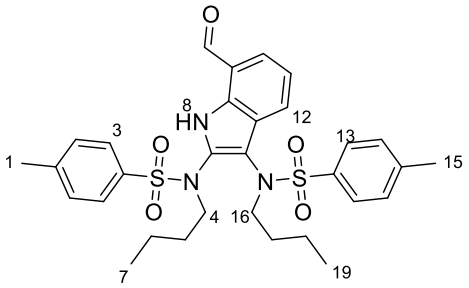
IR (thin film, ν_{max}/cm^{-1}) 2963, 1615, 1575, 1519, 1344, 1155, 1116, 1087, 910, 732, 665;

^{1}H NMR (400 MHz, $CDCl_3$) δ_H 8.20 (1H, s, H8), 8.04 (2H, d, *J* = 8.3 Hz, H14), 7.88 (2H, d, *J* = 8.3 Hz, H3), 7.37 (2H, d, *J* = 8.3 Hz, H15), 7.29 (2H, d, *J* = 8.3 Hz, H2), 7.18 (1H, d, *J* = 8.8 Hz, H9), 6.41 (1H, dd, *J* = 8.8, 2.4 Hz, H10), 5.25 (1H, d, *J* = 2.4 Hz, H13), 3.75 (2H, brs., H17), 3.61 (2H, brs., H4), 3.17 (4H, q, *J* = 7.0 Hz, H11), 2.45 (3H, s, H16), 2.42 (3H, s, H1), 1.64 (2H, brs., H18), 1.32 – 1.14 (4H, m, H5, H19), 1.11 – 0.97 (8H, m, H6, H12), 0.84 (3H, t, *J* = 7.3 Hz, H20), 0.62 (3H, t, *J* = 7.2 Hz, H7);

^{13}C NMR (101 MHz, $CDCl_3$) δ_C 160.1, 159.2, 152.5, 143.4, 143.2, 138.8, 137.7, 135.2, 132.6, 131.7, 129.3, 129.2, 128.8, 128.7, 115.8, 108.2, 101.7, 50.7, 49.6, 44.6, 30.9, 29.5, 21.70, 21.68, 20.2, 20.0, 13.8, 13.7, 12.5;

HRMS (ESI) m/z: $[M + H]^+$ Calcd for $C_{35}H_{47}N_4O_5S_2$ 667.2982; Found 667.2981.

***N,N'*-(7-Formyl-1*H*-indole-2,3-diyl)bis(*N*-butyl-4-methylbenzenesulfonamide), 102**



ZT423

Synthesised from *N*-butyl-*N*-(((*N*-cyclohexyl-4-methylphenyl)sulfonamido)ethynyl)-4-methylbenzenesulfonamide (50 mg, 0.10 mmol, 1.0 eq.), anthranil (20.3 μL, 0.20 mmol, 2.0 eq.), chloro[tris(2,4-di-*tert*-butyl-phenyl)phosphite]gold(I) (4.4 mg, 5.0 μmol, 5 mol%) and silver bis(trifluoromethanesulfonyl)imide (2.0 mg, 5.2 μmol, 5 mol%) in DCE (anhy., 0.2 mL) with general procedure **7.2.3d** at room temperature for 2 h. Column chromatography (silica gel, 10% → 20% EtOAc/pentane) afforded the title compound (59 mg, 99 μmol, 98%) as a yellow solid;

m.p. 73 °C ($CHCl_3$);

R_f 0.28 (20% EtOAc/pentane);

IR (thin film, ν_{max}/cm^{-1}) 3420, 2962, 1673, 1344, 1163, 909, 730, 664;

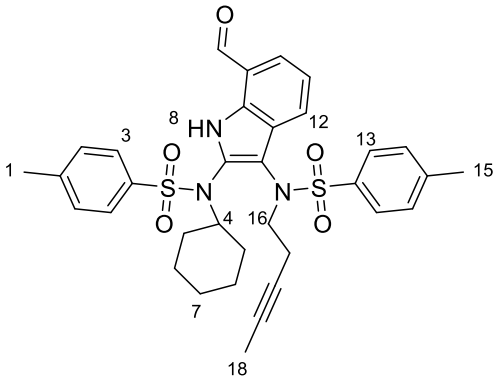
^{1}H NMR (400 MHz, $CDCl_3$) δ_H 10.20 (1H, s, H8), 10.09 (1H, s, H9), 7.78 (2H, d, *J* = 8.2 Hz, H3), 7.66 – 7.57 (3H, m, H12, H13), 7.33 (2H, d, *J* = 8.2 Hz, H2), 7.24 (2H, d, *J* = 8.0 Hz, H14), 7.12 – 7.02 (2H, m, H10, H11), 3.90 – 3.66 (2H, m, H4), 3.61 – 3.48 (1H, m, H16), 3.45 – 3.31 (1H, m, H16), 2.46 – 2.40 (6H, m, H1, H15), 1.56 – 1.43 (2H, m, H5),

1.38 – 1.28 (2H, m, H17), 1.28 – 1.18 (2H, m, H6), 1.16 – 1.05 (2H, m, H18), 0.84 (3H, t, *J* = 7.4 Hz, H7), 0.76 (3H, t, *J* = 7.3 Hz, H19);

^{13}C NMR (101 MHz, $CDCl_3$) δ_C 193.3, 144.5, 143.8, 137.5, 137.0, 132.5, 130.1, 129.7, 129.5, 129.2, 128.0, 127.7, 126.6, 125.9, 120.3, 120.1, 111.4, 51.8, 51.1, 31.4, 30.8, 21.70, 21.66, 19.9, 19.8, 13.8, 13.7;

HRMS (ESI) m/z: $[M + H]^+$ Calcd for $C_{31}H_{38}N_3O_5S_2$ 596.2247; Found 596.2250.

_N_-Cyclohexyl-_N_-(7-formyl-3-((4-methyl-_N_-(pent-3-yn-1-yl)phenyl)sulfonamido)-1_H_-indol-2-yl)-4-methylbenzenesulfonamide, 107



ZT510

Synthesised from *N*-cyclohexyl-4-methyl-*N*-(((4-methyl-*N*-(pent-3-yn-1-yl)phenyl)sulfonamido)ethynyl)benzenesulfonamide (52 mg, 0.10 mmol, 1.0 eq.), benzo[*c*]isoxazole (20 µmol, 0.20 mmol, 2.0 eq.), chloro[tris(2,4-di-*tert*-butylphenyl)phosphite]gold(I) (4.4 mg, 5.00 µmol, 5 mol%) and silver bis(trifluoromethanesulfonyl)imide (2.0 mg, 5.15 µmol**,** 5 mol%) in DCE (anhy., 0.2 mL) with general procedure **7.2.3d**. at room temperature for 18 h. Column chromatography (silica gel, 10% → 20% EtOAc/pentane) afforded the title compound (43 mg, 0.068 mmol, 67%) as a yellow oil;

R_f 0.21 (20% EtOAc/pentane);

IR (thin film, ν_{max}/cm^{-1}) 3422, 2933, 2857, 1672, 1347, 1160, 910, 731, 664;

^{1}H NMR (500 MHz, $CDCl_3$) δ_H 10.07 (1H, s, H9), 9.79 (1H, s, H8), 7.82 (2H, d, *J* = 8.3 Hz, H13), 7.79 (2H, d, *J* = 8.3 Hz, H3), 7.65 (1H, dd, *J* = 7.4, 1.0 Hz, H10), 7.37 (2H, d, *J* = 8.3 Hz, H2), 7.35 – 7.30 (3H, m, H12, H14), 7.12 (1H, app. t, *J* = 7.7 Hz, H11), 3.92 – 3.85 (1H, m, H4), 3.84 – 3.79 (2H, m, H16), 2.48 (3H, s, H1), 2.47 (3H, s, H15), 2.38 – 2.29 (1H, m, H17), 2.27 – 2.18 (1H, m, H17), 2.16 – 2.09 (1H, m, H5), 1.92 – 1.68 (4H, m, H5, H6), 1.60 (3H, t, *J* = 2.5 Hz, H18), 1.56 – 1.45 (2H, m, H5, H7), 1.33 – 1.18 (2H, m, H6), 1.11 – 0.98 (1H, m, H7);

^{13}C NMR (126 MHz, $CDCl_3$) δ_C 193.4, 144.6, 143.9, 137.9, 137.4, 131.0, 130.31, 130.1, 129.8, 129.7, 129.3, 128.3, 127.7, 127.5, 126.0, 120.22, 120.19, 115.0, 76.1, 63.5, 51.0, 33.2, 31.7, 26.4, 26.2, 24.9, 21.8, 21.7, 19.0, 3.6;

HRMS (ESI) m/z: $[M + H]^+$ Calcd for $C_{34}H_{38}N_3O_5S_2$ 632.2247; Found 632.2257.

7.4.9 X-Ray Crystallography

Single crystal X-ray diffraction data were collected using a (Rigaku) Oxford Diffraction SuperNova A diffractometer and reduced using CrysAlisPro. Structures were solved using Super-Flip[239] and refined using CRYSTALS[240, 241]. Data for **88n** and **89** are deposited with the CCDC: CCDC 2213976 and CCDC 2213977.

Table 7.01 Crystal data and structure refinement for **88n.**

CCDC Identification code	CCDC 2213976
Empirical formula	C39 H43 N3 O5 S2
Formula weight	697.92
Temperature	150 K
Wavelength	1.54184 Å
Crystal system	Triclinic
Space group	P -1

Unit cell dimensions	a = 9.7137(2) Å	α= 107.043(3)°.
	b = 11.0676(4) Å	β= 99.017(2)°.
	c = 17.5505(5) Å	γ = 90.606(2)°.
Volume	1778.46(10) $Å^3$	
Z	2	
Density (calculated)	1.303 Mg/m^3	
Absorption coefficient	1.745 mm^{-1}	
F(000)	740	
Crystal size	0.18 x 0.17 x 0.10 mm^3	
Theta range for data collection	4.186 to 76.220°.	
Index ranges	-12<=h<=12, -13<=k<=11, -22<=l<=22	
Reflections collected	43066	
Independent reflections	7365 [R(int) = 0.030]	
Completeness to theta = 73.933°	99.8 %	
Absorption correction	Semi-empirical from equivalents	
Max. and min. transmission	0.84 and 0.67	
Refinement method	Full-matrix least-squares on F2	
Data / restraints / parameters	7365 / 0 / 442	
Goodness-of-fit on F2	0.9916	
Final R indices [I>2sigma(I)]	R1 = 0.0330, wR2 = 0.0895	
R indices (all data)	R1 = 0.0363, wR2 = 0.0927	
Largest diff. peak and hole	0.62 and -0.43 $e.Å^{-3}$	

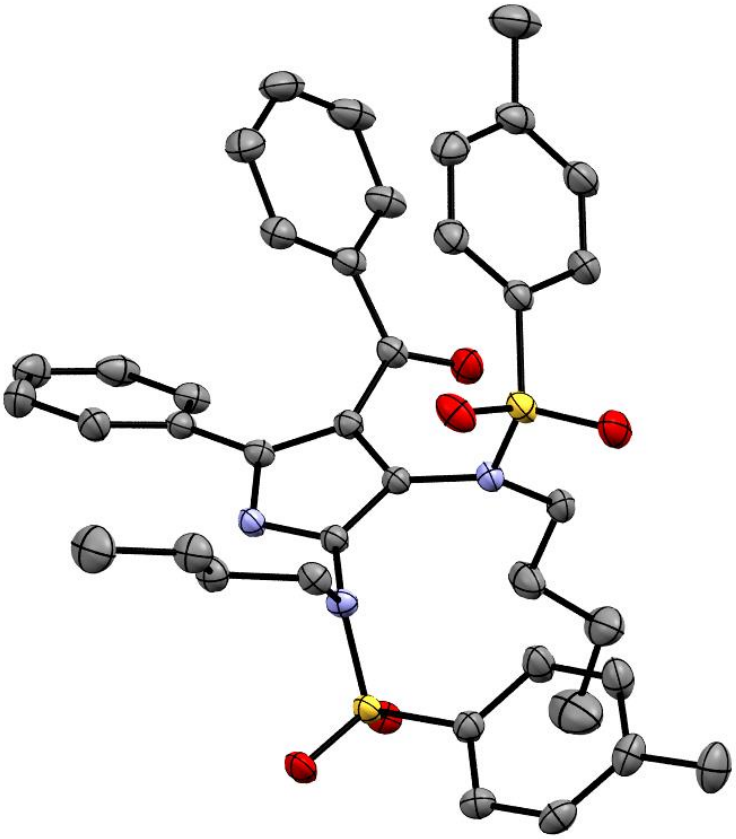


Figure 7.13 The structure of **88n** determined from X-ray diffraction studies, displacement ellipsoids are drawn at 50% probability and hydrogen atoms are omitted for clarity.

Table 7.02 Crystal data and structure refinement for **89.**

CCDC Identification code	CCDC 2213977	
Empirical formula	C27 H35 N3 O5 S2 (C6 H6)	
Formula weight	623.83	
Temperature	150 K	
Wavelength	1.54180 Å	
Crystal system	Triclinic	
Space group	P -1	
Unit cell dimensions	a = 9.2395(2) Å	α= 93.824(2)°.
	b = 13.2474(4) Å	β= 96.199(2)°.
	c = 13.6052(4) Å	γ = 95.206(2)°.
Volume	1543.77(8) $Å^3$	

Z	2
Density (calculated)	1.260 Mg/m^3
Absorption coefficient	1.822 mm^{-1}
F(000)	664
Crystal size	0.04 x 0.18 x 0.30 mm^3
Theta range for data collection	3.277 to 76.267°.
Index ranges	-11<=h<=11, -16<=k<=16, -18<=l<=16.
Reflections collected	38196
Independent reflections	6825 [R(int) = 0.0307]
Completeness to theta = 76.276°	98.9 %
Absorption correction	Semi-empirical from equivalents
Max. and min. transmission	0.93 and 0.75
Refinement method	Full-matrix least-squares on F2
Data / restraints / parameters	6825 / 11 / 401
Goodness-of-fit on F2	0.9958
Final R indices [I>2sigma(I)]	R1 = 0.0307, wR2 = 0.0819
R indices (all data)	R1 = 0.0327, wR2 = 0.0844
Largest diff. peak and hole	0.93 and -0.34 $e.Å^{-3}$

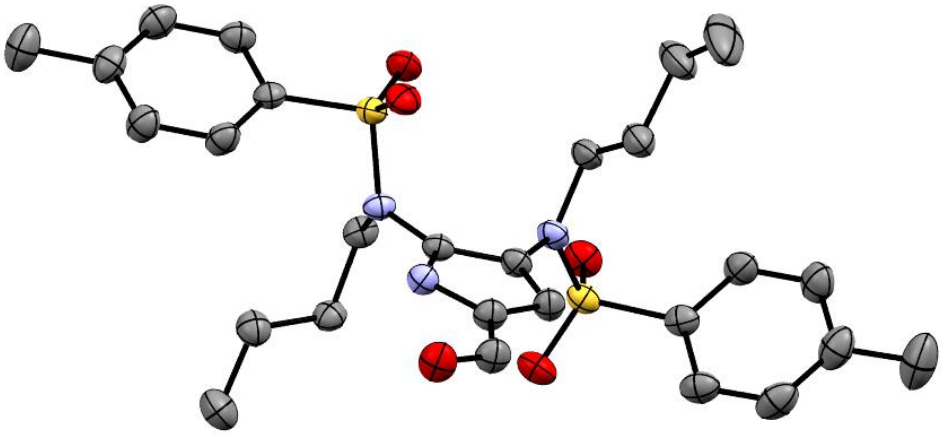


Figure 7.14 The structure of **89** determined from X-ray diffraction studies, displacement ellipsoids are drawn at 50% probability, and hydrogen atoms and residual solvent are omitted for clarity.

7.5 Chapter IV Computational Details

7.5.1 Computational Methods

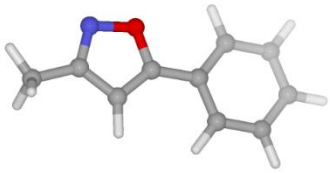
The authors would like to acknowledge the use of the University of Oxford Advanced Research Computing (ARC) facility in carrying out this work. http://dx.doi.org/10.5281/zenodo.22558. All DFT calculations were carried out using the Gaussian 16 program[242] and ORCA (v 5.0.3)[243]. Geometry optimisation of all structures was carried out using the Gaussian 16 program without any constraints of freedom. Each stationary point was confirmed to be either a local minimum or a transition state by vibrational frequency calculations. Domain-based local pair natural orbital coupled cluster theory with single, double, and perturbative triple excitations (DLPNO-CCSD(T))[155] calculations were performed using the ORCA (v 5.0.3) program and def2-TZVPP basis

set[156] for all atoms using 'Tight' convergence criteria. In the geometry optimisation, the IEFPCM method,[244] which is the default SCRF method built in the Gaussian 16 program package, was used to model the solvent effects of 1,2-dichloroethane. For the DLPNO-CCSD(T) calculations, the CPCM method[157] was used to simulate the solvent effects with 1,2-dichloroethane (ε = 10.36) as solvent. Natural Bond Orbital (NBO) analysis was performed using the NBO (version 3)[245] analysis module implemented in Gaussian 16 program package.

7.5.2 Cartesian Coordinates and Energy Data of All Computed Structures

7.5.2a Benchmark Structures

3Me5PhIsoxazole-M06-Opt



C 0.57204700 -0.05351400 -0.00000700
O 1.14172100 -1.27517700 0.00020400
C 2.76058800 0.15332000 -0.00000500
C 1.55198900 0.89650700 -0.00013300
N 2.52656600 -1.14166500 0.00020300
H 1.44496100 1.97404100 -0.00044300
C -0.88332800 0.01096900 -0.00001100
C -1.65719700 -1.15635300 -0.00015800
C -1.52283800 1.25739500 0.00012600
C -3.04540000 -1.07405100 -0.00014800
H -1.16823700 -2.12847400 -0.00027500
C -2.90979200 1.33426200 0.00012100
H -0.93131200 2.17198400 0.00025100
C -3.67568100 0.16874000 -0.00001300
H -3.63814200 -1.98705900 -0.00025400
H -3.39587000 2.30819900 0.00023600
H -4.76252600 0.23001300 -0.00000900
C 4.15579100 0.66530600 -0.00012500
H 4.86950100 -0.16507500 -0.00005200
H 4.34239600 1.28688100 -0.88416600
H 4.34241800 1.28707600 0.88377000

IEFPCM(1,2-dichloroethane)-M06/6-31+G(d):

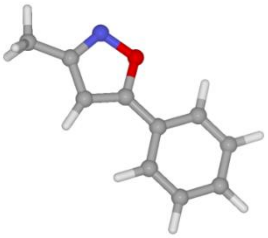
Zero-point correction =	0.166344 (Hartree/Particle)
Thermal correction to Energy =	0.176196
Thermal correction to Enthalpy =	0.177140
Thermal correction to Gibbs Free Energy =	0.130011
Sum of electronic and zero-point Energies =	-515.907996
Sum of electronic and thermal Energies =	-515.898144
Sum of electronic and thermal Enthalpies =	-515.897200
Sum of electronic and thermal Free Energies =	-515.944329
Electronic Energy =	-516.074340

IEFPCM(1,2-dichloroethane)-[Functional]/[Basis Set]//IEFPCM(1,2-dichloroethane)-M06/6-31+G(d):

Electronic Energy (M06-L/6-31+G(d)) =	-516.372414

Electronic Energy (B2PLYPD3/6-31+G(d)) =	-515.371329
Electronic Energy (MP2/6-31+G(d)) =	-514.836128
Electronic Energy (PBE/6-31+G(d)) =	-515.814455
Electronic Energy (PBE0/6-31+G(d)) =	-515.541724
Electronic Energy (TPSS/6-31+G(d)) =	-516.538351
Electronic Energy (DLPNO-CCSD(T)/def2-TZVPP) =	-515.522300

3Me5PhIsoxazole-M06L-Opt

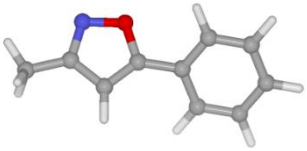


C -0.56894600 -0.05261700 -0.00000700	C 2.91371600 1.33517400 -0.00009000
O -1.13840500 -1.28164000 -0.00009900	H 0.93466100 2.17432500 -0.00016600
C -2.76407700 0.15719500 0.00003300	C 3.68014600 0.16863100 -0.00000800
C -1.55602000 0.89534000 0.00007300	H 3.63970500 -1.98801600 0.00013400
N -2.53573800 -1.14463700 -0.00004900	H 3.39998300 2.30873100 -0.00015500
H -1.44557700 1.97190900 0.00016400	H 4.76671600 0.22937700 -0.00000600
C 0.88196600 0.01236100 -0.00001200	C -4.15917100 0.66760200 0.00008700
C 1.65935000 -1.15650300 0.00006800	H -4.87507600 -0.15875700 0.00008100
C 1.52599300 1.26009600 -0.00009400	H -4.34848000 1.29000100 0.88163000
C 3.04784900 -1.07471900 0.00007000	H -4.34852900 1.29005400 -0.88140700
H 1.16916600 -2.12740000 0.00013400	

IEFPCM(1,2-dichloroethane)-M06L/6-31+G(d):

Zero-point correction =	0.166681 (Hartree/Particle)
Thermal correction to Energy =	0.176514
Thermal correction to Enthalpy =	0.177458
Thermal correction to Gibbs Free Energy =	0.130487
Sum of electronic and zero-point Energies =	-516.205946
Sum of electronic and thermal Energies =	-516.196113
Sum of electronic and thermal Enthalpies =	-516.195169
Sum of electronic and thermal Free Energies =	-516.242140

3Me5PhIsoxazole-MP2-Opt

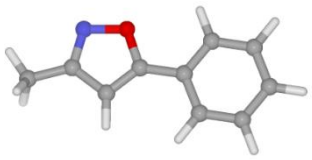


C 0.56905000 -0.03218000 -0.02005300	C -2.94073600 1.29961300 -0.21213800
O 1.13956700 -1.20974300 -0.41968900	H -0.96525200 2.12965900 -0.48439000
C 2.77385400 0.15393600 0.05560100	C -3.69076800 0.14705600 0.05252100
C 1.56382800 0.85818500 0.28955700	H -3.61628500 -1.96561700 0.50001300
N 2.53111600 -1.08575000 -0.36502100	H -3.44366500 2.24473200 -0.40584900
H 1.44957700 1.86905900 0.65918200	H -4.77730300 0.19625300 0.07435200
C -0.89015200 0.02009400 -0.00209200	C 4.17986900 0.62612100 0.23663600
C -1.64206300 -1.13608000 0.27091900	H 4.87938100 -0.16527800 -0.04403000
C -1.54559800 1.23819600 -0.25290400	H 4.37412500 1.50456900 -0.38579700
C -3.03763500 -1.06858000 0.28964900	H 4.36201900 0.90354600 1.27913700
H -1.13483100 -2.07689100 0.47386400	

IEFPCM(1,2-dichloroethane)-MP2/6-31+G(d):

Zero-point correction =	0.166759 (Hartree/Particle)
Thermal correction to Energy =	0.176910
Thermal correction to Enthalpy =	0.177854
Thermal correction to Gibbs Free Energy =	0.130208
Sum of electronic and zero-point Energies =	-514.671322
Sum of electronic and thermal Energies =	-514.661172
Sum of electronic and thermal Enthalpies =	-514.660228
Sum of electronic and thermal Free Energies =	-514.707874

3Me5PhIsoxazole-PBE-Opt

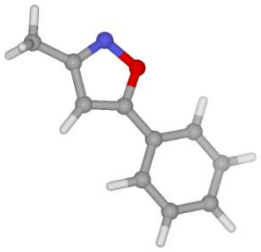


C 0.57243800 -0.05039100 0.00001100	C -2.93897200 1.34309300 0.00025700
O 1.14813300 -1.29102400 0.00044700	H -0.95084200 2.19257100 0.00058600
C 2.78698700 0.15789700 -0.00006100	C -3.71007200 0.16750500 -0.00005500
C 1.57012000 0.90230600 -0.00034000	H -3.66333700 -2.00392900 -0.00057900
N 2.55449400 -1.15280400 0.00042300	H -3.42891200 2.32240700 0.00048700
H 1.46286700 1.98552900 -0.00084200	H -4.80346200 0.22691900 -0.00007900
C -0.88915100 0.01481000 0.00000700	C 4.19430800 0.67213300 -0.00025200
C -1.67128200 -1.16357200 -0.00030600	H 4.91156400 -0.16354200 0.00012800
C -1.54070100 1.27030400 0.00029600	H 4.38234300 1.29678500 -0.89043600
C -3.07024600 -1.08336200 -0.00033200	H 4.38235000 1.29755700 0.88939200
H -1.17965700 -2.14082000 -0.00055000	

IEFPCM(1,2-dichloroethane)-PBE/6-31+G(d):

Zero-point correction =	0.162240 (Hartree/Particle)
Thermal correction to Energy =	0.172366
Thermal correction to Enthalpy =	0.173310
Thermal correction to Gibbs Free Energy =	0.125481
Sum of electronic and zero-point Energies =	-515.654456
Sum of electronic and thermal Energies =	-515.644331
Sum of electronic and thermal Enthalpies =	-515.643387
Sum of electronic and thermal Free Energies =	-515.691216

3Me5PhIsoxazole-PBE/def2-TZVPP-Opt



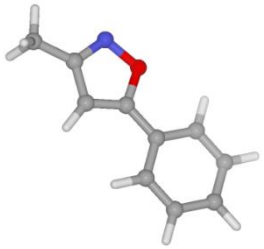
C 0.57103300 -0.05410800 -0.00014500	C -3.05913600 -1.07628200 0.00023700
O 1.14537100 -1.28829300 -0.00030200	H -1.17870900 -2.13195100 0.00020000
C 2.77583200 0.15724100 0.00006000	C -2.92492600 1.33767700 -0.00008700
C 1.56176700 0.89678300 0.00008000	H -0.94437000 2.18032000 -0.00039700
N 2.54550700 -1.14637400 -0.00016600	C -3.69379200 0.16912300 0.00013900
H 1.45084200 1.97486100 0.00002300	H -3.65188300 -1.99179400 0.00041300
C -0.88620500 0.01306000 -0.00008600	H -3.41222400 2.31335000 -0.00016700
C -1.66731500 -1.15808900 0.00011400	H -4.78262500 0.22979400 0.00022900
C -1.53390800 1.26307100 -0.00020200	C 4.17702700 0.67217000 0.00027500

H 4.89164300 -0.15900100 -0.00033300
H 4.36185800 1.29518800 0.88624700
H 4.36169200 1.29631100 -0.88495400

IEFPCM(1,2-dichloroethane)-PBE/def2-TZVPP:

Zero-point correction =	0.161736 (Hartree/Particle)
Thermal correction to Energy =	0.171828
Thermal correction to Enthalpy =	0.172773
Thermal correction to Gibbs Free Energy =	0.125005
Sum of electronic and zero-point Energies =	-515.824875
Sum of electronic and thermal Energies =	-515.814783
Sum of electronic and thermal Enthalpies =	-515.813839
Sum of electronic and thermal Free Energies =	-515.861607

3Me5PhIsoxazole-TPSS-Opt

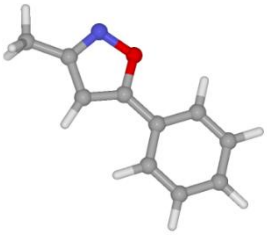


C -0.57115800 -0.04705200 -0.00001600
C 2.94075700 1.34109700 -0.00009800
O -1.14359200 -1.29028300 -0.00012800
H 0.95825100 2.18922900 -0.00020600
C -2.78606200 0.15752700 0.00003700
C 3.70901200 0.16496200 0.00000900
C -1.56983900 0.90114900 0.00009100
H 3.65644500 -2.00050200 0.00018600
N -2.55948900 -1.15205100 -0.00011400
H 3.42999600 2.31420600 -0.00017500
H -1.46408500 1.97881000 0.00021300
H 4.79663200 0.22227600 0.00001800
C 0.89088000 0.01716700 -0.00001400
C -4.19797600 0.67210100 0.00011300
C 1.66985200 -1.16189300 0.00009100
H -4.90791000 -0.16232300 0.00007500
C 1.54341000 1.27094700 -0.00011200
H -4.38144300 1.29285200 0.88704800
C 3.06782100 -1.08404000 0.00010200
H -4.38149200 1.29297400 -0.88672600
H 1.17858900 -2.13269700 0.00017000

IEFPCM(1,2-dichloroethane)-TPSS/6-31+G(d):

Zero-point correction =	0.164270 (Hartree/Particle)
Thermal correction to Energy =	0.174324
Thermal correction to Enthalpy =	0.175268
Thermal correction to Gibbs Free Energy =	0.127604
Sum of electronic and zero-point Energies =	-516.376157
Sum of electronic and thermal Energies =	-516.366103
Sum of electronic and thermal Enthalpies =	-516.365158
Sum of electronic and thermal Free Energies =	-516.412822

3Me5PhIsoxazole-M06/def2-TZVPP-Opt



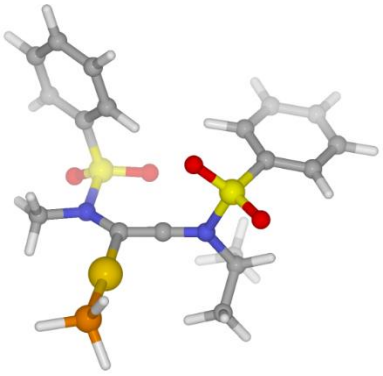
C 0.57159200 -0.05628100 -0.00003900
N 2.51450500 -1.13396400 0.00015700
O 1.13910800 -1.27014500 0.00014000
H 1.43258500 1.96162800 -0.00040800
C 2.74901900 0.15238100 -0.00002400
C -0.87981500 0.01022000 -0.00002900
C 1.54400700 0.89145500 -0.00017500
C -1.65246100 -1.14941300 -0.00013300

C -1.51738300 1.24972000 0.00008100
C -3.03282600 -1.06693100 -0.00008900
H -1.16724700 -2.11630000 -0.00024200
C -2.89635200 1.32708100 0.00011000
H -0.92830700 2.15822900 0.00014000
C -3.65893000 0.16891200 0.00003000
H -3.62319200 -1.97412000 -0.00016800
H -3.37958400 2.29552600 0.00021000
H -4.73953000 0.23053100 0.00006400
C 4.13912000 0.66307700 -0.00004300
H 4.84819400 -0.16239100 -0.00054500
H 4.32325400 1.28274900 -0.87789100
H 4.32360500 1.28172700 0.87848400

IEFPCM(1,2-dichloroethane)-M06/def2-TZVPP:

Zero-point correction =	0.166538 (Hartree/Particle)
Thermal correction to Energy =	0.176310
Thermal correction to Enthalpy =	0.177254
Thermal correction to Gibbs Free Energy =	0.130276
Sum of electronic and zero-point Energies =	-516.078137
Sum of electronic and thermal Energies =	-516.068365
Sum of electronic and thermal Enthalpies =	-516.067421
Sum of electronic and thermal Free Energies =	-516.114399

Int1major-M06-Opt



C 0.01334800 -0.62083300 0.73190300
C 0.92751700 0.30008400 0.74551200
N -0.75250900 -1.60626000 0.48336000
N 0.89332100 1.58908800 1.18175000
S -1.48456700 -1.74157800 -1.15374100
O -1.02034000 -0.55144900 -1.84723800
O -1.13844900 -3.07641500 -1.61703100
S -0.62530300 2.33183300 1.47680100
O -1.57901200 1.22620300 1.44385500
O -0.48414400 3.15911900 2.66542100
C -0.85498500 3.37941700 0.06684600
C -0.83098300 4.76116000 0.23424300
C -1.02394500 2.77975600 -1.18210500
C -0.99980100 5.56741500 -0.88877600
H -0.68907300 5.19142700 1.22340800
C -1.18799400 3.60061500 -2.29151800
H -1.02172400 1.69433800 -1.29305200
C -1.17811100 4.98856300 -2.14345600
H -0.99069500 6.64984800 -0.78053400
H -1.32374300 3.15524300 -3.27479800
C -3.20635800 -1.63961800 -0.79278700
C -3.96456800 -2.80926000 -0.78128300
C -3.74315700 -0.39022700 -0.48076500
C -5.31072100 -2.71663800 -0.44275400
H -3.51140400 -3.76437000 -1.03921600
C -5.08885400 -0.32004800 -0.14265000
H -3.12011500 0.50235600 -0.48869800
C -5.86621000 -1.47887400 -0.12198200
H -5.92574900 -3.61365400 -0.43119100
H -5.53198300 0.64181800 0.10534900
C -1.04908800 -2.70640200 1.47084600
C 0.25232000 -3.37214800 1.86350000
C -1.81892000 -2.12190100 2.63673400
H -1.67498000 -3.42247200 0.92194600
H 0.90846000 -2.66397200 2.38854900
H 0.78107700 -3.75757500 0.98220000
H -1.21882900 -1.35691300 3.14847400
H -2.75931900 -1.66015800 2.30795300
C 2.05257800 2.47629400 1.04974600
H 1.85766900 3.40272300 1.59804800
H 2.25171500 2.70566100 -0.00529300
H -6.91907500 -1.41504500 0.14573400
H -1.30842800 5.62412400 -3.01728100
H 0.04735000 -4.20993900 2.54038300
H -2.05323300 -2.91484900 3.35696700
H 2.92353500 1.99025300 1.49964700
Au 2.65275100 -0.60698400 -0.10405600
P 4.55523000 -1.53090800 -1.11239800
H 4.44181200 -1.86899500 -2.46733800
H 5.69949400 -0.72207600 -1.12015700

H 5.05688500 -2.72008700 -0.5670310

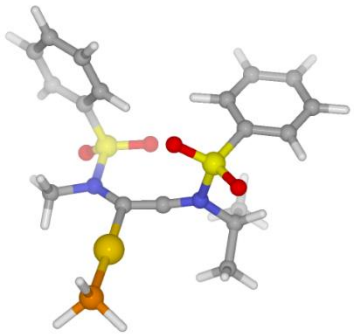
IEFPCM(1,2-dichloroethane)-M06/6-31+G(d)/SDD(Au):

Zero-point correction =	0.385767 (Hartree/Particle)
Thermal correction to Energy =	0.416981
Thermal correction to Enthalpy =	0.417925
Thermal correction to Gibbs Free Energy =	0.319314
Sum of electronic and zero-point Energies =	-2382.157395
Sum of electronic and thermal Energies =	-2382.126182
Sum of electronic and thermal Enthalpies =	-2382.125238
Sum of electronic and thermal Free Energies =	-2382.223849
Electronic Energy =	-2382.543163

IEFPCM(1,2-dichloroethane)-[Functional]/[Basis Set]//IEFPCM(1,2-dichloroethane)-M06/6-31+G(d)/SDD(Au):

Electronic Energy (M06-L/6-31+G(d)/SDD(Au)) =	-2383.259220
Electronic Energy (B2PLYPD3/6-31+G(d)/SDD(Au)) =	-2380.188838
Electronic Energy (MP2/6-31+G(d)/SDD(Au)) =	-2377.519012
Electronic Energy (PBE/6-31+G(d)/SDD(Au)) =	-2381.515737
Electronic Energy (PBE0/6-31+G(d)/SDD(Au)) =	-2380.704334
Electronic Energy (TPSS/6-31+G(d)/SDD(Au)) =	-2383.534099
Electronic Energy (DLPNO-CCSD(T)/def2-TZVPP) =	-2379.877894

Int1major-M06L-Opt



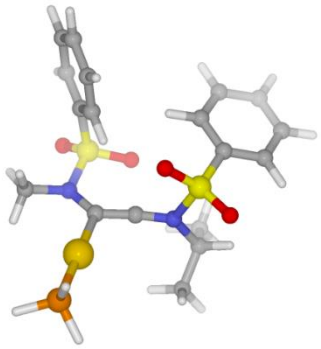
C 0.09647100 -0.69035600 0.87074400
C 0.91393500 0.32384800 0.69068700
N -0.61448600 -1.68646000 0.53762000
N 0.78305300 1.62330700 1.05360000
S -1.32512100 -1.76253300 -1.16738200
O -0.92777900 -0.49127900 -1.75723900
O -0.88626000 -3.04542100 -1.70498400
S -0.77102500 2.26397200 1.47732100
O -1.65624800 1.10135000 1.44772400
O -0.59974500 3.06116500 2.68509500
C -1.13087200 3.34978400 0.12407100
C -1.16829200 4.72515300 0.34702300
C -1.34361700 2.79401100 -1.13930300
C -1.44588200 5.56514200 -0.72920100
H -0.98923100 5.12188600 1.34324700
C -1.61650400 3.64833100 -2.20202000
H -1.28608000 1.71641600 -1.29054900
C -1.66980700 5.02856300 -1.99631200
H -1.48564400 6.64077400 -0.57438500
H -1.78668800 3.23476100 -3.19338700
C -3.05446900 -1.80073000 -0.82678400
C -3.71301700 -3.03169000 -0.83061300
C -3.69765300 -0.60728000 -0.49207500
C -5.06323800 -3.05875500 -0.49465500
H -3.17893500 -3.93965800 -1.10102700
C -5.04629000 -0.65686100 -0.15815100
H -3.15149500 0.33285200 -0.48183900
C -5.72399000 -1.87747400 -0.15702700
H -5.59830500 -4.00524500 -0.49752500
H -5.56842000 0.26030200 0.10327500
C -0.90464600 -2.86254600 1.42782400
C 0.40538400 -3.48987000 1.85623200
C -1.77757400 -2.40494300 2.57878400
H -1.45766700 -3.56552600 0.79174000
H 0.99386900 -2.78457200 2.45577200
H 1.00195100 -3.79460000 0.98952600
H -1.25437100 -1.65291700 3.18177500
H -2.71697800 -1.96666700 2.22241300
C 1.86006000 2.59497500 0.86349400
H 1.61207400 3.50951600 1.40768400
H 1.99558800 2.82620000 -0.19951100
H -6.77831700 -1.90729500 0.10890200

H -1.88438400 5.69028800 -2.83268400
H 0.20864900 -4.37494200 2.46932900
H -2.01689900 -3.25657900 3.22370300
H 2.78604600 2.18895200 1.27783900
Au 2.71150100 -0.44636600 -0.11662500
P 4.67372200 -1.23616900 -1.07000300
H 4.85277200 -1.00192700 -2.43731700
H 5.87539500 -0.73640500 -0.55695300
H 4.91128400 -2.61345200 -1.00524300

IEFPCM(1,2-dichloroethane)-M06L/6-31+G(d)/SDD(Au):

Zero-point correction =	0.386350 (Hartree/Particle)
Thermal correction to Energy =	0.417997
Thermal correction to Enthalpy =	0.418941
Thermal correction to Gibbs Free Energy =	0.318151
Sum of electronic and zero-point Energies =	-2382.874008
Sum of electronic and thermal Energies =	-2382.842361
Sum of electronic and thermal Enthalpies =	-2382.841417
Sum of electronic and thermal Free Energies =	-2382.942207

Int1major-MP2-Opt



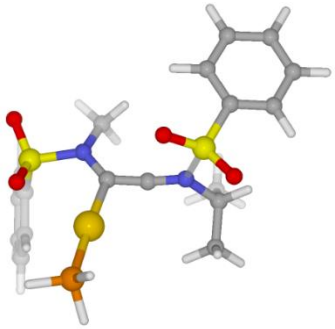
C 0.19877600 -0.67757600 0.68220200
C 0.93760400 0.40121900 0.75940400
N -0.34310800 -1.79098300 0.41948300
N 0.60429800 1.62566900 1.30039000
S -1.09761700 -1.99156100 -1.25008500
O -0.64548700 -0.79505100 -1.95831200
O -0.73107900 -3.35164800 -1.63978100
S -1.05170800 1.96094900 1.56871000
O -1.68115500 0.62813500 1.58566400
O -1.14767900 2.87688300 2.70413500
C -1.54092200 2.82275200 0.09727500
C -2.35157900 3.95653300 0.21948300
C -1.14728200 2.31303600 -1.14800700
C -2.78485200 4.59115000 -0.95053900
H -2.62219100 4.33467800 1.20261300
C -1.58821100 2.96499800 -2.30368500
H -0.51325400 1.43214600 -1.22529400
C -2.40938300 4.09649700 -2.20593100
H -3.41471500 5.47493200 -0.87897900
H -1.29324800 2.58251900 -3.27848000
C -2.80380100 -1.88525500 -0.84638600
C -3.51842100 -3.07231900 -0.63795900
C -3.36747500 -0.61459700 -0.67584300
C -4.85651200 -2.97011400 -0.24529900
H -3.05020500 -4.03924900 -0.80797900
C -4.70425500 -0.54141300 -0.27803100
H -2.78652200 0.28424500 -0.85882900
C -5.44270000 -1.71167400 -0.05546500
H -5.43977900 -3.87437100 -0.08844500
H -5.16804800 0.43268100 -0.14032100
C -0.47121700 -2.92343600 1.40264300
C 0.91594300 -3.27950200 1.91326100
C -1.44529700 -2.50705900 2.49625800
H -0.87189400 -3.75537500 0.81375300
H 1.35344700 -2.43699400 2.45936000
H 1.57725700 -3.55735700 1.08654000
H -1.04651300 -1.65610000 3.05773100
H -2.41529500 -2.21984300 2.07931200
C 1.50267600 2.78189000 1.15503500
H 1.09645700 3.60581200 1.74553400
H 1.59421500 3.08415500 0.10553600
H -6.48268100 -1.64270600 0.25546700
H -2.74911100 4.59829400 -3.10914400
H 0.84150900 -4.12955000 2.59888200
H -1.59230600 -3.34534400 3.18566400
H 2.48011200 2.51476900 1.56213900
Au 2.76072800 -0.04293100 -0.10117100
P 4.79068100 -0.53320700 -1.10625700
H 4.79909400 -0.58866400 -2.50621900
H 5.83722000 0.36158400 -0.84740300
H 5.37421500 -1.76095000 -0.76633200

IEFPCM(1,2-dichloroethane)-MP2/6-31+G(d)/SDD(Au):

Zero-point correction =	0.390931 (Hartree/Particle)

Thermal correction to Energy =	0.422126
Thermal correction to Enthalpy =	0.423070
Thermal correction to Gibbs Free Energy =	0.325011
Sum of electronic and zero-point Energies =	-2377.101045
Sum of electronic and thermal Energies =	-2377.069850
Sum of electronic and thermal Enthalpies =	-2377.068906
Sum of electronic and thermal Free Energies =	-2377.166966

Int1major-PBE-Opt

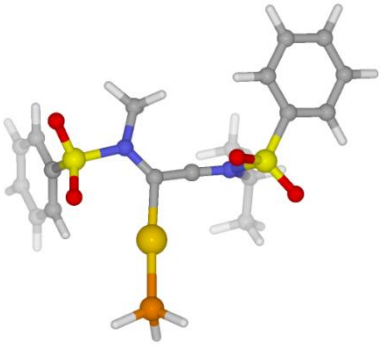


C -0.74136800 0.16486500 0.57838100	H -3.32246500 1.49210100 -1.98793100
C 0.34135400 0.21850100 -0.19769700	C -6.34007500 2.45123900 -0.66353200
N -1.90142300 -0.09918900 1.00153000	H -7.44858500 1.36430200 0.85796300
N 0.77611600 1.35419700 -0.82352700	H -5.03928300 3.30537600 -2.18194900
S -3.19922800 -0.83396900 -0.27692000	C -2.35450900 -0.06621200 2.43771100
O -2.39368800 -0.93288800 -1.51374900	C -1.64322800 -1.17268800 3.22100800
O -3.76955000 -2.01859200 0.40977400	C -2.13299800 1.33482800 3.01191700
S 2.42280300 1.46174300 -1.45378800	H -3.43511400 -0.28168200 2.40160600
O 2.80439700 0.08918700 -1.85195300	H -0.55407000 -0.99484600 3.24378500
O 2.35978100 2.56188600 -2.43989400	H -1.83604900 -2.16296100 2.77741000
C 3.42369100 1.98264200 -0.05852900	H -1.05713500 1.57761000 3.05069800
C 3.57725600 3.35901200 0.18305300	H -2.65127100 2.10045200 2.41101600
C 4.01443700 1.00772400 0.76409300	C 0.05549400 2.62239700 -0.61398300
C 4.34234300 3.76313300 1.28711100	H 0.50950700 3.41123500 -1.22759500
H 3.12600600 4.09552400 -0.48755400	H 0.07920300 2.90569100 0.45399800
C 4.77597000 1.43287000 1.86238000	H -7.09150800 3.24178400 -0.75451100
H 3.89447600 -0.05617000 0.54120600	H 5.53563700 3.12740300 2.98226500
C 4.93694500 2.80430400 2.12477300	H -2.01524300 -1.17803900 4.25910800
H 4.47901100 4.83058200 1.48569600	H -2.53287300 1.36984800 4.03898200
H 5.25098200 0.68841300 2.50881300	H -0.98805600 2.48815200 -0.94030800
C -4.43823500 0.44540900 -0.43732900	Au 1.19606400 -1.68237900 -0.22915800
C -5.58647500 0.38058300 0.37114600	P 2.01345700 -3.84515400 -0.25070000
C -4.21631000 1.48503600 -1.35806100	H 1.15576100 -4.84395000 -0.77424500
C -6.54219400 1.39919700 0.24605300	H 3.19224900 -4.07823600 -1.00125000
H -5.73881600 -0.45456700 1.06037700	H 2.36811300 -4.41814000 0.99579700
C -5.18525500 2.49201600 -1.46475500	

IEFPCM(1,2-dichloroethane)-PBE/6-31+G(d)/SDD(Au):

Zero-point correction =	0.375638 (Hartree/Particle)
Thermal correction to Energy =	0.407973
Thermal correction to Enthalpy =	0.408917
Thermal correction to Gibbs Free Energy =	0.306810
Sum of electronic and zero-point Energies =	-2381.147765
Sum of electronic and thermal Energies =	-2381.115431
Sum of electronic and thermal Enthalpies =	-2381.114487
Sum of electronic and thermal Free Energies =	-2381.216593

Int1major-PBE/def2-TZVPP-Opt

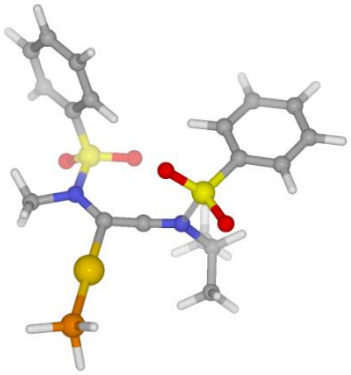


C -0.76260600 0.15347100 0.38306400
C 0.36627500 0.23412600 -0.27880800
N -1.92576100 -0.09452700 0.81391400
N 0.87523900 1.36049600 -0.86563000
S -3.19537800 -0.75658900 -0.39337800
O -2.48067000 -0.75888300 -1.65169600
O -3.67953800 -1.97266100 0.23250100
S 2.49463000 1.42926300 -1.44090600
O 2.86262700 0.07306800 -1.80145900
O 2.48912500 2.49163800 -2.42741600
C 3.46195000 1.94944000 -0.04541600
C 3.64787500 3.31897100 0.17850700
C 4.01423700 0.98555200 0.80663600
C 4.39599800 3.72462100 1.28416600
H 3.23020800 4.05051000 -0.51180900
C 4.76051600 1.40874100 1.90651200
H 3.87496900 -0.07476400 0.60008500
C 4.94805200 2.77335400 2.14679900
H 4.55371900 4.78769400 1.46595900
H 5.20310100 0.66858600 2.57321900
C -4.45297100 0.48211800 -0.38614200
C -5.57834400 0.30073700 0.42728600
C -4.29619800 1.61066700 -1.20183400
C -6.56777400 1.28356500 0.42200300
H -5.68224900 -0.59888200 1.03217500
C -5.29581100 2.58138000 -1.19047600
H -3.42126500 1.71375200 -1.84202900
C -6.42451200 2.41968400 -0.37961700
H -7.45452500 1.15659500 1.04246600
H -5.19618500 3.46319800 -1.82288500
C -2.33584300 -0.05565500 2.26591000
C -1.62644900 -1.17092200 3.02557400
C -2.07486100 1.33314700 2.83571400
H -3.41677100 -0.24990400 2.25595700
H -0.53813000 -1.01859700 3.00812300
H -1.85653800 -2.15405900 2.59673300
H -0.99940100 1.55743700 2.84085500
H -2.59776100 2.10768900 2.26016500
C 0.14318200 2.62682300 -0.71453500
H 0.62507200 3.40398300 -1.31243800
H 0.11096900 2.92823700 0.34281200
H -7.20247700 3.18337300 -0.37854300
H 5.53527500 3.09686300 3.00657200
H -1.95749500 -1.16260400 4.07191600
H -2.43650200 1.36884600 3.87128800
H -0.87882000 2.48385800 -1.08763200
Au 1.16487400 -1.69536700 -0.20454000
P 1.93990700 -3.83411200 -0.10778600
H 1.08352700 -4.84815000 -0.59464400
H 3.12451700 -4.11572200 -0.82600600
H 2.27014300 -4.35106400 1.16615800

IEFPCM(1,2-dichloroethane)-PBE/def2-TZVPP:

Zero-point correction =	0.375272 (Hartree/Particle)
Thermal correction to Energy =	0.407243
Thermal correction to Enthalpy =	0.408187
Thermal correction to Gibbs Free Energy =	0.306801
Sum of electronic and zero-point Energies =	-2381.745780
Sum of electronic and thermal Energies =	-2381.713809
Sum of electronic and thermal Enthalpies =	-2381.712865
Sum of electronic and thermal Free Energies =	-2381.814252

Int1$_{major}$-TPSS-Opt

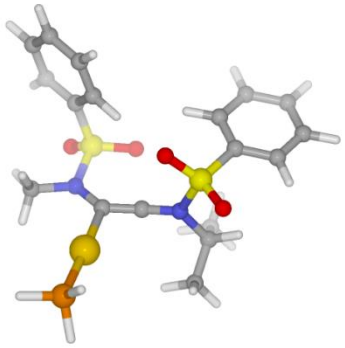


C 0.20968200 -0.58814900 0.88299800
C 0.95405200 0.46566300 0.53266700
N -0.43055100 -1.66420400 0.70508100
N 0.67608200 1.79266800 0.69706100
S -1.21029100 -1.95925500 -1.05876700
O -0.98260400 -0.65275400 -1.70759000
O -0.60633400 -3.21488400 -1.55254500
S -0.87461900 2.28952500 1.37706100
O -1.64128800 1.02236800 1.42113900
O -0.60724100 3.08283500 2.58938300
C -1.52777100 3.36941200 0.10346900
C -1.76604900 4.71336000 0.42791500
C -1.80298400 2.83778900 -1.16803400
C -2.30449700 5.55004800 -0.56035800
H -1.54198600 5.08278700 1.42622000
C -2.33468400 3.69255600 -2.14086200
H -1.60069800 1.79200900 -1.39304700
C -2.58551000 5.04183000 -1.83747800
H -2.50168100 6.59528200 -0.32956400
H -2.55257400 3.30441600 -3.13422800
C -2.94584500 -2.22000700 -0.70795800
C -3.47578600 -3.50546800 -0.90827500
C -3.71936400 -1.14140800 -0.24739000
C -4.83829100 -3.70542300 -0.64930200
H -2.84090500 -4.31079600 -1.27085500
C -5.07624000 -1.36885600 0.01187600
H -3.27324300 -0.16303500 -0.08672300
C -5.63272400 -2.64308000 -0.19009400
H -5.27539400 -4.68942800 -0.80821300
H -5.69750700 -0.54993400 0.36964800
C -0.57514700 -2.79977700 1.69205000
C 0.72724200 -3.61208100 1.72131400
C -0.98436800 -2.24275800 3.06117500
H -1.38710900 -3.41676400 1.28684000
H 1.55485100 -2.99358300 2.09414600
H 0.97858800 -3.99173300 0.72387500
H -0.19208000 -1.60482800 3.47317800
H -1.90789300 -1.65632500 2.99285900
C 1.71930900 2.83904900 0.64341300
H 1.24005700 3.80253300 0.44176500
H 2.39901600 2.60200500 -0.18192000
H -6.68972500 -2.80786300 0.01176400
H -3.00073300 5.69788300 -2.60069300
H 0.60502900 -4.46692000 2.39889600
H -1.14839200 -3.08076100 3.75068100
H 2.26862400 2.89227000 1.59054300
Au 2.79142400 -0.20560900 -0.19913300
P 4.80417600 -0.96433300 -1.06724500
H 4.73789100 -1.74239900 -2.23587100
H 5.73690100 0.01506100 -1.44900100
H 5.59721400 -1.78203000 -0.24369500

IEFPCM(1,2-dichloroethane)-TPSS/6-31+G(d)/SDD(Au):

Zero-point correction =	0.380305 (Hartree/Particle)
Thermal correction to Energy =	0.413055
Thermal correction to Enthalpy =	0.413999
Thermal correction to Gibbs Free Energy =	0.309508
Sum of electronic and zero-point Energies =	-2383.134209
Sum of electronic and thermal Energies =	-2383.101460
Sum of electronic and thermal Enthalpies =	-2383.100515
Sum of electronic and thermal Free Energies =	-2383.205006

Int1major-M06/6-31+G(d)/LANL2DZ-Opt

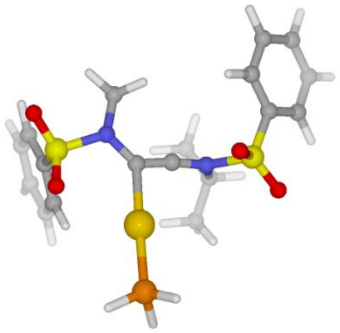


C 0.01930600 -0.62632800 0.76949800	H -3.10922900 0.47694400 -0.45611300
C 0.91732300 0.31035300 0.76140700	C -5.84535500 -1.52848800 -0.14919600
N -0.73715200 -1.61573500 0.50394900	H -5.88625500 -3.65864300 -0.49132500
N 0.87521400 1.60216600 1.18260100	H -5.52879000 0.59065700 0.11492700
S -1.45198200 -1.74094700 -1.14112400	C -1.02319400 -2.73672000 1.46991000
O -0.99410200 -0.53871000 -1.81794500	C 0.28241800 -3.40942700 1.83656600
O -1.08780900 -3.06679700 -1.61692500	C -1.78384100 -2.18182600 2.65585600
S -0.64659800 2.34039600 1.47635000	H -1.65391300 -3.44123200 0.91169900
O -1.59846800 1.23369300 1.43753500	H 0.94172100 -2.71156400 2.37148800
O -0.51038700 3.16520200 2.66731500	H 0.80463100 -3.77402300 0.94252800
C -0.87475800 3.39016100 0.06800600	H -1.17087800 -1.44856200 3.19764700
C -0.85763100 4.77158800 0.23832300	H -2.71591700 -1.69267300 2.34365300
C -1.03858300 2.79190300 -1.18219800	C 2.03214900 2.49249600 1.05130100
C -1.02857100 5.57918600 -0.88341300	H 1.83012800 3.42336200 1.58944800
H -0.71958300 5.20057800 1.22859400	H 2.23763100 2.71300200 -0.00442800
C -1.20528000 3.61408700 -2.29021800	H -6.90132500 -1.47638300 0.10869700
H -1.03153100 1.70659600 -1.29412500	H -1.33476300 5.63838600 -3.01217600
C -1.20239000 5.00179800 -2.13940600	H 0.08519200 -4.26251800 2.49642700
H -1.02501200 6.66144200 -0.77309600	H -2.03225700 -2.99665400 3.34639400
H -1.33755800 3.17005300 -3.27456700	H 2.90167200 2.01395200 1.51193400
C -3.17806100 -1.65991500 -0.79548100	Au 2.64144300 -0.59241700 -0.10329700
C -3.92747200 -2.83515400 -0.80928000	P 4.54534200 -1.51510800 -1.13078700
C -3.72675600 -0.41943500 -0.46913600	H 4.35719700 -2.09312900 -2.39299500
C -5.27765100 -2.75721200 -0.48314200	H 5.59917100 -0.62723900 -1.38323800
H -3.46445300 -3.78292100 -1.07675600	H 5.20447200 -2.54378400 -0.44522100
C -5.07623400 -0.36397200 -0.14380300	

IEFPCM(1,2-dichloroethane)-M06/6-31+G(d)/LANL2DZ(Au):

Zero-point correction =	0.385737 (Hartree/Particle)
Thermal correction to Energy =	0.416992
Thermal correction to Enthalpy =	0.417936
Thermal correction to Gibbs Free Energy =	0.319202
Sum of electronic and zero-point Energies =	-2381.837754
Sum of electronic and thermal Energies =	-2381.806499
Sum of electronic and thermal Enthalpies =	-2381.805555
Sum of electronic and thermal Free Energies =	-2381.904289

Int1$_{major}$-M06/def2-TZVPP-Opt

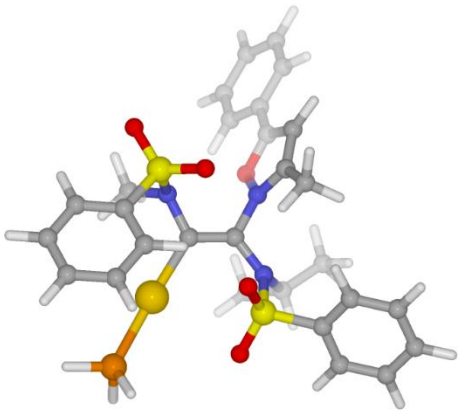


C -0.71070600 0.06965000 -0.05798400	H -3.39645300 0.82309200 -2.14896400
C 0.42539600 0.17747500 -0.62690400	C -6.12617400 2.17527300 -0.67182800
N -1.77178100 -0.11214900 0.61847600	H -7.03323900 1.48088300 1.14304400
N 0.93817900 1.14626500 -1.43788200	H -5.04160400 2.64582400 -2.46281400
S -3.08830100 -1.06636900 -0.06442100	C -1.91304400 0.39003900 2.03257200
O -2.57551200 -1.53751100 -1.30372100	C -0.93668900 -0.34903600 2.91371100
O -3.47669000 -1.95042800 0.98141000	C -1.72833500 1.88725900 2.04794600
S 2.61320800 1.34556400 -1.50813700	H -2.93480400 0.13653300 2.31882100
O 3.18655100 0.03930100 -1.48764800	H 0.09137800 -0.13379700 2.61007000
O 2.84648800 2.23155200 -2.59920700	H -1.09903800 -1.42597800 2.86619600
C 2.97212400 2.17012100 0.00127800	H -0.70484500 2.15216300 1.76921400
C 2.97358900 3.55728700 0.03029100	H -2.41980900 2.38148600 1.36310900
C 3.18345500 1.42047400 1.15119500	C 0.11702400 2.34236100 -1.64077900
C 3.19157300 4.20123900 1.23548200	H 0.58863200 2.99320000 -2.37006200
H 2.82068700 4.12091700 -0.88050900	H -0.02810600 2.88072600 -0.69971400
C 3.39851200 2.07784400 2.34837700	H -6.84757900 2.96916400 -0.81397000
H 3.19775300 0.33909600 1.10323100	H 3.57153600 3.97276400 3.32903900
C 3.39956700 3.46372300 2.38971100	H -1.05764600 -0.02409500 3.94649500
H 3.20328100 5.28229700 1.27073200	H -1.90826200 2.26616800 3.05317200
H 3.57345600 1.50649700 3.25016400	H -0.85015800 2.02585700 -2.02890100
C -4.29971400 0.16495300 -0.31187500	Au 1.24752900 -1.74223800 -0.15080500
C -5.31288100 0.32632800 0.62141100	P 2.07614900 -3.83784400 0.35488600
C -4.18539700 0.98682900 -1.42626700	H 1.38463600 -4.93309100 -0.17540000
C -6.23213200 1.34226000 0.42992800	H 3.38378300 -4.11092400 -0.06265900
H -5.38413700 -0.33834500 1.47172900	H 2.14368600 -4.18690200 1.70871300
C -5.10952200 1.99786300 -1.59965900	

IEFPCM(1,2-dichloroethane)-M06/def2-TZVPP:

Zero-point correction =	0.387085 (Hartree/Particle)
Thermal correction to Energy =	0.417667
Thermal correction to Enthalpy =	0.418611
Thermal correction to Gibbs Free Energy =	0.321496
Sum of electronic and zero-point Energies =	-2382.748640
Sum of electronic and thermal Energies =	-2382.718058
Sum of electronic and thermal Enthalpies =	-2382.717114
Sum of electronic and thermal Free Energies =	-2382.814229

Int2$_{major}$-M06-Opt



C -0.54289800 0.49837700 -0.10933100
C -0.01897700 -0.73107000 -0.30684100
N 0.03797000 1.73350200 -0.43484200
N -0.78066500 -1.84029300 0.19038400
S 1.57504300 2.13175500 0.16918600
O 1.73160200 1.38082000 1.40825500
O 2.56089300 2.00922800 -0.90221900
S -0.45571800 -2.32555400 1.79021900
O -0.60790900 -1.12763800 2.60501700
O -1.27747600 -3.50374200 2.01539800
C 1.25623100 -2.80166400 1.80112100
C 1.59403300 -4.11193900 1.46492300
C 2.22450500 -1.83240400 2.05927200
C 2.94029200 -4.45530900 1.38345500
H 0.81275700 -4.85026900 1.29119500
C 3.56739800 -2.19369700 1.97869000
H 1.93187400 -0.81683400 2.31944600
C 3.92261200 -3.49819000 1.63911400
H 3.22272700 -5.47648000 1.13438700
H 4.33491400 -1.45111900 2.19231800
C 1.42647300 3.86170900 0.55572800
C 1.82309300 4.81249900 -0.38188300
C 0.93229600 4.22814400 1.80613000
C 1.67691100 6.16140000 -0.07180500
H 2.25832100 4.49831800 -1.32896400
C 0.79611000 5.57914800 2.10502400
H 0.69006100 3.46307700 2.54093900
C 1.15634900 6.54225900 1.16308100
H 1.98131900 6.91628000 -0.79398700
H 0.42123600 5.88209200 3.08073400
C -0.43724300 2.48103200 -1.63900900
C -0.60880400 1.56140800 -2.83363500
C -1.68827400 3.28347500 -1.31401600
H 0.36756500 3.18842200 -1.87970300
H -1.40481200 0.82188400 -2.66835400
H 0.32085400 1.01997700 -3.05157100
H -2.55367500 2.63326200 -1.12284900
H -1.52996800 3.92362400 -0.43464600
C -0.91950800 -2.92821700 -0.77896800
H -1.55186300 -3.71149400 -0.35218900
H 0.05706300 -3.34478300 -1.08087500
H 1.04664900 7.59861700 1.40114500
H 4.97413500 -3.77752000 1.58744800
H -0.88102500 2.15210400 -3.71720600
H -1.95198300 3.92914500 -2.16142900
H -1.41135300 -2.51871500 -1.66967100
Au 1.85249400 -1.01664100 -1.18361300
P 4.05661700 -1.22560600 -2.02040300
H 5.00734100 -0.45019200 -1.33436400
H 4.69066300 -2.48033500 -1.99239500
H 4.33293700 -0.84039800 -3.34334200
N -1.87630900 0.61217000 0.42982700
O -2.87544500 0.07042400 -0.34384900
C -2.38369500 1.04288500 1.58262800
C -4.01685800 0.16806300 0.36146100
C -3.75859300 0.78299900 1.56589800
C -5.21832700 -0.35676500 -0.25009100
H -4.45629400 1.00020100 2.36393000
C -5.16927600 -1.01182900 -1.48893800
C -6.44422200 -0.20672900 0.41309700
C -6.33582000 -1.50982300 -2.05165900
H -4.21896500 -1.13144300 -2.00632800
C -7.60561900 -0.70806000 -0.15602700
H -6.49001400 0.30456200 1.37348700
C -7.55258600 -1.35959600 -1.38755300
H -6.29742200 -2.01902000 -3.01226900
H -8.55555900 -0.59008900 0.36072700
H -8.46485700 -1.75231900 -1.83247000
C -1.55590300 1.69013300 2.61958500
H -0.51014900 1.37403200 2.54534000
H -1.62236100 2.78169400 2.50565900
H -1.93409900 1.42342200 3.61175300

IEFPCM(1,2-dichloroethane)-M06/6-31+G(d)/SDD(Au):

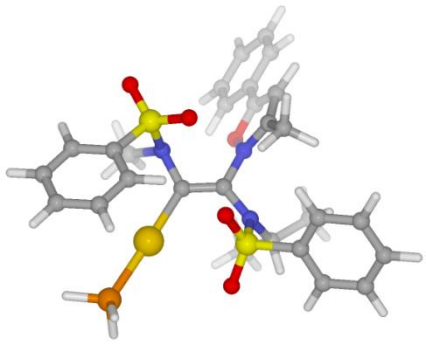
Zero-point correction =	0.557026 (Hartree/Particle)
Thermal correction to Energy =	0.598009
Thermal correction to Enthalpy =	0.598953
Thermal correction to Gibbs Free Energy =	0.480037

Sum of electronic and zero-point Energies =	-2898.043591
Sum of electronic and thermal Energies =	-2898.002609
Sum of electronic and thermal Enthalpies =	-2898.001665
Sum of electronic and thermal Free Energies =	-2898.120581
Electronic Energy =	-2898.600618

IEFPCM(1,2-dichloroethane)-[Functional]/[Basis Set]//IEFPCM(1,2-dichloroethane)-M06/6-31+G(d)/SDD(Au):

Electronic Energy (M06-L/6-31+G(d)/SDD(Au)) =	-2899.651270
Electronic Energy (B2PLYPD3/6-31+G(d)/SDD(Au)) =	-2895.576411
Electronic Energy (MP2/6-31+G(d)/SDD(Au)) =	-2892.389186
Electronic Energy (PBE/6-31+G(d)/SDD(Au)) =	-2897.329210
Electronic Energy (PBE0/6-31+G(d)/SDD(Au)) =	-2896.263955
Electronic Energy (TPSS/6-31+G(d)/SDD(Au)) =	-2900.070425
Electronic Energy (DLPNO-CCSD(T)/def2-TZVPP) =	-2895.438128

Int2$_{major}$-M06L-Opt



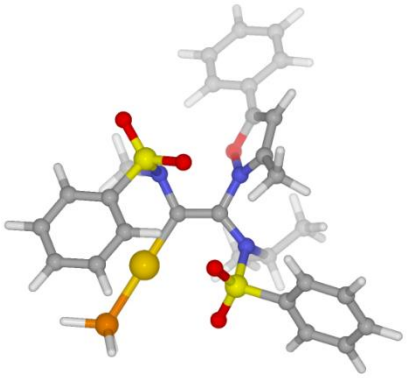
C -0.56135400 0.48671800 -0.12341100	H 1.11763200 7.06486400 -0.86160600
C 0.05159100 -0.71359500 -0.26709600	H 0.14627900 5.86097600 3.15649900
N -0.05672300 1.73489100 -0.50627600	C -0.55704500 2.39046500 -1.75892600
N -0.63895700 -1.83701400 0.31082200	C -0.68063000 1.38052400 -2.88375500
S 1.44022200 2.27236500 0.09385600	C -1.83966800 3.16239200 -1.49482300
O 1.68800300 1.51516300 1.31830200	H 0.22754500 3.10542800 -2.03403700
O 2.41700100 2.28534400 -0.99732900	H -1.45960300 0.63596200 -2.67538000
S -0.24121500 -2.17024300 1.93674500	H 0.26518400 0.84695000 -3.03908100
O -0.38418600 -0.90387200 2.64959800	H -2.68562400 2.49463400 -1.29170200
O -1.03793600 -3.33998500 2.30208200	H -1.72343900 3.84604800 -0.64495500
C 1.47288500 -2.62866700 1.91797700	C -0.65834700 -3.01722200 -0.55582800
C 1.81778700 -3.95025900 1.62751500	H -1.21610100 -3.81565000 -0.06235200
C 2.43969100 -1.63214600 2.06509300	H 0.35818400 -3.36283000 -0.80967300
C 3.16481500 -4.27873200 1.49621400	H 0.35614400 7.63820500 1.43258600
H 1.04285400 -4.70647200 1.51971300	H 5.19482700 -3.55973500 1.54914600
C 3.78316400 -1.97917300 1.93694600	H -0.94928300 1.89345000 -3.81336600
H 2.13975700 -0.60635500 2.26657400	H -2.10289300 3.75725400 -2.37656000
C 4.14376100 -3.29595800 1.65087900	H -1.17481100 -2.74173800 -1.48036300
H 3.44946500 -5.30598200 1.27895600	Au 1.90283500 -0.95357100 -1.17963200
H 4.54820500 -1.21410200 2.05578700	P 4.04069700 -1.25450900 -2.10504400
C 1.11838900 3.97038600 0.51881400	H 5.08981500 -0.56685100 -1.47812400
C 1.27975700 4.96243100 -0.44965900	H 4.57526700 -2.55099400 -2.10590900
C 0.72221700 4.28073300 1.81990200	H 4.27935900 -0.89380400 -3.43822700
C 0.99657100 6.28365200 -0.11462900	N -1.90303900 0.54358900 0.38751000
H 1.63991100 4.70533800 -1.44335100	O -2.84888200 -0.15373100 -0.34965900
C 0.44859300 5.60666300 2.14299500	C -2.47451700 1.07207800 1.47274000
H 0.65552300 3.49807800 2.57124800	C -4.01705900 -0.04517400 0.32425700
C 0.57348400 6.60375500 1.17526600	C -3.82701800 0.71881100 1.45578200

C -5.16175200 -0.71260500 -0.24916100
H -4.56180300 0.98276400 2.20323300
C -5.03966400 -1.47563600 -1.42275300
C -6.41222200 -0.59502900 0.37954800
C -6.15533400 -2.10861300 -1.95434000
H -4.07252600 -1.57012900 -1.91207900
C -7.52148500 -1.23249500 -0.15963700
H -6.51390800 -0.00451600 1.28779300
C -7.39590100 -1.98915200 -1.32580700
H -6.05782600 -2.69927300 -2.86223300
H -8.48762500 -1.13911100 0.33057600
H -8.26715900 -2.48742400 -1.74557400
C -1.69499900 1.87513400 2.43176700
H -0.63438700 1.61230300 2.38449700
H -1.81251900 2.94212800 2.20337700
H -2.06020100 1.70707000 3.44798400

IEFPCM(1,2-dichloroethane)-M06L/6-31+G(d)/SDD(Au):

Zero-point correction =	0.558148 (Hartree/Particle)
Thermal correction to Energy =	0.599200
Thermal correction to Enthalpy =	0.600144
Thermal correction to Gibbs Free Energy =	0.480644
Sum of electronic and zero-point Energies =	-2899.095184
Sum of electronic and thermal Energies =	-2899.054132
Sum of electronic and thermal Enthalpies =	-2899.053188
Sum of electronic and thermal Free Energies =	-2899.172688

Int2$_{major}$-MP2-Opt



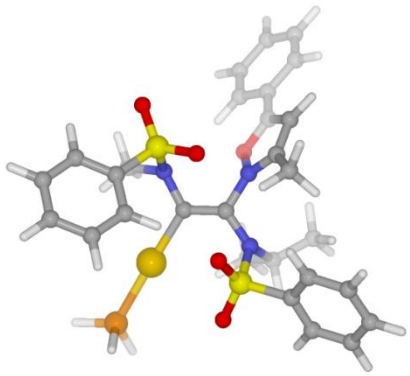
C -0.50099200 0.60028500 -0.12770500
C -0.11540200 -0.69380600 -0.30319800
N 0.19065000 1.77854400 -0.43996500
N -1.03797300 -1.67115500 0.22017200
S 1.81510700 1.92289600 0.05479100
O 1.92260600 1.14296900 1.29503900
O 2.71256400 1.67222900 -1.08629000
S -0.73123300 -2.11517900 1.83690400
O -0.71733600 -0.85198300 2.58802600
O -1.67819700 -3.19253400 2.14258500
C 0.91852000 -2.76861600 1.81224500
C 1.11307400 -4.10125000 1.42401200
C 1.98960800 -1.90649300 2.08168900
C 2.42421600 -4.57729500 1.30651000
H 0.26061000 -4.75732900 1.26148800
C 3.29280200 -2.40513300 1.96737100
H 1.80669800 -0.88041300 2.38600900
C 3.51095500 -3.73181100 1.57138100
H 2.59575300 -5.61418300 1.02444300
H 4.13452600 -1.75462500 2.19839300
C 1.92766100 3.65067300 0.44536500
C 2.38809400 4.54534500 -0.52901400
C 1.60889200 4.06863200 1.74382900
C 2.48436900 5.90198900 -0.20117700
H 2.69991000 4.18185200 -1.50558500
C 1.71936700 5.42703400 2.05527100
H 1.33293700 3.34014100 2.50122200
C 2.13933800 6.34392600 1.08201800
H 2.84138200 6.61010600 -0.94553400
H 1.49118300 5.76800700 3.06273000
C -0.19618400 2.50654600 -1.69557800
C -0.31238600 1.55345100 -2.87733500
C -1.46048000 3.32625700 -1.44827800
H 0.62536000 3.20346100 -1.88925800
H -1.13185700 0.83919200 -2.73690000
H 0.61866500 0.99451300 -3.01469100
H -2.34307100 2.68749300 -1.33141300
H -1.34705400 3.95202900 -0.55615400
C -1.26251900 -2.80581500 -0.69651600
H -1.99746600 -3.47714000 -0.24750400
H -0.33197900 -3.34755100 -0.92036000
H 2.22270000 7.39910600 1.33230400
H 4.52643400 -4.11774100 1.49965300
H -0.51478800 2.12640400 -3.78933900
H -1.64542600 3.98037300 -2.30781700
H -1.66070800 -2.39339200 -1.62788900
Au 1.67602900 -1.23092900 -1.10895100
P 3.76448100 -1.81624100 -1.94659500

H 4.86263500 -1.28720800 -1.25111300
H 4.10112600 -3.17855200 -1.98035000
H 4.07378900 -1.43278200 -3.26069100
N -1.80891000 0.86304500 0.40155400
O -2.85053400 0.35520600 -0.33261800
C -2.25435000 1.47458300 1.50068800
C -3.98879500 0.63797900 0.36715500
C -3.65617300 1.35236200 1.49938900
C -5.22279900 0.12102300 -0.19742100
H -4.33196100 1.69056000 2.27443500
C -5.21284300 -1.10566600 -0.88737400
C -6.41745900 0.84371400 -0.03390600
C -6.40612200 -1.59961200 -1.41768300
H -4.28734800 -1.67106600 -0.97878000
C -7.60481200 0.33084800 -0.56040700
H -6.41313900 1.80293100 0.48140700
C -7.60052700 -0.88554600 -1.25536000
H -6.40758200 -2.54911400 -1.94827100
H -8.53176000 0.88678100 -0.44009900
H -8.52769300 -1.27828300 -1.66664500
C -1.32914100 2.10522000 2.47618300
H -0.35991100 1.60136200 2.45520900
H -1.19991800 3.16829500 2.23974400
H -1.75216700 2.01726700 3.48109800

IEFPCM(1,2-dichloroethane)-MP2/6-31+G(d)/SDD(Au):

Zero-point correction =	0.561891 (Hartree/Particle)
Thermal correction to Energy =	0.603335
Thermal correction to Enthalpy =	0.604279
Thermal correction to Gibbs Free Energy =	0.482480
Sum of electronic and zero-point Energies =	-2891.804940
Sum of electronic and thermal Energies =	-2891.763496
Sum of electronic and thermal Enthalpies =	-2891.762552
Sum of electronic and thermal Free Energies =	-2891.884352

Int2$_{major}$-PBE-Opt



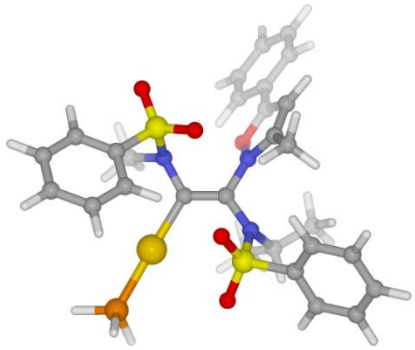
C -0.47347600 0.51063200 -0.09348700
C -0.00426200 -0.75446700 -0.37294500
N 0.16901000 1.72455100 -0.40398700
N -0.72708800 -1.86861100 0.13844200
S 1.78750400 2.00821400 0.18037900
O 1.95816800 1.11925400 1.35147400
O 2.72155700 1.96381100 -0.97370000
S -0.58502100 -2.26482300 1.84816300
O -0.59718700 -0.97403100 2.56843200
O -1.61658500 -3.29734500 2.08562000
C 1.03654800 -3.02207100 2.03827900
C 1.12815600 -4.42158500 2.11320700
C 2.17053800 -2.19306000 2.09133400
C 2.39696100 -5.00476200 2.25183100
H 0.22073300 -5.03181000 2.08659100
C 3.42959800 -2.79652800 2.22930800
H 2.07235800 -1.10461900 2.03870600
C 3.54342200 -4.19509100 2.30920200
H 2.48627400 -6.09354200 2.32272200
H 4.32337500 -2.16647200 2.28649000
C 1.77208900 3.71664300 0.76248900
C 2.09990900 4.75294900 -0.12798700
C 1.50762900 3.96833600 2.11919800
C 2.11414200 6.07315700 0.34591600
H 2.37249300 4.52651600 -1.16290900
C 1.53383100 5.29290600 2.57914400
H 1.32446800 3.13704900 2.80506800
C 1.82373200 6.34398900 1.69302700
H 2.36897200 6.88891700 -0.33794500
H 1.34256900 5.50128600 3.63668900
C -0.27376700 2.55581700 -1.57901500
C -0.55135700 1.69552700 -2.81592500
C -1.45444900 3.46677100 -1.21070000
H 0.59180600 3.19884700 -1.81085300
H -1.42478700 1.03728200 -2.66828900
H 0.31891600 1.06398700 -3.06224800
H -2.37876700 2.89174800 -1.02832400
H -1.22772200 4.07012200 -0.31550000
C -0.73112300 -3.06860600 -0.71995100
H -1.40359900 -3.81691800 -0.27527400

H 0.28357100 -3.49553200 -0.85054300
H 1.84330700 7.37564300 2.05845300
H 4.53007000 -4.65595700 2.42403700
H -0.76421600 2.35045600 -3.67797200
H -1.66240700 4.15973200 -2.04428200
H -1.12519100 -2.78127500 -1.70661300
Au 1.70732400 -1.02138700 -1.49052900
P 3.68770700 -1.25665200 -2.70956300
H 4.89360100 -0.94049400 -2.02945000
H 4.04348300 -2.52050800 -3.25302600
H 3.85193300 -0.44747500 -3.86534500
N -1.78810300 0.68121800 0.47365400
O -2.84241500 0.17131900 -0.30607700
C -2.29418100 1.29294500 1.56009100
C -3.99774300 0.45903700 0.35861100
C -3.69639000 1.17307900 1.51143800
C -5.23862500 -0.01409700 -0.23353100
H -4.39088200 1.53645900 2.26539700
C -5.22933400 -0.87074300 -1.36016500
C -6.47309400 0.38852600 0.32921000
C -6.43686600 -1.31386100 -1.90856800
H -4.27865000 -1.19284000 -1.79507000
C -7.67466200 -0.06072000 -0.22648200
H -6.49300400 1.05732600 1.19531000
C -7.65999100 -0.91161200 -1.34508100
H -6.42481300 -1.97881600 -2.77760500
H -8.62578200 0.25529100 0.21270000
H -8.60262900 -1.26169000 -1.77756800
C -1.43404100 1.95116600 2.57911300
H -0.46967700 1.42997100 2.66703900
H -1.25103300 3.00325800 2.29484800
H -1.94286200 1.93933000 3.55524100

IEFPCM(1,2-dichloroethane)-PBE/6-31+G(d)/SDD(Au):

Zero-point correction =	0.541491 (Hartree/Particle)
Thermal correction to Energy =	0.584455
Thermal correction to Enthalpy =	0.585399
Thermal correction to Gibbs Free Energy =	0.459230
Sum of electronic and zero-point Energies =	-2896.772046
Sum of electronic and thermal Energies =	-2896.729082
Sum of electronic and thermal Enthalpies =	-2896.728138
Sum of electronic and thermal Free Energies =	-2896.854306

Int2$_{major}$-PBE/def2-TZVPP-Opt



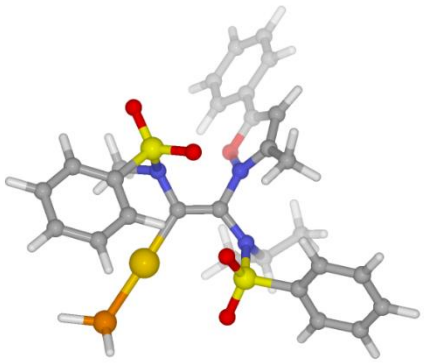
C -0.47607000 0.50608800 -0.08944700
C 0.04195500 -0.73371900 -0.34766800
N 0.12603400 1.73524300 -0.41136200
N -0.63976100 -1.87525300 0.16200100
S 1.69341300 2.09816600 0.16714800
O 1.91434600 1.22746500 1.30734600
O 2.61061800 2.11143100 -0.96258400
S -0.49446400 -2.28700200 1.82202300
O -0.52716100 -1.03634900 2.55562900
O -1.48436200 -3.32099800 2.04902000
C 1.12482000 -3.00407300 1.99811400
C 1.25782900 -4.39662600 2.01497800
C 2.23694900 -2.15895100 2.10052200
C 2.53247600 -4.95148800 2.14011600
H 0.37113100 -5.02652300 1.95487100
C 3.50352300 -2.73148500 2.22478600
H 2.11122900 -1.07639000 2.09827300
C 3.65183600 -4.12168300 2.24357400
H 2.64857300 -6.03525900 2.16491800
H 4.37693600 -2.08543800 2.31915400
C 1.59015800 3.78304100 0.75156900
C 1.87495600 4.83836400 -0.12276700
C 1.30557300 4.02023800 2.10089500
C 1.82673800 6.14847700 0.35472900
H 2.16298000 4.63174300 -1.15283900
C 1.26911900 5.33450800 2.56713700
H 1.15620400 3.18194000 2.77904700
C 1.51654400 6.39745600 1.69398500
H 2.04771600 6.97558600 -0.32011000
H 1.06150000 5.52740400 3.61991200
C -0.36194500 2.54955300 -1.57649000
C -0.57724500 1.69239900 -2.82107000
C -1.59204800 3.38685400 -1.21802400
H 0.46375600 3.24139100 -1.79048400

H -1.40022400 0.97748200 -2.68458600
H 0.32992300 1.12898200 -3.07608400
H -2.48651000 2.76644800 -1.07022600
H -1.41881100 3.98334600 -0.31281400
C -0.67343200 -3.03855100 -0.73897300
H -1.29979400 -3.81427500 -0.28670300
H 0.33550600 -3.43633200 -0.94251200
H 1.48708800 7.42267900 2.06368900
H 4.64464100 -4.56067300 2.34821400
H -0.83341500 2.33996800 -3.67009400
H -1.81471300 4.07992900 -2.04058900
H -1.12622200 -2.72809800 -1.68772800
Au 1.77051000 -0.96277800 -1.45264800
P 3.72777600 -1.16650700 -2.64599700
H 4.92106100 -0.77221200 -1.99202700
H 4.13188700 -2.43708300 -3.12720100
H 3.85904800 -0.41447500 -3.83980500
N -1.79900300 0.62890500 0.46796500
O -2.82933900 0.09494600 -0.31992300
C -2.32501200 1.17872500 1.56995900
C -3.98897900 0.31415000 0.35254800
C -3.71564800 0.99946400 1.52193600
C -5.21126300 -0.18372400 -0.24731200
H -4.42031400 1.31258600 2.28210800
C -5.18456700 -0.94928000 -1.42940500
C -6.44642200 0.10259100 0.36618400
C -6.37301500 -1.41625400 -1.98149100
H -4.23362900 -1.18043900 -1.90821400
C -7.62884600 -0.36920000 -0.19334100
H -6.48141700 0.69796100 1.27853700
C -7.59543600 -1.12856300 -1.36689700
H -6.34711200 -2.00958300 -2.89532400
H -8.58099800 -0.14348500 0.28636100
H -8.52412500 -1.49699900 -1.80314000
C -1.49964100 1.84018000 2.60663300
H -0.50579500 1.38374400 2.65978200
H -1.39448900 2.91008100 2.37232400
H -1.99286700 1.74926600 3.58089500

IEFPCM(1,2-dichloroethane)-PBE/def2-TZVPP:

Zero-point correction =	0.540428 (Hartree/Particle)
Thermal correction to Energy =	0.583132
Thermal correction to Enthalpy =	0.584076
Thermal correction to Gibbs Free Energy =	0.458228
Sum of electronic and zero-point Energies =	-2897.549806
Sum of electronic and thermal Energies =	-2897.507102
Sum of electronic and thermal Enthalpies =	-2897.506158
Sum of electronic and thermal Free Energies =	-2897.632006

$Int2_{major}$-TPSS-Opt



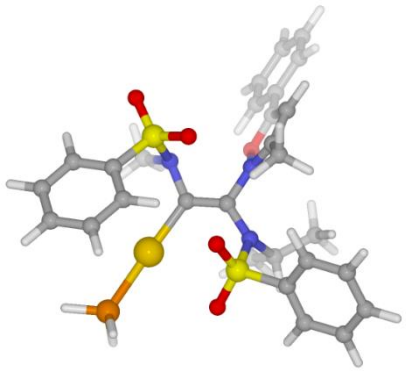
C -0.54179200 0.47986000 -0.06190400
C 0.09231600 -0.71322500 -0.28187600
N -0.07854200 1.76033100 -0.43371500
N -0.54330600 -1.88562900 0.28048100
S 1.46701700 2.30335300 0.12356800
O 1.78504500 1.49609400 1.32259700
O 2.40283500 2.35951700 -1.02801800
S -0.17048000 -2.27087000 1.93055200
O -0.29097300 -1.00331800 2.68289100
O -1.03146200 -3.43243700 2.25873700
C 1.54385200 -2.81006600 1.98931800
C 1.83138900 -4.18415800 1.95658200
C 2.55540800 -1.83577400 2.04053400
C 3.17359100 -4.58977600 1.98761000
H 1.02453000 -4.91290400 1.92750900
C 3.89121000 -2.26185200 2.07113800
H 2.30379500 -0.77785700 2.06602600
C 4.19929000 -3.63204500 2.04547600
H 3.41414000 -5.65151000 1.97417900
H 4.68837300 -1.52177100 2.12139200
C 1.19639400 4.01027900 0.63936800
C 1.37072600 5.04529300 -0.29385300
C 0.88444400 4.27316500 1.98282200
C 1.18937600 6.37060300 0.12610900
H 1.66462300 4.82311700 -1.31729100
C 0.71420300 5.60389000 2.38821900

H 0.80670900 3.45900400 2.69833300
C 0.85636500 6.64928200 1.46116300
H 1.32129400 7.18166000 -0.58784800
H 0.48167700 5.82132400 3.42925700
C -0.62621300 2.46133000 -1.66232900
C -0.75871400 1.49476800 -2.84630300
C -1.93408100 3.20424300 -1.34328300
H 0.13822200 3.20406000 -1.91728100
H -1.53081000 0.73637000 -2.66154700
H 0.19281400 0.98425600 -3.04328700
H -2.76089300 2.50941200 -1.14836400
H -1.80959600 3.86302400 -0.47497500
C -0.52143300 -3.07208500 -0.61338300
H -1.07061200 -3.88238200 -0.12643000
H 0.50682800 -3.38865900 -0.85077000
H 0.72317600 7.68079200 1.78284600
H 5.23913200 -3.95407200 2.07513900
H -1.04634800 2.06349800 -3.74051800
H -2.21689100 3.81984200 -2.20791700
H -1.03577600 -2.79238300 -1.53789900
Au 1.82825100 -0.88984800 -1.38402200
P 3.78854300 -1.14532200 -2.64104100
H 4.94030300 -0.48265300 -2.18200100
H 4.29104700 -2.44867600 -2.80125300
H 3.76673100 -0.71678800 -3.97998700
N -1.87428100 0.48915300 0.50932200
O -2.85267000 -0.15305100 -0.27693300
C -2.45412700 0.99945000 1.60981900
C -4.03379500 -0.03369500 0.39764100
C -3.82450500 0.68376500 1.56518800
C -5.20380900 -0.64710700 -0.21354100
H -4.55460000 0.94139600 2.32035400
C -5.09587500 -1.38076000 -1.41825100
C -6.46555200 -0.50345200 0.40941900
C -6.23508300 -1.96054700 -1.98432100
H -4.12852800 -1.49645700 -1.90242900
C -7.59781200 -1.08790800 -0.16531100
H -6.56069200 0.06211200 1.33420600
C -7.48632500 -1.81686300 -1.36135000
H -6.14729500 -2.52563700 -2.91043700
H -8.56594600 -0.97459200 0.31884200
H -8.37047100 -2.27088700 -1.80567800
C -1.68828400 1.76178400 2.63817400
H -0.63436100 1.47286200 2.63044400
H -1.77683900 2.83771300 2.43372800
H -2.11455500 1.56304800 3.62703800

IEFPCM(1,2-dichloroethane)-PBE/6-31+G(d)/SDD(Au):

Zero-point correction =	0.548409 (Hartree/Particle)
Thermal correction to Energy =	0.591180
Thermal correction to Enthalpy =	0.592124
Thermal correction to Gibbs Free Energy =	0.466322
Sum of electronic and zero-point Energies =	-2899.533865
Sum of electronic and thermal Energies =	-2899.491094
Sum of electronic and thermal Enthalpies =	-2899.490150
Sum of electronic and thermal Free Energies =	-2899.615952

Int2$_{major}$-M06-6-31+G(d)/LANL2DZ-Opt



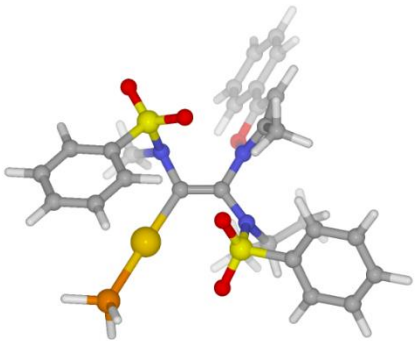
C -0.54352200 0.49786700 -0.11048600
C -0.01920300 -0.73110800 -0.30640600
N 0.03617800 1.73290700 -0.43763700
N -0.77891500 -1.84056300 0.19001400
S 1.57305500 2.13445500 0.16506700
O 1.73398400 1.38023500 1.40157400
O 2.55681700 2.01806600 -0.90881500
S -0.45104800 -2.32625600 1.78942900
O -0.59931600 -1.12772600 2.60390500
O -1.27457300 -3.50275900 2.01649400
C 1.25979600 -2.80571900 1.79527500
C 1.59373800 -4.11762200 1.46160400
C 2.23087700 -1.83676200 2.04402100
C 2.93899300 -4.46324800 1.37335900
H 0.81033000 -4.85518200 1.29438100
C 3.57273700 -2.20033700 1.95667600
H 1.94110800 -0.81979400 2.30214100
C 3.92407600 -3.50660900 1.61979500

H 3.21855400 -5.48554500 1.12573700
H 4.34271500 -1.45809600 2.16267200
C 1.42017200 3.86277600 0.55683200
C 1.80875200 4.81717100 -0.38052800
C 0.93033700 4.22458500 1.81027500
C 1.65899500 6.16480700 -0.06677300
H 2.24124500 4.50692500 -1.33014200
C 0.79044100 5.57441900 2.11275200
H 0.69456200 3.45705500 2.54459900
C 1.14255600 6.54097700 1.17126400
H 1.95727800 6.92240900 -0.78866000
H 0.41899600 5.87380500 3.09087100
C -0.44022700 2.47801700 -1.64267900
C -0.60578900 1.55689600 -2.83693800
C -1.69506100 3.27554100 -1.32028900
H 0.36196300 3.18868600 -1.88229400
H -1.39752000 0.81280300 -2.67150000
H 0.32741800 1.02127300 -3.05429600
H -2.55882900 2.62222200 -1.13250100
H -1.54151100 3.91533500 -0.43982100
C -0.91527000 -2.92865600 -0.77949200
H -1.55041600 -3.71091800 -0.35496300
H 0.06196000 -3.34701000 -1.07722100
H 1.02991800 7.59637400 1.41219400
H 4.97488000 -3.78751300 1.56239800
H -0.88120100 2.14540300 -3.72098900
H -1.95856300 3.92121800 -2.16775800
H -1.40270700 -2.51852900 -1.67229400
Au 1.85172500 -1.01216100 -1.17749800
P 4.07123800 -1.20941700 -2.00908300
H 5.01466800 -0.43828800 -1.30877400
H 4.70947400 -2.46203900 -1.99085500
H 4.35418700 -0.80893900 -3.32586100
N -1.87673400 0.60980500 0.42903100
O -2.87555200 0.06681000 -0.34419700
C -2.38463300 1.04237700 1.58086600
C -4.01716900 0.16510300 0.36068900
C -3.75944400 0.78204500 1.56424000
C -5.21814600 -0.36163600 -0.25014100
H -4.45740900 1.00011300 2.36180300
C -5.16815100 -1.01998200 -1.48722400
C -6.44447700 -0.21026900 0.41194200
C -6.33415400 -1.52009700 -2.04916800
H -4.21748100 -1.14070700 -2.00369600
C -7.60533300 -0.71371800 -0.15641700
H -6.49102000 0.30362000 1.37091200
C -7.55134500 -1.36857500 -1.38613500
H -6.29502100 -2.03191200 -3.00835400
H -8.55560200 -0.59476700 0.35950400
H -8.46319600 -1.76296700 -1.83043500
C -1.55657900 1.69056800 2.61703400
H -0.51118100 1.37304500 2.54352200
H -1.62173000 2.78202100 2.50150500
H -1.93517700 1.42573700 3.60955900

IEFPCM(1,2-dichloroethane)-M06/6-31+G(d)/LANL2DZ(Au):

Zero-point correction =	0.557058 (Hartree/Particle)
Thermal correction to Energy =	0.598039
Thermal correction to Enthalpy =	0.598984
Thermal correction to Gibbs Free Energy =	0.480129
Sum of electronic and zero-point Energies =	-2897.724401
Sum of electronic and thermal Energies =	-2897.683419
Sum of electronic and thermal Enthalpies =	-2897.682475
Sum of electronic and thermal Free Energies =	-2897.801329

Int2$_{major}$-M06/def2-TZVPP-Opt



C -0.53972100 0.48471500 -0.09882700
C 0.02107500 -0.71975600 -0.28334300
N 0.00979100 1.72814800 -0.43119900
N -0.69519200 -1.85717000 0.20393700
S 1.49848900 2.18695900 0.17733500
O 1.67800600 1.45688000 1.39242600
O 2.47486300 2.11298700 -0.86685000
S -0.39603300 -2.33674300 1.77796900
O -0.55432000 -1.17224900 2.58951900
O -1.19187900 -3.49889900 1.99111800

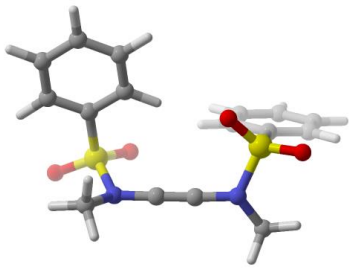
C 1.30394500 -2.79474000 1.78489300
C 1.65612600 -4.09080500 1.43467100
C 2.26721900 -1.83054500 2.04760600
C 2.99621500 -4.42266900 1.34417900
H 0.88585300 -4.82999100 1.25642800
C 3.60510500 -2.17825400 1.95962900
H 1.97262800 -0.82597100 2.32089500
C 3.96741700 -3.46793200 1.60512400
H 3.28301300 -5.43259300 1.08250000
H 4.36397600 -1.43787600 2.17849500
C 1.27779900 3.89473500 0.55994300
C 1.64087900 4.86154700 -0.36563400
C 0.77023000 4.24731800 1.80180500
C 1.45236600 6.19663900 -0.05548300
H 2.08584200 4.56831200 -1.30732700
C 0.59107000 5.58441900 2.10328700
H 0.55465100 3.48059200 2.53302400
C 0.92058600 6.55625700 1.17145300
H 1.73195900 6.95786400 -0.77150400
H 0.20632200 5.87038500 3.07321400
C -0.48545100 2.45023100 -1.63658800
C -0.60592000 1.52670800 -2.82770200
C -1.76988200 3.19681900 -1.33368900
H 0.28601800 3.18683300 -1.86693200
H -1.36748000 0.76019700 -2.66723900
H 0.34175600 1.02754100 -3.03521000
H -2.60819700 2.51522100 -1.17628000
H -1.65928500 3.82535600 -0.44757400
C -0.82866900 -2.92511200 -0.78150800
H -1.43443400 -3.72519500 -0.36456000
H 0.14543300 -3.31649000 -1.09984500
H 0.77784300 7.60187000 1.41097900
H 5.01452700 -3.73699100 1.54600200
H -0.89354800 2.10093900 -3.70837100
H -2.03414700 3.83903500 -2.17417900
H -1.33432900 -2.51627600 -1.65704900
Au 1.90123900 -0.95466400 -1.16122300
P 4.06968400 -1.12899000 -2.01301900
H 5.02912600 -0.34712900 -1.35152100
H 4.71864400 -2.37369600 -1.99734600
H 4.32269800 -0.74637500 -3.33926700
N -1.87934800 0.56058100 0.42580900
O -2.85589900 -0.00471700 -0.34888300
C -2.40098800 0.98484700 1.56568600
C -3.99912000 0.07598800 0.34335600
C -3.76462400 0.69858100 1.54065500
C -5.18505000 -0.47447700 -0.26610400
H -4.47016400 0.90584700 2.32495200
C -5.12592500 -1.12305600 -1.49966300
C -6.40718700 -0.35865600 0.39564200
C -6.27450200 -1.64572100 -2.05713000
H -4.18111600 -1.21794000 -2.01852800
C -7.55067900 -0.88390800 -0.16801500
H -6.46253500 0.14497700 1.35214600
C -7.48565700 -1.52764200 -1.39374400
H -6.22663100 -2.14894000 -3.01335800
H -8.49644100 -0.79172300 0.34846800
H -8.38403600 -1.93946700 -1.83448700
C -1.59591800 1.64131100 2.60598100
H -0.54101100 1.39534500 2.50019800
H -1.73024300 2.72329300 2.53491600
H -1.93651600 1.31887100 3.58799500

IEFPCM(1,2-dichloroethane)-M06/def2-TZVPP:

Zero-point correction =	0.558290 (Hartree/Particle)
Thermal correction to Energy =	0.598781
Thermal correction to Enthalpy =	0.599725
Thermal correction to Gibbs Free Energy =	0.481421
Sum of electronic and zero-point Energies =	-2898.821573
Sum of electronic and thermal Energies =	-2898.781082
Sum of electronic and thermal Enthalpies =	-2898.780138
Sum of electronic and thermal Free Energies =	-2898.898442

7.5.2b Symmetric Yndiamide Cycle

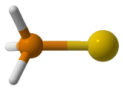
Yndiamide-Symmetric



C -0.58223200 1.87188400 0.17384700
C 0.58267300 1.87200300 -0.17222600
N -1.84453200 1.83684000 0.62936700
N 1.84497200 1.83735200 -0.62778000

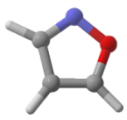
S -2.33406800 0.38689000 1.41414100
O -1.12502500 -0.18318400 1.99161500
O -3.47106100 0.73786300 2.25445900
S 2.33444000 0.38806600 -1.41386200
O 1.12544700 -0.18123100 -1.99220600
O 3.47172100 0.73966900 -2.25352200
C 2.90233600 -0.63702200 -0.08082500
C 4.26626200 -0.87466400 0.06386000
C 1.96365500 -1.12667900 0.82756700
C 4.69703200 -1.64522700 1.14052500
H 4.97171200 -0.46683300 -0.65704700
C 2.41136400 -1.88588100 1.90196800
H 0.90165600 -0.91493700 0.71192600
C 3.77320100 -2.14723000 2.05465600
H 5.75818800 -1.85003300 1.26528000
H 1.69217000 -2.27355400 2.62070700
C -2.90249100 -0.63675800 0.08021700
C -4.26645800 -0.87441700 -0.06406100
C -1.96418800 -1.12534100 -0.82914300
C -4.69765700 -1.64389100 -1.14132800
H -4.97160300 -0.46742500 0.65761700
C -2.41232800 -1.88346800 -1.90412700
H -0.90215400 -0.91357800 -0.71379900
C -3.77420400 -2.14482100 -2.05643200
H -5.75885000 -1.84868600 -1.26579600
H -1.69344100 -2.27030500 -2.62362000
C -2.89125900 2.53605200 -0.13539300
H -3.82671400 2.50704700 0.43038100
C 2.89172400 2.53571000 0.13772800
H 3.82711400 2.50746600 -0.42818600
H 3.03242100 2.07813200 1.12642200
H -4.11800400 -2.74174700 -2.89898400
H 4.11666800 -2.74500300 2.89674200
H 2.58125700 3.57710400 0.25506100
H -3.03181000 2.07964400 -1.12464500
H -2.58087900 3.57762200 -0.25140100
Zero-point correction = 0.300212 (Hartree/Particle)
Thermal correction to Energy = 0.323493
Thermal correction to Enthalpy = 0.324437
Thermal correction to Gibbs Free Energy = 0.244651
Electronic Energy (DLPNO-CCSD(T)/def2-TZVPP) = -1823.397137

PH3Au+



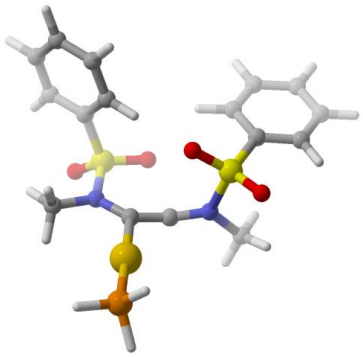
Au -0.44167100 0.00000700 0.00000000
P 1.83971400 0.00001100 -0.00000400
H 2.43240000 0.39290100 1.20353500
H 2.43123200 -1.23932000 -0.26136400
H 2.43264600 0.84571100 -0.94214800
Zero-point correction = 0.028054 (Hartree/Particle)
Thermal correction to Energy = 0.031792
Thermal correction to Enthalpy = 0.032736
Thermal correction to Gibbs Free Energy = 0.000318
Electronic Energy (DLPNO-CCSD(T)/def2-TZVPP) = -477.923766

Isoxazole



C 1.10114500 0.22692000 0.00005900
O 0.55570800 -0.99765200 -0.00019400
C -1.06315600 0.40974100 0.00007600
C 0.13060000 1.17563500 0.00022200
N -0.82725700 -0.87992900 -0.00017500
H 0.24162400 2.25098100 0.00043500
H 2.18342100 0.26057400 0.00007000
H -2.09144800 0.75538500 0.00013500
Zero-point correction = 0.057955 (Hartree/Particle)
Thermal correction to Energy = 0.061537
Thermal correction to Enthalpy = 0.062481
Thermal correction to Gibbs Free Energy = 0.031758
Electronic Energy (DLPNO-CCSD(T)/def2-TZVPP) = -245.648888

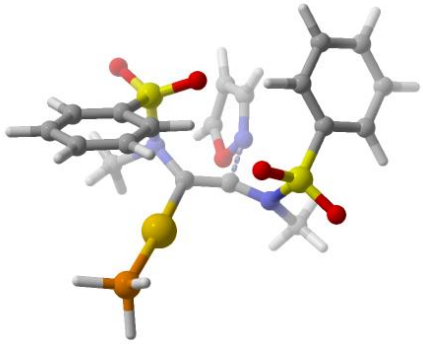
Int1



C -0.15506900 -0.72372700 -1.09211400
C -0.89275700 0.31506300 -0.80039300
N 0.50769700 -1.79566700 -0.90206300
N -0.67575600 1.63829000 -0.99716400
S 1.22134500 -2.10134700 0.73440600
O 0.90896100 -0.89432500 1.48116100
O 0.70037800 -3.39952400 1.13444400
S 0.89872500 2.19789000 -1.39737900
O 1.68932400 0.97607300 -1.52051300
O 0.77652400 3.11737900 -2.51858600
C 1.38623800 3.10460500 0.04369100
C 1.61556200 4.47363500 -0.06215500
C 1.51917300 2.41330000 1.24836700
C 2.00596000 5.16909000 1.07943400
H 1.49354100 4.97859000 -1.01806500
C 1.90698400 3.12495200 2.37737100
H 1.31728600 1.34268600 1.30741300
C 2.15096400 4.49675300 2.29094500
H 2.19506700 6.23869400 1.01964100
H 2.01781900 2.60750000 3.32797100
C 2.94596700 -2.21114200 0.38845400
C 3.53519800 -3.47276900 0.31891900
C 3.65863500 -1.03195300 0.16832600
C 4.89431400 -3.54832500 0.03291400
H 2.94313000 -4.36882800 0.49347900
C 5.01459700 -1.13073700 -0.11963500
H 3.16399600 -0.06305500 0.21223600
C 5.62740600 -2.38258600 -0.18465900
H 5.38015600 -4.52007100 -0.01909900
H 5.59482300 -0.22708000 -0.29224200
C 0.74458800 -2.84863400 -1.90523500
H 0.49897400 -3.82298100 -1.47209100
C -1.69208200 2.65096600 -0.69570400
H -1.35287300 3.62279700 -1.06680900
H -1.86300700 2.71278800 0.38621500
H 6.69025200 -2.44939500 -0.40874300
H 2.45453000 5.04651100 3.17985800
H -2.62184600 2.39535100 -1.21285900
Au -2.71381500 -0.43856300 -0.0055810
P -4.70840000 -1.22146700 0.94305200
H -4.58831100 -1.99732500 2.10355500
H -5.62499500 -0.24424200 1.35308900
H -5.51379300 -2.04020200 0.14016100
H 0.09839800 -2.64674000 -2.76150600
H 1.79397200 -2.82738700 -2.21811300

Zero-point correction = 0.329389 (Hartree/Particle)
Thermal correction to Energy = 0.358120
Thermal correction to Enthalpy = 0.359065
Thermal correction to Gibbs Free Energy = 0.264674
Electronic Energy (DLPNO-CCSD(T)/def2-TZVPP) = -2301.3848001

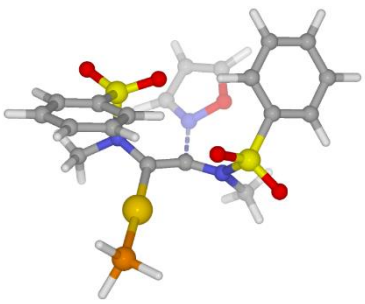
TS1



C 0.86361400 -0.38223400 -1.03629300
C -0.24402100 0.31490200 -0.96533100
N 1.46038700 -1.53780900 -0.95189300
N -0.30696200 1.72421900 -0.91756000
S 1.77704400 -2.21924000 0.66091400
O 0.62259000 -1.83660200 1.45049800
O 2.11917500 -3.59890900 0.37948600
S -0.21832100 2.40066100 0.65499600
O 0.94768600 1.79578900 1.28330700
O -0.32123600 3.83550300 0.45778900
C -1.66866300 1.80905100 1.49226500
C -2.85546100 2.53261700 1.38491900
C -1.60206900 0.59395100 2.17457800
C -4.00601800 2.01958500 1.97692500
H -2.86802100 3.49046800 0.86712800
C -2.76085100 0.09877900 2.76801100
H -0.66009900 0.05170000 2.24863400
C -3.95737900 0.80737900 2.66550300
H -4.93854700 2.57708200 1.91562800
H -2.72033000 -0.83768700 3.32243500
C 3.20440900 -1.32988700 1.20310100
C 4.45615600 -1.72745100 0.73078800
C 3.03769500 -0.24746500 2.06346100
C 5.57219200 -0.99798900 1.12371100
H 4.55318600 -2.60193700 0.08917800
C 4.16831400 0.46395800 2.45407000
H 2.04723300 0.03972900 2.40875500
C 5.42635500 0.09344600 1.98117300
H 6.55940700 -1.29034300 0.77234000
H 4.06133600 1.30810700 3.13283400
C 2.23724400 -2.05786100 -2.08433000
H 3.21624500 -1.56171000 -2.12594900
C -1.33015600 2.31301500 -1.78796400
H -1.25538900 3.40237800 -1.73389200
H -2.34905900 1.98752300 -1.51710900
H 6.30614400 0.65414500 2.29192700
H -4.85745300 0.42186100 3.14223300
H -1.11768400 1.99228700 -2.81337200
Au -1.97800200 -0.87926000 -0.76864500
P -3.95181500 -2.12143000 -0.44100700
H -4.00226800 -2.92030500 0.71324300
H -5.13529600 -1.38012500 -0.28953000
H -4.34923800 -3.04828600 -1.41784600
N 2.36362600 0.96322200 -1.52341700
O 2.10935200 1.39960800 -2.80417700
C 3.00043700 1.93349900 -0.90782600
C 2.61805600 2.62997400 -2.93278500
C 3.20059500 3.03240000 -1.77142800
H 3.69359500 3.97064900 -1.55850600
H 3.27606800 1.80897500 0.13506400
H 2.50044200 3.08445000 -3.90884100
H 2.35438900 -3.13799500 -1.96945800
H 1.68256900 -1.83925100 -3.00180800

Zero-point correction = 0.390333 (Hartree/Particle)
Thermal correction to Energy = 0.422496
Thermal correction to Enthalpy = 0.423441
Thermal correction to Gibbs Free Energy = 0.324279
Electronic Energy (DLPNO-CCSD(T)/def2-TZVPP) = -2547.035438

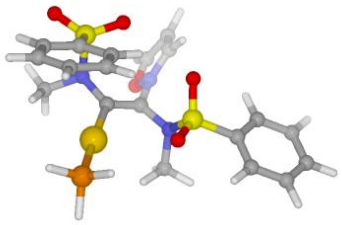
TS1$_{rot}$



C 0.72762100 -0.35057600 -1.23883100
C -0.44726000 0.23718600 -1.17884700
N 1.43457200 -1.41810100 -0.99971800
N -0.64493900 1.62499300 -1.29268900
S 1.65488000 -2.00780900 0.66795400
O 0.50766200 -1.49368700 1.39297600
O 1.88819200 -3.42645400 0.47878900
S -0.29666200 2.55352800 0.11621300
O 0.94918300 2.02756200 0.65360000
O -0.41773900 3.93715900 -0.31100100
C -1.61943500 2.15600300 1.23058300
C -2.78083100 2.92657500 1.21013200
C -1.49603500 1.02406200 2.03571700
C -3.84799600 2.54530500 2.01813600
H -2.83634600 3.81638500 0.58507800
C -2.57086700 0.66049800 2.84233600
H -0.57480600 0.44422200 2.03960000
C -3.74322700 1.41492100 2.82821900
H -4.75964600 3.13941200 2.02315500
H -2.48297700 -0.20933900 3.49153100
C 3.13024600 -1.22156400 1.23119900
C 4.35034600 -1.85766200 1.00464200
C 3.03321600 0.01907100 1.85672800
C 5.51355300 -1.21658900 1.41695600
H 4.38147800 -2.84102500 0.53849000
C 4.20711000 0.64136800 2.26677500
H 2.06534700 0.49437800 2.00239500
C 5.43952600 0.02697400 2.04514100
H 6.47788000 -1.69613400 1.26221700
H 4.15574900 1.60795900 2.76412600
C 2.18866500 -2.12170800 -2.04934300
H 1.93259400 -3.18409800 -2.03414900
C -1.87984700 2.02366500 -1.97836300
H -1.87941600 3.10944600 -2.10991500
H -2.78264000 1.71219600 -1.42625600
H 6.35374600 0.51739700 2.37578200
H -4.57850400 1.12965600 3.46580700
H -1.88731700 1.54832400 -2.96391300
Au -2.03007500 -1.06499000 -0.66876700
P -3.81947700 -2.43475200 0.01198500
H -3.50086400 -3.68113300 0.57437000
H -4.64758200 -1.90376600 1.01497200
H -4.77920200 -2.81651400 -0.93910300
N 2.12316600 1.02439300 -1.84848400
O 3.30842800 0.77044100 -1.20661500
C 2.19891800 2.24457700 -2.32797500
C 4.08413900 1.85541800 -1.31648200
C 3.44715800 2.82826900 -2.02099000
H 3.80477400 3.81544400 -2.27837700
H 1.35220200 2.66340100 -2.85971400
H 5.05880700 1.77766200 -0.85020900
H 3.26617600 -1.99331100 -1.88997600
H 1.91170300 -1.68053000 -3.00992900

Zero-point correction = 0.389394 (Hartree/Particle)
Thermal correction to Energy = 0.421956
Thermal correction to Enthalpy = 0.422900
Thermal correction to Gibbs Free Energy = 0.321974
Electronic Energy (DLPNO-CCSD(T)/def2-TZVPP) = -2547.034823

Int2

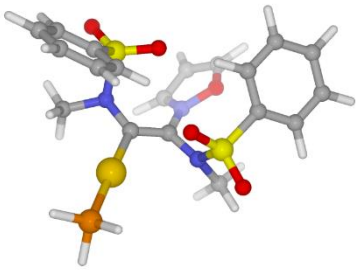


C 0.70258900 1.15387100 -0.75499900
C -0.59631100 0.80387300 -0.86885600
N 1.81332700 0.28296500 -0.77789500
N -1.58493400 1.83114900 -0.76211700
S 2.06141700 -0.57488300 0.67504900
O 1.68613100 0.38076400 1.71538400
O 1.41314500 -1.88467400 0.63189200
S -2.09879000 2.18522900 0.84012200
O -0.90261500 2.57859000 1.57175100
O -3.22803300 3.08558600 0.69065400
C -2.65926100 0.63674600 1.50593300
C -3.98644300 0.25481400 1.31614900
C -1.73121100 -0.19367500 2.13467300
C -4.39068800 -0.99810600 1.76860500
H -4.69046900 0.93829400 0.84388000
C -2.15132600 -1.44507400 2.57848300
H -0.70402500 0.13951600 2.28242700
C -3.47448100 -1.84470300 2.39354700
H -5.42673000 -1.30777200 1.64504200
H -1.44013400 -2.10159000 3.07794000
C 3.81622000 -0.82024600 0.66699500
C 4.32064900 -2.11092800 0.54036500
C 4.64672500 0.29005200 0.81065200
C 5.70160100 -2.28933000 0.55498900
H 3.63916000 -2.95342200 0.44037800
C 6.02195400 0.09680000 0.82298700

H 4.21960900 1.28649200 0.91716700
C 6.54556200 -1.19053000 0.69457300
H 6.11700100 -3.29029800 0.45916200
H 6.68828700 0.94919900 0.93729400
C 2.11842100 -0.42288800 -2.02545800
H 3.10006700 -0.90361800 -1.94182700
C -2.68885000 1.67724400 -1.71883100
H -3.35871500 2.53615300 -1.63307900
H -3.24809300 0.73925800 -1.56121800
H 7.62409100 -1.33628500 0.70620500
H -3.80118500 -2.81871700 2.75607700
H -2.25751000 1.66098200 -2.72466300
Au -1.15471200 -1.21059900 -0.97752300
P -1.74143100 -3.49780900 -0.82550900
H -1.11576500 -4.17422400 0.23627200
H -3.08601200 -3.82284000 -0.57582300
H -1.46539400 -4.37789500 -1.88544600
N 1.07590300 2.53716100 -0.58180800
O 1.00902600 3.34373100 -1.69044700
C 1.45010100 3.24911700 0.46278800
C 1.34982500 4.56645800 -1.27856500
C 1.64686000 4.57664900 0.05294500
H 1.94613700 5.41777700 0.66213400
H 1.53719300 2.76008200 1.42847600
H 1.33605100 5.32886600 -2.04786900
H 1.35918500 -1.18056900 -2.27066600
H 2.16605100 0.31780300 -2.83064800

Zero-point correction = 0.393212 (Hartree/Particle)
Thermal correction to Energy = 0.424862
Thermal correction to Enthalpy = 0.425806
Thermal correction to Gibbs Free Energy = 0.328019
Electronic Energy (DLPNO-CCSD(T)/def2-TZVPP) = -2547.065238

Int2$_{rot}$

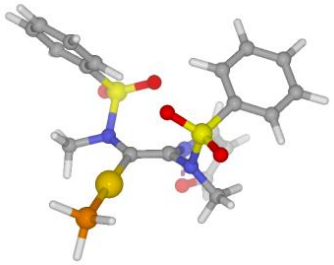


C 0.85929900 -0.23501500 -1.20945400
C -0.44914800 0.12404600 -1.14985300
N 1.36685900 -1.47042700 -0.80753400
N -0.81294500 1.46479100 -1.43105500
S 1.56630100 -1.81416500 0.86692700
O 0.43171000 -1.20374100 1.54457700
O 1.80084100 -3.24704600 0.91492200
S -0.40111400 2.67336700 -0.27346900
O 0.91145100 2.30282400 0.24193400
O -0.60793400 3.94293400 -0.95046800
C -1.60840400 2.48785300 1.01081700
C -2.68710400 3.36762100 1.06560900
C -1.47409400 1.41792000 1.89533500
C -3.65443900 3.17147100 2.04733600
H -2.75253500 4.19439200 0.36034400
C -2.45375000 1.23420100 2.86539000
H -0.62314800 0.74028200 1.83312200
C -3.53823200 2.10772100 2.94049800
H -4.49957700 3.85354800 2.11497600
H -2.36069700 0.41010500 3.57048800
C 3.03749000 -0.96366100 1.37465600
C 4.27190000 -1.57209200 1.15190300
C 2.92734000 0.31403000 1.91759800
C 5.42852300 -0.86785600 1.47150200
H 4.32118400 -2.58580300 0.75710000
C 4.09297900 1.00275600 2.23786000
H 1.94919100 0.76755200 2.06737500
C 5.33747800 0.41604700 2.00996200
H 6.40213400 -1.32821600 1.31507900
H 4.02639800 1.99872300 2.67199000
C 2.21622600 -2.20918000 -1.74371200
H 2.30384500 -3.24474900 -1.40621500
C -2.15800500 1.64651100 -1.99108000
H -2.29519500 2.69764200 -2.26178400
H -2.94287100 1.33266000 -1.28320900
H 6.24603200 0.95756900 2.26871800
H -4.29795400 1.96163600 3.70639300
H -2.23825300 1.03821800 -2.89711500
Au -1.84516800 -1.31173900 -0.54284600
P -3.38262200 -2.95725800 0.16851800
H -3.00339800 -3.74069600 1.27100900
H -4.65611900 -2.53673600 0.58713300
H -3.74325800 -3.96526500 -0.74105200
N 1.84624200 0.66823100 -1.76425500
O 2.98545000 0.90266300 -1.04108300
C 1.81717800 1.48972300 -2.80060800
C 3.63389000 1.88646000 -1.65943900
C 2.95363500 2.30563100 -2.76806600
H 3.23215700 3.07876300 -3.47011400
H 0.98310100 1.45736000 -3.49177400

H 4.57751500 2.16558500 -1.20541100
H 3.22303700 -1.77320500 -1.83972800
H 1.72322900 -2.20469000 -2.72222200

Zero-point correction = 0.392000 (Hartree/Particle)
Thermal correction to Energy = 0.424065
Thermal correction to Enthalpy = 0.425010
Thermal correction to Gibbs Free Energy = 0.325092
Electronic Energy (DLPNO-CCSD(T)/def2-TZVPP) = -2547.068534

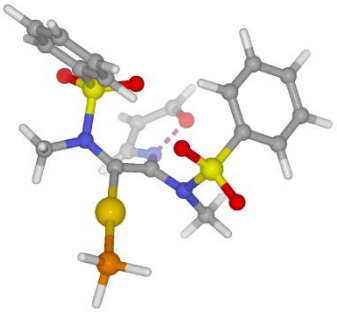
TS2



C -0.81127200 -0.42526100 0.86197300
C 0.56424900 -0.13798000 0.92535900
N -1.22131100 -1.56215400 0.11651500
N 1.01631800 1.05995700 1.36288300
S -1.48779200 -1.31555000 -1.54689500
O -0.38694700 -0.47464700 -1.99961900
O -1.71753900 -2.63827200 -2.10351800
S 0.30039800 2.61605200 0.92716100
O -0.98242500 2.34629400 0.30139100
O 0.41349300 3.46740800 2.09539300
C 1.44089800 3.13146800 -0.32616800
C 2.28134800 4.21309300 -0.08433800
C 1.45371500 2.41753200 -1.52434200
C 3.16067300 4.60047400 -1.09247800
H 2.23696900 4.74000400 0.86739000
C 2.34233500 2.81625300 -2.51513500
H 0.78547400 1.56763200 -1.67758300
C 3.19021800 3.90388200 -2.29849600
H 3.82389800 5.44805000 -0.93304100
H 2.37039600 2.27861200 -3.46066800
C -2.98593100 -0.36463800 -1.65240400
C -4.20968400 -1.01935500 -1.50982300
C -2.90386500 1.01730500 -1.81069500
C -5.37711600 -0.26151200 -1.50499000
H -4.24532900 -2.10474500 -1.42646700
C -4.08064900 1.76168400 -1.80878300
H -1.93425000 1.49838100 -1.92101900
C -5.31109900 1.12442600 -1.65020200
H -6.34126400 -0.75542700 -1.40169800
H -4.03404400 2.84152500 -1.93725500
C -2.00997900 -2.58294800 0.80032200
H -2.16853100 -3.42761700 0.12480100
C 2.43064500 1.19238300 1.74670100
H 2.57151000 2.13611900 2.28243300
H 3.08534300 1.16138400 0.86437900
H -6.22811200 1.71106700 -1.65253800
H 3.88203000 4.21086000 -3.08074200
H 2.67955500 0.37393900 2.42639800
Au 1.84980600 -1.63224400 0.22163700
P 3.23483500 -3.34318200 -0.64454100
H 3.75538200 -4.29172700 0.25050600
H 2.65907500 -4.18790500 -1.60705100
H 4.40738000 -2.95629800 -1.31312600
N -1.68792100 0.15306800 1.69626800
O -1.62249700 -0.44877700 3.25927600
C -2.90547600 0.67271200 1.68897400
C -2.72725800 -0.04580000 3.77408600
C -3.58873200 0.58876700 2.89204000
H -4.55659400 1.01501500 3.11610800
H -1.43460300 -2.92808800 1.66780700
H -2.98695400 -2.20447300 1.14554000
H -3.22324300 1.16871800 0.77106100
H -2.86338500 -0.19507100 4.84665100

Zero-point correction = 0.389878 (Hartree/Particle)
Thermal correction to Energy = 0.421840
Thermal correction to Enthalpy = 0.422784
Thermal correction to Gibbs Free Energy = 0.323482
Electronic Energy (DLPNO-CCSD(T)/def2-TZVPP) = -2547.041019

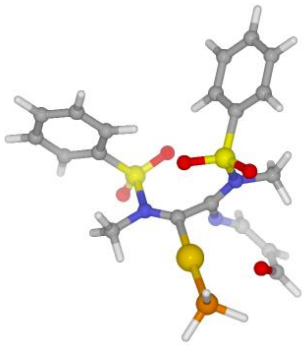
TS2$_{rot}$



C -0.72038400 -0.48079900 1.13446200
C 0.60198500 -0.03753600 0.99276700
N -1.10698200 -1.68958500 0.52861800
N 1.00726900 1.23249600 1.26524700
S -1.34712500 -1.66973100 -1.17165800
O -0.32398200 -0.77213200 -1.69752800
O -1.39217500 -3.07142000 -1.55364200
S 0.16457300 2.66663400 0.69928000
O -1.13932800 2.21960100 0.24598800
O 0.30208200 3.66163700 1.74825200
C 1.16055600 3.11459400 -0.69410400
C 1.91047600 4.28566700 -0.64073400
C 1.16510900 2.26494700 -1.80053200
C 2.68302100 4.62455000 -1.74833500
H 1.87813200 4.91612700 0.24615000
C 1.94775000 2.61849200 -2.89331800
H 0.57551600 1.34559400 -1.80703000
C 2.70077500 3.79365600 -2.86614400
H 3.27235200 5.53898100 -1.73557900
H 1.96716500 1.97544100 -3.77085400
C -2.93305100 -0.92882500 -1.44643700
C -4.07820600 -1.71461200 -1.31815300
C -2.99716600 0.43086500 -1.73906200
C -5.32044300 -1.10961400 -1.47466900
H -3.99434600 -2.78293000 -1.12520600
C -4.24712900 1.01852700 -1.90275100
H -2.08304900 1.01285100 -1.83305900
C -5.40268500 0.25250200 -1.76437100
H -6.22637200 -1.70583700 -1.38468300
H -4.31602600 2.07828700 -2.14085700
C -1.95666600 -2.60317100 1.29214700
H -2.02795900 -3.55187800 0.75398900
C 2.43548600 1.48396200 1.51532000
H 2.55540300 2.48967800 1.93032100
H 3.02320600 1.38992200 0.59110700
H -6.37849000 0.71754100 -1.89459900
H 3.30885200 4.06285300 -3.72784400
H 2.79150600 0.76216800 2.25473600
Au 1.95481600 -1.51152200 0.34743700
P 3.38806300 -3.19963000 -0.46471000
H 3.91521900 -4.12421100 0.45118400
H 2.83310800 -4.06869600 -1.41779000
H 4.56025100 -2.80405700 -1.12878700
N -1.60772400 0.09193500 1.98256600
O -3.05818000 0.69815500 1.40661300
C -1.48199900 0.76311400 3.12083700
C -3.43543800 1.46933100 2.35598500
C -2.53022800 1.62106200 3.39962900
H -2.65661200 2.21472400 4.29423500
H -0.61084200 0.56369200 3.74187300
H -4.44593200 1.87861700 2.29286400
H -2.96474900 -2.19718100 1.46582800
H -1.47276600 -2.78838900 2.25745700

Zero-point correction =	0.390073 (Hartree/Particle)
Thermal correction to Energy =	0.421876
Thermal correction to Enthalpy =	0.422820
Thermal correction to Gibbs Free Energy =	0.324497
Electronic Energy (DLPNO-CCSD(T)/def2-TZVPP) =	-2547.043235

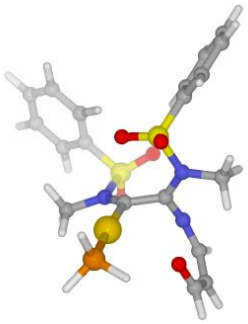
Z-Int3



C -0.42917700 0.47507500 1.23047400
C -0.47359700 -0.75948300 0.38962200
N -0.25193000 1.71100900 0.65126700
N 0.36758600 -1.73379100 0.56610400
S 0.32863400 1.89123900 -0.94718900
O 0.80946400 0.56064500 -1.31814700
O -0.70968400 2.53309700 -1.73752000
S 1.91332800 -1.57914100 1.50362400
O 2.11962600 -0.15148800 1.66962400
O 1.76559100 -2.46546300 2.64283400
C 3.06841000 -2.24008000 0.34656900
C 3.65092300 -3.47752000 0.61258200
C 3.36145900 -1.49478300 -0.79632000
C 4.57508900 -3.97610900 -0.30007300
H 3.39166800 -4.02842600 1.51442800
C 4.28031300 -2.01606600 -1.69849200
H 2.87096000 -0.54013200 -0.98295300
C 4.88471400 -3.24894200 -1.44835600
H 5.05173900 -4.93561800 -0.11284700
H 4.52637000 -1.45763100 -2.59879200
C 1.68849200 3.00987500 -0.77039000
C 1.62350600 4.24916300 -1.40306300
C 2.79369000 2.60706100 -0.02162000
C 2.71218200 5.10845400 -1.28422800
H 0.74174300 4.52901100 -1.97552000
C 3.86877200 3.48026400 0.08913600
H 2.80592500 1.63576600 0.47035000
C 3.82713600 4.72464100 -0.54160700
H 2.68590500 6.08033300 -1.77206100
H 4.74135200 3.18898000 0.66979000
C -0.58351000 2.93389200 1.38577500
H -0.33575900 3.80175400 0.76825400
C 0.18360900 -3.06791800 -0.03109000
H 0.59311500 -3.82493200 0.64456200
H 0.69107400 -3.11464900 -1.00072700
H 4.67368700 5.40251000 -0.45075900
H 5.60580400 -3.64774100 -2.15912000
H -0.88737500 -3.24362100 -0.15478100
Au -2.22375300 -0.88418500 -0.76718200
P -4.20675300 -0.94081700 -2.03392700
H -4.10210100 -0.62985600 -3.39640200
H -4.90443500 -2.15533000 -2.08150600
H -5.21399900 -0.05686200 -1.62257900
N -0.76715600 0.23303700 2.43107000
O -3.40350100 0.98003500 1.45402700
C -1.28921500 0.86530500 3.50505600
C -3.57828600 1.29587500 2.63083900
C -2.56415100 1.32375100 3.65857000
H -2.85552300 1.67994600 4.64452400
H -1.65339100 2.96079300 1.61017000
H 0.00891500 2.98862300 2.30615600
H -0.62813200 0.86573700 4.37668700
H -4.59477000 1.58957200 2.97056400

Zero-point correction =	0.389347 (Hartree/Particle)
Thermal correction to Energy =	0.423035
Thermal correction to Enthalpy =	0.423979
Thermal correction to Gibbs Free Energy =	0.319555
Electronic Energy (DLPNO-CCSD(T)/def2-TZVPP) =	-2547.090366

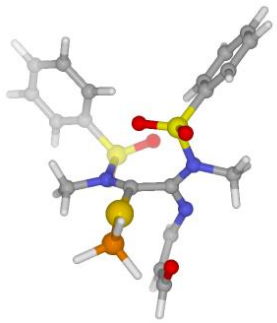
TS_{flip}



C -0.38990300 0.40270700 1.23690100	C 3.93954700 4.74414300 0.03155800
C -0.46780900 -0.75682500 0.30011700	H 2.85326300 6.21927300 -1.10654900
N -0.19246000 1.67745000 0.77108900	H 4.80005900 3.09493800 1.12590100
N 0.34053000 -1.76834100 0.38666300	C -0.60639900 2.80434900 1.60860500
S 0.44293700 1.99919400 -0.78424800	H -0.60574000 3.71522100 1.00281000
O 0.91003400 0.69596200 -1.25382300	C 0.11290100 -3.04208200 -0.31056100
O -0.56017500 2.73211000 -1.53326800	H 0.42134300 -3.86636200 0.34110700
S 1.89533100 -1.73455000 1.34164400	H 0.68696100 -3.06497000 -1.24368500
O 2.12983900 -0.33001600 1.61478400	H 4.78355400 5.40473700 0.22114200
O 1.70405700 -2.70953400 2.39480000	H 5.53436500 -3.63117800 -2.46228200
C 3.03410300 -2.33306500 0.13668500	H -0.95506200 -3.13093400 -0.52443200
C 3.57784300 -3.60427200 0.31222400	Au -2.23679700 -0.64866900 -0.82700800
C 3.35394800 -1.51384300 -0.94687100	P -4.22441600 -0.29782000 -2.03713100
C 4.48899500 -4.06327900 -0.63311800	H -4.12771300 0.31900100 -3.29367400
H 3.30004900 -4.20708600 1.17502700	H -5.04016500 -1.39725100 -2.34629100
C 4.25883500 -1.99748300 -1.88376400	H -5.13510000 0.54537900 -1.38263100
H 2.89195400 -0.53316700 -1.06146300	N -0.72462700 0.15689800 2.42530100
C 4.82377900 -3.26361800 -1.72444100	O -3.38831200 0.67044400 1.36996500
H 4.93718700 -5.04746900 -0.51627200	C -1.47040000 -0.08351900 3.48558800
H 4.52499300 -1.38324400 -2.74114400	C -3.72094900 0.35980600 2.52047000
C 1.80817700 3.07241600 -0.44663200	C -2.84031100 -0.01295000 3.58535700
C 1.77233400 4.36737200 -0.95836800	H -3.27834500 -0.25449100 4.55088800
C 2.88146100 2.59187700 0.30393000	H -1.62508100 2.62516700 1.96838800
C 2.85680400 5.20473700 -0.71379800	H 0.08394100 2.92455400 2.45237500
H 0.91466700 4.70232400 -1.53852600	H -0.89724400 -0.36640400 4.37321900
C 3.95243300 3.44500500 0.54048500	H -4.79957400 0.36898400 2.78727900
H 2.87265600 1.57820900 0.70385100	

Zero-point correction =	0.389679 (Hartree/Particle)
Thermal correction to Energy =	0.422545
Thermal correction to Enthalpy =	0.423489
Thermal correction to Gibbs Free Energy =	0.322514
Electronic Energy (DLPNO-CCSD(T)/def2-TZVPP) =	-2547.078094

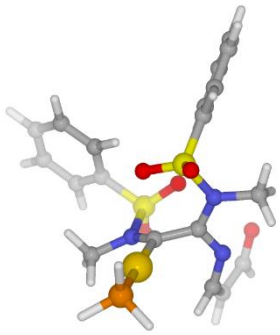
***E*-Int3**



C 0.31646700 -0.43345400 1.32281900
C 0.56754200 0.61278900 0.28797900
N 0.03611500 -1.72113800 0.91274000
N -0.08653400 1.73219800 0.25739700
S -0.66011100 -2.06509000 -0.59638200
O -0.96409400 -0.74761000 -1.15774800
O 0.22124200 -2.97329300 -1.30692300
S -1.65565900 2.02409200 1.14975600
O -2.07378000 0.71019700 1.59664400
O -1.35071600 3.09407700 2.07814500
C -2.68526900 2.60680600 -0.15550700
C -3.03892300 3.95552100 -0.16680800
C -3.11742300 1.70050800 -1.12498900
C -3.86751500 4.40672500 -1.18814900
H -2.68241200 4.62490900 0.61404500
C -3.93729000 2.17666200 -2.14070100
H -2.80578200 0.65666300 -1.09378100
C -4.31040700 3.52089100 -2.16918900
H -4.16781700 5.45177700 -1.21647300
H -4.28772300 1.49477400 -2.91234000
C -2.15040800 -2.92340700 -0.17785700
C -2.30909700 -4.23057600 -0.63058200
C -3.12328700 -2.26888000 0.57837400
C -3.49035500 -4.89898300 -0.32163600
H -1.52292400 -4.70511400 -1.21452300
C -4.29401400 -2.95447200 0.87909600
H -2.96381000 -1.25094600 0.93472200
C -4.47613500 -4.26251000 0.42851700
H -3.63792400 -5.91985500 -0.66753100
H -5.06628100 -2.46677600 1.47030900
C 0.30339900 -2.83003900 1.82894800
H 0.26826300 -3.76769500 1.26589200
C 0.32529800 2.87420600 -0.57263600
H 0.06538800 3.80477600 -0.05808300
H -0.17855700 2.82679500 -1.54488500
H -5.39667800 -4.79120300 0.66881700
H -4.95593100 3.88212200 -2.96748900
H 1.40914600 2.82946200 -0.70644100
Au 2.30649700 0.16968900 -0.81063100
P 4.23755400 -0.52655300 -1.96084200
H 4.08648300 -1.56819400 -2.88857200
H 4.95754100 0.40650000 -2.72254100
H 5.24697600 -1.03974900 -1.13168400
N 0.63351100 -0.22644100 2.53612900
O 3.41092800 -0.29856100 1.74444800
C 1.11267700 0.87920500 3.16713700
C 3.50990500 0.61269100 2.56322900
C 2.40949700 1.28395800 3.22400100
H 2.65108700 2.11984800 3.87768900
H -0.43664300 -2.85158600 2.63788700
H 1.30628900 -2.70094300 2.24875500
H 0.36910200 1.40166700 3.77869800
H 4.51967100 0.97491900 2.85331000

Zero-point correction =	0.389808 (Hartree/Particle)
Thermal correction to Energy =	0.423367
Thermal correction to Enthalpy =	0.424311
Thermal correction to Gibbs Free Energy =	0.321052
Electronic Energy (DLPNO-CCSD(T)/def2-TZVPP) =	-2547.095062

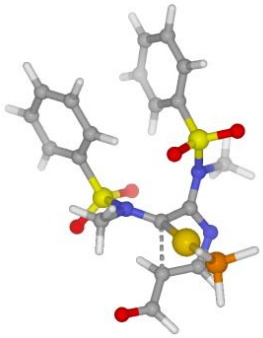
***E*-Int3$_{rot}$**



C -0.37909300 0.21769900 1.42316300	C 4.17465500 4.33813900 -0.05887000
C -0.75811400 -0.65042200 0.27441100	H 3.11117800 6.07818800 -0.76074300
N -0.01838600 1.53826500 1.22895900	H 4.98080300 2.46439500 0.64773000
N -0.09181700 -1.71651000 -0.04383400	C 0.05564300 2.40694200 2.40553100
S 0.19986000 2.20241200 -0.30933500	H 0.35670700 3.41025900 2.08993600
O 0.31074100 1.03412800 -1.19048200	C -0.60625300 -2.74458900 -0.95893000
O -0.84476600 3.18135000 -0.55983200	H -0.19994200 -3.71841000 -0.66747500
S 1.64698200 -2.01243200 0.47512200	H -0.31148100 -2.50883900 -1.98820600
O 2.05651000 -0.74994100 1.04971400	H 5.13248900 4.85269100 -0.00907800
O 1.60818400 -3.25057100 1.22299200	H 4.11216600 -2.85511700 -4.48105700
C 2.40702600 -2.27500200 -1.09569900	H -1.69582200 -2.77385300 -0.87434400
C 2.85215900 -3.55887400 -1.40796000	Au -2.62664100 -0.12192400 -0.52512400
C 2.55012000 -1.19233200 -1.96468500	P -4.66689000 0.66691500 -1.41388800
C 3.47396300 -3.75757900 -2.63602900	H -4.57847300 1.85209500 -2.15891500
H 2.72391300 -4.37311100 -0.69708800	H -5.36372300 -0.16625000 -2.30135100
C 3.16660400 -1.41660200 -3.18967400	H -5.67629000 0.99306400 -0.49634500
H 2.17117200 -0.20571500 -1.69833800	N -0.60097600 -0.19196700 2.60836100
C 3.62727300 -2.69142300 -3.52055100	O 1.58966800 -1.00126100 4.11423600
H 3.83989600 -4.74714900 -2.90070400	C -1.06724400 -1.42568300 2.99080700
H 3.28896300 -0.59197400 -3.88849300	C 0.90742200 -1.97087800 4.38931400
C 1.75476900 3.03663300 -0.17995900	C -0.41222200 -2.26073300 3.82529200
C 1.81137600 4.38048500 -0.54176600	H -0.90323500 -3.18416100 4.12691700
C 2.87648300 2.32650800 0.24858900	H -2.07660000 -1.69078400 2.65027500
C 3.04141400 5.02910100 -0.48125700	H 1.26667400 -2.71516400 5.13559200
H 0.90980200 4.89964800 -0.86074500	H 0.79602900 1.99668200 3.10252200
C 4.09339600 2.99422800 0.30786700	H -0.92146600 2.45845200 2.89705200
H 2.79507200 1.28182700 0.54838100	

Zero-point correction =	0.389385 (Hartree/Particle)
Thermal correction to Energy =	0.423090
Thermal correction to Enthalpy =	0.424034
Thermal correction to Gibbs Free Energy =	0.319763
Electronic Energy (DLPNO-CCSD(T)/def2-TZVPP) =	-2547.093291

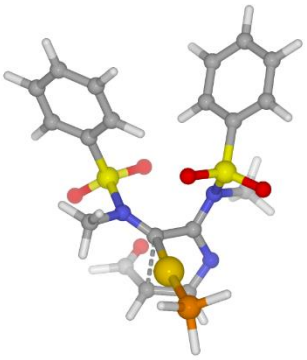
TS3



C 0.54674400 -0.34227900 1.60750000
C 0.94701100 0.47448900 0.43399300
N -0.51554100 -1.20874400 1.62026300
N 0.12318600 1.27412500 -0.25845300
S -0.97282200 -2.13838600 0.24215900
O -0.43205300 -1.43972000 -0.91938800
O -0.58358900 -3.51419200 0.48711600
S -1.12576700 2.20874400 0.55215700
O -1.34805600 1.51532800 1.81530400
O -0.67065700 3.58785500 0.57116100
C -2.51094100 2.04826300 -0.54327000
C -3.50567700 3.01759000 -0.41251600
C -2.62048100 0.98074400 -1.43170900
C -4.65108100 2.89707700 -1.19192700
H -3.38086900 3.85211400 0.27591600
C -3.76640500 0.88904800 -2.21487500
H -1.82978600 0.23610500 -1.51820600
C -4.77883700 1.83766200 -2.08991300
H -5.43985400 3.64138500 -1.10611700
H -3.86609400 0.06810300 -2.92267600
C -2.74394000 -2.01474500 0.28037500
C -3.43284100 -2.98493100 -0.44770100
C -3.39814500 -0.97189300 0.93241600
C -4.81810400 -2.89332700 -0.53040600
H -2.89591400 -3.80064700 -0.92975300
C -4.78549100 -0.90560500 0.84986100
H -2.84023700 -0.22750600 1.49962800
C -5.49079900 -1.85742400 0.11690600
H -5.37383600 -3.64117400 -1.09213600
H -5.31355100 -0.10215800 1.36051900
C -0.84841300 -1.83777000 2.91120500
H -1.76064500 -2.42833900 2.79040300
C 0.58336200 1.87391400 -1.52322900
H -0.18818400 2.53950900 -1.92123900
H 0.75431100 1.06470900 -2.24280200
H -6.57591200 -1.79785100 0.05635800
H -5.67350700 1.75722500 -2.70449200
H 1.49521000 2.45941400 -1.34701000
Au 2.59869700 -0.41394800 -0.58742300
P 4.34641000 -1.49425200 -1.71703400
H 4.53884300 -2.85083900 -1.41773000
H 4.24817300 -1.53428300 -3.11557800
H 5.64395900 -0.98833400 -1.54931600
N 1.33684200 -0.35250300 2.67423600
O 3.30444200 3.24464600 0.41561500
C 2.28151600 0.58413100 2.60963600
C 3.34711100 2.40662000 1.29062000
C 2.15519800 1.69768400 1.78300200
H 1.23329600 2.27829200 1.78746600
H -1.02706500 -1.03941500 3.63820700
H -0.03465000 -2.48443600 3.25364300
H 3.22078500 0.36122800 3.12760800
H 4.31889300 2.08990000 1.73961300

Zero-point correction =	0.389402 (Hartree/Particle)
Thermal correction to Energy =	0.421680
Thermal correction to Enthalpy =	0.422624
Thermal correction to Gibbs Free Energy =	0.324156
Electronic Energy (DLPNO-CCSD(T)/def2-TZVPP) =	-2547.077182

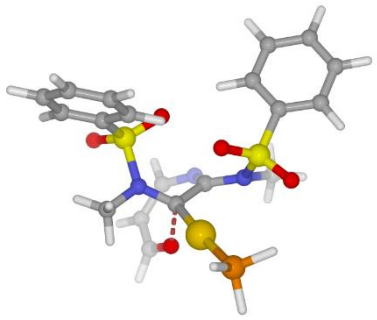
$TS3_{rot}$



C -0.69464000 0.43092000 1.55674800
C -1.00352500 -0.60183000 0.53877700
N 0.39942600 1.26343900 1.50439500
N -0.17813800 -1.51796300 0.01946700
S 0.69026500 2.10604200 0.02591700
O 0.44180700 1.12803000 -1.03034200
O -0.08658400 3.33439400 0.04252600
S 1.30317300 -2.17604300 0.76488400
O 1.75518000 -1.16201600 1.69706000
O 0.97290900 -3.52152000 1.19977500
C 2.39460600 -2.30168400 -0.63220900
C 3.07376800 -3.50945700 -0.78932300
C 2.60433500 -1.21305400 -1.47714200
C 4.00570800 -3.61618500 -1.81726800
H 2.87399000 -4.34304700 -0.11912500
C 3.53395500 -1.34325400 -2.50270900
H 2.03282000 -0.29300200 -1.36125800
C 4.23526000 -2.53728100 -2.66788500
H 4.54975800 -4.54826800 -1.95422300
H 3.70588600 -0.50798200 -3.17869700
C 2.41387900 2.49268000 0.14159400
C 2.80285800 3.77480700 -0.24030800
C 3.32955000 1.51421800 0.52896000
C 4.16136400 4.07702100 -0.24973000
H 2.05546700 4.51570700 -0.51699300
C 4.68065000 1.83951300 0.51963400
H 2.99025900 0.53446600 0.86578000
C 5.09368700 3.11275900 0.12588100
H 4.48942400 5.07130000 -0.54506800
H 5.41313600 1.09708900 0.82993700
C 0.66607900 2.05429700 2.71752700
H 1.63194500 2.55476800 2.60153000
C -0.64144400 -2.31062000 -1.12930700
H 0.02225800 -3.16382400 -1.29670000
H -0.64347900 -1.68045900 -2.02805400
H 6.15424100 3.35732100 0.12144600
H 4.96258200 -2.62912500 -3.47233000
H -1.64812700 -2.69638400 -0.92428900
Au -2.56835600 0.14687200 -0.72895100
P -4.17225800 1.12901300 -2.12732700
H -3.98245000 2.49068500 -2.40512400
H -4.29599900 0.60151300 -3.42120100
H -5.50977400 1.12063300 -1.70420700
N -1.60352700 0.69985600 2.48856800
O -0.53418500 -2.00612000 3.45421900
C -2.59237300 -0.18396700 2.51119900
C -1.35819100 -2.36738500 2.64825900
C -2.41340200 -1.49124700 2.05975800
H -3.30514100 -2.04236900 1.74689500
H -3.57506200 0.19752000 2.80344700
H -1.40752300 -3.42130700 2.30103100
H 0.72772500 1.35335500 3.55545600
H -0.12308100 2.79232100 2.89831700

Zero-point correction =	0.389013 (Hartree/Particle)
Thermal correction to Energy =	0.421362
Thermal correction to Enthalpy =	0.422306
Thermal correction to Gibbs Free Energy =	0.322638
Electronic Energy (DLPNO-CCSD(T)/def2-TZVPP) =	-2547.062741

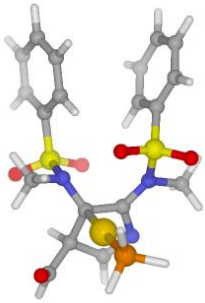
$TS3_{oxazepine}$



C -0.59305800 0.00318800 1.64823300	C -5.20522800 3.15102200 -0.58808700
C 0.68590200 -0.55603200 1.01442400	H -6.67352700 1.65054100 -1.08531600
N -1.81801100 -0.34423900 1.14842500	H -3.54544400 4.43886700 -0.09315200
N 1.71407700 0.34825300 0.80768000	C -2.97140300 -0.29374800 2.05169300
S -2.19891100 -0.21648000 -0.54503100	H -3.80949400 -0.80872200 1.57210100
O -0.97125400 0.21667300 -1.19600400	C 3.02886300 -0.18915900 0.44390300
O -2.84769200 -1.45965500 -0.92220300	H 3.80871400 0.52458500 0.73032900
S 1.61571600 2.07904600 0.75275400	H 3.09052100 -0.38943500 -0.63523100
O 0.20006200 2.40802200 0.68933200	H -5.92749000 3.96527800 -0.59912500
O 2.45280400 2.62647100 1.80942300	H 3.96298600 3.19886700 -4.21803200
C 2.37373000 2.41078500 -0.81420400	H 3.20629700 -1.11554700 0.99807000
C 3.59117700 3.08450000 -0.84393700	Au 0.51584400 -2.17405000 -0.38974100
C 1.70775800 2.01126700 -1.97204500	P 0.16394500 -3.91479800 -1.92646500
C 4.15939100 3.36835000 -2.08267400	H 0.96681400 -3.97406200 -3.07724000
H 4.07286900 3.38391900 0.08523000	H 0.27351300 -5.23875100 -1.47178300
C 2.29337100 2.29936300 -3.19911600	H -1.11773100 -3.93982400 -2.50013300
H 0.75342000 1.48850000 -1.90863400	N -0.56814500 0.66537600 2.76194500
C 3.51319800 2.97506300 -3.25240800	O 1.09706500 -1.54999100 2.31752000
H 5.10825300 3.89841900 -2.13202200	C 0.43836000 0.94244000 3.58870400
H 1.79335600 2.00045300 -4.11817500	C 1.63195300 -1.15275200 3.41572100
C -3.38076900 1.09726200 -0.56128700	C 1.46789500 0.10140500 3.98508600
C -4.71283800 0.80367800 -0.84357400	H 2.08334000 0.38237000 4.83508800
C -2.93399300 2.39018300 -0.28801800	H -3.24880400 0.73957100 2.29633900
C -5.62828500 1.85113400 -0.85985500	H -2.71358700 -0.82866100 2.96965900
H -5.01570200 -0.22065600 -1.05327300	H 0.35238700 1.91941100 4.07190300
C -3.86643800 3.42068600 -0.30265900	H 2.24190400 -1.91502900 3.91539400
H -1.88320100 2.58105400 -0.06937600	

Zero-point correction =	0.389791 (Hartree/Particle)
Thermal correction to Energy =	0.421895
Thermal correction to Enthalpy =	0.422839
Thermal correction to Gibbs Free Energy =	0.323740
Electronic Energy (DLPNO-CCSD(T)/def2-TZVPP) =	-2547.066331

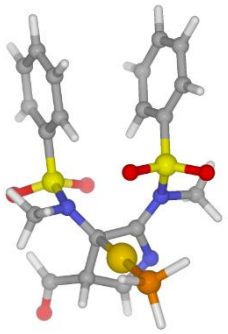
Int4



C -0.67224500 0.07212300 1.58182500
C -0.98034500 -0.92606500 0.57449300
N 0.12150200 1.15836400 1.58472900
N 0.04167700 -1.36817200 -0.33373700
S 0.59025700 2.08697200 0.17466600
O 0.20607100 1.32353300 -1.00067800
O 0.02068300 3.40471600 0.38302000
S 1.28491400 -2.24175300 0.42084700
O 1.44186800 -1.60428800 1.73380100
O 1.01227600 -3.67725600 0.39510400
C 2.69988000 -1.90987000 -0.60251400
C 3.78953000 -2.76235800 -0.42614700
C 2.74628200 -0.81965900 -1.46891000
C 4.96055200 -2.50123800 -1.12934900
H 3.71660400 -3.61757200 0.24421000
C 3.92087000 -0.58409600 -2.17740200
H 1.88044900 -0.17069300 -1.59210000
C 5.02465300 -1.41575000 -2.00251500
H 5.82141100 -3.15461200 -1.00317800
H 3.97112200 0.25840500 -2.86518900
C 2.35271800 2.15586100 0.35015300
C 2.98561500 3.22142200 -0.29054700
C 3.05919500 1.15611100 1.01468200
C 4.37511200 3.27264100 -0.26861900
H 2.40350600 3.99783900 -0.78455900
C 4.44797300 1.23472600 1.03653000
H 2.54461100 0.33054100 1.50694700
C 5.10175700 2.28281000 0.39258300
H 4.89022000 4.09522900 -0.76010200
H 5.01753300 0.46610200 1.55590800
C 0.33128900 1.88455900 2.85721000
H 1.10836900 2.63708000 2.70350400
C -0.39928200 -1.93675100 -1.61182200
H 0.44940200 -2.40508300 -2.12164500
H -0.76727900 -1.11883500 -2.24464600
H 6.18876700 2.33461500 0.41190800
H 5.94095700 -1.22259500 -2.55749300
H -1.18495800 -2.69385900 -1.48376500
Au -2.50932500 0.29822400 -0.50717700
P -4.08039500 1.65148200 -1.58965400
H -5.34994500 1.10380900 -1.82816200
H -4.41962000 2.85948500 -0.96208300
H -3.73651200 2.10478000 -2.87221900
N -1.34062700 -0.16293500 2.78950400
O -3.50140600 -2.38235000 -0.18764900
C -1.91981200 -1.30786700 2.69079200
C -2.99038100 -2.64180600 0.87305500
C -1.71662100 -2.00338800 1.39312000
H -1.02994300 -2.85611400 1.58794100
H 0.66573800 1.16993000 3.61363200
H -0.59112800 2.37576100 3.17892400
H -2.53887600 -1.68616000 3.50668500
H -3.43479900 -3.39752500 1.55707500

Zero-point correction =	0.391396 (Hartree/Particle)
Thermal correction to Energy =	0.423600
Thermal correction to Enthalpy =	0.424544
Thermal correction to Gibbs Free Energy =	0.326479
Electronic Energy (DLPNO-CCSD(T)/def2-TZVPP) =	-2547.116453

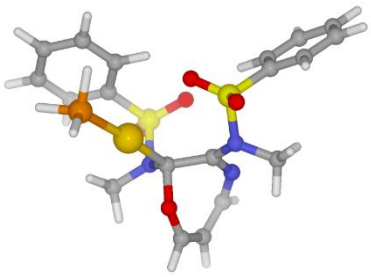
Int4$_{epi}$



C 0.78625700 0.19864100 1.51447000
C 1.14082400 0.98786300 0.34577000
N -0.09927300 -0.80336000 1.71712600
N 0.14030100 1.40016600 -0.59801400
S -0.58365300 -1.96545300 0.51483200
O -0.19640900 -1.42353100 -0.78077000
O -0.01908600 -3.23415800 0.93651400
S -1.17047100 2.30766500 -0.01400300
O -1.24948600 1.96631500 1.40914200
O -1.04272200 3.71622500 -0.38067100
C -2.57946800 1.68027600 -0.90130600
C -3.75062400 2.42526800 -0.75115000
C -2.53827800 0.52111900 -1.66938800
C -4.90984800 1.97992900 -1.37516000
H -3.75020100 3.34190900 -0.16275900
C -3.70579500 0.09755300 -2.29976400
H -1.61783900 -0.04993000 -1.76432000
C -4.88661000 0.81886200 -2.14842700
H -5.83127500 2.54865200 -1.26726400
H -3.68766600 -0.80476600 -2.90853300
C -2.34336800 -1.99305500 0.70876400
C -2.98116500 -3.16114100 0.29139600
C -3.04328700 -0.88367000 1.17963000
C -4.37020400 -3.20746800 0.33901100
H -2.40276900 -4.01790600 -0.05058300
C -4.43082100 -0.95933200 1.23699300
H -2.52342200 0.01753600 1.50728900
C -5.09000200 -2.11096800 0.81111400
H -4.88942100 -4.10842600 0.01949800
H -4.99654300 -0.10957500 1.61437800
C -0.32008900 -1.27456800 3.10297800
H -1.14842400 -1.98744900 3.09874300
C 0.58648900 1.74298900 -1.94861200
H -0.22606000 2.22461800 -2.50249200
H 0.86430400 0.82095600 -2.47749600
H -6.17639700 -2.15862100 0.85670700
H -5.79551700 0.48015200 -2.64252300
H 1.44039600 2.43722400 -1.93716200
Au 2.46830500 -0.56075300 -0.57366700
P 3.92295300 -2.15228500 -1.49295100
H 3.56823500 -3.49181500 -1.27456900
H 4.08559000 -2.13327900 -2.88618200
H 5.25728200 -2.14339400 -1.06168800
N 1.51595300 0.55890100 2.64292400
O 2.66186000 4.28937300 1.39093300
C 2.26065900 1.56210300 2.32037200
C 1.85610400 3.54422300 0.90039200
C 2.13920400 2.02029800 0.91981200
H 3.14501400 1.97041500 0.46410300
H 2.94860600 2.01021700 3.03838000
H 0.92203500 3.89754700 0.42305300
H -0.58903400 -0.41312500 3.71970700
H 0.57670500 -1.75988300 3.49758400

Zero-point correction =	0.391413 (Hartree/Particle)
Thermal correction to Energy =	0.423645
Thermal correction to Enthalpy =	0.424589
Thermal correction to Gibbs Free Energy =	0.326131
Electronic Energy (DLPNO-CCSD(T)/def2-TZVPP) =	-2547.107125

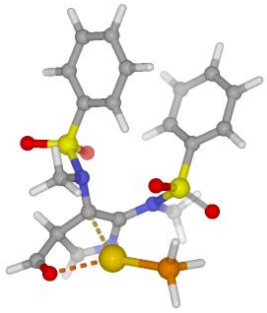
Int4$_{oxazepine}$



C 1.13075200 1.39415600 -0.62515400	C 5.85730200 -0.80114600 2.07007500
C -0.40390700 1.19320900 -0.75970400	H 6.88816600 -1.93240100 0.54889000
N 2.03196700 0.49319300 -1.10457600	H 4.59341200 0.30609100 3.42513000
N -1.09675000 2.00414000 0.24982300	C 3.28314600 1.04529300 -1.65395300
S 2.19496500 -1.15264300 -0.54855800	H 3.79867200 0.25721800 -2.20975800
O 1.04127000 -1.45379400 0.27944500	C -2.47423000 2.37044000 -0.09399100
O 2.48923000 -1.94072000 -1.73256800	H -2.92214100 2.88948100 0.75641800
S -0.91547800 1.52698600 1.87307300	H -3.07661200 1.48926500 -0.36777000
O 0.46145200 1.06227900 1.99998800	H 6.73741600 -0.71247400 2.70405400
O -1.39310200 2.65705400 2.65959800	H -4.36195100 -2.85151800 2.66768100
C -2.00312600 0.15113500 2.16460500	H -2.47419700 3.07448500 -0.93115100
C -3.35979300 0.38432500 2.39338400	Au -1.30659300 -0.72795100 -1.13155900
C -1.47432300 -1.13876800 2.13488300	P -2.46639800 -2.73511000 -1.55091900
C -4.20632200 -0.70603000 2.56577800	H -1.92937500 -3.90790400 -0.99655700
H -3.74897000 1.39838700 2.45550900	H -3.78265600 -2.80306300 -1.06626500
C -2.33276200 -2.21889700 2.32392800	H -2.65669100 -3.13573000 -2.88189800
H -0.40907400 -1.28813300 1.97804200	N 1.55906400 2.57445100 -0.30476400
C -3.69455300 -2.00329800 2.52560400	O -0.56937600 1.86689000 -2.06176400
H -5.26639300 -0.54042500 2.74609700	C 0.99395700 3.75339700 -0.42151100
H -1.93210500 -3.23116800 2.31371000	C -0.43542600 3.16482900 -2.29443000
C 3.63388200 -1.02593000 0.47143600	C 0.15999100 4.10539000 -1.50034600
C 4.82679500 -1.59941800 0.03987800	H 0.03815500 5.15279400 -1.76360300
C 3.52095600 -0.33472300 1.67881000	H 3.93253900 1.43849000 -0.86165600
C 5.94603600 -1.48606000 0.85949600	H 3.02206500 1.84696100 -2.35012100
H 4.87269000 -2.12536500 -0.91168800	H 1.32366900 4.51596000 0.28625200
C 4.65255800 -0.22656800 2.47848700	H -0.89474700 3.43295400 -3.24596800
H 2.57178900 0.10723500 1.98471800	

Zero-point correction =	0.392130 (Hartree/Particle)
Thermal correction to Energy =	0.423559
Thermal correction to Enthalpy =	0.424503
Thermal correction to Gibbs Free Energy =	0.328327
Electronic Energy (DLPNO-CCSD(T)/def2-TZVPP) =	-2547.077551

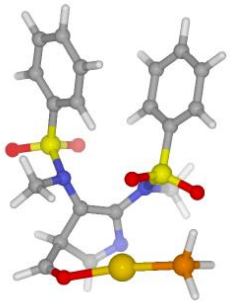
TS4



C 0.73832600 0.12990600 1.60730700
C 0.86642700 1.13931100 0.65108100
N -0.04126100 -0.99414800 1.68497700
N -0.12314900 1.48037100 -0.30116500
S -0.45442200 -1.99576000 0.35605000
O -0.09655100 -1.28852900 -0.86883600
O 0.16450200 -3.29287800 0.59394700
S -1.43937900 2.32475100 0.38945200
O -1.59666800 1.75535400 1.72863400
O -1.23391900 3.76635500 0.27342200
C -2.80164800 1.85043600 -0.65019800
C -3.94460100 2.64432500 -0.55976100
C -2.75719000 0.70648100 -1.44460400
C -5.07591100 2.26770200 -1.27565300
H -3.94358300 3.54303400 0.05550800
C -3.89352400 0.35434500 -2.16693300
H -1.85114700 0.10481500 -1.50187400
C -5.04936000 1.12626500 -2.07662500
H -5.97744000 2.87401300 -1.21561200
H -3.87292600 -0.53257700 -2.79815900
C -2.21423400 -2.14571900 0.51378500
C -2.79053500 -3.26050000 -0.09587400
C -2.97565500 -1.15838900 1.13504500
C -4.17607600 -3.37753000 -0.08629400
H -2.16693600 -4.02552300 -0.55573300
C -4.35980700 -1.30034800 1.14306900
H -2.50665600 -0.29240200 1.60315800
C -4.95641700 -2.40003600 0.53077800
H -4.64623400 -4.24046000 -0.55318200
H -4.97070700 -0.54007200 1.62664800
C -0.18668900 -1.65893500 2.99732200
H -0.97253600 -2.41518300 2.91929200
C 0.33136500 2.03820300 -1.57462300
H -0.53095200 2.32178900 -2.18762600
H 0.88883600 1.25882600 -2.11166300
H -6.04010200 -2.50165500 0.53970800
H -5.93558300 0.84219700 -2.64135200
H 0.96142300 2.93165000 -1.44581700
Au 2.71672700 -0.20191900 -0.62515700
P 2.95213000 -2.33631000 -1.49066100
H 4.22360900 -2.84925500 -1.78913600
H 2.39843000 -3.34915100 -0.69147800
H 2.27195300 -2.53301900 -2.70125300
N 1.52861200 0.37517800 2.75083600
O 3.53093400 1.97843600 -0.20807600
C 2.06177800 1.53252900 2.61459700
C 2.96239400 2.65383400 0.63174000
C 1.70022600 2.21563200 1.32237600
H 1.08080500 3.10683000 1.54258000
H -0.49042200 -0.90849100 3.73215500
H 0.74762900 -2.13687700 3.30547200
H 2.75527100 1.92961200 3.35623000
H 3.40567000 3.61953200 0.93694200

Zero-point correction =	0.391458 (Hartree/Particle)
Thermal correction to Energy =	0.422741
Thermal correction to Enthalpy =	0.423686
Thermal correction to Gibbs Free Energy =	0.327769
Electronic Energy (DLPNO-CCSD(T)/def2-TZVPP) =	-2547.105750

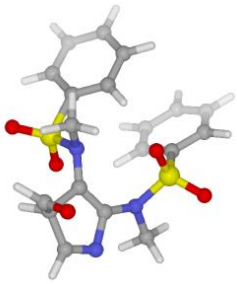
Int5



C -0.62007300 -0.47359800 1.52203200
C -0.38602300 -1.52773300 0.69387800
N 0.04802700 0.73859300 1.65118700
N 0.66739200 -1.74349300 -0.19370000
S 0.16964200 1.78373700 0.33331900
O -0.03413600 0.98550500 -0.87410100
O -0.72721900 2.92463400 0.53404400
S 2.13035400 -2.25176700 0.53745300
O 2.16867700 -1.58317900 1.83362600
O 2.23012300 -3.70606000 0.48460200
C 3.34250800 -1.54761700 -0.55807800
C 4.62311100 -2.09538200 -0.49021700
C 3.04964800 -0.45285700 -1.36964300
C 5.63669300 -1.51801500 -1.24771200
H 4.81826200 -2.96154000 0.14049100
C 4.07227800 0.10046100 -2.13442700
H 2.04107900 -0.04167100 -1.40826500
C 5.36091500 -0.42410600 -2.06752700
H 6.64251700 -1.93092900 -1.20505600
H 3.85757300 0.95113700 -2.77938800
C 1.84733500 2.35150300 0.44347400
C 2.13862300 3.55977500 -0.18974000
C 2.83304900 1.57342400 1.04807600
C 3.45969600 3.99272300 -0.22011400
H 1.34448900 4.15405800 -0.63860300
C 4.14752600 2.02913000 1.01624500
H 2.58709500 0.62847900 1.53414600
C 4.45980400 3.22871100 0.38110300
H 3.70680300 4.93402900 -0.70665200
H 4.92929800 1.43335200 1.48474700
C 0.04962900 1.37611600 2.97684900
H 0.72927600 2.23377300 2.95785400
C 0.34197700 -2.40610100 -1.45115100
H 1.25133700 -2.56614000 -2.03944300
H -0.32976500 -1.75595800 -2.02505300
H 5.49103600 3.57654000 0.35867700
H 6.15681600 0.01746900 -2.66466100
H -0.12299600 -3.39593500 -1.29273100
Au -3.04525100 0.05694200 -0.63693500
P -3.41084000 2.32394400 -0.72086400
H -4.64788800 2.69241200 -1.26991800
H -3.40321800 3.00036100 0.50349400
H -2.49780000 3.04807300 -1.49455900
N -1.68212200 -0.72534400 2.42639900
O -2.98886000 -2.13706800 -0.69329900
C -2.12345800 -1.90240000 2.18912800
C -2.36177800 -2.95614800 -0.03011800
C -1.39198800 -2.59850900 1.05846400
H -0.87711500 -3.50839400 1.41055700
H -2.97372800 -2.32524800 2.72257000
H 0.42956800 0.64632700 3.69928100
H -0.95230000 1.70927700 3.26765000
H -2.54144300 -4.02377500 -0.24594800

Zero-point correction =	0.392801 (Hartree/Particle)
Thermal correction to Energy =	0.424414
Thermal correction to Enthalpy =	0.425358
Thermal correction to Gibbs Free Energy =	0.328034
Electronic Energy (DLPNO-CCSD(T)/def2-TZVPP) =	-2547.114634

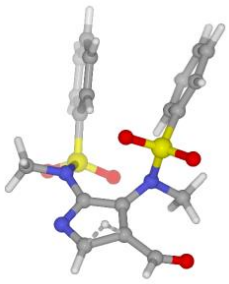
Int6



C 2.08651800 0.98318500 -0.54415600	H -2.42138700 3.35269100 1.51845700
C 2.15525200 -0.28758600 -0.07277600	C -3.12969300 0.91769500 -1.42284200
N 1.02157500 1.87864800 -0.62885200	H -0.98923200 0.64265800 -1.51447800
N 1.13315600 -1.09822900 0.44665000	C -4.18556800 1.54643300 -0.76926500
S 0.05425100 2.28001300 0.69540100	H -4.76473300 2.91528100 0.79515000
O 0.32121100 1.31682300 1.75431300	H -3.32018000 0.23143900 -2.24669800
O 0.18917500 3.70412100 0.96901600	C 1.06833300 2.89475800 -1.68784800
S 0.32524200 -2.05433200 -0.69566000	H 0.07606100 3.34586700 -1.79015900
O 0.27547800 -1.26751700 -1.92483400	C 1.43052200 -1.76983400 1.71130200
O 0.89803600 -3.39881900 -0.74775700	H 0.54442200 -2.30149600 2.07480700
C -1.31123500 -2.17658700 0.00402200	H 1.70224900 -0.99769000 2.43935500
C -2.13741000 -3.15863400 -0.53980600	H -5.20964700 1.35943600 -1.08828900
C -1.76740100 -1.29202600 0.97806500	H -4.95657700 -2.44574800 1.21647300
C -3.45500000 -3.24506600 -0.10444700	H 2.24550700 -2.50483500 1.61008600
H -1.74894400 -3.84563000 -1.29037400	N 3.30804900 1.41306200 -1.11541600
C -3.08384000 -1.40389500 1.41679500	O 4.80295900 -0.38719800 1.65985800
H -1.10678600 -0.52784500 1.38727500	C 4.13032300 0.43528300 -1.01618500
C -3.92605000 -2.36980200 0.87349300	C 4.36873000 -1.18552300 0.86756200
H -4.11292300 -4.00402500 -0.52353000	C 3.55939700 -0.78294700 -0.35868900
H -3.45127500 -0.72056300 2.18065800	H 3.51062400 -1.63567000 -1.05945600
C -1.58710900 2.01795500 0.04326700	H 1.80259100 3.67693900 -1.46834600
C -2.63246300 2.66291200 0.70269500	H 1.32491100 2.39716400 -2.62766500
C -1.81784400 1.14722800 -1.01722700	H 5.16674600 0.52578100 -1.34014600
C -3.93809700 2.41807100 0.29096500	H 4.53817500 -2.27802500 1.00003800

Zero-point correction =	0.362385 (Hartree/Particle)
Thermal correction to Energy =	0.389297
Thermal correction to Enthalpy =	0.390241
Thermal correction to Gibbs Free Energy =	0.304053
Electronic Energy (DLPNO-CCSD(T)/def2-TZVPP) =	-2069.144075

TS5

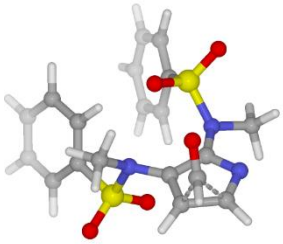


C -1.84609600 -1.56198200 -0.35114700	S 0.50968000 -2.29234000 0.79567400
C -2.19931400 -0.30132500 0.16191700	O 0.07863900 -1.39996900 1.86244100
N -0.58294600 -2.15018800 -0.48185300	O 0.71735800 -3.70335600 1.09133000
N -1.33481800 0.71310300 0.62244300	S -0.86507700 1.79812600 -0.57486700

O -0.75172900 1.00867000 -1.80281600
O -1.71433400 2.98614800 -0.59590000
C 0.76173000 2.30179700 -0.03870600
C 1.29348400 3.41387400 -0.68964600
C 1.49065900 1.59635700 0.91479700
C 2.58826700 3.81832200 -0.38518700
H 0.69515600 3.95538700 -1.42102100
C 2.77822200 2.02629800 1.22453400
H 1.06181000 0.72477800 1.40842900
C 3.32795800 3.12682700 0.57318200
H 3.01670500 4.68210400 -0.89009700
H 3.35556900 1.48564400 1.97286200
C 2.01190900 -1.67972300 0.04974300
C 3.20883600 -2.07101700 0.64772900
C 1.98561600 -0.80262800 -1.03096500
C 4.40467800 -1.56224000 0.15253600
H 3.19981800 -2.77317000 1.48001300
C 3.19171000 -0.31082000 -1.52230700
H 1.03948400 -0.49588000 -1.47845100
C 4.39520400 -0.68465200 -0.93110900
H 5.34726400 -1.85971100 0.60832700
H 3.18215400 0.37979500 -2.36421700
C -0.43133000 -3.18339000 -1.51494900
H 0.63387200 -3.39692800 -1.64829200
C -1.58766400 1.26889300 1.96051200
H -0.86086600 2.06102600 2.16932100
H -1.43325200 0.45711500 2.67943700
H 5.33433000 -0.29232900 -1.31791200
H 4.33843100 3.45172800 0.81581200
H -2.59943700 1.67905900 2.04646100
N -2.88066600 -2.21166200 -0.92800500
O -4.61344000 1.56769600 1.16586300
C -3.93767000 -1.40438000 -0.83733500
C -4.64669300 0.80060000 0.23520300
C -3.58492100 -0.15134500 -0.14801200
H -3.70946600 -0.23935100 -1.44692500
H -0.95590800 -4.10663400 -1.24689700
H -0.83493500 -2.78806200 -2.45139000
H -4.94413300 -1.71395500 -1.11281100
H -5.55066400 0.72774500 -0.41574300

Zero-point correction = 0.359925 (Hartree/Particle)
Thermal correction to Energy = 0.386093
Thermal correction to Enthalpy = 0.387038
Thermal correction to Gibbs Free Energy = 0.304534
Electronic Energy (DLPNO-CCSD(T)/def2-TZVPP) = -2069.106914

TS5'

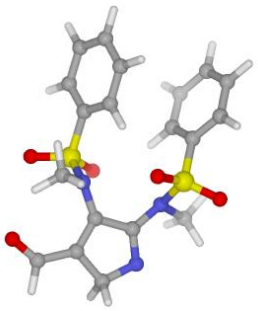


C 2.25644200 0.53347800 -0.62310800
C 2.06259600 -0.78237600 -0.16350600
N 1.32088500 1.56759900 -0.75188900
N 0.91433600 -1.36357600 0.41608200
S 0.46969800 2.15850500 0.58314700
O 0.58012600 1.17704300 1.65389400
O 0.85728800 3.53990800 0.83624500
S -0.07272000 -2.20019300 -0.66778600
O -0.02060200 -1.45501500 -1.92239800
O 0.24724900 -3.62630600 -0.68257400
C -1.68427000 -2.00453400 0.07216500
C -2.68838500 -2.83471100 -0.42318300
C -1.94886000 -1.02349300 1.02418300
C -3.98885800 -2.66708100 0.03899300
H -2.44950000 -3.60202700 -1.15832400
C -3.25289300 -0.88020500 1.49024100
H -1.14971100 -0.38187000 1.39499700
C -4.26962100 -1.69188100 0.99528800
H -4.78362000 -3.30544500 -0.34245000
H -3.47132500 -0.11852700 2.23698200
C -1.20365700 2.18193600 -0.03935300
C -2.10362400 3.02172100 0.61503700
C -1.60759000 1.33684200 -1.06841900
C -3.44046200 3.00208500 0.23209100
H -1.75564400 3.68550600 1.40503300
C -2.94819700 1.33182600 -1.44410600
H -0.89040600 0.68118500 -1.56202000
C -3.86163900 2.15698600 -0.79435300
H -4.15459900 3.65343500 0.73274000
H -3.27536400 0.66644200 -2.24174700
C 1.60193200 2.57706700 -1.77914800
H 0.70439400 3.18501300 -1.93402700
C 1.14059800 -2.02717200 1.70313400
H 0.18806100 -2.38084600 2.11232700
H 1.55986500 -1.28006800 2.38535600
H -4.90952300 2.14521600 -1.08998400
H -5.28836300 -1.56801500 1.35905800
H 1.81780000 -2.88943400 1.61306300

N 3.51474200 0.74205300 -1.05812500
O 4.16252800 -0.02266200 1.79979100
C 4.17565300 -0.41225300 -0.87800200
C 4.49847300 -0.75505300 0.92311900
C 3.31672900 -1.41811600 -0.29557900
H 3.49293500 -2.49242600 -0.25104000
H 2.43907100 3.22494300 -1.49686900
H 1.83924500 2.05176300 -2.70873700
H 5.17228400 -0.57051400 -1.28648200
H 5.37408300 -1.43400200 0.95123700

Zero-point correction = 0.361091 (Hartree/Particle)
Thermal correction to Energy = 0.387282
Thermal correction to Enthalpy = 0.388227
Thermal correction to Gibbs Free Energy = 0.304939
Electronic Energy (DLPNO-CCSD(T)/def2-TZVPP) = -2069.108954

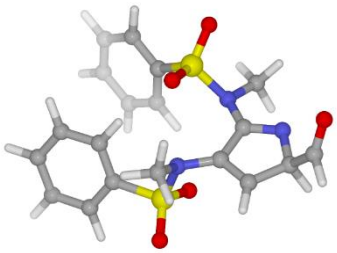
Int7



C -1.86498100 -1.53236800 -0.38994400
C -2.31239500 -0.21252700 0.12874800
N -0.53609500 -1.92083500 -0.64830100
N -1.47785700 0.84075800 0.53127100
S 0.46809500 -2.21712300 0.67783200
O -0.00762800 -1.36552500 1.76378200
O 0.59252600 -3.64935500 0.91275600
S -0.81671800 1.78603000 -0.70338000
O -0.68022200 0.89321800 -1.85144400
O -1.55658400 3.02985200 -0.86111000
C 0.79228500 2.21487300 -0.05817200
C 1.43699400 3.27014200 -0.70245600
C 1.39953500 1.51299800 0.97898700
C 2.72306700 3.61742700 -0.30427300
H 0.93184800 3.81454300 -1.49884500
C 2.67936400 1.88602300 1.38007200
H 0.88461600 0.68595300 1.46675100
C 3.34162200 2.92804900 0.73787500
H 3.23849300 4.43678100 -0.80185800
H 3.16144900 1.34659200 2.19380500
C 2.04126000 -1.63846400 0.06736800
C 3.16738200 -2.07310100 0.76470100
C 2.13895000 -0.76200100 -1.01032300
C 4.41887800 -1.60750900 0.37705500
H 3.06192500 -2.77397900 1.59153600
C 3.40086300 -0.31880100 -1.39653500
H 1.24423400 -0.42555500 -1.53516800
C 4.53444800 -0.73370200 -0.70338600
H 5.30697300 -1.93719400 0.91293100
H 3.49179900 0.36348800 -2.24004500
C -0.37904400 -2.89551300 -1.73767700
H 0.68845900 -3.05825500 -1.91726600
C -1.77827400 1.52049500 1.79873500
H -0.97421000 2.23002800 2.01914700
H -1.78240600 0.75309200 2.58117900
H 5.51712500 -0.37796600 -1.00879400
H 4.34516500 3.20937600 1.05290900
H -2.73228300 2.05607100 1.76229500
N -2.83653400 -2.31946800 -0.69415500
O -4.57799200 1.86460300 0.76075800
C -4.05342500 -1.62146700 -0.38091700
C -4.72088900 0.71297500 0.40542000
C -3.67474500 -0.27602100 0.13915000
H -0.86234300 -3.85031800 -1.50438700
H -0.82850100 -2.45718600 -2.63443100
H -4.63226900 -2.22586100 0.33667900
H -5.74650900 0.31104300 0.22521800
H -4.68836300 -1.53774900 -1.27907600

Zero-point correction = 0.363441 (Hartree/Particle)
Thermal correction to Energy = 0.390037
Thermal correction to Enthalpy = 0.390981
Thermal correction to Gibbs Free Energy = 0.307382
Electronic Energy (DLPNO-CCSD(T)/def2-TZVPP) = -2069.156604

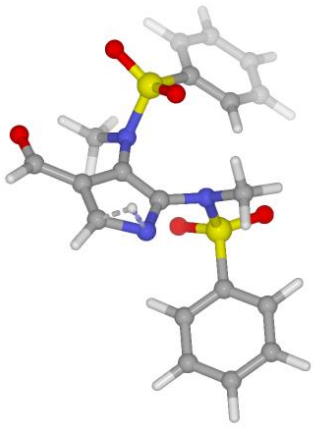
Int7'



C -2.24865100 0.41425800 0.44309100	H 1.75868700 3.68505700 -1.39645700
C -1.97232300 -0.93227600 -0.12086400	C 2.91892700 1.41956100 1.53646100
N -1.32085100 1.44361500 0.64665700	H 0.88666000 0.68240600 1.57146800
N -0.74430700 -1.42616200 -0.62493900	C 3.82494000 2.27451100 0.91574000
S -0.43748300 2.09371900 -0.64504500	H 4.12362100 3.76195600 -0.61919700
O -0.47726600 1.13218600 -1.73943900	H 3.23795900 0.78053100 2.35836800
O -0.87621100 3.46029100 -0.88780900	C -1.68316700 2.43720900 1.66735800
S 0.20004600 -2.20529300 0.53800500	H -0.81853600 3.08166000 1.85550200
O 0.00060300 -1.46008100 1.77827500	C -0.83022000 -2.11182000 -1.91751200
O -0.04305600 -3.64505300 0.53697800	H 0.17222300 -2.40761400 -2.24490100
C 1.85120800 -1.92673600 -0.07535500	H -1.23691300 -1.39612000 -2.63948700
C 2.85214600 -2.71241700 0.49367500	H 4.85771000 2.31196000 1.25844200
C 2.14081600 -0.93283000 -1.00663800	H 5.51596900 -1.33243100 -1.09975300
C 4.17416500 -2.48689500 0.12711500	H -1.45868200 -3.01234900 -1.87328300
H 2.59447300 -3.49191700 1.20930700	N -3.45508500 0.54143300 0.87536100
C 3.46752400 -0.73290300 -1.37793400	O -5.74750700 0.41200400 -0.78813400
H 1.34394100 -0.32476300 -1.43463200	C -4.12129500 -0.70808800 0.62404100
C 4.48019800 -1.50024300 -0.80923600	C -5.36765800 -0.58580200 -0.23833900
H 4.96626300 -3.09025800 0.56643900	C -3.12448500 -1.61705800 -0.02180800
H 3.70636800 0.03698600 -2.10981400	H -3.29643500 -2.65184300 -0.30717300
C 1.20616700 2.17566700 0.04322800	H -2.53680200 3.04710500 1.35324900
C 2.09801200 3.04540300 -0.58308600	H -1.93525900 1.89511200 2.58285800
C 1.59756600 1.36156200 1.10163200	H -4.45385800 -1.15405800 1.58055700
C 3.41578400 3.08715300 -0.14135200	H -5.91712200 -1.55276700 -0.33867900

Zero-point correction =	0.362958 (Hartree/Particle)
Thermal correction to Energy =	0.389612
Thermal correction to Enthalpy =	0.390557
Thermal correction to Gibbs Free Energy =	0.305833
Electronic Energy (DLPNO-CCSD(T)/def2-TZVPP) =	-2069.155127

TS6

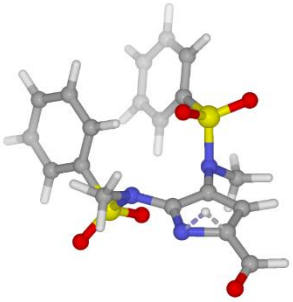


C -1.09568600 3.25571800 0.64030100	C 0.15711000 3.09269400 0.01558600

C 0.39445700 1.70495400 -0.02027200
C -0.71515500 1.08949900 0.57780700
C 0.98786200 4.22031700 -0.39734000
O 2.05092500 4.14743500 -0.97636500
N -0.86134800 -0.28384500 0.84089400
N 1.52058200 1.01597100 -0.48243400
S -1.53364400 -1.20999700 -0.40914700
O -1.33138300 -2.59749000 -0.01330100
O -0.97732000 -0.67395100 -1.64083300
C -3.28208600 -0.88039100 -0.38857800
C -4.11086800 -1.66376300 0.41151700
C -3.78084200 0.17746000 -1.14533300
C -5.47093600 -1.37431700 0.45468600
H -3.69413800 -2.49971000 0.97063700
C -5.14223300 0.45512700 -1.09318800
H -3.10885800 0.75915700 -1.77370200
C -5.98313000 -0.31674200 -0.29369200
H -6.13325400 -1.98165300 1.06867500
H -5.54932100 1.27381700 -1.68357300
S 2.65905400 0.53014200 0.66523000
O 1.95907100 0.55402800 1.94502600
O 3.89062500 1.28564800 0.47969900
C 2.99235600 -1.15335700 0.19206100
C 2.01887100 -2.12135300 0.42228100
C 4.21078900 -1.46356500 -0.40377900
C 2.27136100 -3.43171800 0.03683700
H 1.07391400 -1.84760700 0.88738800
C 4.45504800 -2.78234800 -0.77838200
H 4.94917000 -0.67962500 -0.56134900
C 3.48748100 -3.76044400 -0.56093700
H 1.50949200 -4.19200700 0.19794400
H 5.40351300 -3.04387100 -1.24407800
C 1.99940200 1.21230600 -1.85082700
H 1.11979900 1.30776200 -2.49556800
H 2.54334900 0.31255300 -2.16528900
N -1.66085400 1.98183400 0.95302100
H -1.18635000 2.78411300 1.83178500
H 3.68133100 -4.78868200 -0.86227400
H -7.04856900 -0.09588000 -0.25891500
H 2.63583400 2.09957800 -1.94219100
C -1.21125700 -0.65167600 2.21348900
H -1.18545900 -1.74171500 2.30670700
H -2.20301300 -0.27478900 2.50552900
H -0.44304100 -0.22740700 2.87000000
H -1.74770400 4.12662300 0.64900700
H 0.55748100 5.21352200 -0.12564200

Zero-point correction = 0.359053 (Hartree/Particle)
Thermal correction to Energy = 0.385690
Thermal correction to Enthalpy = 0.386634
Thermal correction to Gibbs Free Energy = 0.301108
Electronic Energy (DLPNO-CCSD(T)/def2-TZVPP) = -2069.106281

TS6’

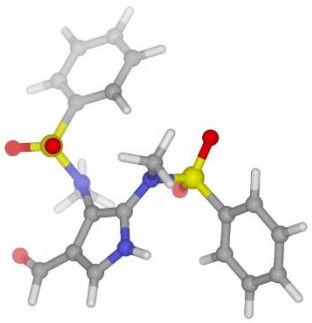


C 2.16060500 0.49999100 -0.17058600
C 1.99702000 -0.81092400 0.35612300
N 1.16989600 1.43205600 -0.51444300
N 0.78537900 -1.42661500 0.74484700
S 0.24261400 2.13111900 0.71756900
O 0.25994700 1.20661800 1.84482000
O 0.64524800 3.51555000 0.92753500
S -0.04531900 -2.18645300 -0.51215700
O 0.19653800 -1.37434200 -1.70219500
O 0.26396500 -3.61253600 -0.55901100
C -1.74216900 -2.01008700 0.00748200
C -2.66746500 -2.82747600 -0.63972500
C -2.13462000 -1.05958000 0.94668100
C -4.01793200 -2.67912800 -0.34446300
H -2.32954400 -3.57231000 -1.35880700
C -3.48901700 -0.93601700 1.24430700
H -1.39554300 -0.42473500 1.43580900
C -4.42684700 -1.73645400 0.59794900
H -4.75183100 -3.30842200 -0.84432500
H -3.80855400 -0.19865000 1.97898200
C -1.37759900 2.15209500 -0.02978200
C -2.31094600 3.01061900 0.54960100
C -1.71466400 1.30686500 -1.08320800
C -3.61443700 3.01079600 0.06572700
H -2.01427300 3.67361600 1.36098900
C -3.02077200 1.32837300 -1.56505300
H -0.97241200 0.63512100 -1.51489600
C -3.96764400 2.17136600 -0.99036500
H -4.35418900 3.67515400 0.50846100
H -3.29663200 0.66996900 -2.38734000

C 1.48851400 2.34043900 -1.62125500
H 0.60713400 2.94862400 -1.84816800
C 0.83064600 -2.17084100 2.00476200
H -0.16890200 -2.54751300 2.24652000
H 1.13812700 -1.46977400 2.78827600
H -4.98850400 2.17831200 -1.36886500
H -5.48475300 -1.62861400 0.83161900
H 1.51920100 -3.02682800 1.96381500
N 3.44054900 0.77761900 -0.44895700
O 6.36227100 0.43916200 -0.32385100
C 4.15462900 -0.45221200 -0.15070300
C 5.62179600 -0.47043500 -0.03152300
C 3.24730100 -1.39936700 0.37319500
H 3.48832100 -2.40885100 0.69500900
H 2.33149800 2.99899000 -1.38283700
H 1.72491500 1.72812500 -2.49820600
H 3.89507300 -0.07872900 -1.32510700
H 6.01124600 -1.44330900 0.34897400

Zero-point correction = 0.359109 (Hartree/Particle)
Thermal correction to Energy = 0.385505
Thermal correction to Enthalpy = 0.386449
Thermal correction to Gibbs Free Energy = 0.302826
Electronic Energy (DLPNO-CCSD(T)/def2-TZVPP) = -2069.100127

Product

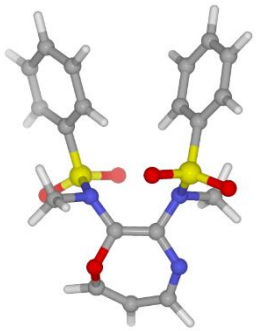


C -1.20865300 3.17626500 0.66008500
C 0.04246000 3.05557700 0.07138200
C 0.34847200 1.65343600 0.03773600
C -0.72206900 0.99289700 0.59482100
C 0.80071700 4.21257900 -0.35447800
O 1.89890100 4.20189000 -0.88882000
N -0.89524300 -0.37472400 0.81813000
N 1.49677300 1.00850300 -0.45477300
S -1.58849100 -1.28014500 -0.43661200
O -1.39110400 -2.67671800 -0.06442900
O -1.03333600 -0.75135300 -1.67451000
C -3.32872300 -0.92209800 -0.39582400
C -4.15675900 -1.68051500 0.43061500
C -3.81762700 0.14382400 -1.15045400
C -5.50876000 -1.35841500 0.49960300
H -3.75126700 -2.51803000 0.99535300
C -5.17133000 0.45372100 -1.06963900
H -3.14925300 0.71109000 -1.79591700
C -6.01229900 -0.29425400 -0.24643600
H -6.17057600 -1.94503700 1.13324300
H -5.57137700 1.27723600 -1.65749500
S 2.73326600 0.63174300 0.60995000
O 2.14423900 0.65401000 1.94760000
O 3.92279800 1.44055500 0.34186400
C 3.12522900 -1.04734600 0.16509200
C 2.18174200 -2.03998100 0.42423100
C 4.35283200 -1.33622600 -0.42140500
C 2.48066400 -3.35363800 0.08568900
H 1.22584900 -1.78093500 0.87791300
C 4.64081600 -2.65802800 -0.75552400
H 5.06718700 -0.53751000 -0.60993700
C 3.70816800 -3.66087500 -0.50313900
H 1.75291800 -4.13933500 0.27918600
H 5.59634600 -2.90118700 -1.21579200
C 1.85624200 1.17194600 -1.86358900
H 0.95369500 0.99171000 -2.45646100
H 2.59805500 0.41313000 -2.14071600
N -1.65845500 1.94186300 0.97312700
H -2.55176100 1.74271000 1.41035900
H 3.93679000 -4.69145600 -0.76857800
H -7.07112200 -0.04887900 -0.19083800
H 2.25596800 2.17360200 -2.06585600
C -1.15558500 -0.81249700 2.19500200
H -1.03890000 -1.89801100 2.25687600
H -2.16127300 -0.53712900 2.54786800
H -0.40288100 -0.33886800 2.83362700
H -1.79049100 4.06602900 0.87186300
H 0.28895700 5.18049800 -0.14974700

Zero-point correction = 0.363461 (Hartree/Particle)
Thermal correction to Energy = 0.390582
Thermal correction to Enthalpy = 0.391526
Thermal correction to Gibbs Free Energy = 0.303204

Electronic Energy (DLPNO-CCSD(T)/def2-TZVPP) = -2069.189018

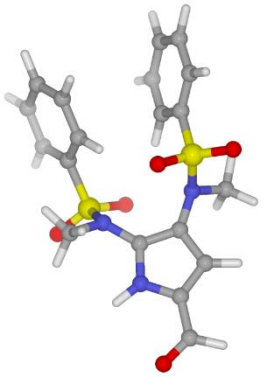
Product$_{oxazepine}$



C -2.07757800 -0.99194500 -0.04174100
C -2.13260700 0.24295800 0.52207700
N -0.84181600 -1.55104000 -0.47586300
N -1.06541100 1.11111600 0.77126100
S 0.07720200 -2.33118000 0.70175100
O 0.00041500 -1.51502500 1.91236200
O -0.26990400 -3.74999300 0.81227600
S -0.57856100 2.08887600 -0.53361800
O -0.55735700 1.23313100 -1.71629800
O -1.37878400 3.31415700 -0.58787100
C 1.07988600 2.52220900 -0.05645700
C 1.56735400 3.74745400 -0.50730100
C 1.87405200 1.63521500 0.66769000
C 2.88982900 4.08239400 -0.23420900
H 0.92087100 4.42810000 -1.05760900
C 3.19141300 1.98828500 0.93895500
H 1.46212500 0.69581800 1.03585200
C 3.69884000 3.20451600 0.48495000
H 3.28612100 5.03460400 -0.58027600
H 3.82144300 1.30760700 1.50850300
C 1.71554100 -2.22615500 0.00485800
C 2.63694100 -3.18367900 0.42574300
C 2.07479400 -1.19363300 -0.85895100
C 3.95077200 -3.09444000 -0.02266500
H 2.32845200 -3.98929000 1.08937300
C 3.39036600 -1.12391200 -1.30700500
H 1.33221200 -0.46892200 -1.19376600
C 4.32600900 -2.06684100 -0.88668000
H 4.68074900 -3.83424100 0.29914200
H 3.68196100 -0.32556400 -1.98715100
C -0.91185600 -2.25818000 -1.76298500
H 0.09358200 -2.55648600 -2.07507200
C -1.12607100 1.80466300 2.06933800
H -0.18091100 2.32454900 2.24920800
H -1.25355300 1.03998600 2.84152500
H 5.35355600 -2.00470600 -1.24010000
H 4.73135400 3.47330500 0.69964900
H -1.95275000 2.52269900 2.11589300
N -3.17518400 -1.79928100 -0.26054300
O -3.35314700 0.65916800 1.04622400
C -4.33620600 -1.34207000 -0.60512700
C -4.17535600 1.00644600 -0.00636000
C -4.70939700 0.04427500 -0.77385200
H -5.45370900 0.30782100 -1.52271300
H -1.30593100 -1.55196600 -2.50141000
H -1.55544000 -3.14418900 -1.71309600
H -5.09190000 -2.09644900 -0.84245600
H -4.38974700 2.07176500 -0.09483700

Zero-point correction = 0.362294 (Hartree/Particle)
Thermal correction to Energy = 0.388936
Thermal correction to Enthalpy = 0.389880
Thermal correction to Gibbs Free Energy = 0.304299
Electronic Energy (DLPNO-CCSD(T)/def2-TZVPP) = -2069.117387

Product'

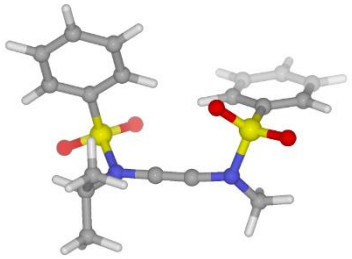


C 2.13018100 0.41944600 -0.13955100	H -1.87482800 3.85011600 1.27481500
C 1.99595900 -0.88458000 0.34509700	C -3.04474200 1.38552400 -1.48835300
N 1.16849100 1.35991900 -0.50796800	H -1.03858500 0.58327000 -1.41533600
N 0.78537700 -1.52466600 0.69027000	C -3.93661400 2.31430100 -0.95949200
S 0.28546000 2.14373600 0.70871000	H -4.22208400 3.92630900 0.44648900
O 0.28283200 1.25047000 1.85972700	H -3.36544500 0.69480400 -2.26675800
O 0.75762100 3.51487600 0.86430500	C 1.41977300 2.14383900 -1.71777800
S -0.08227200 -2.22332100 -0.57360800	H 0.51157800 2.68968400 -1.99353200
O 0.13217200 -1.37072500 -1.74056500	C 0.80941600 -2.29436100 1.93392300
O 0.18734500 -3.65423400 -0.68524800	H -0.18971100 -2.68914600 2.14715100
C -1.76270600 -2.03069000 0.00166800	H 1.09339700 -1.60674900 2.73864600
C -2.72098300 -2.83466600 -0.61304800	H -4.95967800 2.35546700 -1.32958900
C -2.11266300 -1.07436700 0.95215300	H -5.47251100 -1.59488600 0.94762600
C -4.05921600 -2.66703700 -0.27388900	H 1.50895200 -3.14127400 1.89026200
H -2.41663600 -3.58553000 -1.34076300	N 3.45796300 0.66022000 -0.30818200
C -3.45437400 -0.93027300 1.29411200	O 6.26866000 0.49481600 -0.47383100
H -1.34912400 -0.45153100 1.41896800	C 4.18640300 -0.44793800 0.05483900
C -4.42439100 -1.71754200 0.67954500	C 5.62261400 -0.45240300 -0.05327400
H -4.81784200 -3.28680800 -0.74824300	C 3.29198300 -1.42092200 0.46906300
H -3.73865900 -0.18887100 2.03943300	H 3.55345100 -2.41853300 0.80678100
C -1.34064400 2.21070700 -0.02201300	H 2.22626200 2.87990800 -1.58881500
C -2.21768200 3.15469700 0.51025000	H 1.66107600 1.44286900 -2.52484000
C -1.73679800 1.31984900 -1.01621400	H 3.88947700 1.51784500 -0.63462300
C -3.52530700 3.19612200 0.03932300	H 6.11679200 -1.39172900 0.27858200

Zero-point correction =	0.364224 (Hartree/Particle)
Thermal correction to Energy =	0.390898
Thermal correction to Enthalpy =	0.391842
Thermal correction to Gibbs Free Energy =	0.307231
Electronic Energy (DLPNO-CCSD(T)/def2-TZVPP) =	-2069.184559

7.5.2c Non-symmetric Yndiamide Cycle

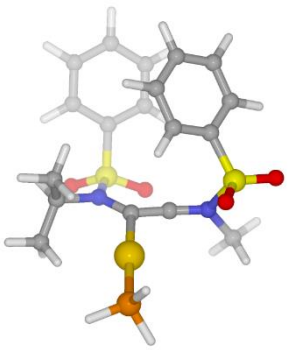
Yndiamide-Non-symmetric



C 0.54816700 1.55081800 -0.38213800
C -0.61540500 1.75942700 -0.09202700
N 1.80326100 1.29908800 -0.76805300
N -1.86538700 1.88920600 0.37641300
S 2.10962900 -0.22002700 -1.49632600
O 0.83635800 -0.66825000 -2.04421100
O 3.27349800 -0.04714900 -2.35655400
S -2.46249100 0.59564600 1.34102000
O -1.29349000 -0.03583100 1.93702100
O -3.51770600 1.15347600 2.17723300
C -3.19649600 -0.50004100 0.15190700
C -4.57968000 -0.65162500 0.12590100
C -2.36272900 -1.13972500 -0.76581700
C -5.13963800 -1.49001600 -0.83468600
H -5.20054400 -0.12566700 0.84800200
C -2.93843900 -1.96590500 -1.72341700
H -1.28347700 -0.99033100 -0.74878100
C -4.32199400 -2.14312300 -1.75416800
H -6.21824800 -1.62866300 -0.86529300
H -2.30260600 -2.47072000 -2.44793900
C 2.55880000 -1.25613100 -0.12767400
C 3.89365700 -1.60193300 0.06116300
C 1.56208000 -1.62493300 0.77559200
C 4.23539600 -2.34523900 1.18815200
H 4.64667200 -1.29339000 -0.66119000
C 1.92060100 -2.35979100 1.89886400
H 0.52590000 -1.32691300 0.62200500
C 3.25357200 -2.71813400 2.10359400
H 5.27274700 -2.62992400 1.35099300
H 1.15624000 -2.65006000 2.61687800
C 2.94885300 2.00889600 -0.11148700
C 2.94941600 3.45145800 -0.57833500
C 2.87957800 1.88276200 1.39915600
H 3.85082400 1.50913200 -0.49007400
H 2.02626400 3.95788200 -0.26339900
H 3.02593200 3.51235700 -1.67031900
H 1.96846600 2.35924000 1.78635100
H 2.88528700 0.83404300 1.72454100
C -2.86765000 2.60004800 -0.43416400
H -3.78147800 2.72439000 0.15380700
H -3.08643000 2.05521400 -1.36256100
H 3.52834200 -3.29269100 2.98607800
H -4.76588300 -2.79358500 -2.50533300
H 3.79724700 3.98892000 -0.13606400
H 3.74271500 2.38631200 1.85175300
H -2.46511300 3.58765500 -0.67348400

Zero-point correction = 0.356059 (Hartree/Particle)
Thermal correction to Energy = 0.382120
Thermal correction to Enthalpy = 0.383065
Thermal correction to Gibbs Free Energy = 0.297123
Electronic Energy (DLPNO-CCSD(T)/def2-TZVPP) = -1901.886252

Int1$_{minor}$

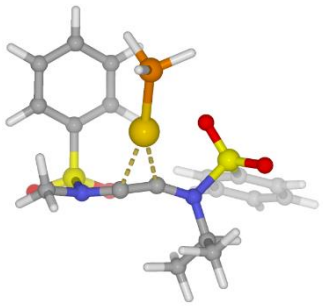


C -0.54506100 -0.61106800 0.52847400
C -0.33463600 0.51284500 1.12312700
N 0.18447900 -1.75542500 0.42253200
N -0.24910300 1.69842500 1.59174000

S 1.54421600 -1.96383600 1.45247900
O 1.40136000 -0.95802600 2.49833800
O 1.57472800 -3.38470800 1.77136900
S 0.02203100 3.05301500 0.43361100
O -1.18495000 3.07186000 -0.37884100
O 0.37696300 4.17896700 1.28005900
C 1.39191200 2.53573500 -0.54696000
C 2.63476000 3.11357600 -0.28891300
C 1.18139900 1.64422200 -1.60176100
C 3.69494200 2.79578100 -1.12974600
H 2.75725000 3.81394600 0.53444000
C 2.26277600 1.31806600 -2.41246100
H 0.19209300 1.23366700 -1.79858500
C 3.50891400 1.89995600 -2.18151900
H 4.66921500 3.25051900 -0.96230200
H 2.12616800 0.62407600 -3.23964200
C 2.98247300 -1.57061700 0.49359400
C 3.44836400 -2.49544600 -0.44193800
C 3.65418600 -0.37841700 0.75375100
C 4.61116700 -2.20345500 -1.14524000
H 2.93087300 -3.43977500 -0.60135300
C 4.83349400 -0.11742700 0.06194700
H 3.27394600 0.31675200 1.50068900
C 5.30574100 -1.02147700 -0.88636000
H 4.98936600 -2.91274900 -1.87835600
H 5.38642300 0.79650700 0.26961100
C -0.18391900 -2.86912800 -0.50195200
C -1.44324600 -3.57719200 -0.04048900
C -0.24641500 -2.36964400 -1.93358100
H 0.64543800 -3.58142300 -0.41849200
H -2.32083800 -2.91339300 -0.08193400
H -1.33310600 -3.94276600 0.98734600
H -1.07797200 -1.66355500 -2.08176400
H 0.68709700 -1.86582600 -2.21783100
C -0.70798300 2.09719500 2.93976200
H -1.67610900 2.60484200 2.86708500
H 0.03203100 2.76327100 3.38865000
H 6.22817900 -0.80857700 -1.42376300
H 4.34643600 1.65211500 -2.83154100
H -1.64738800 -4.43284700 -0.69619600
H -0.40569100 -3.21533800 -2.61382900
H -0.80079800 1.18205400 3.52875000
Au -2.53974500 -0.29976700 -0.20448900
P -4.71480200 0.07817500 -0.99060400
H -5.36700600 -1.01697200 -1.57194700
H -5.65839200 0.49673600 -0.04327100
H -4.86096700 1.05407300 -1.98525500

Zero-point correction =	0.385772 (Hartree/Particle)
Thermal correction to Energy =	0.416729
Thermal correction to Enthalpy =	0.417673
Thermal correction to Gibbs Free Energy =	0.321584
Electronic Energy (DLPNO-CCSD(T)/def2-TZVPP) =	-2379.869854

$TS_{interconv.}$

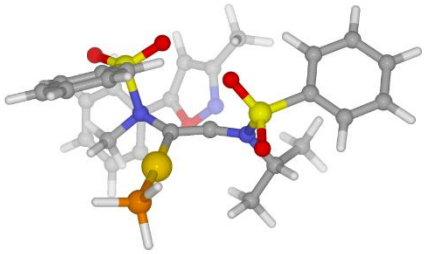


C -0.40566400 -0.17148300 1.01186300
C 0.64585100 0.22512200 1.62666800
N -1.64066800 -0.58155300 0.90837400
N 1.35718100 1.33011300 1.86528800
S -2.22264100 -1.13271900 -0.65438000
O -1.10183200 -0.90528700 -1.55589300
O -2.77275900 -2.45849500 -0.44848400
S 1.00844800 2.71226300 0.83988000
O -0.42595900 2.65691000 0.61352300
O 1.67203100 3.83184200 1.47581400
C 1.85791900 2.26038300 -0.64912200
C 3.21508900 2.56222500 -0.76611100
C 1.17668500 1.52838700 -1.62189600
C 3.90337800 2.10772600 -1.88644800
H 3.71290400 3.16012700 -0.00421600
C 1.88088900 1.08106800 -2.73642800
H 0.11488400 1.31761300 -1.52266700
C 3.23917800 1.36633100 -2.86448500
H 4.95876600 2.34524500 -2.00298500
H 1.35581500 0.51885500 -3.50739700
C -3.52349700 0.02384100 -0.95840600
C -4.81628500 -0.46427400 -1.13055300
C -3.21573400 1.38270000 -1.03153800
C -5.83396900 0.44723600 -1.39705700
H -5.01276900 -1.53241800 -1.05963600
C -4.24666600 2.27630900 -1.29109800
H -2.19892300 1.74083500 -0.86730400
C -5.54856600 1.80820800 -1.47605600

H -6.85186900 0.09113400 -1.53994500
H -4.03338300 3.34155700 -1.34690900
C -2.56447900 -0.66344100 2.09217500
C -2.14095100 -1.82524800 2.96767000
C -2.58550300 0.67100000 2.80915000
H -3.55378100 -0.86539900 1.65581000
H -1.12586700 -1.66466300 3.35809000
H -2.16236600 -2.76961400 2.41087700
H -1.60862700 0.89555300 3.25962900
H -2.84885900 1.49157000 2.13056300
C 2.70028400 1.25359300 2.45119100
H 2.95678700 2.22365300 2.88363800
H 3.44762000 0.96830900 1.69615300
H -6.34982000 2.51568700 -1.68090200
H 3.78387600 1.02462200 -3.74314000
H -2.81717800 -1.91343400 3.82661200
H -3.32270100 0.63844700 3.62024700
H 2.67742500 0.49979500 3.24246100
Au 1.38371100 -1.41161900 0.19241300
P 2.69699500 -2.89258500 -1.05086700
H 3.60012700 -3.71984000 -0.36803700
H 1.99085300 -3.82562400 -1.82418600
H 3.53084300 -2.30584200 -2.01482200

Zero-point correction = 0.385688 (Hartree/Particle)
Thermal correction to Energy = 0.416132
Thermal correction to Enthalpy = 0.417076
Thermal correction to Gibbs Free Energy = 0.322046
Electronic Energy (DLPNO-CCSD(T)/def2-TZVPP) = -2379.867396

TS1$_{major}$

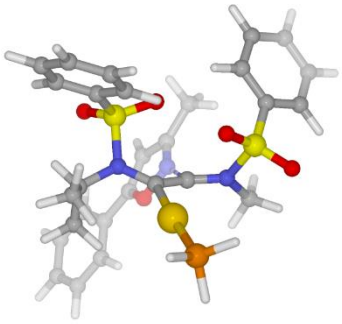


C -0.43179200 -0.74566300 -0.47731400
C 0.35703900 0.29278600 -0.36207300
N -1.61364500 -1.22897400 -0.71870200
N 1.62888400 0.32311300 0.24133100
S -2.98331600 -0.53139700 0.18168700
O -2.39542900 0.02080600 1.38611600
O -3.66959900 0.30379300 -0.79060500
S 1.66502600 0.69006900 1.91182800
O 0.69322900 -0.18580700 2.54263200
O 3.07328900 0.66150200 2.27229200
C 1.06751400 2.36124200 2.01413000
C 1.97048200 3.41316700 1.86891500
C -0.30293000 2.57754100 2.16089300
C 1.48410200 4.71725200 1.86663700
H 3.03676900 3.20986900 1.78231100
C -0.77192500 3.88975700 2.16479000
H -0.98267200 1.73493300 2.28247000
C 0.11732100 4.95333500 2.01512000
H 2.17608200 5.55130200 1.76719400
H -1.83590300 4.07831700 2.30215000
C -3.97726300 -1.93718900 0.56757200
C -5.03244500 -2.27727300 -0.27692500
C -3.66592900 -2.67459900 1.70918600
C -5.77747800 -3.41320800 0.02219200
H -5.26983600 -1.65626900 -1.13884700
C -4.42021900 -3.80683700 1.99148900
H -2.86092300 -2.35445500 2.36779800
C -5.46477100 -4.17835000 1.14466500
H -6.60770600 -3.69778800 -0.62058600
H -4.19971500 -4.39537700 2.87955500
C -1.92772500 -2.05649900 -1.93733200
C -1.02101100 -1.64847800 -3.08022100
C -1.85019900 -3.53829500 -1.61347500
H -2.96040900 -1.78112500 -2.19654100
H 0.02796500 -1.88840400 -2.86098600
H -1.09917100 -0.57388600 -3.29007500
H -0.82387800 -3.82626700 -1.35691200
H -2.50914300 -3.81156700 -0.77886500
C 2.66093200 0.97536800 -0.57013700
H 3.62619700 0.87396600 -0.06534200
H 2.43651500 2.04020700 -0.75410800
H -6.05066400 -5.06727900 1.37043800
H -0.25468500 5.97687100 2.03139000
H -1.31237100 -2.19679700 -3.98408100
H -2.16351500 -4.11660000 -2.49216100
H 2.70789200 0.44951400 -1.53029400
Au -0.55667400 2.05341800 -1.10640000
P -1.58778500 4.06019200 -1.78666500
H -2.81280300 4.36017000 -1.16825300
H -0.87907700 5.24749800 -1.53767900
H -1.92845700 4.24058600 -3.13693700
N 0.81465000 -2.43816900 -0.06374300
O 2.01409400 -2.27316300 -0.73129200
C 1.11205300 -2.84243100 1.16222300
C 3.02181900 -2.57761600 0.10482500
C 2.50674600 -2.96125600 1.31505400

C 4.37758800 -2.42425400 -0.39427100
H 3.04419000 -3.27841300 2.19979800
C 4.64033700 -2.38071300 -1.76956100
C 5.43274200 -2.29903300 0.51843400
C 5.94492900 -2.22508200 -2.22151200
H 3.82125400 -2.48269900 -2.47979300
C 6.73429900 -2.14251100 0.05976100
H 5.22685700 -2.29693300 1.58839200
C 6.99273900 -2.10726900 -1.30962800
H 6.14641400 -2.19960600 -3.29083900
H 7.54962200 -2.03959600 0.77327900
H 8.01365300 -1.98535500 -1.66727100
C 0.02913900 -3.11755700 2.14063300
H -0.63683100 -2.24869700 2.20868300
H -0.55428900 -3.99783700 1.83861700
H 0.44482900 -3.29676700 3.13700800

Zero-point correction = 0.554549 (Hartree/Particle)
Thermal correction to Energy = 0.595736
Thermal correction to Enthalpy = 0.596680
Thermal correction to Gibbs Free Energy = 0.476467
Electronic Energy (DLPNO-CCSD(T)/def2-TZVPP) = -2895.396756

TS1$_{minor}$

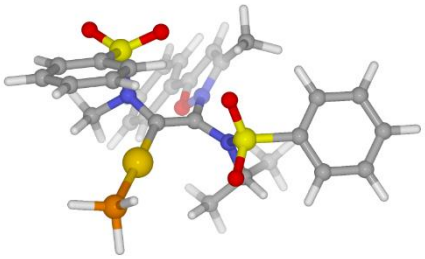


C -0.01749500 0.53284400 -0.86453500
C 0.09287900 -0.66622600 -0.30836900
N 0.60802800 1.40632800 -1.61018400
N -0.49070900 -1.02223500 0.89281400
S 2.28997900 1.87593300 -1.25741100
O 2.79632300 0.85968900 -0.35433600
O 2.85619600 2.08400000 -2.57913300
S -0.28634400 -0.03140300 2.26869300
O 0.33736800 1.20540400 1.81600700
O -1.55199700 -0.00589100 2.98771700
C 0.91593100 -0.92956100 3.21439700
C 0.52042100 -1.65226800 4.33468100
C 2.23536100 -0.91549500 2.76101400
C 1.48129400 -2.39305400 5.01931200
H -0.51753300 -1.62494500 4.66279300
C 3.18092100 -1.65934600 3.45651200
H 2.50976300 -0.33456800 1.87859000
C 2.80265600 -2.39899100 4.57844300
H 1.19584900 -2.96419100 5.90051300
H 4.21745400 -1.66052800 3.12483200
C 2.16752300 3.42754200 -0.41686800
C 2.05870600 4.58908700 -1.18330000
C 2.19550300 3.45240200 0.97652100
C 1.95723500 5.80992300 -0.52592900
H 2.08014700 4.53631000 -2.27051000
C 2.10748100 4.68525300 1.61492000
H 2.26509100 2.52699100 1.54407400
C 1.98287600 5.85553900 0.86804100
H 1.87509100 6.72843500 -1.10331700
H 2.13512900 4.72914000 2.70193200
C -1.02591000 -2.38745600 1.15585500
H -1.40935300 -2.33634200 2.18430900
H 1.91359900 6.81553300 1.37664000
H 3.54846800 -2.98105400 5.11688200
Au 1.40098700 -1.87266900 -1.44644700
P 2.91882500 -3.10541700 -2.75333100
H 3.42702200 -4.30201400 -2.22201700
H 2.49281500 -3.55127900 -4.01506000
H 4.11314300 -2.45503400 -3.10282900
N -1.69048900 1.41722500 -0.19071300
O -2.71628500 0.58784800 -0.58130200
C -2.22480100 2.43031000 0.46870600
C -3.87893500 1.10053400 -0.13581500
C -3.62611900 2.26776500 0.53189600
C -5.09440400 0.36570000 -0.44506100
H -4.33585500 2.94105100 0.99591900
C -5.08460500 -0.68288300 -1.37400300
C -6.29231100 0.71628100 0.19005200
C -6.25905300 -1.36785300 -1.65973500
H -4.15695400 -0.95331200 -1.87598800
C -7.46279600 0.02817200 -0.10031100
H -6.30404000 1.52100500 0.92423400
C -7.44844700 -1.01476300 -1.02513400
H -6.24724800 -2.17963500 -2.38463300
H -8.38930100 0.30327500 0.39992200
H -8.36680000 -1.55355500 -1.25134000
C -0.07645300 2.15246200 -2.67212000
H -0.47024400 3.10152400 -2.28379800

H 0.62322600 2.34082500 -3.49082600
H -0.90612600 1.53955200 -3.03503300
C -2.20688500 -2.64727800 0.23847500
H -2.62803300 -3.64123300 0.43646900
H -2.99142000 -1.89638800 0.39376400
H -1.89835600 -2.61248500 -0.81680600
C 0.01783300 -3.49145800 1.09338200
H 0.31788500 -3.71144500 0.05798300
H 0.91690500 -3.24801600 1.67488800
H -0.41185100 -4.41465300 1.50355200
C -1.40351200 3.53353600 1.02287800
H -1.94551900 4.48348300 0.95553200
H -1.17187800 3.33796800 2.07783300
H -0.44961600 3.62330800 0.49181200

Zero-point correction = 0.554780 (Hartree/Particle)
Thermal correction to Energy = 0.596059
Thermal correction to Enthalpy = 0.597003
Thermal correction to Gibbs Free Energy = 0.477147
Electronic Energy (DLPNO-CCSD(T)/def2-TZVPP) = -2895.394605

Int2$_{major}$

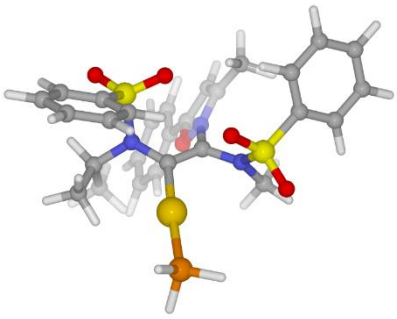


C -0.56666400 0.49476200 -0.07563000
C 0.08213600 -0.67910800 -0.22589700
N -0.11472800 1.76690500 -0.45428100
N -0.59163800 -1.83436200 0.31686100
S 1.34311600 2.37122100 0.15149600
O 1.59969200 1.66376100 1.40189200
O 2.34886500 2.36562700 -0.91020000
S -0.15352800 -2.27951800 1.88754100
O -0.34156200 -1.09229100 2.71377900
O -0.89912300 -3.50040500 2.17897600
C 1.57918800 -2.66432600 1.83375400
C 1.97266000 -3.96093100 1.50376800
C 2.50512600 -1.63834300 2.02486400
C 3.33101500 -4.23468900 1.37142000
H 1.22804300 -4.74316900 1.36643800
C 3.86085100 -1.93063800 1.89439800
H 2.17087200 -0.63082700 2.26764700
C 4.27071300 -3.22234200 1.56731000
H 3.65592000 -5.24342300 1.12410900
H 4.59699200 -1.14331100 2.04735900
C 0.97201500 4.07394700 0.51211900
C 1.23866900 5.05145700 -0.44476300
C 0.42797000 4.39500700 1.75429200
C 0.91445100 6.37482000 -0.16029900
H 1.70537000 4.78364400 -1.39071900
C 0.11247600 5.72167400 2.02729600
H 0.27608800 3.62129200 2.50338300
C 0.34523100 6.70677400 1.06771500
H 1.11527900 7.14846100 -0.89848800
H -0.30711700 5.98740800 2.99543900
C -0.67738400 2.42885200 -1.67189500
C -0.74982000 1.46237900 -2.83946100
C -2.00713900 3.09915800 -1.36053900
H 0.04461500 3.21218300 -1.93717800
H -1.45685000 0.64269400 -2.64902800
H 0.23463000 1.02421300 -3.05046700
H -2.80493200 2.36641000 -1.17707100
H -1.92418100 3.75201100 -0.48030700
C -0.71559900 -2.93215100 -0.64651300
H -1.29012200 -3.74609800 -0.19696500
H 0.26683500 -3.29961400 -0.98795800
H 0.09464500 7.74337600 1.28511600
H 5.33206300 -3.44398100 1.46763400
H -1.09187200 1.99731500 -3.73414000
H -2.32101300 3.71273300 -2.21465400
H -1.26584700 -2.54633600 -1.51300400
Au 1.94090500 -0.88940400 -1.15441500
P 4.08111500 -1.16799900 -2.13079800
H 5.14180700 -0.50586800 -1.49183000
H 4.59542000 -2.47384900 -2.18561400
H 4.28300300 -0.75660700 -3.45739300
N -1.91225200 0.48642100 0.44321700
O -2.83014000 -0.18118800 -0.33006500
C -2.48472900 0.88452200 1.57875600
C -3.98781000 -0.19124900 0.35451800
C -3.82196100 0.47334600 1.54823400
C -5.11145200 -0.85754600 -0.26887000
H -4.55464100 0.63587000 2.32787900
C -4.96150200 -1.52428900 -1.49366600
C -6.36058400 -0.83154900 0.36667400
C -6.05407900 -2.15657600 -2.07149000
H -3.99257100 -1.54849900 -1.98933400
C -7.44735000 -1.46681400 -0.21821700
H -6.48226800 -0.31312600 1.31623300
C -7.29571800 -2.12898700 -1.43653200
H -5.93747100 -2.67470800 -3.02103700

H -8.41596400 -1.44506600 0.27653500
H -8.14932200 -2.62637100 -1.89321600
C -1.75178000 1.64143700 2.61128500
H -0.67234700 1.47497000 2.53492900
H -1.97014300 2.71224700 2.49546300
H -2.09169900 1.33333000 3.60497800

Zero-point correction = 0.556614 (Hartree/Particle)
Thermal correction to Energy = 0.597600
Thermal correction to Enthalpy = 0.598544
Thermal correction to Gibbs Free Energy = 0.479046
Electronic Energy (DLPNO-CCSD(T)/def2-TZVPP) = -2895.438128

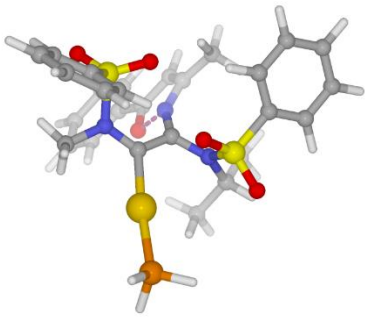
Int2$_{minor}$



C -0.49516200 0.58127000 -0.26690300
C 0.16580400 -0.60484500 -0.26954600
N -0.08652300 1.71355300 -0.98213600
N -0.27377300 -1.58383100 0.66231000
S 1.32106400 2.57403600 -0.59626200
O 2.07632500 1.76139400 0.34647500
O 1.90057700 2.96927900 -1.87734200
S 0.00467500 -1.30771500 2.31210100
O 0.01638300 0.13591100 2.51872700
O -0.94343900 -2.13773000 3.05097100
C 1.64406800 -1.91972900 2.60817000
C 1.81810900 -3.14956300 3.23646600
C 2.71835700 -1.16826100 2.13045400
C 3.11159200 -3.64392900 3.38555400
H 0.95552800 -3.70605900 3.59847300
C 4.00283400 -1.68002000 2.28220600
H 2.55026000 -0.20548800 1.64625100
C 4.19740900 -2.91430600 2.90441800
H 3.26966600 -4.60153700 3.87765800
H 4.85594000 -1.11104400 1.91732100
C 0.82633000 4.05893800 0.24777900
C 0.20521300 5.08105400 -0.47026500
C 1.08788900 4.17297000 1.61123900
C -0.18911400 6.23021000 0.20748400
H 0.04461200 4.99207400 -1.54320900
C 0.69858600 5.33389400 2.27342300
H 1.58621100 3.36272500 2.14045600
C 0.05503900 6.35431600 1.57560900
H -0.67674100 7.03600000 -0.33727700
H 0.90022600 5.43968800 3.33748700
C -0.36974000 -3.02318200 0.26578600
H -0.66107100 -3.53908700 1.18983000
H -0.25025900 7.25871600 2.09858800
H 5.20594800 -3.30751800 3.01949900
Au 1.78914800 -0.83222100 -1.57234000
P 3.60241800 -0.97096400 -3.08454300
H 4.80048500 -1.53648900 -2.62067100
H 3.42349700 -1.69631500 -4.27282200
H 4.07762700 0.24605800 -3.59778400
N -1.82117100 0.68675400 0.28793900
O -2.73604100 -0.14631600 -0.32676800
C -2.47044700 1.50578400 1.12143500
C -3.94461800 0.14311200 0.18169700
C -3.82793700 1.17314400 1.08577300
C -5.06757000 -0.63622800 -0.29608700
H -4.61317900 1.65132800 1.65666600
C -4.93783700 -1.47772300 -1.41062500
C -6.29935800 -0.53485700 0.36582000
C -6.03137900 -2.21132400 -1.85078400
H -3.98671200 -1.54744700 -1.93582000
C -7.38717900 -1.27224700 -0.08115600
H -6.40215100 0.10888500 1.23789000
C -7.25452600 -2.11075500 -1.18791000
H -5.93085800 -2.86234600 -2.71666500
H -8.34061200 -1.19649300 0.43724100
H -8.10892500 -2.68824700 -1.53588300
C -0.94374500 2.19246800 -2.06789100
H -1.82560000 2.72994200 -1.68751300
H -0.37381200 2.85284500 -2.72672500
H -1.26869600 1.32512300 -2.65598100
C -1.50604900 -3.17714300 -0.72986100
H -1.61434400 -4.23302100 -1.00946300
H -2.45484300 -2.82962800 -0.30242800
H -1.30416500 -2.60250900 -1.64608300
C 0.91384800 -3.66121100 -0.25147500
H 1.12426800 -3.37785300 -1.29206900
H 1.79055900 -3.41213000 0.35984700
H 0.78872900 -4.75208900 -0.23138500
C -1.80053200 2.57519500 1.88566100
H -2.39453900 2.82870100 2.76870500

H -0.79989700 2.26527800 2.19872600 H -1.71743100 3.47889700 1.26459900
Zero-point correction = 0.555940 (Hartree/Particle)
Thermal correction to Energy = 0.597205
Thermal correction to Enthalpy = 0.598149
Thermal correction to Gibbs Free Energy = 0.477605
Electronic Energy (DLPNO-CCSD(T)/def2-TZVPP) = -2895.427630

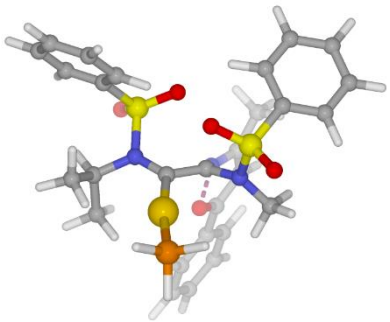
TS2$_{major}$



C -0.41159900 0.46037100 -0.09469600 H -2.77767200 2.28807300 -1.00500500
C 0.25067500 -0.76468600 -0.32282100 H -1.75582100 3.67305700 -0.53211700
N 0.02169200 1.60932300 -0.80523600 C 0.44433300 -3.16122300 0.11611100
N 0.13741300 -1.79290600 0.55266800 H 0.02474500 -3.87128100 0.83625700
S 1.55131200 2.22615000 -0.41748200 H 1.52841200 -3.32056600 0.02656100
O 2.28743700 1.14775600 0.23524400 H 0.72346100 6.23945800 3.43535600
O 2.05963600 2.84210400 -1.63675000 H 5.23517200 -3.80039900 3.36851000
S 0.18573300 -1.60626900 2.29743500 H -1.69847200 1.75845300 -3.75925100
O 0.25213100 -0.18320000 2.57905100 H -2.45280200 3.58238300 -2.15913000
O -0.86586000 -2.44200400 2.84797600 H -0.03972200 -3.33067000 -0.84883700
C 1.77442600 -2.31500100 2.63680100 Au 1.50248100 -0.92085600 -1.99617200
C 1.85019500 -3.52106900 3.32498200 P 3.01185900 -0.90709300 -3.81758600
C 2.90385100 -1.62446700 2.19679000 H 2.55756100 -1.29540100 -5.08894200
C 3.11054500 -4.05061500 3.59057100 H 3.56799400 0.34760200 -4.11724400
H 0.94039900 -4.02369700 3.64930500 H 4.17675400 -1.68559800 -3.72027200
C 4.15199600 -2.17330200 2.46550900 N -1.56959600 0.45439300 0.57681800
H 2.80512600 -0.68107600 1.65584900 O -2.79254200 -0.34894300 -0.27647800
C 4.25299800 -3.37979100 3.16039700 C -2.30882100 1.20271700 1.40629100
H 3.19797000 -4.98934300 4.13371500 C -3.88057000 -0.02413900 0.34563900
H 5.05017300 -1.65505000 2.13562800 C -3.66802300 0.95778100 1.31788000
C 1.31034500 3.49972800 0.79758800 C -5.12466200 -0.70710100 0.00765700
C 0.90282600 4.76583000 0.37927100 H -4.40840200 1.40207300 1.97092200
C 1.52574900 3.20087200 2.14052600 C -5.12724000 -1.71560800 -0.96561600
C 0.68301600 5.74815700 1.33881700 C -6.32174000 -0.35107200 0.64334100
H 0.78150200 4.98181300 -0.68154100 C -6.31167100 -2.36108800 -1.29168900
C 1.31431700 4.19870800 3.08842400 H -4.19580100 -1.98747400 -1.45829700
H 1.84937400 2.20188100 2.42993400 C -7.50382700 -0.99759800 0.31052200
C 0.88769200 5.46362300 2.68962400 H -6.33318800 0.43255400 1.39893900
H 0.36757400 6.74324300 1.03116000 C -7.49959900 -2.00313500 -0.65533800
H 1.48576000 3.98573300 4.14207400 H -6.31110500 -3.14557700 -2.04571100
C -0.77393100 2.26541500 -1.88014900 H -8.43137800 -0.71866000 0.80619900
C -1.12454000 1.26312200 -2.96561100 H -8.42773900 -2.50970300 -0.91396700
C -2.00581300 2.98681800 -1.35259900 C -1.67010100 2.17384900 2.33097300
H -0.09323600 3.00932400 -2.31278800 H -2.41441900 2.55858800 3.03454700
H -1.73609000 0.43941200 -2.57264700 H -0.84668200 1.70666900 2.87960600
H -0.21605400 0.83793700 -3.41446600 H -1.25793800 3.01821300 1.76051200
Zero-point correction = 0.554124 (Hartree/Particle)

Thermal correction to Energy = 0.595328
Thermal correction to Enthalpy = 0.596272
Thermal correction to Gibbs Free Energy = 0.475766
Electronic Energy (DLPNO-CCSD(T)/def2-TZVPP) = -2895.403348

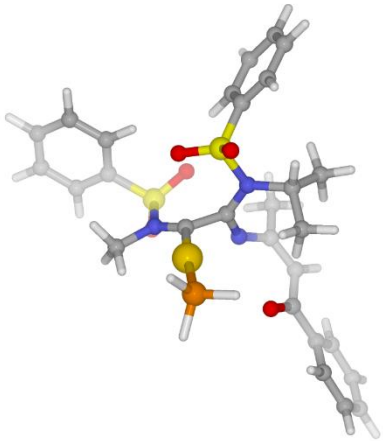
TS2$_{minor}$



C -0.37934300 0.62063200 -0.15465500
C 0.17911900 -0.66927900 -0.19029200
N -0.00369800 1.54665000 -1.15668300
N 0.14693200 -1.44629400 0.91893700
S 1.55309500 2.22164900 -1.09793500
O 2.38759300 1.24179000 -0.41374100
O 1.83656900 2.63715400 -2.46470600
S 0.38499200 -0.81472300 2.53216400
O 0.58854400 0.62098900 2.42224700
O -0.66005900 -1.36579800 3.37885000
C 1.94919300 -1.55460300 2.91718200
C 2.01435900 -2.58942000 3.84359600
C 3.07418700 -1.06846000 2.25069400
C 3.25665700 -3.16165000 4.10744500
H 1.11163800 -2.93000000 4.34850200
C 4.30453500 -1.65127200 2.52759600
H 2.98081600 -0.25959500 1.52354500
C 4.39281500 -2.69598900 3.44959400
H 3.33534500 -3.97133600 4.83006600
H 5.19788000 -1.29031800 2.02192600
C 1.47561300 3.66756500 -0.07074900
C 1.03249800 4.86876700 -0.62415400
C 1.84998500 3.56408000 1.26742900
C 0.94807600 5.99010300 0.19510500
H 0.78442300 4.92701700 -1.68296000
C 1.77065400 4.69789800 2.07061700
H 2.19000400 2.60894000 1.66481900
C 1.31626900 5.90318800 1.53795700
H 0.60965200 6.93770200 -0.21936500
H 2.06742100 4.63896300 3.11621900
C 0.06658000 -2.94115100 0.86640500
H 0.00437900 -3.25053800 1.91797800
H 1.25767900 6.78643700 2.17162400
H 5.36016800 -3.14909700 3.65887900
Au 1.08319300 -1.17507500 -2.01553700
P 2.14101900 -1.46331900 -4.10803000
H 2.66415700 -0.28543700 -4.66674600
H 3.26572800 -2.30164300 -4.18422600
H 1.39478800 -1.95067600 -5.19405200
N -1.50665900 0.82070300 0.54979400
O -2.76318800 -0.04957300 -0.08287300
C -2.16677700 1.81984300 1.15861600
C -3.83215600 0.50332900 0.40647600
C -3.54307700 1.67634500 1.10630100
C -5.11731100 -0.15496700 0.21404000
H -4.24565300 2.32881800 1.60894900
C -5.19130700 -1.34503700 -0.52347800
C -6.28410600 0.40314600 0.75380600
C -6.41687700 -1.96829300 -0.71102900
H -4.28391800 -1.77253800 -0.94676400
C -7.50713400 -0.22332600 0.56019900
H -6.23867600 1.32642200 1.32892200
C -7.57429200 -1.40880300 -0.17067900
H -6.47277200 -2.89238400 -1.28273900
H -8.41089600 0.21168200 0.98175900
H -8.53459400 -1.89885600 -0.32069000
C -1.02537700 2.16967800 -1.98801800
H -1.65699500 2.87686800 -1.42578200
H -0.54535000 2.69877000 -2.81616200
H -1.65997900 1.37749500 -2.40545500
C -1.24041300 -3.33456100 0.20044300
H -1.36599400 -4.42411000 0.23621300
H -2.09110100 -2.86623600 0.71303800
H -1.25514400 -3.02241100 -0.85344000
C 1.28304800 -3.61151700 0.25182800
H 1.32655500 -3.46840700 -0.83700400
H 2.22079700 -3.24540000 0.68930400
H 1.22098400 -4.69209200 0.43476500
C -1.43179800 2.91282900 1.84186700
H -2.13035000 3.52263300 2.42236400
H -0.65574400 2.50424900 2.49723300
H -0.93557400 3.55663800 1.10206600
Zero-point correction = 0.554187 (Hartree/Particle)
Thermal correction to Energy = 0.595431
Thermal correction to Enthalpy = 0.596376

Thermal correction to Gibbs Free Energy = 0.476547
Electronic Energy (DLPNO-CCSD(T)/def2-TZVPP) = -2895.403295

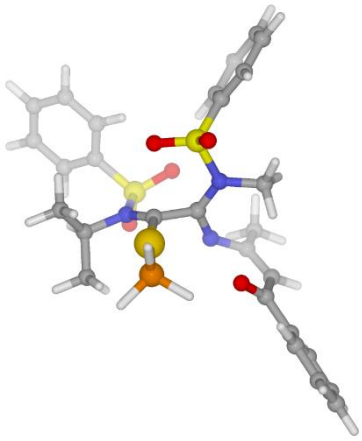
***Z*-Int3$_{major}$**



C 0.06808900 0.43233000 -0.21901000
C -0.42946900 -0.95216900 0.08102300
N -0.29397800 1.47258200 0.64227300
N -1.05422400 -1.65322500 -0.81608400
S -1.80264500 1.40946000 1.43550100
O -2.51261500 0.28036200 0.83751500
O -1.59093200 1.43270700 2.87718300
S -1.74066100 -0.95829200 -2.35414400
O -1.81461000 0.47570700 -2.14748400
O -0.93857600 -1.53818800 -3.41633300
C -3.36179700 -1.65194700 -2.35004600
C -3.63704500 -2.72573600 -3.19508800
C -4.31817600 -1.08984500 -1.50337300
C -4.92500900 -3.25020000 -3.19034200
H -2.86437000 -3.13082000 -3.84554600
C -5.59698300 -1.63373300 -1.51078400
H -4.06252500 -0.25422900 -0.85346200
C -5.89638900 -2.70783600 -2.34970200
H -5.16922500 -4.08347000 -3.84530700
H -6.36304900 -1.21563300 -0.86164100
C -2.54892300 2.93635400 0.94164300
C -2.67459800 3.96228900 1.87422100
C -2.95241600 3.07796700 -0.38633200
C -3.22205900 5.17281900 1.45713600
H -2.35274000 3.81316400 2.90292000
C -3.49771300 4.29258100 -0.78406400
H -2.83237800 2.25688700 -1.09238800
C -3.62791900 5.33598600 0.13430000
H -3.33059800 5.98839100 2.16886600
H -3.82091800 4.42650700 -1.81425500
C 0.64563700 2.50574500 1.20586700
C 1.87649100 1.84031300 1.79009600
C 0.94314000 3.65638500 0.26161100
H 0.08008300 2.92703400 2.04744400
H 2.45744400 1.29927300 1.03359700
H 1.59168000 1.12822000 2.57765400
H 1.65000200 3.38266100 -0.52931000
H 0.02516700 4.05119300 -0.19431000
C -1.30336700 -3.09716500 -0.67984700
H -1.14529100 -3.58180500 -1.64853100
H -2.32760700 -3.27071000 -0.33310900
H -4.05268900 6.28538600 -0.18623600
H -6.90130400 -3.12551600 -2.35002300
H 2.52221600 2.60674800 2.23719900
H 1.40431000 4.46624600 0.84134400
H -0.58844400 -3.50111100 0.04078800
Au 0.31440200 -1.70169300 1.89135100
P 1.24176100 -2.42767700 3.93374700
H 0.34779300 -2.81017000 4.94301800
H 2.09652800 -3.53729800 3.88509400
H 2.03910400 -1.49265300 4.60851100
N 0.95993200 0.41058400 -1.11524300
O 3.45468300 -0.33404500 -0.21549400
C 1.69881300 1.30949100 -1.82740800
C 3.90211900 0.39686300 -1.10766200
C 3.06144500 1.31513100 -1.85798000
C 5.35918800 0.34339900 -1.44105900
H 3.52665500 2.02656100 -2.53600900
C 6.22851700 -0.22831100 -0.50324400
C 5.88390900 0.81445000 -2.65118700
C 7.59163900 -0.31286200 -0.75893300
H 5.81452000 -0.59991100 0.43252200
C 7.24772700 0.71790200 -2.91403700
H 5.22971000 1.23705600 -3.41170400
C 8.10452200 0.16011000 -1.96728500
H 8.25808500 -0.74912600 -0.01646100
H 7.64158600 1.07732200 -3.86332300
H 9.17193800 0.09127400 -2.17160300
C 0.89374400 2.16063000 -2.76615200
H 1.51083400 2.95327700 -3.20226200
H 0.50241500 1.53398000 -3.57907800
H 0.02534500 2.60392600 -2.26296500

Zero-point correction =	0.554989 (Hartree/Particle)
Thermal correction to Energy =	0.596921
Thermal correction to Enthalpy =	0.597865
Thermal correction to Gibbs Free Energy =	0.476191
Electronic Energy (DLPNO-CCSD(T)/def2-TZVPP) =	-2895.450103

_Z_-Int3$_{minor}$



C -0.10335700 0.53714300 0.50747300	Au -0.80655900 -1.55983900 -1.46276800
C 0.41105600 -0.80328100 0.08229100	P -2.30066000 -2.21920400 -3.15725100
N 0.00161200 1.61845600 -0.35281200	H -1.94214100 -1.91553200 -4.47753800
N 1.29609500 -1.43594300 0.78814700	H -2.60785900 -3.58285400 -3.26036400
S 1.16509500 1.67853800 -1.59073100	H -3.58003500 -1.65089200 -3.07743900
O 2.02230900 0.51619100 -1.35899400	N -0.81126800 0.44887700 1.55271300
O 0.47812200 1.81785000 -2.86641700	O -3.17801800 0.24864500 0.11662500
S 2.27192000 -0.64740900 2.09974300	C -1.59325400 1.29856900 2.29111600
O 2.09332100 0.78460600 1.93454500	C -3.71397800 0.73371600 1.12240200
O 1.87833700 -1.32646700 3.32184700	C -2.94683600 1.38598700 2.17295200
C 3.91488800 -1.10144300 1.63563200	C -5.19993900 0.68453500 1.26218900
C 4.58128500 -2.07069000 2.38382300	H -3.46749400 1.99133500 2.91155300
C 4.49532600 -0.46257400 0.53897600	C -5.96917000 0.46339700 0.11291100
C 5.87787500 -2.41076400 2.01303700	C -5.84621200 0.82480500 2.49633700
H 4.09674200 -2.53858400 3.23871800	C -7.35506100 0.40079700 0.19092800
C 5.79060500 -0.81992600 0.18417300	H -5.45905500 0.34881800 -0.84241600
H 3.94175200 0.28006100 -0.03450700	C -7.23388200 0.74716700 2.57767300
C 6.47549400 -1.78991500 0.91693600	H -5.26786000 0.97000300 3.40746700
H 6.42115300 -3.16132400 2.58263400	C -7.99033200 0.54154700 1.42552700
H 6.26646800 -0.33930200 -0.66765700	H -7.94443700 0.24142200 -0.71071000
C 2.03675300 3.18376900 -1.25286800	H -7.72542600 0.84572000 3.54413000
C 2.00721200 4.19770000 -2.20703000	H -9.07615600 0.48877800 1.48908700
C 2.73212200 3.30861000 -0.04975000	C -0.91829000 2.75651500 -0.25916600
C 2.70861700 5.37211100 -1.94783600	H -0.68431600 3.38399300 0.60929200
H 1.44801500 4.06601600 -3.13080600	H -0.82208900 3.36322500 -1.16459300
C 3.42417800 4.48948800 0.19195300	H -1.94409700 2.38245100 -0.20879600
H 2.72652200 2.50384300 0.68488700	C 0.32558200 -3.70909000 0.98820300
C 3.41282200 5.51540700 -0.75438800	H 0.58679500 -4.77265600 1.04560600
H 2.70116000 6.17602000 -2.68067800	H -0.08976500 -3.39910200 1.95526000
H 3.97332200 4.60959100 1.12343900	H -0.45137900 -3.59377000 0.21979700
C 1.57263100 -2.91371700 0.65431300	C 2.18696900 -3.22804400 -0.69484200
H 2.31712200 -3.12773800 1.43058900	H 1.49309100 -3.00568900 -1.51771900
H 3.95762900 6.43655200 -0.55643300	H 3.11314100 -2.66169400 -0.85820500
H 7.48939700 -2.06311200 0.63119200	H 2.42557600 -4.29761200 -0.73468000

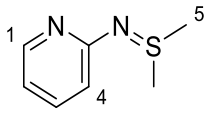
C -0.83911900 1.99820800 3.37866700	H -0.32516600 1.26474000 4.01455100
H -1.50218300 2.61256300 3.99594300	H -0.05415600 2.63547800 2.94461000

Zero-point correction =	0.554952 (Hartree/Particle)
Thermal correction to Energy =	0.596922
Thermal correction to Enthalpy =	0.597866
Thermal correction to Gibbs Free Energy =	0.476299
Electronic Energy (DLPNO-CCSD(T)/def2-TZVPP) =	-2895.458901

7.6 Chapter V Characterisation Data

7.6.1 Sulfilimines

1,1-Dimethyl-*N*-(pyridin-2-yl)-λ^4-sulfanimine, 179a



ZT290

Synthesised from 2-aminopyridine (0.47 g, 5.00 mmol, 1.0 eq.), dimethyl sulfide (0.41 mL, 5.50 mmol, 1.1 eq.). NCS (734 mg, 5.50 mmol, 1.1 eq.) and sodium methoxide solution (25% w/w in MeOH, 1.3 mL, 5.50 mmol, 1.1 eq.) with general procedure **7.2.2d**. Column chromatography (silica gel, 10% MeOH/DCM) afforded the title compound (671 mg, 4.35 mmol, 87%) as a pale-yellow solid.

R_f 0.21 (10% MeOH/DCM);

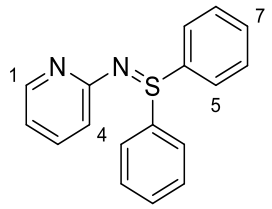
IR (thin film, ν_{max}/cm^{-1}) 3327, 1593, 1489, 1421, 1312, 1145, 904, 772, 731;

^{1}H NMR (400 MHz, $CDCl_3$) δ_H 8.00 – 7.93 (1H, m, H1), 7.29 (1H, ddd, *J* = 8.7, 7.0, 1.9 Hz, H3), 6.64 (1H, d, *J* = 8.4 Hz, H4), 6.48 – 6.41 (1H, m, H2), 2.69 (6H, s, H5);

^{13}C NMR (101 MHz, $CDCl_3$) δ_C 165.5, 147.2, 136.8, 114.2, 111.5, 33.9;

Data are consistent with literature values.[176]

1,1-Diphenyl-*N*-(pyridin-2-yl)-λ^4-sulfanimine, 179a'



ZT549

Modified from a literature procedure.[176] In a heat gun-dried round-bottom flask equipped with a stirrer bar was dissolved diphenyl sulfoxide (1.01 g, 5.00 mmol, 1.0 eq.) in DCM (anhy., 10 mL). A solution of 2-aminopyridine (940 mg, 10.0 mmol) in DCM (anhy., 10 mL) was prepared in a similar way. The sulfoxide solution was then cooled to −78 °C before trifluoromethanesulfonic anhydride (0.94 mL, 5.50 mmol, 1.1 eq.) was added to it dropwise. The reaction mixture was stirred at −78 °C for another 1 h and the 2-aminopyridine solution was added dropwise. The resulting mixture was stirred for another hour at −78 °C, slowly warmed to room temperature and stirred for 4 h. Upon completion, the reaction mixture was diluted with saturated $NaHCO_3$ aqueous solution (15 mL), and extracted three times with DCM. The organic layer was combined, washed with brine, dried over Na_2SO_4, concentrated *in vacuo,* and purified by column chromatography (silica gel, 40% EtOAc/pentane) to afford the title compound (1.07 g, 3.84 mmol, 77%) as a brown solid;

R_f 0.24 (40% EtOAc/pentane);

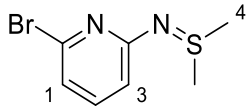
IR (thin film, ν_{max}/cm^{-1}) 3059, 1587, 1475, 1421, 1311, 1299, 909, 737, 688;

^{1}H NMR (400 MHz, $CDCl_3$) δ_H 7.94 (1H, ddd, *J* = 5.2, 1.9, 1.0 Hz, H1), 7.78 – 7.67 (4H, m, H5), 7.48 – 7.42 (6H, m, H6, H7), 7.37 (1H, ddd, *J* = 8.6, 7.0, 1.9 Hz, H3), 6.93 (1H, app. dt, *J* = 8.6, 1.0 Hz, H4), 6.49 (1H, ddd, *J* = 7.0, 5.2, 1.0 Hz, H2);

^{13}C NMR (101 MHz, $CDCl_3$) δ_C 165.4, 147.3, 138.9, 136.8, 131.4, 129.7, 127.7, 114.9, 112.2;

Data are consistent with literature values.[176]

_N_-(6-Bromopyridin-2-yl)-1,1-dimethyl-λ^4-sulfanimine, 179b



ZT513

Modified from a literature procedure.[246] In a heat gun-dried flask was added DMSO (0.77 mL, 10.8 mmol, 2.2 eq.) and DCM (anhy., 2.5 mL). The solution was then cooled to – 78 °C on a dry ice/acetone bath. While stirring, trifluoroacetic anhydride (0.83 mL, 5.97 mmol, 1.2 eq.) was added dropwise, and a white precipitate was formed. In another heat gun-dried vial was added 2-amino-6-bromopyridine (865 mg, 5.00 mmol, 1.0 eq.). The vial was purged under high vacuum for 30 s and backfilled with argon (this cycle was repeated twice more). DCM (anhy., 2.5 mL) and DMSO (1.5 mL) were added, and the resulting solution was then added dropwise to the previously prepared DMSO and trifluoroacetic anhydride solution at – 78 °C. The reaction was stirred at – 78 °C until the white precipitate disappeared. The cooling bath was then removed and a NaOH solution (10 wt% in water, 2.5 mL) was added. The reaction mixture was stirred at room temperature overnight. Upon completion, the reaction mixture was diluted with water, and extracted three times with EtOAc. The organic phase was combined, washed three times with brine, dried over Na_2SO_4, and concentrated *in vacuo*. Column chromatography (silica gel, 10% MeOH/DCM) followed by recrystallization from DCM/pentane afforded the title compound (356 mg, 1.53 mmol, 31%) as a yellow solid.

m.p. 69 – 71 °C;

R_f 0.32 (10% MeOH/DCM);

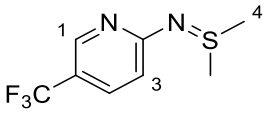
IR (thin film, ν_{max}/cm^{-1}) 3415, 1589, 1425, 1323, 1156, 921, 774, 728;

^{1}H NMR (400 MHz, $CDCl_3$) δ_H 7.13 (1H, dd, *J* = 8.2, 7.3 Hz, H2), 6.61 (1H, dd, *J* = 7.3, 0.7 Hz, H1), 6.56 (1H, dd, *J* = 8.2, 0.7 Hz, H3), 2.74 (6H, s, H4);

^{13}C NMR (101 MHz, $CDCl_3$) δ_C 165.8, 139.2, 138.9, 114.3, 112.6, 33.2;

HRMS (ESI) m/z: $[M + H]^+$ Calcd for $C_7H_{10}{}^{79}BrN_2S$ 232.9743; Found 232.9745.

1,1-Dimethyl-*N*-(5-(trifluoromethyl)pyridin-2-yl)-λ^4-sulfanimine, 179c



ZT561

Synthesised from 5-(trifluoromethyl)pyridin-2-amine (811 mg, 5.00 mmol, 1.0 eq.), dimethyl sulfide (0.41 mL, 5.50 mmol, 1.1 eq.). NCS (734 mg, 5.50 mmol, 1.1 eq.) and sodium methoxide solution (25% w/w in MeOH, 2.3 mL, 10.1 mmol, 2.1 eq.) with general procedure **7.2.2d**. Recrystallisation from Et_2O/pentane afforded the title compound (867 mg, 3.90 mmol, 78%) as a yellow solid;

R_f 0.37 (10% MeOH/DCM);

IR (thin film, ν_{max}/cm^{-1}) 3360, 1608, 1315, 1293, 1105, 1072;

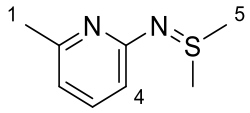
^{1}H NMR (400 MHz, $CDCl_3$) δ_H 8.20 – 8.17 (1H, m, H1), 7.46 – 7.38 (1H, m, H2), 6.62 (1H, d, *J* = 8.8 Hz, H3), 2.71 (6H, s, H4);

^{13}C NMR (101 MHz, $CDCl_3$) δ_C 167.6, 145.0 (q, $^3J_{C–F}$ = 4.5 Hz), 133.4 (q, $^3J_{C–F}$ = 3.1 Hz), 125.3 (q, $^1J_{C–F}$ = 269.9 Hz), 113.9 (q, $^2J_{C–F}$ = 32.6 Hz), 113.6, 33.3;

^{19}F NMR (377 MHz, $CDCl_3$) δ_F -60.86;

Data are consistent with literature values.[176]

1,1-Dimethyl-*N*-(6-methylpyridin-2-yl)-λ⁴-sulfanimine, 179d



ZT548

Synthesised from 6-methylpyridin-2-amine (1.08 g, 10.0 mmol, 1.0 eq.), dimethyl sulfide (0.82 mL, 11.0 mmol, 1.1 eq.). NCS (1.47 g, 11.0 mmol, 1.1 eq.) and sodium methoxide solution (25% w/w in MeOH, 4.6 mL, 20.1 mmol, 2.1 eq.) with general procedure **7.2.2d**. Column chromatography (silica gel, 10% MeOH/DCM) afforded the title compound (1.68 g, 10.0 mmol, quant.) as a yellow oil;

R_f 0.25 (10% MeOH/DCM);

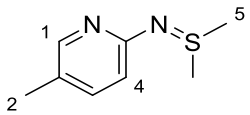
IR (thin film, ν_{max}/cm^{-1}) 3199, 1590, 1556, 1439, 1322, 970, 847, 784, 736;

^{1}H NMR (400 MHz, $CDCl_3$) δ_H 7.21 (1H, dd, *J* = 8.3, 7.1 Hz, H3), 6.47 (1H, d, *J* = 8.3 Hz, H2), 6.33 (1H, d, *J* = 7.1 Hz, H4), 2.71 (6H, s, H5), 2.34 (3H, s, H1);

^{13}C NMR (101 MHz, $CDCl_3$) δ_C 165.0, 155.8, 137.3, 110.8, 110.5, 33.6, 24.3;

Data are consistent with literature values.[176]

1,1-Dimethyl-*N*-(5-methylpyridin-2-yl)-λ⁴-sulfanimine, 179e



ZT552

Synthesised from 5-methylpyridin-2-amine (1.08 g, 10.0 mmol, 1.0 eq.), dimethyl sulfide (0.82 mL, 11.0 mmol, 1.1 eq.). NCS (1.47 g, 11.0 mmol, 1.1 eq.) and sodium methoxide solution (25% w/w in MeOH, 4.6 mL, 20.1 mmol, 2.1 eq.) with general procedure **7.2.2d**. Column chromatography (silica gel, 10% MeOH/DCM) afforded the title compound (1.47 g, 8.74 mmol, 87%) as a yellow oil;

R_f 0.23 (10% MeOH/DCM);

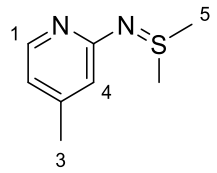
IR (thin film, ν_{max}/cm^{-1}) 3361, 1608, 1475, 1376, 1304, 913, 827;

^{1}H NMR (400 MHz, $CDCl_3$) δ_H 7.83 – 7.78 (1H, m, H1), 7.16 (1H, dd, *J* = 8.5, 2.4 Hz, H3), 6.59 (1H, d, *J* = 8.5 Hz, H4), 2.69 (6H, s, H5), 2.13 (3H, s, H2);

^{13}C NMR (101 MHz, $CDCl_3$) δ_C 163.6, 146.6, 138.3, 120.2, 113.8, 34.0, 17.6;

Data are consistent with literature values.[176]

1,1-Dimethyl-*N*-(4-methylpyridin-2-yl)-λ^4-sulfanimine, 179f



ZT555

Synthesised from 4-methylpyridin-2-amine (1.08 g, 10.0 mmol, 1.0 eq.), dimethyl sulfide (0.82 mL, 11.0 mmol, 1.1 eq.). NCS (1.47 g, 11.0 mmol, 1.1 eq.) and sodium methoxide solution (25% w/w in MeOH, 4.6 mL, 20.1 mmol, 2.1 eq.) with general procedure **7.2.2d**. Column chromatography (silica gel, 10% MeOH/DCM) afforded the title compound (0.71 g, 4.22 mmol, 42%) as a pale-yellow oil;

R_f 0.16 (10% MeOH/DCM);

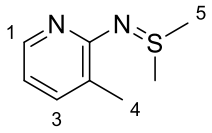
IR (thin film, ν_{max}/cm^{-1}) 3360, 1606, 1396, 1315, 1168, 957, 729;

^{1}H NMR (400 MHz, $CDCl_3$) δ 7.88 – 7.80 (1H, m, H1), 6.51 – 6.45 (1H, m, H4), 6.35 – 6.28 (1H, m, H2), 2.68 (6H, s, H5), 2.16 (3H, s, H3);

^{13}C NMR (101 MHz, $CDCl_3$) δ_C 165.6, 147.7, 146.8, 114.3, 113.4, 34.0, 21.1;

Data are consistent with literature values.[176]

1,1-Dimethyl-*N*-(3-methylpyridin-2-yl)-λ^4-sulfanimine, 179g



ZT557

Synthesised from 3-methylpyridin-2-amine (1.08 g, 10.0 mmol, 1.0 eq.), dimethyl sulfide (0.82 mL, 11.0 mmol, 1.1 eq.). NCS (1.47 g, 11.0 mmol, 1.1 eq.) and sodium methoxide solution (25% w/w in MeOH, 4.6 mL, 20.1 mmol, 2.1 eq.) with general procedure **7.2.2d**. Preparative LPLC (Silia*Sep* PREMIUM silica 24 g, 10% MeOH/DCM) afforded the title compound (1.08 g, 6.42 mmol, 64%) as a yellow oil;

R_f 0.32 (10% MeOH/DCM);

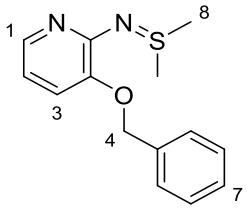
IR (thin film, ν_{max}/cm^{-1}) 3378, 1593, 1407, 1305, 912, 774;

^{1}H NMR (400 MHz, $CDCl_3$) δ_H 7.89 – 7.82 (1H, m, H1), 7.18 – 7.10 (1H, m, H3), 6.45 – 6.36 (1H, m, H2), 2.73 (6H, s, H5), 2.17 (3H, s, H4);

^{13}C NMR (101 MHz, $CDCl_3$) δ_C 164.7, 144.5, 136.2, 122.7, 111.6, 33.9, 18.0;

Data are consistent with literature values.[176]

***N*-(3-(Benzyloxy)pyridin-2-yl)-1,1-dimethyl-λ^4-sulfanimine, 179h**



ZT568

Synthesised from 3-(benzyloxy)pyridin-2-amine (1.00 g, 5.00 mmol, 1.0 eq.), dimethyl sulfide (0.41 mL, 5.50 mmol, 1.1 eq.). NCS (734 mg, 5.50 mmol, 1.1 eq.) and sodium methoxide solution (25% w/w in MeOH, 2.3 mL, 10.1 mmol, 2.1 eq.) with general

procedure **7.2.2d**. Recrystallisation from Et_2O/pentane afforded the title compound (376 mg, 1.44 mmol, 29%) as a yellow solid;

R_f 0.43 (10% MeOH/DCM);

IR (thin film, ν_{max}/cm^{-1}) 3054, 1591, 1436, 1188, 1114, 909, 730;

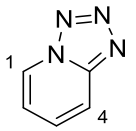
^{1}H NMR (400 MHz, $CDCl_3$) δ_H 7.60 (1H, dd, *J* = 5.1, 1.5 Hz, H1), 7.44 – 7.37 (2H, m, H5), 7.35 – 7.29 (2H, m, H6), 7.28 – 7.22 (1H, m, H7), 6.71 (1H, dd, *J* = 7.6, 1.5 Hz, H3), 6.34 (1H, dd, *J* = 7.6, 5.1 Hz, H2), 5.21 (2H, s, H4), 2.79 (6H, s, H8);

^{13}C NMR (101 MHz, $CDCl_3$) δ_C 157.6, 145.8, 138.7, 137.7, 128.5, 127.5, 126.9, 117.4, 111.1, 70.3, 33.6;

Data are consistent with literature values.[176]

7.6.2 Tetrazolo[1,5-a]pyridines

Tetrazolo[1,5-*a*]pyridine, 183a



ZT558

Synthesised from 2-bromopyridine (0.96 mL, 10.1 mmol, 1.0 eq.), sodium azide (1.96 g, 30.2 mmol, 3.0 eq.), CuI (192 mg, 1.01 mmol, 10 mol%), *N*,*N*′-dimethylethylenediamine (0.16 mL, 1.51 mmol, 15 mol%), and sodium ascorbate (100 mg, 0.50 mmol, 5 mol%) with general procedure **7.2.2e**. Column chromatography (silica gel, Et_2O) afforded the title compound (0.99 g, 8.24 mmol, 82%) as a colourless solid. Single crystals suitable for X-ray crystallography were grown by vapour diffusion of pentane into a concentrated solution of the title compound in Et_2O.

R_f 0.27 (Et_2O);

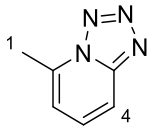
IR (thin film, ν_{max}/cm^{-1}) 3106, 1632, 1492, 1140, 1094, 1015, 912, 768, 752;

^{1}H NMR (400 MHz, $CDCl_3$) δ_H 8.84 (1H, app. dt, *J* = 6.9, 1.2 Hz, H1), 8.08 – 8.00 (1H, m, H4), 7.69 (1H, ddd, *J* = 9.0, 6.7, 1.2 Hz, H3), 7.25 (1H, app. dt, *J* = 6.8, 1.1 Hz, H2);

^{13}C NMR (101 MHz, $CDCl_3$) δ_C 148.7, 132.0, 125.6, 116.7, 116.1;

Data are consistent with literature values.[247]

5-Methyltetrazolo[1,5-*a*]pyridine, 183d



ZT573

Synthesised from 2-bromo-6-methylpyridine (0.57 mL, 5.01 mmol, 1.0 eq.), sodium azide (977 mg, 15.0 mmol, 3.0 eq.), CuI (95 mg, 0.50 mmol, 10 mol%), *N*,*N*′-dimethylethylenediamine (81 μL, 0.75 mmol, 15 mol%), and sodium ascorbate (50 mg, 0.25 mmol, 5 mol%) with general procedure **7.2.2e**. Column chromatography (silica gel, Et_2O) afforded the title compound (547 mg, 4.08 mmol, 81%) as a yellow solid;

m.p.

R_f 0.34 (Et_2O);

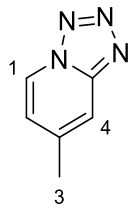
IR (thin film, ν_{max}/cm^{-1}) 3068, 1640, 1509, 909, 800, 730;

^{1}H NMR (400 MHz, $CDCl_3$) δ_H 7.91 (1H, d, *J* = 9.0 Hz, H4), 7.60 (1H, dd, *J* = 9.0, 6.9 Hz, H3), 7.04 – 6.97 (1H, m, H2), 2.95 (3H, s, H1);

^{13}C NMR (101 MHz, $CDCl_3$) δ_C 148.9, 136.9, 131.9, 115.4, 113.2, 17.6;

Data are consistent with literature values.[182]

7-Methyltetrazolo[1,5-*a*]pyridine, 183f



ZT588

Synthesised from 2-bromo-4-methylpyridine (0.56 mL, 5.03 mmol, 1.0 eq.), sodium azide (977 mg, 15.0 mmol, 3.0 eq.), CuI (95 mg, 0.50 mmol, 10 mol%), *N*,*N*′-dimethylethylenediamine (81 μL, 0.75 mmol, 15 mol%), and sodium ascorbate (50 mg, 0.25 mmol, 5 mol%) with general procedure **7.2.2e**. Column chromatography (silica gel, Et_2O) afforded the title compound (502 mg, 3.74 mmol, 75%) as a colourless solid;

R_f 0.32 (Et_2O);

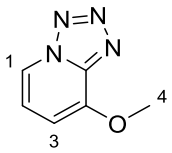
IR (thin film, ν_{max}/cm^{-1}) 3124, 3050, 1648, 1636, 1493, 1096, 797, 735;

^{1}H NMR (400 MHz, $CDCl_3$) δ_H 8.69 (1H, d, *J* = 7.0, H1), 7.77 (1H, s, H4), 7.04 (1H, dd, *J* = 7.0, 1.7 Hz, H2), 2.56 (3H, s, H3);

^{13}C NMR (101 MHz, $CDCl_3$) δ_C 149.1, 143.9, 124.5, 119.4, 114.1, 21.8;

Data are consistent with literature values.[182]

8-Methoxytetrazolo[1,5-*a*]pyridine, 183i



ZT608

Synthesised from 2-bromo-3-methoxypyridine (940 mg, 5.00 mmol, 1.0 eq.), sodium azide (977 mg, 15.0 mmol, 3.0 eq.), CuI (95 mg, 0.50 mmol, 10 mol%), *N*,*N*′-dimethylethylenediamine (81 μL, 0.75 mmol, 15 mol%), and sodium ascorbate (50 mg,

0.25 mmol, 5 mol%) with general procedure **7.2.2e**. Column chromatography (silica gel, EtOAc) afforded the title compound (593 mg, 3.95 mmol, 79%) as a colourless solid;

R_f 0.45 (EtOAc/pentane);

m.p. 191 – 193 °C;

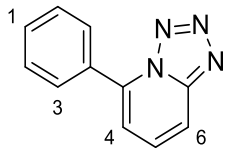
IR (thin film, ν_{max}/cm^{-1}) 3115, 3060, 1573, 1497, 1296, 1220, 1008, 971, 907, 731;

^{1}H NMR (400 MHz, $CDCl_3$) δ_H 8.44 (1H, dd, *J* = 6.8, 0.8 Hz, H1), 7.13 (1H, dd, *J* = 7.7, 6.8 Hz, H2), 6.86 (1H, dd, *J* = 7.7, 0.8 Hz, H3), 4.12 (3H, s, H4);

^{13}C NMR (101 MHz, $CDCl_3$) δ_C 148.5, 144.4, 117.8, 117.2, 107.4, 57.0.

HRMS (ESI) m/z: $[M + H]^+$ Calcd for $C_6H_7N_4O$ 151.0614; Found 151.0613.

5-Phenyltetrazolo[1,5-*a*]pyridine, 183j



ZT612, ZT615

Synthesis of 2-bromo-6-phenylpyridine: Modified from a literature procedure.[248] In a heat gun-dried round-bottom flask was dissolved 2-(dimethylamino)ethan-1-ol (1.5 mL, 15.0 mmol, 3 eq.) in hexane (anhy., 15 mL). The resulting solution was cooled to 0 °C before an *n*-butyllithium solution (1.6 M in hexane, 18.8 mmol, 6.0 eq.) was added dropwise. In a separate heat gun-dried vial was added 2-phenylpyridine (776 mg, 5.00 mmol, 1.0 eq.). The vial was purged under high vacuum for 30 s and backfilled with nitrogen (this cycle was repeated twice more). Hexane (anhy., 5 mL) was added to dissolve the 2-phenylpyridine. A solution of tetrabromomethane (5.80 g, 17.5 mmol, 3.5 eq.) in hexane (anhy., 5 mL) was prepared in a similar way. The 2-phenylpyridine solution was added dropwise to the previously prepared 2-(dimethylamino)ethan-1-ol and *n*-butyllithium mixture at 0 °C. After stirring for 1 h at 0 °C, it was cooled to −78 °C and the previously prepared

tetrabromomethane solution was added dropwise. The resulting reaction mixture was stirred at −78 °C for another hour and gently warmed to room temperature and stirred overnight. Upon completion, the reaction mixture was quenched by slowly adding water, and the aqueous phase was extracted three times with Et_2O. The organic layer was combined, dried over Na_2SO_4, and concentrated *in vacuo* to afford crude 2-bromo-6-phenylpyridine (857 mg, 3.66 mmol, 73%) as a deep orange oil which was used in the next step without further purification.

Synthesis of the title compound: Synthesised from 2-bromo-6-phenylpyridine (857 mg, 3.66 mmol, 1.0 eq.), sodium azide (714 mg, 11.0 mmol, 3.0 eq.), CuI (70 mg, 0.37 mmol, 10 mol%), *N*,*N*′-dimethylethylenediamine (60 μL, 0.75 mmol, 15 mol%), and sodium ascorbate (36 mg, 0.18 mmol, 5 mol%) with general procedure **7.2.2e**. Column chromatography (silica gel, Et_2O) afforded the title compound (384 mg, 1.96 mmol, 53%) as a yellow solid;

R_f 0.44 (Et_2O);

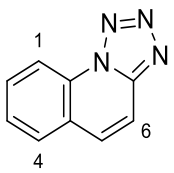
IR (thin film, ν_{max}/cm^{-1}) 3092, 1629, 1487, 1113, 1101, 910, 804, 760, 732, 692;

^{1}H NMR (400 MHz, $CDCl_3$) δ_H 8.08 – 7.95 (3H, m, H3, H6), 7.76 (1H, dd, *J* = 9.0, 7.0 Hz, H5), 7.65 – 7.53 (3H, m, H1, H2), 7.30 (1H, dd, *J* = 7.0, 1.1 Hz, H4);

^{13}C NMR (101 MHz, $CDCl_3$) δ_C 149.4, 139.4, 132.2, 131.1, 130.8, 129.2, 129.1, 115.8, 114.3;

HRMS (ESI) m/z: $[M + Na]^+$ Calcd for $C_{11}H_8N_4Na$ 219.0641; Found 219.0633.

Tetrazolo[1,5-*a*]quinoline, 183k



ZT616

Synthesised from 2-bromoquinoline (857 mg, 5.00 mmol, 1.0 eq.), sodium azide (975 mg, 15.0 mmol, 3.0 eq.), CuI (95 mg, 0.50 mmol, 10 mol%), *N*,*N*′-dimethylethylenediamine (81 μL, 0.75 mmol, 15 mol%), and sodium ascorbate (50 mg, 0.25 mmol, 5 mol%) with general procedure **7.2.2e**. Column chromatography (silica gel, Et_2O) afforded the title compound (734 mg, 4.31 mmol, 86%) as a colourless solid;

R_f 0.65 (Et_2O);

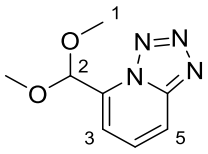
IR (thin film, ν_{max}/cm^{-1}) 3104, 3079, 1613, 1561, 1448, 1278, 1219, 1086, 822, 764;

^{1}H NMR (400 MHz, $CDCl_3$) δ_H 8.69 (1H, d, *J* = 8.3 Hz,), 8.01 – 7.91 (2H, m), 7.91 – 7.84 (2H, m), 7.72 (1H, t, *J* = 7.7 Hz);

^{13}C NMR (101 MHz, $CDCl_3$) δ_C 147.5, 133.4, 131.4, 130.9, 129.1, 128.1, 123.9, 117.0, 112.8;

Data are consistent with literature values.[249]

5-(Dimethoxymethyl)tetrazolo[1,5-*a*]pyridine, 183l



ZT639, ZT640

Synthesis of 2-bromo-6-(dimethoxymethyl)pyridine: in a heat gun-dried round-bottom flask was added 6-bromopicolinaldehyde (0.93 g, 5.00 mmol, 1.0 eq.) and 4-methylbenzenesulfonic acid monohydrate (48 mg, 0.25 mmol, 5 mol%). MeOH (anhy., 10 mL) was added to dissolve the two reagents, followed by the addition of trimethyl orthoformate (2.2 mL, 20.0 mmol, 4 eq.). The reaction mixture was refluxed under nitrogen until completion by TLC. Upon completion, it was cooled to room temperature, and concentrated *in vacuo* to give the crude 2-bromo-6-(dimethoxymethyl)pyridine (assume quantitative yield) as a brown oil which was used in the next step without further purification.

Synthesis of the title compound: Synthesised from 2-bromo-6-(dimethoxymethyl)pyridine (1.16 g, 5.00 mmol, 1.0 eq.), sodium azide (975 mg, 15.0 mmol, 3.0 eq.), CuI (95 mg, 0.50 mmol, 10 mol%), *N*,*N*′-dimethylethylenediamine (81 μL, 0.75 mmol, 15 mol%), and sodium ascorbate (50 mg, 0.25 mmol, 5 mol%) with general procedure **7.2.2e**. Column chromatography (silica gel, Et_2O) afforded the title compound (418 mg, 2.15 mmol, 43% over two steps) as a colourless solid;

m.p. 108 °C;

R_f 0.46 (Et_2O);

IR (thin film, ν_{max}/cm^{-1}) 3080, 2945, 2838, 1374, 1208, 1118, 1100, 1048, 975, 816;

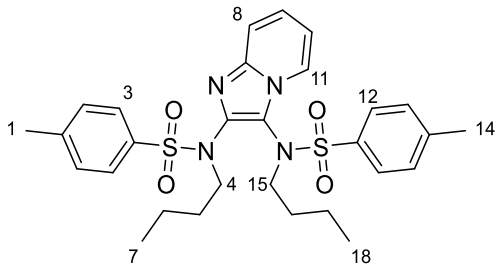
^{1}H NMR (400 MHz, $CDCl_3$) δ_H 8.03 (1H, d, *J* = 9.0 Hz, H5), 7.70 (1H, dd, *J* = 9.0, 7.0 Hz, H4), 7.44 (1H, d, *J* = 7.0 Hz, H3), 6.13 (1H, s, H2), 3.54 (6H, s, H1);

^{13}C NMR (101 MHz, $CDCl_3$) δ_C 148.9, 135.8, 131.6, 115.8, 114.2, 98.3, 55.1;

HRMS (ESI) m/z: $[M + Na]^+$ Calcd for $C_8H_{10}N_4O_2Na$ 217.0696; Found 217.0675;

7.6.3 Gold-catalysed Functionalisation of Yndiamides with Sulfilimines or Tetrazolo[1,5-*a*]pyridines

_N_,_N_′-(Imidazo[1,2-*a*]pyridine-2,3-diyl)bis(_N_-butyl-4-methylbenzenesulfonamide), 180a



ZT502

Synthesised from *N*,*N*′-(ethyne-1,2-diyl)bis(*N*-butyl-4-methylbenzenesulfonamide) (48 mg, 0.10 mmol, 1.0 eq.), 1,1-dimethyl-*N*-(pyridin-2-yl)-λ^4-sulfanimine (31 mg, 0.20 mmol, 2.0

eq.), dichloro(2-pyridinecarboxylato)gold (2 mg, 5.13 μmol, 5 mol%) in toluene (anhy., 0.2 mL) with general procedure **7.2.3e** at 80 °C for 18 h. Column chromatography (silica gel, 20% EtOAc/pentane) afforded the title compound (35 mg, 62 μmol, 61%) as a colourless oil;

ZT574

Synthesised from *N*,*N'*-(ethyne-1,2-diyl)bis(*N*-butyl-4-methylbenzenesulfonamide) (48 mg, 0.10 mmol, 1.0 eq.), tetrazolo[1,5-*a*]pyridine (24 mg, 0.20 mmol, 2.0 eq.), chloro[tris(2,4-di-*tert*-butylphenyl)phosphite]gold(I) (4.4 mg, 5.00 μmol, 5 mol%) and silver bis(trifluoromethanesulfonyl)imide (2 mg, 5.15 μmol, 5 mol%) in DCE (anhy., 0.2 mL) with general procedure **7.2.3f** at 80 °C for 18 h. Column chromatography (silica gel, 10% → 20% EtOAc/pentane) afforded the title compound (39 mg, 68 mmol, 68%) as a colourless oil;

R_f 0.20 (20% EtOAc/pentane);

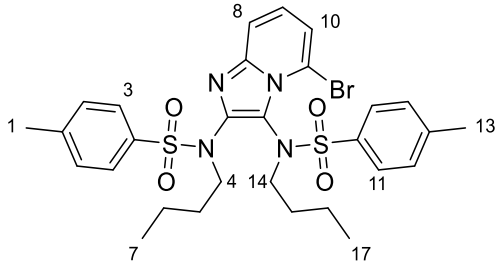
IR (thin film, ν_{max}/cm^{-1}) 2960, 2933, 2874, 1349, 1160, 1090, 911, 814, 732, 668;

^{1}H NMR (400 MHz, $CDCl_3$) δ_C 8.32 (1H, d, *J* = 6.9 Hz, H11), 7.99 (2H, d, *J* = 8.4 Hz, H12), 7.81 (2H, d, *J* = 8.3 Hz, H3), 7.49 (1H, d, *J* = 9.0 Hz, H8), 7.39 (2H, d, *J* = 8.4 Hz, H13), 7.34 – 7.27 (3H, m, H2, H9), 6.94 (1H, td, *J* = 6.8, 1.2 Hz, H10), 4.06 – 3.94 (1H, m, H15), 3.90 – 3.77 (1H, m, H15), 3.32 – 3.20 (1H, m, H4), 3.12 – 2.98 (1H, m, H4), 2.46 (3H, s, H14), 2.43 (3H, s, H1), 1.79 – 1.63 (1H, m, H16), 1.52 – 1.35 (1H, m, H16), 1.33 – 1.23 (2H, m, H17), 1.18 – 1.06 (2H, m, H5), 1.05 – 0.94 (2H, m, H6), 0.83 (3H, t, *J* = 7.3 Hz, H18), 0.66 (3H, t, *J* = 7.2 Hz, H7);

^{13}C NMR (101 MHz, $CDCl_3$) δ_C 144.2, 143.9, 141.0, 138.9, 137.1, 135.8, 130.0, 129.6, 128.9, 127.9, 126.1, 124.3, 118.0, 118.0, 113.2, 52.8, 51.0, 31.4, 29.3, 21.8, 21.7, 20.1, 20.0, 13.8, 13.6;

HRMS (ESI) m/z: $[M + H]^+$ Calcd for $C_{29}H_{37}N_4O_4S_2$ 569.2251; Found 569.2254.

***N*,*N'*-(5-Bromoimidazo[1,2-*α*]pyridine-2,3-diyl)bis(*N*-butyl-4-methylbenzenesulfonamide), 180b**



ZT517

Synthesised from *N*,*N'*-(ethyne-1,2-diyl)bis(*N*-butyl-4-methylbenzenesulfonamide) (48 mg, 0.10 mmol, 1.0 eq.), *N*-(6-bromopyridin-2-yl)-1,1-dimethyl-λ^4-sulfanimine (47 mg, 0.20 mmol, 2.0 eq.), dichloro(2-pyridinecarboxylato)gold (2 mg, 5.13 μmol, 5 mol%) in PhMe (anhy., 0.2 mL) with general procedure **7.2.3e** at 80 °C for 18 h. Column chromatography (silica gel, 10% → 20% EtOAc/pentane) afforded the title compound (63 mg, 97 μmol, 97%) as a brown oil;

R_f 0.17 (20% EtOAc/pentane);

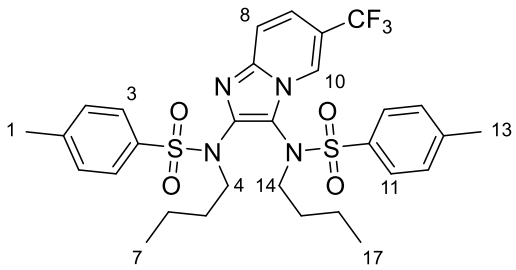
IR (thin film, ν_{max}/cm^{-1}) 2960, 2873, 1344, 1160, 1089, 814, 731, 664;

^{1}H NMR (400 MHz, $CDCl_3$) δ_H 7.92 (2H, d, *J* = 8.3 Hz, H11), 7.77 (2H, d, *J* = 8.3 Hz, H3), 7.49 (1H, dd, *J* = 8.4, 1.7 Hz, H8), 7.35 (2H, d, *J* = 8.3 Hz, H12), 7.29 (2H, d, *J* = 8.3 Hz, H2), 7.18 – 7.10 (2H, m, H9, H10), 4.08 – 3.99 (1H, m, H14), 3.99 – 3.89 (1H, m, H14), 3.19 – 3.08 (1H, m, H4), 2.89 – 2.79 (1H, m, H4), 2.44 (3H, s, H13), 2.42 (3H, s, H1), 1.98 – 1.85 (1H, m, H15), 1.65 – 1.50 (1H, m, H15), 1.41 – 1.27 (2H, m, H16), 1.19 – 1.06 (1H, m, H5), 1.03 – 0.85 (6H, m, H5, H6, H17), 0.64 (3H, t, *J* = 7.2 Hz, H7);

^{13}C NMR (101 MHz, $CDCl_3$) δ_C 143.9, 143.9, 143.0, 141.4, 137.8, 135.9, 129.7, 129.5, 128.9, 128.0, 126.3, 120.7, 119.6, 117.5, 113.3, 54.2, 51.1, 30.2, 28.8, 21.74, 21.69, 20.3, 20.1, 14.0, 13.6;

HRMS (ESI) m/z: $[M + H]^+$ Calcd for $C_{29}H_{36}{}^{79}BrN_4O_4S_2$ 647.1356; Found 647.1361.

***N*,*N*'-(6-(Trifluoromethyl)imidazo[1,2-*a*]pyridine-2,3-diyl)bis(*N*-butyl-4-methylbenzenesulfonamide), 180c**



ZT617

Synthesised from *N*,*N*'-(ethyne-1,2-diyl)bis(*N*-butyl-4-methylbenzenesulfonamide) (48 mg, 0.10 mmol, 1.0 eq.), 1,1-dimethyl-*N*-(5-(trifluoromethyl)pyridin-2-yl)-λ^4-sulfanimine (45 mg, 0.20 mmol, 2.0 eq.), dichloro(2-pyridinecarboxylato)gold (2 mg, 5.13 μmol, 5 mol%) in toluene (anhy., 0.2 mL) with general procedure **7.2.3e** at 80 °C for 18 h. Column chromatography (silica gel, 10% → 20% EtOAc/pentane) afforded the title compound (33 mg, 82 μmol, 81%) as a brown foam;

m.p. 163 – 164 °C;

R_f 0.37 (20% EtOAc/pentane);

IR (thin film, ν_{max}/cm^{-1}) 2962, 2875, 1349, 1321, 1167, 1136, 911, 814, 734, 666;

^{1}H NMR (500 MHz, $CDCl_3$) δ_H 8.49 (1H, s, H10), 7.93 (2H, d, *J* = 8.4 Hz, H11), 7.81 (2H, d, *J* = 8.2 Hz, H3), 7.61 (1H, d, *J* = 9.3 Hz, H8), 7.45 – 7.36 (3H, m, H9, H12), 7.32 (2H, d, *J* = 8.2 Hz, H2), 4.08 – 3.98 (1H, m, H14), 3.92 – 3.83 (1H, m, H14), 3.36 – 3.26 (1H, m, H4), 3.14 – 3.05 (1H, m, H4), 2.46 (3H, s, H13), 2.44 (3H, s, H1), 1.69 – 1.57 (1H, m, H15), 1.50 – 1.38 (1H, m, H15), 1.33 – 1.25 (2H, m, H16), 1.24 – 1.15 (1H, m, H5), 1.14 – 1.06 (1H, m, H5), 1.06 – 0.98 (2H, m, H6), 0.84 (3H, t, *J* = 7.4 Hz, H17), 0.68 (3H, t, *J* = 7.3 Hz, H7);

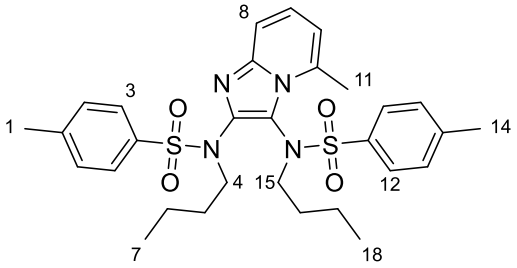
^{13}C NMR (126 MHz, $CDCl_3$) δ_C 144.7, 144.1, 140.8, 140.6, 136.9, 135.8, 130.2, 129.7, 128.8, 127.8, 123.4 (q, $^1J_{C–F}$ = 271.6 Hz), 123.2 (q, $^3J_{C–F}$ = 5.7 Hz), 122.0 (q, $^3J_{C–F}$ = 2.7

Hz), 119.6, 118.9, 117.7 (q, $^2J_{C-F}$ = 34.3 Hz), 52.5, 51.1, 31.3, 29.5, 21.8, 21.7, 20.0, 19.9, 13.7, 13.6;

^{19}F NMR (470 MHz, $CDCl_3$) δ_F -62.31;

HRMS (ESI) m/z: $[M + H]^+$ Calcd for $C_{30}H_{36}F_3N_4O_4S_2$ 637.2125; Found 637.2124.

***N*,*N*'-(5-Methylimidazo[1,2-*a*]pyridine-2,3-diyl)bis(*N*-butyl-4-methylbenzenesulfonamide), 180d**



ZT556

Synthesised from *N*,*N*'-(ethyne-1,2-diyl)bis(*N*-butyl-4-methylbenzenesulfonamide) (48 mg, 0.10 mmol, 1.0 eq.), 1,1-dimethyl-*N*-(6-methyl-pyridin-2-yl)-λ^4-sulfanimine (34 mg, 0.20 mmol, 2.0 eq.), dichloro(2-pyridinecarboxylato)gold (2 mg, 5.13 μmol, 5 mol%) in toluene (anhy., 0.2 mL) with general procedure **7.2.3e** at 80 °C for 18 h. Preparative LPLC (Silia*Sep* PREMIUM silica 12 g) afforded the title compound (eluted at ~20% EtOAc/pentane, 33 mg, 57 μmol, 56%) as a yellow oil; (*E*)-*N*,*N*'-(1-chloroethene-1,2-diyl)bis(*N*-butyl-4-methylbenzenesulfonamide) (eluted at ~15% EtOAc/pentane, 4 mg, 7.8 μmol, 8%) and *N*,*N*'-(ethyne-1,2-diyl)bis(*N*-butyl-4-methylbenzenesulfonamide) (eluted at ~18% EtOAc/pentane, 17 mg, 36 μmol, 36%) were also isolated;

ZT631

Synthesised from *N*,*N*'-(ethyne-1,2-diyl)bis(*N*-butyl-4-methylbenzenesulfonamide) (48 mg, 0.10 mmol, 1.0 eq.), 5-methyltetrazolo[1,5-*a*]pyridine (27 mg, 0.20 mmol, 2.0 eq.), chloro[tris(2,4-di-*tert*-butylphenyl)phosphite]gold(I) (4.4 mg, 5.00 μmol, 5 mol%) and

silver bis(trifluoromethanesulfonyl)imide (2 mg, 5.15 μmol, 5 mol%) in DCE (anhy., 0.2 mL) with general procedure **7.2.3f** at 80 °C for 18 h. Column chromatography (silica gel, 10% → 20% EtOAc/pentane) afforded the title compound (33 mg, 57 mmol, 56%) as an off-colourless solid;

m.p. 79 °C ($CHCl_3$);

R_f 0.23 (20% EtOAc/pentane);

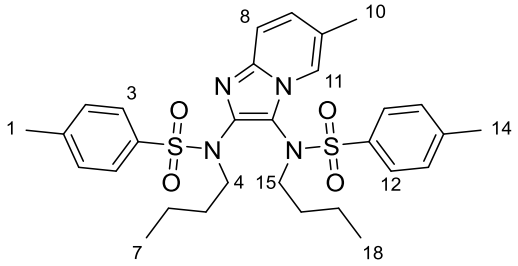
IR (thin film, ν_{max}/cm^{-1}) 2959, 2873, 1343, 1163, 1089, 739, 663

^{1}H NMR (400 MHz, $CDCl_3$) δ_H 8.00 (2H, d, *J* = 8.5 Hz, H12), 7.78 (2H, d, *J* = 8.4 Hz, H3), 7.41 – 7.33 (3H, m, H8, H13), 7.29 (2H, d, *J* = 8.4 Hz, H2), 7.17 (1H, dd, *J* = 9.0, 6.9 Hz, H9), 6.65 (1H, d, *J* = 6.9 Hz, H10), 4.01 – 3.89 (2H, m, H15), 3.18 – 3.06 (1H, m, H4), 3.02 (3H, s, H11), 2.91 – 2.79 (1H, m, H4), 2.46 (3H, s, H14), 2.42 (3H, s, H1), 1.76 – 1.67 (1H, m, H16), 1.60 – 1.46 (1H, m, H16), 1.40 – 1.25 (2H, m, H17), 1.23 – 1.14 (1H, m, H5), 1.04 – 0.89 (3H, m, H5, H6), 0.86 (3H, t, *J* = 7.4 Hz, H18), 0.65 (3H, t, *J* = 7.2 Hz, H7);

^{13}C NMR (101 MHz, $CDCl_3$) δ_C 144.0, 143.9, 142.6, 140.3, 137.5, 137.1, 135.9, 129.9, 129.5, 129.1, 128.1, 126.1, 118.5, 116.3, 115.5, 54.0, 51.3, 30.4, 28.8, 21.73, 21.70, 20.4, 20.22, 20.19, 13.9, 13.6;

HRMS (ESI) m/z: $[M + H]^+$ Calcd for $C_{30}H_{39}N_4O_4S_2$ 583.2407; Found 583.2414.

***N*,*N*'-(6-Methylimidazo[1,2-*a*]pyridine-2,3-diyl)bis(*N*-butyl-4-methylbenzenesulfonamide), 180e**



ZT632

Synthesised from *N*,*N'*-(ethyne-1,2-diyl)bis(*N*-butyl-4-methylbenzenesulfonamide) (48 mg, 0.10 mmol, 1.0 eq.), 1,1-dimethyl-*N*-(5-methyl-pyridin-2-yl)-λ^4-sulfanimine (34 mg, 0.20 mmol, 2.0 eq.), dichloro(2-pyridinecarboxylato)gold (2 mg, 5.13 μmol, 5 mol%) in toluene (anhy., 0.2 mL) with general procedure **7.2.3e** at 80 °C for 18 h. Column chromatography (silica gel, 10% → 20% EtOAc/pentane) afforded the title compound (18 mg, 31 μmol, 31%) as a yellow gum; (*E*)-*N*,*N*'-(1-chloroethene-1,2-diyl)bis(*N*-butyl-4-methylbenzenesulfonamide) (3 mg, 5.9 μmol, 6%) and *N*,*N*'-(ethyne-1,2-diyl)bis(*N*-butyl-4-methylbenzenesulfonamide) (28 mg, 59 μmol, 59%) were also isolated;

m.p. 174 °C;

R_f 0.30 (20% EtOAc/pentane);

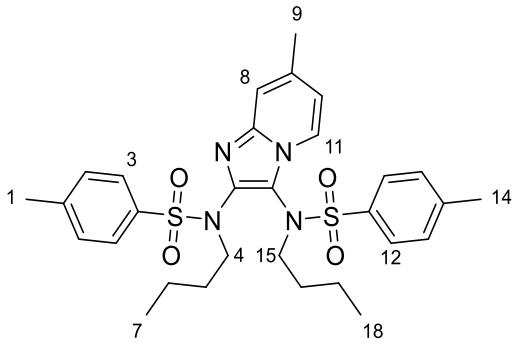
IR (thin film, ν_{max}/cm^{-1}) 2961, 2874, 1345, 1159, 1090, 911, 813, 756, 734, 667;

^{1}H NMR (400 MHz, $CDCl_3$) δ_H 8.03 (1H, s, H11), 7.99 (2H, d, *J* = 8.5 Hz, H12), 7.80 (2H, d, *J* = 8.2 Hz, H3), 7.42 – 7.35 (3H, m, H8, H13), 7.30 (2H, d, *J* = 8.2 Hz, H2), 7.12 (1H, dd, *J* = 9.2, 1.8 Hz, H9), 4.05 – 3.93 (1H, m, H15), 3.90 – 3.77 (1H, m, H15), 3.31 – 3.19 (1H, m, H4), 3.11 – 2.99 (1H, m, H4), 2.46 (3H, s, H14), 2.43 (3H, s, H1), 2.37 (3H, s, H10), 1.77 – 1.63 (1H, m, H16), 1.54 – 1.38 (1H, m, H16), 1.29 (2H, app. sext., *J* = 7.5 Hz, H17), 1.20 – 1.05 (2H, m, H5), 1.04 – 0.93 (2H, m, H6), 0.84 (3H, t, *J* = 7.3 Hz, H18), 0.65 (3H, t, *J* = 7.3 Hz, H7);

^{13}C NMR (101 MHz, $CDCl_3$) δ_C 144.2, 143.8, 140.0, 138.7, 137.3, 135.9, 130.0, 129.6, 129.3, 128.9, 127.9, 123.0, 121.9, 117.6, 117.3, 52.8, 51.1, 31.3, 29.4, 21.8, 21.7, 20.1, 20.0, 18.6, 13.8, 13.6;

HRMS (ESI) m/z: $[M + H]^+$ Calcd for $C_{30}H_{39}N_4O_4S_2$ 583.2407; Found 583.2422.

***N*,*N*'-(7-Methylimidazo[1,2-*a*]pyridine-2,3-diyl)bis(*N*-butyl-4-methylbenzenesulfonamide), 180f**



ZT634

Synthesised from *N*,*N'*-(ethyne-1,2-diyl)bis(*N*-butyl-4-methylbenzenesulfonamide) (48 mg, 0.10 mmol, 1.0 eq.), 1,1-dimethyl-*N*-(4-methyl-pyridin-2-yl)-λ^4-sulfanimine (34 mg, 0.20 mmol, 2.0 eq.), dichloro(2-pyridinecarboxylato)gold (2 mg, 5.13 μmol, 5 mol%) in toluene (anhy., 0.2 mL) with general procedure **7.2.3e** at 80 °C for 18 h. Column chromatography (silica gel, 0% → 10% → 20% EtOAc/pentane) afforded the title compound (15 mg, 26 μmol, 26%) as a colourless solid; (*E*)-*N*,*N*'-(1-chloroethene-1,2-diyl)bis(*N*-butyl-4-methylbenzenesulfonamide) (3 mg, 5.9 μmol, 6%) and *N*,*N*'-(ethyne-1,2-diyl)bis(*N*-butyl-4-methylbenzenesulfonamide) (33 mg, 69 μmol, 69%) were also isolated;

ZT633

Synthesised from *N*,*N'*-(ethyne-1,2-diyl)bis(*N*-butyl-4-methylbenzenesulfonamide) (48 mg, 0.10 mmol, 1.0 eq.), 7-methyltetrazolo[1,5-*a*]pyridine (27 mg, 0.20 mmol, 2.0 eq.), chloro[tris(2,4-di-*tert*-butylphenyl)phosphite]gold(I) (4.4 mg, 5.00 μmol, 5 mol%) and silver bis(trifluoromethanesulfonyl)imide (2 mg, 5.15 μmol, 5 mol%) in DCE (anhy., 0.2 mL) with general procedure **7.2.3f** at 80 °C for 18 h. Column chromatography (silica gel, 0% → 10% → 20% EtOAc/pentane) afforded the title compound (22 mg, 38 mmol, 37%) as a colourless oil; (*E*)-*N*,*N*'-(1-chloroethene-1,2-diyl)bis(*N*-butyl-4-

methylbenzenesulfonamide) (1 mg, 2.0 μmol, 2%) and *N*,*N*'-(ethyne-1,2-diyl)bis(*N*-butyl-4-methylbenzenesulfonamide) (16 mg, 34 μmol, 34%) were also isolated;

m.p. 62 °C ($CHCl_3$);

R_f 0.31 (20% EtOAc/pentane);

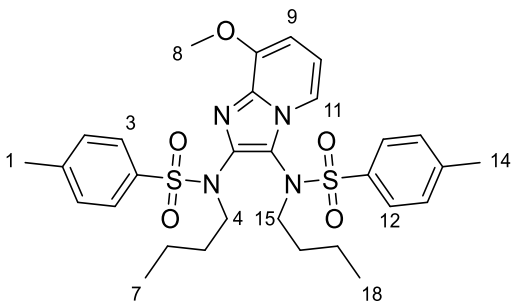
IR (thin film, ν_{max}/cm^{-1}) 2961, 2874, 1350, 1164, 1090, 814, 756, 735, 677, 663;

^{1}H NMR (400 MHz, $CDCl_3$) δ_H 8.20 (1H, d, *J* = 7.0 Hz, H11), 7.98 (2H, d, *J* = 8.3 Hz, H12), 7.80 (2H, d, *J* = 8.2 Hz, H3), 7.38 (d, *J* = 8.3 Hz, 2H, H13), 7.30 (2H, d, *J* = 8.2 Hz, H2), 7.24 (1H, s, H8), 6.77 (1H, dd, *J* = 7.0, 1.8 Hz, H10), 4.05 – 3.93 (1H, m, H15), 3.89 – 3.77 (1H, m, H15), 3.30 – 3.18 (1H, m, H4), 3.08 – 2.97 (1H, m, H4), 2.45 (3H, s, H14), 2.42 (3H, s, H1), 2.41 (3H, s, H9), 1.77 – 1.63 (1H, m, H16), 1.51 – 1.37 (1H, m, H16), 1.36 – 1.20 (2H, m, H17), 1.18 – 1.04 (2H, m, H5), 1.04 – 0.93 (2H, m, H6), 0.83 (3H, t, *J* = 7.4 Hz, H18), 0.65 (3H, t, *J* = 7.3 Hz, H7);

^{13}C NMR (101 MHz, $CDCl_3$) δ_C 144.1, 143.8, 141.4, 138.6, 137.22, 137.17, 135.9, 129.9, 129.5, 128.9, 127.9, 123.6, 117.5, 116.3, 115.8, 52.8, 51.0, 31.4, 29.4, 21.73, 21.68, 21.5, 20.1, 20.0, 13.8, 13.6;

HRMS (ESI) m/z: $[M + H]^+$ Calcd for $C_{30}H_{39}N_4O_4S_2$ 583.2407; Found 583.2395.

***N*,*N*'-(8-Methoxyimidazo[1,2-*a*]pyridine-2,3-diyl)bis(*N*-butyl-4-methylbenzenesulfonamide), 180i**



ZT635

Synthesised from *N*,*N'*-(ethyne-1,2-diyl)bis(*N*-butyl-4-methylbenzenesulfonamide) (48 mg, 0.10 mmol, 1.0 eq.), 8-methoxytetrazolo[1,5-*a*]pyridine (30 mg, 0.20 mmol, 2.0 eq.), chloro[tris(2,4-di-*tert*-butylphenyl)phosphite]gold(I) (4.4 mg, 5.00 μmol, 5 mol%) and silver bis(trifluoromethanesulfonyl)imide (2 mg, 5.15 μmol, 5 mol%) in DCE (anhy., 0.2 mL) with general procedure **7.2.3f** at 80 °C for 18 h. Column chromatography (silica gel, 20% → 40% EtOAc/pentane) afforded the title compound (56 mg, 94 mmol, 93%) as a blue solid;

m.p. 157 – 158 °C;

R_f 0.10 (20% EtOAc/pentane);

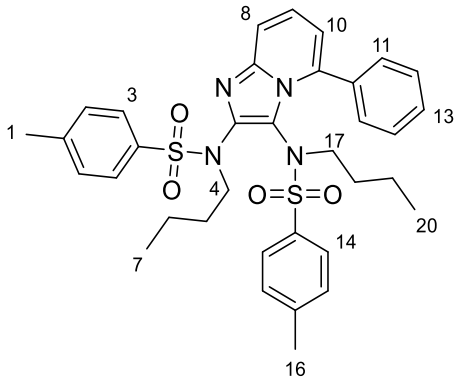
IR (thin film, ν_{max}/cm^{-1}) 2962, 2875, 1553, 1343, 1288, 1163, 1090, 911, 756, 733, 664;

^{1}H NMR (400 MHz, $CDCl_3$) δ_H 8.02 (2H, d, *J* = 8.1 Hz, H12), 7.96 (1H, dd, *J* = 6.8, 1.0 Hz, H11), 7.80 (2H, d, *J* = 8.1 Hz, H3), 7.39 (2H, d, *J* = 8.1 Hz, H13), 7.29 (2H, d, *J* = 8.1 Hz, H2), 6.84 (1H, dd, *J* = 7.8, 6.8 Hz, H10), 6.57 (1H, dd, *J* = 7.8, 1.0 Hz, H9), 4.04 – 3.91 (4H, m, H15, H8), 3.84 – 3.72 (1H, m, H15), 3.38 – 3.26 (1H, m, H4), 3.25 – 3.13 (1H, m, H4), 2.45 (3H, s, H14), 2.41 (3H, s, H1), 1.77 – 1.63 (1H, m, H16), 1.50 – 1.36 (1H, m, H16), 1.30 – 1.21 (2H, m, H17), 1.21 – 1.11 (2H, m, H5), 1.06 – 0.95 (2H, m, H6), 0.81 (3H, t, *J* = 7.3 Hz, H18), 0.66 (3H, t, *J* = 7.3 Hz, H7);

^{13}C NMR (101 MHz, $CDCl_3$) δ_C 149.0, 144.1, 143.8, 138.2, 137.0, 135.5, 135.3, 129.9, 129.6, 129.0, 127.9, 119.0, 117.1, 113.0, 102.4, 56.0, 52.8, 50.9, 31.2, 29.5, 21.7 (2C), 20.1, 20.0, 13.8, 13.6;

HRMS (ESI) m/z: $[M + H]^+$ Calcd for $C_{30}H_{39}N_4O_5S_2$ 599.2356; Found 599.2375.

***N*,*N*'-(5-Phenylimidazo[1,2-*a*]pyridine-2,3-diyl)bis(*N*-butyl-4-methylbenzenesulfonamide), 180j**



ZT637

Synthesised from *N*,*N*'-(ethyne-1,2-diyl)bis(*N*-butyl-4-methylbenzenesulfonamide) (48 mg, 0.10 mmol, 1.0 eq.), 5-phenyltetrazolo[1,5-*a*]pyridine (40 mg, 0.20 mmol, 2.0 eq.), chloro[tris(2,4-di-*tert*-butylphenyl)phosphite]gold(I) (4.4 mg, 5.00 μmol, 5 mol%) and silver bis(trifluoromethanesulfonyl)imide (2 mg, 5.15 μmol, 5 mol%) in DCE (anhy., 0.2 mL) with general procedure **7.2.3f** at 80 °C for 18 h. Preparative LPLC (RediSep Rf Gold® 12 g HP Silica, 30 % EtOAc/pentane) afforded the title compound (59 mg, 91 mmol, 91%) as a yellow gum;

m.p. 155 – 157 °C;

R_f 0.24 (20% EtOAc/pentane);

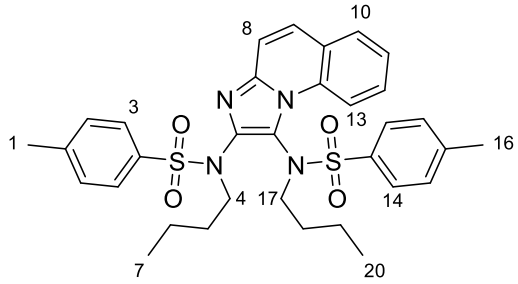
IR (thin film, ν_{max}/cm^{-1}) 2962, 2875, 1347, 1164, 911, 732;

^{1}H NMR (400 MHz, $CDCl_3$) δ_H 7.88 – 7.73 (3H, m, H13, H14), 7.63 – 7.36 (7H, m, H3, H8, H11, H12), 7.32 – 7.27 (3H, m, H9, H15), 7.22 (2H, d, *J* = 8.1 Hz, H2), 6.69 (1H, dd, *J* = 7.0, 1.3 Hz, H10), 3.40 – 3.30 (1H, m, H17), 3.30 – 3.18 (1H, m, H17), 3.13 – 3.01 (1H, m, H4), 2.78 – 2.65 (1H, m, H4), 2.43 (3H, s, H16), 2.38 (3H, s, H1), 1.87 – 1.73 (1H, m, H18), 1.72 – 1.59 (1H, m, H18), 1.28 – 1.13 (3H, m, H5, H19), 0.96 – 0.83 (6H, m, H6, H19, H20), 0.68 (3H, t, *J* = 7.1 Hz, H7);

^{13}C NMR (101 MHz, $CDCl_3$) δ_C 143.8, 143.5, 142.2, 140.1, 139.8, 138.1, 135.8, 135.0, 131.2, 129.5, 129.5, 129.2, 129.1, 128.0, 127.3, 125.5, 120.2, 117.5, 117.2, 53.9, 51.1, 30.5, 29.1, 21.7, 21.6, 20.3, 20.1, 13.8, 13.7;

HRMS (ESI) m/z: $[M + H]^+$ Calcd for $C_{35}H_{41}N_4O_4S_2$ 645.2564; Found 645.2589.

***N*,*N*'-(Imidazo[1,2-*a*]quinoline-1,2-diyl)bis(*N*-butyl-4-methylbenzenesulfonamide), 180k**



ZT644

Synthesised from *N*,*N*'-(ethyne-1,2-diyl)bis(*N*-butyl-4-methylbenzenesulfonamide) (48 mg, 0.10 mmol, 1.0 eq.), tetrazolo[1,5-a]quinoline (86 mg, 0.51 mmol, 5.0 eq.), chloro[tris(2,4-di-*tert*-butylphenyl)phosphite]gold(I) (4.4 mg, 5.00 μmol, 5 mol%) and silver bis(trifluoromethanesulfonyl)imide (2 mg, 5.15 μmol, 5 mol%) in DCE (anhy., 0.2 mL) with general procedure **7.2.3f** at 80 °C for 18 h. Column chromatography (silica gel, 10% → 20% EtOAc/pentane) afforded the title compound (18 mg, 29 mmol, 29%) as an off-colourless solid;

m.p. 210 °C;

R_f 0.25 (20% EtOAc/pentane);

IR (thin film, ν_{max}/cm^{-1}) 2962, 1347, 1166, 910, 732;

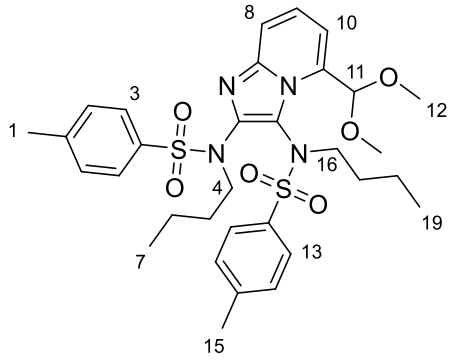
^{1}H NMR (400 MHz, $CDCl_3$) δ_H 8.91 (1H, d, *J* = 8.7 Hz, quinoline Ar*H*), 8.02 (2H, d, *J* = 8.4 Hz, H14), 7.86 (2H, d, *J* = 8.2 Hz, H3), 7.79 (1H, dd, *J* = 7.8, 1.7 Hz, quinoline Ar*H*), 7.62 – 7.55 (2H, m, quinoline Ar*H*), 7.52 – 7.46 (1H, m, quinoline Ar*H*), 7.44 – 7.37 (3H,

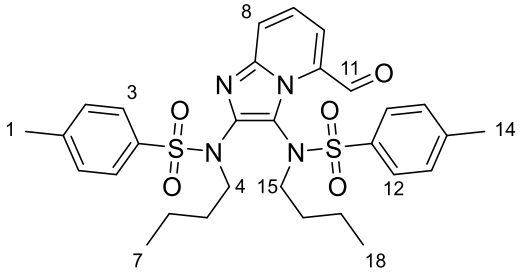
m, quinoline Ar*H*, H15), 7.33 (2H, d, *J* = 8.2 Hz, H2), 4.13 – 3.95 (2H, m, H17), 3.36 – 3.24 (1H, m, H4), 3.22 – 3.10 (1H, m, H4), 2.48 (3H, s, H16), 2.45 (3H, s, H1), 1.74 – 1.63 (1H, m, H18), 1.58 – 1.49 (1H, m, H18), 1.41 – 1.21 (3H, m, H5, H19), 1.21 – 1.10 (1H, m, H5), 1.07 – 0.95 (2H, m, H6), 0.77 (3H, t, *J* = 7.4 Hz, H20), 0.68 (3H, t, *J* = 7.3 Hz, H7);

^{13}C NMR (101 MHz, $CDCl_3$) δ_C 144.3, 143.9, 140.4, 139.8, 137.0, 136.0, 133.7, 129.9, 129.6, 129.3, 129.1, 128.6, 128.3, 128.2, 125.4, 124.7, 121.2, 117.5, 117.4, 53.0, 51.4, 29.6, 29.1, 21.78, 21.76, 20.23, 20.20, 13.8, 13.7;

HRMS (ESI) m/z: $[M + H]^+$ Calcd for $C_{33}H_{39}N_4O_4S_2$ 619.2407; Found 619.2422.

_N_,_N_'-(5-(Dimethoxymethyl)imidazo[1,2-*a*]pyridine-2,3-diyl)bis(*N*-butyl-4-methylbenzenesulfonamide) (left) 180l, and _N_,_N_'-(5-Formylimidazo[1,2-*a*]pyridine-2,3-diyl)bis(*N*-butyl-4-methylbenzenesulfonamide) (right) 180m





ZT643

Synthesised from *N*,*N*'-(ethyne-1,2-diyl)bis(*N*-butyl-4-methylbenzenesulfonamide) (48 mg, 0.10 mmol, 1.0 eq.), 5-(dimethoxymethyl)tetrazolo[1,5-*a*]pyridine (39 mg, 0.51 mmol, 5.0 eq.), chloro[tris(2,4-di-*tert*-butylphenyl)phosphite]gold(I) (4.4 mg, 5.00 μmol, 5 mol%) and silver bis(trifluoromethanesulfonyl)imide (2 mg, 5.15 μmol, 5 mol%) in DCE (anhy., 0.2 mL) with general procedure **7.2.3f** at 80 °C for 18 h. Preparative LPLC (RediSep Rf Gold® 12 g HP Silica, 0% → 40 % EtOAc/pentane) afforded the **180l** (eluted at ~ 35%

EtOAc/pentane, 27 mg, 42 mmol, 42%) as a black solid and **180m** (eluted at ~ 40% EtOAc/pentane, 16 mg, 27 mmol, 27%) as a yellow gum;

Characterisation for **180l**:

m.p. 70 °C ($CHCl_3$);

R_f 0.24 (20% EtOAc/pentane);

IR (thin film, ν_{max}/cm^{-1}) 2962, 1347, 1165, 1089, 911, 732;

^{1}H NMR (400 MHz, $CDCl_3$) δ_H 7.93 (2H, d, *J* = 8.4 Hz, H13), 7.81 (2H, d, *J* = 8.4 Hz, H3), 7.49 (1H, dd, *J* = 8.7, 1.5 Hz, H8), 7.41 – 7.33 (3H, m, H10, H14), 7.32 – 7.27 (3H, m, H2, H9), 6.61 (1H, s, H11), 4.00 – 3.84 (2H, m, H16), 3.51 (3H, s, H12), 3.34 (3H, s, H12), 3.21 – 3.09 (1H, m, H4), 2.90 – 2.78 (1H, m, H4), 2.45 (3H, s, H15), 2.43 (3H, s, H1), 1.96 – 1.81 (1H, m, H17), 1.70 – 1.56 (1H, m, H17), 1.39 – 1.17 (3H, m, H5, H18), 1.06 – 0.85 (6H, m, H6, H18, H19), 0.66 (3H, t, *J* = 7.3 Hz, H7);

^{13}C NMR (101 MHz, $CDCl_3$) δ_C 144.3, 143.9, 142.3, 140.5, 137.3, 136.9, 136.1, 129.9, 129.5, 129.2, 128.3, 125.2, 119.2, 118.8, 113.5, 96.6, 55.5, 53.2, 52.5, 51.4, 29.7, 29.0, 21.8, 21.7, 20.4, 20.2, 14.0, 13.7;

HRMS (ESI) m/z: $[M + H]^+$ Calcd for $C_{32}H_{43}N_4O_6S_2$ 643.2619; Found 643.2620;

Characterisation for **180m**:

m.p. 168 – 170 °C;

R_f 0.54 (40% EtOAc/pentane);

IR (thin film, ν_{max}/cm^{-1}) 2962, 1693, 1347, 1164, 911, 732;

^{1}H NMR (400 MHz, $CDCl_3$) δ_H 11.13 (1H, s, H11), 7.86 (2H, d, *J* = 8.4 Hz, H12), 7.82 (2H, d, *J* = 8.1 Hz, H3), 7.76 – 7.71 (2H, m, H8, H10), 7.40 – 7.35 (3H, m, H9, H13), 7.32 (2H, d, *J* = 8.1 Hz, H2), 4.18 – 4.00 (2H, m, H15), 3.21 – 3.09 (1H, m, H4), 2.70 – 2.56 (1H, m, H4), 2.45 (3H, s, H14), 2.44 (3H, s, H1), 1.76 – 1.54 (2H, m, H16), 1.41 – 1.27

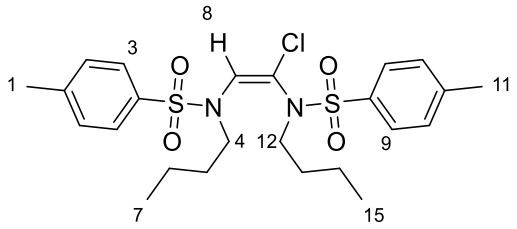
(2H, m, H17), 1.22 – 1.10 (1H, m, H5), 1.01 – 0.82 (6H, m, H5, H6, H18), 0.65 (3H, t, *J* = 7.2 Hz, H7);

^{13}C NMR (101 MHz, $CDCl_3$) δ_C 183.4, 144.8, 144.1, 141.5, 140.7, 136.5, 136.0, 135.5, 130.1, 129.6, 129.1, 128.0, 124.8, 123.9, 119.9, 118.2, 53.0, 51.1, 30.5, 29.0, 21.79, 21.76, 20.1, 20.0, 13.9, 13.6;

HRMS (ESI) m/z: $[M + H]^+$ Calcd for $C_{30}H_{37}N_4O_5S_2$ 597.2200; Found 597.2203.

7.6.4 Miscellaneous

(*E*)-*N*,*N*'-(1-Chloroethene-1,2-diyl)bis(*N*-butyl-4-methylbenzenesulfonamide), 181



ZT298

To a heat gun-dried vial containing a stirrer bar and 3 Å molecular sieves were added *N*,*N*'-(ethyne-1,2-diyl)bis(*N*-butyl-4-methylbenzenesulfonamide) (48 mg, 0.10 mmol, 1.0 eq.) and 1,1-dimethyl-*N*-(pyridin-2-yl)-λ^4-sulfanimine (32 mg, 0.20 mmol, 2.0 eq.). The vial was purged under high vacuum for 30 s and backfilled with argon (this vacuum cycle was repeated twice more). The vial was then moved into the glovebox where $IPrAuNTf_2$ (4 mg, 4.62 μmol, 5 mol%) was added. DCE (anhy., 0.5 M) was added after the vial was removed from the glovebox. The reaction mixture was stirred at 80 °C overnight under an argon atmosphere in the dark. Upon completion, the reaction mixture was concentrated *in vacuo* and purified by column chromatography (silica gel, 10 % EtOAc/pentane) to afford the title compound (32 mg, 64 μmol, 64%) as a colourless oil;

R_f 0.32 (10 % EtOAc/pentane);

IR (thin film, ν_{max}/cm^{-1}) 2960, 1354, 1165, 1090, 910, 815, 730, 660;

^{1}H NMR (400 MHz, $CDCl_3$) δ_H 7.76 (2H, d, *J* = 8.2 Hz, H3), 7.68 (2H, d, *J* = 8.2 Hz, H9), 7.33 (2H, d, *J* = 8.2 Hz, H2), 7.29 (2H, d, *J* = 8.2 Hz, H10), 6.95 (1H, s, H8), 3.73 (2H, brs., H4), 3.10 (2H, brs., H12), 2.43 (3H, s, H1), 2.42 (3H, s, H11), 1.68 (2H, brs., H5), 1.46 – 1.27 (4H, m, H6, H13), 1.28 – 1.16 (2H, m, H14), 0.92 (3H, t, *J* = 7.4 Hz, H7), 0.84 (3H, t, *J* = 7.3 Hz, H15);

^{13}C NMR (101 MHz, $CDCl_3$) δ_C 144.7, 144.2, 136.2, 134.4, 129.9, 129.6, 129.0, 127.7, 127.5, 114.9, 48.8, 46.9, 31.5, 29.5, 21.8, 21.7, 20.2, 20.0, 13.9, 13.8;

HRMS (ESI) m/z: $[M + H]^+$ Calcd for $C_{24}H_{34}ClN_2O_4S_2$ 513.1643; Found 513.1646.

7.6.5 X-Ray Crystallography

Single crystal X-ray diffraction data were collected using a (Rigaku) Oxford Diffraction SuperNova A diffractometer and reduced using CrysAlisPro. Structures were solved using Super-Flip[239] and refined using CRYSTALS[240, 241].

Table 7.03 Crystal data and structure refinement for **183a**.

Empirical formula	C5 H4 N4	
Formula weight	120.11	
Temperature	150 K	
Wavelength	1.54184 Å	
Crystal system	Monoclinic	
Space group	I 2/a	
Unit cell dimensions	a = 7.1726(6) Å	α = 90°.
	b = 7.6686(5) Å	β = 99.606(7)°.
	c = 9.7354(8) Å	γ = 90°.

Volume	527.98(7) $Å^3$
Z	4
Density (calculated)	1.511 Mg/m^3
Absorption coefficient	0.867 mm^{-1}
F(000)	248
Crystal size	0.20 x 0.15 x 0.05 mm3
Theta range for data collection	7.393 to 75.906°.
Index ranges	-8<=h<=8, -5<=k<=9, -12<=l<=12
Reflections collected	2302
Independent reflections	554 [R(int) = 0.038]
Completeness to theta = 75.906°	99.6 %
Absorption correction	Semi-empirical from equivalents
Max. and min. transmission	0.96 and 0.53
Refinement method	Full-matrix least-squares on F2
Data / restraints / parameters	554 / 0 / 45
Goodness-of-fit on F2	1.0519
Final R indices [I>2sigma(I)]	R1 = 0.0450, wR2 = 0.1218
R indices (all data)	R1 = 0.0490, wR2 = 0.1310
Largest diff. peak and hole	0.24 and -0.22 $e.Å^{-3}$

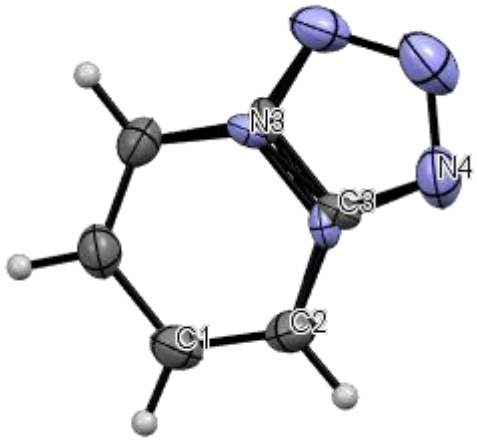
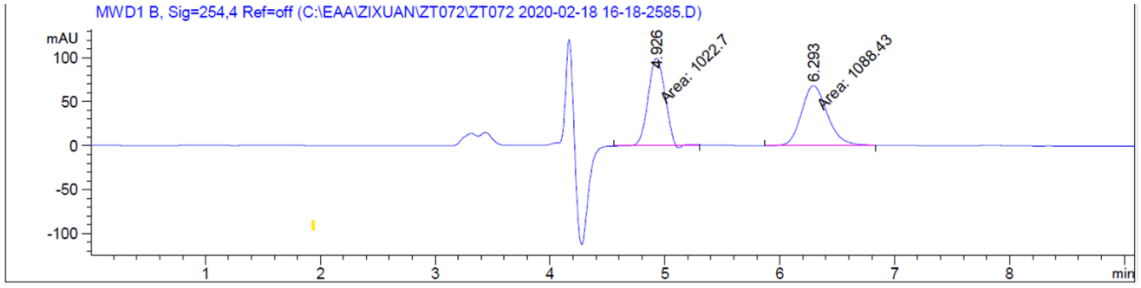


Figure 7.15 The structure of **183a** determined from X-ray diffraction studies, displacement ellipsoids are drawn at 50% probability. Atoms C1, C2, C3, N3 and N4 are generated by symmetry.

7.7 Chapter VI Characterisation Data

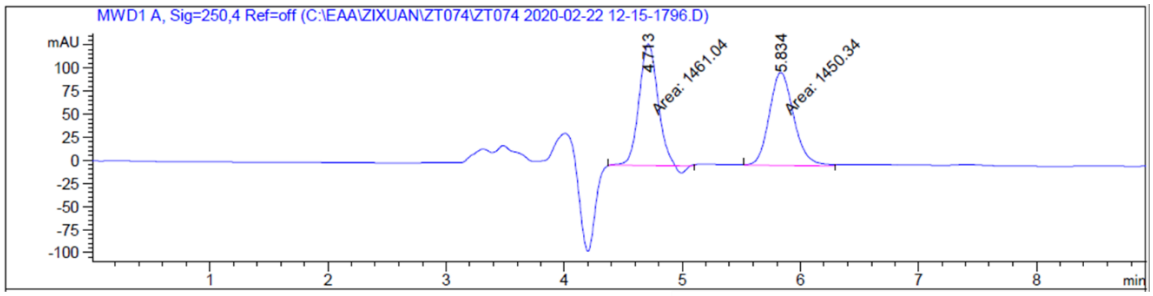
7.7.1 HPLC Traces



Signal 2: MWD1 B, Sig=254,4 Ref=off

Peak #	RetTime [min]	Type	Width [min]	Area [mAU*s]	Height [mAU]	Area %
1	4.926	MM	0.1707	1022.69916	99.87263	48.4432
2	6.293	MM	0.2651	1088.43091	68.43781	51.5568
Totals :				2111.13007	168.31044	

Figure 7.16 HPLC traces of attempted asymmetric gold(I)-catalysed functionalisation of yndiamides and pyridine *N*-oxides with 10 mol% (*S*)-BINOL-PO_2H. (CHIRALPAK® IC, 40% IPA/n-hexane, 1 mL/min).



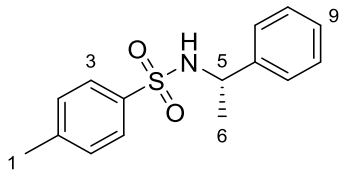
Signal 1: MWD1 A, Sig=250,4 Ref=off

Peak #	RetTime [min]	Type	Width [min]	Area [mAU*s]	Height [mAU]	Area %
1	4.713	MM	0.1848	1461.04187	131.79764	50.1838
2	5.834	MM	0.2400	1450.33801	100.70090	49.8162
Totals :				2911.37988	232.49854	

Figure 7.17 HPLC traces of attempted asymmetric gold(I)-catalysed functionalisation of yndiamides and pyridine *N*-oxides with 20 mol% (*S*)-BINOL-PO_2H. (CHIRALPAK® IC, 40% IPA/n-hexane, 1 mL/min).

7.7.2 Sulfonamides

(S)-4-Methyl-*N*-(1-phenylethyl)benzenesulfonamide, 1x



ZT233

Synthesised from 4-methylbenzenesulfonyl chloride (5.00 g, 26.2 mmol, 1.0 eq.), *(S)*-1-phenylethan-1-amine (3.8 mL, 29.5 mmol, 1.1 eq.), and triethylamine (4.4 mL, 31.6 mmol, 1.2 eq.) with general procedure **7.2.1a**. Recrystallisation from DCM/pentane afforded the title compound (6.95 g, 25.2 mmol, 96%) as a colourless solid.

R_f 0.32 (DCM);

$[\alpha]_D^{25}$ = − 64.60 (*c* 0.01, $CHCl_3$);

IR (thin film, ν_{max}/cm^{-1}) 3273, 2980, 1599, 1329, 1158, 1093, 960, 814, 760, 701, 666;

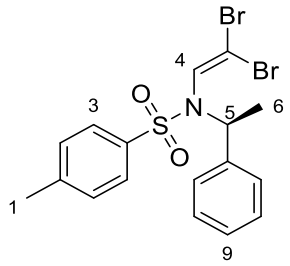
^{1}H NMR (400 MHz, $CDCl_3$) δ_H 7.62 (2H, d, *J* = 8.3 Hz, H3), 7.22 – 7.15 (5H, m, H2, H7, H9), 7.13 – 7.07 (2H, m, H8), 4.94 (1H, d, *J* = 6.7 Hz, H4), 4.46 (1H, app. quin., *J* = 6.8 Hz, H5), 2.38 (3H, s, H1), 1.42 (3H, d, *J* = 6.9 Hz, H6);

^{13}C NMR (101 MHz, $CDCl_3$) δ_C 143.3, 142.2, 137.8, 129.6, 128.7, 127.6, 127.2, 126.3, 53.7, 23.7, 21.6;

Data are consistent with literature values.[250]

7.7.3 1,1-Dibromoenamides

***(S)*-*N*-(2,2-Dibromovinyl)-4-methyl-*N*-(1-phenylethyl)benzenesulfonamide, 2x**



ZT238, ZT239

Synthesised from *(S)*-4-methyl-*N*-(1-phenylethyl)benzenesulfonamide (2.20 g, 8.00 mmol, 1.0 eq.), *n*-butyllithium (1.4 M in hexane, 6.4 mL, 8.96 mmol, 1.1 eq.), BtCHO (1.53 g, 10.4 mmol, 1.3 eq.), tetrabromomethane (7.96 g, 24.0 mmol, 3.0 eq.), triphenylphosphine (12.6 g, 48.0 mmol, 6.0 eq.) with general procedure **7.2.1c**. Column chromatography (silica gel, 10% EtOAc/pentane) afforded the title compound (2.11 g, 4.59 mmol, 57%) as a colourless solid.

m.p. 101 °C;

R_f 0.47 (10% EtOAc/pentane);

$[\alpha]_D^{25}$ = + 27.40 (*c* 0.01, $CHCl_3$);

IR (thin film, ν_{max}/cm^{-1}) 3032, 1598, 1494, 1453, 1352, 1160, 1090, 909, 860, 815, 657;

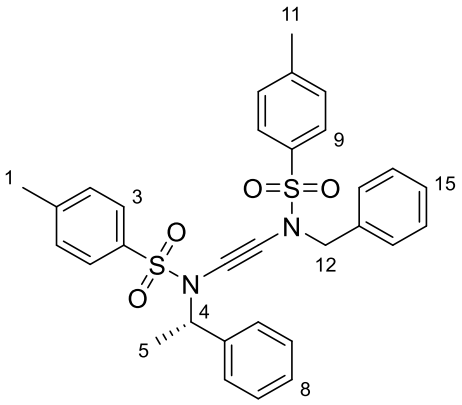
^{1}H NMR (400 MHz, $CDCl_3$) δ_H 7.69 (2H, d, *J* = 8.2 Hz, H3), 7.29 (2H, d, *J* = 8.2 Hz, H2), 7.27 – 7.22 (3H, m, H7, H9), 7.18 – 7.12 (2H, m, H8), 6.29 (1H, s, H4), 5.23 (1H, q, *J* = 7.1 Hz, H5), 2.43 (3H, s, H1), 1.47 (3H, d, *J* = 7.1 Hz, H6).

^{13}C NMR (101 MHz, $CDCl_3$) δ_C 144.1, 138.4, 136.8, 129.8, 128.8, 128.5, 128.3, 128.1, 127.8, 105.1, 59.1, 21.7, 18.0;

HRMS (ESI) m/z: $[M + Na]^+$ Calcd for $C_{17}H_{17}O_2N^{79}Br_2NaS$ 479.9239; Found 479.9240.

7.7.4 Yndiamides

***(S)*-*N*-Benzyl-4-methyl-*N*-(((4-methyl-*N*-(1-phenylethyl)phenyl)sulfonamido)ethynyl)benzenesulfonamide，4x**



ZT241

Synthesised from *N*-benzyl-4-methylbenzenesulfonamide (260 mg, 1.00 mmol, 1.0 eq.), *(S)*-*N*-(2,2-dibromovinyl)-4-methyl-*N*-(1-phenylethyl)benzenesulfonamide (503 mg, 1.10 mmol, 1.1 eq.), CuI (38 mg, 0.20 mmol, 0.20 eq.), 1,10-phenanthroline (72 mg, 0.40 mmol, 0.40 eq.), and Cs_2CO_3 (972 mg, 3.00 mmol, 3.0 eq.) with general procedure **7.2.1d**. Column chromatography (silica gel, 10% DCM + 20% Et_2O/pentane) afforded the title compound (153 mg, 0.27 mmol, 27%) as a yellow solid;

m.p. 148 °C;

R$_f$ 0.53 (10% DCM + 20% Et_2O/pentane);

$[\alpha]^{25}_D$ = + 67.93 (*c* 0.01, $CHCl_3$);

IR (thin film, ν_{max}/cm^{-1}) 2981, 1597, 1416, 1362, 1168, 1089, 910, 814, 730, 699, 660;

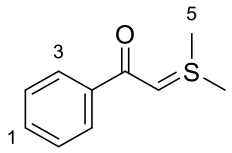
^{1}H NMR (400 MHz, $CDCl_3$) δ_H 7.76 (2H, d, *J* = 8.3 Hz, H3), 7.52 (2H, d, *J* = 8.3 Hz, H9), 7.41 – 7.28 (7H, m, H2, H6, H7, H8), 7.25 – 7.21 (5H, m, H13, H15), 7.16 – 7.08 (2H, m, H14), 5.19 (1H, q, *J* = 7.0 Hz, H4), 4.65 – 4.53 (2H, m, H12), 2.56 (3H, s, H1), 2.51 (3H, s, H11), 1.36 (3H, d, *J* = 7.0 Hz, H5);

^{13}C NMR (101 MHz, $CDCl_3$) δ_C 144.6, 144.2, 140.1, 135.6, 135.1, 134.8, 129.8, 129.4, 128.9, 128.6, 128.4, 128.3, 127.9, 127.8, 127.7, 126.9, 71.6, 67.7, 58.8, 56.0, 21.8, 21.7, 19.7;

HRMS (ESI) m/z: $[M + Na]^+$ Calcd for $C_{31}H_{30}O_4N_2NaS_2$ 581.1539; Found 581.1539;

7.7.5 Transfer Reagents

2-(Dimethyl-λ^4-sulfaneylidene)-1-phenylethan-1-one, 185



ZT505

Modified from a literature procedure.[251] In a round-bottom flask was dissolved dimethyl(2-oxo-2-phenylethyl)sulfonium bromide (2.55 g, 9.76 mmol, 1.0 eq.) in 1M NaOH (20 mL, 20.0 mmol, 2.1 eq.). The reaction mixture was stirred at room temperature for 1 h and then it was extracted three times with $CHCl_3$. The organic phase was combined, dried over

Na_2SO_4 and concentrated *in vacuo* to afford the title compound (1.29 g, 7.16 mmol, 73%) as a yellow solid;

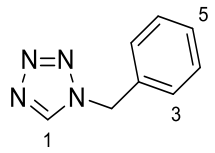
IR (thin film, ν_{max}/cm^{-1}) 3373, 1509, 1488, 1392, 991, 854, 705;

^{1}H NMR (400 MHz, $CDCl_3$) δ_H 7.80 – 7.73 (2H, m, H3), 7.36 – 7.29 (3H, m, H1, H2), 4.30 (1H, s, H4), 2.96 (6H, s, H5);

^{13}C NMR (101 MHz, $CDCl_3$) δ_C 183.2, 141.0, 129.6, 128.0, 126.4, 50.8, 28.5;

^{1}H NMR data are consistent with literature values, while one ^{13}C NMR peak (δ_C = 50.8 ppm) failed to match that from the literature (δ_C = 52.0 ppm).[252]

1-Benzyl-1*H*-tetrazole



ZT533

Modified from a literature procedure.[253] In a round-bottom flask was dissolved benzylamine (1.1 mL, 10.0 mmol, 1.0 eq.) in acetic acid (4 mL). Triethyl orthoformate (2.5 mL, 15.0 mmol, 1.5 eq.) was added to the solution followed by sodium azide (845 mg, 13.0 mmol, 1.3 eq.). The reaction mixture was then heated to 80 °C and stirred overnight. Upon completion, it was cooled to room temperature and carefully quenched with dilute $NaHCO_3$ solution (5 % w/w in water, ~ 30 mL). The resulting solution was then extracted three times with EtOAc, dried over Na_2SO_4, concentrated *in vacuo*, and purified by column chromatography (silica gel, 20 % → 40 % EtOAc/pentane) to afford the title compound (831 mg, 5.19 mmol, 52%) as a colourless solid;

IR (thin film, ν_{max}/cm^{-1}) 3113, 1163, 1003, 726, 708;

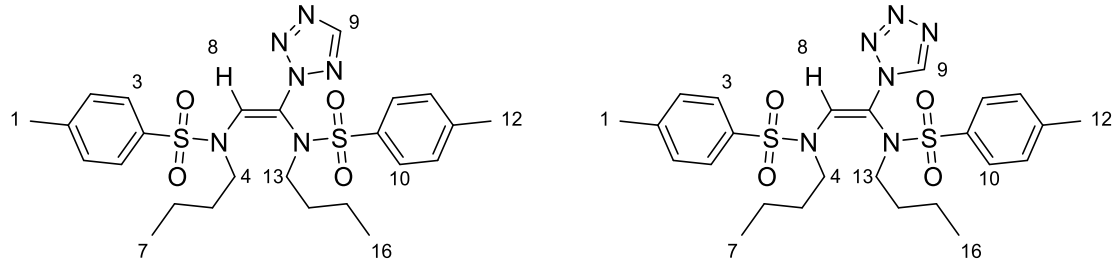
^{1}H NMR (400 MHz, $CDCl_3$) δ_H 8.50 (1H, s, H1), 7.47 – 7.36 (3H, m, H4, H5), 7.33 – 7.27 (2H, m, H3), 5.59 (2H, s, H2);

^{13}C NMR (101 MHz, $CDCl_3$) δ_C 142.5, 132.9, 129.60, 129.58, 128.4, 52.4;

Data are consistent with literature values.[254]

7.7.6 Gold-Catalysed Functionalisaion Products

(*Z*)-*N*,*N*'-(1-(2*H*-tetrazol-2-yl)ethene-1,2-diyl)bis(*N*-butyl-4-methylbenzenesulfonamide) (left) 188, and (*Z*)-*N*,*N*'-(1-(1*H*-tetrazol-1-yl)ethene-1,2-diyl)bis(*N*-butyl-4-methylbenzenesulfonamide) (right) 189



ZT531-A (left), ZT531-B(right)

To a heat gun-dried vial containing a stirrer bar and 3 Å molecular sieves were added *N*,*N*'-(ethyne-1,2-diyl)bis(*N*-butyl-4-methylbenzenesulfonamide) (48 mg, 0.10 mmol, 1.0 eq.) and tetrazole (14 mg, 0.20 mmol, 2.0 eq.). The vial was purged under high vacuum for 30 s and backfilled with argon (this vacuum cycle was repeated twice more). The vial was then moved into glovebox where chloro[tris(2,4-di-tert-butylphenyl)phosphite]gold(I) (4.4 mg, 5.00 μmol, 5 mol%) and silver bis(trifluoromethanesulfonyl)imide (2 mg, 5.15 μmol, 5 mol%) were added. DCE (anhy., 0.5 M) was added after the vial was removed from the glovebox. The reaction mixture was stirred at 80 °C for 2 h under nitrogen atmosphere in the dark. Upon completion, the reaction mixture was concentrated *in vacuo* and purified by preparative LPLC (RediSep Rf Gold® 12 g HP Silica, 20 % EtOAc/pentane) to give **188** (21 mg, 38 μmol, 38%) as a colourless solid (single crystals suitable for X-ray crystallography were grown by vapour diffusion of pentane into a concentrated solution of the title compound in chloroform) and **189** (15 mg, 27 μmol, 27%) as a colourless solid.

Characterisation for **188**:

m.p. 124 – 126 °C;

R_f 0.39 (20% EtOAc/pentane);

IR (thin film, ν_{max}/cm^{-1}) 2961, 1356, 1166, 1088, 944, 732, 715, 665;

^{1}H NMR (400 MHz, $CDCl_3$) δ_H 8.26 (1H, s, H9), 7.77 (2H, d, *J* = 8.4 Hz, H3), 7.64 (1H, s, H8), 7.39 – 7.30 (4H, m, H2, H10), 7.16 (2H, d, *J* = 8.1 Hz, H11), 3.89 (2H, brs., H4), 3.48 (1H, brs., H13), 3.15 (1H, brs., H13), 2.44 (3H, s, H1), 2.39 (3H, s, H12), 1.94 (1H, brs., H5), 1.68 (1H, s, H5), 1.38 (4H, brs., H6, H14), 1.14 (2H, app. sext., *J* = 7.4 Hz, H15), 0.95 (3H, t, *J* = 7.4 Hz, H7), 0.77 (3H, t, *J* = 7.3 Hz, H16).

^{13}C NMR (101 MHz, $CDCl_3$) δ_C 152.1, 144.9, 144.5, 135.6, 134.7, 130.2, 129.5, 128.7, 128.1, 127.6, 115.5, 49.6, 47.1, 31.5, 29.6, 21.8, 21.7, 20.1, 20.0, 13.9, 13.7;

HRMS (ESI) m/z: $[M + Na]^+$ Calcd for $C_{25}H_{34}N_6O_4S_2Na$ 569.1975; Found 569.2002.

Characterisation for **189**:

m.p. 60 – 62 °C;

R_f 0.27 (20% EtOAc/pentane);

IR (thin film, ν_{max}/cm^{-1}) 2961, 1353, 1167, 1087, 911, 732, 709, 667;

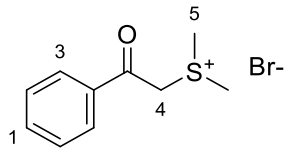
^{1}H NMR (400 MHz, $CDCl_3$) δ_H 8.58 (1H, s, H9), 7.72 (2H, d, *J* = 8.1 Hz, H3), 7.35 (2H, d, *J* = 8.1 Hz, H2), 7.18 (2H, d, *J* = 8.2 Hz, H11), 7.11 (2H, d, *J* = 8.2 Hz, H10), 7.02 (1H, s, H8), 3.83 (2H, t, *J* = 8.1 Hz, H4), 3.21 – 3.12 (2H, m, H13), 2.44 (3H, s, H1), 2.38 (3H, s, H12), 1.79 (2H, brs., H5), 1.39 (2H, h, *J* = 7.6 Hz, H6), 1.31 – 1.22 (2H, m, H14), 1.08 – 0.92 (5H, m, H7, H15), 0.72 (3H, t, *J* = 7.3 Hz, H16);

^{13}C NMR (101 MHz, $CDCl_3$) δ_C 145.2, 145.1, 144.3, 135.8, 134.7, 130.3, 130.1, 127.6, 127.3, 127.3, 112.9, 49.8, 47.0, 31.3, 29.7, 21.8, 21.7, 19.9, 19.8, 13.9, 13.7;

HRMS (ESI) m/z: $[M + Na]^+$ Calcd for $C_{25}H_{34}N_6O_4S_2Na$ 569.1975; Found 569.1996;

7.7.7 Miscellaneous

Dimethyl(2-oxo-2-phenylethyl)sulfonium bromide



ZT504

Modified from a literature procedure.[255] In a round-bottom flask was dissolved 2-bromoacetophenone (1.99 g, 10.0 mmol, 1.0 eq.) in acetone (10 mL). Dimethyl sulfide (1.5 mL, 20.4 mmol, 2.0 eq.) was added and the reaction mixture was stirred at room temperature for 4 h. Upon completion, the reaction mixture was filtered, and the collected precipitate was washed with Et_2O and dried in air to afford the title compound (2.55 g, 9.76 mmol, 98%) as a colourless solid;

IR (thin film, ν_{max}/cm^{-1}) 3003, 2987, 2908, 1672, 1341, 1216, 993, 755, 692;

^{1}H NMR (400 MHz, DMSO) δ_H 8.07 – 8.01 (2H, m, H3), 7.81 – 7.75 (1H, m, H1), 7.68 – 7.60 (2H, m, H2), 5.65 (2H, s, H4), 3.03 (6H, s, H5);

^{13}C NMR (101 MHz, DMSO) δ_C 191.4, 135.1, 133.9, 129.2, 128.7, 52.9, 24.6;

Data are consistent with literature values.[256]

7.7.8 X-Ray Crystallography

Single crystal X-ray diffraction data were collected using a (Rigaku) Oxford Diffraction SuperNova A diffractometer and reduced using CrysAlisPro. Structures were solved using Super-Flip[239] and refined using CRYSTALS[240, 241].

Table 7.04 Crystal data and structure refinement for **188**.

Empirical formula	C25 H34 N6 O4 S2	
Formula weight	546.71	
Temperature	150 K	
Wavelength	1.54184 Å	
Crystal system	Triclinic	
Space group	P -1	
Unit cell dimensions	a = 8.6418(2) Å	α= 74.161(2)°.
	b = 10.0254(3) Å	β= 81.593(2)°.
	c = 17.0728(5) Å	γ = 73.947(2)°.
Volume	1363.49(7) $Å^3$	
Z	2	
Density (calculated)	1.332 Mg/m^3	
Absorption coefficient	2.122 mm^{-1}	
F(000)	580	
Crystal size	0.21 x 0.20 x 0.07 mm^3	
Theta range for data collection	4.734 to 75.898°.	
Index ranges	-10<=h<=10, -9<=k<=12, -18<=l<=21	
Reflections collected	15292	
Independent reflections	5616 [R(int) = 0.026]	
Completeness to theta = 74.380°	99.5 %	
Absorption correction	Semi-empirical from equivalents	
Max. and min. transmission	0.86 and 0.77	
Refinement method	Full-matrix least-squares on F2	
Data / restraints / parameters	5616 / 0 / 334	
Goodness-of-fit on F2	0.9993	

Final R indices [I>2sigma(I)]	R1 = 0.0330, wR2 = 0.0833
R indices (all data)	R1 = 0.0370, wR2 = 0.0878
Largest diff. peak and hole	0.33 and -0.35 e.Å^{-3}

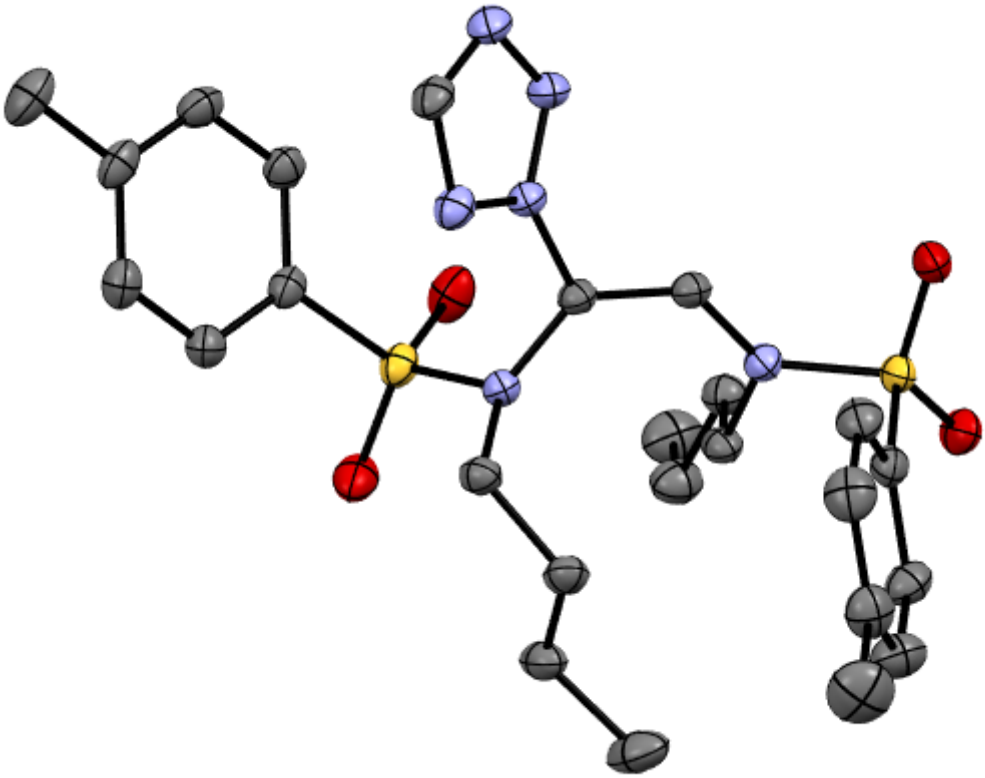


Figure 7.17 The structure of **188** determined from X-ray diffraction studies, displacement ellipsoids are drawn at 50% probability and hydrogen atoms are omitted for clarity.

Reference

1. Z. Janousek, J. Collard and H. G. Viehe, *Angew. Chem., Int. Ed. Engl.*, 1972, **11**, 917-918.
2. B. Witulski and T. Stengel, *Angew. Chem. Int. Ed.*, 1998, **37**, 489-492.
3. J. D. Rainier and J. E. Imbriglio, *Org. Lett.*, 1999, **1**, 2037-2039.
4. M. O. Frederick, J. A. Mulder, M. R. Tracey, R. P. Hsung, J. Huang, K. C. M. Kurtz, L. Shen and C. J. Douglas, *J. Am. Chem. Soc.*, 2003, **125**, 2368-2369.
5. X. Zhang, Y. Zhang, J. Huang, R. P. Hsung, K. C. M. Kurtz, J. Oppenheimer, M. E. Petersen, I. K. Sagamanova, L. Shen and M. R. Tracey, *J. Org. Chem.*, 2006, **71**, 4170-4177.
6. J. R. Dunetz and R. L. Danheiser, *Org. Lett.*, 2003, **5**, 4011-4014.
7. T. Hamada, X. Ye and S. S. Stahl, *J. Am. Chem. Soc.*, 2008, **130**, 833-835.
8. A. Coste, G. Karthikeyan, F. Couty and G. Evano, *Angew. Chem. Int. Ed.*, 2009, **48**, 4381-4385.
9. K. Jouvin, A. Coste, A. Bayle, F. Legrand, G. Karthikeyan, K. Tadiparthi and G. Evano, *Organometallics*, 2012, **31**, 7933-7947.
10. X. Zeng, Y. Tu, Z. Zhang, C. You, J. Wu, Z. Ye and J. Zhao, *J. Org. Chem.*, 2019, **84**, 4458-4466.
11. S. J. Mansfield, R. C. Smith, J. R. J. Yong, O. L. Garry and E. A. Anderson, *Org. Lett.*, 2019, **21**, 2918-2922.
12. E. Godin, J. Santandrea, A. Caron and S. K. Collins, *Org. Lett.*, 2020, **22**, 5905-5909.
13. G. Evano, B. Michelet and C. Zhang, *C. R. Chim.*, 2017, **20**, 648-664.
14. G. Evano, N. Blanchard, G. Compain, A. Coste, C. S. Demmer, W. Gati, C. Guissart, J. Heimburger, N. Henry, K. Jouvin, G. Karthikeyan, A. Laouiti, M. Lecomte, A. Martin-Mingot, B. Métayer, B. Michelet, A. Nitelet, C. Theunissen, S. Thibaudeau, J. Wang, M. Zarca and C. Zhang, *Chem. Lett.*, 2016, **45**, 574-585.
15. G. Evano, A. Coste and K. Jouvin, *Angew. Chem. Int. Ed.*, 2010, **49**, 2840-2859.
16. K. A. DeKorver, H. Li, A. G. Lohse, R. Hayashi, Z. Lu, Y. Zhang and R. P. Hsung, *Chem. Rev.*, 2010, **110**, 5064-5106.
17. C. C. Lynch, A. Sripada and C. Wolf, *Chem. Soc. Rev.*, 2020, **49**, 8543-8583.
18. Q. Li, L. Han, L. Zhao, Y. Hou and R. Sharma, *Synth. Commun.*, 2021, **51**, 2754-2781.

19. Z. L. Xinyue Zhou, Xiao-Na Wang, *Chinese J. Org. Chem.*, 2021, **41**, 1288-1318.
20. S. Shandilya, M. Protim Gogoi, S. Dutta and A. K. Sahoo, *Chem. Rec.*, 2021, **21**, 4123-4149.
21. H. Chechik-Lankin, S. Livshin and I. Marek, *Synlett*, 2005, **2005**, 2098-2100.
22. B. Gourdet and H. W. Lam, *J. Am. Chem. Soc.*, 2009, **131**, 3802-3803.
23. B. Gourdet, M. E. Rudkin, C. A. Watts and H. W. Lam, *J. Org. Chem.*, 2009, **74**, 7849-7858.
24. S. J. Mansfield, DPhil Thesis, University of Oxford, 2019.
25. S. J. Mansfield, K. E. Christensen, A. L. Thompson, K. Ma, M. W. Jones, A. Mekareeya and E. A. Anderson, *Angew. Chem. Int. Ed.*, 2017, **56**, 14428-14432.
26. P. J. Smith, DPhil Thesis, University of Oxford, 2022.
27. O. Garry, Master's Thesis, University of Oxford, 2018.
28. J. Ragus, PartII Thesis, University of Oxford, 2022.
29. N. B. Desai, N. McKelvie and F. Ramirez, *J. Am. Chem. Soc.*, 1962, **84**, 1745-1747.
30. P. J. Smith, Z. Tong, J. Ragus, P. Solon, K. W. Shimkin and E. A. Anderson, *Org. Lett.*, 2022, **24**, 7522-7526.
31. O. L. Garry, S. J. Mansfield and E. A. Anderson, *Synthesis*, 2021, **53**, 4221-4230.
32. A. Mekareeya, P. R. Walker, A. Couce-Rios, C. D. Campbell, A. Steven, R. S. Paton and E. A. Anderson, *J. Am. Chem. Soc.*, 2017, **139**, 10104-10114.
33. P. J. Smith, Y. Jiang, Z. Tong, H. D. Pickford, K. E. Christensen, J. Nugent and E. A. Anderson, *Org. Lett.*, 2021, **23**, 6547-6552.
34. P. A. Wender and T. J. Williams, *Angew. Chem. Int. Ed.*, 2002, **41**, 4550-4553.
35. R. N. Straker, Q. Peng, A. Mekareeya, R. S. Paton and E. A. Anderson, *Nat. Commun.*, 2016, **7**, 10109.
36. W. Schwemberger and W. Gordon, *Chem. Zentralbl.*, 1935, **106**, 514-514.
37. J. H. Teles, S. Brode and M. Chabanas, *Angew. Chem. Int. Ed.*, 1998, **37**, 1415-1418.
38. E. Mizushima, K. Sato, T. Hayashi and M. Tanaka, *Angew. Chem. Int. Ed.*, 2002, **41**, 4563-4565.
39. R. Dorel and A. M. Echavarren, *Chem. Rev.*, 2015, **115**, 9028-9072.
40. D. J. Gorin and F. D. Toste, *Nature*, 2007, **446**, 395-403.
41. W. Zi and F. Dean Toste, *Chem. Soc. Rev.*, 2016, **45**, 4567-4589.
42. E. Jiménez-Núñez and A. M. Echavarren, *Chem. Commun.*, 2007, 333-346.
43. A. Fürstner, *Chem. Soc. Rev.*, 2009, **38**, 3208-3221.

44. A. Fürstner and P. W. Davies, *Angew. Chem. Int. Ed.*, 2007, **46**, 3410-3449.
45. C. Obradors and A. M. Echavarren, *Chem. Commun.*, 2014, **50**, 16-28.
46. A. Hoffmann-Röder and N. Krause, *Org. Biomol. Chem.*, 2005, **3**, 387-391.
47. A. S. K. Hashmi and G. J. Hutchings, *Angew. Chem. Int. Ed.*, 2006, **45**, 7896-7936.
48. A. S. K. Hashmi, *Chem. Rev.*, 2007, **107**, 3180-3211.
49. L. Fensterbank and M. Malacria, *Acc. Chem. Res.*, 2014, **47**, 953-965.
50. N. D. Shapiro and F. D. Toste, *J. Am. Chem. Soc.*, 2007, **129**, 4160-4161.
51. G. Li and L. Zhang, *Angew. Chem. Int. Ed.*, 2007, **46**, 5156-5159.
52. S. Bhunia, P. Ghosh and S. R. Patra, *Adv. Synth. Catal.*, 2020, **362**, 3664-3708.
53. Z. Zheng, X. Ma, X. Cheng, K. Zhao, K. Gutman, T. Li and L. Zhang, *Chem. Rev.*, 2021, **121**, 8979-9038.
54. L. W. Ye, X. Q. Zhu, R. L. Sahani, Y. Xu, P. C. Qian and R. S. Liu, *Chem. Rev.*, 2021, **121**, 9039-9112.
55. L. Ye, L. Cui, G. Zhang and L. Zhang, *J. Am. Chem. Soc.*, 2010, **132**, 3258-3259.
56. L. Zhang, *Acc. Chem. Res.*, 2014, **47**, 877-888.
57. L. Ye, W. He and L. Zhang, *J. Am. Chem. Soc.*, 2010, **132**, 8550-8551.
58. J. A. Burkhard, C. Guérot, H. Knust and E. M. Carreira, *Org. Lett.*, 2012, **14**, 66-69.
59. J. Cai, X. Wang, Y. Qian, L. Qiu, W. Hu and X. Xu, *Org. Lett.*, 2019, **21**, 369-372.
60. K. Ji, Y. Zhao and L. Zhang, *Angew. Chem. Int. Ed.*, 2013, **52**, 6508-6512.
61. C. Shu, R. Liu, S. Liu, J.-Q. Li, Y.-F. Yu, Q. He, X. Lu and L.-W. Ye, *Chem. Eur. J.*, 2015, **10**, 91-95.
62. L. Ye, W. He and L. Zhang, *Angew. Chem. Int. Ed.*, 2011, **50**, 3236-3239.
63. C. Shu, L. Li, Y.-F. Yu, S. Jiang and L.-W. Ye, *Chem. Commun.*, 2014, **50**, 2522-2525.
64. C. Shu, L. Li, X.-Y. Xiao, Y.-F. Yu, Y.-F. Ping, J.-M. Zhou and L.-W. Ye, *Chem. Commun.*, 2014, **50**, 8689-8692.
65. Y. Wang, K. Ji, S. Lan and L. Zhang, *Angew. Chem. Int. Ed.*, 2012, **51**, 1915-1918.
66. G. Henrion, T. E. J. Chavas, X. Le Goff and F. Gagosz, *Angew. Chem. Int. Ed.*, 2013, **52**, 6277-6282.
67. D. Qian and J. Zhang, *Chem. Commun.*, 2012, **48**, 7082-7084.
68. K. Ji, F. Yang, S. Gao, J. Tang and J. Gao, *Chem. Eur. J.*, 2016, **22**, 10225-10229.
69. P. W. Davies, A. Cremonesi and N. Martin, *Chem. Commun.*, 2011, **47**, 379-381.
70. R. B. Dateer, K. Pati and R.-S. Liu, *Chem. Commun.*, 2012, **48**, 7200-7202.

71. S. Shi, T. Wang, W. Yang, M. Rudolph and A. S. K. Hashmi, *Chem. Eur. J.*, 2013, **19**, 6576-6580.
72. A. Y. Dubovtsev, D. V. Dar'in and V. Y. Kukushkin, *Org. Lett.*, 2019, **21**, 4116-4119.
73. C.-F. Xu, M. Xu, Y.-X. Jia and C.-Y. Li, *Org. Lett.*, 2011, **13**, 1556-1559.
74. L.-Q. Yang, K.-B. Wang and C.-Y. Li, *Eur. J. Org. Chem.*, 2013, **2013**, 2775-2779.
75. Z. F. Al-Rashid and R. P. Hsung, *Org. Lett.*, 2008, **10**, 661-663.
76. F. Pan, S. Liu, C. Shu, R.-K. Lin, Y.-F. Yu, J.-M. Zhou and L.-W. Ye, *Chem. Commun.*, 2014, **50**, 10726-10729.
77. L. Li, C. Shu, B. Zhou, Y.-F. Yu, X.-Y. Xiao and L.-W. Ye, *Chem. Sci.*, 2014, **5**, 4057-4064.
78. C. H. Shen, L. Li, W. Zhang, S. Liu, C. Shu, Y. E. Xie, Y. F. Yu and L. W. Ye, *J. Org. Chem.*, 2014, **79**, 9313-9318.
79. M. D. Santos and P. W. Davies, *Chem. Commun.*, 2014, **50**, 6001-6004.
80. J. D. Priest, L. Male and P. W. Davies, *Tetrahedron*, 2021, **78**, 131757.
81. K.-B. Wang, R.-Q. Ran, S.-D. Xiu and C.-Y. Li, *Org. Lett.*, 2013, **15**, 2374-2377.
82. A. Buzas, F. Istrate, X. F. Le Goff, Y. Odabachian and F. Gagosz, *J. Organomet. Chem.*, 2009, **694**, 515-519.
83. S. Couty, C. Meyer and J. Cossy, *Angew. Chem. Int. Ed.*, 2006, **45**, 6726-6730.
84. H.-S. Yeom and S. Shin, *Org. Biomol. Chem.*, 2013, **11**, 1089-1092.
85. F. Sánchez-Cantalejo, J. D. Priest and P. W. Davies, *Chem. Eur. J.*, 2018, **24**, 17215-17219.
86. P. H. Kaur and P. W. Davies, *Synlett*, 2021, **32**, 897-900.
87. A. Mukherjee, R. B. Dateer, R. Chaudhuri, S. Bhunia, S. N. Karad and R.-S. Liu, *J. Am. Chem. Soc.*, 2011, **133**, 15372-15375.
88. P.-P. Ruan, C.-H. Shen, L. Li, C.-Y. Liu and L.-W. Ye, *Org. Chem. Front.*, 2016, **3**, 989-993.
89. B.-H. Zhu, C.-M. Wang, H.-Y. Su and L.-W. Ye, *Chin. J. Chem.*, 2019, **37**, 58-62.
90. D. V. Patil, S. W. Kim, Q. H. Nguyen, H. Kim, S. Wang, T. Hoang and S. Shin, *Angew. Chem. Int. Ed.*, 2017, **56**, 3670-3674.
91. Y. Deng, J. Zhang, B. Bankhead, J. P. Markham and M. Zeller, *Chem. Commun.*, 2021, **57**, 5254-5257.
92. M. A. T. Blaskovich, *J. Med. Chem.*, 2016, **59**, 10807-10836.

93. P. Neumann-Staubitz and H. Neumann, *Curr. Opin. Struct. Biol.*, 2016, **38**, 119-128.
94. K. D. Collins and F. Glorius, *Nat. Chem.*, 2013, **5**, 597-601.
95. T. Gensch, M. Teders and F. Glorius, *J. Org. Chem.*, 2017, **82**, 9154-9159.
96. S. G. Dawande, V. Kanchupalli, J. Kalepu, H. Chennamsetti, B. S. Lad and S. Katukojvala, *Angew. Chem. Int. Ed.*, 2014, **53**, 4076-4080.
97. T. Ankner and G. Hilmersson, *Org. Lett.*, 2009, **11**, 503-506.
98. D. Campeau, D. F. León Rayo, A. Mansour, K. Muratov and F. Gagosz, *Chem. Rev.*, 2021, **121**, 8756-8867.
99. F.-L. Hong and L.-W. Ye, *Acc. Chem. Res.*, 2020, **53**, 2003-2019.
100. F. Pan, C. Shu and L. W. Ye, *Org. Biomol. Chem.*, 2016, **14**, 9456-9465.
101. A. H. Zhou, Q. He, C. Shu, Y. F. Yu, S. Liu, T. Zhao, W. Zhang, X. Lu and L. W. Ye, *Chem. Sci.*, 2015, **6**, 1265-1271.
102. F. Hu and M. Szostak, *Adv. Synth. Catal.*, 2015, **357**, 2583-2614.
103. D. B. Huple, S. Ghorpade and R.-S. Liu, *Adv. Synth. Catal.*, 2016, **358**, 1348-1367.
104. L. Li, T.-D. Tan, Y.-Q. Zhang, X. Liu and L.-W. Ye, *Org. Biomol. Chem.*, 2017, **15**, 8483-8492.
105. X.-Y. Xiao, A.-H. Zhou, C. Shu, F. Pan, T. Li and L.-W. Ye, *Chem. Asian. J.*, 2015, **10**, 1854-1858.
106. R. L. Sahani and R.-S. Liu, *Angew. Chem. Int. Ed.*, 2017, **56**, 1026-1030.
107. R. D. Kardile, B. S. Kale, P. Sharma and R.-S. Liu, *Org. Lett.*, 2018, **20**, 3806-3809.
108. A. S. Kulandai Raj, K.-C. Tan, L.-Y. Chen, M.-J. Cheng and R.-S. Liu, *Chem. Sci.*, 2019, **10**, 6437-6442.
109. P. E. Simm, P. Sekar, J. Richardson and P. W. Davies, *ACS Catal.*, 2021, **11**, 6357-6362.
110. S. S. Giri and R.-S. Liu, *Chem. Sci.*, 2018, **9**, 2991-2995.
111. H. Jin, L. Huang, J. Xie, M. Rudolph, F. Rominger and A. S. Hashmi, *Angew. Chem., Int. Ed. Engl.*, 2016, **55**, 794-797.
112. H. Jin, B. Tian, X. Song, J. Xie, M. Rudolph, F. Rominger and A. S. K. Hashmi, *Angew. Chem. Int. Ed.*, 2016, **55**, 12688-12692.
113. Z. Zeng, H. Jin, K. Sekine, M. Rudolph, F. Rominger and A. S. K. Hashmi, *Angew. Chem. Int. Ed.*, 2018, **57**, 6935-6939.
114. M.-H. Tsai, C.-Y. Wang, A. S. Kulandai Raj and R.-S. Liu, *Chem. Commun.*, 2018, **54**, 10866-10869.

115. Z. Zeng, H. Jin, M. Rudolph, F. Rominger and A. S. K. Hashmi, *Angew. Chem. Int. Ed.*, 2018, **57**, 16549-16553.
116. Y.-C. Hsu, S.-A. Hsieh and R.-S. Liu, *Chem. Eur. J.*, 2019, **25**, 5288-5297.
117. L. Song, X. Tian, M. Rudolph, F. Rominger and A. S. K. Hashmi, *Chem. Commun.*, 2019, **55**, 9007-9010.
118. X. Tian, L. Song, K. Farshadfar, M. Rudolph, F. Rominger, T. Oeser, A. Ariafard and A. S. K. Hashmi, *Angew. Chem. Int. Ed.*, 2020, **59**, 471-478.
119. P. D. Jadhav, X. Lu and R.-S. Liu, *ACS Catal.*, 2018, **8**, 9697-9701.
120. W. Xu, J. Zhao, X. Li and Y. Liu, *J. Org. Chem.*, 2018, **83**, 15470-15485.
121. R. Vanjari, S. Dutta, B. Prabagar, V. Gandon and A. K. Sahoo, *Chem. Asian. J.*, 2019, **14**, 4828-4836.
122. V. Bhardwaj, D. Gumber, V. Abbot, S. Dhiman and P. Sharma, *RSC Adv.*, 2015, **5**, 15233-15266.
123. M. d. C. A. D. Bianco, D. I. L. F. Marinho, L. V. B. Hoelz, M. M. Bastos and N. Boechat, *Pharmaceuticals*, 2021, **14**, 893.
124. G. Li Petri, V. Spano, R. Spatola, R. Holl, M. V. Raimondi, P. Barraja and A. Montalbano, *Eur. J. Med. Chem.*, 2020, **208**, 112783.
125. E. Barnea, S. Majumder, R. J. Staples and A. L. Odom, *Organometallics*, 2009, **28**, 3876-3881.
126. R.-J. Tang, T. Milcent and B. Crousse, *J. Org. Chem.*, 2018, **83**, 930-938.
127. L. De Luca, G. Giacomelli and A. Porcheddu, *J. Org. Chem.*, 2002, **67**, 6272-6274.
128. T. Javorskis and E. Orentas, *J. Org. Chem.*, 2017, **82**, 13423-13439.
129. C. Shu, Y.-H. Wang, C.-H. Shen, P.-P. Ruan, X. Lu and L.-W. Ye, *Org. Lett.*, 2016, **18**, 3254-3257.
130. G.-X. Ru, T.-T. Zhang, M. Zhang, X.-L. Jiang, Z.-K. Wan, X.-H. Zhu, W.-B. Shen and G.-Q. Gao, *Org. Biomol. Chem.*, 2021, **19**, 5274-5283.
131. J. Zhang, Y. Li, C. Zhang, X.-N. Wang and J. Chang, *Org. Lett.*, 2021, **23**, 2029-2035.
132. S. Kobayashi, K. Arai, T. Yamakawa, Y.-J. Chen, M. M. Salter and Y. Yamashita, *Adv. Synth. Catal.*, 2011, **353**, 1927-1932.
133. T. Sammakia and R. S. Smith, *J. Org. Chem.*, 1992, **57**, 2997-3000.
134. M. Vadivelu, S. Sampath, K. Muthu, K. Karthikeyan and C. Praveen, *J. Org. Chem.*, 2019, **84**, 13636-13645.

135. B. Lu, Y. Li, Y. Wang, D. H. Aue, Y. Luo and L. Zhang, *J. Am. Chem. Soc.*, 2013, **135**, 8512-8524.
136. Y. Wang, A. Yepremyan, S. Ghorai, R. Todd, D. H. Aue and L. Zhang, *Angew. Chem. Int. Ed.*, 2013, **52**, 7795-7799.
137. L. Zhou, L. Yang, S. Dai, Y. Gao, R. Fang, A. M. Kirillov and L. Yang, *Catal. Sci. Technol.*, 2020, **10**, 240-251.
138. K. Ji, J. Nelson and L. Zhang, *Beilstein J. Org. Chem.*, 2013, **9**, 1925-1930.
139. Z. Dong, C.-H. Liu, Y. Wang, M. Lin and Z.-X. Yu, *Angew. Chem. Int. Ed.*, 2013, **52**, 14157-14161.
140. S. A. Rzhevskiy, A. N. Philippova, G. A. Chesnokov, A. A. Ageshina, L. I. Minaeva, M. A. Topchiy, M. S. Nechaev and A. F. Asachenko, *Chem. Commun.*, 2021, **57**, 5686-5689.
141. M. Skaria, Y.-C. Hsu, Y.-T. Jiang, M.-Y. Lu, T.-C. Kuo, M.-J. Cheng and R.-S. Liu, *Org. Lett.*, 2020, **22**, 4478-4482.
142. R. Fang, K. Liu, A. M. Kirillov and L. Yang, *J. Org. Chem.*, 2022, **87**, 7193-7201.
143. Y. Zhao and D. G. Truhlar, *Theor. Chem. Acc.*, 2008, **120**, 215-241.
144. Y. Zhao and D. G. Truhlar, *J. Chem. Phys.*, 2006, **125**, 194101.
145. J. P. Perdew, K. Burke and M. Ernzerhof, *Phys. Rev. Lett.*, 1997, **78**, 1396-1396.
146. C. Adamo and V. Barone, *J. Chem. Phys.*, 1999, **110**, 6158-6170.
147. J. Tao, J. P. Perdew, V. N. Staroverov and G. E. Scuseria, *Phys. Rev. Lett.*, 2003, **91**, 146401.
148. S. Grimme, *J. Chem. Phys.*, 2006, **124**, 034108.
149. S. Grimme, S. Ehrlich and L. Goerigk, *J. Comput. Chem.*, 2011, **32**, 1456-1465.
150. L. Goerigk and S. Grimme, *J. Chem. Theory Comput.*, 2011, **7**, 291-309.
151. M. Head-Gordon and T. Head-Gordon, *Chem. Phys. Lett.*, 1994, **220**, 122-128.
152. W. J. Hehre, R. Ditchfield and J. A. Pople, *J. Chem. Phys.*, 1972, **56**, 2257-2261.
153. D. Andrae, U. Häußermann, M. Dolg, H. Stoll and H. Preuß, *Theor. Chim. Acta.*, 1990, **77**, 123-141.
154. G. Scalmani and M. J. Frisch, *J. Chem. Phys.*, 2010, **132**, 114110.
155. D. G. Liakos, Y. Guo and F. Neese, *J. Phys. Chem. A.*, 2020, **124**, 90-100.
156. F. Weigend and R. Ahlrichs, *Phys. Chem. Chem. Phys.*, 2005, **7**, 3297-3305.
157. V. Barone and M. Cossi, *J. Phys. Chem. A*, 1998, **102**, 1995-2001.
158. M. Cossi, N. Rega, G. Scalmani and V. Barone, *J. Comput. Chem.*, 2003, **24**, 669-681.

159. CYLview20, C. Y. Legault, Université de Sherbrooke, 2020 (http://www.cylview.org)
160. T. H. Dunning and P. J. Hay, in *Methods of Electronic Structure Theory*, ed. H. F. Schaefer, Springer US, Boston, MA, 1977, DOI: 10.1007/978-1-4757-0887-5_1, pp. 1-27.
161. P. J. Hay and W. R. Wadt, *J. Chem. Phys.*, 1985, **82**, 270-283.
162. W. R. Wadt and P. J. Hay, *J. Chem. Phys.*, 1985, **82**, 284-298.
163. P. J. Hay and W. R. Wadt, *J. Chem. Phys.*, 1985, **82**, 299-310.
164. GaussView, Version 6.1, R. Dennington, T. A. Keith and J. M. Millam, Semichem Inc., Shawnee Mission, KS, 2016
165. D. J. Gorin, N. R. Davis and F. D. Toste, *J. Am. Chem. Soc.*, 2005, **127**, 11260-11261.
166. X.-N. Wang, H.-S. Yeom, L.-C. Fang, S. He, Z.-X. Ma, B. L. Kedrowski and R. P. Hsung, *Acc. Chem. Res.*, 2014, **47**, 560-578.
167. Y. Tokimizu, S. Oishi, N. Fujii and H. Ohno, *Org. Lett.*, 2014, **16**, 3138-3141.
168. C. Shu, Y. H. Wang, B. Zhou, X. L. Li, Y. F. Ping, X. Lu and L. W. Ye, *J. Am. Chem. Soc.*, 2015, **137**, 9567-9570.
169. B. Zhou, Y.-Q. Zhang, X. Liu and L.-W. Ye, *Sci. Bull.*, 2017, **62**, 1201-1206.
170. C.-H. Shen, Y. Pan, Y.-F. Yu, Z.-S. Wang, W. He, T. Li and L.-W. Ye, *J. Organomet. Chem.*, 2015, **795**, 63-67.
171. Y. Pan, G.-W. Chen, C.-H. Shen, W. He and L.-W. Ye, *Org. Chem. Front.*, 2016, **3**, 491-495.
172. W.-B. Shen, Q. Sun, L. Li, X. Liu, B. Zhou, J.-Z. Yan, X. Lu and L.-W. Ye, *Nat. Commun.*, 2017, **8**, 1748.
173. X. Tian, L. Song and A. S. K. Hashmi, *Chem. Eur. J.*, 2020, **26**, 3197-3204.
174. C. Li and L. Zhang, *Org. Lett.*, 2011, **13**, 1738-1741.
175. X. Tian, L. Song, M. Rudolph, F. Rominger, T. Oeser and A. S. K. Hashmi, *Angew. Chem. Int. Ed.*, 2019, **58**, 3589-3593.
176. X. Tian, L. Song, M. Rudolph, Q. Wang, X. Song, F. Rominger and A. S. K. Hashmi, *Org. Lett.*, 2019, **21**, 1598-1601.
177. X. Tian, L. Song, C. Han, C. Zhang, Y. Wu, M. Rudolph, F. Rominger and A. S. K. Hashmi, *Org. Lett.*, 2019, **21**, 2937-2940.
178. X. Tian, L. Song, M. Rudolph, F. Rominger and A. S. K. Hashmi, *Org. Lett.*, 2019, **21**, 4327-4330.

179. J. Panda, B. P. Raiguru, M. Mishra, S. Mohapatra and S. Nayak, *ChemistrySelect*, 2022, **7**, e202103987.
180. A. S. K. Hashmi, J. P. Weyrauch, M. Rudolph and E. Kurpejović, *Angew. Chem. Int. Ed.*, 2004, **43**, 6545-6547.
181. M. Chen, N. Sun, H. Chen and Y. Liu, *Chem. Commun.*, 2016, **52**, 6324-6327.
182. S. Roy, H. Khatua, S. K. Das and B. Chattopadhyay, *Angew. Chem. Int. Ed.*, 2019, **58**, 11439-11443.
183. H. Khatua, S. K. Das, S. Roy and B. Chattopadhyay, *Angew. Chem. Int. Ed.*, 2021, **60**, 304-312.
184. T. Sasaki, K. Kanematsu and M. Murata, *Tetrahedron*, 1971, **27**, 5359-5366.
185. M. TiŠLer, *Synthesis*, 1973, **1973**, 123-136.
186. M. Kanyalkar and E. C. Coutinho, *Tetrahedron*, 2000, **56**, 8775-8777.
187. W. Zordok, *Int. J. Sci. Res. Manag.*, 2012.
188. W. Zordok, *J. Indian Chem. Soc.*, 2013, **90**, 197-209.
189. L. Pollegioni and S. Servi, *Methods Mol. Biol.*, 2012.
190. V. A. Soloshonok and K. Izawa, *Asymmetric synthesis and application of α-amino acids*, ACS Publications, 2009.
191. Y.-M. Wang, A. D. Lackner and F. D. Toste, *Acc. Chem. Res.*, 2013, **47**, 889-901.
192. J.-Q. Zhang, Y. Liu, X.-W. Wang and L. Zhang, *Organometallics*, 2019, **38**, 3931-3938.
193. R. L. LaLonde, Z. J. Wang, M. Mba, A. D. Lackner and F. D. Toste, *Angew. Chem. Int. Ed.*, 2010, **49**, 598-601.
194. G. L. Hamilton, E. J. Kang, M. Mba and F. D. Toste, *Science*, 2007, **317**, 496-499.
195. S. Handa, D. J. Lippincott, D. H. Aue and B. H. Lipshutz, *Angew. Chem. Int. Ed.*, 2014, **53**, 10658-10662.
196. C. Shu, C.-Y. Shi, Q. Sun, B. Zhou, T.-Y. Li, Q. He, X. Lu, R.-S. Liu and L.-W. Ye, *ACS Catal.*, 2019, **9**, 1019-1025.
197. T. Lauterbach, S. Gatzweiler, P. Nösel, M. Rudolph, F. Rominger and A. S. K. Hashmi, *Adv. Synth. Catal.*, 2013, **355**, 2481-2487.
198. J. Liu, M. Chen, L. Zhang and Y. Liu, *Chem. Eur. J.*, 2015, **21**, 1009-1013.
199. W. Rao, M. J. Koh, D. Li, H. Hirao and P. W. H. Chan, *J. Am. Chem. Soc.*, 2013, **135**, 7926-7932.
200. C. Zhang, K. Hong, S. Dong, M. Liu, M. Rudolph, M. C. Dietl, J. Yin, A. S. K. Hashmi and X. Xu, *ACS Catal.*, 2023, **13**, 4646-4655.

201. Y.-R. Zhao, L. Li, G.-Y. Xu and J. Xuan, *Adv. Synth. Catal.*, 2022, **364**, 506-511.
202. J. K. Laha, S. Sharma and N. Dayal, *Eur. J. Org. Chem.*, 2015, 7885-7891.
203. K. A. DeKorver, M. C. Walton, T. D. North and R. P. Hsung, *Org. Lett.*, 2011, **13**, 4862-4865.
204. A. E. Pasqua, M. Matheson, A. L. Sewell and R. Marquez, *Organic Process Research & Development*, 2011, **15**, 467-470.
205. Stephen J. Connon and Anthony F. Hegarty, *Eur. J. Org. Chem.*, 2004, **2004**, 3477-3483.
206. T. V. Hansen, P. Wu and V. V. Fokin, *J. Org. Chem.*, 2005, **70**, 7761-7764.
207. G. Poissonnet, *Synth. Commun.*, 1997, **27**, 3839-3846.
208. E. P. McCarney, C. S. Hawes, S. Blasco and T. Gunnlaugsson, *Dalton Trans.*, 2016, **45**, 10209-10221.
209. M. J. Harper, E. J. Emmett, J. F. Bower and C. A. Russell, *J. Am. Chem. Soc.*, 2017, **139**, 12386-12389.
210. D. J. Scott, M. J. Fuchter and A. E. Ashley, *Angew. Chem. Int. Ed.*, 2014, **53**, 10218-10222.
211. G. Laudadio, E. Barmpoutsis, C. Schotten, L. Struik, S. Govaerts, D. L. Browne and T. Noël, *J. Am. Chem. Soc.*, 2019, **141**, 5664-5668.
212. L. Lu, C. Chen, H. Jiang and B. Yin, *J. Org. Chem.*, 2018, **83**, 14385-14395.
213. X. Qi, F. Yu, P. Chen and G. Liu, *Angew. Chem. Int. Ed.*, 2017, **56**, 12692-12696.
214. R. Liu, Z. Wei, J. Wang, Y. Liu and H. Xue, *Chem. Commun.*, 2020, **56**, 5038-5041.
215. J. Cui, Q. Jia, R.-Z. Feng, S.-S. Liu, T. He and C. Zhang, *Org. Lett.*, 2014, **16**, 1442-1445.
216. B. Wu, X. Yang and M. Yan, *J. Med. Chem.*, 2019, **62**, 7751-7768.
217. W. Zhao, X. Wang and C. Yang, *Synth. Commun.*, 2014, **44**, 150-160.
218. J. B. McManus and D. A. Nicewicz, *J. Am. Chem. Soc.*, 2017, **139**, 2880-2883.
219. K. Yonekura, Y. Yoshimura, M. Akehi and T. Tsuchimoto, *Adv. Synth. Catal.*, 2018, **360**, 1159-1181.
220. J. Motoyoshiya, N. Sakai, M. Imai, Y. Yamaguchi, R. Koike, Y. Takaguchi and H. Aoyama, *J. Org. Chem.*, 2002, **67**, 7314-7318.
221. A. Nikbakht, K. Amiri, H. Khosravi, Y. Zhou, S. Balalaie and B. Breit, *Org. Lett.*, 2021, **23**, 3343-3348.
222. X. Chen, J. T. Merrett and P. W. Hong Chan, *Org. Lett.*, 2018, **20**, 1542-1545.

223. K. K. Pasunooti, B. Banerjee, T. Yap, Y. Jiang and C.-F. Liu, *Org. Lett.*, 2015, **17**, 6094-6097.
224. O. Debleds, E. Gayon, E. Ostaszuk, E. Vrancken and J.-M. Campagne, *Chem. Eur. J.*, 2010, **16**, 12207-12213.
225. G. R. Kumar, Y. K. Kumar and M. S. Reddy, *Chem. Commun.*, 2016, **52**, 6589-6592.
226. S. Pusch, D. Schollmeyer and T. Opatz, *Org. Lett.*, 2016, **18**, 3043-3045.
227. S. Mondal, S. Biswas, K. G. Ghosh and D. Sureshkumar, *Chem. Asian. J.*, 2021, **16**, 2439-2446.
228. A. A. G. Fernandes, A. F. da Silva, C. Y. Okada Jr., V. Suzukawa, R. A. Cormanich and I. D. Jurberg, *Eur. J. Org. Chem.*, 2019, **2019**, 3022-3034.
229. H. Jiao, Z. Xinting, Y. Wenquan and C. Junbiao, *Chinese J. Org. Chem.*, 2018, **38**, 3236-3241.
230. K. K.-Y. Kung, V. K.-Y. Lo, H.-M. Ko, G.-L. Li, P.-Y. Chan, K.-C. Leung, Z. Zhou, M.-Z. Wang, C.-M. Che and M.-K. Wong, *Adv. Synth. Catal.*, 2013, **355**, 2055-2070.
231. P. V. Khairnar, T.-H. Lung, Y.-J. Lin, C.-Y. Wu, S. R. Koppolu, A. Edukondalu, P. Karanam and W. Lin, *Org. Lett.*, 2019, **21**, 4219-4223.
232. P. Kumar and M. Kapur, *Org. Lett.*, 2019, **21**, 2134-2138.
233. S. Tang, J. He, Y. Sun, L. He and X. She, *Org. Lett.*, 2009, **11**, 3982-3985.
234. S. Murarka and A. Studer, *Org. Lett.*, 2011, **13**, 2746-2749.
235. M. Kitamura, R. Sakata, N. Tashiro, A. Ikegami and T. Okauchi, *Bull. Chem. Soc. Jpn.*, 2015, **88**, 824-833.
236. Y. Pei and B. O. S. Wickham, *Tetrahedron Lett.*, 1993, **34**, 7509-7512.
237. J. Ye, X. Yang, M. Xu, P. K.-s. Chan and C. Ma, *Eur. J. Med. Chem.*, 2019, **182**, 111635.
238. A. P. Kozikowski, S. Tapadar, D. N. Luchini, K. H. Kim and D. D. Billadeau, *J. Med. Chem.*, 2008, **51**, 4370-4373.
239. L. Palatinus and G. Chapuis, *J. Appl. Cryst.*, 2007, **40**, 786-790.
240. P. W. Betteridge, J. R. Carruthers, R. I. Cooper, K. Prout and D. J. Watkin, *J. Appl. Cryst.*, 2003, **36**, 1487.
241. R. I. Cooper, A. L. Thompson and D. J. Watkin, *J. Appl. Cryst.*, 2010, **43**, 1100-1107.

242. Gaussian 16, Rev. C.01, M. J. Frisch, G. W. Trucks, H. B. Schlegel, G. E. Scuseria, M. A. Robb, J. R. Cheeseman, G. Scalmani, V. Barone, G. A. Petersson, H. Nakatsuji, X. Li, M. Caricato, A. V. Marenich, J. Bloino, B. G. Janesko, R. Gomperts, B. Mennucci, H. P. Hratchian, J. V. Ortiz, A. F. Izmaylov, J. L. Sonnenberg, Williams, F. Ding, F. Lipparini, F. Egidi, J. Goings, B. Peng, A. Petrone, T. Henderson, D. Ranasinghe, V. G. Zakrzewski, J. Gao, N. Rega, G. Zheng, W. Liang, M. Hada, M. Ehara, K. Toyota, R. Fukuda, J. Hasegawa, M. Ishida, T. Nakajima, Y. Honda, O. Kitao, H. Nakai, T. Vreven, K. Throssell, J. A. Montgomery Jr., J. E. Peralta, F. Ogliaro, M. J. Bearpark, J. J. Heyd, E. N. Brothers, K. N. Kudin, V. N. Staroverov, T. A. Keith, R. Kobayashi, J. Normand, K. Raghavachari, A. P. Rendell, J. C. Burant, S. S. Iyengar, J. Tomasi, M. Cossi, J. M. Millam, M. Klene, C. Adamo, R. Cammi, J. W. Ochterski, R. L. Martin, K. Morokuma, O. Farkas, J. B. Foresman and D. J. Fox, Gaussian, Inc., Wallingford CT, 2016

243. F. Neese, F. Wennmohs, U. Becker and C. Riplinger, *J. Chem. Phys.*, 2020, **152**, 224108.

244. J. Tomasi, B. Mennucci and R. Cammi, *Chem. Rev.*, 2005, **105**, 2999-3094.

245. A. E. Reed, L. A. Curtiss and F. Weinhold, *Chem. Rev.*, 1988, **88**, 899-926.

246. A. K. Sharma, T. Ku, A. D. Dawson and D. Swern, *J. Org. Chem.*, 1975, **40**, 2758-2764.

247. O. García Mancheño and C. Bolm, *Org. Lett.*, 2007, **9**, 2951-2954.

248. L. Vandromme, H.-U. Reißig, S. Gröper and J. P. Rabe, *Eur. J. Org. Chem.*, 2008, **2008**, 2049-2055.

249. S. Liu, D. Lentz and C. C. Tzschucke, *J. Org. Chem.*, 2014, **79**, 3249-3254.

250. D. Sarkar, M. K. Ghosh and N. Rout, *Tetrahedron Lett.*, 2018, **59**, 2360-2364.

251. C. Ye, B.-G. Cai, J. Lu, X. Cheng, L. Li, Z.-W. Pan and J. Xuan, *J. Org. Chem.*, 2021, **86**, 1012-1022.

252. H. Nambu, Y. Onuki, N. Ono, K. Tsuge and T. Yakura, *Chem. Commun.*, 2019, **55**, 6539-6542.

253. K. Grammatoglou and A. Jirgensons, *J. Org. Chem.*, 2022, **87**, 3810-3816.

254. E. Duchamp and S. Hanessian, *Org. Lett.*, 2020, **22**, 8487-8491.

255. H. Qin, Y. Jia, N. Wang, Z.-X. Jiang and Z. Yang, *Chem. Commun.*, 2020, **56**, 8265-8268.

256. Z. Cao, D. Shi, Y. Qu, C. Tao, W. Liu and G. Yao, *Molecules*, 2013, **18**, 15717-15723.